

THE JOURNAL OF PHYSICAL CHEMISTRY

Volume 68, Number 2 February, 1964

Application of Significant Structure Theory to Water	R. P. Marchi and Henry Eyring	221
The Kinetics of the Reaction between Vanadium(II) and Vanadium(IV)	T. W. Newton and F. B. Baker	228
Kinetics of Ethylene Hydrogenation over Alumina	J. H. Sinfelt	232
Diffusion in Liquid Hydrocarbon Mixtures	Anthony L. Van Geet and Arthur W. Adamson	238
On the Photochemistry of Aqueous Solutions of Chloride, Bromide, and Iodide Ions	Joshua Jortner, Michael Ottolenghi, and Gabriel Stein	247
Heat Capacities and Thermodynamic Properties of Globular Molecules. X. Fusion of Pentaerythrityl Fluoride	John C. Trowbridge and Edgar F. Westrum, Jr.	255
Job's Method of Continuous Variations with Ion Exchange for the Study of Complexes in Solution	Stanley Bukata and Jacob A. Marinsky	258
Metastable Ions in Mass Spectrometry	G. A. Muccini, W. H. Hamill, and R. Barker	261
An Extension of the Conjugation Theory of Electron-Transfer Reactions	P. V. Manning, R. C. Jarnagin, and M. Silver	265
Kinetics of Ring-Opening and Vinyl Polymerizations without Termination Reactions	L. F. Beste and H. K. Hall, Jr.	269
Second Acid Dissociation of N,N-Di(2-hydroxyethyl)glycine and Related Thermodynamic Quantities from 0 to 55°	S. P. Datta, A. K. Grzybowski, and Roger G. Bates	275
Further Observations of the Stabilities and Reactivities of Gaseous Boroxines	Richard F. Porter and Suresh K. Gupta	280
Kinetics of the Reactions of Elemental Fluorine with Zirconium Carbide and Zirconium Diboride at High Temperatures	A. K. Kuriakose and J. L. Margrave	290
A Study of Selected Ions in the Mass Spectra of Benzenethiol and Deuterated Benzenethiol	D. G. Earnshaw, G. L. Cook, and G. U. Dinneen	296
Quenching of the Scintillation Process in Plastics by Organometallics	Stanley R. Sandler and K. C. Tsou	300
The ³¹ P _i Mercury-Photosensitized Decomposition of Monosilane	H. Niki and Gilbert J. Mains	304
The Effects of Linear Energy Transfer in the Radiation-Induced Polymerization of Several Vinyl Compounds	J. Fock, A. Henglein, and W. Schnabel	310
An Effusion Study of the Decomposition of Copper(II) Bromide	R. R. Hammer and N. W. Gregory	314
The Gas Phase Reactions of Recoil Sulfur Atoms with Carbon Monoxide and Carbon Dioxide	Edward K. C. Lee, Y. N. Tang, and F. S. Rowland	318
On the Viscosity of Branched Polymers Produced by High-Energy Irradiation	J. G. Spiro, D. A. I. Goring, and C. A. Winkler	323
Proton Magnetic Resonance Spectra of Aromatic and Aliphatic Thiols.	Sheldon H. Marcus and Sidney I. Miller	331
Studies of Chemically Reacting Systems on Sephadex. II. Molecular Weights of Monomers in Rapid Association Equilibrium	D. J. Winzor and H. A. Scheraga	338
Hydrogenolysis of Ethane over Supported Platinum	J. H. Sinfelt	344
Electron Paramagnetic Resonance Study of the Photolysis of Nitromethane, Methyl Nitrite, and Tetranitromethane at 77°K.	Benon H. J. Bielski and Richard B. Timmons	347
On the Sonochemical Formation of Hydrogen Peroxide in Water	M. Anbar and I. Pecht	352
Solvolysis of the Tetrachloronickelate(II) Anion	Charles P. Nash and Myrna S. Jenkins	356
Photometric Study of the Reaction of Iodine with Active Nitrogen	C. G. Freeman and L. F. Phillips	362
The Extraction of Acids by Basic Organic Solvents. IV. Tributyl Phosphate and Trioctyl Phosphine Oxide-HAuCl ₄ and HAuBr ₄	M. I. Tocher, D. C. Whitney, and R. M. Diamond	368

No. **40** in the
**ADVANCES IN
CHEMISTRY
SERIES**

MASS SPECTRAL CORRELATIONS

by **FRED W. McLAFFERTY**, Dow Chemical Company

This compilation gives the empirical and structural formulas of ions that might be found at a particular m/e in a mass spectrum plus an indication of how each such ion might have arisen. It contains a wide variety of compound types. Some 4,000 mass spectra are referenced.

The author has drawn freely from his extensive background in mass spectrometry as well as from the efforts and ideas of colleagues and co-workers. He pulls together heretofore scattered information between two covers, the first time such a file has been published.

You can find possible ion structures and precursor molecules for each of the prominent ions in the mass spectrum of an unknown compound with a further indication of the general probability of their occurrence. Space has been left throughout the table for added correlations from your own personal file of spectra.

Newcomers to the field will find this book indispensable. Experts will find it a timesaver in interpreting the spectrum of an unfamiliar compound when information is lacking on the history of the sample. Laboratory directors will want copies for staff members. Why not put this volume to work for **you**?

117 pages.

Paper bound.

Price: \$4.75

Order from:

Special Issues Sales/American Chemical Society
1155 Sixteenth Street, N.W./Washington, D.C. 20036

The Effect of Pressure on the Dissociation of Lanthanum Ferricyanide Ion Pairs in Water S. D. Hamann, P. J. Pearce, and W. Strauss	375
Reactions of Deuterium Atoms with Olefins in Liquid Propane at 90°K. Relative Rate Constants of the Addition T. T. Kassal and M. Szwarc	381
Calculation of the Ostwald Solubility Coefficient for Hydrogen Atoms and the Absolute Rate Constants of Their Addition to Propylene M. Szwarc	385
Calorimetric Investigations of Molten Salts Teh Hu, Hon Chung Ko, and Loren G. Hepler	387
On the Mechanism of Fluorescence Quenching. Tyrosine and Similar Compounds Jehuda Feitelson	391
Activity, Density, and Relative Viscosity Data for Several Amino Acids, Lactamide, and Raffinose in Aqueous Solution at 25° H. David Ellerton, Gundega Reinfelds, Dennis E. Mulcahy, and Peter J. Dunlop	398
The Mutual Frictional Coefficients of Several Amino Acids in Aqueous Solution at 25° H. David Ellerton, Gundega Reinfelds, Dennis E. Mulcahy, and Peter J. Dunlop	403

NOTES

The Solubility of Mercury in Hydrocarbons Robert R. Kuntz and Gilbert J. Mains	408
Ionization of Some Weak Acids in Water-Heavy Water Mixtures Pentti Salomaa, Larry L. Schaleger, and F. A. Long	410
Particle to Particle Migration of Hydrogen Atoms on Platinum-Alumina Catalysts from Particle to Neighboring Particles S. Khoobiar	411
Hardly Band Extinction Coefficients of Ozone in the Gas Phase and in Liquid Nitrogen, Carbon Monoxide, and Argon William B. DeMore and Odell Raper	412
Concerning the Densities and Temperature Coefficients of Liquid Barium and Calcium A. V. Grosse and P. J. McGonigal	414
The Kinetics of the Periodate Oxidation of 2-Aminoethanol George Dahlgren and John Hodsdon	416
Transport of Aqueous Solutions at a Mercury-Glass Interface, Induced by Electric Polarization Robert J. Good and William G. Givens	418
Deactivation of Palladium-Alumina Catalysts Donald G. Manly and Fred J. Rice, Jr.	420
The Electric Dipole Moment and Molecular Conformation of the Heterocycle Boron-Oxygen-Nitrogen-Boron- Oxygen-Nitrogen H. Bradford Thompson, Lester P. Kuhn, and Masahiro Inatome	421
Participation of the SO ₂ ⁻ Radical Ion in the Reduction of <i>p</i> -Nitrophenol by Sodium Dithionite C. R. Wasmuth, Charles Edwards, and Richard Hutcherson	423
Nuclear Magnetic Resonance Studies of Ion-Exchange Resins. II. Electrolyte Invasion Robert H. Dinius and Gregory R. Choppin	425
Thermodynamic Study of Germanium Monotelluride Using a Mass Spectrometer R. Colin and J. Drowart	428
Heat Capacities and Thermodynamic Properties of Globular Molecules. XI. Melting of 3-Azabicyclo[3.2.2]nonane Claus A. Wulff and Edgar F. Westrum, Jr.	430
The Synthesis and Infrared and Nuclear Magnetic Resonance Spectra of Ammonium Dicyanamide James W. Sprague, Jeanette G. Grasselli, and William M. Ritchey	431
A New Class of Photochromic Substances: Metal Carbonyls M. A. El-Sayed	433
Electrolyte-Solvent Interaction. XIII. Conductance of Amine Picrates in Ethylene Chloride at 25° James J. Zwolenik and Raymond M. Fuoss	434

COMMUNICATIONS TO THE EDITOR

Reduction of Platinum Oxide by Organic Compounds. Catalytic Self-Activation in Deuterium Exchange Reactions J. L. Garnett and W. A. Sollich	436
Carbon-13 Chemical Shifts and Intramolecular Hydrogen Bonding G. E. Maciel and G. B. Savitsky	437
Plutonyl Species in Molten Chloride Salt Solutions J. L. Swanson	438
On the Delayed Fluorescence of Pyrene Solutions. A Correction J. B. Birks	439

AUTHOR INDEX

- Adamson, A. W., 238
 Anbar, M., 352
 Baker, F. B., 228
 Barker, R., 261
 Bates, R. G., 275
 Beste, L. F., 269
 Bielski, B. H. J., 347
 Birks, J. B., 439
 Bukata, S., 258
 Choppin, G. R., 425
 Colin, R., 428
 Cook, G. L., 296
 Dahlgren, G., 416
 Datta, S. P., 275
 DeMore, W. B., 412
 Diamond, R. M., 368
 Dinius, R. H., 425
 Dinneen, G. U., 296
 Drowart, J., 428
 Dunlop, P. J., 398, 403
 Earnshaw, D. G., 296
 Edwards, C., 423
 Ellerton, H. D., 398, 403
 El-Sayed, M. A., 433
 Eyring, H., 221
 Feitelson, J., 391
 Fock, J., 310
 Freeman, C. G., 362
 Fuoss, R. M., 434
 Garnett, J. L., 436
 Givens, W. G., 418
 Good, R. J., 418
 Goring, D. A. I., 323
 Grasselli, J. G., 431
 Gregory, N. W., 314
 Grosse, A. V., 414
 Grzybowski, A. K., 275
 Gupta, S. K., 280
 Hall, H. K., Jr., 269
 Hamann, S. D., 375
 Hamill, W. H., 261
 Hammer, R. R., 314
 Henglein, A., 310
 Hepler, L. G., 387
 Hodsdon, J., 416
 Hu, T., 387
 Hutcherson, R., 423
 Inatome, M., 421
 Jarnagin, R. C., 265
 Jenkins, M. S., 356
 Jortner, J., 247
 Kassal, T. T., 381
 Khoobiar, S., 411
 Ko, H. C., 387
 Kuhn, L. P., 421
 Kuntz, R. R., 408
 Kuriakose, A. K., 290
 Lee, E. K. C., 318
 Long, F. A., 410
 Maciel, G. E., 437
 Mains, G. J., 304, 408
 Manly, D. G., 420
 Manning, P. V., 265
 Marchí, R. P., 221
 Marcus, S. H., 331
 Margrave, J. L., 290
 Marinsky, J. A., 258
 McGonigal, P. J., 414
 Miller, S. I., 331
 Muccini, G. A., 261
 Mulcahy, D. E., 398, 403
 Nash, C. P., 356
 Newton, T. W., 228
 Niki, H., 304
 Ottolenghi, M., 247
 Pearce, P. J., 375
 Pecht, I., 352
 Phillips, L. F., 362
 Porter, R. F., 280
 Raper, O., 412
 Reinfelds, G., 398, 403
 Rice, F. J., Jr., 420
 Ritchey, W. M., 431
 Rowland, F. S., 318
 Salomaa, P., 410
 Sandler, S. R., 300
 Savitsky, G. B., 437
 Schaleger, L. L., 410
 Scheraga, H. A., 338
 Schnabel, W., 310
 Silver, M., 265
 Sinfelt, J. H., 232, 344
 Sollich, W. A., 436
 Spiro, J. G., 323
 Sprague, J. W., 431
 Stein, G., 247
 Strauss, W., 375
 Swanson, J. L., 438
 Swzarc, M., 381, 385
 Tang, Y. N., 318
 Thompson, H. B., 421
 Timmons, R. B., 347
 Tocher, M. I., 368
 Trowbridge, J. C., 255
 Tsou, K. C., 300
 Van Geet, A. L., 238
 Wasmuth, C. R., 423
 Westrum, E. F., Jr., 255, 430
 Whitney, D. C., 368
 Winkler, C. A., 323
 Winzor, D. J., 338
 Wulff, C. A., 430
 Zwolenik, J. J., 434

THE JOURNAL OF PHYSICAL CHEMISTRY

Registered in U. S. Patent Office © Copyright, 1964, by the American Chemical Society

VOLUME 68, NUMBER 2 FEBRUARY 15, 1964

Application of Significant Structure Theory to Water¹

by R. P. Marchi² and Henry Eyring

Department of Chemistry, University of Utah, Salt Lake City, Utah (Received October 17, 1963)

A quantitative model embodying the principles of significant structure theory is proposed for liquid water. The model considers water to be composed primarily of two species: a nonrotating hydrogen-bonded species and a rotating monomer. Since the resulting partition function is a function of temperature and volume, all thermodynamic variables may be computed. Calculated results agree reasonably well with experimental quantities.

Introduction

This paper is another in a continuing series of publications³ on the application of the theory of significant structures to various classes of liquids. A review article⁴ has recently been published which explains the origin and meaning of the various factors in the partition function and summarizes the previous applications of the theory.

Due to its wide availability and unusual properties, water has always provided an interesting scientific challenge. During the years a great number of qualitative and quantitative theories have been proposed to explain the properties of water and to elucidate its structure. Rather than review the numerous papers on water, the reader's attention is called to several papers⁵⁻⁷ which contain reviews of previous work in the field.

Dr. M. A. Eliason, working in this laboratory some years ago, was concerned with the water problem and carried out some interesting preliminary investigations.

In general, there have been two main approaches to liquid water. Frank⁸ has called them the "uniformist" or average approach and the "mixture" approach. The uniformist view assumes that liquid water is composed of water molecules which have more or less the same properties. The mixture approach assumes water to be composed of at least two species.

In fact there will be exchange reactions between the species so that an average over a long period of time must show all the molecules to have the same properties. An instantaneous picture, however, reveals different types of water molecules. The instantaneous picture model which we are proposing falls into the "mixture" class.

The Model

We visualize water to be composed primarily of two

- (1) This work partially supported by U. S. Army Ordnance Contract Number DA-ARO(D)-31-124-0298.
- (2) National Institutes of Health Postdoctoral Fellow for 1963.
- (3) H. Eyring, T. Ree, and N. Hirai, *Proc. Natl. Acad. Sci. U. S.*, **44**, 683 (1958); E. J. Fuller, T. Ree, and H. Eyring, *ibid.*, **45**, 1594 (1959); C. M. Carlson, H. Eyring, and T. Ree, *ibid.*, **46**, 333 (1960); T. R. Thomson, H. Eyring, and T. Ree, *ibid.*, **46**, 336 (1960); C. M. Carlson, H. Eyring, and T. Ree, *ibid.*, **46**, 649 (1960); H. Eyring and T. Ree, *ibid.*, **47**, 526 (1961); T. S. Ree, T. Ree, and H. Eyring, *ibid.*, **48**, 501 (1962); D. Henderson, H. Eyring, and D. Felix, *J. Phys. Chem.*, **66**, 1128 (1962); S. Chang, T. Ree, H. Eyring, and I. Matzner, "Progress in International Research on Thermodynamic and Transport Properties," American Society of Mechanical Engineers, New York, N. Y., 1962, p. 88; H. Eyring, D. Henderson, and T. Ree, *ibid.*, p. 340.
- (4) H. Eyring and R. P. Marchi, *J. Chem. Educ.*, in press.
- (5) G. Neméthy and H. Scheraga, *J. Chem. Phys.*, **36**, 3382 (1962).
- (6) F. S. Feates and D. J. G. Ives, *J. Chem. Soc.*, 2798 (1956).
- (7) H. M. Chadwell, *Chem. Rev.*, **4**, 375 (1927).
- (8) H. S. Frank, "Desalination Research Conference," Publication 942 of National Academy of Science—National Research Conference, 1962, p. 141.

species. One species is the tetrahedrally hydrogen-bonded water molecule which will be called the "ice-like" component. By the term "ice-like" we are not implying that these water molecules have the same spatial arrangement as is found in ice; rather, it is meant that the water molecule is hydrogen bonded to its neighbors. The other primary component of water is assumed to be a freely rotating monomer. With respect to the ice-like component the monomer will have a higher entropy and will pack more tightly. The ice-like components, due to the tetrahedral hydrogen bonding, pack in a very bulky way creating voids or interstitial sites. Some or all of these voids are occupied by rotating monomers. As the temperature increases, more and more water molecules break their hydrogen bonds and become freely rotating monomers. At temperatures above 250° water will be composed almost entirely of the rotating monomers and will behave much like a normal liquid. An equilibrium constant can be written which gives the relative concentration of the two species. In general, the pictorial concept of this model is qualitatively the same as those proposed earlier by Samoilov,⁹ Pauling,¹⁰ and Danford and Levy.¹¹

More specifically, we feel the following qualitative description of water can be given. Upon melting, the water molecules rearrange themselves from the hexagonal packing of Ice I into a more dense though still tetrahedrally hydrogen-bonded form which has a molar volume approximately 20% smaller. The structure perhaps is analogous to that of Ice III¹² or along the lines of the model proposed by Danford and Levy. At the same time, the melting process introduces enough fluidized vacancies to cause a 10% increase in volume. The net result is a 10% contraction in the volume. At the melting point the rotating monomers constitute a few per cent of the water molecules. As the temperature rises, more water molecules move into the interstitial sites thus decreasing the net volume, but at the same time fluidized vacancies are being introduced. Apparently below 4° the filling of interstitial sites overshadows the introduction of vacancies so that there is a net decrease in volume. Above 4° water begins to behave as a normal liquid. Due to the increase in concentration of the monomers with rising temperature, it will be necessary for the structure of the ice-like component to change to accommodate more rotating monomers. This would account for the various properties¹³ which reveal structure changes and the minimum in the heat capacity curve around 35°.¹⁴

In a normal liquid it is usually found that the molecules rotate. In those cases when hydrogen bonds can be formed, it becomes advantageous for a molecule to

form them since this will lower the Helmholtz free energy of the system at the expense of entropy. When a water molecule forms four hydrogen bonds, there is a large increase in the internal energy, enough to compensate for the loss in entropy. Very little is gained if one or two of these hydrogen bonds are broken, since the rotational or librational motion is still rather constrained and yet there has been a loss in energy equivalent to the breaking of one or two bonds. A water molecule that has only one hydrogen bond will possess a reasonable amount of freedom, but of the five possible species, we think that the monomer and the tetrahedrally hydrogen-bonded water molecule will be the two predominant species.

The existence of a freely rotating monomer in liquid water has been a widely discussed possibility. The experimental evidence for such a species rests on some neutron scattering studies by Hughes, Palevsky, *et al.*,¹⁵ and some low frequency Raman scattering by Stoicheff¹⁶ in Ottawa. Neither of these experiments is conclusive since the experimental observations are subjected to various interpretations. Frank¹⁷ has discussed the question of whether or not direct spectral evidence could be definitely obtained for a monomer. The existence of a rotating monomer seems plausible since most of the water molecules will be completely hydrogen bonded (at low temperatures) so that the monomer will have no choice but to remain a monomer. Furthermore, if the monomer is surrounded by the ice-like components, it will be in a more or less homogenous field and will rotate almost, if not completely, freely. At high temperatures water behaves as a normal liquid so that a rotating monomer seems very plausible.

The features of our model which are essential to the partition function are the following. Water is composed of two species, one of which rotates. The concentration of the rotating component increases with temperature. With these concepts and by making use of significant structure theory, we can write the partition function as shown in the equation

- (9) O. Samoilov, *Zh. Fiz. Khim.*, **20**, 1411 (1946).
- (10) L. Pauling, "The Nature of the Chemical Bond," Third Ed., Cornell University Press, Ithaca, N. Y., 1960, p. 472.
- (11) M. D. Danford and H. A. Levy, *J. Am. Chem. Soc.*, **84**, 3965 (1962).
- (12) W. B. Kamb and S. K. Datta, *Nature*, **187**, 140 (1960).
- (13) M. Magat, *Trans. Faraday Soc.*, **33**, 114 (1937).
- (14) D. C. Ginnings and G. T. Furukawa, *J. Am. Chem. Soc.*, **75**, 522 (1953).
- (15) D. J. Hughes, H. Palevsky, W. Kley, and E. Tunkelo, *Phys. Rev.*, **119**, 872 (1960).
- (16) B. Stoicheff, unpublished work; see footnote 23 of ref. 12; also ref. 5 and 14.
- (17) See ref. 5 and footnote 18 of H. S. Frank and A. S. Quist, *J. Chem. Phys.*, **34**, 604 (1961).

$$f_{\text{H}_2\text{O}} = f_s^{Nv_s/V} f_g^{\frac{N}{2} \frac{v-v_s}{v}} \quad (1)$$

where

$$f_g = \left[\frac{(2\pi m_1 kT)^{3/2} eV}{h^3} f_{\text{vib}} f_{\text{rot}} \right]^2 + \frac{(2\pi m_2 kT)^{3/2} eV}{h^3} \frac{eV}{N/2} f_{\text{vib}}^2 f_{\text{rot}}^2 \frac{8\pi^2 I kT}{2h^2} \frac{e^{D/RT} - 1}{1 - e^{-h\nu/kT}} \quad (2)$$

Here f_{vib} is the partition function for three degrees of internal freedom and is given by

$$f_{\text{vib}} = \prod_{i=1}^3 (1 - \exp(-h\nu_i/kT))^{-1} \quad (3)$$

and f_{rot} is the partition function for a three dimensional rigid rotator

$$f_{\text{rot}} = \frac{(8\pi^2 kT)^{3/2} (\pi ABC)^{1/2}}{2h^3} \quad (4)$$

The three intramolecular vibration frequencies and the principal moments of inertia were taken to be the same as in the vapor state: $\omega_1 = 3652$, $\omega_2 = 1595$, $\omega_3 = 3756$ cm^{-1} ; $A = 1.024 \times 10^{-40}$, $B = 1.921 \times 10^{-40}$, $C = 2.947 \times 10^{-40}$, $I = 3.365 \times 10^{-39}$ c.g.s.

f_g (eq. 2) is the gas-like portion of the partition function, and, since water is known to associate in the gas phase, contains terms for the monomer and the dimer species. The monomer term is squared so that when f_g is raised to the $N/2$ power, the correct number of degrees of freedom ($9N$) will be obtained. The dimer term contains the factor $N/2$ since there are $N/2$ dimer molecules. The factor $(e^{D/RT} - 1)$ (where D is the dissociation energy) arises in the following manner.

Assume that the potential well between two molecules may be represented by a simple parabola so that a harmonic oscillator model may be used. The partition function for all energy levels is

$$\sum_{n=0}^{\infty} e^{-\frac{n h \nu}{kT}} = \frac{1}{1 - e^{-h\nu/kT}} \quad (5)$$

but we wish to consider only those energies for which the two molecules are associated. Accordingly, we must subtract those terms having an energy greater than D . Thus

$$\frac{1 - e^{-D/RT}}{1 - e^{-h\nu/kT}} \quad (6)$$

For energies greater than D the dimer will dissociate into monomers. Therefore, we must add a term for the monomers. If we now include the translational

partition function, we obtain for a system of monomers and dimers

$$\frac{(2\pi m_1 kT)^{3/2} V}{h^3} e^{-D/RT} + \frac{8\pi^2 I kT}{2h^2} \frac{1 - e^{-D/RT}}{1 - e^{-h\nu/kT}} \quad (7)$$

In obtaining eq. 7, it was tacitly assumed that the zero point energy level would be taken as the zero of energy and no correction was made for the hindering of the rotation of the individual molecules forming the dimer. It is more customary to take the energy level at which the two molecules separate as the zero. To do this we must multiply eq. 7 by $e^{D/RT}$ obtaining

$$\frac{(2\pi m_1 kT)^{3/2} V}{h^3} + \frac{8\pi^2 I kT}{2h^2} \frac{e^{D/RT} - 1}{1 - e^{-h\nu/kT}} \quad (8)$$

which is the form used in eq. 2.

The question frequently arises as to why eq. 1 is written as a product while eq. 2 is written as a sum. This is because there are two ways of obtaining the average properties of a system. Gibbs pointed this out many years ago. Given a system of molecules, one can observe one molecule for a great length of time and obtain the average properties of the system by averaging the properties of the one molecule over time. This gives rise to a sum of states. A common example of this procedure is the partition function for a simple harmonic oscillator. The other way of averaging is to take an instantaneous picture of many molecules. Some molecules will be in one state and other molecules in other states. To obtain the average properties, an instantaneous average must in this case be taken over the molecules in all of space. The resulting partition function will be a product of partition functions for each molecular state with each state properly weighted. An example of this type of averaging is the partition function for a mixed ideal gas. Each of these ways of averaging can be carried out correctly and both will give the same result provided the relaxation time of the system is short compared with the length of time over which the system is averaged. Thus, Boltzmann's ergodic hypothesis is reasonable for a system of molecules, since they suffer a great number of collisions.

With regard to significant structure theory, the space averaging procedure has been used. An instantaneous picture of a liquid reveals that while some of the molecules are completely surrounded by molecules, others are adjacent to a fluidized vacancy. That is, some of the molecules are vibrating about some point in space (behaving in a solid-like manner) while others are exhibiting translational degrees of freedom (gas-like behavior). Therefore, the liquid partition func-

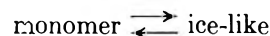
tion is written as a product of solid-like and gas-like partition functions (eq. 1) each weighted by their respective fractions, V_s/V and $V - V_s/V$. Since this partition function has been so successful, it seems reasonable to assume that the number of molecules in states intermediate to solid-like and gas-like behavior may be neglected. In considering the dimer term in the gas-like portion of the partition function (eq. 2), a time averaging procedure was chosen and, thus, a sum of terms. Certainly, to be correct, trimer and higher terms should also be included. However, it seems reasonable to assume that a molecule will spend very little time in highly polymerized configurations, since the concentration of dimers in water vapor¹⁸ at the boiling point is only about 1%.

With our visualization of water as being composed of two species, we can write the solid-like portion, f_s , of the partition function either by means of a time average or a space average. If we use a time average, we obtain the form

$$f_s = \frac{e^{E_s/RT}}{(1 - e^{-\theta/T})^3} \left[1 + n \frac{V - V_s}{V} e^{-\frac{\alpha E_s V_s}{RT(V - V_s)}} \right] \times f_{\text{vib}} \left[\frac{1 - e^{-E_0/RT}}{(1 - e^{-\theta/T})^3} + e^{-E_0/RT} f_{\text{rot}} \right] \quad (9)$$

The origin of the first three factors (partition function for an Einstein solid, the degeneracy term and the partition function for three degrees of internal freedom, eq. 3) is given elsewhere.⁴ The remaining factor is a time average of one molecule assuming that only the two extreme states (either a molecule is completely hydrogen bonded and so its remaining three degrees of freedom are represented by an Einstein oscillator or it is not hydrogen bonded and is completely free to rotate) need be considered. E_0 is the energy required for a molecule to transfer from a completely bonded state to a freely rotating state. Examination of the last factor in eq. 9 shows that when T is small, eq. 9 reduces to the partition function of a molecule which has six degrees of external vibration and three of internal vibration. When T is large, eq. 9 becomes the partition function of a molecule which has three degrees of external vibration, three of internal vibration, and three of rotational freedom. Intermediate temperatures yield a partition function for a molecule which has properties which are a combination of the two limiting states. By using the time-averaging method, it is tacitly assumed that the external vibrational degrees of freedom are the same for the ice-like component and the monomer, *i.e.*, they have the same Einstein characteristic temperature, θ . Likewise, it is assumed that the same degeneracy term and the same value for E_s is applicable

for both species. Since the relative concentration of the two species changes with temperature, E_s and V_s will also vary with temperature. Thus, if the following equilibrium is considered



an equilibrium constant can be written.

$$K = \frac{[\text{ice-like}]}{[\text{monomer}]} = e^{-\frac{\Delta H}{RT}} e^{\frac{\Delta S}{R}} e^{-\frac{P\Delta V}{RT}} \quad (10)$$

Then

$$E_s = \frac{KE_{s_1} + E_{s_2}}{1 + K}$$

$$V_s = \frac{KV_{s_1} + V_{s_2}}{1 + K} \quad (11)$$

where E_{s_1} and V_{s_1} are the sublimation energy and solid volume of the ice-like component.

Using a space-averaging procedure, the following form is obtained for f_s

$$f_s = \left\{ \frac{e^{E_{s_1}/RT}}{(1 - e^{-\theta_1/T})^3} \left[1 + n_1 \frac{V - V_{s_1}}{V} e^{-\frac{\alpha_1 E_{s_1} V_{s_1}}{RT(V - V_{s_1})}} \right] \times f_{\text{vib}} \right\}^{\rho} \left\{ \frac{e^{E_{s_2}/RT}}{(1 - e^{-\theta_2/T})^3} \times \left[1 + n_2 \frac{V - V_{s_2}}{V} e^{-\frac{\alpha_2 E_{s_2} V_{s_2}}{RT(V - V_{s_2})}} \right] f_{\text{vib}} f_{\text{rot}} \right\}^{(1-\rho)} \quad (12)$$

The first factor is the partition for the ice-like component, and it is weighted by its relative concentration, ρ , which may be obtained from eq. 10: $\rho = K/1 + K$. To avoid considering librational degrees of freedom and for simplicity, six degrees of freedom for the ice-like component have been treated as Einstein oscillators. The remaining factor is the partition function for the freely rotating monomer and so contains a partition function for a three dimensional rigid rotator. V_s is assumed to be a simple linear combination of the V_s values of the two species

$$V_s = \rho V_{s_1} + (1 - \rho) V_{s_2} \quad (13)$$

All calculations were performed on an IBM 1620 or 7090 computer. Values for the parameters for eq. 1, 2, and 9 are shown in Table I. The results are given in Fig. 1-4, which show Helmholtz free energy, entropy, pressure, and volume *vs.* temperature, respectively.

(18) C. Herzberg, "Molecular Spectra and Molecular Structure," Vol. II, D. Van Nostrand Company, Princeton, N. J., 1945, p. 161; K. K. Kelley, "Contributions to the Data on Theoretical Metallurgy," U. S. Dept. of Interior, Bureau of Mines, Bulletin 477, 1950, p. 50.

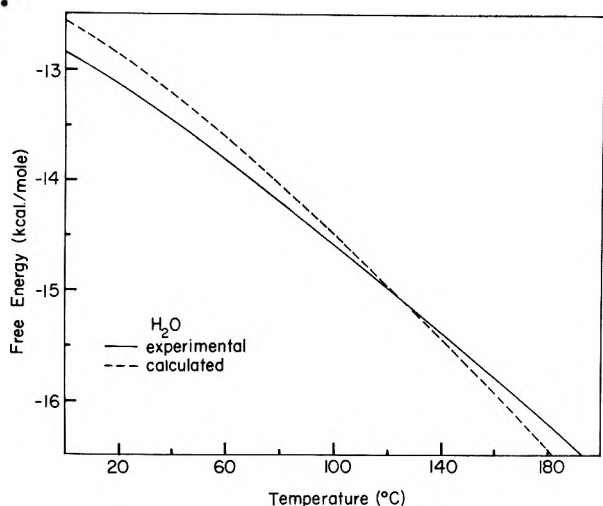


Figure 1. Helmholtz free energy vs. temperature; experimental values are from Dorsey.¹⁹

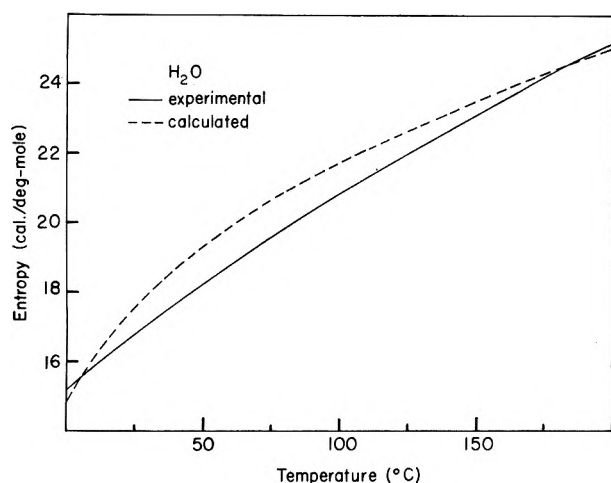


Figure 2. Entropy vs. temperature; experimental values are from Dorsey¹⁹ and Bureau of Mines.¹⁸

Experimental quantities were taken from Dorsey.¹⁹ The error in the free energy is greatest at the melting point and is about 300 cal. The maximum error in the entropy occurs near the boiling point and amounts to 0.9 e.u. out of 22 e.u. The normal boiling point occurs at 98°, and at 150° the pressure is approximately

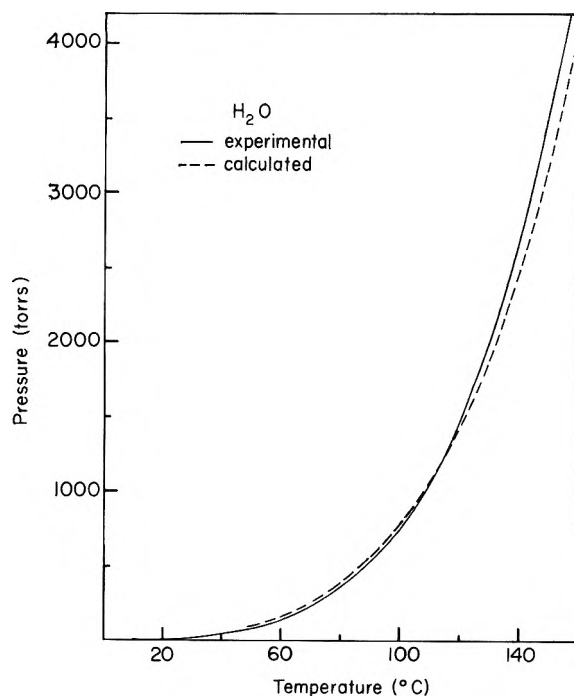


Figure 3. Pressure (mm.) vs. temperature; experimental values from Dorsey.¹⁹

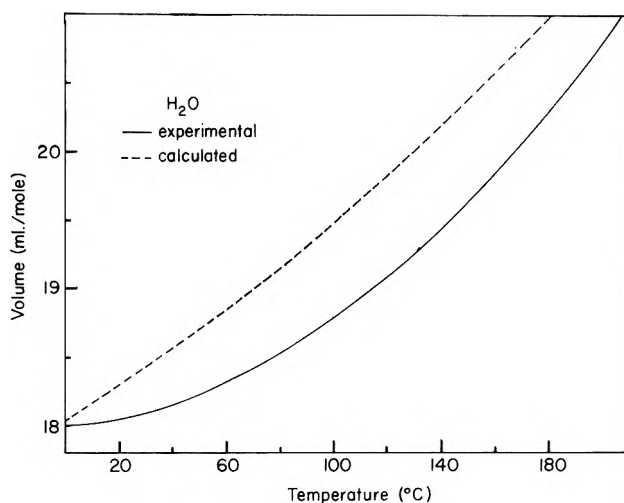


Figure 4. Molar volume vs. temperature; experimental values from Dorsey.¹⁹

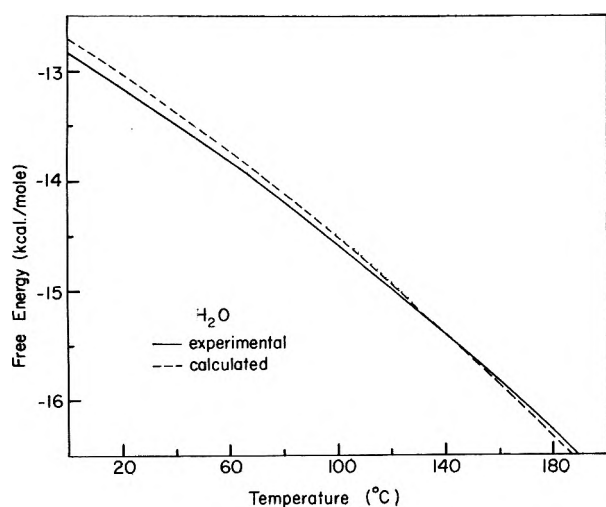
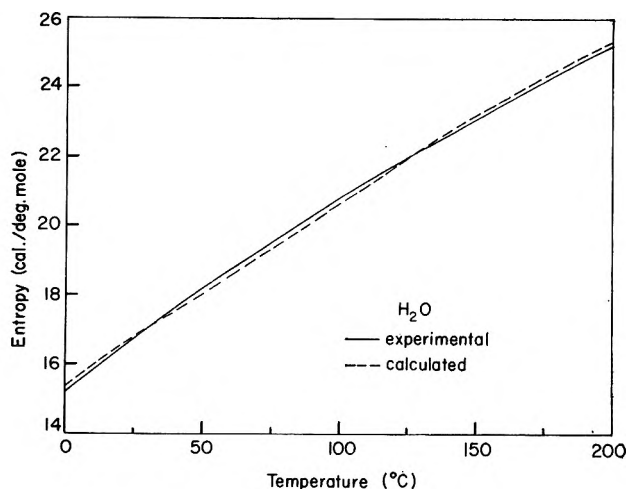
300 mm. too low. The volume curve exhibits no minimum at 4°, and near the boiling point the molar volume is too high by about 0.7 ml./mole. The critical temperature is 18% too large, the critical volume and entropy are approximately 10% too large, and the critical pressure is 65% too large.

Table I: Parameters for Equations 1, 2, 9, and 10

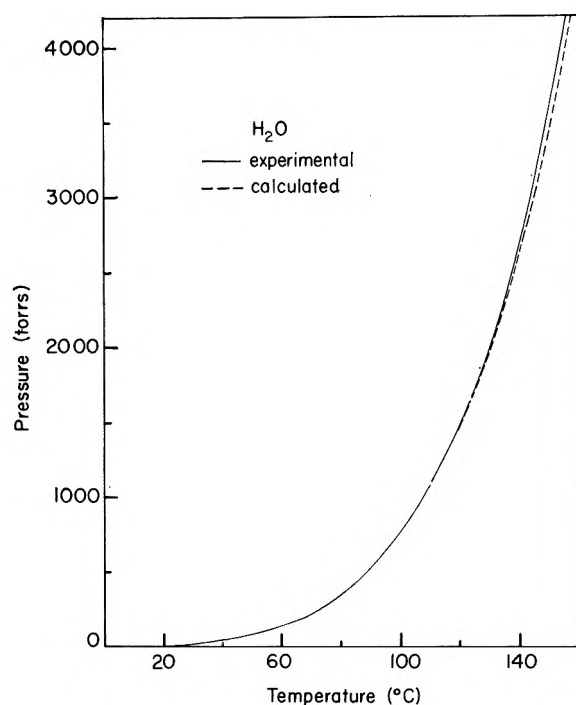
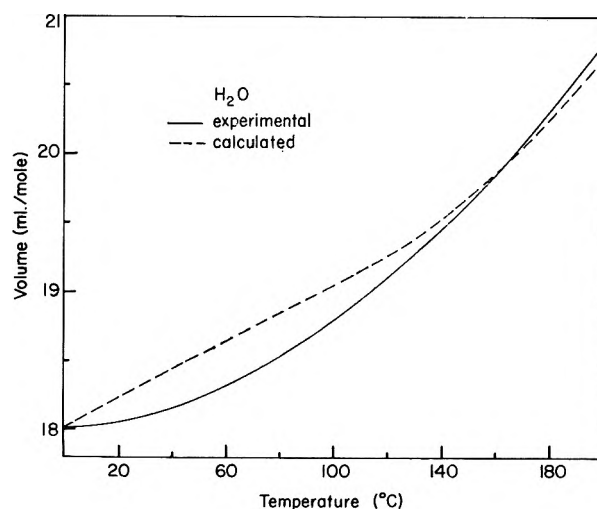
$E_{s1} = 10.794$ kcal.	$n = 11.0$
$E_{s2} = 9.6283$ kcal.	$\theta = 213.0$
$V_{s1} = 17.805$ ml./mole	$a = 1.0 \times 10^{-8}$
$V_{s2} = 17.670$ ml./mole	$D = 3.7$ kcal.
$\nu = 1.798 \times 10^{12}$ sec. ⁻¹	$E_0 = 270$ cal.
$\Delta S = -18.02$ e.u.	$\Delta H = -3.89$ kcal.

(19) N. Dorsey, "Properties of Ordinary Water-Substance," Reinhold Publishing Corporation, New York, N. Y., 1940.

แผนกห้องสมุด กรมวิทยาศาสตร์
กระทรวงอุตสาหกรรม

Figure 5. Helmholtz free energy *vs.* temperature.Figure 6. Entropy *vs.* temperature.

Calculated properties based on the space-averaging procedure (eq. 1, 2, and 12) are shown in Fig. 5-8. The values of the appropriate parameters are given in Table II. In all cases the properties calculated by means of a space average are better than those obtained from a time-averaging method. The maximum error in free energy has been reduced to 125 cal. and in the entropy to 0.2 e.u. The boiling point is obtained almost exactly, and at 150° the pressure is too low by 90 mm. The maximum error in volume over most of the liquid range (250° temperature span) is 0.3 ml./mole, but still does not exhibit the minimum at 4°. The calculated and observed critical properties are shown in Table III. Figure 9 is a plot of the equilibrium constant (eq. 10) *vs.* temperature. The quantity $1/1 + K$ gives the per cent monomer concentration.

Figure 7. Pressure *vs.* temperature.Figure 8. Molar volume *vs.* temperature.

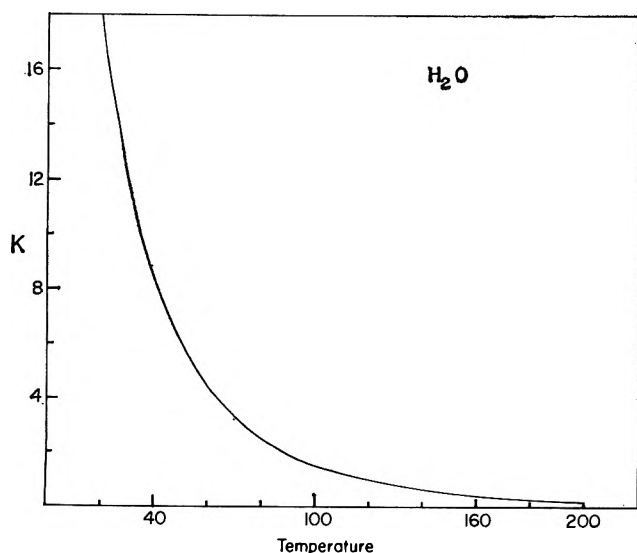
The monomer concentration at the melting point is approximately 2.5%, 40% at the boiling point, and at 250° the monomer concentration is about 90%. The calculated entropy of vaporization is 26.14 e.u. The observed value is 26.02 e.u.

Discussion

Of the two approaches used here for water, the space-averaging procedure was found to be superior to the process of taking a time average. This was to be ex-

Table II: Parameters for Equations 1, 2, 10, and 12

$n_1 = 12.0$	$E_{s_1} = 10.794 \text{ kcal.}$	$a_1 = 9.255 \times 10^{-8}$	$\theta_1 = 221.51$	$V_{s_1} = 17.61 \text{ ml./mole}$
$n_2 = 8.0$	$E_{s_2} = 9.6543 \text{ kcal.}$	$a_2 = 1.000 \times 10^{-4}$	$\theta_2 = 230.40$	$V_{s_2} = 17.11 \text{ ml./mole}$
$\nu = 1.798 \times 10^{12} \text{ sec.}^{-1}$		$D = 3.7 \text{ kcal.}$	$\Delta S = -17.3 \text{ e.u.}$	$\Delta H = -6.9 \text{ kcal.}$

**Figure 9.** Equilibrium constant (eq. 10) for parameters given in Table II vs. temperature.**Table III:** Critical Properties

	Calcd.	Obsd.	$\Delta, \%$
$T_c, ^\circ\text{K.}$	718.7	647.2	11
$V_c, \text{ml./mole}$	60.26	55.85	7.9
$P_c, \text{mm.}$	257,048	165,976	55
$S_c, \text{e.u.}$	36.69	33.84	8.4

pected since experience has shown that space averaging does not require as detailed a description of a system as time averaging. Absolute reaction rate theory is a good example of this. Approaching kinetics by means of a time average essentially requires a solution to the quantum mechanical many body problem. On the other hand, reaction rate theory looks only at the initial reactants and the activated complex. However, this tremendous simplification is somewhat offset by the introduction of a transmission coefficient. So it is not surprising that with the same amount of information (*i.e.*, assumption of two species) the space-averaging procedure yields better agreement with experimental observations.

The model presented in this paper yields excellent agreement with experiment except for such properties

as the volume and quantities involving the second derivative, such as the heat capacity at constant volume. The calculated heat capacity is found to be 10 cal./deg. instead of the observed 18 cal./deg. It is to be expected that if the calculated volume is wrong, C_v will also be wrong, since both are very structure-dependent quantities. Structure dependence comes into significant structure theory by means of the quantity V_s . Due to the fact that water is a strongly associated liquid, V_s will have an unusual functional behavior. With liquid argon one can assume that V_s is constant and still obtain close agreement with reality. With water we have assumed that V_s is a simple linear combination (eq. 11 or 13) of the V_s values of the two species. For water with all its unusual structural behavior this is an oversimplifying assumption, since V_s should be rather strongly temperature dependent. Other workers^{5,17} have essentially assumed an *a priori* behavior for V_s and duplicated the experimental variation of V quite closely.

In developing a theory of liquids there are really two problems involved. First, a theory of solids is needed to determine quantities such as V_s and E_s . With the previous liquids treated by significant structure theory, a theory of solids was not needed, since there were no drastic rearrangements upon melting. Thus, the parameters required in this liquid theory could be closely approximated by the properties of the solid at the melting point. With liquids such as water we have a much different situation, since at the melting point there is a fundamental structure change. A theory of solids is needed then to calculate the molar volume of the ice-like component of water and how it varies with temperature. When this quantity is known, the unusual volume behavior of liquid water will follow in a natural way.

The other main problem in developing a liquid theory is accounting for the excess volume, $V - V_s$. For a model to qualify as a reasonable representation of the liquid state, it must be able to explain how a liquid utilizes the excess volume. Theories which neglect this concept are not liquid theories but rather are theories of superheated solids or supercooled gases. A rigorous approach to liquids which utilizes pair potentials is impressive, but only if it is an attempt to explain liquids and not superheated solids. If cell

or lattice models sometimes give reasonable agreement with experimentally determined quantities, it cannot be taken as an indication of their validity, since it is to be expected that the properties of a superheated solid will not differ greatly from those of a liquid.

In summary, we have proposed a model of liquid water which by using the theory of significant structures has assumed that water is composed primarily of two species: an ice-like component (but we are not imply-

ing that the spatial arrangement is the same as ice) and a freely rotating monomer. The model demonstrates reasonable agreement with experiment. A model successfully applied to one liquid means little, but this model is strengthened since significant structure theory has been applied successfully to so many classes of liquids. Certainly, this is not the final work on water, but it opens up an interesting line of approach.

The Kinetics of the Reaction between Vanadium(II) and Vanadium(IV)¹

by T. W. Newton and F. B. Baker

University of California, Los Alamos Scientific Laboratory, Los Alamos, New Mexico
(Received September 30, 1963)

The kinetics of the reaction $V(II) + V(IV) = 2V(III)$ have been studied in acid perchlorate solutions from 0.2 to 2.0 *M* in $HClO_4$ over a temperature range from 0.4 to 34.5° at $\mu = 2.0 M$. The rate law is $-d[V(IV)]/dt = (k_0 + k_1[H^+])[V(II)][V(IV)]$. The k_0 term accounts for nearly all of the rate, and values of ΔH^* and ΔS^* for this path were found to be 12.3 ± 0.1 kcal./mole and -16.5 ± 0.3 e.u. Chloride ion increases the rate slightly while sulfate increases the rate markedly. The effect of ionic strength was studied between 0.2 and 2.0 *M* at 25° and is in accord with the extended form of the Debye-Hückel equation.

Introduction

The kinetics of the reaction between V(II) and V(IV) have been studied in order to learn the rate law and the thermodynamic quantities of activation for comparison with other oxidation-reduction reactions. Earlier workers have reported that the reaction is rapid² or instantaneous.³ Recently, however, catalytic polarographic currents for the reduction of V(III) in the presence of V(IV) have been used to estimate the rate of the reaction in sulfate solutions.⁴

In the present work it was found that the rate of the reaction in perchlorate solutions is conveniently measurable using spectrophotometric techniques. The reaction proceeds partly by way of a highly colored intermediate which has been identified as a hydrolytic

dimer of V(III). A study of the properties of this substance will be published elsewhere.⁵

Experimental

Reagents. V(IV) perchlorate solutions were prepared from V(V) in $HClO_4$ by electrolytic reduction at a mercury cathode. Small amounts of V(III) were

- (1) Work done under the auspices of the U. S. Atomic Energy Commission.
- (2) K. V. Krishnamurty and A. C. Wahl, *J. Am. Chem. Soc.*, **80**, 5921 (1958).
- (3) W. R. King, Jr., and C. S. Garner, *J. Phys. Chem.*, **58**, 29 (1954).
- (4) J. W. Olver and J. W. Ross, Jr., *ibid.*, **66**, 1699 (1962).
- (5) T. W. Newton and F. B. Baker, *Inorg. Chem.*, in press.

removed by reaction with V(V). The V(V) solutions were prepared by the dissolution of V_2O_5 in $HClO_4$. The V(IV) solutions were analyzed by reduction to V(II) on zinc amalgam, adding an aliquot to excess standard Ce(IV) in 5 *M* H_2SO_4 , and back-titrating with standard Fe(II) to the ferroin end point. The V(II) solutions were prepared by the reduction of V(IV) on zinc amalgam. All of the V(II) solutions were protected from air oxidation by means of blankets of argon. The $HClO_4$, $LiClO_4$, and $NaClO_4$ solutions were prepared and standardized as described previously.⁶

Procedure. Appropriate amounts of V(II), V(IV), $HClO_4$, and salt ($LiClO_4$ or $NaClO_4$) stock solutions were brought to the desired temperature and mixed in special absorption cells. The solutions and cells were thoroughly swept with argon before use. The cells were either two-chambered for hand mixing or arranged for injection with mechanical stirring. The cells were positioned in a small thermostat in the light beam of the Cary recording spectrophotometer, Model 14. Additional details have been given in previous articles.^{6,7}

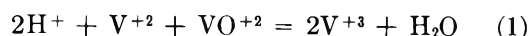
The reaction was followed at 7600 Å. where the absorption is due primarily to V(IV). After the final absorbance readings were made, an aliquot of the mixture was added to excess standard Ce(IV) in 6 *M* H_2SO_4 , and back-titrated with standard Fe(II) in order to determine the initial V(II) concentration. The initial V(IV) concentration was computed from the amount and concentration of the stock solution used.

The concentration units used here are moles per liter (*M*) at 23°. The actual concentrations are slightly different at different temperatures, for example, being about 1% higher at 0°.

The apparent second-order rate constants were calculated from the absorbance data using the method of least squares described previously.⁶

Catalytic Impurities. The possibility of catalytic impurities was investigated by comparing the rates obtained using specially prepared reagents with those obtained using the reagents described above. The use of recrystallized $VO(ClO_4)_2$, recrystallized $LiClO_4$, or redistilled $HClO_4$ gave essentially the same rates as the use of the ordinary preparations. V(II) prepared electrolytically gave the same results as that prepared on zinc amalgam. To minimize air oxidation, the V(II) solutions were transferred using hypodermic syringes; replacing the stainless steel needle with a glass one was without effect.

Stoichiometry. The oxidation potentials of the various vanadium couples in acid solution⁸ are such that the reaction



goes to completion. V(II) is unstable with respect to oxidation by H^+ and both V(II) and V(III) can be oxidized by ClO_4^- ; however, the rates of these reactions are low. It is reported that in HCl solutions V(II) is oxidized at a rate <1%/month at 25° and about 11%/month at 50°.³ The oxidation by ClO_4^- is relatively more rapid; in 1 *M* $HClO_4$ the rate of oxidation of V(II) is about 0.12%/min. and of V(III) about 0.03%/min. at 50°. At 25° we have found the rate of oxidation of V(II) by ClO_4^- to be <1%/hr. in 2 *M* $HClO_4$.

The highly colored intermediate mentioned above does not affect the determination of the kinetics at 7600 Å. Its absorption maximum is at 4250 Å. and its maximum concentration is very low. In 0.2 *M* $HClO_4$ solutions at 25° which are 5×10^{-3} *M* in V(II) and V(IV), we estimate the concentration of the complex to be less than 4×10^{-5} *M*.

These considerations show that the side reactions mentioned will not significantly affect the stoichiometry indicated by reaction 1.

Results

The Rate Law. Absorbance vs. time data for all of the rate runs were in satisfactory agreement with the second-order rate law

$$-d[V(IV)]/dt = -d[V(II)]/dt = k'[V(II)][V(IV)] \quad (2)$$

Further confirmation of this rate law was obtained in an experiment in which the total vanadium concentration was increased from 0.012 to 0.057 *M*. This change in concentration was found to increase k' , the apparent second-order rate constant, by only about 6%. Further experiments with added Zn(II) showed that this increase was predominantly a medium effect.

The rate was found to be independent of the V(III) in an experiment in which 0.013 *M* V(III) was replaced by 0.013 *M* La(III). This change caused a decrease in k' of only about 1.3%, well within the experimental error.

The effect of hydrogen ion concentration on the rate was found to be quite small. The data in Table I show that increasing the $HClO_4$ concentration from 0.2 to 2.0 *M* at constant ionic strength increased the

(6) T. W. Newton and F. B. Baker, *J. Phys. Chem.*, **67**, 1425 (1963).

(7) T. W. Newton, *ibid.*, **62**, 943 (1958).

(8) W. M. Latimer, "Oxidation Potentials," Second Ed., Prentice-Hall, Inc., New York, N. Y., 1952.

average rate by about 7% at 0° and 10% at 34.5°. The rate law, including the hydrogen ion dependence, may be written

$$-d[V(IV)]/dt = (k_0 + k_1[H^+])[V(II)][V(IV)]$$

or, since neither vanadium species is appreciably hydrolyzed in the acid concentration range studied

$$-d[V(II)]/dt = (k_0 + k_1[H^+])[V^{+2}][VO^{+2}] \quad (3)$$

Table I: Apparent Second-Order Rate Constants at Various HClO₄ Concentrations and Temperatures. Conditions: $\mu = 2.0$ (LiClO₄), $4.8 \times 10^{-3} M$ V(II), $7.0 \times 10^{-3} M$ V(IV). The units are $M^{-1} \text{ min.}^{-1}$

HClO ₄ , M	—0.4°—		—12.8°—		—24.8°—		—34.5°—	
	Obsd.	Calcd. ^a	Obsd.	Calcd.	Obsd.	Calcd.	Obsd.	Calcd.
0.2	14.3	13.7	38.1	38.2	93.4	94.8	188.9	187.9
	14.0		37.2		95.7		189.8	
1.0	15.2 ^b	14.8	38.7	39.4	97.2	97.3	194.5	192.3
	14.0	14.3	39.2 ^c	40.3	95.9		192.7	
2.0	15.3	14.9	41.4	40.9	101.1	100.5	199.3	197.8
	14.9		39.7		99.2		202.4	

^a Calculated from the activation parameters in Table V. ^b Determined at 0.8°. ^c Determined at 13.1°.

Catalysis by Anions. The effects of the anions Cl⁻ and SO₄⁻² were briefly investigated; the results are summarized in Tables II and III.

Table II: Apparent Second-Order Rate Constant at Various HCl Concentrations. Conditions: $\mu = 2.0$ (HClO₄), $4 \times 10^{-3} M$ V(II), $7.1 \times 10^{-3} M$ V(IV), 24.8°

HCl, M	0.00	0.02	0.06	0.10	0.20	0.30	0.50
$k', M^{-1} \text{ min.}^{-1}$	96.3	99.5	103	104	109	112	118
Calcd. eq. 10	98.0	99.4	102	104	109	113	118

Table III: Apparent Second-Order Rate Constants at Various Sulfate Concentrations. Conditions: $4.9 \times 10^{-3} M$ V(II), $7.0 \times 10^{-3} M$ V(IV), 24.8°, $\mu \sim 0.8 M$

HClO ₄	Concentrations, M						Rate constant, $M^{-1} \text{ min.}^{-1}$
	H ₂ SO ₄	Na ₂ SO ₄	NaClO ₄	H ⁺	HSO ₄ ⁻	SO ₄ ^{-2a}	
0.493	0	0	0.299	0.493	0	0	40.5
.467	0.022	0	.297	.493	0.018	0.004	73.6
.364	.110	0	.281	.493	.091	.018	217
0	.475	0.075	.057	.493	.457	.093	732
0.250	0	0	.599	.25	0	0	39.7
.233	0.013	0	.539	.25	0.009	0.004	70
.166	.065	0	.523	.25	.046	.018	196
0	.241	0.083	.322	.25	.232	.093	772

^a [H⁺], [HSO₄⁻], and [SO₄⁻²] were calculated assuming K_a of HSO₄⁻ to be 0.1 M.

Ionic Strength Dependence. The effect of ionic strength was investigated at 24.8° in 0.2 M HClO₄. Both LiClO₄ and NaClO₄ were used to vary μ between 0.2 and 2.0 M. The results of these experiments are summarized in Table IV. It is seen that substituting NaClO₄ for LiClO₄ has very little effect on the rate constants.

Table IV: Effect of Ionic Strength on the Apparent Second-Order Rate Constants. Conditions: 0.20 M HClO₄, $3.9 \times 10^{-3} M$ V(II), $8.0 \times 10^{-3} M$ V(IV), 24.8°

Ionic strength, μ, M	LiClO ₄ solutions $k', M^{-1} \text{ min.}^{-1}$		NaClO ₄ solutions $k', M^{-1} \text{ min.}^{-1}$	
	Obsd.	Calcd. ^a	Obsd.	Calcd.
0.20	20.0, 20.2	20.2	20.3, 20.5	20.7
.49	31.1	31.2	32.4	31.3
.92	46.5, 46.2	45.8	45.6	45.2
1.28	60.3	59.0	58.0, 59.4	57.7
2.00	89.9, 89.3	91.2	84.9, 87.6	88.3

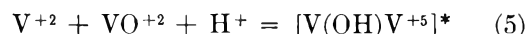
^a Calculated from an extended Debye-Hückel equation using the parameters given in the text.

Discussion

Activation Processes. The empirical rate law, eq. 3, shows that the principal net activation process is



and that the two hydrogen ions required for the over-all reaction are acquired after the rate-determining step. The minor term in the rate law, $k_1[H^+]$, can be due to an additional reaction path with the net activation process



or it might equally well be due to a small medium effect.

The temperature dependence of the rate has been interpreted under the assumption that both k_0 and k_1 follow the equation⁹

$$k_i = (k_B/h)T \exp(\Delta S_i^*/R) \exp(-\Delta H_i^*/RT) \quad (6)$$

A least-squares program was used to find values of ΔS_0^* , ΔH_0^* , ΔS_1^* , and ΔH_1^* which minimize the sum of the squares of the per cent deviations between the observed and calculated rate constants at all values of [H⁺] and temperature simultaneously.³ The results of this calculation are included in Table V. The

(9) S. Glasstone, K. Laidler, and H. Eyring, "The Theory of Rate Processes," McGraw-Hill Book Co., Inc., New York, N. Y., 1941, p. 196.

calculated rate constants given in Table I are based on these thermodynamic quantities of activation.

Table V: Thermodynamic Quantities of Activation, 25°

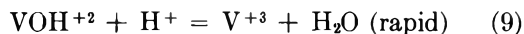
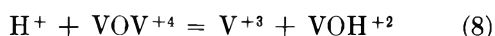
Reaction path	Net act. process	ΔS , e.u.	ΔH^* , kcal./mole	ΔF^* , kcal./mole	$S^*_{\text{complex}, a}$, e.u.
k_0	(4)	-16.5 ± 0.3^b	12.3 ± 0.1	17.2	-65
$k_1[\text{H}^+]$	(5)	-31.6 ± 6.4	9.8 ± 1.8	19.2	-81

^a The formal ionic entropy of the activated complex, $S^*_{\text{complex}} = \Delta S^* + \sum S^0_{\text{reactants}}$. $S^0_{\text{V}^{+2}}$ was estimated to be -23 ± 3 and $S^0_{\text{VO}^{+2}}$ is reported to be -26 ± 3 e.u. See M. J. LaSalle and J. W. Cobble, *J. Phys. Chem.*, **59**, 519 (1955).

^b The uncertainties listed are the standard deviations determined by the least-squares program.

Although the values found for ΔS_1^* and ΔH_1^* are quite reasonable, it should be re-emphasized that they may not actually apply to net activation process 5 because of medium effects.

It has been shown⁵ that about half of the reaction between V(II) and V(IV) proceeds by way of the colored intermediate mentioned previously. The most likely mechanism is



Thus, eq. 4 actually represents the formation of more than one activated complex with the formula $[\text{VOV}^{+4}]$ and the activation parameters listed in Table V are average values. Such a possibility is present, of course, in many reactions but is mentioned here specifically because the intermediate is actually detectable.

Chloride Catalysis. The small effect of chloride ion, shown in Table II, is consistent with the equation

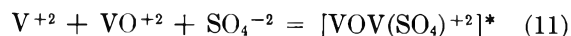
$$k' \text{ (in Cl}^-) = k_0'(1 + 2.46[\text{Cl}^-]) / (1 + 1.71[\text{Cl}^-]) \quad (10)$$

where k_0' is the rate constant in the absence of chloride ion. This expression suggests that there is a path involving chloride ion as well as a small amount of chloride complexing of one or both of the reactants. On the other hand, some or all of the effect may be due to the change in medium when chloride ion is substituted for perchlorate ion.

The small effect of chloride observed here is in accord with an inner-sphere activated complex bridged with the vanadyl oxygen. This follows from the observa-

tion that Cl^- catalyzes the reactions of $\text{Co}(\text{NH}_3)_6^{+3}$ with V^{+2} and with Cr^{+2} , which involve outer-sphere activated complexes,¹⁰ and the observation that for inner-sphere activated complexes, Cl^- enhances the rate if it is in the bridging position but has only a small effect if it is in a ligand position.¹¹

Sulfate Catalysis. The data in Table III show that small amounts of sulfate markedly increase the rate of reaction between V(II) and V(IV) and that the rate is essentially independent of $[\text{H}^+]$ and $[\text{HSO}_4^-]$ at constant $[\text{SO}_4^{-2}]$. The rate was found to be nearly linear in $[\text{SO}_4^{-2}]$ up to concentrations of 0.018 M, but at 0.093 M the rate is somewhat below the line. This latter deviation is probably due to a small amount of sulfate complexing or to the ever possible medium effect. These results lead to the conclusion that the activation process



is important in the presence of SO_4^{-2} at concentrations as low as 0.004 M. This conclusion is contrary to that reached by Olver and Ross,⁴ who believe that activation process 4 is predominant even in high sulfate concentrations and that a bisulfate group is present in the activated complex rather than the sulfate group which is indicated in (11). We are unable to follow their arguments since the compositions of their experimental solutions were not given.

It is to be noted, however, that the reaction rates determined by the catalytic reduction currents and those determined directly by spectrophotometry agree fairly well in solutions of the same composition. Olver and Ross found the apparent second-order rate constant to be $10 \text{ M}^{-1} \text{ sec}^{-1}$ at 25° in a solution which was 0.4 M H_2SO_4 and 0.15 M NaHSO_4 . The fourth solution listed in Table III has essentially this same composition; the apparent second-order rate constant for it was found to be $732 \text{ M}^{-1} \text{ min}^{-1}$ or $12.2 \text{ M}^{-1} \text{ sec}^{-1}$.

Ionic Strength Dependence. The data in Table IV can be described satisfactorily by the extended form of the Debye-Hückel equation

$$\log k' = \log k_0' + \frac{0.509\Delta z^2\mu^{1/2}}{1 + 0.329a\mu^{1/2}} + B\mu \quad (12)$$

For the LiClO_4 solutions $k_0' = 3.27$, $a = 9.17 \text{ \AA.}$, and $B = 0.2 \text{ M}^{-1}$; these parameters reproduce the experimental data with a mean deviation of 1.2% and

(10) A. Zwickel and H. Taube, *J. Am. Chem. Soc.*, **83**, 793 (1961).

(11) R. K. Murmann, H. Taube, and F. A. Posey, *ibid.*, **79**, 262 (1957).

a maximum deviation of 2.2%. For the NaClO_4 solutions, the corresponding parameters are $3.57 M^{-1} \text{ min.}^{-1}$, 10.3 \AA. , $0.2 M^{-1}$, 2.0% mean deviation, and 4.0% maximum deviation. The calculated values given in Table IV were obtained using these parameters in eq. 12.¹²

Acknowledgments. The authors wish to acknowledge many helpful discussions with Dr. C. E. Holley, Jr.,

and especially with Dr. J. F. Lemons, under whose general direction this work was done.

(12) NOTE ADDED IN PROOF.—A least-squares method for determining the parameters k_0' , \bar{a} , and B in eq. 12 has been provided by P. McWilliams of the Statistical Section of this laboratory. Results of treating the data in this way are for LiClO_4 solutions: $3.02 M^{-1} \text{ min.}^{-1}$, 8.96 \AA. , and $0.180 M^{-1}$, and for NaClO_4 solutions: $3.06 M^{-1} \text{ min.}^{-1}$, 8.82 \AA. , and $0.161 M^{-1}$. The data were fitted well within their experimental errors; the mean and maximum deviations were 0.7 and 1.7% for LiClO_4 and 1.2 and 1.6% for NaClO_4 .

Kinetics of Ethylene Hydrogenation over Alumina

by J. H. Sinfelt

Esso Research and Engineering Company, Linden, New Jersey (Received September 27, 1963)

The kinetics of hydrogenation of ethylene were studied over alumina in the temperature range 120 to 430°. The rate measurements were made in a flow reactor at atmospheric pressure using helium as a diluent. The rate of hydrogenation to ethane was found to be first order in hydrogen partial pressure and to vary approximately with the square root of the ethylene partial pressure. The apparent activation energy of the reaction was observed to decrease with increasing temperature. At the lowest temperatures the apparent activation energy was about 9 kcal./mole, but approached zero at temperatures above about 300°. Possible explanations for the variation in apparent activation energy are discussed. It is suggested that the mechanism of hydrogenation of ethylene over alumina involves reaction of a hydrogen molecule from the gas phase with an adsorbed ethylene molecule.

Alumina has been shown to be a catalyst for the hydrogenation of ethylene at temperatures in the range of 250 to 500°.¹ However, very little information appears to be available on the kinetics of the reaction over alumina, in marked contrast to the situation with metal catalysts, where many investigations have been reported, the results of which have been summarized by Eley² and Bond.³

Although alumina is a very inactive catalyst for the hydrogenation of ethylene when compared with noble metals such as platinum or palladium, a study of the kinetics is still of interest from a mechanistic viewpoint. Furthermore, alumina is widely used as a catalyst or support for a variety of hydrocarbon reactions, many

of which are carried out in the presence of hydrogen at conditions where the hydrogenation properties of alumina can have a bearing on the results. For example, in the cracking of hydrocarbons over alumina catalysts, hydrogen pressure has been shown to have a marked effect on the distribution between saturated and unsaturated hydrocarbons in the products, and to have a pronounced effect on the rate of cracking.⁴

- (1) V. C. F. Holm and R. W. Blue, *Ind. Eng. Chem.*, **43**, 501 (1951); S. G. Hindin and S. W. Weller, *J. Phys. Chem.*, **60**, 1501 (1956).
- (2) D. D. Eley, "Catalysis," Vol. III, Reinhold Publishing Corp., New York, N. Y., 1955, pp. 49-77.
- (3) G. C. Bond, "Catalysis by Metals," Academic Press, New York, N. Y., 1962, pp. 239-252.

An infrared study of the chemisorption of ethylene on alumina has recently been reported by workers in this laboratory.⁵ This work led to some interesting conclusions regarding the configuration of the surface species resulting from the chemisorption of ethylene. The kinetic study of ethylene hydrogenation reported in the present paper was carried out over one of the same aluminas used in the infrared studies. By investigating the kinetics of the hydrogenation in addition to the infrared study of the chemisorption of ethylene, it was hoped to elucidate the ethylene-hydrogen-alumina system in more detail than would be possible from either approach taken by itself.

Experimental

Apparatus and Procedure. The reaction rate data were obtained in a flow reactor system at atmospheric pressure. The reactor was a 1.0-cm. stainless steel tube approximately 8.0 cm. in length and was mounted vertically inside a small electrical oven. The catalyst occupied a space about 1.5 cm. in length midway along the length of the reactor tube. A fritted stainless steel disk served to support the catalyst in the reactor, and quartz wool was packed on top of the catalyst to keep it in place. A 3-mm. axial thermowell housing an iron-constantan thermocouple extended upward through the fritted steel disk, the tip of the thermocouple being located at the center of the catalyst bed. The reaction gases were passed downflow through the catalyst bed, and the reaction products were analyzed by a chromatographic unit connected to the outlet of the reactor. The chromatographic column, which was 0.6 cm. in diameter and 1 m. in length, was packed with 100 mesh silica gel and operated at 40°. Helium was used as the carrier gas, and a thermal conductivity detector was used with the column.

The flow rates of the reactant gases, ethylene and hydrogen, along with helium diluent, were measured with orifice type flow meters employing manometers. The total gas flow rate was maintained at 1 l./min. throughout. In a typical run, the reactant gases were passed over the catalyst for a period of 3 min. prior to sampling the products for a chromatographic analysis. The ethylene was then cut out and the hydrogen flow continued for 10 min. prior to another run. By this procedure, it was possible to minimize variation in catalyst activity from period to period. As a further insurance against the complications due to varying catalyst activity, measurements at any given conditions were in most cases bracketed by measurements at a standard set of conditions. In this way the effect of changing a variable could be determined more reliably by comparing a given run

period with the standard condition periods run immediately before and after the run period in question.

Materials. The ethylene used in this work was obtained from the Matheson Co. No hydrocarbon impurities were detected in a chromatographic analysis of the ethylene, and it is estimated that any ethane present amounted to less than 0.01%. High purity hydrogen obtained from the Linde Company was further purified by passing it through a Deoxo unit containing palladium catalyst to remove trace amounts of oxygen as water, prior to drying with a molecular sieve.

The alumina catalyst used in this work was prepared from β -alumina trihydrate, obtained from the Davison Chemical Co., by heating in air for 4 hr. at 600°. X-Ray diffraction measurements showed the alumina resulting from this treatment to be η -alumina. The B.E.T. surface area was 295 m.²/g. The maximum concentration of impurities in the alumina, including Fe, Cu, Si, Mg, Ca, and Na, is estimated to be less than 0.1 wt. %. After the alumina was charged to the reactor, hydrogen was passed over the alumina at a rate of 200 cc./min. for 3 hr. at 500° prior to making any reaction rate measurements. The alumina was used in the form of small granules, with an average particle size of 0.3 mm.

Results

The hydrogenation of ethylene to ethane over the alumina catalyst used in this study was investigated over the temperature range 120 to 430°. The reaction took place cleanly with little formation of side products except possibly for small amounts of methane at the highest temperatures investigated.

The kinetic data were all obtained at low conversion levels (0.03 to 3.0%, except for one point at 9.3%), so that the rates are initial rates of reaction. The reaction rates were determined from the relation

$$r = \frac{F}{W} X \quad (1)$$

where F represents the feed rate of ethylene to the reactor in gram moles per hour, W represents the weight in grams of alumina, and X represents the fraction of the ethylene converted to ethane. The reaction rate r is then expressed as gram moles of ethylene hydrogenated per hour per gram of alumina.

In the actual determination of reaction rates, the alumina was first treated with flowing hydrogen at

(4) J. H. Sinfelt and J. C. Rohrer, *J. Phys. Chem.*, **65**, 2272 (1961); **66**, 1559 (1962).

(5) P. J. Lucchesi, J. L. Carter, and D. J. C. Yates, *ibid.*, **66**, 1451 (1962).

500° for 3 hr., after which the reactor was cooled to a convenient reaction temperature to begin a series of measurements of rates as a function of hydrogen and ethylene partial pressures. Since preliminary experiments showed that such a series of measurements over an extended period of time resulted in some decline in the catalytic activity of the alumina, it was decided to bracket all the reaction periods with periods at a standard set of conditions. This made it possible to detect variations in catalyst activity during the course of the measurements. The procedure is illustrated in Table I, which presents data for a typical

Table I: Typical Sequence of Rate Measurements for Ethylene Hydrogenation at 205°

p_H , atm.	p_E , atm.	$r \times 10^{10}$
0.20	0.030	1.04
0.90	0.030	4.16
0.20	0.030	0.85
0.20	0.0070	0.41
0.20	0.030	0.83
0.20	0.20	1.82
0.20	0.030	0.94
0.20 ^b	0.030	0.74
0.060	0.030	0.22
0.20	0.030	0.75
0.20	0.100	0.91
0.20	0.030	0.77
0.20	0.20	1.29
0.20	0.030	0.80
0.20	0.010	0.45
0.20	0.030	0.78

^a Gram moles ethylene hydrogenated per gram of alumina per hour. ^b H₂ flow of 50 cc./min. over the alumina maintained overnight prior to this reaction period.

sequence of reaction periods at 205° to determine the effects of hydrogen and ethylene partial pressures, p_H and p_E , respectively, on the rates. The activity of the alumina is seen to vary slightly, as shown by the repeated observations at the standard conditions ($p_H = 0.20$ atm., $p_E = 0.030$ atm.). During the course of the measurements shown in Table I, the activity of the alumina decreased by about 25%, with a major part of the decline occurring between the seventh and eighth periods shown, which corresponded to an overnight break in the sequence of measurements. During the break, a flow of hydrogen was maintained over the alumina. The reason for the slight decrease in activity is not known.

The effect of hydrogen or ethylene partial pressure on rate of hydrogenation was determined simply by

comparing the rate at a particular set of conditions with the average of the rates at the standard conditions immediately before and after the period in question. For each set of conditions the rate r relative to the rate r_0 at the standard conditions can be expressed by the ratio r/r_0 . This procedure serves to minimize the complications due to varying catalyst activity. The results on the effects of hydrogen and ethylene partial pressures on rates at 205° are presented in this form in Fig. 1 and 2, along with similar results obtained at 403°.

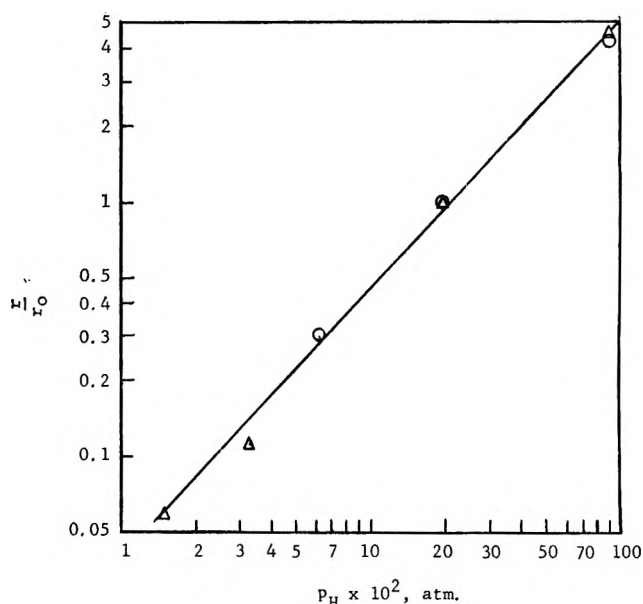


Figure 1. Effect of H₂ partial pressure on rate of hydrogenation at $p_E = 0.030$ atm.: O, 205°; Δ, 403°.

In the logarithmic plot of r/r_0 vs. p_H at constant p_E in Fig. 1, a single line fits the data for both temperatures. The slope of the line is approximately one, indicating that the rate of hydrogenation is first order in hydrogen partial pressure. In Fig. 2 a similar plot of r/r_0 vs. p_E at constant p_H indicates that the average order with respect to ethylene partial pressure is about 0.4 to 0.5 over the range of ethylene partial pressures investigated. While the data suggest that temperature may have an effect on the average order with respect to ethylene partial pressure, the effect is small and the results at both temperatures can be represented reasonably well by a single curve through the data.

The effect of temperature on the rate of hydrogenation is shown in the Arrhenius plot in Fig. 3. The data in this plot were obtained in two ways: by making successive measurements at the different temperatures in a rising temperature sequence followed by a succession of measurements in a falling temperature sequence.

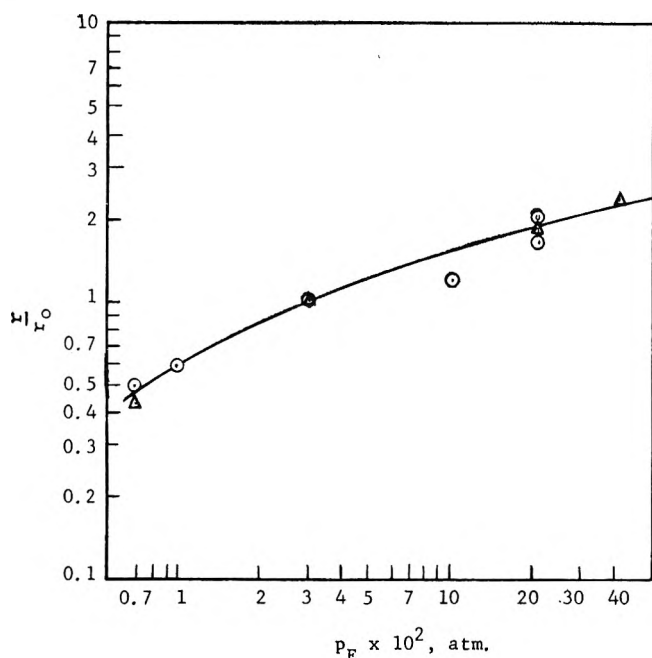


Figure 2. Effect of C_2H_4 partial pressure on rate of hydrogenation at $p_H = 0.20$ atm.: O, 205°; Δ, 403°.

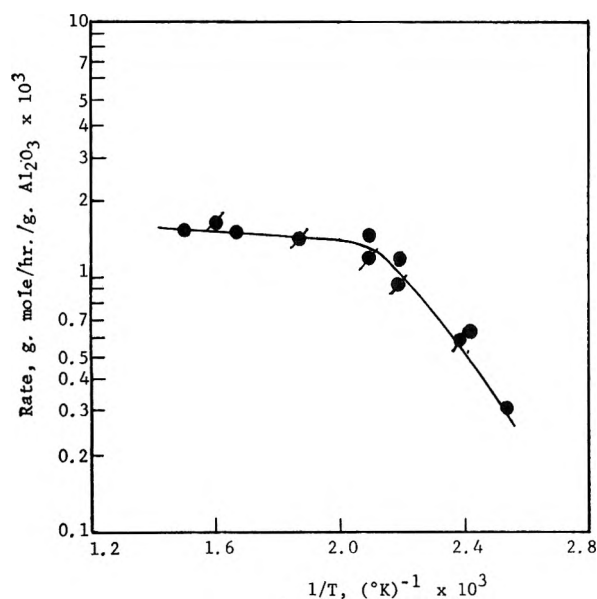


Figure 3. Effect of temperature on C_2H_4 hydrogenation over Al_2O_3 ; H_2 pressure = 0.20 atm., C_2H_4 pressure = 0.20 atm.: ●, points taken in ascending temperature sequence; ●, points taken in descending temperature sequence.

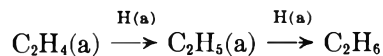
The data obtained during the rising temperature sequence are distinguished from those obtained during the falling temperature sequence by different types of symbols in the plot. Both sets of data fall along the same curve reasonably well, and this serves as a

measure of the reproducibility of the results. The interesting feature of the results is that the slope of the Arrhenius line falls off at the higher temperatures, rather than remaining constant over the whole range of temperatures. This type of behavior is similar to that which has frequently been observed in ethylene hydrogenation over metal catalysts^{2,3} and will be discussed in a subsequent part of the paper. The apparent activation energy of the reaction decreases from about 9 kcal./mole at the lowest temperatures studied to essentially zero at temperatures above about 300°.

Discussion

A number of mechanisms have been proposed for the hydrogenation of ethylene over metal catalysts.^{2,3} An important question which arises in a discussion of the mechanism is the following: does the reaction involve (a) the interaction of adsorbed ethylene with adsorbed hydrogen, or (b) the collision of a molecule of one of the reactants from the gas phase with a molecule of the other on the surface?

On the alumina used in this work, it has been observed in a separate study in this laboratory⁶ that the extent of adsorption of hydrogen is very small compared to the adsorption of ethylene, the coverage by hydrogen being about 1% that of ethylene at 250° and 11 mm. pressure. The alumina surface would therefore be expected to be much more heavily covered with ethylene than with hydrogen during hydrogenation. Thus, if a mechanism of type (b) above applies, it seems likely that the reaction would involve collision of a hydrogen molecule from the gas phase with adsorbed ethylene, rather than the reverse. However, it is conceivable that a mechanism of type (a) above might apply, in which both the ethylene and hydrogen would be adsorbed prior to reaction. One might postulate that hydrogen atoms on the surface, formed by the dissociative chemisorption of hydrogen molecules, react with adsorbed ethylene molecules in a stepwise manner, leading first to the formation of an adsorbed ethyl radical and finally to ethane.

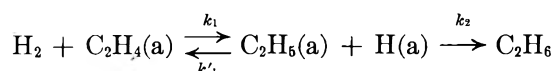


The symbol (a) here refers to an adsorbed species. However, if adsorption equilibria were maintained between the hydrogen atoms on the surface and hydrogen molecules in the gas, the concentration of adsorbed hydrogen atoms would be proportional to the square root of the hydrogen pressure, and it would be difficult to account for the observed first-order dependence of the rate on hydrogen pressure. While

(6) V. Kevorkian, unpublished work, 1962.

this latter objection could be eliminated by postulating that the above reaction involved simultaneous, rather than consecutive, addition of hydrogen atoms to the ethylene, it would seem that the simultaneous addition would be less likely to be an elementary step in the reaction. Furthermore, the formation of ethyl radicals on the surface of alumina has been demonstrated by infrared studies.⁵

While the detailed mechanism of ethylene hydrogenation over alumina cannot be established conclusively from the results of this work, it would appear that the simplest mechanism which could account for the observed kinetics would be one involving reaction of hydrogen molecules from the gas phase with adsorbed ethylene. This proposal is similar to that advanced by Twigg⁷ to account for the kinetics of ethylene hydrogenation over nickel catalysts. Such a mechanism is illustrated as



Here k_1 , k'_1 , and k_2 are rate constants for the various reaction steps. If we let θ_E , θ_x , and θ_H represent the fractions of the surface covered by C_2H_4 , C_2H_5 , and H , respectively, the following steady-state equation for the formation of $\text{C}_2\text{H}_6(\text{a})$ can be written

$$\frac{d\theta_x}{dt} = k_1 p_{\text{H}} \theta_E - k'_1 \theta_x \theta_H - k_2 \theta_x \theta_H = 0 \quad (2)$$

The rate of formation of ethane is given by

$$r = k_2 \theta_x \theta_H \quad (3)$$

Solving eq. 2 for θ_x and substituting in eq. 3, we obtain for the rate

$$r = \frac{k_1 k_2}{k'_1 + k_2} p_{\text{H}} \theta_E \quad (4)$$

Equation 4 accounts for the first-order dependence on hydrogen partial pressure and also gives a way of accounting for the complex dependence of the rate on temperature. If k_2 is large compared to k'_1 at low temperatures, the rate law reduces to the expression $r = k_1 p_{\text{H}} \theta_E$ and the over-all activation energy E simply reflects the temperature dependence of k_1 ; *i.e.*, $E = E_1$. However, if k'_1 increases faster with temperature than k_2 (*i.e.*, $E'_1 > E_2$), then at a sufficiently high temperature k'_1 will become large compared to k_2 and the rate law will reduce to $r = (k_1 k_2 / k'_1) p_{\text{H}} \theta_E$. Under these conditions the over-all activation energy E becomes $E = E_1 + E_2 - E'_1$. Since E'_1 is by hypothesis larger than E_2 , the activation energy E will be lower than E_1 , and hence lower than the activation energy for the low

temperature range. This agrees with the decrease in apparent activation energy with increasing temperature which was observed in the present work.

A decrease in the coverage of the surface by ethylene as the temperature is increased could also lead to a decrease in the apparent activation energy, as has sometimes been suggested for metal catalysts.² Thus, at the lowest temperatures investigated, it is conceivable that the active sites are almost completely covered with ethylene and that the extent of coverage decreases with increasing temperature until at sufficiently high temperatures the surface is only sparsely covered. It might then be expected that the kinetics would be zero order in ethylene at the low temperatures and approach first order at the high temperatures. Unfortunately, data are not available on the order with respect to ethylene at the lowest temperatures of this work, but with regard to any simple explanation of the temperature dependence solely in terms of ethylene coverage, it is difficult to account for the fact that the order remains effectively constant at about 0.4 to 0.5 over the wide temperature range of 205 to 403°. This may be a consequence of a nonuniform surface.⁸

The possibility that the decrease in apparent activation energy at the higher temperatures is related to a pore diffusion limitation has been considered, but does not appear likely. Effectiveness factors calculated by the method of Weisz and Prater⁹ are close to unity, indicating that pore diffusion is not limiting.

In our kinetic analysis, we have suggested that the rate of hydrogenation at low temperatures is simply equal to the rate of the step, $\text{H}_2 + \text{C}_2\text{H}_4(\text{a}) \rightarrow \text{C}_2\text{H}_5(\text{a}) + \text{H}(\text{a})$. The activation energy of the reaction should then correspond to the energy which must be acquired by a gas phase hydrogen molecule in order to react with an adsorbed ethylene molecule upon collision. From kinetic theory we can calculate the number of hydrogen molecules colliding with the surface with the required activation energy E , using the formula

$$1/4 n \bar{c} \exp(-E/RT) \quad (5)$$

where n is the concentration of molecules in the gas and \bar{c} is the average speed of the molecules, given by $(8RT/\pi M)^{1/2}$. At 125° and $p_{\text{H}} = 0.20$ atm., the collision frequency, taking E equal to the experimental activation energy of 9 kcal./mole, turns out to be 2.1×10^{18} molecules/sec./cm.². The observed reaction rate at these conditions, and at $p_{\text{E}} = 0.20$ atm., is $1.8 \times$

(7) G. H. Twigg, *Discussions Faraday Soc.*, 8, 152 (1950).

(8) M. Boudart, *A.I.Ch.E. J.*, 2, 62 (1956).

(9) P. B. Weisz and C. D. Prater, *Advan. Catalysis*, 6, 143 (1954).

10^{10} molecules/sec./cm.², which is a factor of 10^8 lower than the calculated collision frequency. In calculating the number of activated collisions by formula 5, we have assumed that the apparent activation energy of 9 kcal./mole derived from experiment was the true activation energy. It could be that the value of 9 kcal./mole is somewhat lower than the true value since the experimental activation energy does not allow for the possible effect of temperature on the degree of coverage of the surface by ethylene. However, even if the true activation energy were as much as 10 kcal. higher than this value, the observed rate would still be about 10^2 to 10^3 times lower than the calculated frequency of activated collisions. The low "steric factor" suggests that only a small fraction of the adsorbed ethylene molecules is reactive. It seems possible that much of the ethylene is adsorbed dis-

sociatively, leading to extensive coverage of the surface by acetylenic residues, which are not likely to be involved directly in the hydrogenation reaction, but rather serve to deactivate a large part of the surface.

To summarize briefly, the present work has extended the studies on ethylene hydrogenation kinetics, about which much has been reported for metal catalysts, to a different type of catalyst. The kinetics have been investigated over a much wider range of conditions than is usual. Furthermore, although alumina is a much less active hydrogenation catalyst than metals such as platinum and nickel, several features of the kinetics are similar to what has been observed over metal films, including the magnitude of the apparent activation energy and the interesting fall-off in activation energy with increasing temperature.

Diffusion in Liquid Hydrocarbon Mixtures

by Anthony L. Van Geet¹ and Arthur W. Adamson

Department of Chemistry, University of Southern California, Los Angeles, California (Received April 22, 1963)

The tracer and the mutual diffusion coefficients for the liquid system *n*-octane–*n*-dodecane are reported as a function of composition, at 25°, along with viscosity, density, and refractive index. In addition, the tracer diffusion of *n*-octadecane at 25° in various *n*-octane–*n*-dodecane mixtures was determined. The diaphragm cell technique was employed and the radioactivity measurements were made by means of a carefully optimized liquid scintillation counting procedure that obviated the need for coincidence and cooling features. By employing tritium and carbon-14 labeling simultaneous tracer diffusions could be studied. A number of regularities are observed in the data. The activation energies are the same, at a given composition, for the three diffusion coefficients in the *n*-octane–*n*-dodecane system. From this and other observations it appears that the elementary act in the diffusion of *n*-alkanes is the motion of a segment and that at any given composition this motion is primarily determined by the average chain length of the mixture. Thus, at any given composition, the segment length is the same for the tracer diffusion of *n*-octane and *n*-dodecane. Empirical modifications of equations for diffusion in two-component systems are produced on this basis which allow the prediction of any diffusion coefficient at any composition of *n*-alkanes provided only that appropriate self-diffusion coefficients of pure *n*-alkanes are known.

Introduction

An important purpose of diffusion studies in this laboratory has been the testing of models for diffusion in liquids. By the term "models" is meant formulations which go beyond phenomenology to imply specific molecular mechanisms for transport. An example is the application of transition state methods by Eyring and co-workers.² In the treatments of Lamm³ and Laity⁴ which are based on nonequilibrium thermodynamics, the diffusion process is described by pairwise friction coefficients, but the mechanism of diffusion remains unspecified. In some aspects, these treatments are combined in an approach developed in this laboratory.^{5–8} With these and other treatments mentioned later, the recurrent problem has been an excess of theoretical variables, necessitating the use of semi-empirical simplifications which make truly diagnostic tests of validity difficult.

To make any progress at all one should have, in a binary system, at least a knowledge of the differential and the two tracer⁹ diffusion coefficients, and the viscosity as a function of composition. Complete tem-

perature dependencies and, in fact, thermal diffusion coefficients are desirable. For very few systems do the data available approach this standard. Complete diffusion-composition data have been determined for the water-sucrose system,⁶ but the interpretation of results was complicated by presence of various diffusion species resulting from hydration and association,⁷ which caused difficulties in applying the so-called thermodynamic term. Johnson and Babb¹⁰ reported two

- (1) Department of Chemistry, State University of New York, Buffalo, N. Y. Based on a dissertation for the Ph.D. degree at the University of Southern California.
- (2) See S. Glasstone, K. J. Laidler, and H. Eyring, "The Theory of Rate Processes," McGraw-Hill Book Co., New York, N. Y., 1941.
- (3) O. Lamm, *Acta Chem. Scand.*, **6**, 1331 (1952).
- (4) R. W. Laity, *J. Phys. Chem.*, **63**, 80 (1959).
- (5) A. W. Adamson and R. R. Irani, *J. Chim. Phys.*, **55**, 102 (1958).
- (6) R. R. Irani and A. W. Adamson, *J. Phys. Chem.*, **62**, 1517 (1958).
- (7) R. R. Irani and A. W. Adamson, *ibid.*, **64**, 199 (1960).
- (8) A. W. Adamson, *Trans. AIME*, **219**, 158 (1960).
- (9) Following a suggestion of R. Mills, the term "self-diffusion" is reserved for one-component systems.

of the three diffusion coefficients in various benzene-carbon tetrachloride mixtures. Recently, Mills¹¹ has obtained complete diffusion-composition data for the benzene-diphenyl system.

The system *n*-octane-*n*-dodecane was chosen for the present study as one not complicated by association, and for which deviations from ideality are not large. It was hoped to determine whether pairwise interaction quantities are indeed good physical approximations and if so, how they couple to interrelate the three diffusion coefficients. In addition, since hydrocarbon mixtures are quite regular in their properties, it was hoped that at least some general and useful semiempirical relationships would be found.

Experimental

Chemicals. Olefin-free *n*-octane, *n*-dodecane, and *n*-octadecane were obtained from Humphrey-Wilkinson Co., North Haven, Conn. Purity was checked by one or more of the following methods, as needed, to ensure less than 0.6% impurity: refractive index, vapor phase chromatography, melting point, and density. The reference standard of *n*-dodecane was that obtained as a narrow middle cut from reduced pressure distillation in an efficient column, and of *n*-octane, as specified 99.8% pure liquid from the Phillips Petroleum Co.

Carbon-14 labeled *n*-octane and *n*-dodecane, and random tritium labeled toluene were supplied by the Isotope Specialties Co., while the New England Nuclear Corp. supplied C₆H₅C¹⁴OOH and random tritium labeled *n*-octadecane. The disintegration rate of the radiotoluene and benzoic acid was specified to 10% and 5% accuracy, respectively. Correction was made for the decay of the tritium standard with time.

Procedure. Viscosities of *n*-alkane mixtures were measured by means of an Ostwald type viscometer calibrated with a *n*-dodecane standard containing less than 0.05% impurity. Densities were determined with a 10-cm.³ pycnometer, and both measurements were made in a water thermostat good to $\pm 0.03^\circ$.

Diffusion coefficients were measured by the previously described diaphragm cell technique^{12,13} using Stokes type cells.¹³ The 25-cm.³ cell compartments were separated by a 2-mm. thick Pyrex 39570 (30M) sintered glass diaphragm, and each was stirred magnetically at 60 r.p.m. The opening of each compartment was fitted precisely with a Teflon stopper, the upper one of which in turn contained a capillary bore to allow for liquid volume changes.

The cells were calibrated by allowing 0.1 *M* potassium chloride to diffuse into water and taking the integral diffusion coefficient to be 1.87×10^{-5} cm.²/sec.¹⁴ at 25°.

The operating procedure was as follows. Solution was first introduced into the bottom compartment so as to fill it and saturate the diaphragm; the cell was then equilibrated in the water thermostat, and the top compartment rinsed with its solution and filled. This procedure avoided any thermal volume changes in the bottom compartment after the solution had been added to the top one, and thus eliminated a source of thermal mixing. After filling and final thermal equilibration, the capillary in the top Teflon plug was sealed off by means of a rubber policeman.

To avoid evaporation, when 60° runs were involved, the top compartment was filled from a hypodermic needle connected by a copper tube to a storage flask immersed in the thermostat. During the operation, the solution destined for the top compartment dropped in temperature to 57°. Special care was needed to exclude moisture from the solutions during filling and, in addition, they were dried before use with calcium chloride packed in a filter-paper bag.

Typically, the diffusion runs were stopped after 2 to 4 days, by emptying the top compartment, using a hypodermic syringe. The cell was then removed from the thermostat and, after cooling to room temperature, the bottom solution was drained out. All such solutions and other mixtures for analysis were stored in narrow-mouth screw-cap bottles having a 1-mm. Teflon washer in the cap. Ordinary caps, stoppers, etc., were unusable, but the Teflon washer technique was found to eliminate evaporation completely.

In the case of the mutual diffusion runs, the more dense liquid was placed in the bottom compartment. Typically, the concentration difference between the top and bottom compartment dropped from an initial 20% to between 5 and 10% by weight at the end of the run. In the tracer experiments, the labeled solution was placed in the bottom compartment. This was also true where two tracer diffusions were determined simultaneously; both the C¹⁴ labeled *n*-octane and the tritium labeled *n*-octadecane were incorporated in the bottom solution.

Analyses. The potassium chloride solutions for the diffusion cell calibrations were standardized by titration with 0.02 *M* silver nitrate. The composition of the hydrocarbon mixtures from the diffusion runs was determined by means of a differential refractometer¹⁴

(10) P. A. Johnson and A. L. Babb, *J. Phys. Chem.*, **60**, 14 (1956).

(11) R. Mills, *ibid.*, **67**, 600 (1963).

(12) R. Mills and A. W. Adamson, *J. Am. Chem. Soc.*, **77**, 3454 (1955).

(13) R. H. Stokes, *ibid.*, **72**, 763, 2243 (1950).

(14) A. L. Van Geet, Research Report No. 4, May, 1960 (Science Library, University of Southern California).

sensitive to a refractive index difference of one place in the fifth decimal. The instrument was thermostated to $25.0 \pm 0.1^\circ$, and at this temperature the concentration dependence of the refractive index of *n*-octane-*n*-dodecane mixtures was found to be

$$n = n_{C_8} + 0.02444W_2 - 0.00081(1 - W_2)W_2 \quad (1)$$

or

$$n = n_{C_8} + 0.02444F_2 + 0.00078(1 - F_2)F_2 \quad (2)$$

where n_{C_8} refers to the refractive index of pure *n*-octane, and W_2 and F_2 , to the mass and volume fractions of *n*-dodecane, respectively.

The radioactivity of the hydrocarbon samples was determined by means of a liquid scintillation counter assembly developed for the purpose.¹⁵ Briefly, it was possible to avoid both coincidence circuitry and cooling equipment by specially selecting the Dumont 6292 photomultiplier for low noise, and by careful optimizing of signal to noise ratio by choice of high voltage and discriminator settings.

Samples were counted in a conical flask of 35 ml. volume, coated with a suspension of titanium dioxide in clear Tygon lacquer (found to have optimum reflecting ability), and placed on top of the photomultiplier with microscope oil as optical coupler. Detection efficiency was determined by adding known amounts of the benzoic acid- C^{14} or the toluene- H^3 standard to 20 ml. of POPOP solution (5.76 g./l. of *p*-terphenyl and 0.81 g./l. of 1,4-bis(2,5-phenyl xzoyl)-benzene in reagent grade toluene). It was routinely possible to operate at room temperature at a detection efficiency for C^{14} of 83% (and dark noise level of 30 c.p.m.) and a detection efficiency of 10% for tritium (and dark noise level of 90 c.p.m.). Stability was good, especially for C^{14} counting, and, for example, at the usual total count level used, which corresponded to a theoretical 0.3% standard deviation for random fluctuations, actual results were reproducible to between 0.3 and 1.1%. Background was reasonably low, amounting to 150 c.p.m. for carbon-14 and 230 c.p.m. for tritium. Efficiency was not greatly sensitive to the proportion of hydrocarbon in the POPOP, although calibration curves were obtained; usually a 1:2 ratio was used.

In the case of the simultaneous tracer diffusion runs, the counter was first made insensitive to tritium activity by raising the base discrimination level; this reduced the efficiency for carbon-14, but only to 60%. The sample solution was then counted at the usual discriminator setting, whereby both tritium and carbon-14 activity were detected. The tritium activity was

then obtained by difference, after efficiency correction was made.

Calculation of the Diffusion Coefficients. In mutual diffusion, the diaphragm cell method gives an integral diffusion coefficient[†] for the concentration range C_q to C_p , related to the differential coefficient (which is a function of concentration) and to the measured concentrations as¹⁶

$$\bar{D} = (C_p - C_q)^{-1} \int_{C_q}^{C_p} D_{12} dC = (Kt)^{-1} \ln z \quad (3)$$

where

$$z = (C_p - C_q)/(C_r - C_s) \quad (4)$$

Here, C denotes the moles per cm.³ of one of the components (volume fraction could equally well be used), and the indices p and q denote initial bottom and top solutions, respectively, and r and s, the final bottom and top solutions, respectively. \bar{D} and D_{12} are the integral and differential mutual diffusion coefficients (the latter defined by Fick's law), t is the time in seconds, and K is the diffusion cell constant, in cm.⁻².

In the derivation of eq. 3 it has been assumed that \bar{D} is constant during the diffusion run. This assumption is approximately obeyed if only a small amount of material is allowed to diffuse through the diaphragm, so z is close to one. For z -values between 2 and 4 as were actually used, it is usually necessary to replace $\bar{D}t$ in eq. 3 by $\int \bar{D} dt$. However, it happens that D_{12} varied linearly with volume fraction, so that \bar{D} for the range F_q to F_p is equal to D_{12} at the mean volume fraction and is constant during a diffusion run.

Actually, since, as shown by eq. 2, refractive index was almost linear in volume fraction, z was approximated by $(n_p - n_q)/(n_r - n_s)$. The error in the calculated \bar{D} did not exceed 0.2%, and it was advantageous to be able to determine the refractive index differences directly by means of the differential refractometer.

Tracer diffusion coefficients were calculated in two ways. First, eq. 3 was used directly, with

$$z = R_p/(R_r - R_s) \quad (5)$$

where R refers to the c.p.m. in a reference volume of hydrocarbon solution (here, $R_q = 0$). Alternatively, by material balance

$$V_p R_p = V_r R_r + V_q R_s$$

where V denotes the volume of the indicated compartment (the free pore volume of the diaphragm, 0.3

(15) See A. L. Van Geet, "Diffusion in Hydrocarbons," Dissertation, University of Southern California, 1961, for detailed performance and calibration data.

(16) J. H. Northrop and M. L. Anson, *J. Gen. Physiol.*, **12**, 543 (1929).

ml., is included in V_p). The quantity z may then be expressed as

$$z = R_p/[R_p - (1 + V_q/V_p)R_a] \quad (6)$$

Owing to counting errors, the two procedures generally gave slightly different answers, and the two D -values were averaged.

Estimates of Errors and Optimum Diffusion Time. The uncertainty in a D -value depends not only on the accuracy of the analyses of the two compartments, but also on diffusion time, and there exists an optimum time such that the standard deviation ΔD is at a minimum.

In the case of radioactive samples, the error in the count rate is given by $\Delta R = rR$, where r in our case was essentially constant at 0.01, with R in c.p.m. The error propagated into D is then obtained by appropriate differentiation of eq. 3, which gives

$$\Delta D/D = (\Delta z/z)/\ln z = rf(z)/\ln z \quad (7)$$

If z is calculated¹⁴ from eq. 5, then

$$f(z) = 1/2(2z^2 + 6)^{1/2} \quad (8)$$

and if z is calculated from the average of eq. 5 and 6, then

$$f(z) = 1/2(5z^2 - 8z + 5)^{1/2} \quad (9)$$

In the case of eq. 8, the minimum in $\Delta D/D$ is at $z = 3.5$, or $DKt = 1.25$; however, the standard deviation ΔD only increases by 10% when $DKt = 0.88$ or 1.72. With eq. 9 the corresponding 10% limits are at $DKt = 0.47$ and 1.19, and for both equations $\Delta D/D = 2.4r$ at these limits. Thus with $r = 1\%$, the error in tracer diffusion coefficient becomes about 2.4%, which is consistent with the data in Table II.

Similarly, the error in D_{12} has been determined in relation to the error Δn in the refractive index measurement ($n_p - n_a$). This last error is approximately independent of ($n_p - n_a$), so $\Delta D/D$ is again given by eq. 7, with $r = \Delta n/(n_p - n_a)$. Here $f(z) = (z^2 + 1)^{1/2}$, from which the minimum $\Delta D/D$ is at $DKt = 1.11$, and the 10% limits are at $DKt = 0.74$ and 1.61. With $\Delta n/(n_p - n_a) = 0.3\%$, $\Delta D/D$ is 0.95% at the 10% limits. The situation is similar in the case of the calibration by means of potassium chloride diffusion.

Activation energies are obtained in our case from diffusion coefficients at two temperatures, and as would be expected, errors in D become magnified. Calculation¹⁵ of the activation energy error ΔE shows that

$$\Delta E/R = [(T_1 T_2)/(T_1 - T_2)](\Delta D/D)(2)^{1/2} \quad (10)$$

All tracer diffusion coefficients were measured in duplicate, so that $\Delta D/D = 2.4\%/ \sqrt{2}$, or 1.7%, and with

T_1 and T_2 equal to 298 and 333°K., ΔE becomes about 140 cal. This is what is observed, as evident in Fig. 2.

An additional source of error stems from the fact that when diffusion commences, the diaphragm is filled with bottom solution, some of which immediately diffuses out as the system approaches a steady-state condition. Since eq. 3 implies steady-state conditions at all times, some error is involved in its use here. It has been estimated, however, that this error is less than 0.2% provided that DKt exceeds 0.7.¹⁴

Results

Physical Properties of n -Octane- n -Dodecane Mixtures.

The measured densities of n -octane- n -dodecane mixtures are given, within experimental error, by the relationship

$$1/\rho = W_1/\rho_1^0 + W_2/\rho_2^0 + W_1 W_2 \Delta V \quad (11)$$

where ρ_i^0 is the density of the indicated pure component. Our densities for pure n -octane and n -dodecane agreed with literature ones¹⁷ to within the experimental error of 0.0002 g./cm.³. The term $W_1 W_2 \Delta V$ is the excess volume, and ΔV has the values -0.0024 cm.³/g. and -0.0065 cm.³/g. at 25 and 60°, respectively. Partial molar volumes calculated from eq. 11 (see ref. 15 for tabulations) agree well with literature data.^{17,18} They are nearly constant at $V_1 = 163$ cm.³/mole and $V_2 = 228$ cm.³/mole (25°).

The viscosities of these mixtures can be represented to within the experimental error by an equation suggested by Adamson⁸

$$\varphi = F_1 \varphi_1 + F_2 \varphi_2 + F_1 F_2 \Delta \varphi \quad (12)$$

The measured fluidities of pure n -octane and n -dodecane, φ_1 and φ_2 , agree with literature values to within 0.5%.¹⁷ They are 1.951 and 0.7257 cp.⁻¹ at 25°, respectively, and 2.805 and 1.228 cp.⁻¹ at 60°, respectively. The interaction term, $\Delta \varphi$, has the values -0.44 and -0.41 cp.⁻¹ at 25 and 60°, respectively. In the present system, eq. 12 works equally well if weight fractions are used, provided that the values of $\Delta \varphi$ are taken to be -0.35 and -0.38 , at the two respective temperatures.

If molar refractions are additive, then it follows from eq. 2 that refractive index should be nearly linear in volume fraction. Thus $R = \Sigma N_i R_i$, with $R_i = V_i (n_i^2 - 1)/(n_i^2 + 2)$ and N denoting mole fraction. In the present case, where the refractive indices of the pure

(17) American Petroleum Institute, Project 44, 1952.

(18) A. Desmyter and J. H. van der Waals, *Rec. trav. chim.*, **77**, 53 (1958).

components are not very different, one obtains the approximate form

$$n = \sum N_i V_i n_i / V = \sum F_i n_i \quad (13)$$

where $V = \sum N_i V_i$ is the molar volume of the mixture.

Diffusion Coefficients. The mutual and tracer diffusion data for the *n*-octane-*n*-dodecane system are summarized in Tables I and II, and those for diffusion of a trace amount of *n*-octadecane in *n*-octane-*n*-dodecane mixtures in Table III.¹⁹ The general behavior is shown in Fig. 1, and, qualitatively, is as would be expected. Thus the tracer diffusion coefficients of *n*-octane and *n*-dodecane approach the mutual diffusion coefficient at compositions approaching pure *n*-dodecane and *n*-octane, respectively, and so meet the phenomenological expectation. Interestingly, the mutual diffusion coefficient is linear with volume fraction (and hence with weight but not with mole fraction) within experimental error.

By least-squares analysis, the following straight lines were fitted to the data: at 25°, $D_{12} = (1.4569 \pm 0.0032) - (0.576 \pm 0.011)(F_2 - 0.4540) = (1.719 - 0.576F_2) \times 10^{-5}$ cm.²/sec.; at 60°, $D_{12} = (2.4239 \pm 0.0051) - (0.671 \pm 0.019)(F_2 - 0.4085) = (2.698 - 0.671F_2) \times 10^{-5}$ cm.²/sec. The data fit these regression lines with a standard deviation ("about" the regression)

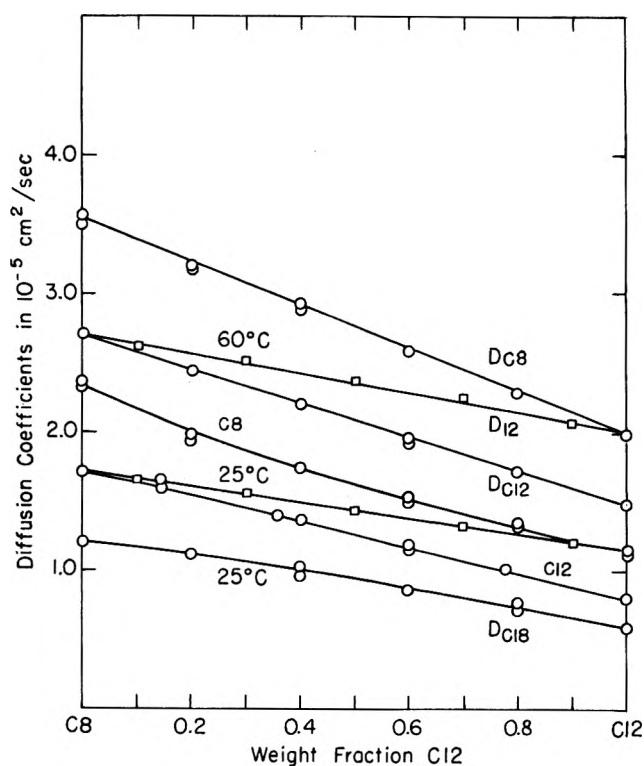


Figure 1. Diffusion coefficients in the system *n*-octane-*n*-dodecane.

Table I: Mutual Diffusion Coefficients in the System C₈-C₁₂

W ₂ , weight fraction C ₁₂ in %	N ₂ , mole fraction C ₁₂ in %	F ₂ , volume fraction C ₁₂ in %		D ₁₂ , 10 ⁻⁵ cm. ² /sec.	
		25°	60°	25°	60°
10.06	6.98	9.50	9.43	1.667	2.627
				1.644	2.613
				1.678	2.637
30.06	22.37	28.74	28.58	1.570	2.520
				1.543	2.518
50.06	40.20	48.48	48.27	1.441	2.374
				1.434	2.374
70.06	61.08	68.72	68.54	1.320	2.253
				1.322	2.253
90.06	85.88	89.47	89.40	1.208	2.070
				1.200	

Table II: Tracer Coefficients in the System C₈-C₁₂

W ₂ , % C ₁₂	N ₂ , % C ₁₂	F ₂ (25°), % C ₁₂	D _{C8}		D _{C12}		D _{C18} , 25°
			25°	60°	25°	60°	
0	0	0	2.368	3.535	1.718	2.728	1.209
			2.348	3.570	1.719	2.720	1.200
20	14.37	18.97	1.951	3.208	1.580	2.445	1.115
			1.982	3.195	1.546	2.449	1.137
40	30.90	38.45	1.746	2.888	1.350	2.206	1.027
			1.744	2.923	1.372	2.204	0.955
60	50.16	58.45	1.524	2.585	1.149	1.933	0.866
			1.502	2.589	1.164	1.952	0.847
80	72.85	78.96	1.345	2.287	1.002	1.715	0.773
			1.327	2.290	0.988	1.729	0.726
100	100	100	1.148	1.982	0.818	1.480	0.594
			1.136	1.988	0.809	1.485	0.613

Table III: System C₈-C₁₈ or C₁₂

N _{C8}	N _{C12}	N _{C18}	D _{C18} , 60°
0	100	0	1.039
60	0	40	1.052
60	0	40	1.043
60	0	40	1.025
0	0	100	0.525
0	0	100	0.532

of ± 0.011 and $\pm 0.016 \times 10^{-5}$ cm.²/sec. at 25 and 60°, respectively.

The activation energies for the three diffusion coef-

(19) It should be noted that our value for the self-diffusion coefficient for *n*-octane at 25° does not agree with that of 2.00×10^{-5} cm.²/sec. reported by D. C. Douglass and D. W. McCall, *J. Phys. Chem.*, **62**, 1102 (1958). However, if their self-diffusion coefficients for various *n*-alkanes are plotted against carbon number, it is seen that their *n*-octane value is out of line. The interpolated value does agree with ours both in the case of *n*-octane and in the case of *n*-dodecane (which they did not measure).

Table IV: Diffusion and Viscosity Activation Energies in the System C₈-C₁₂

W ₂ , % C ₁₂	Mutual diffusion	Activation energy, kcal.			Viscosity
		Tracer diffusion			
		C ₈	C ₁₁	C ₁₈	
10.06	2.58				
30.06	2.72				
50.06	2.83				
70.06	3.01				
90.06	3.06				
0		2.31	2.61		2.05
20		2.75	2.51		2.19
40		2.88	2.72		2.29
60		3.03	2.91		2.55
80		3.04	3.00		2.72
100		3.12	3.39	3.07	2.96

ficients of the *n*-octane-*n*-dodecane system are summarized in Table IV and plotted against composition in Fig. 2. Because of the relatively small variation in E , and the magnified experimental error (see Experimental), it is not possible to decide between mole fraction and volume fraction as the natural composition unit. Interestingly, however, the activation energies for the three diffusion coefficients fall on the same approximate line and thus appear to be determined entirely by the composition and not by the type of diffusion process (*vide infra*). Finally, as might be expected, the viscosity activation energies parallel those for diffusion.

Discussion

*Diffusion in *n*-Alkanes as a Segmental Motion.* It seems quite significant that the activation energies for diffusion in the *n*-octane-*n*-dodecane system are the same for a given composition, irrespective of the type of diffusion involved. As discussed below, it seems clear that in a two-component system three basic types of interactions are involved, *i.e.*, 1-2, 1-1, 2-2, and that diffusion (as well as viscosity) should be treated in terms of pairwise frictions. Mutual diffusion involves only 1-2 type interactions, while the two tracer diffusions involve 1-2 and 1-1, and 1-2 and 2-2, type interactions, respectively. In the present case, the activation energy appears to be the same for 1-2, 1-1, and 2-2 type processes for any given composition, which suggests that in the case of *n*-alkanes, the rate-determining step is the same in each case. This rate-determining step might well be the activated displacement of a segment of a hydrocarbon chain. Actually, it would be difficult to visualize the motion of a long chain hydrocarbon molecule in any other way.

If the rate-determining step is characterized entirely

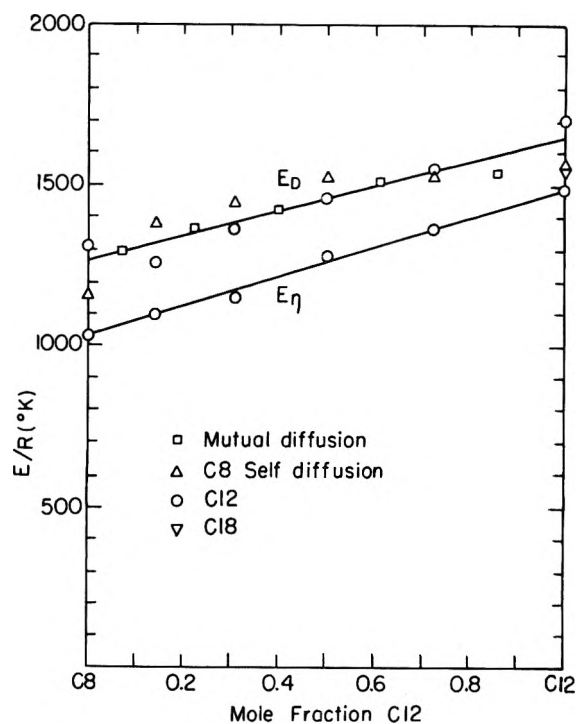


Figure 2. Diffusion and viscosity activation energies in the system *n*-octane-*n*-dodecane.

by the nature of the local environment, then one would expect that tracer diffusion of *any* *n*-alkane in *n*-octane-*n*-dodecane mixtures would have activation energies falling on the line in Fig. 2. As indicated in the figure, this is in fact what we observed in the case of dilute *n*-octadecane in *n*-octane-*n*-dodecane mixtures. In fact, the above observation suggests further that to a good approximation the local environment is determined by the average molar chain length, \bar{v} , where $\bar{v} = \sum N_i v_i$. Thus the activation energy for diffusion in *n*-dodecane should be the same as for diffusion in 50% *n*-octane-*n*-dodecane. This is just the principle of congruence discussed further below.

Although the activation energies are the same, the three diffusion coefficients at a given composition are numerically different, and it is evidently in the pre-exponential factor that molecular size enters. This role of chain length can be estimated as follows.

We suppose that a molecule C_vH_{2v+2} diffuses through the quasi-independent motion of q segments (where $q < v$), the length of each being $l = v/q$. If one segment moves a distance λ in the x -direction, the center of volume of the molecule then moves a distance λ/q , and if the frequency of such displacements is k sec.⁻¹, then the mean square displacement in 1 sec. will be $\bar{x}^2 = kq(\lambda/q)^2 = k\lambda^2l/v$. The diffusion coefficient is then

$$D = \frac{1}{2}(lk\lambda^2/v) \quad (14)$$

and on this basis the diffusion coefficient of a n -alkane should vary inversely as its chain length. While the motion of adjacent segments can certainly not be entirely independent, the degree of restriction, except for end effects, should be independent of chain length. Equation 14 is in fact approximately obeyed for C-5 to C-10 n -alkanes, using Douglass and McCall's data¹⁹ (ours for n -octane), in that a plot of D vs. $1/v$ is linear. Furthermore, one predicts from eq. 14 that at any given composition, the ratio of tracer diffusion coefficients in n -octane- n -dodecane mixtures should be $D_{C_8}/D_{C_{12}} = 12/8$ or 1.5. The actual ratio varies from 1.3 to 1.4.

Viscosity may likewise be viewed in terms of segmental motion. According to Eyring, *et al.* (see ref. 2, p. 482), the viscosity is given by

$$\eta = \frac{\lambda_1 kT}{\lambda_2 \lambda_3 \lambda^2 k} \quad (15)$$

where the values of λ are now taken to refer to the segment q . If the frequency factor is taken to be the same in both, it may be eliminated from eq. 14 and 15 and, if, in addition, the molar volume is set equal to $Nq\lambda_1\lambda_2\lambda_3$, then one obtains

$$\eta D = \frac{1}{2}\lambda_1^2 RT/V \quad (16)$$

If λ_1^3 is now assumed to be proportional to V/N , then eq. 16 becomes

$$\eta D \sim RT/(V^{1/3}N^{2/3}) \quad (17)$$

If the usual differential procedure to obtain activation energies, that is $E = -R[\partial \ln D/\partial(1/T)]_p$, is applied to eq. 17, and the appropriate values of the molar volumes at 25 and 60° are inserted, then for our n -octane- n -dodecane system we would predict that $(E_D - E_\eta) = 550$ cal. This is somewhat larger than the 350-450 cal. difference found experimentally and comparison with the prediction derived from eq. 16 (taking λ_1 to be temperature independent) is much better.

In summary, then, we are inclined to agree with Douglass and McCall¹⁹ that motion is segmental even in short chain n -alkanes, rather than only with very long ones, as Eyring, *et al.*, suggest.² In our system, one would expect that the volume of activation, $\Delta V^* = -RT(\partial \ln D/\partial p)_T$, is proportional to the length l of the diffusing segment: $l/v \sim \Delta V^*/V$. McCall and co-workers²⁰ find that ΔV^* increases with the chain length v . One would expect that the energy of activation is about proportional to ΔV^* . Thus the observed increase of the activation energy with the average molar chain length of the medium is interpreted as an increase of the length l of the diffusing segment.

The Principle of Congruence. Our conclusion that the local environment as given by the average chain length, \bar{v} , largely determines the character of the elementary segmental motions can be considered as an extension of the principle of congruence proposed by Brønsted and Koefoed.²¹ It is tempting to generalize further to postulate that all transport properties of such mixtures are determined primarily by v . Thus the viscosity of an equimolar mixture of n -octane and n -dodecane is in fact only 2.8% higher than that of pure n -decane. At 60°, the difference is only 1.0%.

In the case of tracer diffusion, the principle holds within our experimental error. The identity of activation energies for all diffusion processes occurring in a mixture of given \bar{v} was cited above. As a further example, the tracer diffusion coefficient of n -octadecane in n -dodecane is the same as in the congruent mixture of n -octane and n -octadecane (Table III).

The principle of congruence can be extended further to relate the tracer diffusion coefficients in a given mixture

$$\sum N_{i v_i} D_{C_{v_i}} = \bar{v} D_{C_{\bar{v}}} = \bar{v} D_C^0 \quad (18)$$

Here, $D_{C_{\bar{v}}}$ is the chain length weighted tracer diffusion coefficient which, for the case where v is integer, is equal to the self-diffusion coefficient of corresponding chain length pure n -alkane. As an illustration, a mixture of 60 mole % n -octane and 40 mole % n -octadecane is congruent with n -dodecane, and $0.6 \times 8 \times D_{C_8} + 0.4 \times 18 \times D_{C_{18}} = 12D_{C_{12}}$, or $0.4D_{C_8} + 0.6D_{C_{18}} = D_{C_{12}} = D_{C_{12}}^0$. It may be seen from Table II that this holds within experimental error. Mutual diffusion, which involves an added thermodynamic factor, is better treated in terms of the equations in the next sections.

Tests of Diffusion Models. Using a statistical mechanical approach, Bearman²² obtained the following relationships

$$D_1 V_1 = D_2 V_2 = (D_{12}/B_{12}) V_1 V_2 / V \quad (19)$$

Here, V denotes the total molar volume, and B_{12} is the rational thermodynamic term, *i.e.*, $B_{12} = (N_1/RT) d\mu_1/dN_1 = (N_2/RT) d\mu_2/dN_2$. In this approach, the assumptions limit the conclusions to a model which is approximately that of a regular solution. Specifically, it is assumed that the radial distribution function is independent of compositions and that volumes are additive. These specifications would seem to be met

(20) D. W. McCall, D. C. Douglass, and E. W. Anderson, *Phys. Fluids*, **2**, 87 (1959).

(21) J. N. Brønsted and J. Koefoed, *Kgl. Danske Videnskab. Selskab. Mat.-fis. Med.*, **22**, No. 17, 1 (1946).

(22) R. J. Bearman, *J. Phys. Chem.*, **65**, 1961 (1961).

reasonably well in our case of *n*-alkane mixtures and accordingly it is of interest to test some of Bearman's relationships. One expectation is that the ratio D_1/D_2 be essentially constant and equal to the ratio of molar volumes. This is essentially the prediction made above on the basis of segmental motion as the transport mechanism, and the ratio of molar volumes, 1.4, does approximate the nearly constant ratio D_1/D_2 . Bearman provides a second expectation, namely that the product $D_1\eta$ should be independent of composition. This prediction is only approximately obeyed. Both the products $D_{C_2}\eta$ and $D_{C_{11}}\eta$ vary by about 30% over the entire composition range, as against a twofold opposite variation in the D 's separately. The viscosity factor thus overcorrects for the variation. Other simple formulations, such as that of Eyring, *et al.*,² and the Stokes-Einstein equation also suggest approximate constancy of $D\eta$ products, so this test is not very diagnostic.

From eq. 19, it follows that

$$(D_{12}/B_{12})V_1V_2/V = F_2D_1V_1 + F_1D_2V_2$$

or

$$D_{12} = (N_2D_1 + N_1D_2)B_{12} \quad (20)$$

This relationship, as well as eq. 19, have been obtained in a different and probably less rigorous manner by Hartley and Crank.²³ The thermodynamic factor, B_{12} , in the system *n*-octane-*n*-dodecane follows from the data of Brønsted and Koefoed²¹: $B_{12} = 1 + 0.0356N_1N_2$. This relationship also applies to 60° since the temperature coefficient of B_{12} is very small.²⁴ Equation 20 can then be tested empirically by calculating D_{12} from the tracer diffusion data. We find the average deviation from the experimental D_{12} to be -0.63% at 25° and -0.72% at 60°. Statistically, these differences are insignificant at the 90% probability level. Empirically, the following relationship fits the data also, the average deviations being +0.35% and +0.37% at the two temperatures

$$D_{12} = F_2D_1 + F_1D_2 \quad (21)$$

Equation 19 holds fairly well. D_{12} may be calculated from D_1 or from D_2 . In the first case, the average deviations from the experimental D_{12} are -4.6 and -4.1% at the two temperatures; in the second case they are +2.0 and +1.6%.

A more general approach retains the pairwise friction coefficients as separate parameters. The treatments of Lamm³ and Laity⁴ are examples, and using the latter, if the friction factor R_{11} is taken to be independent of composition, then the relationship is obtained

$$1/D_1 = F_1/D_1^0 + N_2B_{12}/D_{12} \quad (22)$$

and similarly for D_2 . The tracer diffusion coefficients predicted by eq. 22 do not agree well with our data, the maximum deviation being 18%. Following Lamm, as an empirical modification, one can assume that R_{11} is proportional to viscosity, so that $R_{11} = R_{11}^0\eta/\eta_1$ where η_1 refers to the viscosity of pure component. This leads to the equation

$$1/D_1 = (F_1/D_1^0)(\eta/\eta_1) + N_2B_{12}/D_{12} \quad (23)$$

and correspondingly for D_2 . This equation now represents our data quite well at 25°; in the case of the 60° data, deviations up to 4.4% occur.

Another approach, proposed in this laboratory,⁵⁻⁸ resembles the above, although the language of absolute rate theory was used. The important difference, however, is that it is specified that the 1-1, 1-2, and 2-2 pairwise interactions occur with the *local* restriction of no net volume flow, rather than that the restriction is a collective one imposed trivially by the laboratory frame of reference chosen. One then obtains the equation

$$D_1 = F_1D_1^0(\eta_1/\eta) + F_2D_{12}/A_1 \quad (24)$$

which, like eq. 23, includes an added assumption that the 1-1 friction coefficient is proportional to viscosity. The term A_1 is the concentration based thermodynamic factor ($A_1 = N_2B_{12}/F_2$).

In a system such as the present one, where the diffusion coefficients of the two pure components are not greatly different, the difference in form between eq. 23 and eq. 24 is more apparent than real, and both equations fit our data equally well. No test of local *vs.* collective prohibition of net volume flow is thus provided.

Empirically, eq. 20, 21, 23, and 24 are about equally useful. The first two, however, require the knowledge of mutual and tracer diffusion coefficient as a function of concentration and then predict the second tracer diffusion coefficient. The second pair of equations is less demanding in that a knowledge of the mutual diffusion coefficients as a function of concentration plus the self-diffusion coefficients for the two pure liquids (which can be obtained by the spin-echo method as an alternate to the relatively difficult tracer studies) suffices to give both tracer diffusion coefficients as a function of composition.

(23) See, for example, J. Crank, "The Mathematics of Diffusion," Clarendon Press, Oxford, 1956, p. 225.

(24) J. H. van der Waals and J. J. Hermans, *Rec. trav. chim.*, **69**, 949, 971 (1950).

Returning to eq. 19, the tracer diffusion of dilute n -octadecane in a mixture of n -octane and n -dodecane is predicted quite well, *i.e.*, $D_{C_{18}}V_{C_{18}} = D_{C_8}V_{C_8} = D_{C_{12}}V_{C_{12}}$, in any given composition. Equation 19 may also be used to predict mutual diffusion coefficients. Observing that D_{12} varies linearly with volume fraction, then

$$D_{12} = F_1D_1^0V_1/V_2 + F_2D_2^0V_2/V_1 \quad (25)$$

The entire set of diffusion data for the C_8 - C_{12} system may now be calculated from D_1^0 and D_2^0 alone, and these calculated values agree with the experimental ones with a maximum deviation of 6% and an average of 3%. Equations 19 and 25 provide an approximate basis for estimating the diffusional behavior of any n -alkane mixture, provided the appropriate self-diffusion

coefficients are known. In combination with Douglass and McCall's data and reasonable extrapolations of it, the practical usefulness of these approximations should be considerable. Further, these equations can be extended to multicomponent n -alkane mixtures as well.

Acknowledgment. The measurement of the tracer diffusion coefficients of dilute n -octadecane in various n -octane- n -dodecane mixtures was carried out by Mr. Bruce W. Davis in partial fulfillment of an M.S. degree in chemistry. Assistance of Miss Valeria Artel in some of the gas chromatographic measurements is gratefully acknowledged. Finally, we are greatly indebted to the American Petroleum Institute and to the Petroleum Research Fund of the American Chemical Society for financial support.

On the Photochemistry of Aqueous Solutions of Chloride, Bromide, and Iodide Ions

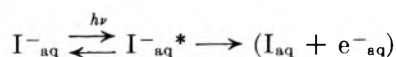
by Joshua Jortner, Michael Ottolenghi, and Gabriel Stein

Department of Physical Chemistry, Hebrew University, Jerusalem, Israel (Received April 27, 1968)

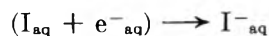
The photochemistry of aqueous solutions of Cl^- , Br^- , I^- and OH^- was investigated at 2537, 2288, and 1849 Å., in the temperature range 5–37°. The excited halide ions dissociate into a halogen atom and a solvated electron. Scavengers for solvated electrons, such as H_3O^+ , N_2O , or acetone compete with the secondary diffusive recombination of these but do not interact with the spectroscopic excited state. Cl atoms dehydrogenate ethanol and methanol, while I atoms appear to be unable to do so at all wave lengths. For Br atoms, however, the results indicate that at 2288 Å., formed in their lower energy $^2\text{P}_{1/2}$ state, they do not dehydrogenate the scavengers but may be able to do so when formed in the higher energy $^2\text{P}_{3/2}$ state at 1849 Å. The effects of temperature, wave length, added salt, and type of halide ion indicate that the atom–electron pair is formed from the excited ion in a distinct step. This process, essentially one of charge asymmetrization, competes with the deactivation of the excited ion. The value of the limiting constant quantum yield, Γ , obtained at high scavenger concentrations depends on this competition.

Introduction

In previous work,^{1–5} the photochemistry of the iodide ion was investigated at 2537 Å. in aqueous solutions at 25°. The effect of different scavengers on the quantum yields of the products indicated that there was no interaction between the scavenger and the spectroscopic excited state of the ion. The experimental results could be explained, however, in terms of a dissociation of the excited ion into an iodine atom and a solvated electron produced in close proximity. This nonhomogeneous initial distribution of radicals is often referred to using the colorful expression of radicals formed in a solvent cage. The radical formation process competes with the decay of the excited state, back to the ground state ion



where the parentheses stress the fact that I_{aq} and e^-_{aq} are formed in pairs. Various scavengers were shown to capture e^-_{aq} , thus preventing the recombination



Such a recombination of original partners is known as “secondary (diffusive) recombination.” The term “primary recombination,” describing recombination between radicals not yet separated by a solvent molecule, is somewhat misleading, as primary recombination is the kinetic equivalent to the deactivation of the excited state. Radicals which escape secondary recombination achieve a homogeneous distribution and, if no scavenger is present, will ultimately undergo a “bulk recombination” process.

A quantitative kinetic analysis, based on Noyes' approach for the treatment of scavenging competing with secondary recombination of radicals,^{6,7} relating the quantum yield of the products to the scavenger concentration, was carried out,^{1–5} and found to agree

- (1) J. Jortner, M. Ottolenghi, R. Levine, and G. Stein, *J. Phys. Chem.*, **65**, 1232 (1961).
- (2) J. Jortner, M. Ottolenghi, and G. Stein, *ibid.*, **66**, 2029 (1962).
- (3) J. Jortner, M. Ottolenghi, and G. Stein, *ibid.*, **66**, 2037 (1962).
- (4) J. Jortner, M. Ottolenghi, and G. Stein, *ibid.*, **66**, 2042 (1962).
- (5) J. Jortner, M. Ottolenghi, J. Rabani, and G. Stein, *J. Chem. Phys.*, **37**, 2488 (1962).
- (6) R. M. Noyes, *J. Am. Chem. Soc.*, **77**, 2042 (1955).
- (7) R. M. Noyes, *ibid.*, **78**, 5486 (1956); cf. J. C. Roy, R. R. Williams, and W. H. Hamill, *ibid.*, **76**, 3274 (1954).

with the experimental results. Similar mechanisms, resulting in the formation of solvated electrons, appear to operate in the photochemistry of I^- in D_2O , methanol, ethanol, 1-propanol, and methyl cyanide as solvents.⁸

The purpose of the present work was to investigate whether the above conclusions are specific to the I^- ion or if the formation of solvated electrons is also common to other ions, characterized by charge transfer to the solvent (c.t.s.) bands. A second object was to get a closer insight of the detailed mechanism of the transition from the spectroscopic excited state to the reactive radical pair. We therefore investigated the effects of ultraviolet radiation on aqueous solutions of Cl^- , Br^- , and I^- , with special attention to the effects of changing wave length, temperature, and added salts on the photochemistry of the three halide ions, as well as some experiments on solutions of the OH^- ion.

Experimental

Light Sources and Actinometry: 2537 Å. A low pressure mercury arc lamp was used. Details of the irradiation technique, filtration of light at other wave lengths, and actinometry were as described previously.^{1,2} The light intensity was 1.5×10^{-6} einstein $l^{-1} \text{ sec}^{-1}$.

2288 Å. An Osram-Cd/1 cadmium arc lamp was used operated at 12 v. (through a choke from the 220 v. mains) and 1.5 amp. a.c. There is no emission below 2000 Å. The light intensity at 2144 Å. was found to be less than 5% of that at 2288 Å. and is included with the latter. Our solutions did not absorb any of the lines emitted above 2650 Å. Actinometry was carried out by means of uranyl oxalate solution, using for the quantum yield of the actinometer the value⁹ of 0.55 for 2288 Å. In a first experiment the actinometric solution in the reaction vessel was irradiated directly. In a second experiment a 1-cm. path length 4 *N* acetic acid solution filter,¹⁰ absorbing all the light below 2400 Å., was inserted between the reaction vessel and the lamp. The chemical change on illumination was determined in both cases by titration with 0.01 *N* $KMnO_4$ solution. From the difference between the two values, the light intensity at 2288 Å. was determined as 3.4×10^{-7} einstein $l^{-1} \text{ sec}^{-1}$.

1849 Å. A low pressure Hg vapor lamp was used. In the case of Cl^- and Br^- solutions, there was no need to filter out radiation at higher wave lengths since these were not absorbed. For I^- solutions an X-ray irradiated LiF crystal filter was used as recommended by Weeks, Gordon, and Meaburn.¹¹

At this wave length 10^{-2} *M* methanol dissolved in

water¹² was used as an actinometer, measuring the hydrogen yield. The light intensity calculated was 8×10^{-8} einstein $l^{-1} \text{ sec}^{-1}$, assuming a quantum yield of 0.65 for the actinometer.^{12b}

Reaction Vessels and Thermostatic Arrangements. The reaction vessels were adapted from 1-cm. optical path length spectrophotometer cells, since effectively total absorption in these could be obtained in all cases. The reaction cells were seated inside square copper blocks through which thermostated water was circulated. The temperature was constant inside the reaction cells to within $\pm 0.5^\circ$ of the stated values.

Gas Analysis. Reaction yields were determined from the amounts of gaseous products: H_2 and N_2 formed. H_2 was determined using a McLeod gage and separately using a Pirani gage. Agreement between the two methods indicated the purity of the gaseous product. N_2 from H_2O containing solutions was determined after freezing out H_2O in a CO_2 -acetone-cooled trap and only then N_2O in a liquid air-cooled trap. Agreement between readings on the McLeod and Pirani gages indicated the purity of the product. To check our results control combustion experiments were carried out showing the absence of O_2 in all experiments. Experiments were designed so that simultaneous evolution of N_2 and H_2 should not take place. Iodine liberated was determined as I_3^- by spectrophotometry.¹

Materials used were Analar grade. Distilled water was redistilled from alkaline permanganate followed by distillation from dilute phosphoric acid.

Results

Comparison of the Photochemistry of I^- Solutions at 2537, 2288, and 1849 Å. The results of experiments in which aqueous I^- solutions at 25° were irradiated with light of 2537 Å., in the presence of various scavengers, were described previously.¹⁻⁵ In all scavenger systems the limiting quantum yield of the final products, Γ , reached at high scavenger concentrations, was found to be $\Gamma = 0.29$. Thus the yield of formation of the pair ($I_{aq} + e^-_{aq}$) from the excited state is 0.29.

In the present experiments at 2288 Å. and 25° , two systems were investigated. (a) H_3O^+ is used as the

- (8) J. Jortner, M. Ottolenghi, and G. Stein, *J. Phys. Chem.*, **67**, 1271 (1963).
- (9) C. R. Masson, V. Boekelheide, and W. A. Noyes, Jr., in A. Weissberger, Ed., "Technique of Organic Chemistry," Vol. II, Interscience Publishers, Inc., New York, N. Y., 1956, p. 295.
- (10) E. J. Bowen, "The Chemical Action of Light," Oxford University Press, London, 1946, p. 283.
- (11) J. L. Weeks, S. Gordon, and G. M. A. C. Meaburn, *Nature*, **191**, 1186 (1961).
- (12) (a) L. Farkas and Y. Hirschberg, *J. Am. Chem. Soc.*, **59**, 2450 (1937); (b) J. H. Baxendale, *Trans. Faraday Soc.*, **56**, 37 (1960).

scavenger,^{3,5} $e^-_{aq} + H_3O^+ \rightarrow H + H_2O$, converting the solvated electron into an H atom, and 1 M methanol as the H atom scavenger converting it to molecular hydrogen.³ Experiments were carried out at pH 0.82 and 1.65, using H_2SO_4 to set the pH. In both experiments, where $[I^-] = 0.01 M$, the value for the quantum yield of H_2 , $\gamma(H_2)$, was 0.25 ± 0.01 . Thus the yield is independent of $[H^+]$ in this range, and $\Gamma = \gamma(H_2)$ so that $\Gamma = 0.25 \pm 0.01$. (b) Here N_2O is used as the scavenger of e^-_{aq} ,³ according to $e^-_{aq} + N_2O \rightarrow O^- + N_2$. Solutions containing $[I^-] = 0.1 M$ were irradiated in the presence of $2.10^{-2} M N_2O$. The quantum yield of I_2 , $\gamma(I_2)$, was 0.23 ± 0.01 , and the quantum yield of N_2 , $\gamma(N_2) = 0.24 \pm 0.01$. As $[N_2O]$ is sufficient for total electron scavenging, we may again assume $\gamma(N_2) = \Gamma$. The values of Γ determined in the two independent scavenging systems are thus in fair agreement. We conclude, in view of the uncertainty of $\pm 10\%$ in the actinometry at 2288 Å., that the values of Γ do not differ significantly from those at 2537 Å.

At 1849 Å. control experiments were first carried out to show the efficiency of the X-irradiated LiF filters in removing light at 2537 Å. Solutions of 0.15 M I^- were irradiated at pH 2 in the presence of 1 M methanol through 5-mm. path length of 0.1 N NaCl solution (to remove light at 1849 Å.) and through the LiF filter. At twice the usual dose of irradiation, H_2 was not evolved. Without the NaCl filter $\gamma(H_2) = \Gamma = 0.97$ was obtained at pH 2. In order to determine the value of the "experimental residual yield,"¹² γ_r^{ex} , (i.e., the yield at high pH values when practically any efficient scavenger for the radicals, except the solvent itself, is absent) experiments were carried out in 0.15 N I^- and 1 M ethanol solutions at pH 11.9, using NaOH (OH^- does not contribute significantly to the absorption in this case). $\gamma_r^{ex}(H_2) = 0.04$ was found.

The Photochemistry of Br^- at 2288 and at 1849 Å. At 2288 Å., 0.5 M KBr solutions containing 1 M methanol were irradiated. The pH values were set using H_2SO_4 , $2.5 \times 10^{-3} M$ acetate or phosphate buffers, or NaOH. The absorption of all these solutions without added KBr was negligible compared with their absorption when KBr was added. The quantum yield of H_2 evolution remained constant during irradiation, up to hydrogen concentrations of $10^{-4} M$. The dependence of $\gamma(H_2)$ on the pH is shown in Fig. 1 and indicates that at 25° $\Gamma = 0.50 \pm 0.01$, while the constant experimental residual yield obtained at pH > 7 is $\gamma_r^{ex} = 0.025$ (an additional experimental point at pH 11 giving the same value is not shown in the graph). In Fig. 2, $1 + \log [1 - (\gamma(H_2)/\Gamma)]$ is plotted

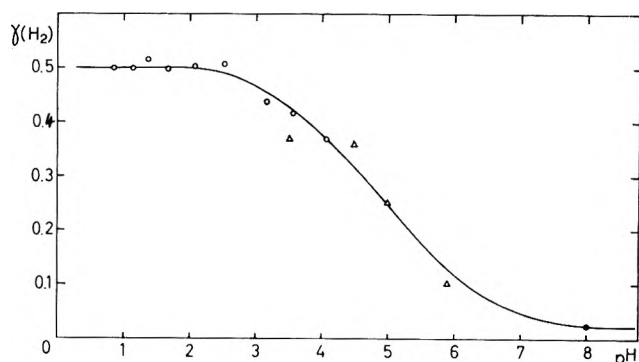


Figure 1. The pH dependence of the quantum yield of H_2 in the photochemistry of KBr (0.5 M) at 2288 Å. in the presence of 1 M methanol: O, pH adjusted with H_2SO_4 ; ●, pH adjusted with $2.5 \times 10^{-3} M K_2HPO_4/NaH_2PO_4$ buffer; Δ, pH adjusted with $2.5 \times 10^{-3} M CH_3COOH/CH_3COONa$ buffer.

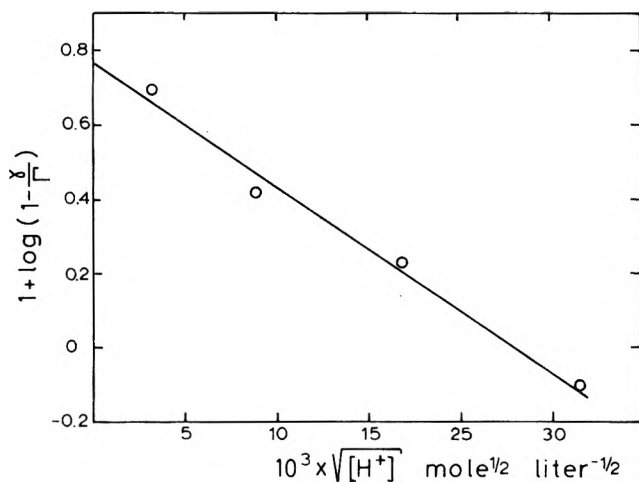


Figure 2. The plot of the experimental results of Fig. 1 according to the cage scavenging eq. 1.

as a function of $\sqrt{[H^+]}$. This plot is according to the general scavenging equation²

$$\ln \left(1 - \frac{\gamma(H_2)}{\Gamma} \right) = \ln \beta' - \frac{2a}{\beta'} \sqrt{\pi k_{H^+ + e^-_{aq}} [H^+]} \quad (1)$$

which describes the competition between the scavenging process $H^+ + e^-_{aq} \rightarrow H$ and the secondary recombination $Br_{aq} + e^-_{aq} \rightarrow Br^-_{aq}$. a is a parameter defined by Noyes,^{6,7} and $\beta' = 1 - \gamma_r/\Gamma$. γ_r is the total yield of solvated electrons and halogen atoms which escape secondary recombination, and diffuse into the bulk, when no external scavenger is present. The intercept of the straight line gives $\beta' = 0.58 \pm 0.05$ and hence $\gamma_r = 0.21 \pm 0.03$. It can be seen that γ_r^{ex} is much smaller than γ_r . This is due to the

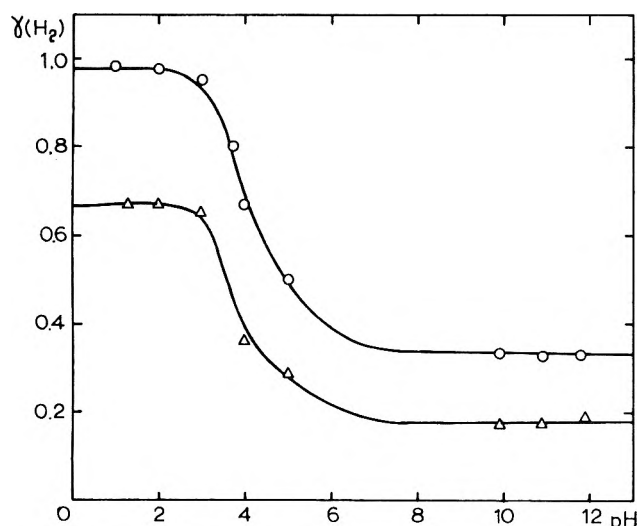


Figure 3. Hydrogen quantum yields in the photochemistry of 0.5 M KBr (Δ) and 0.5 M KCl (O) at various pH values, in the presence of 1 M CH_3OH .

bulk recombination Br (or Br_2^-) + $e^-_{\text{aq}} \rightarrow \text{Br}^-$ which competes with the processes by which, in this pH range, e^-_{aq} is converted to hydrogen with the participation of the solvent. From the slope and from this value of β' , we obtain $2a\sqrt{\pi k_{\text{H}^+ + e^-_{\text{aq}}}} = 44 \text{ l.}^{1/2} \text{ mole}^{-1/2}$.

At 1849 Å., 0.5 M solutions of KBr were irradiated in the presence of 1 M methanol. At this wavelength pH values were set using H_2SO_4 (pH < 4), 2.5×10^{-3} M acetate buffer (pH 5.0), and KOH (pH > 9). The dependence of $\gamma(\text{H}_2)$ on pH is shown in Fig. 3. Since $\epsilon^{1849}_{\text{Br}^-} = 1 \times 10^4 \text{ cm.}^{-1} \text{ mole}^{-1} \text{ l.}$, the absorption of light by components other than Br^- may be neglected. Even that of acetate,¹³ with $\epsilon^{1849} = 1 \times 10^3$, may be neglected at the concentration employed, as¹³ can be OH^- . From the values of $\gamma(\text{H}_2)$ at low pH one gets $\Gamma = 0.69 \pm 0.01$. Experiments were also carried out using N_2O as the scavenger for e^-_{aq} . In the presence of N_2O at a partial pressure of 360 mm., from solutions of 0.5 M KBr, at 25° $\gamma(\text{H}_2) = \Gamma = 0.68 \pm 0.04$ was obtained. Since¹⁴ $\epsilon^{1849}_{\text{N}_2\text{O}} = 40$, the absorption due to N_2O may be neglected.

Photochemistry of Cl^- Solutions at 1849 Å. Solutions of 0.5 M KCl were irradiated at this wavelength in the presence of 1 M methanol as H atom scavenger, at varying pH values. The results are shown in Fig. 3, pH values being set as in the Br^- system. Since¹³ $\epsilon^{1849}_{\text{Cl}^-} = 3800 \text{ cm.}^{-1} \text{ mole}^{-1} \text{ l.}$, the absorption of light due to the added sulfate, acetate, and hydroxyl ions may be neglected. Additional experiments at pH 12 using 0.25 M KCl gave $\gamma(\text{H}_2) = 0.366$, as in the case of 0.5 M KCl solutions.

Using 0.5 M KCl solutions at pH 11.9 in the presence of 360 mm. pressure of N_2O we get $\Gamma = \gamma(\text{N}_2) = 0.99 \pm 0.04$ for this scavenger of solvated electrons.

Experiments were also carried out at pH 11.9 in 0.5 M KCl solutions containing 1 M methanol with the addition of 1.10^{-3} M acetone, which^{15,16} captures e^-_{aq} without yielding H_2 , but reacts more slowly with H atoms.¹⁶ Irradiations at 1849 Å. were in the presence of the X-irradiated LiF crystal filter, to eliminate light at 2537 Å. which might cause photolysis of the acetone, while at 1849 Å. at the concentrations employed the absorption by acetone itself may be neglected. The results in the presence of acetone showed the reduction of $\gamma(\text{H}_2)$, the experimental residual yield of H_2 , from ~ 0.33 to less than 0.03, demonstrating that the residual yield involves solvated electrons.

Photochemistry of OH^- at 1849 Å. The absorption spectrum of aqueous solutions of OH^- shows great similarity to that of the halogens (e.g., it is affected similarly by changes in temperature¹⁷) and is attributed to a c.t.t.s.-type transition. At 1849 Å. in solutions of 0.1 M KOH containing N_2O at 520 mm. pressure, $\gamma(\text{N}_2)$ was found to be 0.5.

The Effect of Alcohol Concentration Some experiments have been carried out in order to clarify the role of the added ethyl alcohol on the experimental residual yield, i.e., on the constant, pH independent yield of H_2 observed at pH > 8. The solutions employed contained varying amounts of ethanol and 5×10^{-2} M NH_4Cl at pH 7.8. It has been shown⁵ that NH_4^+ acts as a scavenger for solvated electrons, converting them to H atoms. The low concentration of NH_4^+ employed by us was not sufficient for competing with secondary recombination of electrons but sufficient to prevent electron capture by impurities in the bulk. The results for solutions of I^- , Br^- , and Cl^- at various wave lengths are reported in Table I.

The Effect of Temperature on the Quantum Yield at 2537, 2288, and 1849 Å. (a) **Iodide at 2537 Å. 1. In the Presence of N_2O .** In the region of complete scavenging of e^-_{aq} , i.e., solutions of 0.15 N KI at a partial pressure of $P_{\text{N}_2\text{O}} = 400$ mm. in unbuffered, nearly neutral solutions, the results shown in Fig. 4 were obtained between 5 and 37°. The solubility of N_2O changes with temperature in this range.¹⁸ Plot-

(13) G. K. Rollefson and M. Burton, "Photochemistry and the Mechanism of Chemical Reactions," Prentice-Hall, Inc., New York, N. Y., 1941.

(14) M. Zelikoff, K. Watanabe, and E. C. Y. Inn, *J. Chem. Phys.*, **21**, 1643 (1953).

(15) J. T. Allan and G. Scholes, *Nature*, **187**, 218 (1960).

(16) J. Rabani and G. Stein, *J. Chem. Phys.*, **37**, 1865 (1962).

(17) J. Jortner, B. Raz, and G. Stein, *ibid.*, **34**, 1455 (1961).

Table I: The Effect of Ethanol Concentration on the H_2 Quantum Yield in the Photochemistry of KBr (0.5 M), KCl (0.5 M), and KI (0.15 M) in Solutions Containing $5 \times 10^{-2} M NH_4^+$ at pH 7.8

C ₂ H ₅ OH, mole l. ⁻¹	$\gamma(H_2)$			
	Br ⁻ (1849 Å.)	Br ⁻ (2288 Å.)	I ⁻ (2537 Å.)	Cl ⁻ (1849 Å.)
0.1	0.096	0.080	0.060	0.170
0.3	0.112	0.081
0.6	0.061	...
1.0	0.150	0.078	...	0.390
3.3	0.199	0.088	0.069	...

ting Seidell's data for our conditions we found that within this range, even at the highest temperature, $[N_2O]$ did not decrease below the concentration required for complete scavenging.

2. *In the Presence of H₂SO₄.* In Fig. 5 the complete scavenging curves are given for the H^+ concentration range from 2 to $10^{-4} N H_2SO_4$, between 5 and 37°. In

Table II: The Temperature Dependence of Γ in the Photochemistry of I⁻, Br⁻, and Cl⁻

Temp., °C.	I ⁻ at 2537 Å.		Br ⁻ at 2288 Å.	Br ⁻ at 1849 Å.	Cl ⁻ at 1849 Å.
	N ₂ O as scavenger for e ⁻ _{aq}	H ₃ O ⁺ as scavenger for e ⁻ _{aq}			
5	0.190	0.205	0.37	0.48	0.90
15	0.230	0.245	0.41	0.56	0.94
25	0.290	0.293	0.50	0.67	0.98
35	0.55	0.72	0.98
37	0.362	0.350

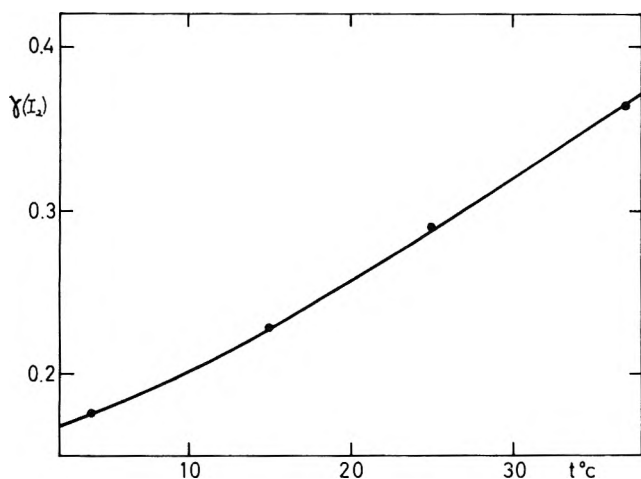


Figure 4. Temperature dependence of I_2 quantum yields in the photochemistry of I⁻ at 2537 Å. $P_{N_2O} = 600$ mm.; total scavenging is assumed so that $\gamma(I_2) = \Gamma$.

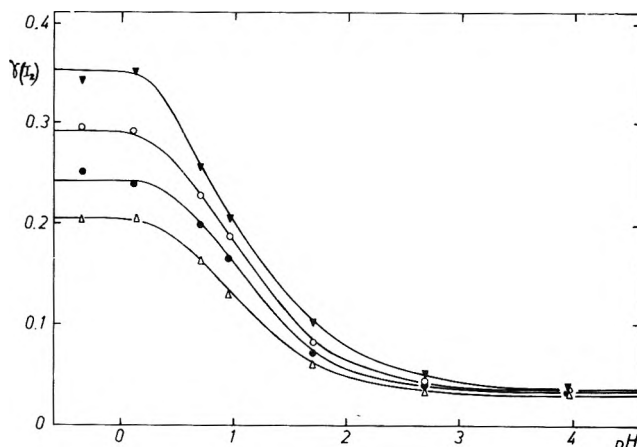


Figure 5. Scavenging of H atoms by H_3O^+ (see ref. 1) at various temperatures: Δ , 5°; \bullet , 15°; \circ , 25°; \blacktriangledown , 37°.

Table II values of Γ , the limiting quantum yields for the two cases, are compared.

(b) *Bromide at 2288 and 1849 Å.* Solutions of 0.5 M Br⁻ were irradiated in the presence of 1 M methanol at pH 1.8, in the temperature range 5 to 35°. The results are shown in Table II.

(c) *Chloride at 1849 Å.* Solutions of 0.5 M Cl⁻ were irradiated in the presence of 1 M methanol at pH 1.8 in the temperature range 5 to 35°. The results are shown in Table II.

Effects of Added Salts on the Quantum Yield. We investigated the effect of large amounts of added salts on the limiting quantum yield Γ in view of the investigation of the effect of such additions on the spectrum¹⁹ of I⁻

When 0.15 M KI solutions were irradiated at 2537 Å. and 25°, in the presence of 5 M HCl and 9 M LiCl, and 2.5 M HCl and 9 M LiCl, $\gamma(H_2)$ remained constant at 0.298 ± 0.002 . Similarly, when up to 1 M KBr was added, $\gamma(H_2) = 0.293 \pm 0.003$ was obtained using 1.78 M H₂SO₄ as the scavenger, and $\gamma(I_2) = 0.293 \pm 0.003$ using 590 mm. pressure of N₂O.

Discussion

1. *The Reactivity of the Halogen Atoms in the Photochemistry of the Halides.* The photochemical results for Br⁻ at 2288 Å. show a close similarity to those of I⁻ at 2537 Å.¹⁻⁴ Thus we may assume again the formation of the pair (X + e⁻_{aq}) with e⁻_{aq} scavenged by H₃O⁺ or N₂O. The scavenging by H₃O⁺ is shown by the dependence of $\gamma(H_2)$ on pH in Fig. 1. Figure 2 shows that Noyes' scavenging kinetics are obeyed.

(18) A. Seidell, "Solubilities of Inorganic and Organic Compounds," Supplement to Third Ed., D. Van Nostrand, New York, N. Y., 1955.

(19) G. Stein and A. Treinin, *Trans. Faraday Soc.*, 56, 1393 (1960).

Table III: Values of the Experimental Parameters γ_r^{ex} , Γ , and $\gamma_r^{\text{ex}}/\Gamma$ in the Photochemistry of I^- , Br^- , and Cl^- at Various Wave Lengths

Parameter	System				
	I^- , 2537 Å.	Br^- , 2288 Å.	I^- , 1849 Å.	Br^- , 1849 Å.	Cl^- , 1849 Å.
Γ	0.29	0.5	0.97	0.67	0.98
γ_r^{ex}	0.015	0.025	0.039	0.175	0.34
$\gamma_r^{\text{ex}}/\Gamma$	0.05	0.05	0.04	0.26	0.35

Table III summarizes the values of Γ , γ_r^{ex} (the experimental, constant, residual yield at high pH values), and those of the parameter $\gamma_r^{\text{ex}}/\Gamma$. This parameter represents the fraction of radicals which ultimately escape secondary recombination. It should be noted that the value of the ratio $\gamma_r^{\text{ex}}/\Gamma$ is exceptionally high for Cl^- and Br^- at 1849 Å., compared with those for I^- at 2537 and 1849 Å. and for Br^- at 2288 Å. Our explanation of this phenomenon is as follows. In the case of Cl^- , not only H atoms but Cl atoms also dehydrogenate the alcohol as shown by Berces and Trotman-Dickenson.²⁰ In our system the scavenging of Cl atoms competes with the recombination $\text{Cl} + e_{\text{aq}}^- \rightarrow \text{Cl}^-$. Assuming that the radicals formed in the dehydrogenation process are relatively poor scavengers of e_{aq}^- , this will increase the efficiency of the processes by which e_{aq}^- is converted to molecular hydrogen at this pH. In the absence of an efficient scavenger, solvated electrons in aqueous solutions will react with the solvent yielding molecular hydrogen. Matheson and Rabani (private communication) studied this reaction by means of electron pulse techniques and found that a second-order reaction occurs with a rate constant $k_{e_{\text{aq}}^- + e_{\text{aq}}^-} \cong 10^{10} \text{ mole}^{-1} \text{ sec}^{-1}$. However, in our photochemical experiments the rate of formation of e_{aq}^- is lower by mean orders of magnitude, so that a first-order reaction: $e_{\text{aq}}^- + \text{H}_2\text{O} \rightarrow \text{H} + \text{OH}_{\text{aq}}^-$, may play a role. Such a process agrees with the results of Lifshitz and Stein (to be published), who studied deuterium isotope effects in the radiation chemistry of aqueous systems. Acetone, $10^{-3} M$, practically eliminates any hydrogen evolution. This is consistent with e_{aq}^- being responsible, by reacting with the solvent water, for the formation of H_2 in this pH range. As previously stated, acetone acts as an efficient electron scavenger in a process that does not lead to gas evolution.

Unlike the case for Cl, energetic reasons prevent the dehydrogenation of the alcohol by I and ground state Br atoms ($\text{C-H} = 97 \text{ kcal.}$, $\text{H-I} = 71 \text{ kcal.}$, and $\text{H-Br} = 87 \text{ kcal.}$, while $\text{H-Cl} = 102 \text{ kcal.}$). Considering the behavior of the Br^- system at 1849 Å. where

the ratio $\gamma_r^{\text{ex}}/\Gamma$ is similar to the one in the Cl^- system rather than to that of Br^- at 2288 Å., we suggest that Br atoms formed at 1849 Å. are capable of dehydrogenating the alcohol while those formed at 2288 Å. behave like I atoms and are incapable of reaction with the aliphatic scavenger. This assumption is supported by the spectroscopic studies which indicate that the Br atom formed at 2288 Å. is in the $^2\text{P}_{3/2}$ state while at 1849 Å. it appears in the $^2\text{P}_{1/2}$ atomic state. Since $E^{\text{Br}^2\text{P}_{1/2}} - E^{\text{Br}^2\text{P}_{3/2}} = 10 \text{ kcal.}$, the reaction between the alcohol and the $^2\text{P}_{1/2}$ Br atom can no more be excluded. In the case of I^- , even if I is formed in the $^2\text{P}_{1/2}$ state (at 1849 Å.), $E^{\text{I}^2\text{P}_{1/2}} - E^{\text{I}^2\text{P}_{3/2}} = 21 \text{ kcal.}$ and the dehydrogenation process does not occur.

These views are also supported by the experimental results presented in Table I. It can be seen that in the case of I^- at 2537 Å. and of Br^- at 2288 Å., the quantum yields are almost unaffected by the alcohol concentration (the small rise at 3.3 M $\text{C}_2\text{H}_5\text{OH}$ may be due to an increase in Γ which markedly depends on the solvent⁸). However, when going over to Cl^- and Br^- at 1849 Å., $\gamma(\text{H}_2)$ increases significantly with the alcohol concentration. According to our previous arguments this is consistent with the existence of the scavenging process $\text{X} + \text{C}_2\text{H}_5\text{OH} \rightarrow \text{X}^- + \text{H}^+ + \text{C}_2\text{H}_4\text{OH}$ where X represents Cl or $^2\text{P}_{1/2}$ Br atoms. When X is an I ($^2\text{P}_{3/2}$ or $^2\text{P}_{1/2}$) or a $^2\text{P}_{3/2}$ Br atom the process does not take place and the alcohol concentration does not affect the results.

2 The Dissociation of the Excited State. The investigations of the spectra of I^- , Br^- , Cl^- , and OH^- in aqueous solution,^{21,22} and the effects of changes in temperature,²³ solvent,²⁴ and added ions,¹⁶ are consistent with the assumption that on the absorption of a light quantum the ground state ion, occupying a cavity defined by the surrounding oriented water molecules, goes over into an excited state in which according to the Frank-Condon principle the atomic nuclei have preserved their previous positions. This excited (c.t.t.s. state consists of an electron in a 2s orbital in the coulombic, spherically symmetrical, field of the oriented solvent medium.²² The excited electron in this orbital is confined over the first layer of water molecules of hydration, its mean radius being $R_{\text{ex}} \cong 5.8 \text{ Å.}$ Previous work^{2,3} showed that electron scavengers, H^+_{aq}

(20) T. Berces and A. F. Trotman-Dickenson, *J. Chem. Soc.*, 4281 (1961).

(21) G. Stein and A. Treinin, *Trans. Faraday Soc.*, 55, 1087 (1959).

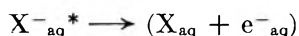
(22) R. L. Platzman and J. Franck, "Farkas Memorial Volume," Jerusalem, 1952, p. 21.

(23) (a) M. Smith and M. C. R. Symons, *Discussions Faraday Soc.*, 24, 206 (1957); (b) G. Stein and A. Treinin, *Trans. Faraday Soc.*, 55, 1091 (1959).

(24) I. Burak and A. Treinin, *ibid.*, in press.

or N_2O , could not directly interact with this excited state to scavenge the excited electron from it. The reason for this is not likely to be an energetic one, since the reaction $e^- + H^+_{aq} \rightarrow H$ is exoergic by ~ 50 kcal. for an unbound electron. In the first excited state the energy of binding of the electron is²¹ only ~ 35 kcal. It appears rather that the reason is one of time scale. The velocity of decay of the excited state to the ground state is too great for scavengers such as H^+_{aq} at concentrations of the order of 1–4 *M* to compete with it. The situation in the case of this "primary recombination" is similar to that for the so-called primary (nondiffusive) cage recombination in the photochemistry of, *e.g.*, diatomic molecules and others in solution²⁵ where scavengers able to compete with it could not be found.

The results in the present and previous^{2,5} work indicate however that there is a process able to compete with the decay of the excited state. This process leads to the formation of a halogen atom and a solvated electron, e^-_{aq} , in close proximity.



The two fragments now begin a random walk diffusion process; the distribution of radicals tending to become homogeneous. In previous papers^{1–5} we considered the possibility of a direct interaction of the scavenger with the excited state of the ion (preventing "primary recombination") or, alternatively, homogeneous scavenging in the bulk of the solution, occurring after a presumably fast diffusion of the radical partners from each other, so that secondary recombination would be of low probability. Neither of these possibilities accounts for the experimental results obtained in the previous or in the present work. The results, however, are in good agreement with a mechanism of scavenging processes, competing with secondary recombination of the parent atom and the solvated electron. Three regions of changing quantum yield may be observed. At high scavenger concentrations secondary recombination is effectively prevented and a plateau of limiting quantum yield, Γ , is reached. The situation is of total scavenging and the value of Γ corresponds to the yield of formation of the atom-electron pairs. At lower scavenger concentrations the quantum yield decreases with the decrease in the scavenger concentration, in quantitative agreement with the theoretical predictions on the effect of scavengers on secondary recombination.^{2–4,6,7} Finally, at very low scavenger concentrations, one should expect to reach a region in which scavenging competes with bulk recombination and homogeneous kinetics applies. However, our experimental results in this region are not accurate

enough to confirm such an assumption. The pH-independent residual yield obtained above pH 7 is due to the fact that the water solvent itself acts as a scavenger to solvated electrons and a condition of zero scavenger concentration cannot be achieved.

The formation of e^-_{aq} from the primary excited state occurs in competition with the decay to the ground state which is rapid enough to prevent direct scavenging from the spectroscopic excited state. It involves a process of asymmetrization, in which the electronic charge is no more spherically symmetrical around the halogen atom (a 2s electron bound in the polarization field of the original ion) but a solvated, self-trapped electron in its lowest (1s) energy level. It should be noted²⁴ that in both cases the same effective charge $Z_{eff} = [(1/D_{op}) - (1/D_s)] = 0.5$ (where D_{op} and D_s represent the optical and static dielectric constants of water) determines the field in which the electron is bound. The main difference between the states is the type of electronic orbital, 2s in the excited state of the ion, with the neutral atom at the center, and in the case of the solvated electron, which has been displaced relative to the atom.

The Effect of Temperature on Γ . Considering the formation of the pair $(X + e^-_{aq})$ as a process resulting from the competition between a thermal deactivation and a thermal asymmetrization, we allocate an activation energy E_1 to the first process and E_2 to the second. Thus denoting the rate of decay to the ground state by

$$A = k_1 \exp(-E_1/RT)$$

and the rate of asymmetrization by

$$B = k_2 \exp(-E_2/RT)$$

(where k_1 and k_2 contain transmission coefficients and entropy factors), the limiting quantum yield, Γ , will be given by

$$\Gamma = \frac{B}{A + B} = \frac{1}{1 + (A/B)} = \frac{1}{1 + \frac{k_1}{k_2} \exp \frac{(E_2 - E_1)}{RT}}$$

Denoting $\Delta E = (E_2 - E_1)$ and $k_1/k_2 = C$

$$\ln \{ (1/\Gamma) - 1 \} = \ln C + (\Delta E/R)1/T \quad (2)$$

Figure 6 shows the plots of $\log \{ (1/\Gamma) - 1 \}$ vs. $1/T$ for I^-_{aq} at 2537 Å. and for Br^-_{aq} at 2288 Å. The slopes give $\Delta E = 4.9$ kcal. mole⁻¹ for I^-_{aq} and $\Delta E = 4.0$ kcal. mole⁻¹ for Br^-_{aq} . For Cl^-_{aq} at 1849 Å. the quantum yield approaches 1, and the change with

(25) J. Franck and E. Rabinowitch, *Trans. Faraday Soc.*, **30**, 120 (1934).

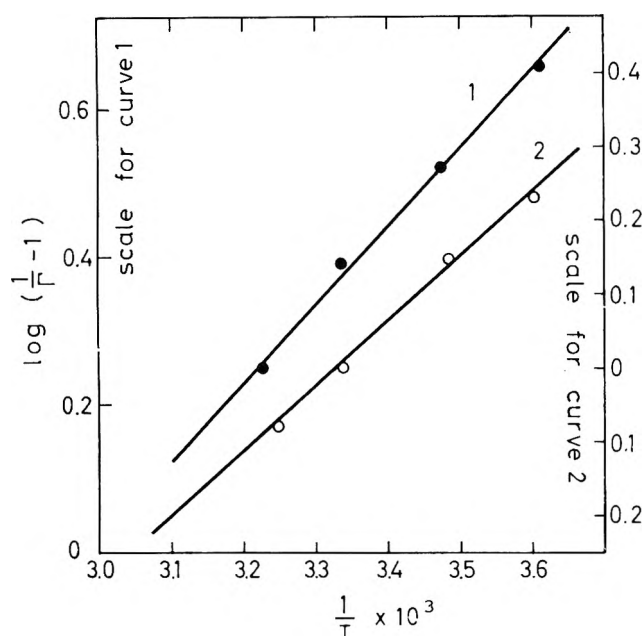


Figure 6. Test of eq. 2 for the temperature dependence of Γ in the photochemistry of I^- at 2537 Å. and Br^- at 2288 Å.

temperature is too small for the derivation of a reliable value of ΔE .

These results therefore prove that at least one of the competing processes involves an activation energy. However, only the difference ΔE may be calculated and the separate values E_1 and E_2 cannot be evaluated from our experimental results. The exact nature of the two processes is still not completely clear. The radiationless deactivation may resemble that of excited centers in ionic crystals in which energy may be needed to reach a cross section point of the energy curve with that of the ground state. The configuration coordinate may be one depending on the relative distance between the first hydration layer and the central atom (or ion). The asymmetrization process is essentially one of relative diffusion of X and the expanded electronic orbital, whose efficiency will be determined by the diffusion rate of the less mobile species. It is difficult to say which of the two will be the more mobile, as the diffusion coefficient of solvated electrons is not known. It should also be noted that both diffusive displacements may be abnormal, that of X in the sense that the atom must diffuse out of a cavity around which solvent molecules were organized by the original field of the ion. In the case of the electronic charge the displacement must be accompanied by a transition to the ground, 1s, state of the solvated electron.

The Dependence of Γ on Wave Length, Type of Halide Ion, and Added Salts. Passing from 2537 to 2288 Å. the absorption, in the case of I^-_{aq} , is always in the

same band, leading to the formation of a 2s electron and a $^2P_{3/2}$ iodine atom. Spectroscopic studies²¹ showed that the main reason for the broadening of the absorption band is due to changes in the ground state of the ion. In solution the ions are situated in cavities bound by the solvent water; the broad absorption band is due to the distribution of the equivalent radii of such cavities. According to this theory, changes of equivalent radius affect mainly the energy of binding in the ground state. The excited state, and in particular the energy of binding of the excited electron, remains largely unaffected. The present results agree with this assumption and may be interpreted as showing that the increased energy of $h\nu$ at 2288 Å. compared with 2537 Å. is needed in the case of I^-_{aq} to raise the electron to about the same level from a deeper ground state in the potential well formed by the oriented solvent.

Proceeding to 1849 Å., Γ rises considerably, its ratio to γ_r^{ex} remaining the same as at 2537 and 2288 Å. At 1849 Å., the absorption is in a band which may pertain to another transition.²⁶ In this the excited electron may go to a higher, *e.g.*, 3s state in the potential well described by the Franck-Platzman theory. Two reasons may then contribute to the higher value of Γ : lower recombination probably to the ground state and higher efficiency of the reaction leading to the formation of the solvated electrons from the excited state.

As to the change of Γ in the series I^- at 2537 Å., Br^- at 2288 Å., and Cl^- at 1849 Å., all these transitions yield a 2s state of the excited electron and the $^2P_{3/2}$ state of the halogen atom. Nevertheless, the efficiency of the asymmetrization of the first excited state to yield a solvated electron and a halogen atom increases in the series $I^-_{aq} < Br^-_{ac} < Cl^-_{aq}$. Two causes may contribute to this. The process of asymmetrization may involve the movement of the halogen atom, which will be easier for the light Cl than for the heavier Br or I.

A second cause may be a different rate of deactivation, A , decreasing in the order I^- , Br^- , Cl^- . However the lack of values of k_1 and E_1 prevents a quantitative analysis of such an effect.

The complete lack of salt effects on Γ , even in highly concentrated solutions, is consistent with the spectroscopic studies¹⁹ which claim that added salts may influence the ground state of the ion (*i.e.*, the effective cavity radius) but do not effect markedly the excited state, the changes in D_{op} and D_s with addition of salts being negligible. Our photochemical results show that both A and B may remain unaffected by foreign ions and are also consistent with the fact that the excited

(26) G. Scheibe, *Z. physik. Chem.*, **35**, 355 (1929).

state is not affected by high concentrations of the salts now employed.

After the completion of this manuscript Hart and Boag's work²⁷ appeared, showing the absorption spectrum of the hydrated electron in water and in aqueous solutions irradiated with pulses of ionizing radiation. Subsequently, Matheson and Rabani²⁸ found spectroscopic evidence for the formation of sol-

vated electrons in the flash photolysis of aqueous solutions, including those of halide ions. These results give strong support for the views expressed in the present and previous^{1-5,8} papers.

(27) E. J. Hart and J. W. Boag, *J. Am. Chem. Soc.*, **84**, 4090 (1962).

(28) M. S. Matheson and J. Rabani, to be published.

Heat Capacities and Thermodynamic Properties of Globular

Molecules. X. Fusion of Pentaerythrityl Fluoride¹

by John C. Trowbridge and Edgar F. Westrum, Jr.

Department of Chemistry, University of Michigan, Ann Arbor, Michigan (Received June 3, 1963)

The heat capacity of crystalline and liquid $C(CH_2F)_4$ has been determined by adiabatic calorimetry from 295 to 385°K. The small entropy of fusion, 3.35 cal./mole °K., at the 367.43°K. triple point temperature confirms the plastically crystalline nature of this substance.

Introduction

Low temperature heat capacity studies on pentaerythritol² and the pentaerythrityl halides³ revealed the presence of a transition at 249.40°K. to the plastically crystalline state in pentaerythrityl fluoride, $C(CH_2F)_4$, with 12.66 cal./mole °K. entropy of transition.⁴ Study of the thermodynamics of the fusion process was undertaken to provide a basis for further correlation of the crystal II \rightarrow crystal I transition in the fluoride with that in pentaerythritol and to give an added test of the proposed mechanism of transition in the former.

Experimental

Calorimetric Sample. The identical sample used previously⁴ was loaded in the nitrogen atmosphere of the drybox. For these measurements 58.6279 g. (*in vacuo*) of pentaerythrityl fluoride were used.

Further indication of purity is provided by the fractional fusion studies.

Calorimeter and Thermostat. The Mark IV intermediate temperature thermostat and silver calorimeter W-22⁵ were used in these measurements with the quasi-adiabatic technique previously employed.⁶ The calorimetric system had previously been calibrated⁷ with the Calorimetry Conference Sample of synthetic sapphire.⁸

(1) This work was supported in part by the United States Atomic Energy Commission.

(2) E. F. Westrum, Jr., and D. H. Payne, *J. Phys. Chem.*, in press.

(3) D. H. Payne and E. F. Westrum, Jr., *ibid.*, **66**, 748 (1962).

(4) E. F. Westrum, Jr., and D. H. Payne, *ibid.*, in press.

(5) J. C. Trowbridge and E. F. Westrum, Jr., *ibid.*, **67**, 2381 (1963).

(6) E. F. Westrum, Jr., J. B. Hatcher, and D. W. Osborne, *J. Chem. Phys.*, **21**, 419 (1953).

(7) E. F. Westrum, Jr., and J. C. Trowbridge, to be published.

(8) G. T. Furukawa, T. B. Douglas, R. E. McCoskey, and D. C. Ginnings, *J. Res. Natl. Bur. Std.*, **57**, 67 (1956).

For thermal conduction 12.5 cm. pressure of helium gas at 300°K. was put into the sample space before sealing off the calorimeter.

Results

Heat Capacity. The experimental heat capacities are presented in Table I in chronological order in terms of the ice point as 273.15°K., the defined thermochemical calorie as 4.184 j., and a molecular weight of 144.119 g. Adjustments (which amounted to less than 0.01% over the entire temperature range investigated) were applied to the data for the finite temperature increments used. No correction was made for sublimation or vaporization since no adequate representation of the vapor pressure as a function of temperature was available. However, this emendation is estimated from rough vapor pressure values to be less than 0.05%. Figure 1 shows the experimentally determined heat

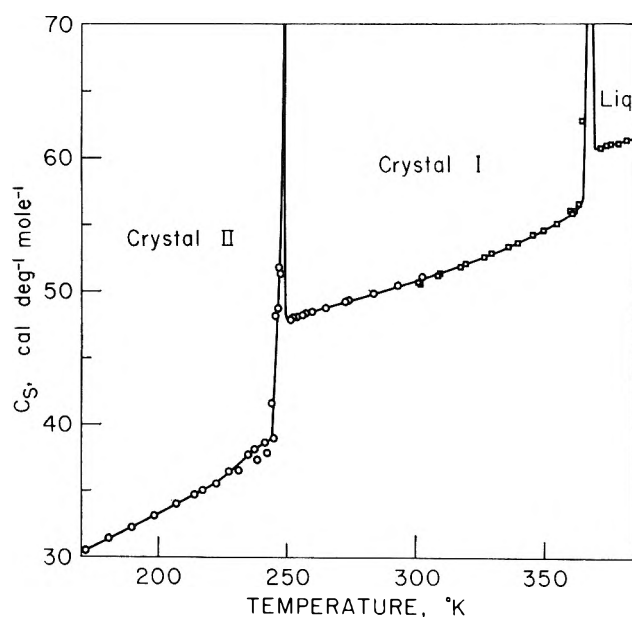


Figure 1. Heat capacity of pentaerythrityl fluoride: O, cryogenic data of Westrum and Payne⁴; □, data from this research.

capacities together with some of the low temperature values.⁴ The nearly 0.18% discrepancy in the heat capacities measured by the two instruments at the point of overlap has a negligible effect on the thermodynamic functions. These data are considered to be characterized by a probable error of 0.1%. A further test of the measurement and computation procedure is afforded by the enthalpy-type run B indicated in Table II and its comparison with the enthalpy of the regular runs and the integral of the smoothed heat capacity

curve. Smoothed heat capacities from a least-squares-fit curve through the experimental data are presented at selected temperatures in Table III.

Table I: Heat Capacity of Pentaerythrityl Fluoride. (Units: cal., mole, °K.)

\bar{T}	C_p	\bar{T}	C_p	\bar{T}	C_p
Series I		Series III		373.39	60.99
301.31	50.67	362.88	56.64	377.85	61.15
309.07	51.37	363.75	62.83	381.04	61.36
319.34	52.12	364.35	73.13	Series VII	
329.28	52.91	Series IV		300.98	50.71
339.28	53.70	Fusion Run D		308.62	51.27
349.19	54.63	Fusion Run E		317.15	51.90
Fusion Runs A		Series V		326.40	52.65
371.04	60.80	Fusion Runs E		335.74	53.44
374.97	61.09	Series VI		345.08	54.30
Series II		Series VI		354.38	55.15
Enthalpy Run B		Series VI		360.82	56.05
Fusion Runs C		Series VIII		Fusion Run F	
371.13	60.74	369.18	59.83		
374.93	61.07	369.99	60.30		
		Fusion runs			
\bar{T}	ΔT	C_p^a	\bar{T}	ΔT	C_p
Runs A		Runs E			
359.43	10.293	(56.17)	367.02	0.030	1450
365.39	1.682	(165.1)	367.04	0.023	1900
366.46	0.523	576	367.05	0.024	1790
366.80	0.213	1440	367.07	0.026	1690
366.99	0.164	1970	367.09	0.026	1660
368.08	1.954	(139.4)			
Runs C					

(Cf. Table IV)

^a Values in parentheses involve finite temperature increments in regions of high curvature.

Melting. The triple point of this sample occurs at 367.06°K. with an enthalpy increment of 1230 cal./mole and a corresponding entropy of melting of 3.35 cal./(mole °K.). Molal heat capacities as high as 1900 cal./(mole °K.) were observed and thermal equilibrium was attained typically only after a 3.5-hr. period in this region. It was consequently desirable to obtain several enthalpy increment runs through the entire melting regions. Such runs (D and F) are compared with the sum of the enthalpy increments of the series of heat capacity runs through the transition region as shown in Table II.

Table II: Enthalpy and Entropy Increments of Pentaerythrityl Fluoride. (Units: cal., mole, °K.)

Designation	Number of runs	T_{final}	T_{initial}	$H^{\circ}_{275} - H^{\circ}_{265}$	$S^{\circ}_{275} - S^{\circ}_{265}$
Fusion					
Series I(A)	8	376.89	354.28	2387.7	6.518
Runs C	9	376.82	364.25	(2367.1) ^a	(6.462) ^a
Run D	1	369.17	362.68	2381.7	6.502
Run F	1	374.80	353.21	2385.2	6.511
Average:				2384.9	6.510
Crystal I					
$H^{\circ}_{300} - H^{\circ}_{280}$					
Series I	3	364.57	334.46	1629.0	
Series VI	4	362.64	331.07	1629.2	
Runs B	1	364.26	328.38	1629.2	
Average:				1629.1	
Numerical quadrature of smoothed curve: 1629.0					

^a Rejected from average by Chauvenet's criterion.

Table III: Thermodynamic Functions of Pentaerythrityl Fluoride. ($C_5H_8F_4$; 1 mole = 144.119 g. Units: cal., mole, °K.)

T	C_p	S°	$H^{\circ} - H^{\circ}_0$	$-(G^{\circ} - H^{\circ}_0)/T$
Crystal I				
298.15 ^a	50.71	69.31	11333	31.30
300	50.82	69.63	11427	31.53
310	51.47	71.30	11939	32.79
320	52.15	72.95	12457	34.02
330	52.91	74.56	12982	35.22
340	53.76	76.16	13515	36.40
350	54.76	77.73	14058	37.56
360	55.94	79.27	14611	38.69
367.06	(56.84)	80.45	15030	39.50
Liquid				
367.06	(60.61)	83.80	16259	39.50
370	60.69	84.21	16413	39.81
380	61.31	85.83	17024	41.03

^a From Westrum and Payne.⁴

Fractional melting data from Table IV for this sample of pentaerythrityl fluoride show that the reciprocal fraction melted ($1/F$) is not a linear function of temperature and suggests that the impurity forms a solid solution with the sample. By applying the method of Mastrangelo and Dornte⁹ to correct for the presence of solid solution, the sample was found to contain 0.0018 mole fraction of impurity. Furthermore, the triple point of this sample is 367.06°K. and that of the pure substance extrapolated is 367.43°K.

Table IV: Fractional Melting of Pentaerythrityl Fluoride. (Units: cal., mole, °K.)

\bar{T}	ΔT	C_p	ΔH_{excess}	$1/F$	T_{final}
Fusion Runs C					
364.54	0.588	74.21	21.53	56.062	364.834
364.93	0.248	92.06	32.69	36.920	365.052
365.52	0.985	176.5	153.11	7.884	366.012
366.32	0.620	477.9	411.71	2.932	366.612
366.76	0.259	1170	699.42	1.726	366.888
368.06	2.339	257.4	1227.05		369.226
Triple point; this sample				(1.000)	367.06
Triple point; pure compound				(0.000)	367.43

Thermodynamic Properties. The thermodynamic properties calculated by quadrature of the experimental heat capacity data on a digital computer are also provided at selected temperatures in Table III. Nuclear spin and isotopic mixing contributions have not been included in the entropy or in the free energy function. The tabulated functions are based on the low temperature values for the enthalpy and entropy obtained by Westrum and Payne⁴ below 300°K.

Discussion

Upon taking into account only the changes in the symmetry features on traversing the solid II \rightarrow I transition in pentaerythrityl fluoride, Westrum and Payne⁴ could account for the magnitude and mechanism of the transition. This mechanism then was applied to the solid phase anomaly in pentaerythritol, $C(CH_2OH)_4$, studied by Nitta, *et al.*,¹⁰ and found to predict exactly the experimental results after correction terms were added for the additional symmetry modes available to the hydrogen atoms.

Having experimentally determined the fusion properties of pentaerythrityl fluoride, a further check is now possible on the effects of the hydrogen atoms in pentaerythritol. Because of the proximity in size of oxygen and fluorine atoms, the basic lattice heat capacity should be the same in both cases with differences in entropies due only to symmetry factors. Westrum and Payne⁴ showed that this difference in configurational entropy would be $R \ln 2 + 4R \ln 3 = 10.11$ cal./mole °K.). The entropies of transition and fusion in pentaerythritol are, respectively, 22.8 and 3.2 cal./mole °K.), while the corresponding increments are

(9) S. V. R. Mastrangelo and R. W. Dornte, *J. Am. Chem. Soc.*, **77**, 6200 (1955).

(10) I. Nitta, T. Watanabe, S. Seki, and M. Momotani, *Proc. Japan Acad.*, **26**, 1019 (1950).

12.66 and 3.35 cal./ (mole °K.), respectively, for pentaerythryl fluoride. A sum of the two transitions in each of these substances gives the disorder present above their common lattice energy. Subtracting this sum for the fluoride from that of the alcohol gives $26.0 - 16.0 = 10.0$ cal./ (mole °K.). This is well within experimental error of the 10.1 cal./ (mole °K.) calcu-

lated by Westrum and Payne and, as such, is further evidence for the proper choice of mechanism for the observed transitions.

Acknowledgment. This work was performed under the auspices of the United States Atomic Energy Commission. The authors are indebted to Dr. Elfreda Chang for assistance in the evaluation of the data.

Job's Method of Continuous Variations with Ion Exchange for the Study of Complexes in Solution

by Stanley Bukata^{1,2} and Jacob A. Marinsky³

Department of Chemistry, State University of New York at Buffalo, Buffalo, New York (Received June 18, 1963)

The use of ion-exchange properties for determining the nature of complex species in solution by Job's continuous variations method has been developed. The Cu^{+2} -EDTA, Ca^{+2} -EDTA, and Ca^{+2} -citrate systems were studied to demonstrate the method. The results obtained were in agreement with the results of earlier investigations of these systems.

Introduction

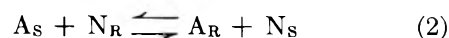
Job's method of continuous variations⁴ of isomolar solutions has been used frequently for the study of complexes in solution. Solution properties, which are linear functions of the concentrations of the species involved, are analyzed in applying the method. Some properties which have been employed are refractive index,⁵ heat of mixing,⁶ density,⁷ dielectric constant,⁸ and light absorption.^{9,10} A solution property adaptable to Job's method and not previously discussed in the literature is ion exchange. The discussion below is given for cation exchange but would be similar for anion exchange.

Let mixtures be made by the addition of x ml. of B to $(V_T - x)$ ml. of A when both solutions are at a concentration of M moles/l. The symbol V_T corresponds to the total volume of the mixtures which is presumed to be essentially constant in the absence of appreciable volume change on mixing. Allow these isomolar solutions to undergo cation exchange with a suitable

resin. Assume that A and B react to form a single complex according to



Further, assume A undergoes cation exchange according to the equation



- (1) Union Carbide Predoctoral Fellow, 1961-1962.
- (2) This paper is based on a portion of a dissertation submitted by S. Bukata in partial fulfillment of the requirements for the degree of Doctor of Philosophy.
- (3) Correspondence to be addressed to this author.
- (4) P. Job, *Ann. Chem.*, **9**, 113 (1928).
- (5) G. Spacu and E. Popper, *Bul. soc. stiinta Cluj.*, **7**, 400 (1934).
- (6) M. M. Chauvenet, P. Job, and G. Urbain, *Compt. rend.*, **171**, 855 (1920).
- (7) Y. Wormser, *Bull. soc. chim. France*, **15**, 395 (1948).
- (8) N. Q. Trinh, *Compt. rend.*, **226**, 403 (1948).
- (9) W. C. Vosburgh and G. R. Cooper, *J. Am. Chem. Soc.*, **63**, 437 (1941).
- (10) R. K. Gould and W. C. Vosburgh, *ibid.*, **64**, 1630 (1942).

where the subscripts S and R refer to the solution and resin phase, respectively. The cation N must not form a complex with B and B and AB_n are expected to be excluded from the resin, being anionic or neutral entities. In the presence of excess N, the ion exchange may often be represented by a linear equation

$$A_R = k_D A_S \quad (3)$$

where A_R is the concentration of A in the resin phase at equilibrium and A_S is the concentration of A in the solution phase. At equilibrium, eq. 1, 2, and 3 must be satisfied simultaneously. Let

$$C_1 = (A_S) \quad (4)$$

$$C_2 = (B) \quad (5)$$

$$C_3 = (AB_n) \quad (6)$$

where the parentheses signify millimolar concentration. Then for any mixture

$$C_1 = M(V_T - x) - C_3 - k_D C_1 \quad (7)$$

$$C_2 = Mx - nC_3 \quad (8)$$

$$C_1 C_2^n = K C_3 \quad (9)$$

where K is the equilibrium constant for reaction 1. The condition for a maximum or a minimum in the curve of C_3 plotted against x is

$$\frac{dC_3}{dx} = 0 \quad (10)$$

Differentiating eq. 7, 8, and 9 with respect to x

$$(1 + k_D) \frac{dC_1}{dx} = -M - \frac{dC_3}{dx} \quad (11)$$

$$\frac{dC_2}{dx} = M - n \frac{dC_3}{dx} \quad (12)$$

$$C_1(nC_2^{n-1}) \frac{dC_2}{dx} + C_2^n \frac{dC_1}{dx} = K \frac{dC_3}{dx} \quad (13)$$

At $dC_3/dx = 0$, the position of the maximum or minimum

$$(1 + k_D) \frac{dC_1}{dx} = -M V_T \quad (14)$$

and

$$\frac{dC_2}{dx} = M \quad (15)$$

substituting these values into (13)

$$(1 + k_D) C_1 n = C_2 \quad (16)$$

and using eq. 7, 8, and 9

$$n = \frac{x}{V_T - x} \quad (17)$$

Thus, where C_3 is a maximum or a minimum, n can be determined by use of eq. 17.

In general, C_3 is not measured directly; instead use is made of the ion-exchange property of the solution to evaluate C_3 .

Letting Y equal the difference between the observed removal from solution of A by exchange with N and by complexing with B $\{M(V_T - x) - k_D C_1 - C_3\}$ and the calculated removal of A without complex formation $\{m(V_T - x) - k_D C_1\}$ then

$$Y = \frac{C_3}{1 + k_D} \quad (18)$$

in a concentration region in which eq. 3 holds. Differentiating eq. 18 with respect to x

$$\frac{dY}{dx} = \frac{1}{1 + k_D} \frac{dC_3}{dx} \quad (19)$$

where $dC_3/dx = 0$, $dY/dx = 0$, a plot of Y vs. x will have a maximum or a minimum with C_3 and eq. 17 continues to be valid.

Experimental

Several aqueous systems in which the complex species were already well defined were studied to test the above treatment. Dowex-50-4x in the sodium form was used throughout. The concentration regions studied were where the ion exchange was governed by a linear rela-

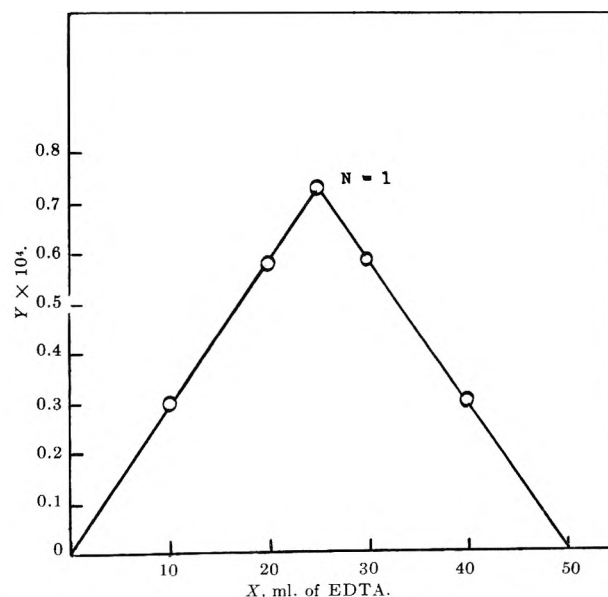


Figure 1. Cu^{+2} -EDTA system, Job's plot.

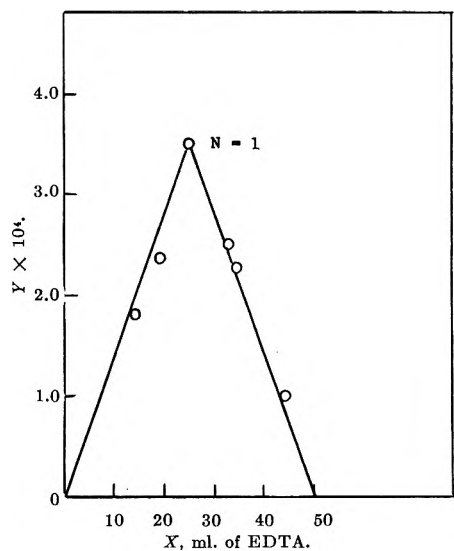


Figure 2. Ca^{+2} -EDTA system, Job's plot.

tion. Constant ionic strength was maintained in the solutions. The total volume of solutions used was 50 ml.

Results

Job's plot for the Cu^{+2} -EDTA system is given in Fig. 1. Cupric nitrate (0.01 M) and the disodium salt of ethylenediaminetetraacetic acid ($\text{Na}_2\text{H}_2\text{EDTA}$) (0.01 M) were used. An ionic strength of 0.52 was maintained by means of sodium nitrate. The maximum occurs at $x = 25$ corresponding to $n = 1$ in agreement with the literature.

Figure 2 is Job's plot for the Ca^{+2} -EDTA system at an ionic strength of 0.62; $n = 1$ in agreement with the literature.

Job's plot for the Ca^{+2} -citrate system at a pH of 6.6 to 7.2 is given in Fig. 3. Sodium citrate solutions were used as the source of ligand. A maximum occurs where $n = 1$ but as x increases, the curve does not drop as

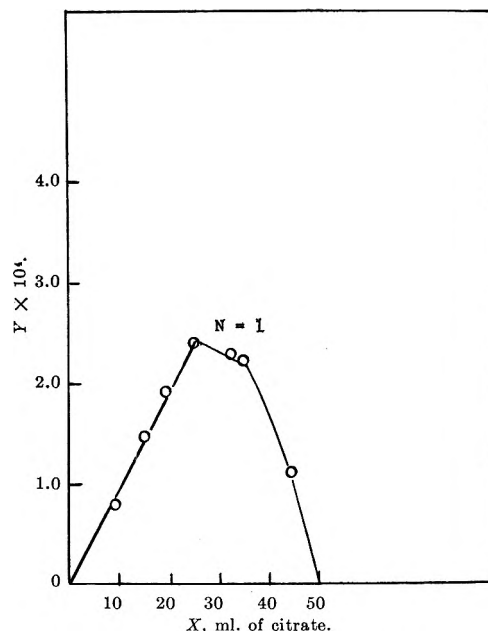


Figure 3. Ca^{+2} -citrate system, Job's plot.

sharply as would be expected for the existence of just one complex species. We attribute this behavior to the presence of more than one complex. The existence of two calcium-citrate complexes has been noted in the literature.¹¹

The results obtained are in agreement with the literature. The treatment given is limited to systems where only one predominant complex is formed. The method should be useful for those systems where other functions of the concentration are not linear or involve large experimental difficulties or costly equipment.

Acknowledgment. Financial support through Contract No. AT(30-1)-2269 with the U. S. Atomic Energy Commission is gratefully acknowledged.

(11) J. Schubert and J. W. Richter, *J. Phys. Colloid Chem.*, **52**, 350 (1948).

Metastable Ions in Mass Spectrometry¹

by G. A. Muccini,² W. H. Hamill, and R. Barker

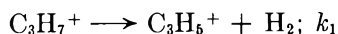
*Department of Chemistry and Radiation Laboratory, University of Notre Dame, Notre Dame, Indiana
(Received June 21, 1963)*

The first-order decay constant k_1 has been measured for the metastable transition, $C_3H_7^+ \rightarrow C_3H_6^+ + H_2$. For the series from propane to *n*-decane, k_1 varies from $0.46 \pm 0.24 \times 10^6$ sec.⁻¹ for *n*-pentane to $0.72 \pm 0.23 \times 10^6$ sec.⁻¹ for *n*-heptane. No trend is apparent. The variation of k_1 with the energy of the ionizing electrons, using *n*-hexane, increases with decreasing ionizing voltage. The pressure dependence of the diffuse peak at mass number 39.1 shows that the metastable transition is not a collision-induced dissociation.

Introduction

The ions formed by electron impact in a mass spectrometer can be classified as: stable, with insufficient excitation energy to decompose before collection; unstable, with enough energy to decompose before leaving the ionization chamber; and metastable, with intermediate energy which decomposes in transit. Those which decompose after acceleration but prior to magnetic deflection are usually focused at a peak of non-integral mass. The relationship between the apparent mass of a metastable ion, m^* , the mass of the parent ion before dissociation, m_0 , and the mass of the fragment ion, m , is given by $m^* = m^2/m_0$. In this work $m^* = 39.1$.

The metastable decomposition



is characteristic of the 43-ion from many hydrocarbons.³ It is to be expected that k_1 , determined by the method of Hipple,⁴ will depend upon the internal energy metastable ion.⁵ The present report considers k_1 for the *n*-alkanes, propane to decane inclusive, using 70-v. electrons, and also various electron energies for *n*-hexane.

Experimental

Propane and heptane were Phillips research grade of 99% purity. Other alkanes were Matheson research grade. All hydrocarbons were used as received, after degassing several times to remove air.

A CEC Model 21-103A mass spectrometer was modified for electromagnetic scanning and for measurements at ionizing voltage from 5 to 100 v. In addition, the two

repeller plates were connected together and powered by a battery. The range 0.25–10 v. was used.

The sample was introduced in the inlet system of the mass spectrometer in the usual way and the pressure measured by the micromanometer. The ion-accelerating voltage was maintained at 2260 v., and the ionizing voltage at 70 v. except for *n*-hexane. Electromagnetic scanning was employed and only the ions with mass numbers from 36 to 44, the region of interest in this study, were recorded. Two runs were made at each repeller setting.

In experiments with *n*-hexane this procedure was repeated for each setting of the ionizing voltage, all other instrumental parameters being constant. The electron energy scale was calibrated against the ionization potential of argon and corrected for varying repeller voltage from the parameters of the ion source which are given below.

Treatment of Results. The time, t_2 , at which metastable ions reach the analyzer region has been given by Hipple⁴ as

$$t_2 \text{ (sec.)} = t_x + t_1 = \frac{v_2 - v_1}{a_2} + t_1 \quad (1)$$

- (1) The work was supported in part by the Radiation Laboratory of the University of Notre Dame, operated under contract with the U. S. Atomic Energy Commission.
- (2) From the M.S. dissertation of G. A. Muccini.
- (3) E. G. Bloom, F. L. Mohler, J. H. Lengel, and E. C. Wise, *J. Res. Natl. Bur. Std.*, **40**, 437 (1948).
- (4) J. A. Hipple, *Phys. Rev.*, **71**, 594 (1947).
- (5) L. S. Kassel, *J. Phys. Chem.*, **32**, 225 (1928); "Kinetics of Homogeneous Gas Reactions," Reinhold Publishing Corp., New York, N. Y., 1932, Chapter 5.

where the quantities involved are

$$v_2 \text{ (cm./sec.)} = (2a_2l_2 + 2a_1s_1)^{1/2} \quad (2)$$

$$v_1 \text{ (cm./sec.)} = (2a_1s_1)^{1/2} = \frac{2s_1}{t_1} \quad (3)$$

$$a_1 \text{ (cm./sec.}^2) = \frac{eE_1}{300m_0}; \quad a_2 \text{ (cm./sec.}^2) = \frac{eE_2}{300m_0} \quad (4)$$

m_0 is the mass of metastable ions $C_3H_7^+$ and a_1 and a_2 are accelerations imparted to the ions of mass m_0 by the repeller and accelerating fields, respectively. As shown in Fig. 1, E_1 and E_2 (v./cm.) are the fields due to the repeller voltage and the ion-accelerating voltage, respectively. Also, $s_1 = 0.135 \pm 0.002$ cm. is the distance between the center of the electron beam and the first accelerating slit, $l_1 = 0.260 \pm 0.005$ cm. is the repeller plate to exit slit separation, while $l_2 = 0.68 \pm 0.01$ cm. is the distance between the first and second accelerating slits. The single variable in these equations is the repeller field E_1 ; therefore, the variation in t_2 is a function of E_1 only. For these experiments $t_1 = 3.5 \times 10^{-6} E^{-1/2}$ and t_2 is only slightly greater, ranging from 3.7 to 0.7×10^{-6} sec. Let ϵ

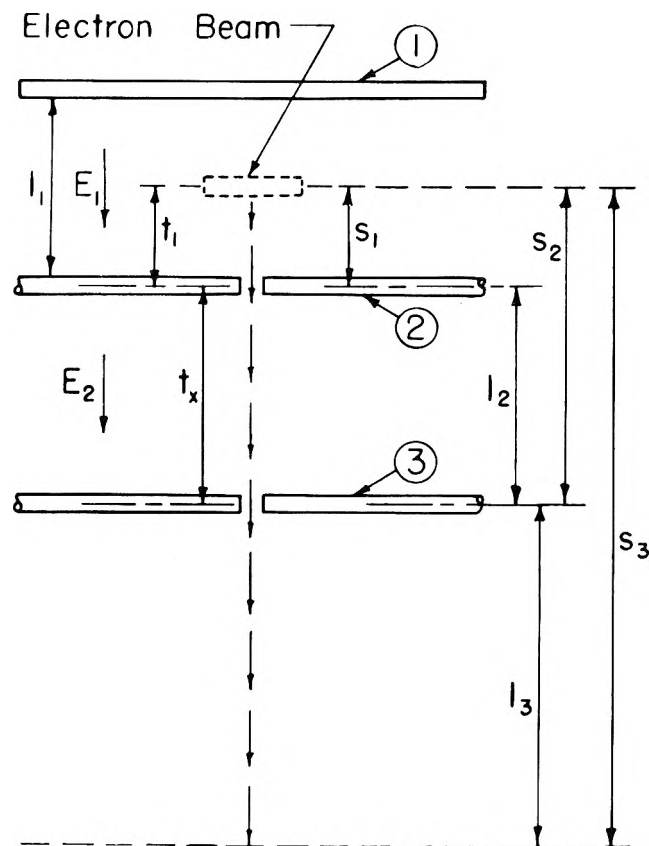


Figure 1. Schematic diagram of ion source to relate the time of dissociation in terms of the geometry and accelerating fields.

represent a particular value of E_1 , then $t_2(\epsilon)$ is the time of flight at repeller field ϵ .

The rate equation for a metastable decomposition, which takes into account peak height normalization, is given by

$$2.302 \log \frac{n'(\epsilon)}{\alpha'(\epsilon)} = k[t_2(\epsilon) - t_2(\epsilon_0)] \quad (5)$$

where $n'(\epsilon)$ is the number of ions in the metastable state which decompose just beyond the last accelerating slit and contribute to the measured 39.1-ion current normalized to the number at $\epsilon = 1$ v. cm.⁻¹, $\alpha'(\epsilon)$ is the correction for repeller field dependent collection efficiency, and $t_2(\epsilon_0)$ is constant with respect to variation in ϵ .⁶ If we plot $\log n'(\epsilon)/\alpha'(\epsilon)$ vs. $t_2(\epsilon)$, we should obtain a straight line from which k can be calculated. For the particular metastable decomposition reported here

$$n'(\epsilon) = \frac{39.1 \text{ peak height at } \epsilon}{39.1 \text{ peak height at } \epsilon_0} \quad (6)$$

and

$$\alpha'(\epsilon) = \frac{43 \text{ peak height at } \epsilon}{43 \text{ peak height at } \epsilon_0} \quad (7)$$

The experimental results for the determination of the rate constant of the $C_3H_7^+$ metastable ion dissociation in each of the hydrocarbons studied appear as plots of the logarithm of the normalized metastable peak height vs. t_2 in Fig. 2. The rate constants k , determined by eq. 5, are shown in Table I, together with the estimated error associated with each value.

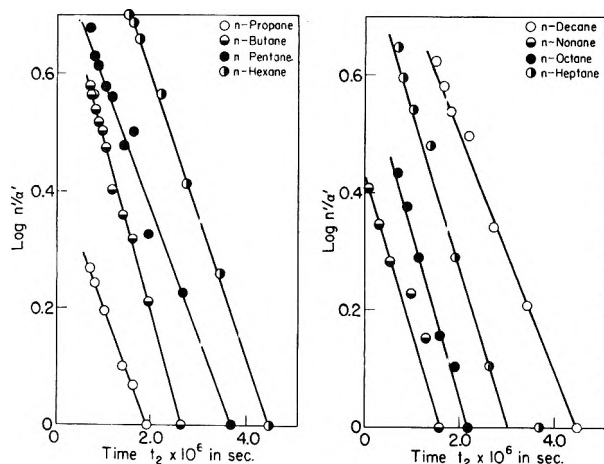


Figure 2. $\log n'/\alpha'$ vs. t_2 for n -hydrocarbons C_3 to C_{10} : abscissa for n -hexane = graph value - 0.8; abscissa for n -nonane = graph value + 0.6; abscissa for n -decane = graph value = 0.8.

(6) For details of the calculation, cf. ref. 4.

Table I: Decay Constant k of the $C_3H_7^+$ Metastable Ion for Each Hydrocarbon Studied

<i>n</i> -Hydrocarbon	Decay constant, $k \times 10^{-6}, \text{sec.}^{-1}$
Propane	0.53 ± 0.1
Butane	0.69 ± 0.1
Pentane	0.46 ± 0.1
Hexane	0.55 ± 0.1
Heptane	0.72 ± 0.1
Octane	0.63 ± 0.1
Nonane	0.67 ± 0.1
Decane	0.51 ± 0.1

Table II: Decay Constant for $C_3H_7^+ \rightarrow C_3H_5^+ + H_2$ Metastable Decomposition from *n*-Hexane at Various Ionizing Voltages

Ionizing voltage	Decay constant, $\text{sec.}^{-1} \times 10^6$
12.5	3.11
15.0	2.49
20.0	0.94
30.0	0.74
50.0	0.71
70.0	0.55
90.0	0.71

Redetermination of the measurement of *n*-butane at accelerating voltages of 2260 and 756 v. subsequently gave⁷ $k_1 = 0.9 \pm 0.2$ and $0.6 \pm 0.2 \times 10^6 \text{sec.}^{-1}$. For *n*-pentane, also at 2260 and 756 v., $k_1 = 0.7 \pm 0.2$ and $0.5 \pm 0.2 \times 10^6 \text{sec.}^{-1}$.

Experimental values of the logarithm of the normalized metastable peak height for *n*-hexane at different ionizing voltages are plotted vs. t_2 in Fig. 3. The corresponding rate constants appear in Table II. It is evident that the rate constant k_1 increases with decreasing ionizing voltage for *n*-hexane. To verify this result, the rate constant for *n*-propane at 30 v. ionizing voltage was measured and found to be $0.81 \times 10^6 \text{sec.}^{-1}$ as compared to a value of $0.53 \times 10^6 \text{sec.}^{-1}$ at 70 v.

The possibility that the increase in the rate constant with decreasing ionizing voltage could be attributed to space-charge effects arising from the electron beam was examined by observing deuteriomethane at different ionizing voltages using 7 v. repeller voltage and an

inlet sample pressure of 267 μ . The cross section of the reaction $CD_4^+ + CD_4 \rightarrow CD_5^+ + CD_3$ is sensitive to change in the velocity of CD_4^+ and therefore to space charge.⁸ At ten ionizing voltages from 12 to 90 v., the $CD_5^+ - CD_4^+$ ratio was 1.7×10^{-3} with an average deviation $\pm 0.05 \times 10^{-3}$. This indicates that appreciable space-charge effects do not occur under our experimental conditions.

The possibility that collision processes could contribute to the peak at $m/e = 39.1$ was tested by measuring the height of the peak at different inlet pressures of xenon or methanol, all other parameters being unchanged. The inlet pressure of *n*-hexane, which was used in these experiments, was kept constant at 26.1 μ , without change in 39.1 peak height.

Discussion

An evident limitation of this work arises because conventional instrumentation constrains the range of measurement of k to the neighborhood of 10^6sec.^{-1} and therefore the measured values of k_1 for metastable ion decompositions necessarily lie within a narrow range, regardless of the original molecule. Since Fig. 3 indicates the possibility of measuring at least a 5-fold range of k_1 , we consider the constancy of k_1 values in Table I to be significant.

Another difficulty with the interpretation of k_1 values in this work is that decompositions following electron impact in a mass spectrometer occur in a collision-free environment and may not be rate-determined, and that the rate may not be a smooth function of the energy. Such a proposal by Steiner, *et al.*,⁹ has not been elaborated or substantiated and our own measurements do not cover a sufficient range in time to provide a

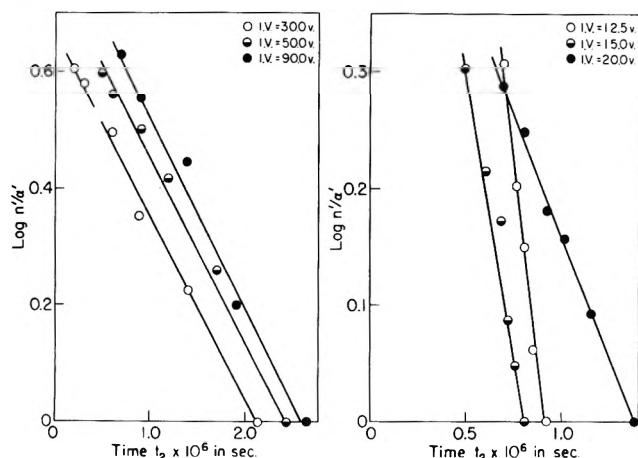


Figure 3. $\text{Log } n'/\alpha'$ vs. t_2 for *n*-hexane at different ionizing voltages: abscissa for I.V. 30 v. = graph value + 0.5; abscissa for I.V. 50 v. = graph value + 0.2; abscissa for I.V. 15 v. = graph value + 0.2.

- (7) These measurements were made with a CEC 21-103C mass spectrometer at the Mellon Institute.
- (8) D. A. Kubose and W. H. Hamill, *J. Am. Chem. Soc.*, **85**, 125 (1963).
- (9) B. Steiner, C. F. Piese, and M. G. Ingraham, *J. Chem. Phys.*, **34**, 189 (1961).

convincing empirical validation of first-order decay. Their description¹⁰ of the dissociative process does not account for the constancy of our parameter k_1 . For want of a better description of the time-dependent process or of contrary evidence, we persist in terms of the first-order process.

Both the invariance of k_1 with carbon number and dependence upon electron energy which were observed in this work are inconsistent with the assumption of rapid relaxation of electronic to vibrational energy.¹¹ Let us assume for the moment that constant k_1 corresponds to constant vibrational energy of the 43*-ion and that randomization of energy precedes formation of the 43*-ion. Since the activation energy difference for producing metastable 43*-ions and stable 41-ions from ground state 43-ions in butane is *ca.* 2 e.v.,¹² it would be expected that more than 4 e.v. of excess energy would be required for the 43*-ion from octane. This is not the case. On the other hand, if 43*-ions form promptly, the activation energy must be accounted for by electronic excitation.

Using the RPD method, it has been found recently that there are discontinuities in the 43-ion abundance curves among others at 2.6 (*n*-octane), 2.0 (*n*-butane), 2.3 (*n*-propyl alcohol), 2.3 (*n*-propyl chloride), 2.4 (*n*-propyl bromide), and 2.3 e.v. (*n*-propyl iodide¹³) above threshold. There is other evidence that appearance potentials by the RPD method reliably measure excited states of fragment ions.¹³ Coggeshall¹⁴ has shown that other metastable decompositions (*e.g.*, $m^* = 31.9$ from butane) involve ions of two or three classes, based upon structure in the rate curves.

We explain the substantial constancy of k_1 for various alkanes in terms of a common (or predominant) electronic state of the 43*-ion from the various *n*-alkanes. Also, the fairly coarse structure of the ion abundance curves provides a partial explanation of the remarkable constancy in the relative peak heights at 43, 41, and 39.1 mass units for many hydrocarbons for each of which the energy distribution from various sources would have to be the same.¹⁵ Since the combined 43- and 41-ion abundances approximate one-third of all ions for these hydrocarbons, the effects being considered are not minor.

The larger k_1 at low electron energy could arise from another metastable electronic state of 43⁺ which could very well decay at a faster rate than the higher state. Measurements reported here do not demonstrate abrupt differences in k_1 , but such discontinuities have since been found,¹⁴ although it has not yet been shown whether vibrational or electronic excitation is responsible.

-
- (10) "The particular dissociation which occurs is determined by whichever reaction coordinate happens to reach a critical extension first." Reference 9, p. 219.
- (11) H. M. Rosenstock, M. B. Wallenstein, A. L. Wahrhaftig, and H. Eyring, *Proc. Natl. Acad. Sci. U. S.*, **38**, 667 (1952).
- (12) R. E. Fox and A. Langer, *J. Chem. Phys.*, **18**, 460 (1950).
- (13) Unpublished measurements by S. Tsuda, C. E. Melton, and G. F. Hennion, Jr.
- (14) N. D. Coggeshall, *J. Chem. Phys.*, **37**, 2167 (1962).
- (15) In the A.P.I. Project Catalog of Mass Spectral Data, the 39.1/43 peak height ratios at normal electron energies are constant within 15%, which indicates that the ratio of metastable to stable 43*-ions is nearly constant for the C₃ to C₁₂ *n*-alkanes.

An Extension of the Conjugation Theory of Electron-Transfer Reactions¹

by P. V. Manning, R. C. Jarnagin, and M. Silver

*Departments of Chemistry and Physics, University of North Carolina, Chapel Hill, North Carolina
(Received July 22, 1963)*

The conjugation theory of electron-transfer reactions formulated by Halpern and Orgel has been extended for effects other than variations in the mobile bond order of the bridging ligand. Electrostatic effects on the rate of formation and mean lifetime of the activated complex are included. The results are applied to the oxidation of aqueous Cr^{2+} by $(\text{NH}_3)_6\text{CoL}^{2+}$ in which L represents a series of nonhalogenated carboxylic acids and diacids. If those ligands with possible ring-stabilized transition states and those with steric barriers to conjugative planarity are excluded, then the treatment allows proper ranking of ligands according to their efficiency as mediators in charge-transfer reactions.

Introduction

The electron-transfer reaction between aqueous Cr^{2+} and pentaamminecobalt(III) with various bridging ligands occupying the sixth octahedral site of the cobalt has been studied by a number of workers. Taube, *et al.*,² have demonstrated that the oxidation-reduction reaction occurs more rapidly for certain conjugated diacid ligands than for the corresponding nonconjugated ligands. This and other evidence led Taube to propose a conjugation mechanism for these reactions.³

Steps toward putting the conjugation mechanism of electron transfer into quantitative form were taken by Halpern and Orgel.⁴ They showed that for a given pair of metal centers, the probability for electron transfer will depend upon the mobile bond order (m.b.o.) of the ligand bridging the metal centers in the activated complex. The m.b.o. for a system in which the metal centers are attached to atoms r and s of the ligand in the activated complex is defined as

$$p_{rs} = \sum_i N_i C_{ir} C_{is}$$

in which N_i is the number of electrons in the i th molecular orbital, and C_{ir} and C_{is} are the coefficients of the r th and s th atoms in the LCAO approximation to the molecular orbital of the ligand. Fraser⁵ measured rate constants for the aqueous $\text{Cr}^{2+} + (\text{NH}_3)_6\text{CoL}^{2+}$ reaction with a series of conjugated diacids as bridging ligands. He found no correlation in observed rate constants with the m.b.o. of the ligands.

In the present work the conjugation theory of Halpern and Orgel is taken as a starting point, and an attempt is made to extend the theory. Electrostatic effects on the rate of formation and mean lifetime of the activated complex are considered and a ranking of predicted rates is compared to experimental results.

The manner of inclusion of electrostatic effects in the derived rate constant relations assumes ionic behavior describable by the usual ionic strength and dielectric treatments and requires use of the charge product of the reactants forming the expected transition state, $(\text{H}_3\text{N})_6\text{CoL}^{2+} \cdots \text{Cr}^{2+}$. There was doubt concerning the $4+$ character of the transition state due to recent experimental evidence of possible perchlorate ion association with aqueous Cr^{2+} ,⁶ and no direct experimental demonstration of conventional electrostatic behavior existed. Therefore, to remove doubt concerning the charge product of the reactants and to demonstrate the applicability of an electrostatic approach, the rate constants for the reaction were determined as a function of ionic strength employing acetate and fumarate as bridging ligands.

- (1) Partially supported by the Army Research Office (Durham).
- (2) See, for instance: H. Taube, *Advan. Inorg. Chem. Radiochem.*, **1**, 1 (1959).
- (3) R. T. M. Fraser, D. K. Sebera, and H. Taube, *J. Am. Chem. Soc.*, **81**, 2906 (1959).
- (4) J. Halpern and L. E. Orgel, *Discussions Faraday Soc.*, **29**, 32 (1960).
- (5) R. T. M. Fraser, *J. Am. Chem. Soc.*, **83**, 4920 (1961).
- (6) J. A. Jackson, J. F. Lemons, and H. Taube, *J. Chem. Phys.*, **38**, 836 (1963).

Experimental

The ionic strength dependence was determined by varying the NaClO_4 concentration in the reaction mixture. Preparation of reactants, kinetic measurements, and calculations were carried out by standard methods.⁷ A Cary Model 14 spectrophotometer with temperature-controlled cell was used for spectral measurements. The rate dependence upon ionic strength for both reactions obeyed an equation due to Davies⁸ for ionic reactions in aqueous solution at 25°.

$$\log k_{bi} = \log k_0 + Z_A Z_B \left(\frac{I^{1/2}}{1 + I^{1/2}} - 0.20I \right)$$

Plots of $\log k_{bi}$ vs. $f(I)$ are shown in Fig. 1 and 2. The straight lines and parameter values of the figures result from a standard curve fitting of the experimental data. Since the fumarate reaction is pH dependent with a rate constant of the form

$$k_{bi} = k_1 + k_2[\text{H}^+] + k_3[\text{H}^+]^{-1}$$

the kinetics were measured at pH 1.73, chosen to minimize $k_2[\text{H}^+] + k_3[\text{H}^+]^{-1}$ with respect to k_1 . At this pH approximately 85% of the reaction occurs by the acid independent paths with net specific rate k_1 and consisting of contributions from both adjacent and remote attack.

Attempts were also made to show the anticipated linear dependence of $\ln k_{bi}$ on the inverse dielectric constant, $1/D$. However, addition of either alcohol or dioxane to dilute solutions of the Co(III) or Cr(II) resulted in nonstoichiometric behavior and irreproducible rate constants.

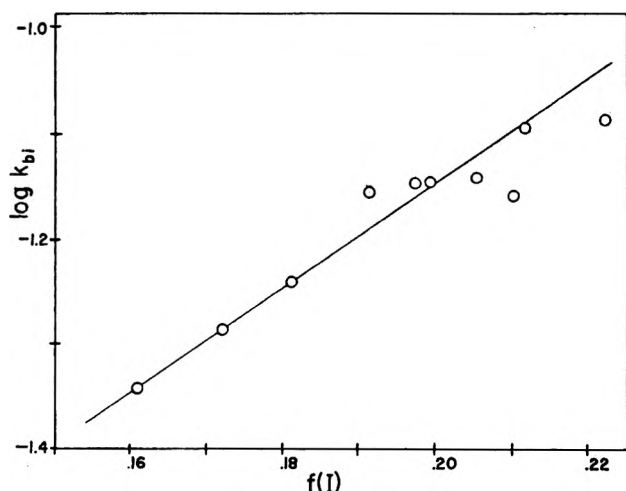


Figure 1. Ionic strength dependence for rate of aqueous $\text{Cr}^{2+} + (\text{NH}_3)_5\text{CoC}_2\text{H}_3\text{O}_2^{2+}$ in NaClO_4 : $Z_A Z_B = 5.1$; $\log k_0 = -2.15$; $T = 25^\circ$.

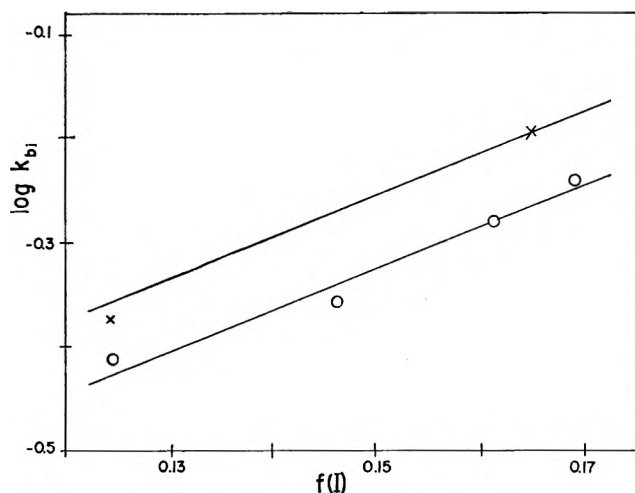


Figure 2. Ionic strength dependence for rate of aqueous $\text{Cr}^{2+} + (\text{NH}_3)_5\text{Co-trans-C}_4\text{H}_3\text{O}_4$ in NaClO_4 : \circ , $Z_A Z_B = 4.1$; $\log k_0 = -0.95$; $T = 20^\circ$; \times , $Z_A Z_B = 4.1$; $\log k_0 = -0.85$; $T = 25^\circ$.

Extension of the Conjugation Theory. The basic assumption of the conjugation theory is that the probability of electron transfer during the lifetime of the activated complex is small. Thus

$$k_{bi} = k_f P \quad (1)$$

in which k_{bi} is the observable second-order rate constant, k_f the rate constant for the formation of the activated complex, and P the probability for decomposition of the activated complex to form products. For reaction at $I = 0$

$$k_0 = k_{f0} P \quad (2)$$

Halpern and Orgel obtained an expression for P for a symmetric activated complex

$$P \cong (C_1 p_{r0} \tau)^2 \quad (3)$$

in which τ is the mean lifetime of the activated complex, and C_1 is a constant approximately independent of the particular ligand.

If the noncoulombic interaction between the aqueous Cr^{2+} and the ligand carboxyl group is constant for the ligands to be compared, then τ_0 may be defined as the mean lifetime of the activated complex for uncharged reactants. For charged reactants

$$\tau \cong \tau_0 e^{-Z_A Z_B e^2 / DkT r_{AB}} \quad (4)$$

in which r_{AB} is the distance separating the reacting metal centers in the activated complex.

The Bronsted-Christiansen-Scatchard equation is⁹

(7) D. K. Sebera and H. Taube, *J. Am. Chem. Soc.*, **83**, 1785 (1961).

(8) C. W. Davies, *J. Chem. Soc.*, 2093 (1938).

$$\ln k_{f0} = \ln k_{f0} \Big|_{D=\infty} - \frac{Z_A Z_B \epsilon^2}{DkT r_{AB}} \quad (5)$$

This electrostatic result is presumably adequate over certain concentration ranges and is partially justified since the primary salt effect was experimentally shown to follow a straightforward electrostatic model. On combining (2), (3), (4), and (5) one obtains

$$\ln k_0 = C_0 + \ln p_{rs}^2 - \frac{3Z_A Z_B \epsilon^2}{DkT r_{AB}} \quad (6)$$

Define M , related to $\log k_0$ by

$$M \equiv \log p_{rs}^2 - \frac{3Z_A Z_B \epsilon^2}{2.3DkT r_{AB}} \quad (7)$$

For large values of M one expects a fast reaction and *vice versa*; thus M values should allow correlation of zero ionic strength reaction rates taking into account both the conjugative effects of bridging ligands and electrostatic effects on the formation and mean lifetime of the transition state complex.

The m.b.o., p_{rs} , was calculated by an LCAO technique. Variations in the carbon-carbon resonance integrals with bond length were allowed for by a method due to Mulliken.¹⁰ Empirical values for the resonance and coulomb integrals were used to account for heteroatom effects.¹¹ The secular equations were solved by similarity transformation of the secular matrix on the University of North Carolina Univac 1105 computer employing the numerical method of Jacobi.¹² Ligand contributions to r_{AB} were determined from Dreiding models. If several ligand configurations were possible, the one giving the largest value of r_{AB} consistent with steric considerations was used.

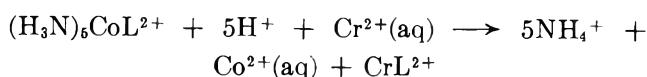
Metal-oxygen bond distances could only be estimated. Data are available for similar Co(II) and (III)-O distances,¹³ but the Cr^{2+} -O distance is not known. The values used, (Cr-O) = 2.4 Å. and (Co-O) = 2.3 Å., are perhaps on the order of 0.1 Å. large for a ground state complex but probably are appropriate for the transition state. It should be noted that a ranking of rate constants by these results is unchanged for $\pm 15\%$ change in the metal oxygen distances.

Results and Discussion

Table I lists most of the experimental rate constants available for which L is a nonhalogenated organic acid. No pH dependence is observed for adjacent attack, but pH dependent terms arise if remote attack occurs. Table I lists only the pH independent contributions to the rate constants. The data of Table I were determined for $I = 1.0$; therefore, quantitative comparison of rate constants to M -

values is not possible. However, an ordering of M -values should show some correlation to an ordering of rate constants if the theory is a sufficient approximation.

Table I: pH Independent Rate Constants for the Reaction



$$I = 1.0$$

L	T, °C.	k_1 , l. mole ⁻¹ sec. ⁻¹	Reference
Naphthyl-1-carboxylato	21	0.07	b
o-Phthalato	25	0.075	e
1-Carboxynaphthyl-4-carboxylato	21	0.08	b
1-Carboxynaphthyl-5-carboxylato	21	0.08	b
2-Carboxynaphthyl-6-carboxylato	21	0.08	b
2-Carboxybiphenyl-2'-carboxylato	21	0.10	b
Naphthyl-2-carboxylato	21	0.11	b
p-Hydroxybenzoato	25	0.13	c
m-Phthalato	25	0.13	a
Benzoato	25	0.14	b
Acetato	25	0.18	a
Fumarato	25	1.32	a
Maleato	25	>30	a
Oxalato	23	>33	d
4-Carboxybiphenyl-4'-carboxylato	21	Fast	b
p-Phthalato	16.6	36	a

^a Reference 7. ^b Reference 5. ^c Reference 14. ^d H. Taube, *J. Am. Chem. Soc.*, **77**, 448 (1955). ^e H. Taube, *Can. J. Chem.*, **37**, 129 (1959).

Since nonelectrostatic effects must remain essentially constant for the reactions to be compared, ligands capable of forming ring stabilized activated complexes should be excluded from consideration.¹⁴ This limitation excluded the oxalato and maleato complexes. In addition to the above restriction, ligands with steric barriers to planarity were excluded.¹⁵ The remaining

- (9) E. S. Amis, "The Kinetics of Chemical Change in Solution," The Macmillan Co., New York, N. Y., 1949, p. 77.
- (10) A. Streitwieser, "Molecular Orbital Theory for Organic Chemists," John Wiley and Sons, New York, N. Y., 1961, pp. 103-105.
- (11) A. Streitwieser, *ibid.*, p. 135.
- (12) "Modern Computing Methods," Second Ed., Philosophical Library, New York, N. Y., 1961, p. 29.
- (13) "Tables of Interatomic Distances and Configuration in Molecules and Ions," L. E. Sutton, Ed., Special Publication No. 11; The Chemical Society, London, 1958.
- (14) Evidence for this type of activated complex for some α -hydroxyacids is given by R. T. M. Fraser in "Advances in the Chemistry of Coordination Compounds," S. Kirschner, Ed., The Macmillan Co., New York, N. Y., 1961, p. 77.
- (15) Molecular models were used to determine such steric barriers.

Table II: Comparison of Ranking According to Experiment and Model

L	k_1^a l. mole ⁻¹ sec. ⁻¹	p_{rs}^2	log p_{rs}^2	$r_{AB}/\text{\AA}$.	$-\frac{1.3Z_A Z_B e^2 d}{DkT r_{AB}}$	M
2-Carboxynaphthyl-6-carboxylato	0.10 ^b	1.58 × 10 ⁻⁴ (remote)	-3.80	14.3 (remote)	-2.54	-6.35
		4.47 × 10 ⁻² (adj.)		5.6 (adj.)		
<i>p</i> -Hydroxybenzoato	0.13	4.28 × 10 ⁻²	-1.37	5.6	-6.50	-7.87
Naphthyl-2-carboxylato	0.13 ^b	4.42 × 10 ⁻²	-1.35	5.6	-6.50	-7.85
<i>m</i> -Phthalato	0.13	4.43 × 10 ⁻² (adj.)	-1.35	5.6 (adj.)	-6.50	-7.85
		2.17 × 10 ⁻⁵ (remote)		10.2 (remote)		
Benzoato	0.14	4.37 × 10 ⁻²	-1.36	5.6	-6.50	-7.86
Acetato	0.18	5.29 × 10 ⁻²	-1.28	5.6	-6.50	-7.78
Fumarato	1.32	2.13 × 10 ⁻³ (remote)	-2.67	9.9 (remote)	-3.68	-6.35
		4.68 × 10 ⁻² (adj.)		5.6 (adj.)		
4-Carboxybiphenyl-4'-carboxylato	Fast	6.02 × 10 ⁻⁵ (remote)	-4.22	16.4 (remote)	-2.22	-6.44
		4.40 × 10 ⁻² (adj.)		5.6 (adj.)		
<i>p</i> -Phthalato	Fast ^c	1.45 × 10 ⁻³ (remote)	-2.84	12.0 (remote)	-3.04	-5.88
		5.22 × 10 ⁻² (adj.)		5.6 (adj.)		

^a $I = 1.0$, $T = 25^\circ$. ^b Estimated from data at 21° . ^c Estimated from data at 16.6° . ^d r_{AB} in \AA , $T = 25^\circ$, term = $-36.4/r_{AB}$.

complexes are listed in order of increasing rate constant in Table II.

Two M -values may be calculated for the diacid ligands, one corresponding to reaction through the adjacent carboxyl, the other through the remote carboxyl. In each case the more positive M -value was used to rank the reaction rate since the larger M -value corresponds to the fastest reaction path. In only one case was the remote path less favorable than the adjacent. For the *m*-phthalato complex a considerably larger M -value is obtained for the adjacent path, thus indicating that the principal contribution to the observed rate should be *via* the adjacent carboxyl. Experiment shows no pH dependence for this reaction and presumably the principal path is *via* the adjacent carboxyl.⁷

The advantages of the extended theory are apparent. Although 2-carboxynaphthyl-6-carboxylato fails to correlate and the M -value for the 4-carboxybiphenyl-4'-carboxylato is somewhat small, the p_{rs}^2 values alone give no correlation. The electrostatic term alone also fails to give the proper correlation and further indicates a several order of magnitude jump in rate constant from acetate to fumarate and from 2-carboxynaphthyl-6-carboxylato to *p*-hydroxybenzoato which are not observed.

A final indication that this model includes some of the proper factors is shown by the zero ionic strength rate constants. Co was evaluated using eq. 6 and the data from Fig. 1 determining k_0 for the acetato complex. This value of Co (12.8) was then used to calculate k_0 for the fumarato complex using structural and m.b.o. parameters for the fumarato bridge. The computa-

tion gives $k_{0(\text{calcd})} \approx 0.19$ l. mole⁻¹ sec.⁻¹ compared with the experimental value $k_0 \approx 0.14$ l. mole⁻¹ sec.⁻¹.¹⁶

The *a priori* exclusion of a number of bridge ligands may have been too severe; however, those reactions excluded due to a possible ring stabilized activated complex occur more rapidly than their M -values would suggest. For example, p_{rs}^2 for the maleato bridge is close to that for fumarato, but r_{AB} for maleato is smaller. Thus maleato has a more negative M -value and is expected to react more slowly than fumarato while in fact it reacts at least 25 times faster.

An indication of the rational nature of the steric barrier exclusion is obtained on examination of the experimental k_2 values. The k_2 contribution to the observed rate is linearly dependent on the H⁺ concentration and has been interpreted as arising from increased conjugation due to protonation of the adjacent carboxyl group.¹ The *o*-phthalato and 2-carboxybiphenyl-2'-carboxylato bridges have large barriers to conjugative planarity and their observed k_2 values are almost zero. Thus even if adjacent protonation occurs, it apparently fails to increase conjugation between the remote metal centers sufficiently for reaction to take place *via* that path.

If one now accepts that the M -value criterion gives a qualitative ranking for the rate of pH independent remote attack, then the values for the 1-4 and 1-5 dicarboxynaphthyls should be too large since small barriers to remote conjugation exist. This proves to be the case. The appropriate values are as follows

(16) From Fig. 2 after correction for 15% reaction by pH dependent paths.

L	p_{rs}^2	r_{AB}	M
1-Carboxynaphthyl-4-carboxylato	6.31×10^{-4}	12.0 Å.	-6.23
1-Carboxynaphthyl-5-carboxylato	8.54×10^{-6}	12.3 Å.	-7.03

indicating rates five to ten times larger than observed.

Conclusions

These results indicate that a combined conjugation-electrostatic theory of electron transfer has some validity. By modification of the Halpern-Orgel scheme to include reasonable electrostatic effects, one is able to order correctly, with one major exception, bridging ligands as to effectiveness as mediators in oxidation-

reduction reactions between Cr(II) and Co(III). The inadequacies of the treatment arise in part from the details of computation. The mobile bond order, p_{rs} , depends upon the degree of the M.O. approximation used; this is especially true for the larger ligands. The microscopic dielectric constant used in (4) is surely too large, but as usual no adequate microscopic constant is available. Perhaps improvement of the M.O. calculations and improvement of the electrostatic treatment along lines set by Kirkwood¹⁷ could produce substantial numerical agreement with experiment.

(17) F. H. Westheimer and J. G. Kirkwood, *J. Chem. Phys.*, **6**, 513 (1938).

Kinetics of Ring-Opening and Vinyl Polymerizations

without Termination Reactions

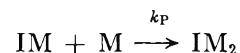
by L. F. Beste and H. K. Hall, Jr.

Pioneering Research Division, Textile Fibers Dept., E. I. du Pont de Nemours and Company, Inc., Wilmington 98, Delaware (Received July 22, 1963)

A new and accurate mathematical method for calculating the initiation and propagation rate constants for competitive, consecutive, second-order polymerizations is derived. The only data required are the initial concentrations of monomer and initiator and values of monomer concentration at various times. The method is sensitive to departures from the postulated kinetic scheme; application to several studies reported in the literature proves that those reactions do not obey the simplest kinetics. The relationship of these methods to those of earlier workers is discussed. An exact and convenient method is presented for calculating the extent of reaction as a function of time, given the rate constants and initial concentrations.

Introduction

The kinetics of ring-opening and vinyl polymerizations in which no termination reaction occurs have not been studied extensively. The simplest formulation of such polymerization kinetics would be



(I = initiator, M = cyclic or vinyl monomer). Chain termination is considered not to occur.

We propose to find k_I and k_P from a knowledge only

of the initial concentrations and of monomer concentration at various times. If some bulk property of the polymerizing mixture—such as volume contraction or heat evolved—is used to measure the progress of the reaction, there will be two cases in which the monomer concentration can be obtained easily. First, if the changes in bulk property associated with the initiation and propagation reactions are equal, the over-all change will be proportional to the disappearance of monomer. Second, under polymerization conditions, *i.e.*, $(M)_0/(I)_0 \gg 100$, the observed change will be almost completely that of the propagation reaction. As described below, some studies require data obtained with comparable initiator and monomer concentrations to determine k_I . A specific analytical technique, such as infrared spectroscopy, must then be used to determine the monomer concentration.

Calculation of the Rate Constants. Initiator can react only with monomer at a rate controlled by the rate constant k_I

$$-\frac{d(I)}{dt} = k_I(I)(M) \quad (1)$$

Monomer reacts not only with initiator but also with reactive ends of polymer molecules of every size. The concentration of polymer molecules is given by $(I)_0 - (I)$, where $(I)_0$ is the concentration of initiator at the start of the reaction. The propagation reaction is controlled by the rate constant k_P so that the rate of disappearance of monomer is

$$-\frac{d(M)}{dt} = k_I(I)(M) + k_P(M)[(I)_0 - (I)] \quad (2a)$$

$$\equiv (k_I - k_P)(I)(M) + k_P(M)(I)_0 \quad (2b)$$

The kinetics of this reaction might be described as first order with a sliding rate constant, a rate constant initially equal to $k_I(I)_0$ and moving toward (but never quite reaching) $k_P(I)_0$. That is, at zero time

$$-\frac{d \ln (M)}{dt} = k_I(I)_0 \quad (3)$$

After a long time, if the initiator is essentially used up

$$-\frac{d \ln (M)}{dt} \rightarrow k_P(I)_0 \quad (4)$$

However, as shown below, a sizable amount of initiator will remain unreacted under some conditions. Of course, if k_I and k_P happen to be equal, the monomer concentration *vs.* time can be plotted as a first-order reaction with an apparent rate constant equal to $k(I)_0$. Integrating (1)

$$\ln \left[\frac{(I)}{(I)_0} \right] = -k_I \int_0^t (M) dt \quad (5)$$

or

$$(I) = (I)_0 \exp \left[-k_I \int_0^t (M) dt \right] \quad (6)$$

Equation 2b may be rewritten

$$-\frac{d \ln (M)}{dt} = (k_I - k_P)(I) + k_P(I)_0 \quad (7)$$

Substituting (6) for (I)

$$-\frac{d \ln (M)}{dt} = (k_I - k_P)(I)_0 \exp \left[-k_I \int_0^t (M) dt \right] + k_P(I)_0 \quad (8)$$

Dividing by $(I)_0$ and subtracting k_P from both sides gives

$$-\frac{1}{(I)_0} \frac{d \ln (M)}{dt} - k_P = (k_I - k_P) e^{-k_I \int_0^t (M) dt} \quad (9)$$

or its negative

$$\frac{1}{(I)_0} \frac{d \ln (M)}{dt} + k_P = (k_P - k_I) e^{-k_I \int_0^t (M) dt} \quad (10)$$

The logarithmic forms of eq. 9 and 10 are

$$\log \left(\frac{-1}{(I)_0} \frac{d \ln (M)}{dt} - k_P \right) = \log (k_I - k_P) - \frac{k_I}{2.303} \int_0^t (M) dt \quad (11a)$$

or

$$\log \left(\frac{1}{(I)_0} \frac{d \ln (M)}{dt} + k_P \right) = \log (k_P - k_I) - \frac{k_I}{2.303} \int_0^t (M) dt \quad (11b)$$

These are the solutions; if k_I is greater than k_P , (11a) is used; contrariwise, (11b).

The procedure is as follows. First plot $\log (M)$ *vs.* t . If the curve is concave upward, k_I is greater than k_P ; if it is concave downward, the reverse is true. Next, obtain slopes, $d \ln (M)/dt$, plot the slopes against t , and smooth to eliminate scatter. To illustrate, let us suppose that k_I is greater than k_P (11a). Divide the slopes by $-(I)_0$ to yield a series of positive numbers. From each of these numbers subtract an assumed constant value of k_P and plot the result on semi-

logarithmic paper against $\int_0^t (M) dt$. (The integrals may be obtained from the plot of (M) vs. t with a planimeter or a computer.) When the correct value of k_P has been chosen, a linear plot of $\log [-1/(I)_0 (d \ln (M))/dt - k_P]$ vs. $\int_0^t (M) dt$ will be obtained.

Because of experimental scatter in the data, linearity is not a sensitive test for the accuracy of k_P . There is a far better test. Namely, $k_I = -2.303$ times the slope of the plot (which is always negative) and the intercept must equal $\log (k_I - k_P)$. How well this works may be seen in Fig. 1. The correct values are

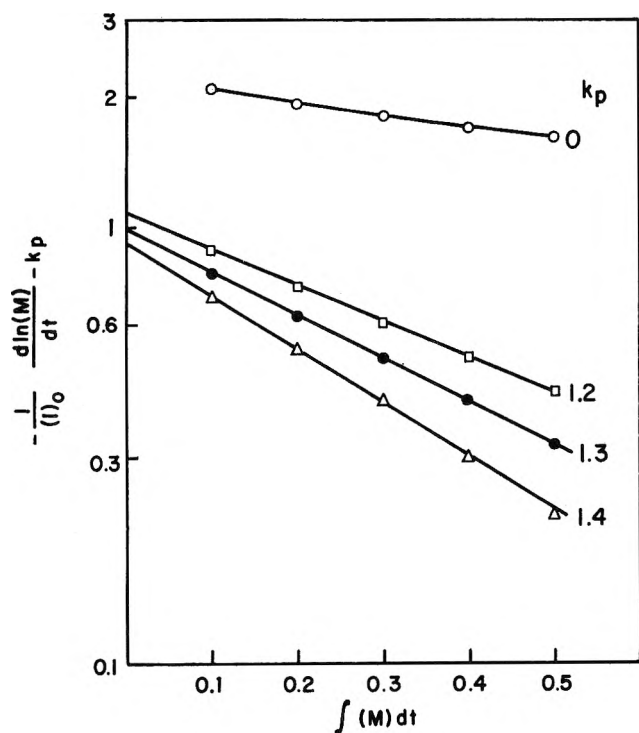


Figure 1. Plot to illustrate method.

$k_I = 2.303$ and $k_P = 1.303$. (The values of $-1/(I)_0 (d \ln (M))/dt$ are denoted by circles.) If k_P is assumed to be 1.2, the upper set of squares will be obtained. A straight line drawn through these points (the slight curvature would not be excessive for experimental data), has slope = -0.826 , $k_I = 1.9$, and $k_I - k_P = 1.9 - 1.2 = 0.7$. The intercept at 1.08 is obviously much too high. Similarly, with $k_P = 1.4$, the slope = -1.232 , $k_I = 2.84$, and the intercept should be 1.44, but is only 0.93. With $k_P = 1.303$, the slope is -1.000 , k_I (from the slope) is 2.303, and the intercept should, and does, equal 1.000. This necessity

to obtain agreement between slope and intercept is the most powerful element in the method.

When the rate constants are similar in value, as here, the error in the method appears not to be above 1%; experimental error will be superimposed on this. As the rate constants diverge in value, the accuracy decreases.

The limiting case in which either of the rate constants is zero is consistent with this treatment. If k_I is zero, no reaction will occur. The initial slope will be zero, so its logarithm cannot be plotted. If k_P is zero, the scheme reduces to that of a bimolecular reaction, with $k_2 = k_1$. Such data could be treated according to the method indicated and would be an unusual way of obtaining the rate constant for a second-order reaction.

Preliminary Deductions from the Experimental Data.

A. *Log (M) vs. Time.* The direction of curvature of this plot shows which rate constant is the larger, as mentioned above. The curve can in no case contain an inflection point.

This last criterion is very useful, as a brief application to literature data will show. Breitenbach and Allinger have described the polymerization of phenylalanine N-carboanhydride by *p*-chloroaniline in nitrobenzene solution in terms of the kinetic scheme of the present report.¹ Semilogarithmic plots of their monomer concentrations against time are sigmoid, so the postulated kinetics cannot apply. The data of Ballard and Bamford² for a similar polymerization also give sigmoid curves when plotted in this fashion. Lundberg and Doty have concluded on other grounds that a more complex kinetic scheme is required for N-carboanhydride polymerization.³

The polymerization of caprolactam, initiated by carboxylic acids or amines, was also subjected to this test. Majury⁴ considered the simple formulation of the present paper, but rejected it because it did not explain the variation of polymerization rate with catalyst concentration. Semilogarithmic plots of his data were markedly sigmoid, confirming his conclusion.

B. *log { -1/(I)₀ (d ln (M))/dt } vs. ∫(M) dt.* It will save time in doubtful cases if this plot is made early in the analysis (e.g., the circles in Fig. 1). If the slope is negative, the slope must gradually decrease (first derivative negative, second derivative positive). If the slope is positive, it must also decrease (first

- (1) J. W. Breitenbach and K. Allinger, *Monatsh.*, **84**, 1103 (1953).
- (2) D. G. H. Ballard and C. H. Bamford, *Proc. Roy. Soc. (London)*, **A223**, 495 (1954).
- (3) R. D. Lundberg and P. Doty, *J. Am. Chem. Soc.*, **79**, 3961 (1957).
- (4) T. G. Majury, *J. Polymer Sci.*, **31**, 383 (1958).

derivative positive, second derivative negative). If this behavior is not found, the postulated kinetic scheme is not obeyed, and a solution will not be obtained with any value of k_P .

C. Preliminary Estimates of k_I and k_P . A fairly good estimate of k_I can be obtained from the slope of $\ln (M)$ vs. t at zero time [slope = $-k_I(I)_0$]. Also, when (11a) is used, it is clear that k_P cannot be so large as to make any of the values of the ordinate negative. When (11b) is used, k_P must be large enough so that addition of k_P will make even the lowest value of the ordinate positive.

Another estimate of k_P can be gotten from the plot of (M) vs. t . It can be shown that if $k_I > k_P$, there can be no inflection point in this plot. If $k_P > k_I$, there will be an inflection point unless

$$\frac{(I)_0}{(M)_0} > \frac{(k_P - k_I)}{k_I} \quad (12)$$

If k_P is greater than k_I , and there is no inflection point, (12) provides a means for estimating the highest possible value of k_P in advance of the detailed analysis. Proof of these statements will be omitted.

Reconstruction of the (M) vs. Time Curve from the Rate Constants. The relation between monomer concentration and time can be obtained if the time variable is transformed in the manner introduced by Wideqvist.⁵

Rearrange eq. 9 as

$$\frac{d(M)}{(M) dt} = -k_P(I)_0 - (k_I - k_P)(I)_0 e^{-k_I \int (M) dt} \quad (13)$$

The independent variable is changed by letting

$$\int_0^t (M) dt \equiv n \quad (14)$$

It follows that

$$(M) dt \equiv dn \quad (15)$$

and

$$\frac{d(M)}{(M) dt} \equiv \frac{d(M)}{dn} \quad (16)$$

Substituting into (13)

$$\frac{d(M)}{dn} = -k_P(I)_0 - (k_I - k_P)(I)_0 e^{-k_I n} \quad (17)$$

which integrates readily to

$$(M) = (M)_0 - k_P(I)_0 n + \left(1 - \frac{k_P}{k_I}\right)(I)_0(e^{-k_I n} - 1) \quad (18)$$

After plotting (M) vs. n , the values of t corresponding to various values of (M) can be determined by means of the relationship

$$t = \int_0^n dt = \int_0^n \frac{dn}{(M)} \quad (19)$$

Calculation of Extent of Reaction of Monomer with Initiator or with Polymer Ends. We wish to know what fraction of the monomer has reacted with initiator and also what fraction with active polymer ends, given k_I , k_P , and (M) as a function of time. Dividing (2b) by (1) gives

$$\frac{d(M)}{d(I)} = \left(1 - \frac{k_P}{k_I}\right) + \frac{k_P(I)_0}{k_I(I)} \quad (20)$$

which easily integrates to

$$(M) - (M)_0 = \left(1 - \frac{k_P}{k_I}\right) [(I) - (I)_0] + \frac{k_P}{k_I}(I)_0 \ln \left[\frac{(I)}{(I)_0}\right] \quad (21)$$

Let X_M = total fraction of monomer reacted = $[(M)_0 - (M)]/(M)_0$; X_I = fraction of monomer reacted with initiator; X_P = fraction of monomer reacted with polymer; [$X_I + X_P = X_M$]. Dividing the negative of eq. 21 by $(M)_0$ gives

$$X_M = \frac{1}{(M)_0} \left(1 - \frac{k_P}{k_I}\right) [(I)_0 - (I)] + \frac{k_P(I)_0}{k_I(M)_0} \ln \left[\frac{(I)_0}{(I)}\right] \quad (22)$$

To use this equation to obtain values of (I) from known values of (M) , it would be advisable to plot a curve of values of (M) calculated from various assumed values of (I) and interpolate the known values of (M) at the time of interest. In units of concentration, the amount of monomer reacted with initiator at any time is $(I)_0 - (I)$. The fraction of monomer reacted with initiator is then

$$X_I = \frac{(I)_0 - (I)}{(M)_0} \quad (23)$$

This is the first term in (22). Subtracting this leaves

$$X_P = \frac{(I)_0}{(M)_0} \frac{k_P}{k_I} \left\{ \ln \left[\frac{(I)_0}{(I)}\right] + \frac{(I)}{(I)_0} - 1 \right\} \quad (24)$$

Polymerization Rates. The polymerization will proceed at nearly its final propagation rate, namely,

(5) (a) S. Wideqvist, *Acta Chem. Scand.*, **4**, 1216 (1950); (b) *Arkiv Kemi*, **8**, 325 (1955); (c) *ibid.*, **8**, 545 (1955).

$k_P(I)_0(M)_t$, during most of the run if two easily obtainable conditions are met: (1) the initiator is of roughly comparable reactivity to the growing polymer chain; and (2) the initiator is present initially at low concentration, as is invariably the case in making high polymer.

For calculation purposes, let us assume that the observed rate of polymerization will be indistinguishable from $-k_P(M)(I)_0$ when the initiator is 90% reacted, *i.e.*, $(I) = 0.1(I)_0$. Assuming that $(M)_0 = 1$ mole/l., $(I)_0 = 2.3 \times 10^{-3}$ mole/l., and $k_P = 10$ l./mole⁻¹ min.⁻¹, we calculate from eq. 21 the monomer concentration $(M)_t$ at which the polymerization rate appears to equal the propagation rate.

k_I , l. mole ⁻¹ min. ⁻¹	$(M)_t$
100	0.998
5	0.991
1	0.965
0.1	0.674
0.05	0.352

The results show that the maximum polymerization rate is reached within the first few per cent of reaction unless k_I takes on very small values. Therefore, many reactive catalysts will all give about the same polymerization rate in practice. This point has also been noted by earlier workers^{6,7} for analogous kinetic situations.

Because of these facts, difficulty in obtaining k_I will be encountered whenever a small concentration of initiator is employed. Unless k_I is very much smaller than k_P , the plot of $\ln(M)$ *vs.* t will apparently become linear soon after the start of the reaction and will remain linear thereafter. The apparently constant slope, of course, is equal to $-k_P(I)_0$ with good accuracy. For accurate evaluation of k_I when k_I and k_P are of comparable magnitude, experimental data obtained with high $(I)_0$ must be obtained. Then the reaction of I with M will play an important role, and k_I can be measured.

Persistence of Initiator. The concentration of initiator which must persist to infinite time is easily found by setting (M) equal to zero in eq. 21. Under conditions leading to high polymer, persistence of initiator will be no problem unless the initiator is far less reactive than the polymer ends. It is sometimes necessary to start with higher concentrations of initiator, either to determine k_I , to prepare very low polymer, or to keep the polymer in solution. As an example, let $(M)_0 = (I)_0 = 0.1$ mole/l., $k_I = 2$, $k_P = 8$ l./mole min.; (I) cannot fall below 0.057, or 57% of the starting value.

Ballard and Bamford² prepared low polymers (about tetramer) *in situ* by the reaction of appropriate quantities of monomer and initiator. The low polymers were then used to determine k_P for the polymerization of N-carboanhydrides. Appreciable quantities of initiator may still be present during the determination of k_P , however, particularly if $k_P > k_I$.

Comparison with Mathematical Methods of Earlier Workers. Previous investigators have obtained the rate constants for this kinetic situation by several approximate methods. Breitenbach and Allinger^{1,8} constructed a plot of $\ln(M)$ against time for each run. The initial slope of the curve was taken to be $-k_I(I)_0$ and the slope near the end $-k_P(I)_0$. As noted above, the value of k_I so obtained will be fairly good, although the experimental error may be high. However, the value of k_P is likely to be seriously in error because of persistence of initiator.

Ballard and Bamford² used low molecular weight polymer as an initiator. The reaction followed accurate first-order kinetics with a rate constant taken to be equal to $k_P(I)_0$. They then used this value of k_P for runs with other initiators, obtained k_I from the initial slopes, and checked their values by reconstructing a plot of (M) *vs.* time through a process of numerical integration. This procedure is satisfactory from a mathematical viewpoint, although it would clearly be preferable to obtain k_I and k_P from a single run.

Another mathematical analysis of these kinetics was carried out by Bauer and Magat.⁶ They presented curves showing concentration and rate relationships for various assumed values of the ratio k_P/k_I . They further showed that knowledge of *both* $(M)_t$ and $(I)_t$, together with a determination of the time at which the polymerization rate passes through a maximum, permits the calculation of both k_P and k_I . However, in many cases such data would be extremely difficult to obtain experimentally.

Application of Present Method to Literature Experimental Data. We had hoped to find experimental data in the literature which could be subjected to the treatments presented in this paper. However, there does not appear to be any record of a polymerization reaction which follows these simple kinetics. More complicated kinetics are observed for the polymerization of various α -amino acid N-carboanhydrides by

(6) E. Bauer and M. Magat, *J. chim. phys.*, **47**, 841 (1950).

(7) G. Gee, W. C. E. Higginson, and G. T. Merrall, *J. Chem. Soc.*, **13**, 435 (1959).

(8) See also E. Katchalski and M. Sela, "Advances in Protein Chemistry," Vol. 13, Academic Press, New York, N. Y., 1958, p. 304.

amines³ and by alkoxides,⁹ of caprolactam by water¹⁰ and by amines,⁴ of ethylene oxide by alkoxides,⁷ and of siloxanes by hydroxide ion.¹¹ We also attempted to apply our method to recorded data on anionic polymerizations of vinyl monomers. However, anionic polymerizations of methyl methacrylate¹² and isoprene¹³ by butyllithium also follow more complicated kinetics. At present, then, the treatment can be used to assess departures from the simple kinetics set down in the Introduction.

Appendix

Differential Equations in Only One Variable. Differentiation of (9) and rearrangement gives a differential equation in (M)

$$\frac{d^2 \ln (M)}{dt^2} + k_I \frac{d(M)}{dt} + k_I k_P (I)_0 (M) = 0 \quad (A1)$$

Theoretically, two points from the plot of (M) vs. t , together with the derivatives, will suffice to solve (A1). Practically, the second derivative will change so slowly that the calculated rate constants will have low accuracy, *even if* eq. A1 is strictly true for the reaction. If one has extremely good data and access to a high-speed computer, it will occasionally be worthwhile to fit the curve of (M) vs. t to a high-order power series in (M) and then differentiate analytically. Comparison of results gotten with different pairs of points will indicate the reliability of the results.

Separation of (21) according to functions of (I) gives

$$(M) = \left\{ (M)_0 - \left(1 - \frac{k_P}{k_I} \right) (I)_0 - \frac{k_P}{k_I} (I)_0 \ln (I)_0 \right\} + \left(1 - \frac{k_P}{k_I} \right) (I) + \frac{k_P}{k_I} (I)_0 \ln (I) \quad (A2)$$

which may be represented schematically thus

$$(M) = A + B(I) + C \ln (I) \quad (A3)$$

Substitution of (A3) into (1) gives a differential equation in (I) only

$$\frac{d(I)}{A(I) + B(I)^2 + C(I) \ln (I)} = -k_I dt \quad (A4)$$

This equation has appeared a number of times in the literature, but it has not been integrated. If one has data for the disappearance of (I) only, (A4) could be solved for the two rate constants by the method suggested above for (A1).

-
- (9) M. Idelson and E. R. Blout, *J. Am. Chem. Soc.*, **80**, 2387 (1958).
 (10) (a) D. Heikens and P. H. Hermans *J. Polymer Sci.*, **44**, 429 (1960); (b) F. Wiloth, *Kolloid-Z.*, **160**, 48 (1958).
 (11) W. T. Grubb and R. C. Osthoff, *J. Am. Chem. Soc.*, **77**, 1405 (1955).
 (12) D. L. Glusker, I. Lysloff, and E. Stiles *J. Polymer Sci.*, **49**, 315 (1961).
 (13) (a) F. J. Welch, *J. Am. Chem. Soc.*, **81**, 1345 (1959); (b) H. Sinn and W. Hofmann, *Makromol. Chem.*, **56**, 234 (1962).

Second Acid Dissociation of N,N-Di(2-hydroxyethyl)glycine and Related Thermodynamic Quantities from 0 to 55°

by S. P. Datta, A. K. Grzybowski, and Roger G. Bates

Department of Biochemistry, University College, London, and Solution Chemistry Section, National Bureau of Standards, Washington, D. C. (Received August 7, 1963)

The thermodynamic second acid dissociation constant of N,N-di(2-hydroxyethyl)glycine (R^\pm), a useful buffer substance for biochemical studies, has been determined from e.m.f. measurements in cells without liquid junction, using hydrogen and silver-silver chloride electrodes. Measurements were made from 0 to 55° at 5° intervals. The second acid dissociation constant (the equilibrium constant for the process $R^\pm \rightleftharpoons R^- + H^+$) is given by $pK_{2a} = 1329.602/T + 4.01592 - 0.00047606T$. The thermodynamic quantities associated with the second acid dissociation have been calculated from the values of pK_{2a} and are compared with those for the acidic dissociation of triethanolammonium ion. When allowance is made for electrostatic contributions to the changes of entropy and enthalpy, there remain large temperature-dependent changes which are similar for the two compounds.

Introduction

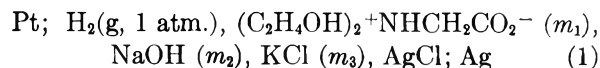
N,N-Di(hydroxyethyl)glycine (R^\pm) is a solid, water-soluble compound easily prepared in a pure state. The second acidic dissociation, namely



takes place in weakly alkaline solutions, making this a useful buffer system for biochemical studies.¹ Although the value of pK_{2a} of N,N-di(2-hydroxyethyl)glycine (8.333 at 25°) is 0.258 unit higher than the pK_a of the protonated form of 2-amino-2-(hydroxymethyl)-1,3-propanediol (tris), making the compound less suitable than tris as a buffer in the region pH 7 to 7.5, the glycine derivative does not contain a primary amino group and thus does not react with carbonyl compounds. The occurrence of such reactions is one of the disadvantages in the use of tris as a buffer for the study of enzyme-catalyzed reactions.² In this respect, triethanolamine is a very suitable buffer substance ($pK_a = 7.762$ at 25°)³ but has the disadvantages of being a viscous liquid difficult to purify and of being unstable to light and air.

Method

The dissociation constant was determined by the measurement of the e.m.f. of cells without liquid junction of the type



where m is the molality. Two series of measurements were made, the first at University College, London, using the apparatus and techniques previously described⁴ and the second at the National Bureau of Standards, with the apparatus and techniques also described in earlier publications.⁵

In both series of measurements the ratio of the concentration of the dipolar ion (R^\pm) to that of the buffer anion (R^-) was approximately 3:1. In the first series, the ratio of the chloride ion concentration to that of the buffer anion was approximately 5:1, while in the second it was approximately 3:1. High values of the ratios acid/base and chloride/base were used in order to minimize complex formation between the buffer anion and silver ions.⁴ In the first (London) series, the e.m.f. was measured from 5 to 55° at 10° intervals,

- (1) A. L. Remisov, *Biokhimiya*, 25, 323 (1960).
- (2) H. R. Mahler, *Ann. N. Y. Acad. Sci.*, 92, 426 (1961).
- (3) R. G. Bates and G. F. Allen, *J. Res. Natl. Bur. Std.* 64A, 343 (1960).
- (4) See, for example, S. P. Datta and A. K. Grzybowski, *Trans. Faraday Soc.*, 54, 1179 (1958).
- (5) R. G. Bates and H. B. Hetzer, *J. Phys. Chem.*, 65, 667 (1961).

while in the second (Washington) series, measurements were made from 0 to 50° at 5° intervals.

From the equations for the e.m.f. of cell 1 and for the second dissociation of the amino acid (R^\pm) one can write

$$pK_{2a} = \frac{(E - E^\circ)F}{RT \ln 10} + \log \frac{m_{R^\pm} m_{Cl^-}}{m_{R^-}} + \log \frac{\gamma_{R^\pm} \gamma_{Cl^-}}{\gamma_{R^-}} \quad (2)$$

The concentration terms have the following values: $m_{R^\pm} = (m_1 - m_2 - m_{H^+} + m_{OH^-})$, $m_{R^-} = (m_2 + m_{H^+} - m_{OH^-})$, and $m_{Cl^-} = m_3$. In the solutions studied, the terms m_{H^+} and m_{OH^-} were so small and so nearly equal that they were ignored in the calculation of the results. The buffer anion reacts with silver ion to form the two complexes AgR and AgR_2^- . In order to evaluate the extent of these reactions in the solution studied, the stepwise formation constants of both these complexes were determined from glass electrode pH measurements during the titration, with a standard solution of sodium hydroxide, of the dipolar buffer ion in the presence of silver nitrate by methods previously described.⁶ The values found for the logarithms of the first and second formation constants were 3.18₁ and 1.84₆, respectively, at 25°.

The much smaller stability of the 2:1 complex relative to that of the 1:1 complex is in contrast with earlier results for some other amino acids,⁶ but it is in agreement with the order of the stabilities of the 1:1 and 2:1 complexes of N,N-di(2-hydroxyethyl)glycine with other metal ions.⁷ Calculations have shown that the amount of complex formation in the solutions studied here is too slight to have a significant effect on m_{R^-} and m_{Cl^-} .

If γ_{R^\pm} is assumed to be unity, the last term of eq. 2 should be directly proportional to the ionic strength. Thus plots of y , namely

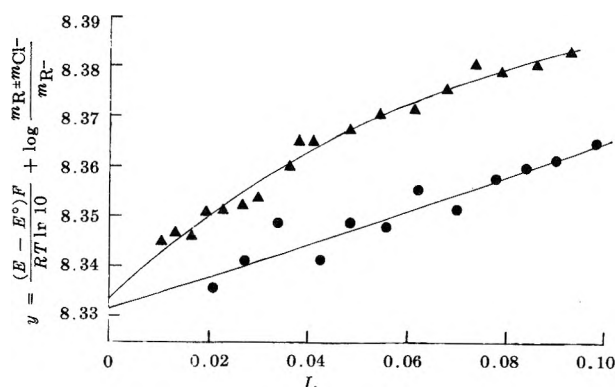


Figure 1. Plots of the extrapolation function y (eq. 3) against the ionic strength: ●, series 1; ▲, series 2.

$$y \equiv \frac{(E - E^\circ)F}{RT \ln 10} + \log \frac{m_{R^\pm} m_{Cl^-}}{m_{R^-}} \quad (3)$$

against ionic strength should also be straight lines cutting the y -axis at the value of pK_{2a} . As shown in Fig. 1, the points obtained with the first series of solutions appear to lie on a straight line, but those obtained with the second series do not. Consequently, the same extrapolation formula was applied as was used in determining the second dissociation constants of glycine, sarcosine, and N,N-dimethylglycine,⁴ namely

$$pK_{2a} = y + BI + CI^{3/2} \quad (4)$$

In eq. 4, B and C are arbitrary constants, the values of which were determined by the method of least squares, and I is the ionic strength.

Experimental

N,N-Di(hydroxyethyl)glycine was prepared by the method of Khromov and Remisov⁸ by the reaction of sodium chloroacetate with diethanolamine. It was recrystallized several times from 80% methanol. The melting point was 190° (cor.). The material used for the first series contained 3.16×10^{-5} mole of chloride per gram, and this amount was allowed for in the calculation of the concentrations. The material used for the second series was further recrystallized from water; it was free from chloride and had a melting point of 192–194° (cor.) when dry. This value is not greatly different from other values given in the literature, namely 190–192° when recrystallized from 80% methanol,⁸ 190–191° from 60% ethanol,⁹ and 193–195° from aqueous ethanol.¹⁰

The equivalent weight of the N,N-di(2-hydroxyethyl)glycine was determined by titrating (with approximately 0.1 M sodium hydroxide) samples consisting of 4.1 to 4.8 mmoles of the amino acid dissolved in 100 ml. of 0.05 M cupric chloride. The end point was established by glass electrode measurements of the pH change. There is a sharp inflection near pH 4.5 where the neutralization of the protons liberated by the formation of the 1:1 complex of Cu(II) and amino acid is complete.⁷ The equivalent weight found for the material used in the first series, after allowance for the chloride content, did not differ significantly from the expected value of 163.175, while for the material used

- (6) S. P. Datta and A. K. Grzybowski, *J. Chem. Soc.*, 1091 (1959).
- (7) S. Chaberek, Jr., R. C. Courtney, and A. E. Martell, *J. Am. Chem. Soc.*, 75, 2185 (1953).
- (8) N. V. Khromov and A. L. Remisov, *Zh. Obshch. Khim.*, 23, 598 (1953).
- (9) M. Izumi, *Pharm. Bull. (Tokyo)*, 2, 275 (1954).
- (10) M. Pascal, *Compt. rend.*, 245, 1318 (1957).

in the second series it was 163.302. The standard error of this mean value was 0.085. The impurity in the second sample was considered to be water, and these equivalent weights were used in calculating the concentrations. In order to correct the weight of the amino acid to vacuum, its density was determined by weighing in benzene and found to be 1.226.

Carbonate-free solutions of sodium hydroxide were prepared by diluting appropriate amounts of a saturated solution with carbon dioxide-free water. Their concentrations were determined by titration with standard hydrochloric acid, the end point being detected by glass electrode pH measurements. Fused potassium chloride was prepared by the method of Pinching and Bates.¹¹

All twelve solutions of the first series were prepared individually, while for the second series four stock solutions were prepared and the other fourteen solutions obtained from them by weight dilution. Each cell contained a pair of hydrogen electrodes and a pair of silver-silver chloride electrodes, and the observed e.m.f. was not accepted unless the duplicate measurements agreed to better than 0.05 mv. The values of E° were obtained from the equation of Bates and Bower¹² relating E° to temperature. The values of the fundamental constants used were those given by Bates and Gary.¹³

Results

The e.m.f. data for the thirty solutions at twelve temperatures are too voluminous for inclusion here. They were used to calculate y (eq. 3), and the values of y thus obtained were plotted against the ionic strength. As an example, the plots for both series at 25° are shown in Fig. 1. The values of pK_{2a} , that is, the value of y at zero ionic strength, were determined from eq. 4.

The values of pK_{2a} from both series, namely pK_{2a} (obsd.), are shown in Table I, which also gives an estimate of σ , the standard deviation of the points from the fitted lines,¹⁴ and $\sqrt{V(y_0)}$, the standard error of the intercepts calculated as previously described.¹⁵ In Table I are also listed the values of pK_{2a} , namely pK_{2a} (calcd.), derived from an equation of the form suggested by Harned and Robinson.¹⁶ The resulting equation, the constants of which were determined from the values of pK_{2a} (obsd.) from both sets by the method of least squares, is

$$pK_2(\text{calcd.}) = 1329.602/T + 4.01592 - 0.00047606T \quad (5)$$

where T is the Kelvin temperature ($t^\circ\text{C.} + 273.15$). The deviations between the observed and calculated values are also given.

It will be noted that the estimates of σ are slightly higher for series 1 (London) than for series 2 (Washington), $\sigma_{av} = 0.0030$ and 0.0022 , respectively. Thus the scatter in the results is somewhat larger in the first series. The standard errors of the intercepts are, however, nearly three times as large for series 1 as for series 2, $\sqrt{V(y_0)}$ (av.) being 0.0066 as compared with 0.0024. The reason for this difference lies mainly in the different ranges of ionic strengths covered in the two series. In both, the highest ionic strength was between 0.09 and 0.10, but in series 1 the lowest ionic strength was 0.02086, while in series 2 it was 0.010450. The fact that the range of ionic strengths covered in series 2 extended to lower values, together with the greater number of solutions measured, allows the value of the intercept to be fixed with more certainty than in the first series. When the number of solutions is reasonably large, it is the first factor which is of greater importance.¹⁵

The agreement between the two series is good, considering that the measurements were made with different materials and apparatus and in different laboratories. Series 1 gives pK_{2a} values slightly lower than those from series 2. The smallest difference is at 5° (0.0016 pK unit) and the largest at 45° (0.0068 pK unit). Nevertheless, there is no valid reason for considering the results of the two series to be significantly different, for at no temperature do the pK_{2a} values differ by more than the sum of the two values of $\sqrt{V(y_0)}$ at that temperature. Consequently, the data from the two series were combined to obtain the constants of eq. 5. At those temperatures where there were two values for pK_{2a} (obsd.), an average value, weighted in proportion to the reciprocals of the $\sqrt{V(y_0)}$ values, was used.

The pK_{2a} values shown in Table I may be compared with the values of Remisov¹ at an ionic strength of 0.033, namely $pK_{2a}' = 8.35$ at 20° and 8.15 at 37°, and of Chaberek, Courtney, and Martell,⁷ $pK_{2a}' = 8.08$ at 30° at an ionic strength of 0.1.

The values of the thermodynamic quantities associated with the dissociation process $R^\pm \rightleftharpoons R^- + H^+$ are given in Table II. They were calculated from eq. 5 by application of the usual formulas. The standard errors were derived by the equations given by Please.¹⁴

(11) G. D. Pinching and R. G. Bates, *J. Res. Natl. Bur. Std.*, **37**, 311 (1946).

(12) R. G. Bates and V. E. Bower, *ibid.*, **53**, 283 (1954).

(13) R. G. Bates and R. Gary, *ibid.*, **65A**, 495 (1961).

(14) N. W. Please, *Biochem. J.*, **56**, 196 (1954).

(15) Equation 7 in S. P. Datta and A. K. Grzybowski, *J. Chem. Soc.*, 792 (1963).

(16) H. S. Harned and R. A. Robinson, *Trans. Faraday Soc.*, **36**, 973 (1940).

Table I: Values of pK_{2a} ^a

<i>t</i> , °C.	Series 1			Series 2			$pK_{2a}(\text{calcd.})$	$10^4\Delta(\text{series 1})$	$10^4\Delta(\text{series 2})$
	$pK_{2a}(\text{obsd.})$	$10^4\sigma$	$10^4\sqrt{V(y_0)}$	$pK_{2a}(\text{obsd.})$	$10^4\sigma$	$10^4\sqrt{V(y_0)}$			
0				8.7530	23	26	8.7536		-6
5	8.6624	31	69	8.6640	24	27	8.6637	-13	+3
10				8.5777	21	23	8.5769		+8
15	8.4911	33	72	8.4938	21	23	8.4930	-19	+8
20				8.4133	20	22	8.4119		+14
25	8.3317	31	70	8.3337	19	21	8.3335	-18	+2
30				8.2560	24	26	8.2576		-16
35	8.1805	29	64	8.1832	23	26	8.1840	-35	-8
37							8.1552		
40				8.1134	23	25	8.1127		+7
45	8.0387	27	61	8.0455	20	22	8.0436	-49	+19
50				7.9795	25	27	7.9766		+29
55	7.9097	27	59				7.9115	-18	
	$\sigma_{av} = 0.0030; \sqrt{V(y_0)_{av}} = 0.0066$			$\sigma_{av} = 0.0022; \sqrt{V(y_0)_{av}} = 0.0024$			$\sqrt{V(pK)} = 0.0015$		

^a $pK_{2a}(\text{obsd.})$ was obtained from eq. 4 and $pK_{2a}(\text{calcd.})$ from eq. 5; σ is the standard deviation about the fitted lines in eq. 4, $\sqrt{V(y_0)}$ is the standard error of the intercept, $\Delta = pK_{2a}(\text{obsd.}) - pK_{2a}(\text{calcd.})$, and $\sqrt{V(pK)}$ is the standard deviation from the line of eq. 5.

Table II: Thermodynamic Quantities for the Second Acid Dissociation of N,N-Di(2-hydroxyethyl)glycine. ($T = ^\circ\text{K.}$)

	Value at 25°
$\Delta G^\circ = 25.4555 + 0.076886T - 0.0000091143T^{2a}$	47.569 kJ. mole ⁻¹
$\Delta H^\circ = 25.4555 + 0.0000091143T^{2a}$	26.266 kJ. mole ⁻¹
$\Delta S^\circ = -76.886 + 0.01823T^b$	-71.45 j. deg. ⁻¹ mole ⁻¹
$\Delta C_p^\circ = 0.01823T^b$	5.4 j. deg. ⁻¹ mole ⁻¹

Standard errors, in j.

<i>t</i> , °C.	$\sigma(\Delta G^\circ)$	$\sigma(\Delta H^\circ)$	$\sigma(\Delta S^\circ)$	$\sigma(\Delta C_p^\circ)$
0	6	153	0.54	5.2
25	4	44	0.15	5.6
55	6	172	0.54	6.2

^a In kJ. mole⁻¹. ^b In j. deg.⁻¹ mole⁻¹.

Extrapolation Lines. The difference between the slopes of the two extrapolation lines (Fig. 1) presumably resides in the last term of eq. 2, that is to say, the activity coefficients do not vary with ionic strength in the same manner in both series. The concentration ratio of buffer dipolar ion to buffer anion was the same (approximately 3:1) in both series, but the ratio of the chloride ion concentration to that of the buffer anion was higher (approximately 5:1) in series 1 than in series 2 (approximately 3:1). It may therefore be inferred that the activity coefficient terms in eq. 2 are affected not only by the ionic strength but also by the concentrations of the various ions present. In the absence of any data on the activity coefficient of any ionized form

of the N,N-di(2-hydroxyethyl)glycine molecule, no detailed discussion of this difference is possible.

Curved extrapolations of this kind have been observed previously with glycine^{4,17} and a number of its derivatives,⁴ and they raise the question of the reliability of the thermodynamic ionization constants calculated from such e.m.f. data. Some comfort in this respect may be derived from the comparatively good agreement between the thermodynamic pK_{2a} values calculated from the two sets of experiments reported here.

Thermodynamic Quantities. An interesting feature of the thermodynamic quantities associated with the second dissociation of N,N-di(2-hydroxyethyl)glycine is the large negative and virtually constant value of ΔS° over the temperature range studied. The constancy of the entropy is reflected in the very small value of ΔC_p° , which does not differ significantly from zero. An aromatic acid of the same charge type, 4-amino-3-methylbenzenesulfonic acid, has recently been found to have a positive entropy of ionization,¹⁸ resembling 2-amino-2-(hydroxymethyl)-1,3-propanediol (tris) in this respect.⁵

The present results may be compared with those for the dissociation of the triethanolammonium ion,³ a compound of similar structure. Values for both compounds are shown in Table III, from which it is seen that the thermodynamic quantities for the two

(17) E. J. King, *J. Am. Chem. Soc.*, **73**, 155 (1951).(18) S. D. Morrett and D. F. Swinehart, *J. Phys. Chem.*, **67**, 717 (1963).

dissociation processes are very different. For the dissociation of triethanolammonium ion, ΔS° is larger (less negative) and increases rapidly with increasing temperature (large positive ΔC_p°) and ΔH° is larger and increases with increasing temperature. These differences between the two compounds must be associated with the presence of the CH_2COO^- group in N,N-di(2-hydroxyethyl)glycine and are probably due to the electrostatic interaction of the carboxylate ion with water. To confirm that this is so, the electrostatic contribution to the thermodynamic quantities was calculated by applying the Born equation¹⁹ to the triethanolammonium, the hydronium, and the N,N-di(2-hydroxyethyl)glycinate ions, and the Scatchard-Kirkwood equation²⁰ to the dipolar ion.

Table III: Observed, Electrostatic, and Nonelectrostatic Thermodynamic Quantities Associated with the Second Acid Dissociation of 1 Mole of N,N-Di(2-hydroxyethyl)glycine and the Dissociation of 1 Mole of Triethanolammonium Ion³ at 25°

	N,N-Di(2-hydroxyethyl)- glycine	Triethanolammonium ion
ΔG° , kj.		
(Obsd.)	47.57	44.49
(El.)	9.63	3.98
(Non.)	37.94	40.51
ΔH° , kj.		
(Obsd.)	26.27	33.45
(El.)	-3.41	-1.41
(Non.)	29.68	34.86
ΔS° , j. deg. ⁻¹		
(Obsd.)	-71.4	-36.4
(El.)	-43.7	-18.1
(Non.)	-27.7	-18.3
ΔC_p° , j. deg. ⁻¹		
(Obsd.)	5.4	52
(El.)	-66.3	-27
(Non.)	71.7	79

The calculation was made in the manner already described.^{21,22} Values of the bulk dielectric constant were taken from the work of Malmberg and Maryott,²³ and the radius of the H_3O^+ ion was taken as 0.86 Å. by interpolation in Pauling's table²⁴ of crystal radii for a univalent cation of mass 19. There are no data available for the radius of the triethanolammonium ion nor for that of the substituted ammonium ion form of N,N-di(2-hydroxyethyl)glycine, but the radii of these ions are likely to be very much the same. They were both taken to be equal to that of the ammonium ion,

namely 1.4 Å,²⁵ for this calculation. The radius of the carboxylate ion and the distance between it and the substituted ammonium ion were taken as 1.23 and 3.17 Å., respectively, as was done for glycine.²⁶

The electrostatic thermodynamic quantities ΔG° (el.), ΔH° (el.), ΔS° (el.), and ΔC_p° (el.) calculated in this way are given in Table III.²⁷ By subtracting these from the observed values, the so-called "nonelectrostatic" thermodynamic quantities, ΔG° (non.), etc., were obtained. These nonelectrostatic quantities, also given in Table III, are seen to be very similar for both compounds. The value of ΔS° (non.) is larger (less negative) than ΔS° (obsd.) and increases with increasing temperature, while ΔC_p° (non.) is large and positive.

This approximate agreement may be taken as evidence that the same effect is responsible for the nonelectrostatic changes in each instance—possibly the so-called "iceberg effect,"²⁸ a concept introduced by Frank and Evans²⁹ to account for the large decrease in entropy which occurs when noble gases, hydrocarbons, etc., are dissolved in water. These authors postulate that the presence of such solutes stabilizes regions of ice-like water structure around the dissolved molecules. With rise in temperature, this structure would break down as a result of increased thermal agitation ("melting of the icebergs"), and hence ΔC_p° (non.) would be large and positive. In the compounds under consideration here, the iceberg effect is postulated to arise from the hydrocarbon substituents on the nitrogen atoms.

It is noteworthy that ΔC_p° (non.) for N,N-di(2-hydroxyethyl)glycine is lower than for its nonhydroxylated structural analogs (N,N-dimethylglycine, ΔC_p° (non.) = +115 j. mole⁻¹ deg.⁻¹; trimethylammonium ion, ΔC_p° (non.) = +177 j. mole⁻¹ deg.⁻¹, both at 25°),²⁸ possibly because the interaction of the

(19) M. Born, *Z. Physik.*, **1**, 45 (1920).

(20) G. Scatchard and J. G. Kirkwood, *Physik. Z.*, **33**, 297 (1932).

(21) S. P. Datta and A. K. Grzybowski, *Biochem. J.*, **78**, 289 (1961).

(22) S. P. Datta and A. K. Grzybowski, *J. Chem. Soc.*, 3068 (1962).

(23) C. G. Malmberg and A. A. Maryott, *J. Res. Natl. Bur. Std.*, **50**, 1 (1956).

(24) L. Pauling, "The Nature of the Chemical Bond," 3rd Ed., Cornell University Press, Ithaca, N. Y., 1960, p. 514.

(25) A. F. Kapustinsky, *Acta Physicochim. URSS*, **14**, 503 (1941).

(26) E. J. Cohn, *Ann. Rev. Biochem.*, **4**, 93 (1935).

(27) Once ΔG° (el.) is determined at any one temperature, the values of the other electrostatic thermodynamic quantities are fixed by the temperature coefficient of the dielectric constant.

(28) S. P. Datta and A. K. Grzybowski, *Trans. Faraday Soc.*, **54**, 1188 (1958).

(29) H. S. Frank and M. W. Evans, *J. Chem. Phys.*, **13**, 507 (1945).

hydroxyl groups with water is antagonistic to iceberg formation. Unfortunately, no data are available for N,N-dimethylglycine itself.

Acknowledgment.—The authors thank Miss Anna Straker for the calculations in this work. They are

also grateful to the Wellcome Trust for a travel grant to S. P. D. which made this collaboration possible. Some of the equipment used in London was provided by the Central Research Fund of the University of London.

Further Observations of the Stabilities and Reactivities of Gaseous Boroxines^{1a}

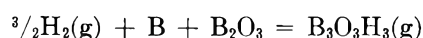
by Richard F. Porter^{1b} and Suresh K. Gupta

Department of Chemistry, Cornell University, Ithaca, New York (Received August 9, 1963)

Gaseous $B_3O_3H_3$ (boroxine) produced in a high temperature reaction of $H_2O(g)$ with elemental boron is thermodynamically unstable with respect to $B_2H_6(g)$ and $B_2O_3(s)$ at room temperature. Molecules of $B_3O_3H_3$ produced at high temperatures exhibit kinetic stability at low temperature. Condensation of gas to solid boroxine provides a kinetic path to B_2H_6 and boric oxide. Molar free energy and enthalpy relationships for $B_3O_3H_3(g)$, $B_3O_3H_3(s)$, and $\frac{1}{2}B_2H_6(g) + B_2O_3(s)$ have been established. Heats of formation of solid and gaseous boroxine are -301.7 ± 2.5 and -291.0 ± 2.0 kcal./mole, respectively, at 298°K. Gaseous boroxine reacts with HCl at high temperatures to produce mono-, di-, and trichloroboroxine. Low pressure reactions of BCl_3 with liquid B_2O_3 produce $B_3O_3Cl_3(g)$ and $B_4O_4Cl_4(g)$. For the reactions $BCl_3(g) + B_2O_3(l) = B_3O_3Cl_3(g)$ and $\frac{4}{3}BCl_3(g) + \frac{4}{3}B_2O_3(l) = B_4O_4Cl_4(g)$, $\Delta H^\circ_{1000^\circ K.} = 16.6 \pm 2.5$ kcal./mole and $\Delta H^\circ_{1125^\circ K.} = 30.8 \pm 5.0$ kcal./mole, respectively. Heats of formation at 298°K. of gaseous mono-, di-, and trichloroboroxine are -314.5 ± 4.0 , -342.2 ± 4.0 , and -378.8 ± 3.5 kcal./mole, respectively. The heat of formation of $B_4O_4Cl_4(g)$ is -494.0 ± 6.0 kcal./mole at 1125°K.

Introduction

Gaseous boroxine has been observed as the major product generated in a high temperature reaction of H_2 with B- B_2O_3 mixtures.² The thermal stability of $B_3O_3H_3$ was demonstrated in studies of the reaction



At a temperature of about 1400°K. the equilibrium constant for the reaction has been found to be of the order of unity. Indirect evidence of the stability of $B_3O_3H_3(g)$ is also noted by observation of the reaction

product isolated in a trap at low temperatures. Investigation of the behavior of the solid has led to some perplexing problems. On warming to room temperature, the solid decomposes to yield diborane and a solid residue. These effects indicated that a more thorough study of the thermodynamic behavior of boroxine would be of value. At present there is little or no information on the chemical behavior of this substance.

(1) (a) Work supported by the Advanced Research Projects Agency; (b) Alfred P. Sloan Fellow.

(2) W. P. Sholette and R. F. Porter, *J. Phys. Chem.*, **67**, 177 (1963).

The present study, therefore, was undertaken for the purpose of examining the condensation–evaporation behavior of boroxine and investigating the chemical properties of the gaseous molecule. During the course of this study, several derivatives of boroxine have been observed and thermodynamic data for a number of these have been obtained.

Experimental

Boroxine was produced by the reaction described previously. In these experiments $\text{H}_2\text{O}(\text{g})$ was passed over a heated sample of elemental boron mixed with boric oxide powder. In the reaction with $\text{H}_2\text{O}(\text{g})$ additional boron oxide is produced along with $\text{H}_2(\text{g})$. The exit of the furnace tube was connected by means of a U-tube and stopcocks to the inlet valve of a mass spectrometer.³ With this assembly it was possible to observe reaction products while experimental conditions were altered. The assembly is illustrated in Fig. 1. Water vapor maintained at room temperature was introduced through a glass frit into the reaction zone which was usually held at a temperature of about 1325°K. The water source was then cut off after a few minutes and the reaction products were examined mass spectrometrically. It is important to note that the reaction products, as they are observed, are essentially at room temperature. The initial hydrogen pressure as observed with H_2^+ was very high and the abundance of $\text{B}_3\text{O}_3\text{H}_3$ as noted by the intensity of $\text{B}_3\text{O}_3\text{H}_2^+$ was two to three orders of magnitude lower than H_2^+ . The $\text{B}_3\text{O}_3\text{H}_2^+/\text{H}_2^+$ ratio increased slowly with time. This was attributed to the difference in rates of diffusion from the hot reaction zone. A small proportion of $\text{B}_3\text{O}_4\text{H}_3$ (hydroxyboroxine) was also observed but in general the ratio of $\text{B}_3\text{O}_4\text{H}_2^+/\text{B}_3\text{O}_3\text{H}_2^+$ was less than 0.05. With fresh samples of B– B_2O_3 mixtures in the reaction chamber, reaction with water was always complete; traces of unreacted water were observed only after several series of measurements with one sample. Diborane also was not observed in the

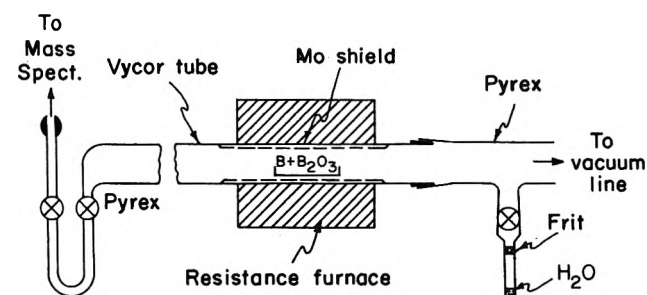


Figure 1. High temperature assembly for preparation of gaseous $\text{B}_3\text{O}_3\text{H}_3$.

early stages of the reaction but was observed after several quantities of boroxine had been generated from one reactant mixture. The trap located between the reaction zone and the mass spectrometer was used to condense $\text{B}_3\text{O}_3\text{H}_3(\text{g})$. This tube also served as a means of introducing solids that undergo reaction with gaseous $\text{B}_3\text{O}_3\text{H}_3$ generated in the hot zone.

A series of experiments was also undertaken to examine the reactions of gaseous boroxine with other reactive gases. The results presented here relate primarily to reactions with $\text{HCl}(\text{g})$. The experimental arrangement is similar to that used previously. This consisted of a Knudsen-type oven mounted to a gas inlet system. Product and unreacted gases leaving the cell are ionized by electron bombardment and the positive ion mass spectrum is observed.³ For these experiments, effusion cells were constructed of compacted boron nitride. Several small chips of BN were also placed in the cell. The mounting stem and cover for the cell were made of molybdenum.

A molybdenum cylinder surrounding the cell was used as a conducting shield for electron-bombardment heating. The assembly is illustrated in Fig. 2. Not shown in the figure are the radiation shields that enclose the oven. Temperatures were recorded with a platinum, platinum–rhodium thermocouple. The advantage of BN cells was that they provided a large

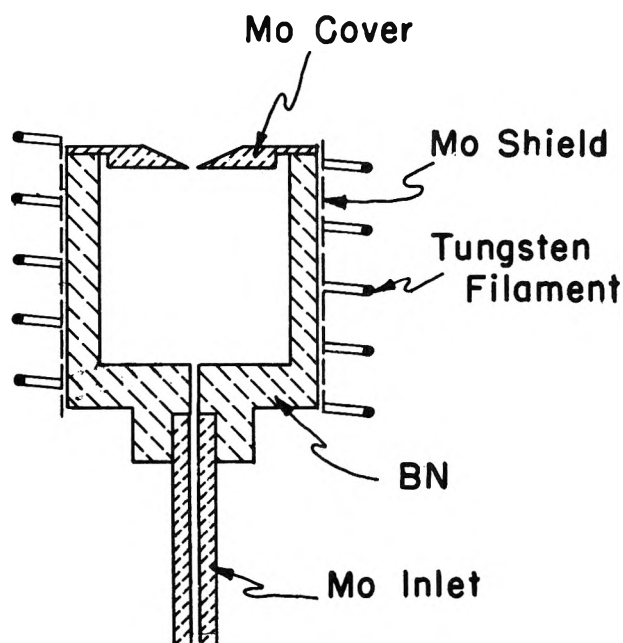


Figure 2. Effusion oven for mass spectrometric studies of reactions of gaseous boroxine.

(3) R. F. Porter and R. C. Shoonmaker, *J. Phys. Chem.*, **62**, 234 (1958).

reactant surface in which boron is essentially at unit activity (note that BN decomposes to $B(s) + N_2(g)^4$). Decomposition or reduction of the BN to produce $N_2(g)$ became a limitation for good vacuum conditions at temperatures above about $1300^\circ K$.

Condensation Behavior of $B_3O_3H_3(g)$. Previous studies of the condensation behavior of $B_3O_3H_3(g)$ were concerned with trapping of solid only at liquid nitrogen temperatures. More detailed information of the temperature–pressure relationship has now been obtained. In these experiments a source of gaseous $B_3O_3H_3$ was produced as described previously except that the U-tube was immersed in a series of “slush baths” at temperatures between 25 and -85° . A series of coolants was prepared from ethanol–Dry Ice, chloroform–Dry Ice, and acetone–Dry Ice mixtures. For these experiments the best conditions for observation were during the initial runs where the only other product was noncondensable $H_2(g)$. Data were taken by observing the intensity of $B_3O_3H_2^+$ (the major ion fragment of $B_3O_3H_3$) as the temperature of the coolant

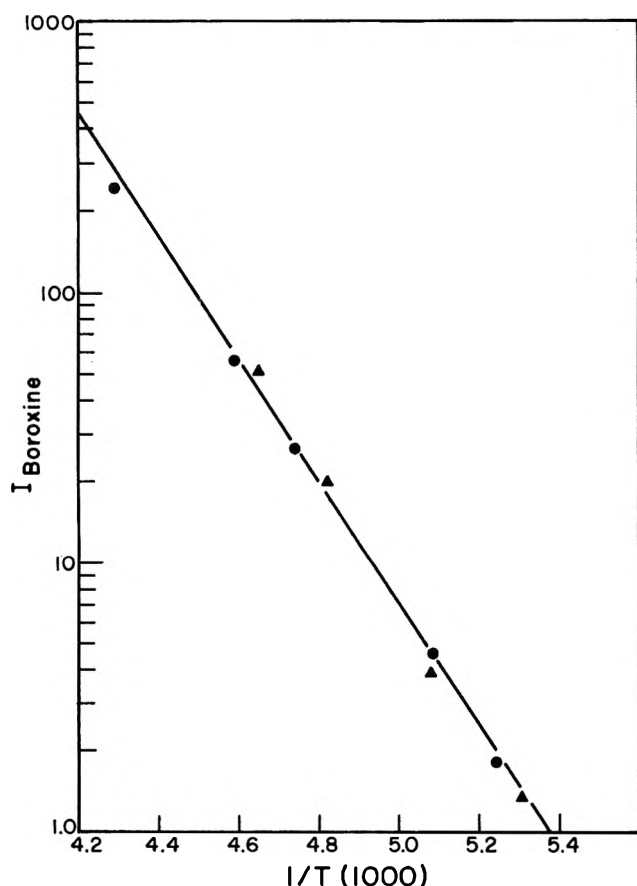


Figure 3. Mass spectrometric data illustrating condensation behavior of boroxine gas: ●, data are for $B_3O_3D_3$; ▲, data are for $B_3O_3H_3$.

was changed. The temperature was first lowered and then gradually raised to check reproducibility. A series of ion current–temperature measurements is given in Fig. 3. A decrease of the $B_3O_3H_2^+$ peak was rarely observed for trap temperatures above -40° . Below this temperature condensation behavior appears to be normal. It should be emphasized that the measurement corresponds to what must be taken as a limiting condensation pressure. As we note later the evaporation behavior is much more complex.

From rough pressure calibrations, we estimate that the pressure of $B_3O_3H_3$ in the system was generally between 0.1 and 0.5 torr for most of these experiments. This pressure range would also correspond roughly to the vapor pressure for the highest temperature at which condensation was observed. The extrapolation of the intensity–temperature curve to higher temperature indicates that a very much higher pressure of $B_3O_3H_3$ is possible at room temperature in a Pyrex system.

Evaporation Behavior of Solid $B_3O_3H_3$. For examination of solid–vapor reactions of boroxine, it was necessary to isolate solid samples in an external system similar to that indicated in Fig. 1. The experimental conditions were identical with those employed for study of the condensation reaction except that the product gases were continually pumped through the system. Samples of solid were condensed in a U-tube which could be easily joined to the inlet system to the mass spectrometer. For a reaction temperature of about $1300^\circ K$, with inlet water vapor at room temperature, it was possible to isolate about 100 mg. of solid in a period of 1.5 to 2 hr. The solid sample was held at liquid nitrogen temperature during transfer to the mass spectrometer inlet.

Samples then were warmed to about -80° and evaporation was followed by monitoring the mass spectrum. It was generally observed that $B_2H_6(g)$ was present in the U-tube when warmed to -85° . The $B_2H_6(g)$ pressure was found to be independent of temperature until the tube had reached a temperature of about 0° . A rapid decomposition was then observed and the $B_2H_5^+$ rose abruptly. The high pressure of B_2H_6 in the trap at -85° must result from condensation of B_2H_6 formed by dissociation of solid condensed on warmer sections of the system above the trap during preparation. This may be due to the small amount of hydroxyboroxine which should have a higher condensation temperature than boroxine. To avoid this problem, samples

(4) (a) P. Schissel and W. Williams, *Bull. Am. Phys. Soc.*, **4**, 139 (1959); (b) L. H. Dreger, V. V. Dadape, and J. L. Margrave, *J. Phys. Chem.*, **66**, 1556 (1962).

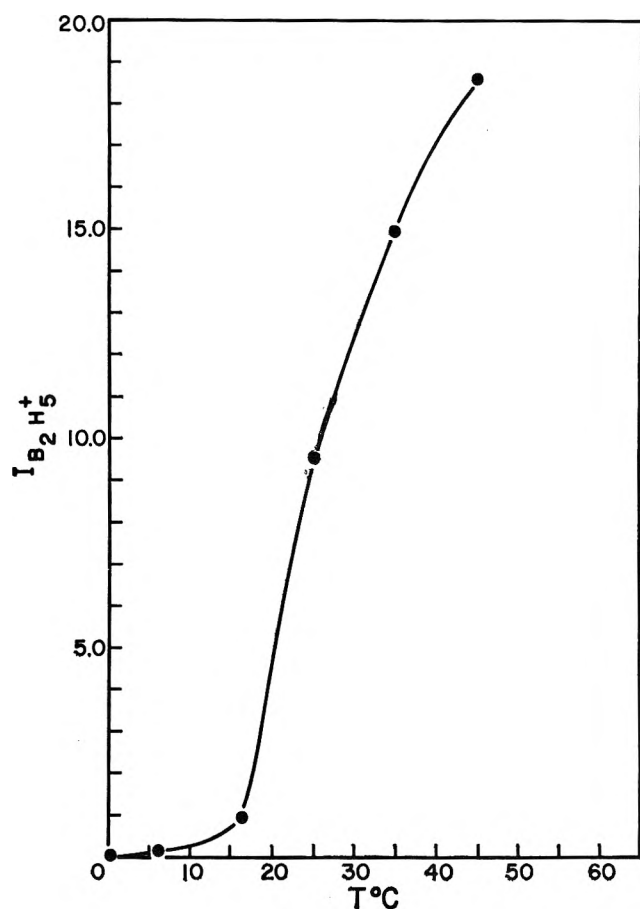


Figure 4. Mass spectrometric data illustrating evaporation behavior of boroxine solid to diborane.

were subsequently prepared by holding the trap at -85° while B_2H_6 was removed by pumping. Evaporation behavior of these samples is illustrated by the data in Fig. 4 where we plot the intensity of $B_2H_5^+$ vs. temperature. These experimental data were obtained by successively replacing a cooler trap by a warmer trap. The point corresponding to the threshold for decomposition was found to depend to some extent on the warming rate. A sample held for several hours in a closed U-tube at -25° was also found to undergo partial decomposition. At temperatures between -85 and -40° , $B_3O_3H_3(g)$ was not detectable. The partial pressure of $B_3O_3H_3(g)$ for samples at 25° was about 0.01 that of $B_2H_6(g)$. Thus it is evident that the condensation–evaporation processes are not reversible. The relative change in intensities of $B_2H_5^+$ and $B_3O_3H_2^+$ was also studied as a function of temperature (see Fig. 4). This was achieved by immersing the U-tube in an oil bath which could be heated to temperatures of about 150° . The ratio $B_3O_3H_2^+/B_2H_5^+$ increased very slightly but for temperatures

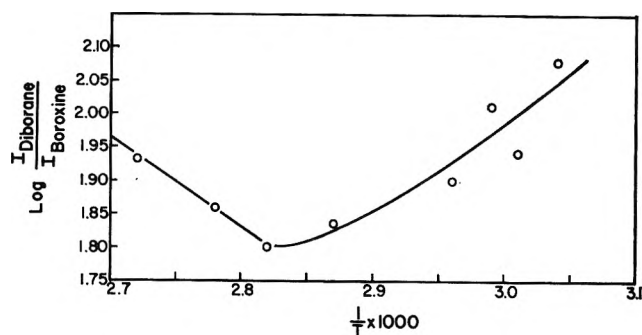
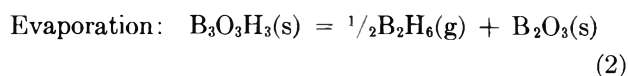
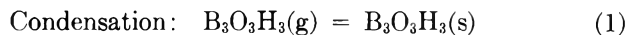


Figure 5. Temperature dependence data for evaporation products of solid boroxine.

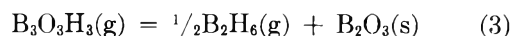
above about 80° this ratio was nonreproducible and usually tended to decrease with an increase in temperature (Fig. 5).

In some experiments after diborane had been pumped from the U-tube, it was found that reheating the residue yielded additional B_2H_6 . This effect indicates that the solid residue behaves thermodynamically like a solid solution of boroxine in boric oxide although the structure of this material is still unknown.⁵

Thermodynamics of Condensation–Evaporation Reactions. Formally, we may consider the reactions



It will also be convenient to consider the reaction



From the temperature dependence curve for condensation of boroxine, we obtain a corresponding heat of condensation. A series of six runs gives an average value of $\Delta H_1^{\circ} = -10.7 \pm 0.5$ kcal./mole. Experiments with deuterated boroxine gave the same value within the experimental error quoted (see Fig. 3). This value is comparable in magnitude to heats of sublimation of similar molecules.⁶ During the course of the experiment liquefaction was never observed either on condensation or during evaporation.

We have evaluated the heat for reaction 3 by the third-law procedure in which ΔF_3 , computed from equi-

(5) S. K. Gupta and R. F. Porter, *J. Phys. Chem.*, **67**, 1286 (1963). There is no intention to imply here that boroxine rings are necessarily retained in the residue after the initial rapid decomposition of the solid. When B_2H_6 is removed from the system, the new decomposition pressure of B_2H_6 is always less than its initial value. This behavior is similar to that associated with a two-component system in which the thermodynamic activities are changing as the composition is altered.

(6) Benzene, which is isoelectronic with boroxine, has a heat of sublimation of about 10.5 kcal./mole.

librium constants, is combined with entropy data. Since it was impossible to extend the temperature dependence curve for reaction 3 to cover a wide range of temperature, calculations of ΔH_3 from slope measurements were un dependable. The following procedure was employed for obtaining equilibrium data. Samples of vapor from solid boroxine, maintained at a constant temperature, were analyzed mass spectrometrically. The pressure of $B_2H_6(g)$ in the U-tube was then determined manometrically. Diborane was pumped from the system; the samples were reheated and the procedure was repeated. From the ratios of total ion current of boroxine to diborane the partial pressure of $B_3O_3H_3(g)$ was calculated, assuming equal ionization cross sections for the two gases. Equilibrium constants, entropy increments,⁷ and heats of reaction are summarized in Table I. The uncertainty in cross section results in an uncertainty in ΔF° of about $RT \ln 2.0 = 0.4$ kcal./mole. An error which cannot be estimated directly results from uncertainty in the thermodynamic activity of $B_2O_3(s)$, which is presumed to be lower than unity if taken relative to crystalline B_2O_3 . This correction should be such as to lower the absolute values of ΔF_3° and ΔH_3° .

Table I: Thermochemical Data for Reaction 3; Data Obtained in Experiments on the Decomposition of Solid Boroxine

Temp., °K.	$P_{B_2H_6}$, atm.	$I_{boroxine}/$ $I_{diborane}$	$P_{boroxine}$, atm.	$-\Delta F^\circ$, kcal./ mole	$-\Delta S^\circ$, e.u.	$-\Delta H^\circ$, kcal./ mole
258	7.0×10^{-7}	5.5×10^{-4}	3.9×10^{-5}	4.5	27.2	11.6
300	1.2×10^{-1}	6.8×10^{-4}	8.3×10^{-5}	4.9	27.2	13.0
348	4.6×10^{-3}	4.2×10^{-2}	1.9×10^{-4}	4.1	27.2	13.6

Reactions of B_2H_6 with Boric Acid and Amorphous Boric Oxide. Further information related to the stability of gaseous boroxine was obtained by examination of the reactions of B_2H_6 with boric acid and glassy boric oxide. For these experiments B_2H_6 was introduced into an evacuated bulb containing either samples of boric acid or boric oxide in large excess. The boric acid used was Mallinckrodt reagent grade. Boric oxide was prepared by dehydration of fused boric acid and then was powdered. The mass spectrum of reaction products was checked periodically while the reaction vessel was maintained at room temperature. The pressure of B_2H_6 was measured in a simple manometer at the conclusion of a mass spectrometric experiment. For experiments with low pressures of B_2H_6 , the gas pressure was fixed prior to observations by expanding the gas at a previously known pressure into

an auxiliary system of known volume. Mass spectral data for one series of experiments with B_2H_6 and boric acid are listed in Table II. Ion peaks at $m/e = 29$ and 45 have been attributed to $HBOH^+$ and $B(OH)_2^+$, respectively. The low relative intensity of H_2^+ showed that little hydrolysis of B_2H_6 had occurred.

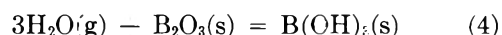
Table II: Typical Mass Spectrum of Products in the Reaction of B_2H_6 with Boric Acid ($P_{B_2H_6} = 4.0$ torr; $T = 300^\circ K.$) (Pertinent Peaks Only)

m/e	Ion peak	Relative intensity
2	H_2^+	27.6
27	$^1B_2H_6^+$	100.0
28	$^1B_2H_6^+ + N_2^+ + CO^+$	2.0
29	H^1BOH^+	0.21
45	$^1B(OH)_2^+$	0.13
83	$^1B_4O_3H_2^+$	0.11

For thermochemical calculations, these data were treated in the same way as that employed for the boroxine decomposition reactions. However, we are now in a better position to define the thermodynamic activity of B_2O_3 in the system. We may write for reaction 3

$$K_{eq} = \frac{(P_{B_2H_6})^{1/2}(a_{B_2O_3})}{P_{B_3O_3H_3}}$$

For reactions of B_2H_6 with $B(OH)_3$, $a_{B_2O_3}$ can be calculated from the standard free energy change of the reaction

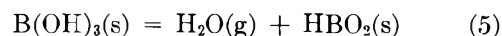


and the partial pressure of H_2O in the system. For reaction 4 we have

$$\Delta F^\circ = \bar{F}_{B_2O_3} + 3\bar{F}_{H_2O} - F^\circ_{B_2O_3} - 3F^\circ_{H_2O} =$$

$$RT \ln a_{B_2O_3} + 3RT \ln a_{H_2O} = -14.0 \text{ kcal.}$$

where the standard state of B_2O_3 is taken relative to the crystalline form. Taking the vapor pressure of H_2O from the reaction



as 2.4×10^{-3} atm.,⁸ we then obtain on setting $\ln P_{H_2O} =$

(7) J.A.N.A. F. Thermochemical Data, Thermal Laboratory, Dow Chemical Co., Midland, Mich., 1960.

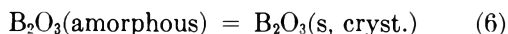
(8) S. Bezzi, *Gazz. Chim. Ital.*, 65, 766 (1935). In a separate experiment the H_2O pressure developed in a closed system containing excess boric acid was measured in a differential manometer. The static pressure as measured against a column of Octoil eventually approached a value of 1.3×10^{-3} atm. Although the rate of attainment of equilibrium is apparently slow at room temperature, the measurement should confirm the value derived from Bezzi's data to at least within a factor of two.

Table III. Thermochemical Data for Reaction 3; $T = 300^\circ\text{K}$., Ionizing Electron Energy = 75 v.

Initial system	$P_{\text{B}_2\text{H}_6}$, atm.	$I_{\text{boroxine}}/I_{\text{diborane}}$	P_{boroxine} , atm.	$-\Delta F^\circ$, kcal./mole	$-\Delta S^\circ$, e.u.	$-\Delta H^\circ$, kcal./mole
$\text{B}_2\text{H}_6(\text{g}) + \text{B}(\text{OH})_3(\text{s})^a$	5.8×10^{-2}	6.9×10^{-4}	4.0×10^{-5}	1.9	27.2	10.1
	5.3×10^{-2}	2.3×10^{-4}	1.2×10^{-5}	2.5	27.2	10.7
	5.3×10^{-2}	2.1×10^{-4}	1.1×10^{-5}	2.6	27.2	10.8
	5.3×10^{-3}	7.8×10^{-4}	4.1×10^{-6}	2.5	27.2	10.7
$\text{B}_2\text{H}_6(\text{g}) + \text{B}_2\text{O}_3(\text{gl})^b$	1.3×10^{-1}	1.1×10^{-3}	1.4×10^{-4}	4.7	21.5	11.1
	5.0×10^{-2}	8.8×10^{-4}	4.4×10^{-5}	5.1	21.5	11.5
	1.2×10^{-2}	1.3×10^{-3}	1.6×10^{-5}	5.3	21.5	11.7
	4.7×10^{-3}	1.8×10^{-3}	8.7×10^{-6}	5.3	21.5	11.7
	1.1×10^{-3}	1.7×10^{-3}	1.8×10^{-6}	5.8	21.5	12.2

^a Standard state taken relative to crystalline B_2O_3 . ^b Standard state taken relative to glassy B_2O_3 .

In $a_{\text{H}_2\text{O}}$, $RT \ln a_{\text{B}_2\text{O}_3} = -3.3$ kcal./mole at 298°K . From the observed pressure data for B_2H_6 and $\text{B}_3\text{O}_3\text{H}_3$ we can then compute ΔF_3° . Results of these computations are given in Table III. For reaction of B_2H_6 with boric oxide we assume that B_2O_3 is amorphous. Equilibrium constants were calculated on this assumption. Thermal data⁷ are available for the reaction



to convert the data from amorphous B_2O_3 to crystalline B_2O_3 . These data are also summarized in Table III. It is evident that the data derived from the boroxine decomposition (Table I) give higher absolute values of ΔH_3° than that derived from data for the B_2H_6 - $\text{B}(\text{OH})_3$ reaction. From these latter data we select a value of $\Delta H_3^\circ = -10.7 \pm 1.5$ kcal./mole. With heats of formation of -305.3^7 and 7.5 kcal./mole for $\text{B}_2\text{O}_3(\text{s})$ and $\text{B}_2\text{H}_6(\text{g})$, this value for ΔH_3° leads to a heat of formation of -291.0 ± 2.0 kcal./mole for $\text{B}_3\text{O}_3\text{H}_3(\text{g})$ at 298°K . With a heat of formation of -301 kcal./mole of glassy B_2O_3 , the data for the $\text{B}_2\text{H}_6(\text{g})$ - $\text{B}_2\text{O}_3(\text{gl})$ reaction lead to a heat of formation of -285.7 kcal./mole for $\text{B}_3\text{O}_3\text{H}_3(\text{g})$. However, since the data in Table I establish an upper limit to the magnitude of ΔH_3° , we place more emphasis on the results of the B_2H_6 - $\text{B}(\text{OH})_3$ reaction. Barring uncertainties in the thermal data for glassy B_2O_3 , the discrepancy in the B_2H_6 - $\text{B}_2\text{O}_3(\text{gl})$ data suggests that the samples of B_2O_3 as prepared by dehydration of boric acid are probably not in a well defined thermodynamic state. However, these data set a firm upper limit on the heat of formation of $\text{B}_3\text{O}_3\text{H}_3(\text{g})$.

Reactions of $\text{B}_3\text{O}_3\text{H}_3(\text{g})$ with $\text{HCl}(\text{g})$. The reactions of gaseous boroxine with HCl were studied by passing HCl - H_2O gas mixtures through an effusion oven of boron nitride (Fig. 2). Reactant gases were generated by evaporation from an aqueous solution of HCl which was held in a glass tube joined to an inlet valve

of the mass spectrometer. The $\text{HCl}/\text{H}_2\text{O}$ ratio in the gas was adjusted by changing the concentration of HCl in this solution. Under the conditions of these experiments $\text{H}_2\text{O}(\text{g})$ reacted completely to give gaseous $\text{B}_3\text{O}_3\text{H}_3$ and a high yield of H_2 . A portion of the mass spectrum of reaction products is shown in Fig. 6. It is evident from the complexity of this spectrum that ion species arise from several molecular precursors. The isotope structure in several of these ion clusters could be used to determine the number of B and Cl

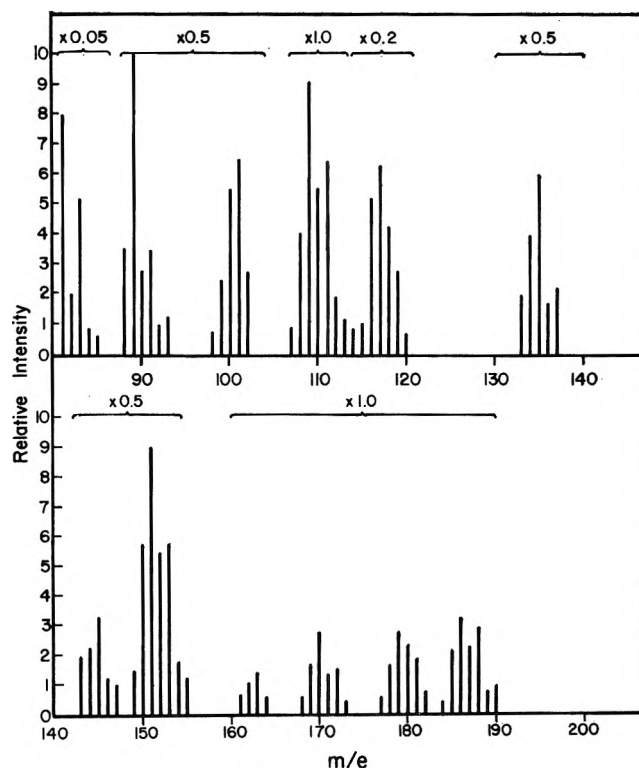
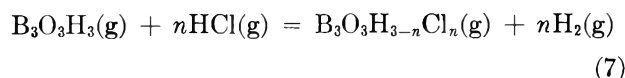


Figure 6. Portion of mass spectrum of products of the reaction of $\text{B}_3\text{O}_3\text{H}_3(\text{g})$ with $\text{HCl}(\text{g})$.

atoms by comparison of experimental intensities with that calculated from statistical contributions from ^{10}B , ^{11}B , ^{35}Cl , and ^{37}Cl isotopes. Groups at $m/e = 115$ –120, 149–156, and 184–192 were shown to arise from the molecules $\text{B}_3\text{O}_3\text{H}_2\text{Cl}$, $\text{B}_3\text{O}_3\text{HCl}_2$, and $\text{B}_3\text{O}_3\text{Cl}_3$, respectively. These groupings bear a resemblance to the mass spectra of the fluoroboroxines where the parent minus hydrogen peaks also predominate.⁹ In experiments with a high inlet ratio of HCl to H_2O $\text{BCl}_3(\text{g})$ was also observed as a product. For study of $\text{B}_3\text{O}_3\text{H}_2\text{Cl}(\text{g})$, it was advantageous to decrease the inlet HCl/ H_2O ratio to cause a decrease in the BCl_3^+ contribution that overlaps the monochloro spectrum. Changes in the HCl/ H_2O ratio also affect the relative abundances of the chloroboroxines.

For thermochemical purposes it is convenient to treat the data for the following general reaction.



To a fair approximation we may set $P_{\text{B}_3\text{O}_3\text{H}_{3-n}\text{Cl}_n}/P_{\text{B}_3\text{O}_3\text{H}_3}$ equal to $I_{\text{B}_3\text{O}_3\text{H}_{3-n}\text{Cl}_n}/I_{\text{B}_3\text{O}_3\text{H}_3}$, where the latter ratio refers to the relative total ion current ratio for chloroboroxine to boroxine. The equilibrium constant for reaction 7 may then be formulated

$$K_{\text{eq}} = \left(\frac{P_{\text{H}_2}}{P_{\text{HCl}}} \right)^n \left(\frac{I_{\text{B}_3\text{O}_3\text{H}_{3-n}\text{Cl}_n}}{I_{\text{B}_3\text{O}_3\text{H}_3}} \right)$$

The pressure ratio of H_2 to HCl was obtained from the relationship

$$P_{\text{H}_2}/P_{\text{HCl}} = 2.1(I_{\text{H}_2}/I_{\text{HCl}+})$$

which has been established previously by calibration.⁹ Equilibrium constants evaluated by this procedure are given in Table IV. The constant involving monochloroboroxine could be determined in the absence of the other two species by reducing the HCl/ H_2O ratio in the reactant gas. The constants for the di- and trichloroboroxines could be determined only when both species were present. The data in Table IV were obtained under conditions where the intensity of $\text{B}_3\text{O}_3\text{Cl}_2\text{H}$ was about four times that of $\text{B}_3\text{O}_3\text{Cl}_3$. A small error is introduced due to the presence of a fragment contribution at $\text{B}_3\text{O}_3\text{Cl}_2^+$ from $\text{B}_3\text{O}_3\text{Cl}_3$. These constants can be judged to be reliable to only within a factor of two. Entropy increments for reaction 7 were computed from tabulated data for HCl and H_2 ,⁷ estimated entropies of boroxine² and trichloroboroxine,⁷ and a correction for symmetry change.

With estimated enthalpy corrections to convert from 1200 to 298°K. we obtain from the ΔH° values in Table IV heats of formation at 298°K. of -314.5 ,

Table IV: Thermochemical Data for the Reaction: $\text{B}_3\text{O}_3\text{H}_3(\text{g}) + n\text{HCl}(\text{g}) = \text{B}_3\text{O}_3\text{H}_{3-n}\text{Cl}_n(\text{g}) + n\text{H}_2(\text{g})$ ($n = 1, 2$, and 3)

n	T , °K.	K	$-\Delta F^\circ$, kcal./mole	$-\Delta S^\circ$, e. u.	$-\Delta H^\circ$, kcal./mole
1	1090	0.381	-2.2	2.98	1.1
1	1150	0.337	-2.5	2.98	0.9
2	1150	0.116	-4.9	8.15	4.4
3	1150	0.035	-7.6	15.50	10.2

-342.2 , and -371.9 kcal./mole for gaseous mono-, di-, and trichloroboroxine, respectively. The over-all uncertainty is about ± 4.0 kcal./mole in each value.

From the mass spectra (Fig. 6) we can also identify by isotope analysis the groupings at $m/e = 176$ –183, 143–147, and 160–165 due to $\text{B}_4\text{O}_4\text{Cl}_2\text{H}^+$, $\text{B}_4\text{O}_4\text{ClH}_2^+$, and $\text{B}_4\text{O}_4\text{FClH}^+$, respectively. The first two presumably arise from the precursors $\text{B}_4\text{O}_4\text{Cl}_2\text{H}_2$ and $\text{B}_4\text{O}_4\text{ClH}_3$. The third is an impurity.

Reactions of $\text{BCl}_3(\text{g})$ with $\text{B}_2\text{O}_3(\text{l})$. It has been known for some time that the volatility of B_2O_3 is enhanced in the presence of BCl_3 .¹⁰ It has generally been assumed that this is due to the formation of $\text{B}_3\text{O}_3\text{Cl}_3(\text{g})$ by analogy to the reaction of BF_3 and B_2O_3 to produce $\text{B}_3\text{O}_3\text{F}_3(\text{g})$. With a minor modification of the effusion assembly (Fig. 2) it was possible to examine the BCl_3 – B_2O_3 reaction at pressures of about 10^{-5} atm. and lower. Similar studies of the BF_3 – B_2O_3 reaction have been reported earlier.¹¹ For the present work Trona BCl_3 was liquefied and redistilled into an evacuated copper tube fitted with a Hoke valve. This all-metal assembly was silver-soldered to a Kovar tube extending from the inlet valve of the effusion cell. The copper tube with BCl_3 was held in a Dry Ice trap to maintain a vapor pressure of about 3.0 torr. The effusion oven was constructed of BN and samples of boric oxide were prepared by dehydration of fused boric acid.

Mass spectra of reaction products were found to depend upon the temperature of the effusion cell. For reaction temperatures between about 800 and 1100°K., the highest value m/e observed corresponds to $\text{B}_3\text{O}_3\text{Cl}_3^+$. For temperatures above 1100°K., the mass spectrum changes and higher molecular weight ion clusters appear. Analysis of the isotope structure for the grouping of $m/e = 210$ to 218 shows clearly that the ionic species is $\text{B}_4\text{O}_4\text{Cl}_3^+$. A typical spectrum of reaction products obtained at about 1200°K. is shown in Table V.

(9) R. F. Porter and W. P. Sholette, *J. Chem. Phys.*, **37**, 198 (1962).

(10) J. Goubeau and H. Keller, *Z. anorg. allgem. Chem.*, **265**, 73 (1951).

(11) R. F. Porter, D. R. Bidinosti, and K. F. Watterson, *J. Chem. Phys.*, **36**, 2104 (1962).

Table V: Mass Spectrum of Products in the Reaction of $\text{BCl}_3(\text{g})$ with $\text{B}_2\text{O}_3(\text{l})$ ($T = 1200^\circ\text{K.}$); 75 v. Ionization Energy

Ion	Relative intensity
BCl_2^+	100.0
$\text{B}_2\text{O}_2\text{Cl}^+$	17.4
B_2OCl_2^+	1.6
BCl_3^+	14.3
$\text{B}_2\text{O}_2\text{Cl}_2^+$	1.1
B_2OCl_3^+	27.1
$\text{B}_3\text{O}_3\text{Cl}_2^+$	44.7
$\text{B}_3\text{O}_3\text{Cl}_2\text{F}^+$	2.2 ^a
B_2OCl_4^+	3.3
$\text{B}_3\text{O}_3\text{Cl}_3^+$	38.9
$\text{B}_4\text{O}_4\text{Cl}_2\text{F}^+$	1.5 ^a
$\text{B}_3\text{O}_2\text{Cl}_4^+$	3.6
$\text{B}_4\text{O}_4\text{Cl}_3^+$	23.3
$\text{B}_4\text{O}_4\text{Cl}_4^+$	0.6

^a Impurity.

The temperature dependence of $\text{B}_3\text{O}_3\text{Cl}_3^+$ on BCl_2^+ (from BCl_3) shows an obvious break and an increase in slope for temperatures above 1100°K. (see Fig. 7). These observations taken collectively indicate that

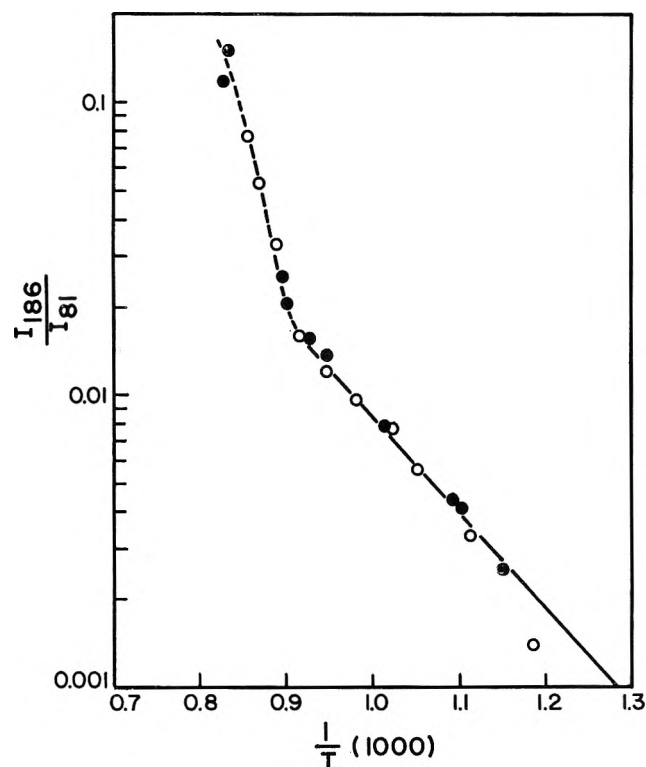
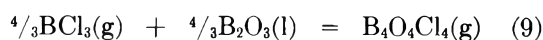


Figure 7. Temperature dependence of $\log I_{\text{B}_3\text{O}_3\text{Cl}_3^+} (m/e = 186)/I_{\text{BCl}_2^+} (m/e = 81)$ as observed for the reaction of $\text{BCl}_3(\text{g})$ with $\text{B}_2\text{O}_3(\text{l})$.

the reaction product in the low temperature range is $\text{B}_3\text{O}_3\text{Cl}_3(\text{g})$ and in the high temperature range is predominantly $\text{B}_4\text{O}_4\text{Cl}_4(\text{g})$. Both species are precursors to $\text{B}_3\text{O}_3\text{Cl}_3^+$. Ion fragmentation of these molecules apparently occurs primarily by loss of Cl , BO_2 , BOCl , and BOCl_2 units. The main reactions may be written



The difference in power dependence in the pressure of BCl_3 for the reactions is to be noted. For high BCl_3 pressures we expect the yield of $\text{B}_4\text{O}_4\text{Cl}_4(\text{g})$ to increase relative to that of $\text{B}_3\text{O}_3\text{Cl}_3(\text{g})$. This pressure effect was also noted by a tendency for the temperature dependence curve of $\text{B}_3\text{O}_3\text{Cl}_3^+/\text{BCl}_2^+$ to flatten off at the highest temperatures. Under these conditions the equilibrium pressure of BCl_3 is low due to the high yield of product and the $4/3$ power dependence becomes more evident.

Enthalpy increments for reactions 8 and 9 were determined from the changes in relative equilibrium constants with temperature (second-law procedure). For reaction 8, one gaseous molecule of reactant produces one molecule of product. Thus in the expression

$$K_{\text{eq}} = P_{\text{B}_3\text{O}_3\text{Cl}_3}/P_{\text{BCl}_3}$$

we may replace the pressure ratio by an ion intensity ratio and a proportionality constant which, for a fixed ionization voltage, is insensitive to changes in ionization current and ion detection efficiency. The low temperature portion of the $I_{\text{B}_3\text{O}_3\text{Cl}_3^+}/I_{\text{BCl}_2^+}$ vs. $1/T$ curve (Fig. 7) was used to determine ΔH_8° . A correction which tends to decrease this value slightly is due to the onset of reaction 9, which has a steeper temperature dependence. This correction is within experimental error and a value of $\Delta H_8^\circ = +16.6 \pm 2.5$ kcal./mole for $T = 1000^\circ\text{K.}$ is obtained.

For reaction 9, the equilibrium constant may be set proportional to $(I_{\text{B}_4\text{O}_4\text{Cl}_4^+})/(I_{\text{BCl}_2^+})^{4/3}$. The temperature dependence of this quantity is shown in Fig. 8. The $\text{B}_4\text{O}_4\text{Cl}_3^+$ ion was selected in preference to $\text{B}_3\text{O}_3\text{Cl}_3^+$ since the latter must be corrected for a contribution from $\text{B}_3\text{O}_3\text{Cl}_3$. The measurements are more accurate for the trimer than for the tetramer since we have a smaller workable temperature range in the latter case. It should also be noted that the pressure of unreacted BCl_3 is small for temperatures above 1300°K. From the curve in Fig. 8 we obtain $\Delta H_9^\circ = 30.8 \pm 5.0$ kcal./mole for an average temperature of 1125°K.

Heats of formation of $\text{B}_3\text{O}_3\text{Cl}_3(\text{g})$ and $\text{B}_4\text{O}_4\text{Cl}_4(\text{g})$ derived from ΔH_8° and ΔH_9° and heats of formation of

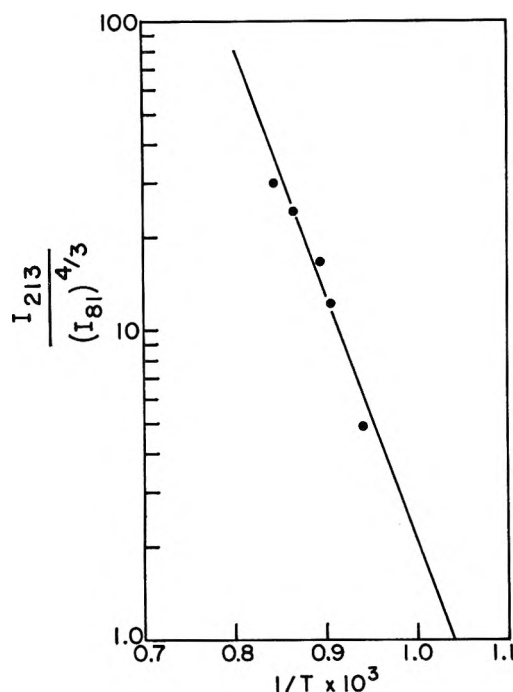


Figure 8. Temperature dependence data for the reaction $\frac{1}{3}\text{BCl}_3(\text{g}) + \frac{1}{3}\text{B}_2\text{O}_3(\text{l}) = \text{B}_4\text{O}_7(\text{g})$. Ion intensities for B_4O_7 and BCl_3 were measured at $m/e = 213$ and $m/e = 81$.

liquid B_2O_3 and BCl_3 are -377.6 ± 3.5 kcal./mole at 1000°K . and -494.0 ± 6.0 kcal./mole at 1125°K ., respectively. When corrected to 298°K ., the former value becomes -378.8 ± 3.5 kcal./mole.

Discussion

A summary of the enthalpy and free energy relationships for species in the boroxine system is illustrated in Fig. 9. The heat of formation of solid boroxine may be taken as -301.7 ± 2.5 kcal./mole at 298°K . Uncertainties in the determination of ΔH° values do not permit us to state with confidence that $\frac{1}{2}\text{B}_2\text{H}_6(\text{g}) - \text{B}_2\text{O}_3(\text{s})$ is definitely below solid boroxine on the enthalpy scale. The order given in Fig. 9 implies that solid boroxine is metastable at all temperatures. The figure shows, however, that $\text{B}_3\text{O}_3\text{H}_3(\text{g})$ is thermodynamically stable with respect to B_2O_3 and B_2H_6 at high temperatures although it may be noted that the pressure of $\text{B}_2\text{H}_6(\text{g})$ is calculated from J.A.N.A.F. data⁷ to be less than 10^{-20} atm. at 1400° when the H_2 pressure over boron is about 10^{-5} atm. Since the present experiments indicate that gaseous $\text{B}_3\text{O}_3\text{H}_3$ at the pressures generated is thermodynamically unstable with respect to $\text{B}_2\text{H}_6(\text{g})$ and $\text{B}_2\text{O}_3(\text{s})$ at room temperature, the persistence of a high concentration of $\text{B}_3\text{O}_3\text{H}_3(\text{g})$ implies a certain degree of kinetic stability. This seems reasonable since the decomposition to B_2H_6 and a solid from the gas phase most probably involves a

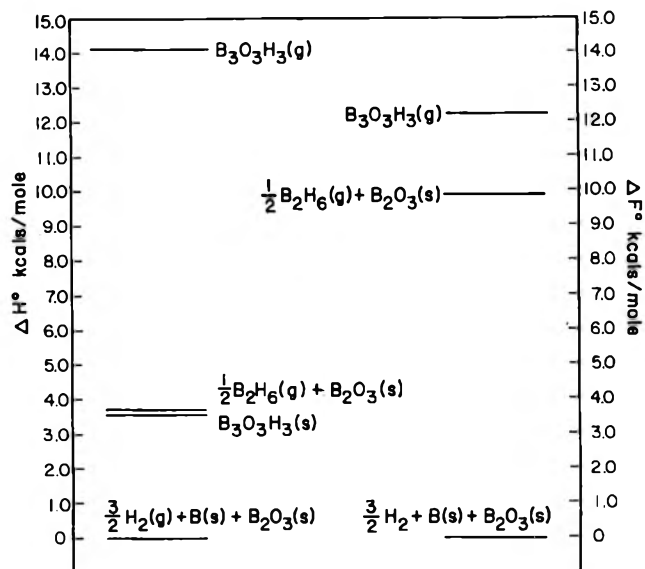
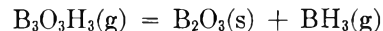


Figure 9. Enthalpy and free energy relationships for solid boroxine and its evaporation products.

complicated mechanism. One possibility is that $\text{BH}_3(\text{g})$ is an intermediate. With the available heats of formation of $\text{B}_2\text{O}_3(\text{s})$ and $\text{BH}_3(\text{g})$ ⁷ we calculate for the reaction



$\Delta H^\circ_{298} = +3.7$ kcal./mole. Condensation of the gas thus appears to provide a means by which the equilibrium condition can be attained. Our heat of formation for $\text{B}_3\text{O}_3\text{H}_3(\text{g})$ is less negative than that previously reported² from considerations of the high temperature reaction of H_2 on $\text{B}-\text{B}_2\text{O}_3$ mixtures (*i.e.*, -302 ± 7 kcal./mole). The more negative value implies that $\text{B}_3\text{O}_3\text{H}_3(\text{g})$ should be in a very high yield in the equilibrium reaction of $\text{B}_2\text{H}_6(\text{g})$ and $\text{B}_2\text{O}_3(\text{s})$. On the other hand, the less negative value implies $\text{B}_3\text{O}_3\text{H}_3(\text{g})$ will not be present in very high yields in the reactions at high temperatures. This discrepancy cannot be accounted for by uncertainties in the thermal data for $\text{B}_2\text{H}_6(\text{g})$ or $\text{B}_2\text{O}_3(\text{s})$. In our calculation we have used for the heat of formation of $\text{B}_2\text{H}_6(\text{g})$ the value of $+6.73$ kcal./mole (relative to amorphous boron) as determined by Prosen and co-workers.¹² Gunn and Green¹³ have recently obtained a value of $+5.0 \pm 0.4$ kcal./mole. This latter value raises the absolute value for the heat of formation of $\text{B}_3\text{O}_3\text{H}_3(\text{g})$ by about 0.9 kcal./mole. The major source of the discrepancy apparently is in the $T\Delta S$ term assumed in the reaction

(12) B. J. Prosen, W. E. Johnson, and F. Y. Pergiel, *J. Res. Natl. Bur. Std.*, **61**, 247 (1958).

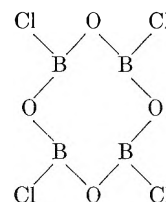
(13) S. R. Gunn and L. G. Green, *J. Phys. Chem.*, **65**, 779 (1961).

of $H_2(g)$ with $B-B_2O_3$ mixtures at temperatures near $1400^\circ K$. Uncertainties in the equilibrium constant cannot alone account for the differences. Most likely the absolute entropy of gaseous boroxine is higher at $1400^\circ K$. than previously assumed. This suggests the need for more complete structural data for the molecule. In a recent communication Lee, Bauer, and Wiberley¹⁴ have reported that gaseous boroxine is produced in explosions of B_5H_9 and O_2 . The infrared spectrum obtained by these workers is consistent with D_{3h} symmetry for the boroxine ring. It is also interesting to note that $B_3O_3H_3(g)$ produced at pressures suitable for infrared detection decomposes in a matter of minutes to $B_2H_6(g)$ and B_2O_3 . These results also are in accord with our observations of the thermodynamic stability of $B_3O_3H_3(g)$.

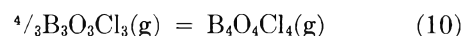
Comparison of the heat of formation of $B_3O_3Cl_3(g)$ determined from $HCl-B_3O_3H_3$ equilibria with that from determined data for the $BCl_3-B_2O_3$ reaction is satisfactory although the latter value should be considered the more reliable.

The importance of $B_4O_4Cl_4$ relative to $B_3O_3Cl_3$ is surprising in view of previous observations concerning the stabilities of the trimeric species $B_3O_3F_3$ ^{11,15,16} and $B_3O_3(OH)_3$.¹⁷ A re-examination of the $H_2O(g)-B$ system has revealed the existence of $B_4O_4H_4(g)$ as a product at a temperature of $1260^\circ K$. However, the highest intensity ratio of $B_4O_4H_3^+/B_3O_3H_2^+$ was only about 7.0×10^{-3} . Although it may be reasonable to assume that the trimeric boroxine structure is planar, it seems unlikely that the tetrameric molecule could maintain a planar arrangement due to strain resulting from the increase in bond angles. Most probably the structure is intermediate between a

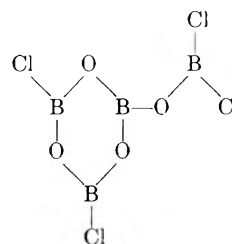
planar configuration and one in which the boron atoms are tetrahedrally arranged, as in B_4Cl_4 .¹⁸



The thermal data indicate that the reaction



is endothermic to the extent of about 8 kcal./mole. This may be an indication of weakening of bond strength accompanying an increase in ring size. Other possible structures, however, including



cannot be eliminated on the basis of the present observations.

- (14) G. H. Lee, W. H. Bauer, and S. E. Wiberley, *J. Phys. Chem.*, **67**, 1742 (1963).
- (15) D. L. Hildenbrand, L. P. Theard, and A. M. Saul, XVIII International Congress of Pure and Applied Chemistry, Montreal, 1961.
- (16) M. Farber, *J. Chem. Phys.*, **36**, 661 (1962).
- (17) D. J. Meschi, W. A. Chupka, and J. Berkowitz, *ibid.*, **33**, 530 (1960).
- (18) M. Atoji and W. N. Lipscomb, *ibid.*, **21**, 172 (1953).

Kinetics of the Reactions of Elemental Fluorine with Zirconium Carbide and Zirconium Diboride at High Temperatures

by A. K. Kuriakose and J. L. Margrave

Departments of Chemistry, University of Wisconsin, Madison, Wisconsin, and Rice University, Houston, Texas (Received August 12, 1963)

Kinetic studies have been made on the reactions of elemental fluorine with zirconium carbide and zirconium diboride up to about 950° and at various fluorine partial pressures using a thermogravimetric method. At a fluorine partial pressure of 31 torr (in helium) and between 278 and 410°, zirconium carbide forms soft and fluffy scales of zirconium tetrafluoride and the reaction rate is linear. An activation energy of 22 kcal./mole is calculated for this process. Zirconium diboride under the above-mentioned conditions does not react to any measurable extent. Above 700° both ZrC and ZrB₂ react with fluorine to form only volatile products and the samples lose weight during fluorination. The reaction rates are again linear except for a slight decrease due to the change in surface area of the specimens with time. With a fluorine partial pressure of 2.8 torr, the activation energies for fluorination of both ZrC and ZrB₂ above 700° are essentially zero. The rate-determining process above 700° is probably only the diffusion of fluorine to the sample surface through the gaseous reaction products. For ZrC at 350° and for ZrB₂ at 700° the rate of fluorination is approximately proportional to the square root and for ZrC at 700° it is proportional to the 1.5 power of the fluorine partial pressure.

Introduction

Although there have been extensive studies of rates of oxidation and nitridation of metals and compounds, there have been very few studies of reaction rates with fluorine. Haendler, *et al.*,¹⁻⁵ have, however, investigated the reaction of fluorine with several metals and some of their compounds in an attempt to synthesize and characterize metallic fluorides. They observed that fluorine reacts with zirconium metal above 190° and that the fluoride coating prevents complete reaction. They also noticed that zirconium dioxide does not react with fluorine at 100°, but converts to zirconium tetrafluoride above 250°. There have also been several other reports⁶⁻¹⁷ on the interaction of fluorine under different conditions, with various types of materials. As for kinetic studies with metals, the reactions of fluorine with copper^{18,19} and nickel²⁰⁻²² have been worked out in some detail.

The reactions between fluorine and ZrC and ZrB₂ are complicated because of the variety of possible solid and gaseous products. Also, ZrF₄ sublims above 600°. Zirconium carbide is known to be decomposed by

halogens and oxidizing agents,²⁶ in general, and hence, a rather vigorous exothermic reaction is to be expected with fluorine. However, no previous data are available on the rates of reaction of fluorine with ZrC and ZrB₂.

- (1) H. M. Haendler and W. J. Bernard, *J. Am. Chem. Soc.*, **73**, 5218 (1951).
- (2) H. M. Haendler, W. L. Patterson, Jr., and W. J. Bernard, *ibid.*, **74**, 3167 (1952).
- (3) H. M. Haendler, S. F. Bertram, R. S. Becker, W. J. Bernard, and S. W. Bukata, *ibid.*, **76**, 2177 (1954).
- (4) H. M. Haendler, L. H. Towler, E. F. Bennett, and W. L. Patterson, Jr., *ibid.*, **76**, 2178 (1954).
- (5) H. M. Haendler, S. F. Bertram, W. J. Bernard, and D. Kippax, *ibid.*, **76**, 2179 (1954).
- (6) R. M. Gunzik and C. E. Feider, NACA-TN-3333, September, 1954.
- (7) L. Stein and R. C. Vogel, ANL-5441, May, 1955.
- (8) H. G. Price, Jr., and H. W. Douglass, NACA-RM-E57 G18, November, 1956.
- (9) J. Fischer and R. K. Steunenberg, *J. Am. Chem. Soc.*, **79**, 1876 (1957).
- (10) M. J. Steindler and R. C. Vogel, ANL-5632, January, 1957.
- (11) G. L. Ericson, W. K. Boyd, and P. D. Miller, NP-6729, April, 1958.

Apparatus and Experimental Procedure

The arrangement of the fluorination furnace is shown in Fig. 1. The reaction chamber consisted of a nickel tube 30.5 cm. long with 2.5 cm. i.d. and 0.3 cm. wall thickness. Heating was done by a Kanthal wire-wound furnace, and the temperature measured with a Pt vs. Pt-10% Rh thermocouple introduced from the bottom of the furnace tube through a 0.6-cm. nickel tube, closed at the top end. The metal joints of the furnace tube were made gas-tight with Teflon gaskets.

The flow of fluorine gas was regulated by a Matheson fluorine pressure reducing valve and metered by a Fisher-Porter borosilicate glass flow meter containing a sapphire float which was calibrated periodically. The fluorine was mixed with purified dry helium gas, metered by another flow meter, in various proportions to obtain the desired fluorine partial pressures. The excess fluorine from the exit was allowed to react with the ammonia fumes over a concentrated NH_4OH solution.

Before commencing the reaction, the nickel furnace tube was passivated by treating it with pure fluorine at 500–600° to form a protective coating of nickel

fluoride. The process was carried out during a period of 3 days by intermittently admitting fluorine for 2 or 3 hr. each time. Also, before starting any run, a mixture of fluorine and helium was passed through the already passivated furnace tube, heated at the desired temperature for nearly 0.5 hr. to 1 hr. as required, until fluorine was detected coming out of the combustion tube in large amounts, as indicated by use of KI paper. After passivation at the required temperature, the system was evacuated and flushed with helium several times, and the sample to be fluorinated was suspended from the helical spring by means of a 0.18-mm. nickel wire, in the atmosphere of flowing helium gas. After about 10 min., fluorine was admitted, along with the helium, and a timer started simultaneously. The partial pressure of fluorine was calculated from the individual flow rates of fluorine and helium at atmospheric pressure. Any reaction of the fluorine with the nickel suspension wire was neglected on the grounds that the surface area of the nickel wire exposed in the hot zone of the furnace was negligibly small compared to the relatively large area of the specimen. The change in extension of the spring was observed by means of a cathetometer and the smallest measurable weight change was 0.05 mg. No temperature correction on the spring was needed since it was maintained at constant (room) temperature. Readings were taken at suitable intervals of time. The silica spring was protected from attack by fluorine by having a blanket of dry nitrogen in the form of a slow, steady

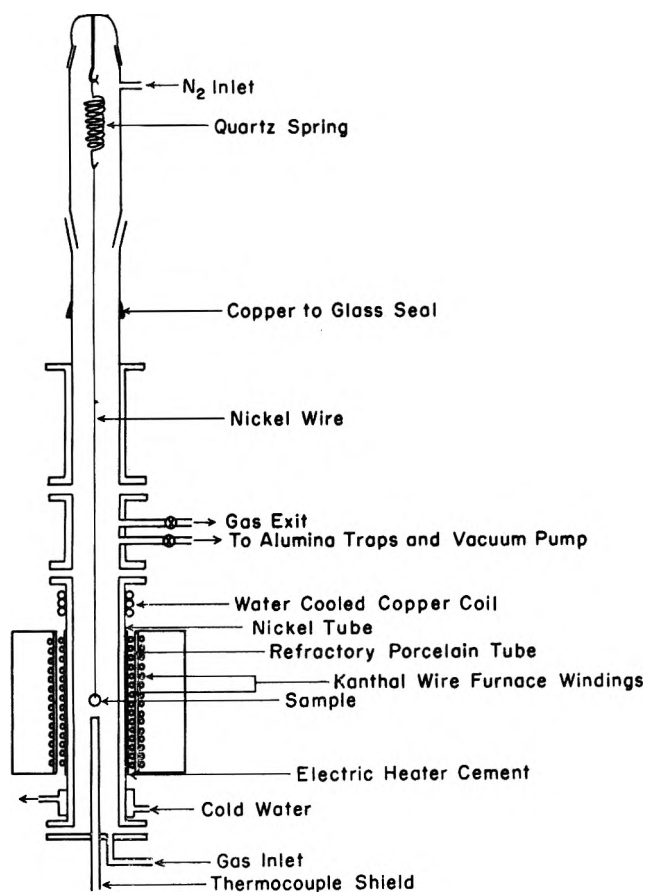


Figure 1. Fluorination furnace set-up.

- (12) E. L. White and F. W. Fink, "Proceedings of the Propellant Thermodynamics and Handling Conference," Special Report 12, Engineering Experimental Station, The Ohio State University, 1959, pp. 161–181.
- (13) C. F. Hale, E. J. Barber, H. A. Bernhardt, and K. E. Rapp, K-1459, September, 1960.
- (14) F. W. Fink, TID-5935, May, 1960.
- (15) R. B. Jackson, Final Report NP-8845, Allied Chemical Corp., General Chemical Division, New York, N. Y., 1960.
- (16) F. W. Fink, TID-13206, June, 1961.
- (17) A. P. Litman and A. E. Goldman, ORNL-2832, June, 1961.
- (18) P. M. O'Donnell and A. E. Spakowski, NASA Technical Note D-768, April, 1961.
- (19) P. E. Brown, J. M. Crabtree, and J. F. Duncan, *J. Inorg. Nucl. Chem.*, **1**, 202 (1955).
- (20) R. K. Steunenberg, L. Seiden, and H. E. Griffin, ANL-5924 (1958).
- (21) R. L. Jarry and W. H. Gunther, ANL-6477 (1961).
- (22) C. F. Hale, E. J. Barber, H. A. Bernhardt, and K. E. Rapp, AECD-4292, July, 1959.
- (23) K. A. Sense, M. J. Snyder, and J. W. Klegg, Rept. AECD-BMI 3708 (1953).
- (24) K. A. Sense, M. J. Snyder, and R. B. Filbert, *J. Phys. Chem.*, **58**, 995 (1954).
- (25) K. A. Sense, R. E. Bowman, R. W. Stone, M. J. Snyder, and R. B. Filbert, Rept. BMI 1064 (1956).
- (26) P. Schwarzkopf and R. Kieffer, in "Refractory Hard Metals," The Macmillan Company, New York, N. Y., 1953, p. 95.

stream sent from the top of the system. At the conclusion of the run, the fluorine was cut off and helium and nitrogen continued to flow until the exit gas was free of fluorine.

The zirconium carbide and zirconium diboride samples, in the form of small disks weighing about 0.2 to 0.4 g., were cut from electron-beam melted rods and polished by grinding on abrasive cloth. The ZrC was 99.5+ % pure with traces of Ti, Si, B, Fe, and N in the order of 0.1% and less and O, Al, Sn, Mg, Ca, Mn, Cu, Mo, Ag, Hf, and Pb in the order of 0.01 to 0.001%. The zirconium diboride was of composition $ZrB_{1.95}$ with 1.7% Hf and 200 p.p.m. of carbon as impurities. The polished ZrB_2 had a shining mirror-like appearance while the ZrC had a shining metallic gray color. Surface areas of the specimens were determined by measuring the geometrical dimensions.

Results and Discussion

A preliminary examination showed that ZrC would burn in fluorine or in an atmosphere rich in fluorine, at about 250–300°. On the other hand, ZrB_2 did not catch fire in pure fluorine at a pressure of 1 atm., but it broke into bits at about the same temperature. Thus, the fluorination of these materials was examined at low fluorine partial pressures where the reactions could be effectively controlled.

Reaction between ZrC and Fluorine at 278–410°. Initial experiments with ZrC and F_2 under a low partial pressure of F_2 (31 mm.) indicated that the reaction was rather smooth at about 300° with a regular increase in weight. The reproducibility of the results was checked at 300° and found to be within 20%. With the same fluorine partial pressure, the reaction was conducted at various temperatures ranging from 278 to 410°. Above 410° the reaction rate was too fast to measure by this technique. The weight increase per unit area of ZrC with time at the various temperatures is illustrated in Fig. 2. There is no question regarding the linearity of the reaction with time and since the extent of reaction is small, the area change in the specimens is not of any importance. Abrupt breaks at and above 334° indicate the crumbling away of part of the fluoride layer formed on the ZrC. Thick scales of ash-gray zirconium fluoride were observed on the surface of the ZrC after reaction. The adhesion of the scales was very poor and the material was soft and fluffy. The reacted samples had a sandwich appearance and their volumes had increased markedly because of the fluffiness of the ZrF_4 formed. The scales were apparently uniform and there were no visible cracks on them except at the edges, where the inner core was practically naked. Viewed under a microscope, the layers were made up of fine

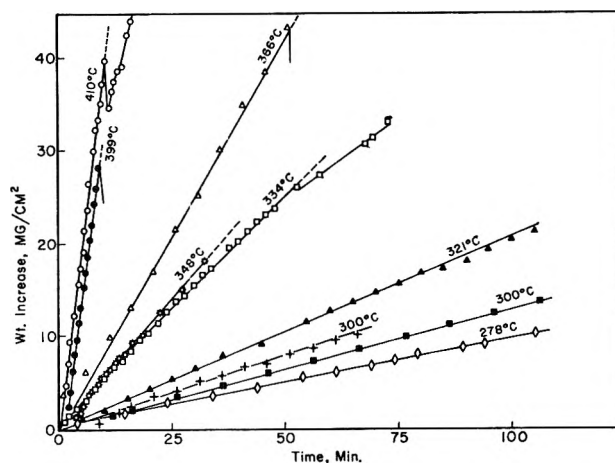


Figure 2. Linear plot for ZrC- F_2 reaction; fluorine partial pressure, 31 mm.

sugar-like crystals uniformly formed without any cracks. It appears that the unreacted ZrC was in direct contact with the fluorine atmosphere, in spite of the fluoride coating, and thus showed a linear rate of reaction.

It is not possible to say whether either zirconium or carbon in the system is preferentially attacked by fluorine, since the gaseous products were not analyzed. X-Ray analysis of the inner core and the outer layer might show some evidence regarding this question; the coating gave an X-ray pattern characteristic of ZrF_4 . The fact that the inner core is rough and black when once the fluoride scales are removed suggests the possibility that the Zr is reacting faster than the carbon.

From the slopes of the straight lines in Fig. 2, the linear rate constants for the reactions were estimated, not taking into account the volatile products. The values obtained are displayed in Table I. The activation energy computed by a least square method is 22.1 ± 1.6 kcal./mole.

Table I: Linear Rate Constants for the ZrC- F_2 Reaction at Various Temperatures (Fluorine Partial Pressure, 31 mm.)

Temp., °C.	Linear rate constant, k_1 , mg./cm. ² /min.
278	0.0995
300	0.1282
300	0.1515
321	0.2010
334	0.5069
348	0.5526
366	0.8450
399	3.4545
410	3.6786

$$\Delta E_a = 22.1 \pm 1.6 \text{ kcal./mole.}$$

Fluorination of ZrB_2 and ZrC above 600° . Zirconium diboride is apparently not attacked by fluorine under a low partial pressure (31 mm. of F_2 ; 709 mm. of helium) below 500° . Since zirconium fluoride is very volatile above 700° , practically no fluoride coating is formed on the boride or carbide surfaces above this temperature and hence the samples are found to lose weight during fluorination. The loss in weight can be measured and used for calculating the rates of the reactions. Figures 3 and 4 present plots of the weight loss/cm.² of the samples with time in minutes, at 600 – 900° for ZrB_2 and 700 – 950° for ZrC , respectively, with a fluorine partial pressure of 2.7 mm. of Hg (736 mm. of helium). The slight curvature in the lines is assumed to be due to the change in surface area of the specimens with the extent of corrosion. Hence, the rate constants for these reactions were calculated at zero time on the basis of a linear rate law, using the equation

$$\Delta w/A = B + Ct - Dt^2 + Et^3 \quad (1)$$

where Δw is the weight loss; A , the initial surface area; t , the time; and B , C , D , and E are constants with C being the linear rate constant $k_{1,t=0}$.

Equation 1 was derived assuming that the length and radius of the cylindrical specimen vary linearly with time, as treated subsequently.

The linear rate of reaction at the surface of a cylinder may be expressed by the equation

$$\frac{d(\Delta w)}{dt} = k2\pi r(r + l) \quad (2)$$

where Δw represents the weight change; k , the linear rate constant; and r and l , the radius and length of the cylinder, respectively.

Assuming that the cylinder is corroded at constant rate from all sides

$$\frac{dr}{dt} = \frac{1}{2} \frac{dl}{dt} = k' \quad (3)$$

where k' is the rate constant for the change in radius and length. Integrating (3)

$$r = r_0 - k't \quad (4)$$

$$l = l_0 - 2k't \quad (5)$$

where r_0 and l_0 represent the initial radius and length of the cylinder. Substituting (4) and (5) in (2)

$$\frac{d(\Delta w)}{dt} = k2\pi(r_0 - k't)(r_0 + l_0 - 3k't) \quad (6)$$

Integrating (6) with respect to t

$$\Delta w = k[2\pi r_0(r_0 + l_0)t - \pi k'(4r_0 + l_0)t^2 + 2\pi k'^2 t^3] + B \quad (7)$$

where B is a constant.

Equation 7 is of the same form as (1) and

$$\left[\frac{d(\Delta w)}{dt} \right]_{t=0} = k[2\pi r_0(r_0 + l_0)] \quad (8)$$

and the value within the brackets in (8) is the initial surface area of the cylinder.

The values for the zero-time rate constants were calculated with a Control Data 1604 computer and they are presented in Tables II and III.

The reaction rates of both ZrB_2 and ZrC with fluorine were not strongly temperature dependent above 600° and the activation energies calculated were essentially zero. Among the possible explanations for this unusual behavior are: (1) there might be extensive surface heating because of the highly exothermic reaction so that all the processes are really occurring at some high

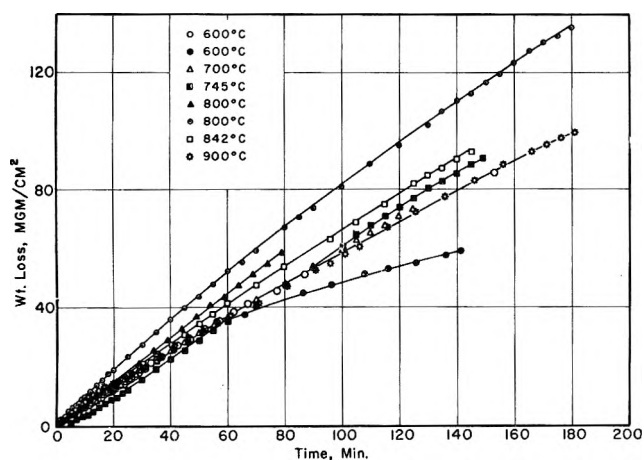


Figure 3. ZrB_2 - F_2 reaction at various temperatures, linear plot; fluorine partial pressure, 2.7 mm.

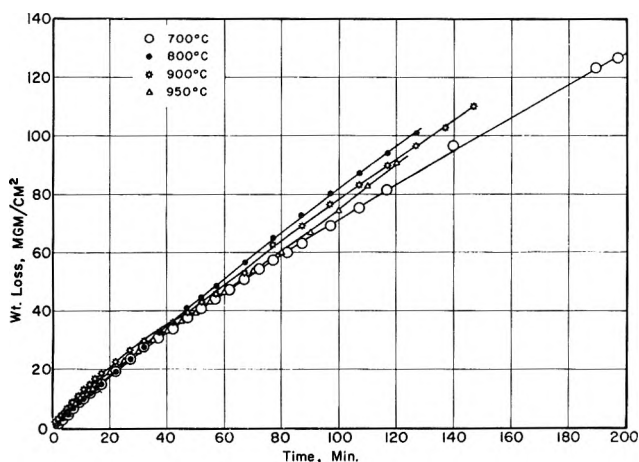


Figure 4. ZrC - F_2 reaction at 700 – 950° ; fluorine partial pressure, 2.7 mm.

Table II: Linear Rate Constants at Zero-Time ($k_{1,t=0}$) ZrB₂-F₂ Reaction at 600-900° ($P_{F_2} = 2.7$ mm.)

Thermo-couple temp., °C.	Corrected surface temp., °C.	Apparent $k_{1,t=0}$, mg./cm. ² /min.	Corrected rate constant, mg./cm. ² /min.
600	...	0.6028	...
600	...	0.7734	...
700	720	0.6354	0.8226
745	765	0.5313	0.7219
800	825	0.9435	1.0101
800	825	0.6842	0.7642
842	867	0.7265	0.8982
900	925	0.5916	0.7468

Table III: Linear Rate Constants at Zero-Time ($k_{1,t=0}$) ZrC-F₂ Reaction at 700-950° ($P_{F_2} = 2.7$ mm.)

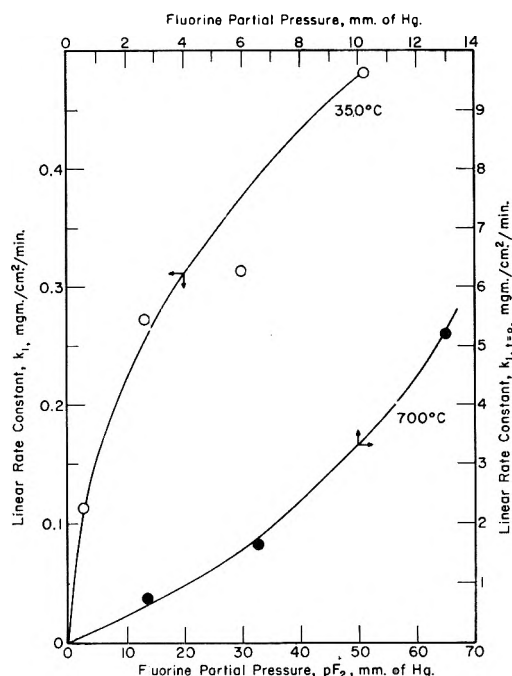
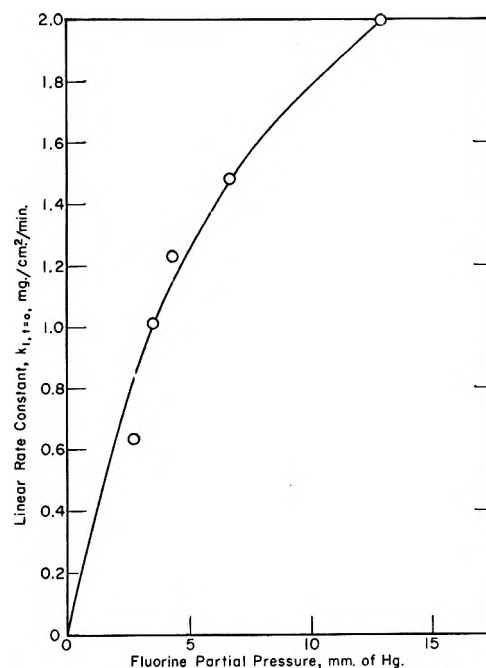
Thermo-couple temp., °C.	Corrected surface temp., °C.	Apparent $k_{1,t=0}$, mg./cm. ² /min.	Corrected rate constant, mg./cm. ² /min.
700	715	0.7565	0.9112
800	815	0.8764	0.9756
900	920	0.9058	1.0466
950	970	0.9697	1.0480

temperature essentially independent of the furnace temperature recorded by the thermocouple; (2) the rate of reaction might be limited by the rates of diffusion of F₂ to the surface and/or products (ZrF₄, BF₃, and CF₄) from the surface; and (3) the observed weight change could be too fast because of reaction of the nickel suspension wire or too slow because of deposition of NiF₂ from the walls and sleeve or ZrF₄ from the sample on the wire. Therefore, several special experiments were performed.

In order to decide if the temperature measured with the thermocouple was close to the actual temperature of the sample, the apparatus was modified by attaching a glass window to the bottom of the furnace to allow observation of the actual surface temperature of the specimen during the reaction, by means of an optical pyrometer. The entire kinetic runs were not repeated, but the steady-state temperatures of samples before and after admitting fluorine were measured. As soon as the fluorine was introduced, there was a sudden rise in temperature, 15 to 20° in the case of ZrC and 20 to 25° for ZrB₂, at a fluorine partial pressure of 2.7 torr, in the temperature range 700-900°. The temperature remained practically constant during the reaction. The same sample or samples of nearly identical dimensions were used in each case. The corrected tem-

peratures for various runs are given in the second column of Tables II and III.

A quantitative evaluation of the rate of reaction of the nickel suspension wire with fluorine showed that

Figure 5. The effect of fluorine partial pressure on the ZrC-F₂ reaction.Figure 6. Effect of fluorine partial pressure on the ZrB₂-F₂ reaction at 700°.

it was negligible in these experiments. The deposition of nickel fluoride and/or ZrF_4 from the walls of the nickel furnace tube or the sample, on the cooler parts of the nickel wire, was appreciable at all temperatures above 600° and a correction was applied for the calculated rate constants by assuming the rate of deposition to be linear with time. The linear rate constant for the deposition was calculated by carefully removing the deposit from the nickel wire and weighing it at the end of each run. This value was added to the value $k_{1,t=0}$ in order to obtain the corrected rate constant. The resultant rate constants for ZrB_2 and ZrC are recorded in the last column of Tables II and III.

The activation energies for the reaction of fluorine with ZrC or ZrB_2 are practically zero in the temperature range 600 – 950° , but the reaction is not explosive at the low fluorine partial pressure used. The likely explanation is: (1) that the reaction rate is controlled only by the diffusion of fluorine in the gas phase to the surface of the samples which involves a very low or no activation energy; and (2) that the concentration of fluorine at the surface is insufficient for an explosive reaction.

The Effect of Fluorine Partial Pressure on the Fluorination of ZrC and ZrB_2 . The nature of the dependence of the rate of reaction of fluorine with ZrC on the fluorine partial pressure was investigated at two tem-

peratures, 350 and 700° , since the mechanism of fluorination at these two temperatures is distinctly different. For ZrB_2 the effect of fluorine partial pressure was studied only at 700° .

The actual temperatures of the reactions at 700° under various fluorine partial pressures were not identical. The temperature rise in each case was proportional to the fluorine partial pressure, but it did not affect the results since the reactions were almost independent of temperature.

The rate constants for the reactions were calculated as indicated earlier and the results are graphically presented in Fig. 5 and 6 for ZrC and ZrB_2 , respectively. For ZrC at 350° and for ZrB_2 at 700° , the rate of fluorination is approximately proportional to the square root, and for ZrC at 700° it is proportional to the 1.5 power of the fluorine partial pressure.

Acknowledgments. The authors are pleased to acknowledge the financial support of this work by the United States Air Force under a subcontract with A. D. Little, Inc., and administered by Dr. Leslie A. McClaine. Samples and analyses were furnished through the courtesy of Dr. George Feick and computer work was conducted in the Wisconsin Numerical Analysis Laboratory with the assistance of Mr. Thomas F. Jambois. The fluorination furnace was originally designed and constructed by Dr. T. C. M. Pillay.

A Study of Selected Ions in the Mass Spectra of

Benzenethiol and Deuterated Benzenethiol

by D. G. Earnshaw, G. L. Cook, and G. U. Dinneen

Laramie Petroleum Research Center, Bureau of Mines, U. S. Department of the Interior, Laramie, Wyoming¹
(Received August 12, 1963)

Partial mass spectra are presented for benzenethiol, C_6H_5SH , and deuterated benzenethiol, C_6H_5SD . The changes in ion intensities that result from deuterium labeling were studied to determine the structure of the parent ion before fragmentation. A seven-membered ring structure for the parent ion is proposed as precursor for some of the ions studied, whereas the six-membered ring structure for the parent is proposed as precursor for the other ions. Appearance potentials were obtained for several product ions from deuterated benzenethiol, C_6H_5SD , and were used to determine heats of formation of the ions and establish processes by which they are formed. The parent ion is the only intermediate between the molecule, C_6H_5SD , and the product ions at $m/e = 34, 45, 46, 67, 77, 84, 85,$ and 109 . A proposed process for the formation of each of the ions is discussed. When ring cleavage of the parent ion takes place, ring closure in one of the fragments also takes place.

Introduction

Part of the research done by the Bureau of Mines is concerned with sulfur compounds in petroleum and shale oil. Mass spectrometry has had an important role in this work.^{2,3} A study of benzenethiol is reported in this paper as an addition to this work.

Mass spectra of benzenethiol (C_6H_5SH) and deuterated benzenethiol (C_6H_5SD) were compared to determine which fragment ions contained the deuterium. From this information the structure of the precursor ion can be postulated. For example, the parent ion of benzenethiol might expand to a seven-membered ring before fragmentation, similarly to the ring expansion that has been proposed for alkylbenzenes⁴ and alkylthiophenes.³

Appearance potentials of selected ions were measured to determine heats of formation using the thermochemical equation

$$\Delta H_f (\text{product ion}) = \Delta H_f (\text{precursor}) + \Delta H_f - \Delta H_f (\text{neutral fragment})$$

where ΔH_f is heat of formation and ΔH is heat of reaction, which is equal to the appearance potential of the product ion minus the appearance potential of the precursor. It was assumed that substituting deuterium

for hydrogen in benzenethiol had a negligible thermochemical effect. The proposed structure of the product ion, proposed structure of the neutral fragment, and the process of their formation were accepted if the value of ΔH_f (product ion), determined from the equation, agreed with the value of ΔH_f taken from the literature for the same ion.

Experimental

The benzenethiol used in this study was a standard sample prepared as a part of the work of American Petroleum Institute Research Project 48A at Laramie, Wyo. The deuterated benzenethiol was prepared by shaking 5 ml. of the benzenethiol three successive times with equal volumes of D_2O . Conversion from C_6H_5SH to C_6H_5SD was 95% as determined by low-ionizing-voltage mass spectrometry and nuclear magnetic resonance spectrometry.

The spectra of the thiols were obtained at 70 v. using a Consolidated Electrodynamics Corp. 21-103C mass

- (1) The work upon which this report is based was done under a cooperative agreement between the Bureau of Mines, U. S. Department of the Interior, and the University of Wyoming.
- (2) I. W. Kinney and G. L. Cook, *Anal. Chem.*, **24**, 1391 (1952).
- (3) G. L. Cook and N. G. Foster, *Proc. Am. Pet. Inst., Sect. III*, **41**, 199 (1961).
- (4) P. N. Rylander, S. Myerson, and H. M. Grubb, *J. Am. Chem. Soc.*, **79**, 842 (1957).

spectrometer with the sample inlet system at room temperature. Prior to obtaining the spectrum of the labeled thiol, the inlet system was conditioned to reduce the deuterium-hydrogen exchange. The spectrum of the C_6H_5SD was calculated by removing the contribution of C_6H_5SH from the spectrum of the impure sample.

Appearance potentials were obtained with repellers set at 2 v. and with the ionizing voltage meter replaced by a Hickok Model 534 voltmeter having 0-20 and 0-50 v. ranges. Appearance potential curves were obtained using a method similar to that of Lossing, Tickner, and Bryce⁵ except that the ionizing voltage which gave 0.1% ion abundance was taken as the appearance potential instead of the voltage that gave 1.0%.

The ionizing-voltage scale was calibrated using benzene as the primary standard. A mixture of benzene and benzenethiol was run, and appearance potential curves were plotted for both parent ions. The voltage scale was shifted so that the parent ion of benzene appeared at 9.2 e.v.⁶ The appearance potential of the benzenethiol parent ion then was read directly from the voltage scale. In subsequent runs to determine the appearance potential of each fragment ion from C_6H_5SD , the appearance potential of the parent ion was used as a secondary standard.

Results

Partial spectra of C_6H_5SH and C_6H_5SD are shown in Table I. Columns two and four show the polyisotopic patterns using the parent peaks as a base. Columns three and five show the monoisotopic patterns after correcting the spectra for the isotopes C^{13} , S^{33} , and S^{34} .

All of the ions produced by a given process from C_6H_5SH appear at a single m/e , but some of the ions produced by the same process from C_6H_5SD appear at the next higher m/e because they contain a deuterium atom in the place of hydrogen. As the number of ions so displaced could not be determined directly, the method of Dibeler and Mohler⁷ was used to determine the contribution of nondeuterated and deuterated ions to each selected m/e in the spectrum of C_6H_5SD . These data then were regrouped as shown in Table II to show the intensities for ions from C_6H_5SH and intensities for the same ions from C_6H_5SD divided into a non-deuterated and a deuterated portion.

The appearance potentials, proposed processes, and ΔH_f values for selected product ions from C_6H_5SD are shown in Table III. The accuracy of the values shown in the second column is estimated at ± 0.2 e.v. The determined values of ΔH_f (product ion) shown in Table III were obtained from the thermochemical equation

Table I: Partial Spectra of C_6H_5SH and C_6H_5SD

m/e	Relative ion intensities			
	C_6H_5SH		C_6H_5SD	
	Polyisotopic	Monoisotopic	Polyisotopic	Monoisotopic
15	0.47	0.47	0.29	0.29
16	0.03	0.02	0.17	0.17
27	1.76	1.74	1.80	1.78
28	0.07	0.04	0.39	0.35
32	1.81	1.81	1.79	1.79
33	2.07	2.05	0.30	0.29
34	0.47	0.37	2.76	2.68
35	0.12	0.03	0.49	0.45
38	5.64	5.50	5.12	4.98
39	15.14	14.96	11.20	11.04
40	0.93	0.44	3.89	3.53
45	11.27	11.26	9.59	9.48
46	0.35	0.10	2.52	2.31
49	1.88	1.87	2.08	2.07
50	10.52	10.43	12.36	12.25
51	14.02	13.56	16.36	15.83
52	1.28	0.68	2.25	1.52
65	10.38	10.36	6.13	6.09
66	27.90	27.33	3.13	2.80
67	1.67	0.15	28.30	28.14
68	0.62	0.58	1.75	0.20
69	11.43	11.41	9.46	9.42
77	13.78	13.68	9.32	9.22
78	2.45	1.55	7.13	6.52
79	0.15	...	2.02	1.52
81	2.38	2.34	1.90	1.88
82	3.49	3.36	2.72	2.61
83	1.51	1.23	1.37	1.15
84	12.59	12.37	4.71	4.53
85	0.77	0.07	8.88	8.59
108	2.68	2.65	1.60	1.58
109	23.48	23.27	9.14	9.02
110	100.00	98.16	11.41	10.67
111	8.36	...	100.00	98.78
112	4.63	...	7.80	...
113	0.34	...	4.60	...

using 1.1 e.v. as the ΔH_f for benzenethiol⁸ and literature values of ΔH_f for neutral fragments from the processes shown. The ΔH_f values shown in the last

- (5) F. P. Lossing, A. W. Tickner, and W. A. Bryce, *J. Chem. Phys.*, **19**, 1254 (1951).
- (6) F. H. Field and J. L. Franklin, "Electron Impact Phenomena and the Properties of Gaseous Ions," Academic Press, New York, N. Y., 1957, p. 242.
- (7) V. H. Dibeler and F. L. Mohler, *J. Res. Natl. Bur. Std.*, **45**, 441 (1950).
- (8) D. W. Scott, J. P. McCullough, W. N. Hubbard, J. F. Messerly, I. A. Hossenlopp, F. R. Frow, and G. Waddington, *J. Am. Chem. Soc.*, **78**, 5463 (1956).

column were taken directly from the literature or calculated by the method of group equivalents.⁹⁻¹¹

Table II: Ratios of Intensities of Nondeuterated to Deuterated Ions from C_6H_5SD

m/e	Empirical formula	Intensity of ions from C_6H_5SH	Intensity of ions from C_6H_5SD	Ratio of intensities of ions from C_6H_5SD
33	SH^+	2.1	0.2	0.11
34	SD^+	..	1.9	..
45	CSH^+	11.3	9.1	4.14
46	CSD^+	..	2.2	..
66	$C_5H_6^+$	27.3
67	$C_5H_5D^+$..	27.3	..
77	$C_6H_5^+$	13.7	8.0	1.40
78	$C_6H_4D^+$..	5.7	..
84	$C_4H_5S^+$	12.4	3.6	0.41
85	$C_4H_3DS^+$..	8.8	..
109	$C_6H_5S^+$	23.3	10.2	0.78
110	$C_6H_4DS^+$..	13.1	..
110	$C_6H_5SH^+$	98.2
111	$C_6H_5SD^+$..	98.2	..

Discussion

Several processes were considered for each of the ions from deuterated benzenethiol. The processes shown in Table III gave determined values of ΔH_f (product ion) that agreed with the literature values to within 0.7 e.v. All other processes considered gave values differing by at least 2.3 e.v. from the literature values. In every case the parent ion, $C_6H_5SD^+$, was the only intermediate between the molecule and the product ion; furthermore, ring cleavage in the parent ion was always followed by ring closure in one of the products, thus lowering ΔH for the process.

The data in Tables II and III were used to postulate the structure of the parent ion before fragmentation. The observed appearance potentials and intensities for some product ions could be accounted for by a precursor with a structure similar to the conventional structure of the benzenethiol molecule, shown in Fig. 1A. However, the intensities and appearance potentials of other product ions could result only from a parent ion structure in which the five hydrogens and the deuterium were equivalent. One such structure is the seven-membered ring, Fig. 1B, analogous to the tropylium ion proposed by Rylander and co-workers.⁴ Although the deuterium is shown on a specific carbon in Fig. 1B, it could be associated with any carbon. In the sub-

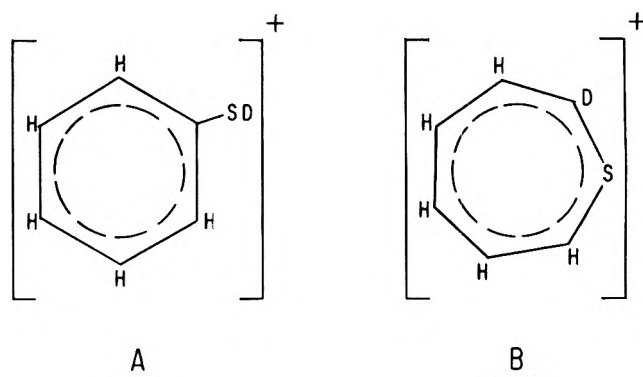


Figure 1. Two proposed structures for the parent ion of C_6H_5SD .

sequent discussion of specific ions, structure 1B will be used to represent structures in which the hydrogens and deuterium are equivalent.

$m/e = 33$ and 34 . The m/e 34 ion, SD^+ , is produced by direct cleavage of the carbon-sulfur bond in structure 1A. Data in Table II show the almost complete change from SH^+ production in $C_6H_5SH^+$ to SD^+ production in $C_6H_5SD^+$.

$m/e = 45$ and 46 . Simple ring cleavage of structure 1A would produce CSD^+ ions only, but the data in Table II show that the ratio of intensities of CSH^+ ion to CSD^+ ion from C_6H_5SD is 4.1. Ring cleavage of structure 1B would produce CSH^+ ions and CSD^+ ions in the intensity ratio of 5, which is close to the observed ratio of 4.1. The postulation of the same precursor for both ions is supported by the fact that they have identical appearance potential curves.

The values of ΔH_f for CSH^+ and CSD^+ shown in Table III were determined using a ΔH_f for the cyclopentadienyl radical of 1.5 e.v. obtained by group equivalent methods. The good agreement between the determined values of the CSH^+ and CSD^+ ions and the literature value¹² for the CSH^+ ion supports the process proposed in Table III.

$m/e = 67$. The 67 ion must be $C_5H_5D^+$, as all five hydrogens and the deuterium are required to produce it. A ΔH_f of 10.7 e.v. was determined for the 67 ion using a ΔH_f for the neutral fragment, CS^+ , of 2.3 e.v.⁶ This ion could have either a cyclic or noncyclic structure, but the cyclic structure is more likely because the determined value of ΔH_f for the 67 ion was within 0.7 e.v. of the literature value for the cyclopentadiene ion, whereas it differed by more than 2 e.v. from ΔH_f

(9) J. L. Franklin, *J. Chem. Phys.*, **21**, 2029 (1953).

(10) J. L. Franklin, *Ind. Eng. Chem.*, **41**, 1070 (1959).

(11) J. L. Franklin and F. H. Field, *J. Am. Chem. Soc.*, **75**, 2819 (1953).

(12) See ref. a in Table III.

Table III: Appearance Potentials, Proposed Processes, and Heats of Formation for Selected Ions from C₆H₅SD

<i>m/e</i>	Appearance potential, e.v.	Proposed process	—Δ <i>H</i> _f (product ion), e.v.—	
			Determined	Literature
45	12.7	C ₆ H ₅ SD → C ₆ H ₅ SD ⁺ → CSH ⁺ + cyclo-C ₅ H ₄ D·	12.4	12.4 ^a
46	12.7	C ₆ H ₅ SD ⁺ → CSD ⁺ + cyclo-C ₅ H ₅ ·	12.4	12.4 ^a
67	11.9	C ₆ H ₅ SD ⁺ → cyclo-C ₅ H ₅ D ⁺ + CS·	10.7	10.0 ^b
77	13.3	C ₆ H ₅ SD ⁺ → C ₆ H ₅ ⁺ + SD·	12.7	13.1 ^c
84	11.8	C ₆ H ₅ SD ⁺ → cyclo-C ₄ H ₄ S ⁺ + C ₂ HD	10.5	10.1 ^d
85	11.8	C ₆ H ₅ SD ⁺ → cyclo-C ₄ H ₃ DS ⁺ + C ₂ H ₂	10.5	10.1 ^d
109	12.2	C ₆ H ₅ SD ⁺ → C ₆ H ₅ S ⁺ + D·	11.0	11.0 ^e
111	8.5	C ₆ H ₅ SD ⁺	9.6	...

^a An average of three values for the CSH⁺ ion reported by B. G. Hobrock and R. W. Kiser, *J. Phys. Chem.*, **66**, 1648 (1962). ^b See ref. 6, p. 264. ^c See ref. 6, p. 266. ^d See ref. 6, p. 301. ^e See ref. 9 and 11.

values for noncyclic structures calculated by group equivalents.⁹⁻¹¹

m/e = 77 and 78. The 77 ion, C₆H₅⁺, can be accounted for by simple bond cleavage of structure 1A. The resulting phenyl ion has a Δ*H*_f of 12.7 e.v. determined using a Δ*H*_f of 1.7 e.v. for the ·SD radical.¹³ The good agreement shown in Table III between the determined and literature value of Δ*H*_f indicates a simple cleavage of the carbon-sulfur bond to produce the phenyl ion at *m/e* = 77 and the ·SD radical.

Some migration of the deuterium evidently takes place prior to the formation of the 78 ion, C₆H₄D⁺, as the parent ion must lose SH·, not SD·, to account for the composition expressed by the formula C₆H₄D⁺. The 77 and 78 ions have different shaped appearance potential curves and occur in the ratio 1.4; but if the 77 ions and 78 ions were to come from the seven-membered ring structure, they should have identical appearance potential curves and occur in the ratio 0.2. Thus, although it is evident that some exchange of hydrogen and deuterium does take place in the parent ion, ring expansion with subsequent production of 77 and 78 ions is unlikely and no process for the 78 ions is proposed.

m/e = 84 and 85. The 84 ions, C₄H₄S⁺, and the 85 ions, C₄H₃DS⁺, have identical appearance potential curves showing that they have the same precursor. Both the 84 ions, C₄H₄S⁺, and the 85 ions, C₄H₃DS⁺, can be accounted for by simple cleavage of structure 1B, but only the 85 ions can be accounted for by simple cleavage of structure 1A. The observed ratio of the intensities of 84 ions to 85 ions is 0.42, in fair agreement with the ratio of 0.50, which would be expected from structure 1B.

The 84 ions, C₄H₄S⁺, and the 85 ions, C₄H₃DS⁺, have the thiophene structure and the neutral fragment is acetylene. Using a Δ*H*_f of 2.4 e.v.¹³ for acetylene, the determined value of Δ*H*_f for the 84 and 85 ions agrees

well with the literature value of Δ*H*_f for the thiophene ion, as shown in Table III.

m/e = 109 and 110. The 109 ion, C₆H₅S⁺, is produced by loss of D· from C₆H₅SD⁺. Using a Δ*H*_f for D· of 2.3 e.v.,¹³ the determined Δ*H*_f for the 109 ion is identical with the literature value shown in Table III. The 110 ion, C₆H₄SD⁺, is produced by loss of H· from C₆H₅DS⁺. Interference at *m/e* 110 from the undeuterated molecular ion, C₆H₅SH⁺, precluded the measurement of the appearance potential and determination of Δ*H*_f for the deuterated fragment ion C₆H₄SD⁺.

The 109 ions could not all be produced from structure 1B by loss of D·, because the corresponding loss of H· should be five times as great, giving 109 ions and 110 ions in the ratio of 0.2. Actually, the 109 and 110 ions occur in the ratio of 0.8 (Table II). Therefore, a 13.1% intensity for the 110 ions (C₆H₄DS⁺) arising from structure 1B would imply that of the 10.2% intensity recorded for the 109 ions (C₆H₅S⁺) 2.6% should also arise from structure 1B. The remaining 7.6% of 109 ions would then arise from some other structure. No evidence is seen for the 109 ions arising from two different structures; thus, structure 1A is proposed as a precursor for both the 109 ions, C₆H₅S⁺, and the 110 ions, C₆H₄SD⁺.

m/e = 111. The parent ion, C₆H₅SD⁺, of deuterated benzenethiol, has a determined Δ*H*_f of 9.6 e.v. as shown in Table III. This value was calculated using a Δ*H*_f of 1.1 e.v. for the compound.⁸

Conclusions

For all the processes studied, two nonequivalent forms of the parent ion are the only intermediates between the molecule and the fragment ions. When

(13) See ref. 6, p. 129.

ring cleavage occurs in the parent ion, ring closure occurs in one of the products, thereby lowering the total energy required for the reaction. The processes and structure proposed are those which best fit the thermochemical data. It has been shown that some of the

ions from C_6H_5SD issue from the six-membered ring structure where the hydrogen and deuterium are not equivalent, but other ions issue from another structure, such as the seven-membered ring, where the hydrogens and deuterium are equivalent.

Quenching of the Scintillation Process in Plastics by Organometallics¹

by Stanley R. Sandler and K. C. Tsou

Central Research Laboratory, Borden Chemical Company, Philadelphia, Pennsylvania, and Harrison Department of Surgical Research, School of Medicine, University of Pennsylvania, Philadelphia, Pennsylvania
(Received August 12, 1963)

Organometallics of the group II, IVA, and VA metals were found to be quenchers for the scintillation process in polyvinyltoluene plastics. Copolymerizing vinyltoluene and *p*-triphenyltinystyrene produced a slight increase in the degree of quenching above triphenyl-4-ethylphenyltin. In addition, copolymerizing *p*-triphenylleadstyrene with vinyltoluene also produced slightly more quenching than triphenyl-4-ethylphenyllead physically dissolved in the plastic scintillator. A modified Stern-Volmer relationship was used to correlate the scintillation quenching of the organometallics and the atomic number. The mechanism of energy transfer and quenching are discussed in relation to the results found in this investigation.

Introduction

The earliest work describing quenching by organometallics in plastics was reported by Pichat, Pesteil, and Clement,² who had found that the addition of hexahydrobenzoates of lead and bismuth, triphenylmethyllead, or lead naphthenate causes serious quenching in the polystyrene scintillator containing 1,1,4,4-tetraphenylbutadiene. More recently, Baisle³ evaluated diphenylmercury and Hyman⁴ evaluated triphenylbismuth, tetraphenyllead, and various lead methacrylates in polyvinyltoluene scintillators and found the organometallics to be quenchers of the light output.

In aromatic solutions, organometallic compounds were found not to act as scintillators⁵ but as quenchers of the light output.⁶⁻⁸

In the present investigation, the group IVA and VA organometallics were evaluated in polyvinyltoluene plastics toward β -irradiation of Pa^{234} . The scintilla-

tion efficiency and the ultraviolet and fluorescence spectral data of the organometallics has been used to attempt a description of the probable mechanism of energy transfer and quenching.

- (1) This work was supported by the U. S. Atomic Energy Commission under Contract No. AT (30-1)-1931.
- (2) L. Pichat, P. Pesteil, and J. Clement, *J. Chim. Phys.*, **50**, 26 (1953).
- (3) L. J. Baisle, *J. Chem. Phys.*, **27**, 801 (1957).
- (4) M. Hyman and J. J. Ryan, *IRE, Trans. Nucl. Sci.*, **5**, 87 (1958).
- (5) H. Gilman, E. A. Weipert, and F. N. Hayes, *J. Org. Chem.*, **23**, 860 (1958).
- (6) F. H. Brown, M. Furst, and H. Kallmann in "Organic Scintillation Detectors," TID 7612, U. S. Atomic Energy Commission 1961, p. 3T.
- (7) V. N. Kerr, F. N. Hayes, and D. Ott, *Intern. J. Appl. Radiation Isotopes*, **1**, 284 (1957).
- (8) J. L. Kropp and M. Burton, *J. Chem. Phys.*, **37**, 1752 (1962).

Experimental

Vinyltoluene monomer was obtained in 99.9% purity from the Dow Chemical Co. and distilled through a 3-ft. Nester-Faust spinning-band column. The di-, tri-, and tetraarylmethyls were obtained from commercial sources and repeatedly recrystallized. The syntheses of the new compounds are described below.

Preparation of Triphenyl-4-ethylphenyllead. To an ether solution of 4-ethylphenylmagnesium bromide (0.27 M) was added 102.3 g. (0.215 mole) of triphenyllead chloride in ether. The solution was refluxed for 3-4 hr. and then hydrolyzed with aqueous ammonium chloride to yield 63.6 g. (54.6%), m.p. 75-77°. *Anal.* Calcd. for $C_{26}H_{24}Pb$: C, 57.50; H, 4.42; Pb, 38.10. Found: C, 56.98; H, 3.89; Pb, 37.28.

Preparation of Triphenyl-4-ethylphenyltin. To 0.27 mole of 4-ethylphenylmagnesium bromide was added an equimolar amount of triphenyltin chloride in ether. The reaction was worked up as in the preceding preparation to yield 53.7 g. (55%), m.p. 83-84°. *Anal.* Calcd. for $C_{26}H_{24}Sn$: C, 68.70; H, 5.27; Sn, 26.00. Found: C, 68.06; H, 5.07; Sn, 26.19.

Preparation of p-Triphenylleadstyrene and p-Triphenyltinstyrene. The following procedure for monomer synthesis represents an improvement over that reported in the literature.^{9,10}

p-Chlorostyrene was treated with the theoretical amount of magnesium in 50 ml. of tetrahydrofuran. A few milliliters of methyl iodide was used to initiate the formation of the Grignard reagent. The *p*-chlorostyrene was added in 100 ml. of tetrahydrofuran (THF) at such a rate that the reaction mixture refluxed. Heating was necessary throughout the reaction. After all the *p*-chlorostyrene had been added the solution was refluxed for 15-20 min. and the solution turned a clear dark green color. Triphenyllead chloride or triphenyltin chloride was dissolved in 100 ml. of THF and added dropwise. After the latter was added, the solution was kept at 50-66° for 1-1.5 hr. and then cooled with ice. The reaction mixture was hydrolyzed with aqueous ammonium chloride and the organic layer separated. The water layer was extracted twice with 100 ml. of ether. The combined organic layer was attached to an aspirator and the THF and ether were removed. Then petroleum ether (60-30°) was added to the residue to extract the product. The product was recrystallized from petroleum ether or isopropyl alcohol to yield either 77% *p*-triphenylleadstyrene, m.p. 112-113° (lit.⁹ m.p. 107-109°), $\lambda_{\max}^{CHCl_3}$ 258 m μ (ϵ 28,700), or 46% *p*-triphenyltinstyrene, m.p. 104-105° (lit.¹⁰ m.p. 105.5-108°), $\lambda_{\max}^{CHCl_3}$ 258 m μ (ϵ 23,000).

An excess of magnesium in this preparation tends to give lower yields, possibly due to the formation of hexaphenylditin or hexaphenyldilead and their cleavage products.¹¹

The polyvinyltoluene scintillators were prepared as previously described¹² and evaluated toward β -irradiation of Pa^{234} , 2.3 Mev., 0.01 mc.

The fluorescence spectra were obtained using an Aminco-Bowman spectrophotofluorometer equipped with a xenon light source, and the ultraviolet spectra were obtained with a Beckman DK-U spectrophotometer.

Results

In an effort to understand the scintillation process of organometallic scintillators a series of molecules containing different heavy atoms was evaluated. For this study aryl metals such as $(C_6H_5)_nM$ were chosen so that $n = 2$ for the group IIB series, 4 for group IVA, and 3 for group VA. The organometallics were dissolved in vinyltoluene containing 3% *p*-terphenyl and 0.05% POPOP (1,4-bis(2,5-phenyloxazolyl)benzene) and polymerized at 100-110° under vacuum for 7 days. A series of various concentrations (0-15%) was used in most cases. The scintillation plastics were machined to 0.5 × 0.813 in. and evaluated relative to an anthracene crystal of the same size with a Pa^{234} β , 2.3 Mev. source (0.01 mc.). A plot of the dif-

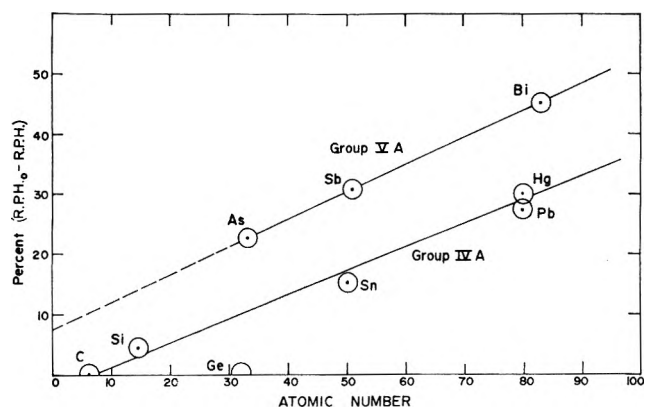


Figure 1. The difference in relative pulse height of organometallic loaded scintillators and unloaded scintillators ($R.P.H._o - R.P.H.$) is plotted against the atomic number for the group IVA and group VA metals.

- (9) H. G. Pars, W. A. Graham, E. R. Atkinson, and C. C. Morgan, *Chem. Ind.* (London), 693 (1960).
- (10) J. R. Leebrick and H. E. Ramsden, *J. Org. Chem.*, **23**, 935 (1958).
- (11) C. Tamborski and E. J. Salaski, *J. Am. Chem. Soc.*, **83**, 373 (1961).
- (12) R. K. Swank and W. L. Buck, *Phys. Rev.*, **91**, 928 (1953).

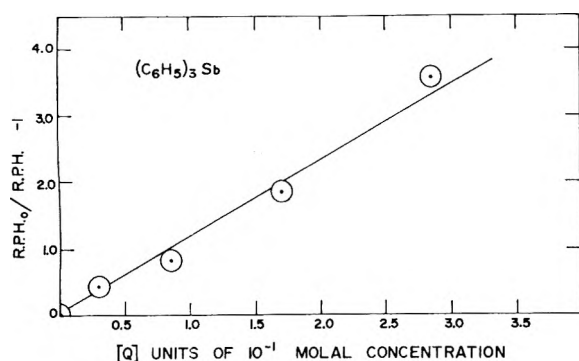


Figure 2. $R.P.H._0/R.P.H. - 1$ vs. concentration of triphenylstibine $[Q] \times 10^{-1} m$.

ference of the relative pulse height of scintillators containing 0.14 m concentration of the organometallic compared to an unloaded scintillator vs. the atomic number gave a straight line for the group IVA and another line for the group VA metals as shown in Fig. 1. It is interesting that the group VA metals are greater quenchers than group IVA with tetraphenylmethane and tetraphenylgermanium showing no quenching.

The study of the effect on the quenching process by incorporation of lead or tin organometallics in the polymer backbone was made possible by copolymerizing p -triphenyltinstyrene or p -triphenylleadstyrene with vinyltoluene. The results are shown in Table I.

Table I: Quenching Constants of Organometallics in Polyvinyltoluene Scintillation Plastics Containing 3% p -Terphenyl and 0.05% POPOP

Quencher	Atomic number of metal	Quenching constant ^a $\times 10^1$
$(C_6H_5)_4C$	6	0
$(C_6H_5)_4Si$	14	0
$(C_6H_5)_4Ge$	32	0
$(C_6H_5)_4Sn$	50	0.210
$(C_6H_5)_3Sn-C_6H_4CH=CH_2$	50	0.097
$(C_6H_5)_3SnC_6H_4C_2H_5$	50	0.030
$(C_6H_5)_4Pb$	82	0.55
$(C_6H_5)_3PbC_6H_4CH=CH_2$	82	0.72
$(C_6H_5)_3PbC_6H_4C_2H_5$	82	0.57
$(C_6H_5)_2Hg$	80	2.86 ^b
$(C_6H_5)_3As$	33	0.66
$(C_6H_5)_3Sb$	51	1.11
$(C_6H_5)_3Bi$	83	5.84

^a Calculated from the relative pulse height data. ^b The quenching constant for $(C_6H_5)_2Hg$ apparently was lower at low concentrations (0–0.15 m) and was calculated to be 0.55.

The degree of quenching by the organometallics was evaluated using the relative pulse height data and the Stern–Volmer¹³ type relationship

$$\frac{R.P.H._0}{R.P.H.} - 1 = k_q[Q] \quad (1)$$

where $R.P.H._0$ is the relative pulse height of a standard scintillator containing no organometallic evaluated toward $Pa^{234}\beta$; $R.P.H.$ is the relative pulse height of an organometallic loaded scintillator. The determination of relative pulse height is that recommended by Swank and Buck,¹² using anthracene crystal of the same size as standard. k_q is the quenching constant and $[Q]$ is the concentration of the organometallic in moles. A plot of $R.P.H._0/R.P.H. - 1$ vs. $[Q]$ for triphenylstibine is shown in Fig. 2 as a representative plot to indicate the method for all the materials studied. The quenching constants are tabulated in Table I.

The ultraviolet and fluorescence spectral properties of the fluor and organometallics are shown in Table II.

Table II: Spectral Properties of Fluors and Quenchers

Compound	Ultraviolet ^a absorption		Fluorescence ^c emission		
	range	λ_{max} , $m\mu$	ϵ_{max}	range	λ_{max} , $m\mu$
p -Terphenyl	210–310	279	30,800	310–445	350
Polyvinyltoluene	290–345	322	310–425	350
Poly- p -triphenylleadstyrene ^b	250–385	322	300–600	370
Poly- p -triphenyltinstyrene ^b	250–400	330	315–530	398
Triphenyl-4-ethylphenyltin	225–285	259	1,720	350–525	385
Triphenyl-4-ethylphenyllead	200–300	257	2,110	290–550	360
Tetraphenyllead	200–280	258	2,130	275–500	360
Tetraphenyltin	240–290	260	1,335	280–500	345
Tetraphenylgermanium	230–290	252	1,555	310–425	350
Tetraphenylsilicon	243–300	266	1,390	295–490	348
Tetraphenylmethane	230–300	256	1,910	290–425	335
Triphenylarsine	200–290	248	13,540	290–475	347
Triphenylstibine	200–300	255	13,870	290–475	345
Triphenylbismuth	200–315	280	4,840	310–435	350
Diphenylmercury	200–280	258	1,370	300–430	348

^a The ultraviolet spectra were determined in chloroform using the Beckman DKU spectrophotometer. ^b Spectral properties of the solid polymer obtained using the Aminco–Bowman spectrophotofluorometer. ^c The fluorescence spectra were obtained in chloroform.

Discussion

The results in Fig. 1 indicate that the relative pulse height is lowered with an increase in the atomic number of the organometallic for the group IVA and VA series.

(13) O. Stern and M. Volmer, *Z. Physik*, 20, 183 (1919).

Diphenylmercury is also included and falls on the line for the group IVA metallics since the atomic number of mercury (80) is close to that of lead (82).

From the results in Fig. 1 the group VA triaryl organometallics appear to be more effective quenchers than the group IVA tetraaryl organometallics. The relationship derived from Fig. 1 ($R.P.H._0 - R.P.H. = k'Z$) can be combined with the Stern-Volmer relationship (eq. 1) to give

$$\frac{k'Z}{R.P.H.} = k_q[Q] \quad (2)$$

where k' , Z , and $R.P.H.$ are the proportionality constant, atomic number, and relative pulse height at 0.14 m organometallics, respectively. The other quantities are the same as described earlier. It is seen from the derived relationship that the quenching constant should increase with an increase in Z and more so with a decrease in $R.P.H.$ Since k' can be evaluated for the group IVA ($k' = 0.384$) and group VA ($k' = 0.50$)

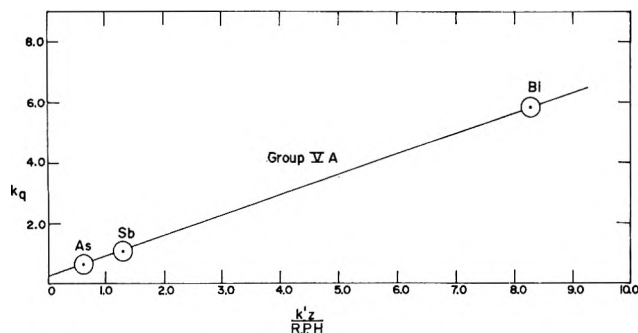


Figure 3. The quenching constant k_q for the organometallics as shown in Table I vs. $k'Z/R.P.H.$ for the group VA metals.

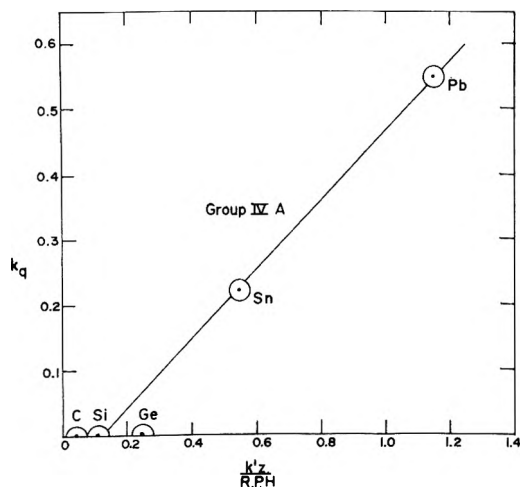
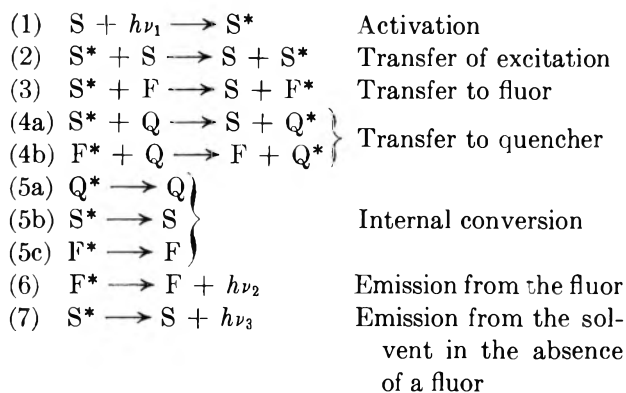


Figure 4. The quenching constant k_q for the organometallics as shown in Table I vs. $k'Z/R.P.H.$ for the group IVA metals.

organometallics from Fig. 1 it can be used to prepare a plot of $k'Z/R.P.H.$ vs. k_q , as shown in Fig. 3 and 4. In most cases knowing the value of k' and the $R.P.H.$ at 0.14 m concentration is enough to determine the k_q of the organometallic from Fig. 3 and 4.

The observed quenching of the scintillation process by the above organometallics may be due to a decrease in the fluorescence by an internal conversion mechanism as has been suggested for oxygen.¹⁴

The scintillation mechanism incorporating a quencher can be described for convenience as



The evidence presented in this investigation suggests that steps 4a, 4b, and 5a are involved in quenching by organometallics in plastics.

In order for energy transfer to occur from an excited donor to an acceptor, as in step 3, the fluorescence spectrum of the donor must overlap the absorption spectrum of the acceptor.¹⁵ It is seen from an examination of Table II that the spectral absorption properties of triphenylbismuth are similar to that of *p*-terphenyl. However, since the former is a poor fluorescence emitter, as the concentrations of triphenylbismuth is increased above *p*-terphenyl the former will capture most of the excitation of the solvent and re-emit very little. This masking effect by an inefficient fluor leads to quenching of the scintillation process by steps 4b and 5a. On the other hand, the organometallics may have an absorption spectrum overlapping the solvent as does poly-*p*-triphenylleadstyrene and poly-*p*-triphenyltinstyrene so that there exists a competition for the excitation energy of the solvent polyvinyltoluene. If, for example, poly-*p*-triphenylleadstyrene re-emits very little of its energy to *p*-terphenyl then quenching of the scintillation process will occur.

If energy transfer occurred along the polymer backbone then introducing a quencher into the polymer by

(14) E. J. Bowen and H. A. Williams, *Trans. Faraday Soc.*, **35**, 765 (1939).

(15) T. Forster, "Fluoreszenz Organischer Verbindungen," Vandenhoeck and Ruprecht, Göttingen, Germany, 1951.

copolymerization may show a reduction in efficiency compared to physically dissolving the quencher. A slight reduction was observed since *p*-triphenyltinstyrene shows a small reduction in efficiency compared to triphenyl-4-ethylphenyltin as seen in Table I. In addition, *p*-triphenylleadstyrene shows slightly more quenching than triphenyl-4-ethylphenyllead. Since energy transfer probably takes place by a π -bond overlap between the excited solvent and fluor, the quencher

competes for this orbital overlap whether physically dissolved or as part of a polymer molecule. This is likely the reason that Kerr, Hayes, and Ott⁷ have found that the aromatic quenchers have a greater detrimental effect on the scintillation process than similarly substituted aliphatic compounds.

Acknowledgment. We are grateful to Dr. B. D. Halpern for his interest and helpful suggestions in this work.

The 3P_1 Mercury-Photosensitized Decomposition of Monosilane

by H. Niki and Gilbert J. Mains

Department of Chemistry, Carnegie Institute of Technology, Pittsburgh 13, Pennsylvania
(Received August 21, 1963)

The 3P_1 Hg-sensitized decomposition of SiH_4 and a 1:1 SiH_4 - SiD_4 mixture was studied at 1 cm. pressure and 25°. Quantum yields of hydrogen and disilane were estimated to be 1.8 and 0.6, respectively, at low conversion, but are subject to considerable uncertainty. Polymeric silicon hydride was deposited on the walls as the reaction proceeded toward a photostationary state. The uniformity of the polymeric film is taken as evidence that the "zebra" effect is not important in his system. The failure of a large concentration of ethylene to reduce the yield or isotopic distribution of hydrogens from the decomposition of the SiH_4 - SiD_4 mixture indicates that the reaction between atomic hydrogen and monosilane is very rapid. Monosilane may find future use as an efficient hydrogen atom scavenger.

Introduction

Silicon hydrides are the closest structural analogs of paraffin hydrocarbons. While the decomposition of small paraffin hydrocarbons has been studied by direct photolysis,^{1,2} mercury sensitized photolysis,³⁻⁵ direct radiolysis,⁶ and mercury-sensitized radiolysis,⁵ no comparable investigations have been reported for the silanes. Because the silanes are thermodynamically unstable relative to the elements at room temperature, and because olefinic compounds, a serious complication in interpreting hydrocarbon systems, are absent among the silicon hydrides, the photochemistry of silanes is of considerable interest. This laboratory has initiated a systematic study of the photochemistry and radiation chemistry of silanes. The data given here represent the first part of this study.

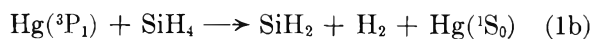
Emelús and Stewart⁷ initially reported the mercury-photosensitized decomposition of monosilane into hydrogen and a brown film of polymeric silicon hydride. The empirical formula of the solid hydride varied from $\text{SiH}_{0.91}$ to $\text{SiH}_{0.43}$ depending upon the extent of conversion. According to these authors, the polymeric film was opaque to ultraviolet light and its deposition

- (1) J. R. McNesby and H. Okabe, *J. Chem. Phys.*, **34**, 668 (1961).
- (2) B. Mahan and R. Mandal, *ibid.*, **37**, 207 (1962).
- (3) R. Back and Van der Auwera, *Can. J. Chem.*, **40**, 2339 (1962).
- (4) L. Dorfman, E. Spittler, P. Jordan, and M. Sauer, *J. Phys. Chem.*, in press.
- (5) G. J. Mains and A. S. Newton, *ibid.*, **65**, 212 (1961).
- (6) P. Ausloos and S. G. Lias, *J. Chem. Phys.*, **38**, 2207 (1963).
- (7) H. J. Emelús and K. Stewart, *Trans. Faraday Soc.*, **32**, 1577 (1936).

rendered extensive decomposition of monosilane impossible. White and Rochow,⁸ in a more recent study aimed at the synthesis of organosilicon compounds, reported the formation of ethylsilane, *n*-butylsilane, and 1,4-disilylbutane in the mercury-photo-sensitized reaction between monosilane and ethylene. On this basis, they suggested the primary process



although earlier workers⁷ could not rule out the molecular formation of hydrogen, *viz.*



and subsequent reactions of the SiH_2 intermediate. In an attempt to learn more about the primary process and the reaction mechanism, the authors have studied the mercury-photo-sensitized decomposition of monosilane and a monosilane: monosilane- d_4 mixture at 25°.

Experimental

Monosilane was prepared by the reaction of silicon tetrachloride (Fisher Laboratory, technical grade) with a suspension of lithium aluminum hydride in diethyl ether.⁹ The monosilane product was purified by bulb-to-bulb distillation at -160° and found to contain 0.2% disilane by mass spectroscopy. Monosilane- d_4 was prepared by the same method using lithium aluminum deuteride (Metal Hydrides, Inc., 97% purity). The mass spectrum of monosilane was in excellent agreement with that reported by Stone.¹⁰ In both SiH_4 and SiD_4 the presence of parent peaks was doubtful. Monosilane slowly decomposes at 25° and must be purified prior to each experiment.

Ethylene and isobutane were taken from Matheson lecture bottles, subjected to bulb-to-bulb distillation, and were found to be mass spectrometrically pure. Bethlehem Apparatus Co. triple-distilled mercury was used without further purification. Hydrogen and deuterium were purified by passage through a palladium thimble.

The silane was loaded into cylindrical reaction vessels, 30 mm. in diameter and 160 mm. long, constructed of Vycor. Conventional vacuum techniques were employed except for the use of appropriate shields and covers to protect the experimenter from explosions should the line accidentally rupture and admit air. (In one case air was accidentally admitted to a 1-l. bulb containing SiH_4 at a pressure of 2 cm. A flame front moved through the vessel but the vessel did not rupture.) Mercury (0.25 μl .) was added to the reaction vessel prior to evacuation and loading with silanes. The irradiations were performed at $25 \pm 2^\circ$ using a Hanovia SC-2537 low pressure mercury lamp described

earlier.¹¹ The average light intensity in the reaction vessel was at least 1.08×10^{17} photons $\text{cc.}^{-1} \text{min.}^{-1}$ by propane actinometry.¹² (At these high intensities the quantum yield of hydrogen is less than 0.5 and intensity dependent. Therefore, the value of I_a cited here is the minimum value. In the authors' opinion it is unlikely to be in error by more than a factor of two.)

All analyses were performed using a Consolidated Electro-dynamics Corp. Model 21-103C mass spectrometer.

Results and Discussion

The initial product distribution of the 3P_1 Hg-sensitized decomposition of monosilane at 1.0 cm. pressure and 25° is shown in Fig. 1. Estimated quantum yields of hydrogen, disilane, and trisilane are 1.8, 0.6, and 0.06 molecules per absorbed photon, respectively, assuming the minimal value of I_a and complete quenching by the

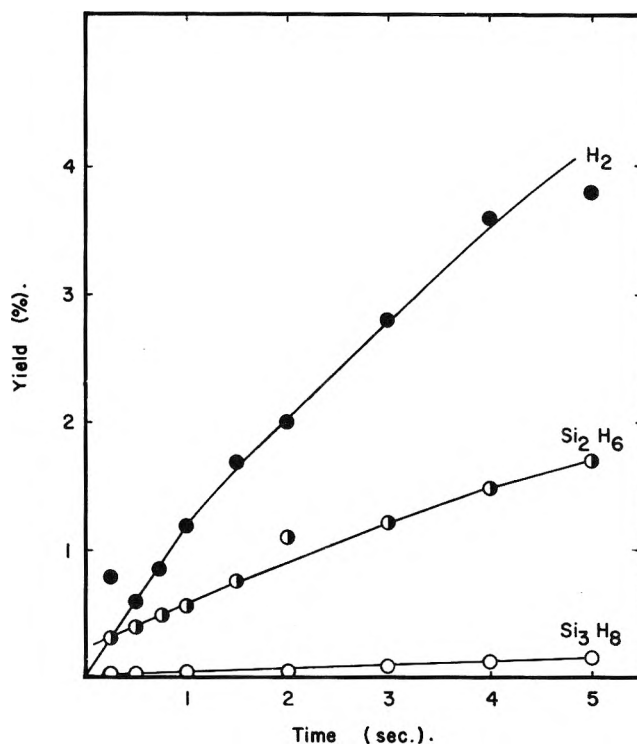
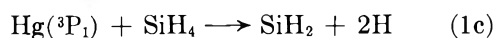


Figure 1. Mercury-sensitized photolysis of monosilane at 1 cm. pressure and 25°; product yields vs. time.

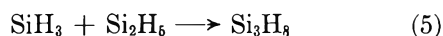
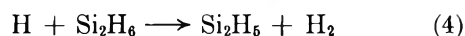
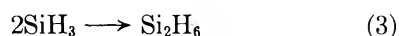
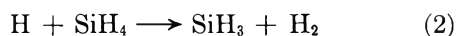
- (8) D. White and E. G. Rochow, *J. Am. Chem. Soc.*, **76**, 3897 (1954).
- (9) A. E. Finholt, A. C. Bond, Jr., K. E. Wilzbach, and H. I. Schlessinger, *ibid.*, **69**, 2692 (1947).
- (10) F. G. A. Stone, W. C. Steele, and L. D. Nicholas, *ibid.*, **84**, 4441 (1962).
- (11) H. Niki, G. J. Mains, and M. H. J. Wijnen, *J. Phys. Chem.*, **67**, 11 (1963).
- (12) S. Bywater and E. W. R. Steacie, *J. Chem. Phys.*, **19**, 319 (1951).

silanes. Although the quenching cross section for SiH_4 has not been directly determined, it has been estimated¹³ from the data of Emel us and Stewart to be the same as CH_4 , *i.e.*, 0.06 \AA^2 . Such a low value implies incomplete energy transfer from the excited mercury atoms in the experiments reported here. In view of these facts, the calculated quantum yields of H_2 , Si_2H_6 , and Si_3H_8 are subject to considerable uncertainty. However, if the value of 1.8 for the quantum yield is correct, it is possible to rule out reactions 1a and 1b as the *exclusive* primary processes. Primary processes of the types



should also be invoked. (An alternate explanation for a large quantum yield of hydrogen, a chain propagation reaction such as a reaction between SiH_3 and SiH_4 to yield Si_2H_6 and a hydrogen atom, can be ruled out on energetic grounds.) It is clear that a decision on the relative importance of reactions 1a to 1c cannot be reached until a more precise determination of the quantum yield has been made. This determination is now in progress and the results will be published in a subsequent report from this laboratory.

Secondary reactions such as



can account for the products at very low conversion where the material balance is good. At higher conversions, *i.e.*, greater than 0.2%, the material balance becomes poor and polymeric silanes build up as a yellow film on the walls of the reaction vessel. If the radiation is continued for a longer period of time, the gaseous products are observed to reach the stationary state (see Fig. 2) attributed by Emel us and Stewart⁷ to the opaque nature of the film. That this conclusion was invalid was demonstrated by pumping off the gaseous products after the stationary state was attained and refilling the reaction vessel with pure hydrogen. When this system of polymeric film and hydrogen (which still contained a drop of liquid mercury from the original filling) was irradiated using 2537-  light, *the polymeric film was removed*. Subsequent analysis of the gas at the completion of the irradiation revealed the formation of monosilane, disilane, trisilane, and tetrasilane. When the experiment was repeated using deuterium instead of hydrogen, the silane products were

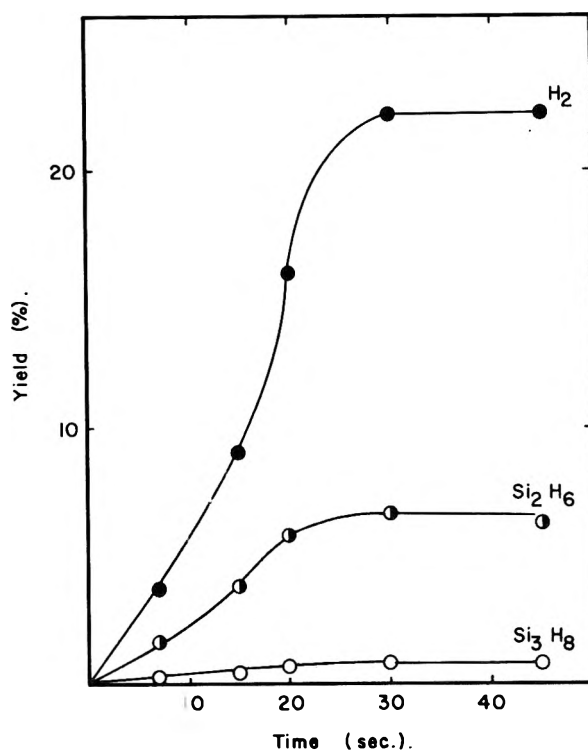


Figure 2. Mercury-sensitized photolysis of monosilane at 1 cm. pressure and 25°; product yields *vs.* time.

almost completely deuterated.¹⁴ It is clear that these observations require the polymeric film to transmit ultraviolet light. Therefore, the stationary state observed by Emel us and Stewart is a photostationary state and not due to the opacity of the film.

The mechanism of deposition or removal of the polymeric silicon hydride "mirror" has not been established. A reasonable mechanism involves the vapor phase build-up of higher silanes in low photostationary state concentrations until a silane is reached for which the primary mechanism of removal from the vapor phase is condensation on the wall rather than further reaction in the vapor phase. Once this silane is deposited on the wall it is subject to intense bombardment by hydrogen atoms (*vide infra*) and excited mercury atoms which could give rise to the cross-linked polymeric state of the deposit. Thus, one would expect the hydrogen content of the polymer to decrease as the extent of the reaction increased, a prediction consistent with the observations of Emel us and Stewart.⁷ If this mechanism is correct, the silane undergoing condensa-

(13) Y. Rouseau, O. Strausz, and H. Gunning, *J. Chem. Phys.*, **39**, 962 (1963).

(14) Some of these deuterated silanes have not been prepared by other methods. We propose to use this technique to synthesize these compounds for physicochemical study.

tion must be at least Si_6H_{14} or larger, since the lower silanes have appreciable vapor pressures¹⁶ at 25° and, therefore, would be detected by mass spectrometry. While traces of Si_4H_{10} and Si_5H_{12} were detected, higher silanes were not. The removal of the "mirror" could similarly be visualized as the surface production of high vapor pressure silanes which, upon desorption, diffuse into the bulk of the vessel and out of the reaction zone near the illuminated surfaces.

In several experiments a rectangular Pyrex plate was inserted in the reaction vessel to observe the density of polymeric film deposition as a function of radial distance from the center of the reaction vessel and, since the vessel was inserted in the center of the helical lamp, as a function the distance along the axis of the reaction vessel. The polymer film was found to decrease in density approximately exponentially from the walls as shown in Fig. 3. No axial variation in film density was observed. These densitometer experiments verify earlier conclusions¹⁶ that the "zebra" effect¹⁷ need not be considered when using helical lamps. It is worth mentioning that the polymeric silicon film exhibited the high electrical conductivity associated with its metalloid nature. No quantitative studies of the electrical characteristics of the film were made.

In an effort to establish the extent to which molecular elimination, reactions 1b and 1d, accounted for the formation of hydrogen, a 1:1 mixture of SiH_4 and SiD_4 was subjected to mercury-photosensitized decomposition at 25° and 1.0 cm. pressure. Since mass spectral patterns are not available for partially deuterated disilane and trisilane, only the isotopic distribution of hydrogen was determined. The data are

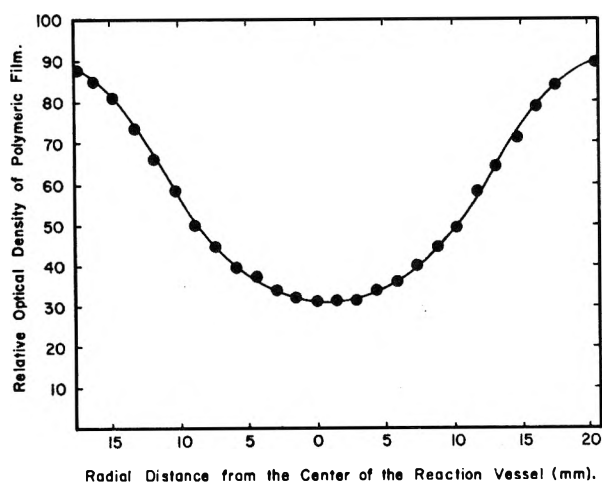


Figure 3. Relative density of polymeric film deposition vs. radial distance from the center of the reaction vessel.

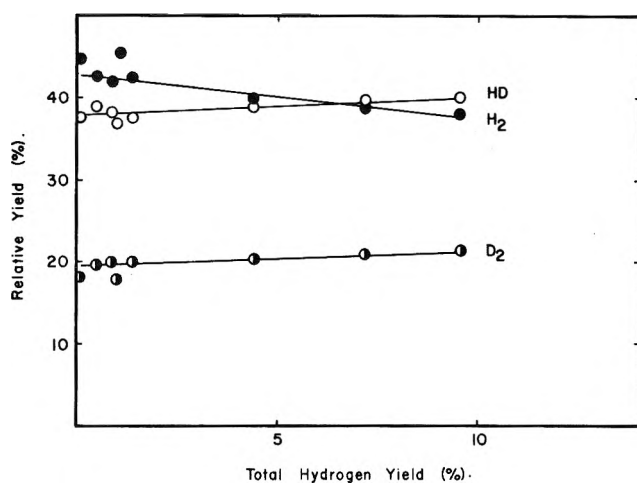


Figure 4. Distribution of H_2 , HD, and D_2 in mercury-sensitized decomposition of the equimolar mixture of SiH_4 and SiD_4 at 1 cm. pressure and 25° .

summarized in Fig. 4 as a function of the extent of reaction. The extremely high yield of HD even at 0.1% decomposition rules out the formation of hydrogen by reactions 1b and 1d exclusively, as the mercury-photosensitized H_2 - D_2 exchange is negligible at these pressures and reaction times.¹⁸ It is difficult to estimate the extent to which isotopic scrambling occurred with monosilane, as mass spectral patterns are not available for SiH_3D , SiD_2H_2 , and SiD_3H . However, the absence of a significant shift in the mass peak pattern of the 1:1 mixture following photolysis indicates that the exchange was less than a few per cent at the lowest conversions. It seems reasonable to conclude that secondary reactions involving hydrogen atoms, such as reactions 2, 4, and higher homologs, are involved in the formation of hydrogen.

It is interesting to note that the isotopic distribution of hydrogen is not greatly shifted even when the reaction has yielded almost 5% hydrogen. This behavior must be contrasted with the mercury-sensitized photolysis of hydrocarbons, such as ethane-ethane- d_6 mixtures,¹⁹ in which mercury-sensitized exchange of the H_2 , HD, D_2 products occurs whenever the yield of product hydrogen approaches 1%. If the increased HD observed in Fig. 4 at 5% hydrogen yield is attributed to H_2 - D_2 mercury-photosensitized exchange starting to occur, the $^3\text{P}_1$ Hg quenching cross section

(15) A. Stock, "Hydrides of Boron and Silicon," Cornell University Press, Ithaca, N. Y., 1933.

(16) R. Doepker and G. J. Mains, *J. Am. Chem. Soc.*, **83**, 294 (1961).

(17) R. M. Noyes, *ibid.*, **81**, 566 (1959).

(18) H. Niki and G. J. Mains, unpublished results.

(19) J. Pirog and G. J. Mains, unpublished results.

of monosilane must be about five times that of ethane. However, in view of the fact that an appreciable fraction of the disilanes formed at this high conversion was $\text{Si}_2\text{D}_6\text{H}$, the validity of the assumption that the shift in H_2 , HD, D_2 distribution is due to mercury-photo-sensitized H_2 - D_2 exchange is in doubt.

Because the relative yield of D_2 in the experiments reported in Fig. 4 was five to ten times larger than that observed in analogous hydrocarbon systems,^{4,6,18} molecular elimination reactions, such as (1b) and (1d), could not be ruled out. Therefore, it was decided to add 4% ethylene to scavenge the atomic hydrogen in the SiH_4 - SiD_4 system. Thus, if reactions 1b and 1d were important, the isotopic distribution of hydrogen should be simply H_2 and D_2 . To the authors' astonishment, neither the yield nor the isotopic distribution of hydrogen changed. In order to confirm this observation, a series of experiments was performed in which the percentage of ethylene was varied. The results of these experiments are given in Fig. 5. It is clear that ethylene, effective in scavenging the hydrogen atoms produced in mercury-sensitized photolysis of hydrocarbons at concentrations below 0.1%, must be present in excess of 10%, to modify even slightly the distribution of hydrogen in silane systems. Furthermore, in the presence of 22% ethylene both HD and D_2 yields are reduced, whereas the H_2 yield is increased, implying the effect of ethylene is to compete with monosilane in quenching the excited mercury atom scavenger. These observations indicate that reaction 2 is much faster than reaction 6.

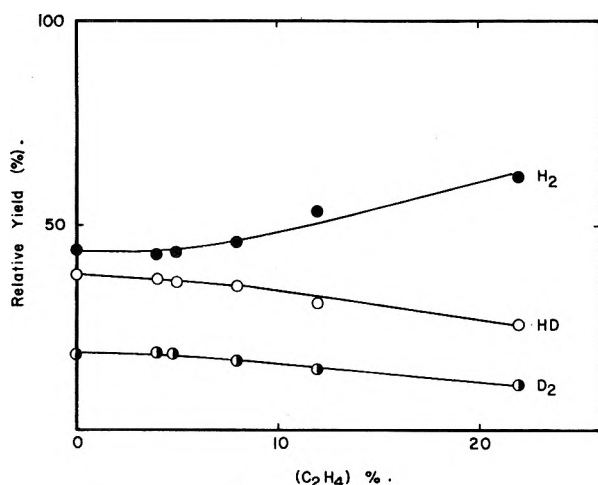


Figure 5. Effect of ethylene on the distribution of H_2 , HD, and D_2 in the mercury-sensitized decomposition of the equimolar mixture of SiH_4 and SiD_4 at 1 cm. pressure and 25° .

and, therefore, monosilane is a more efficient scavenger of hydrogen atoms than ethylene. The empirical equation of Spirin²⁰ predicts an activation energy of 0.5 kcal./mole for reaction 2, a value consistent with the observations reported here. A few experiments were performed in an effort to check the validity of the conclusion that reaction 2 is very rapid. In these experiments, the isotopic composition of the hydrogen evolved from the mercury-photo-sensitized decomposition of 10 cm. of isobutane containing 0.4 to 1.0 cm. of SiD_4 was studied. In these experiments the decomposition was less than 0.2%. The addition of SiD_4 reduced the total hydrogen yield to less than half the amount expected in the absence of monosilane. The isotopic composition of the gas was H_2 :HD: D_2 = 50:40:10 and was found to be essentially independent of initial composition over the range studied. The reason for the decrease in yield is not clear. It is possible that rapid attainment of a silicon polymer-silane photostationary state is responsible for the decreased quantum efficiency. Future studies planned in this laboratory will consider this problem. Regardless of the mechanistic explanation for the yield reduction, the presence of relatively large yields of HD and D_2 are *prima facie* evidence for participation of SiD_4 in the reaction system at relatively low concentrations. While it has not been established that this participation is exclusively *via* hydrogen atom reactions such as reaction 2, the authors are presently inclined to favor this explanation.

It is interesting to note that White and Rochow⁸ did not find any reaction with methane, ethane, propane, or isobutane when they illuminated mixtures of these alkanes with monosilane and mercury vapor. In view of the suggested rapidity of reaction 2, this observation is understandable. Future attempts to synthesize SiH_3R compounds from alkanes, RH, and monosilane should be carried out with the alkane in great excess. As noted in the Introduction, experiments such as these are part of this laboratory's program of study of the silanes.

Conclusions and Summary

The $^3\text{P}_1$ mercury-sensitized decomposition of monosilane yields hydrogen and higher condensation products, Si_2H_6 , Si_3H_8 , etc. As in the analogous hydrocarbon system, methane,⁵ the dimer, and trimer condensation products achieve a photostationary state. However, in the case of monosilane, the formation of large yields of polymeric silicon hydride with considerable metallic character is observed, whereas in the case

(20) Yu. L. Spirin, *Russ. J. Phys. Chem.*, **36**, 636 (1962).

of methane, high condensation polymers may be inferred from the material balance, but their yields are quite small. The polymeric silicon hydride was removed by the reactions of atomic hydrogen formed by $^3\text{P}_1$ Hg sensitization of hydrogen, indicating the polymeric silicon hydride does not extinguish the 2537-Å light even when it appears opaque to visible light.

The primary process(s) are uncertain but may involve the formation of several hydrogen atoms if the estimated high quantum yield of hydrogen is verified in future studies. Whether or not molecular hydrogen formation occurs could not be ascertained because it was not possible to scavenge the atomic hydrogen using very high concentrations of ethylene; therefore, the reaction between atomic hydrogen and monosilane was

presumed to be very rapid. This conclusion was supported by calculation of the activation energy and by experiments using SiD_4 -isobutane mixtures. This suggests that monosilane may find considerable future use as a hydrogen atom scavenger.

Acknowledgments. This research was supported by a contract from the U. S. Atomic Energy Commission and grateful acknowledgment is made thereto. We also wish to express our gratitude to Professor Alan MacDiarmid, University of Pennsylvania, for some early samples of monosilane and disilane and for advice in handling these compounds. Thanks are also due to Dr. Van Dyke for preparation of these samples, and to Mr. S. Wrbican for careful determination of the mass spectra of the product gases.

The Effects of Linear Energy Transfer in the Radiation-Induced Polymerization of Several Vinyl Compounds

by J. Fock, A. Henglein, and W. Schnabel

Hahn-Meitner-Institut für Kernforschung, Berlin-Wannsee, Germany (Received August 22, 1963)

The radiation-induced polymerization of styrene, methyl methacrylate, and vinyl acetate containing small amounts of triethyl borate has been studied. At the same absorbed dose rate, the rate of polymerization by the high LET particles from the reaction $B^{10}(n,\alpha)Li^7$ was found to be much lower than by γ -rays, while the average molecular weight of the polymer formed was higher. The results are explained by assuming that only free radicals in the tracks of fast δ -electrons are able to initiate long-chain polymerization. The fraction f of the energy of the heavy particles that is effective in producing polymerization amounts to 0.16 for styrene, 0.09 for methyl methacrylate, and 0.04 for vinyl acetate (if f is made equal to unity in the case of γ -rays). It is shown that f decreases with increasing radiation sensitivity ($G(R)$ value) of a monomer. The minimum kinetic energy of the δ -electrons which participate in the initiation of long-chain polymerization is calculated to be 170–240 e.v., depending on the nature of the monomer.

Introduction

In a recent paper,¹ an investigation of the polymerization of acrylonitrile containing 5 wt. % of triethyl borate under the influence of γ -rays and of thermal neutrons was reported. A very pronounced LET effect was found, since a 15 times higher absorbed dose of the He–Li particles from the nuclear reaction $B^{10} + n \rightarrow He^4 + Li^7$ was necessary to initiate the polymerization with the same rate as with Co^{60} γ -radiation. The average molecular weight of the polymer formed by heavy particle radiation was found to be higher than in the case of γ -rays at the same absorbed dose rate. These results were interpreted as a homogeneous polymerization of acrylonitrile, *i.e.*, the growing of the chains far away from the tracks of the He–Li particles. The failure of a large fraction of the absorbed heavy particle energy to initiate the polymerization could be understood if it is assumed that only fast δ -electrons are able to produce long chains of the polymer. Radicals which are formed within the main tracks of the He–Li particles are deactivated by mutual interaction before they reach any appreciable chain length. It could be calculated that as an average only those δ -electrons which have a kinetic energy exceeding 215 e.v. escape the tracks and initiate polymerization. It seems interesting to

compare these results with the classical work of Dale, Gray, and Meredith² on the deactivation of carboxypeptidase in aqueous solution by X- and α -rays. In this case, the low LET component of the α -rays was also found to be more effective than the primary particles.

Similar effects of the linear energy transfer of the radiation have now been observed in the polymerization of other monomers, such as styrene, methyl methacrylate, and vinyl acetate. The principal experimental procedure consisted of irradiating (a) the pure monomer by Co^{60} γ -radiation, (b) the monomer containing a few per cent of triethyl borate by γ -rays in order to study the influence of the additive on the polymerization, (c) the monomer containing triethyl borate by thermal neutrons from a nuclear reactor, and (d) the pure monomer in the same position in the reactor in order to correct the results from (c) for the contribution of the γ -background.

- (1) A. Henglein, J. Fock, and W. Schnabel, *Macromol. Chem.*, **63**, 1 (1963).
- (2) W. M. Dale, L. H. Gray, and W. J. Meredith, *Phil. Trans. Roy. Soc. London*, **A242**, 33 (1950).

Experimental

The details of the experimental procedures have been described in the earlier report and are therefore only briefly mentioned here. The γ -irradiations were carried out in the field of a Co^{60} source of 150 c. The neutron irradiations were carried out in the thermal column of the Hahn-Meitner-Institut nuclear reactor where the intensity of fast neutrons was negligible. All samples were surrounded by bismuth in order to decrease the intensity of the γ -background of the thermal column. As can be seen from Table I, the

Table I: Conditions in the Irradiation of Vinyl Acetate Containing 5 wt. % of Triethyl Borate in the Thermal Column of the Berlin Nuclear Reactor

Distance from core, cm.	Thermal neutron flux, (n./cm. ² sec.) $\times 10^{-9}$	Absorbed γ dose rate, rad./sec.	Absorbed He-Li dose rate, rad./sec.
127	10.7	0.59	58.2
132	8.97	0.39	48.8
141	3.25	0.23	17.6
146	2.07	0.08	11.3

absorbed dose due to the γ -background amounted to only a few per cent of the absorbed He-Li dose. In order to correct the observed rate of polymerization for the contribution of the γ -background, a sample containing the pure monomer without boron ester was also irradiated as described in the earlier report. The sample (1 cc.) was irradiated in an evacuated and sealed soft glass vessel. Since the boron content of the samples was rather low, the attenuation of the neutron flux amounted to less than 15% and the distribution of the neutron flux within the sample can be regarded as uniform. The absorbed dose rate was calculated from the relationship

dose rate (rad/hr.) =

$$5.77 \times 10^{-6} \frac{\phi(1 - e^{-\sigma N})E}{\rho} \quad (1)$$

where ϕ is the slow neutron flux in n./cm.² sec, σ the cross section of the $\text{B}^{10}(\text{n},\alpha)\text{Li}^7$ reaction (7.55×10^{-22} cm.²), N the number of boron atoms in 1 cc. of the sample, E the kinetic energy (2.35 Mev.) of the product nuclei of the nuclear reaction, and ρ the density of the sample. Both gold foil activation and the Fricke dosimeter containing boric acid³ were used to determine the thermal neutron flux. γ -Doses were determined with the normal Fricke dosimeter.

The polymers formed were separated by precipitation and their yields determined by a gravimetric method. The intrinsic viscosity was used as a measure of the average molecular weight. Viscosities were determined in methanol in the case of polyvinyl acetate and in benzene in the cases of polystyrene and polymethyl methacrylate.

Experimental Results

The rate of polymerization generally depends on the absorbed dose rate DR according to

$$r = k_1 \times \text{DR}^a \quad (2)$$

where a is a constant exponent over a wide range of the absorbed dose rate. A similar relationship is observed for the dependence of the average molecular weight of the polymer on the dose rate

$$\bar{M} = k_2 \times \text{DR}^{-b} \quad (3)$$

In order to determine the exponent a , the polymerization rate is plotted as a function of the absorbed dose rate in Fig. 1, 2, and 3. The data include the results obtained in the γ -irradiation of the pure and boron-containing monomers (\times , \circ) as well as the results of the He-Li irradiations already corrected for the contribution of the γ -background (\square). In the case of vinyl acetate, an exponent a of exactly 0.5 was obtained. This is as expected if the growing chains are deactivated by reactions among themselves. In the cases of styrene and methyl methacrylate, the slope of the curves decreases with increasing dose rate. This effect is well known and explained by the inefficiency of the monomer to scavenge all primary free radicals

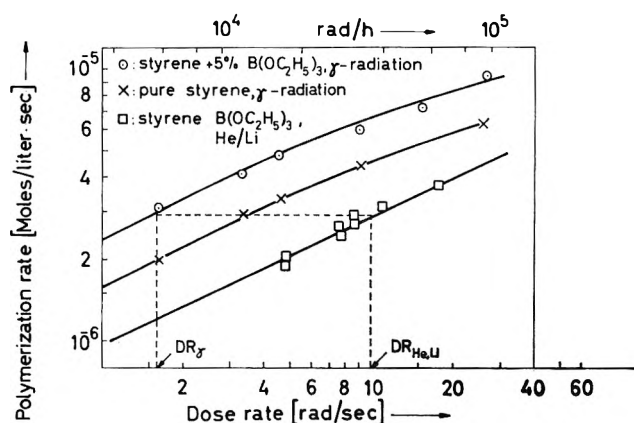


Figure 1. The rate of polymerization of styrene as a function of the absorbed dose rate by γ -rays and He-Li particles.

(3) R. H. Schuler and N. F. Barr, *J. Am. Chem. Soc.*, **78**, 5756 (1956).

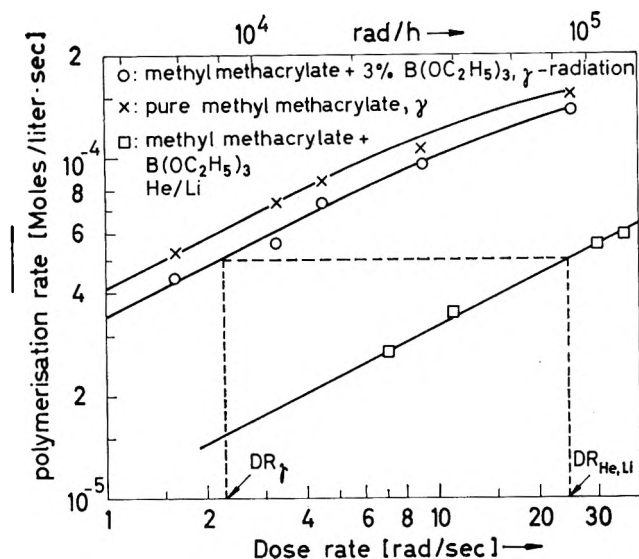


Figure 2. The rate of polymerization of methyl methacrylate as a function of the absorbed dose rate by γ -rays and He-Li particles.

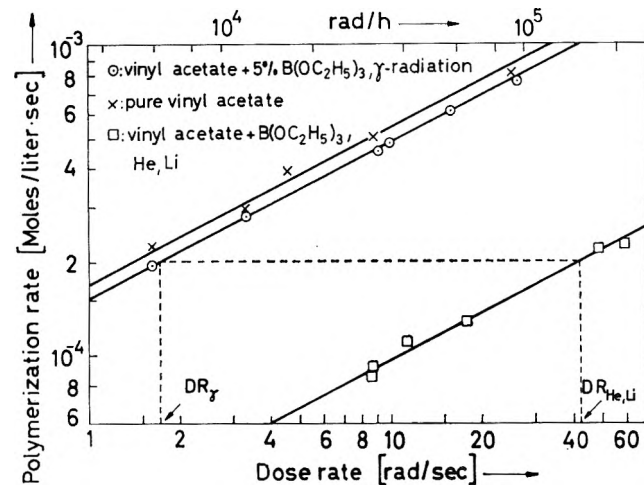


Figure 3. The rate of polymerization of vinyl acetate as a function of the absorbed dose rate by γ -rays and He-Li particles.

at high dose rates.⁴ The average of the slopes here amounts to about 0.4 over the dose range studied. The exponent a is found to have the same value in the γ and He-Li particle irradiation of each of the monomers studied.

The diagrams also show how the γ -polymerization is influenced by the addition of small amounts of triethyl borate. The rate of polymerization in styrene is strongly increased, which is not unexpected since the radiation stability of boron ester is much lower than that of the aromatic styrene molecule. The rate of polymerization of the two other monomers is slightly decreased by the addition of boron ester. Strictly

speaking, we are not investigating LET effects in pure monomers but in monomers containing small amounts of an additive. This difference is not significant in the cases of vinyl acetate and methyl methacrylate, but it is important in the case of styrene.

If a comparison is carried out at constant absorbed dose rate, it is found that the rate of polymerization always is smaller in the case of the He-Li particles than γ -rays. It is more convenient for the quantitative discussion to compare the dose rates DR_γ and $DR_{\text{He-Li}}$ which lead to the same rate of polymerization (see figures). The ratio f of these dose rates may be called the energy utilization of the He-Li particles with respect to the initiation of polymerization by γ -rays. The value of f is listed in Table II for the He-Li particle-induced polymerization of acrylonitrile as well as of the monomers mentioned in Fig. 1-3.

Table II: $G(R)$ Value (Number of Radicals Produced per 100 e.v. of Absorbed γ -Radiation), f -Factor (Energy Utilization), and W_1 (Minimum δ -Electron Energy) in the Polymerization of Various Vinyl Compounds by He-Li Particles

Monomer	$G(R)$	f	W_1
Styrene	0.69	0.16	170
Methyl methacrylate	5.5-11.5	0.09	205
Acrylonitrile	2.4-5.0	0.07	215
Vinyl acetate	9-12	0.04	240

The table shows that the f -factor is quite different for the monomers studied. The most pronounced LET effect (small value of f) was found to occur in vinyl acetate while the smallest difference in the rates of polymerization by γ and He-Li radiation was observed in styrene.

The intrinsic viscosities of the polymers formed in the experiments described by Fig. 1-3 are plotted vs. the absorbed dose rate in Fig. 4. It can be seen that the average molecular weight always decreases with increasing dose rate as is expected from eq. 3. The slope of the straight lines in Fig. 4, *i.e.*, the exponent b in eq. 3, has the same value for γ and heavy particle irradiation. In the cases of styrene and methyl methacrylate, the average molecular weight is considerably higher in the formation of the polymer by He-Li particles if the comparison is carried out at the same over-all absorbed dose rate. In the case of vinyl acetate, only a slight increase of the intrinsic viscosity

(4) A. Chapiro, "Radiation Chemistry of Polymeric Systems," Interscience Publishers, New York, N. Y., London, 1962, p. 163.

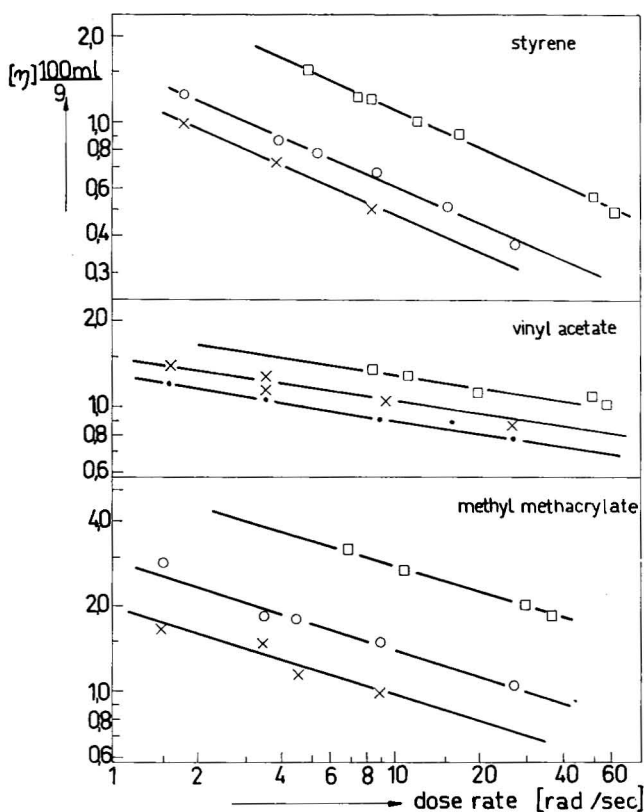


Figure 4. The intrinsic viscosity of the polymers formed by γ - and by He-Li radiation as a function of the absorbed dose rate: (X) pure monomer, γ -rays; O, monomer containing boron ester, γ -rays; \square , monomer containing boron ester, He-Li particles).

with increasing LET is observed. This may be due to the fact that the growing radicals are mainly deactivated by chain transfer in vinyl acetate.⁵

The effect of triethyl borate on the average molecular weight of the polymers formed by γ -irradiation is rather difficult to understand. For instance, the molecular weight of polystyrene is a little higher in the presence of 5 wt. % of the additive, although one would expect from the strong increase in the rate of polymerization (Fig. 1) that shorter chains are formed in the presence of triethyl borate. It seems, therefore, that the effect of triethyl borate on the rate of initiation is complex. However, the influence of the triethyl borate on the mechanism of the polymerization is not important in the comparisons between the effects of γ -rays and He-Li particles since the additive was present at the same concentration.

Discussion

If the growing chains are deactivated by chains or radicals originating from the same track of a high LET particle, the exponents a and b should be equal to 1.0 and 0, respectively. Furthermore, the average molec-

ular weight of the polymer would be expected to be much lower than in the case of γ -irradiation. Since a was found to be independent of the type of radiation and since the average molecular weight increases with decreasing dose rate and is higher than in the case of γ -irradiation, it must be concluded that the chains are growing and are deactivated far away from the tracks of the He-Li particles. In order to explain the low rate of polymerization at high linear energy transfer, the absorbed dose rate may be presented as the sum of the two terms $(DR_{\text{He-Li}} \times f) + (DR_{\text{He-Li}}(1 - f))$. The first term is the dose rate which effectively initiates long chain polymerization. It is identified as the rate of energy dissipation of the He-Li particle for the production of fast δ -electrons which sufficiently escape the tracks. The fraction $DR(1 - f)$ is the rate of energy dissipation within the main track of the particles. It is used to produce secondary electrons of less than about 100 e.v. of kinetic energy which cannot escape the tracks. If the dose rates for equal rates of polymerization by γ -rays and He-Li particles are compared, one obtains the relation

$$k_1 DR_\gamma^a = k_1 DR_{\text{He-Li}}^a f^a \quad (4)$$

from which it follows that

$$f = \frac{DR_\gamma}{DR_{\text{He-Li}}} \quad (5)$$

as already mentioned in the Experimental part.

This reaction mechanism, in a rather schematic way, postulates that only those free radicals will initiate long chains of polymerization which are formed in the δ -ray tracks. However, it may occasionally occur that a free radical produced in the main track escapes the interaction with another radical during the expansion of the track by diffusion and contributes to the formation of a chain that grows into the bulk of the liquid. The probability of this contribution will increase with decreasing linear free radical density along the track. This quantity, however, is determined by the radiation sensitivity of the monomer. The $G(R)$ value, *i.e.*, the number of free radicals produced per 100 e.v. of absorbed energy, may be taken as a measure of the radiation sensitivity. It must therefore be expected that there exists a relationship between the factor f and the $G(R)$ value of a vinyl compound, *i.e.*, f should become smaller with increasing free radical yield.

The relationship between f and $G(R)$ can be recognized from the data in Table II. $G(R)$ has been measured by various authors using different techniques

(5) L. Kuchler, "Polymerisationskinetik," Springer-Verlag, Berlin, 1951, p. 116.

such as the polymerization method or the consumption of dissolved DPPH.⁴ In some cases, the $G(R)$ values reported to date differ considerably. However, the predicted dependence of f on $G(R)$ is readily recognized from Table II.

The fraction of particle energy which is used to produce δ -electrons of kinetic energies between the upper value $W_{\max} = (4m/M)E$ and a lower value W_1 can easily be calculated by using the classical approximation of the energy transfer in a heavy particle-electron collision¹

$$\eta_{\delta} = \frac{1}{2} \frac{\ln W_{\max} - \ln W_1}{\ln W_{\max} - \ln I} \quad (6)$$

Here M and E are the mass and kinetic energy of the

heavy particle, m the electron mass, and I the average ionization potential of the stopping atoms (about 50 e.v. in organic materials). Since the initial kinetic energy of the He-Li particles amounts to about 1 Mev., a value for E of 0.5 Mev. may be taken as representative. By substituting η_{δ} in eq. 6 by the f -factor, W_1 can be calculated. This energy then may be interpreted as the minimum kinetic energy of a δ -electron to participate in the initiation of long-chain polymerization. Table II shows the value of W_1 calculated from the observed f -factor for several monomers. These numbers, of course, have only a formal meaning in terms of schematicized description of the tracks of a heavy particle. At least, they indicate the order of magnitude of the energy of secondary electrons necessary to initiate polymerization.

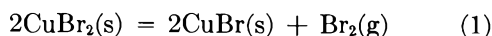
An Effusion Study of the Decomposition of Copper(II) Bromide

by R. R. Hammer and N. W. Gregory

Department of Chemistry, University of Washington, Seattle 5, Washington (Received August 26, 1963)

A torsion effusion study of the reaction $2\text{CuBr}_2(\text{s}) = 2\text{CuBr}(\text{s}) + \text{Br}_2(\text{g})$ leads to values of $\Delta H^\circ = 23.4$ kcal. and $\Delta S^\circ = 43$ e.u. at 298°K. Results are compared with earlier investigations at higher temperatures. The condensation coefficient for the process appears to be of the order of 0.1 at 50° and to decrease as the temperature increases. Apparent values for the activation enthalpies and entropies for the vaporization and condensation processes are calculated.

The decomposition of copper(II) bromide has been



studied by a number of investigators. Equilibrium pressures of bromine reach 1 atm. at *ca.* 280°. At this and lower temperatures, neither of the solid compounds has a vapor pressure which contributes significantly to the total equilibrium pressure in the system. No evidence to suggest that the two solids are significantly soluble in each other has been found. Equilibrium data have been reported by Jackson,¹ Shchukarev and

Oranskaya,² and Barret and Guenebaut-Thevenot,³ all of whom used a diaphragm gage technique in the temperature interval between 130 and 316°. The results are not in good agreement. Studies of the rate of decomposition have been made by Barret and co-workers.⁴

(1) C. G. Jackson, *J. Chem. Soc.*, **99**, 1066 (1911).

(2) S. M. Shchukarev and M. A. Oranskaya, *Zh. Obshch. Khim.*, **24**, 1926 (1954).

(3) P. Barret and N. Guenebaut-Thevenot, *Bull. soc. chim. France*, **409** (1957).

Extrapolation of existing data suggests that equilibrium bromine pressures for (1) should be in the effusion range around 70°. We have made an effusion study of the reaction to test further the applicability of the effusion method to this type of vaporization process^{5,6} and to extend the temperature range over which measurements have been made to increase the reliability of the thermodynamic constants indicated for the reaction. From the reported rate studies, the condensation coefficient is expected to be small; variation of effusion steady-state pressures with cell orifice dimensions may provide further information concerning the kinetics of the reaction.

Experimental

The torsion effusion apparatus has been described previously.⁷ Either a 1- or 2-mil tungsten wire, depending on orifice diameters, was used as a torsion fiber. The torsion constants were determined by calibration of the apparatus by measurement of the vapor pressures of zinc and mercury.⁸

CuBr₂ was prepared by reaction of Baker's reagent grade bromine and Baker's analyzed CuBr. The reactants were sealed in a thick-walled Pyrex tube; liquid bromine was held at a temperature which gave ca. 10 atm. bromine pressure and the copper bromides at the other end of the tube were held at 330° (for about 3 days). The bromine, previously dried over P₂O₅, was distilled into the initially evacuated reactor; in the distillation approximately the first and last 20% of the bromine was discarded. The CuBr was baked out at 400° under high vacuum for 8 hr. prior to the reaction. The product was a black crystalline material of relatively small particle size (ca. a few tenths of a millimeter average dimensions). This material was transferred to the effusion cells in a drybox. Cell orifices were temporarily sealed with Apiezon Q to keep moisture from the sample while mounting the cell on the torsion fiber. CuBr₂ samples were also prepared by evaporation of alcohol or of a water solution of Merck CuBr₂. This material was found to require long periods of drying before results similar to those from samples prepared under anhydrous conditions were obtained. Most of the measurements were made with the latter.

Preliminary studies showed that for relatively small samples, ca. 0.5 g. or less, steady-state effusion pressures rose as the cell temperature was increased, but after a constant temperature had been established, measured pressures dropped steadily with time. For larger samples, from 1 to 3 g., the steady-state pressures leveled off and remained constant and reproducible, in general until about 10% of the sample had decomposed, after which they began to decrease slowly. It is con-

cluded that these larger samples provided an effective surface area for the reaction which remained virtually constant in the initial stages of the decomposition. Steady-state pressures (which fell off with time) for the smaller samples were less than the time-independent level established with the larger samples. After appreciable amounts of CuBr₂ have decomposed, a number of complicating features arise which could account for the gradual fall-off, e.g., recession of the reacting surfaces into crevices and pores, changing condensation and/or vaporization coefficients, slow diffusion of bromine through layers of the reaction product, etc. The CuBr₂ prepared from solution, after being thoroughly dried, was found to maintain steady-state pressures (the same as those above the material prepared by direct bromination) for a somewhat longer time, until samples were about 15% decomposed.

All results quoted below represent steady-state effusion pressures from large samples in the time-independent region of a pressure vs. time curve. These pressures were found to be the same for different samples and to be reproduced when a given temperature was approached from either higher or lower values.

Effusion cells were cylindrical, ca. 4 cm. long, with cross-sectional areas and orifice areas indicated below. Orifices (two of nearly identical area) were placed about 1.5 cm. from the point of suspension at the center and were located on opposite sides near opposite ends of the cell. Orifice Clausing factors (included in the calibration) were virtually unity. Cells were suspended in a horizontal position with the solid sample distributed along the bottom.

Table I: Cell and Torsion Fiber Characteristics

Cell	Sum of areas of both orifices, $A_0 \times 10^4 \text{ cm.}^2$	$\frac{A_0 \times 10^4}{A_c}$	Torsion constant k , mm. radian ⁻¹ ($P = k\theta$)
1 (Quartz)	375	78	0.0232
2 (Pyrex)	71.5	9.8	0.0634
3 (Pyrex)	83.6	11.5	0.0616
4 (Pyrex)	20.9	2.4	0.0114

^a A_c is cell cross-section area. A 2-mil tungsten fiber, length 60 cm., was used for cells 1, 2, and 3; 1-mil fiber for cell 4.

- (4) P. Barret and R. Perret, *Bull. soc. chim. France*, 1459 (1957); P. Barret and L. Bonnetain, *ibid.*, 576 (1961); P. Barret and R. Perret, *Compt. rend.*, 248, 97 (1959).
- (5) E. Kay and N. W. Gregory, *J. Phys. Chem.*, 62, 1079 (1958).
- (6) R. R. Hammer and N. W. Gregory, *ibid.*, 66, 1705 (1962).
- (7) R. J. Sime and N. W. Gregory, *ibid.*, 64, 86 (1960).
- (8) Data for zinc were taken from results of R. F. Barrow, *et al.*; *Trans. Faraday Soc.*, 51, 1354 (1955); K. K. Kelley, U. S. Bureau of Mines Bulletin 385, 1935. Data for mercury from R. H. Busey and W. F. Giaque, *J. Am. Chem. Soc.*, 75, 806 (1953).

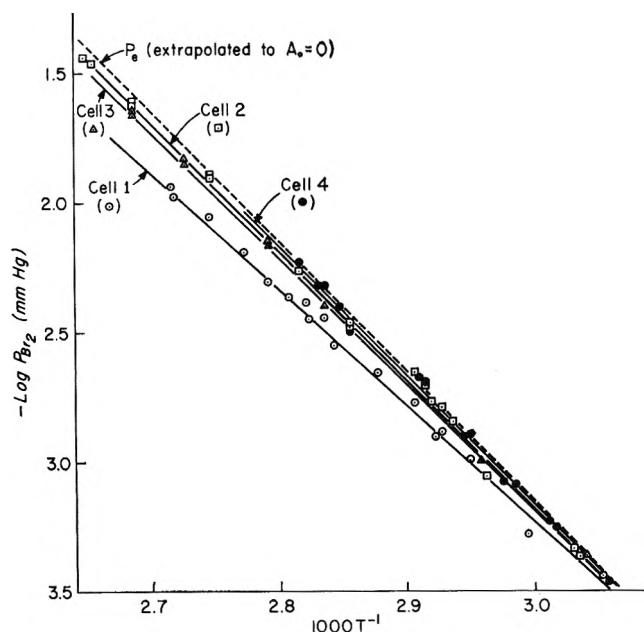


Figure 1. Effusion steady-state pressures for reaction 1.

Results and Discussion

Steady-state pressures were found to be dependent on effusion cell geometry. Independently, the data from each cell were found to correlate well with an equation of the form $\log P(\text{mm.}) = -AT^{-1} + B$, and are shown in Fig. 1. Values of the constants A and B in these equations, determined by least squares, and the standard deviations of $\log P$ are: cell, A , B , σ : 1, 4570, 10.48, 0.031; 2, 4987, 11.79, 0.025; 3, 4918, 11.57, 0.042; 4, 5020, 11.90, 0.023. The corresponding lines are shown on Fig. 1.

At each of the seven temperatures listed in Table II, steady-state pressures were calculated from the least-squares equations for each cell. These values were found to extrapolate to an apparent value of the equilibrium pressure for zero orifice area in a satisfactory fashion with the simple equation

$$P_e = P_s \left(1 + \frac{A_0}{\alpha A_s} \right) \quad (2)$$

where α is the condensation coefficient, the fraction of the molecules striking the reacting surface which condense, and A_s is the effective surface area. As has been pointed out by a number of authors,⁹ eq. 2 can only be expected to give a reasonable extrapolation if P_s is near the equilibrium pressure, *i.e.*, if α is not too small, and for proper cell designs. α and A_s must also be effectively constant at a given temperature. Equation 2 appears to be a satisfactory approximation for the time-independent steady-state pressures measured for the copper bromide system. Apparent values of

α , if A_s is taken as the cell cross-sectional area, are given in Table II.

Table II: Apparent Values of P_e and α for Reaction 1

$t, ^\circ\text{C.}$	$P_e \times 10^3, \text{mm.}$	$\alpha \times 10^2$
50	0.23	13
60	0.73	4.8
70	1.8	2.7
80	4.8	1.9
90	12	1.5
100	28	1.2
110	63	1.0

P_e values in Table II may be represented by the equation $\log P = -5056T^{-1} + 12.01$; the constants correspond to values of $\Delta H^\circ = 23.2$ kcal. mole⁻¹ and $\Delta S^\circ = 41.8$ e.u., mean values for the temperature range indicated.

The results of the various investigators are shown in Fig. 2. Independent second-law treatments of each set of data give the following values for ΔH° (kcal.) and ΔS° (e.u.) (Br_2 at 1 atm. taken as standard state) at mean experimental temperatures, respectively: 21.7, 38¹; 16.5, 28²; 19.3, 34³; this work, 23, 42. A third law correlation can be made using published free energy functions. Kelley and King¹⁰ recommend a value of S°_{298} for $\text{CuBr}(s)$, of 23.0 ± 0.2 , based on data

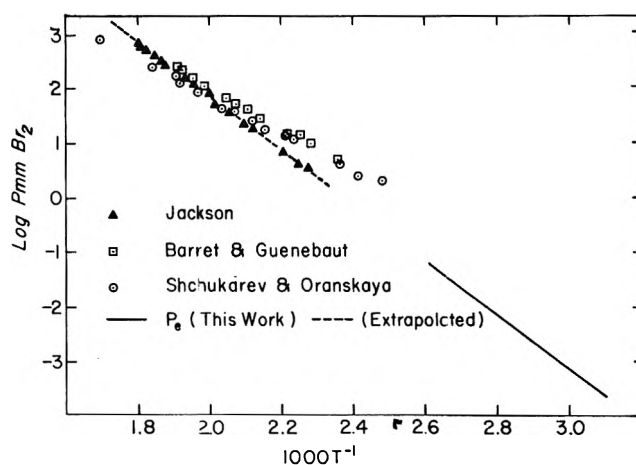


Figure 2. Comparison of the bromine pressures reported by various investigators.

(9) See, for example, K. Motzfeldt, *J. Phys. Chem.*, **59**, 139 (1955); L. Brewer and J. S. Kane, *ibid.*, **59**, 105 (1955); J. H. Stern and N. W. Gregory *ibid.*, **61**, 1226 (1957); G. M. Rosenblatt, *J. Electrochem. Soc.*, **110**, 563 (1963).

(10) K. K. Kelley and E. G. King, U. S. Bureau of Mines Bulletin 592, 1961.

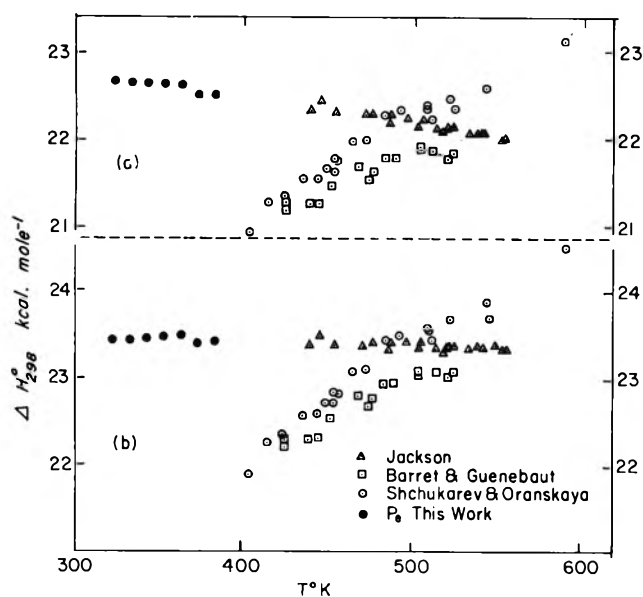


Figure 3. Third-law comparison of the results of various investigators: (a) using free energy functions for CuBr_2 estimated in ref. 14; (b) using free energy functions for CuBr_2 reduced by one unit from those in ref. 14.

of Hu and Johnston.¹¹ This value is slightly higher than the 21.9 e.u. given by Wagman, *et al.*,¹² based on earlier work. Lewis, Randall, Pitzer, and Brewer¹³ also give 23 e.u. and estimate that the free energy function $-(F^\circ - H^\circ_{298})/T$ is 24 for $\text{CuBr}_2(\text{s})$ at 500°K. Brewer, Somayajulu, and Brackett,¹⁴ in a general review of the thermodynamic properties of metal dihalides, estimate the corresponding free energy function for $\text{CuBr}_2(\text{s})$ as 32 at 298°K. and 34 at 500°K. These quantities may be combined with well known values for bromine and, by interpolation and extrapolation, used to evaluate ΔH°_{298} for (1) from ΔF° at each of the experimental temperatures of the various investigators. Results are shown in Fig. 3. For the particular choice of free energy functions cited, all sets of data show some temperature dependence (Fig. 3a). Our results and those of Jackson correlate very well if the entropy estimates for CuBr_2 are lowered by *ca.* one unit, Fig. 3b. In the latter case we obtain $\Delta H^\circ_{298} \pm 23.4$ kcal., in good agreement with 23.6 kcal. predicted from early determinations of heats of formation (Sabatier, Thomsen),¹² and $\Delta S^\circ_{298} = 43$ e.u.

The condensation coefficient appears to decrease with increase in temperature. From the slope of the line obtained by plotting $\ln \alpha$ vs. T^{-1} , the apparent enthalpy ΔH_c^* and entropy ΔS_c^* of activation (relative to the gas) for condensation are -6.4 kcal. and -26 e.u., respectively¹⁵; corresponding values for vaporization (relative to the solid) are $\Delta H_v^* = 17$ kcal. and $\Delta S_v^* = 4$ e.u. The enthalpy of activation for vaporization obtained in this manner is the same as that determined by Barret and Perret⁴ from free evaporation experiments. The area of their evaporating surfaces was not defined and hence their results cannot be used to estimate α for comparison with the present work.

It is to be recognized that the value of α given here was obtained by assignment of the cross-sectional area of the effusion cell as the effective area of the vaporizing and condensing surface. The actual value may well be larger and hence α may actually be smaller. The associated entropies of activation are similarly uncertain. The excellent correspondence of ΔH_v^* with results of free evaporation experiments suggests that this quantity is relatively insensitive to the magnitude of the surface area. It should also be kept in mind that the apparent values of α and its temperature dependence are characteristic of the system only in the region where the effusion steady-state pressures were independent of sample size and degree of decomposition (less than 10%). Under these conditions, however, α appears reasonably independent of the degree of decomposition, and extrapolation of effusion steady-state pressures to obtain equilibrium values appears quite satisfactory for the copper(II) bromide decomposition reaction.

Acknowledgment. Financial assistance for this work was received from the National Science Foundation.

- (11) J. Hu and H. L. Johnston, *J. Am. Chem. Soc.*, **74**, 4771 (1952).
- (12) D. D. Wagman, *et al.*, National Bureau of Standards Circular 500, 1952.
- (13) G. N. Lewis, M. Randall, K. S. Pitzer, and L. Brewer, "Thermodynamics," 2nd Ed., McGraw-Hill Publishing Co., New York, N. Y., 1961.
- (14) L. Brewer, G. R. Somayajulu, and E. Brackett, *Chem. Rev.*, **63**, 111 (1963).
- (15) N. W. Gregory, *J. Phys. Chem.*, **67**, 618 (1963).

The Gas Phase Reactions of Recoil Sulfur Atoms with Carbon Monoxide and Carbon Dioxide¹

by Edward K. C. Lee, Y. N. Tang, and F. S. Rowland

Department of Chemistry, University of Kansas, Lawrence, Kansas (Received September 3, 1963)

Recoil S^{35} atoms from the nuclear reaction $Cl^{35}(n,p)S^{35}$ have been produced in $CO-C_2F_4Cl_2$ and $CO_2-C_2F_4Cl_2$ gaseous mixtures. Carbonyl sulfide (OCS^{35}) has been isolated from each system by radio-gas chromatography. The reaction with CO_2 is probably initiated by an energetic species and accounts for about 2% of the total S^{35} . The reaction with CO is probably a scavenger reaction for thermal S^{35} atoms and accounts for as much as an estimated 85% of the total S^{35} production. The yield is greatly reduced in the simultaneous presence of O_2 and CO . The very high yield of OCS^{35} from CO systems indicates a convenient synthetic method of preparation for this labeled molecule.

Introduction

The sulfur atom created by the nuclear reaction $Cl^{35}(n,p)S^{35}$ has a recoil energy of about 31 kev.,² easily sufficient to break the atom loose from the original bonding environment of the Cl^{35} . This reaction is thus a good potential source for study of the atomic reactions of sulfur, complementing the studies carried out by other methods, *e.g.*, the photolysis of carbonyl sulfide ($O=C=S$).³⁻⁵ Comparisons of experimental results obtained with different sources of sulfur atoms should greatly facilitate the detailed understanding of the chemical reactions involved. The nuclear recoil atoms have the particular asset that they possess high kinetic energies and can perhaps undergo chemical reactions unavailable to atoms of lesser energy.

Recoil $Cl^{35}(n,p)S^{35}$ atoms have previously been studied in various solid phases, but gas phase experiments have been only briefly mentioned.² The $S^{34}(n,\gamma)S^{35}$ nuclear reaction has been used in gas phase experiments with sulfur-containing molecules.⁶

We have observed a large, anomalous radioactivity peak in the study of recoil tritium reactions with certain halocarbons, especially CF_3Cl , and have identified this activity as OCS^{35} . Since the radioactivity found as this compound represented an appreciable fraction of the total estimated S^{35} yield, it was apparent that a rather specific chemical reaction was involved. Furthermore, the freon-type molecules are easy to handle *in vacuo* and make good targets for neutron ir-

radiation, permitting advantageous gas phase experiments with recoil S^{35} atoms.

The study of gas phase high energy chemical reactions through nuclear recoil nuclides has been carried out extensively with several radioactive species, especially C^{11} , C^{14} , T , and the halogens.⁷⁻¹⁰ The current studies of S^{35} reactions are following the pattern established in these earlier hot atom experiments. In order to take advantage of the precision in analysis offered by radio-gas chromatography, these experiments have involved the study of the formation of OCS^{35} from S^{35}

- (1) This research was supported by U. S. Atomic Energy Commission Contract No. AT-(11)-407, and by fellowship support from the Pan American Petroleum Foundation (E. K. C. L.).
- (2) R. H. Herber, "Chemical Effects of Nuclear Transformations," Vol. 2, International Atomic Energy Agency, Vienna, 1961, p. 201.
- (3) O. P. Strausz and H. E. Gunning, *J. Am. Chem. Soc.*, **84**, 4080 (1962).
- (4) A. R. Knight, O. P. Strausz, and H. E. Gunning, *ibid.*, **85**, 1207 (1963).
- (5) A. R. Knight, O. P. Strausz, and H. E. Gunning, *ibid.*, **85**, 2349 (1963).
- (6) M. L. Hyder and S. S. Markowitz, UCRL-10,360-Revised' 1962.
- (7) M. Henchman, D. Urech, and R. Wolfgang, "Chemical Effects of Nuclear Transformations," International Atomic Energy Agency, Vienna, 1961, pp. 83, 99; F. S. Rowland, J. K. Lee, B. Musgrave, and R. M. White, *ibid.*, Vol. 2, p. 67.
- (8) A. P. Wolf, *ibid.*, Vol. 2, p. 3; C. Mackay, M. Pandow, P. Polak, and R. Wolfgang, *ibid.*, Vol. 2, p. 17.
- (9) J. Willard, *ibid.*, Vol. 1, p. 218.
- (10) E. Rack and A. Gordus, *J. Chem. Phys.*, **34**, 1855 (1961); *J. Phys. Chem.*, **65**, 945 (1961).

reactions with CO and CO₂. Freon-114 (1,2-dichlorotetrafluoroethane) has been used as the chlorine-containing target for the thermal neutron reaction.

Experimental

S³⁵ Production Rate. The S³⁵ production rate can be calculated as about 270 d.p.m. of S³⁵/min./cm.³ STP of target molecule for irradiation under our typical conditions,¹¹⁻¹³ approximately 20 times the rate observed for the S³⁴(n,γ) reaction for sulfur of natural isotopic abundance. Integral neutron doses of the order of 3 × 10¹⁴ n./cm.² produce conveniently measurable amounts of activity.

Chemicals. Freon-114, C₂F₄Cl₂ (Matheson Co.), was used without additional purification, except for degassing *in vacuo* at -196°. Carbon dioxide, carbon monoxide, and oxygen were used directly from the tanks. The stated purity of each gas is: CO, C.P. grade, 99.5% minimum purity; CO₂, Bone Dry grade, 99.8% minimum purity; C₂F₄Cl₂, 95.0% minimum purity; oxygen (Airco), 99% minimum purity.

Carbonyl sulfide was prepared for gas chromatographic calibration by treating KSCN with dilute sulfuric acid.¹⁴

Sample Preparation and Irradiations. All samples were prepared by the techniques developed for recoil tritium irradiations. The irradiation bulbs, made from 1720 Pyrex glass, had volumes of 10-15 ml. and were equipped with break-seals.

The samples were irradiated in the Lazy Susan facility of the TRIGA reactor of the Omaha VA Hospital at an ambient temperature of 20°. The nominal flux of 1.0 × 10¹¹ n./cm.²/sec. was reduced to 5.5 × 10¹⁰ n./cm.²/sec. by the B¹⁰ content of the Pyrex 1720 glass.¹⁵

Radio-gas Chromatography. The irradiated samples were stored for 3 weeks to allow decay of possible short-lived species and then were analyzed by radio-gas chromatography.¹⁶

Two gas chromatographic columns were used for separation of the various components. The activity peak emerged only shortly before the large macroscopic peak of C₂F₄Cl₂ on each column (DMS column: OCS at 42 min., C₂F₄Cl₂ at 44 min.; Safrole column: OCS at 58 min., C₂F₄Cl₂ at 62 min.). As with many halocarbons,¹⁶ C₂F₄Cl₂ acts as a quenching agent when macroscopic amounts are present in the counting volume. The tail of the OCS³⁵ peak was partially quenched in the DMS runs because of incomplete separation, and all quantitative measurements were made with the Safrole column.

The characteristics of these two g.l.c. columns are: (a) 50-ft. Safrole column, 30% by weight on firebrick,

0°, helium flow rate 0.48 ml./sec., (He + C₃H₈) flow rate, 1.43 ml./sec.; (b) 50-ft. dimethylsulfolane column, 30% by weight on firebrick, 24°, helium flow rate 0.43 ml./sec., (He + C₃H₈) flow rate, 1.05 ml./sec.

The irradiated sample bulbs were broken open within a vacuum line, and an aliquot (43%) of the contents was transferred to the gas chromatographic injection loop. After g.l.c. separation of the molecular components, propane was added to the helium flow gas to give a good proportional counting gas.¹⁶

The β-activity of S³⁵ (*E*_{βmax} = 0.167 Mev.) was measured by internal, flow, proportional counting, in the same counting arrangement used for tritium assay. For purposes of estimation of the per cent of total activity found as OCS³⁵, the counting efficiency was assumed to be 100% within the 85-ml. activity volume of the counter. Corrections were made for S³⁵ decay after irradiation; the loss of activity by recoil to the walls was assumed to be negligible for this recoil energy and the gas pressures involved.

Identification of Radioactivity as S³⁵. Although no other long-lived active isotope was expected in such yield from nuclear reactions with the known components, the counting system is indiscriminate and furnishes no check information on the identity of the radioactivity. Carrier carbonyl sulfide was added to one sample, and both it and its accompanying radioactivity were trapped from the g.l.c. flow stream with a liquid N₂ trap. The contents were chemically converted to BaSO₄,¹⁷ mounted on an aluminum planchet, and counted with a Sharp Low Beta counter. The subsequent decay curve confirmed the radioactivity as S³⁵, in a yield corresponding to that observed in the radio-gas chromatography.

Radiation Damage. Radiolysis will be caused in these samples by the general background level of irradiation and by the (n,p) reaction itself. No precise measurements are available about over-all per cent decomposition, but this level is less than 0.1% as measured by the appearance of minor peaks. The radiolysis problem is not completely negligible, however, for

(11) S³⁵: half-life 86.4 days¹²; thermal neutron cross section for Cl³⁵(n,p)S³⁵ = 0.30 ± 0.01 barn¹³; neutron flux, 5 × 10¹⁰ n./cm.²/sec.; assuming two Cl atoms per molecule.

(12) R. D. Cooper and E. S. Cotton, *Science*, **129**, 1360 (1959).

(13) H. Berthet and J. Rossel, *Helv. Phys. Acta*, **28**, 265 (1955); the value 0.17 ± 0.04 is frequently quoted.

(14) See J. W. Mellor, "A Comprehensive Treatise on Inorganic and Theoretical Chemistry," Vol. 5. Longmans, Green and Co., New York, N. Y., 1924, p. 972.

(15) E. K. C. Lee and F. S. Rowland, *J. Am. Chem. Soc.*, **85**, 897 (1963).

(16) J. K. Lee, *et al.*, *Anal. Chem.*, **34**, 741 (1962).

(17) See F. T. Treadwell and W. T. Hall, "Analytical Chemistry," Vol. 2, John Wiley and Sons, New York, N. Y., 1951, p. 690, for the procedure.

the presence of O_2 apparently facilitates radiolytic formation of CO_2 from CO and removal of CO_2 . These radiation chemistry conclusions are necessarily qualitative, since the experiments were not specifically designed for such studies. The per cent radiolytic effect on CO and CO_2 may be 10–15%, through preferential reactions of some radiolytic reactive species.

The recoil tritium studies in which OCS^{35} was first identified were carried out with CF_3Cl , CHF_2Cl , CH_2FCl , and CH_2Cl_2 . The amount of OCS^{35} found in each sample varied widely, but corresponded to >75% of the S^{35} produced in CF_3Cl , and about 50% with CHF_2Cl . None of these samples contained more than 0.1% CO or CO_2 , indicating that the scavenger action of very minor components must be quite substantial.

Results

A typical irradiation in these experiments created about 10^5 d.p.m. of S^{35} activity, which should be subsequently found distributed among various sulfur-containing species. Since the number of possible compounds is relatively large, and the gas chromatographic separations are not yet worked out ($S^{35}O_2$, $S^{35}CCl_2$, S^{35} -containing halocarbons, etc.), the initial studies have been limited to the measurement of OCS^{35} . Other active compounds of comparable volatility could have been observed, but none was found by our present experimental techniques. The observed yields of OCS^{35} from CO and CO_2 mixtures with $C_2F_4Cl_2$ are listed in Tables I and II.

Table I: $O=C=S^{35}$ Yields from Recoil S^{35} in $CO-C_2F_4Cl_2$ Mixtures

Sample no.	Pressures, cm.			Observed activity, ^a counts	Relative $O=C=S^{35}$ activity ^b	% yield ^b
	$C_2F_4Cl_2$	CO	O_2			
318	67.0	10.8	0	35,420 ± 200	2280 ± 20	85
319	69.6	7.6	0	29,270 ± 180	1680 ± 10	63
320	76.7	1.1	0	17,360 ± 140	866 ± 8	32
321	62.9	15.8	1.3	9920 ± 100	583 ± 6	22
322	72.2	6.5	1.3	2210 ± 60	103 ± 3	3.8
323	77.9	1.6	1.3	1290 ± 50	64 ± 3	2.4

^a Actual number of counts observed in the 85-ml. counter during the passage of the $O=C=S^{35}$ peak. ^b Relative activity, defined as 10^3 times d.p.m./min. of irradiation at 5.5×10^{10} n./cm.²/sec., per cm.³/cm. of $C_2F_4Cl_2$ pressure. If all of the calculated S^{35} activity appeared as $O=C=S^{35}$, the relative activity would be 2680. The relative activity has been obtained from the observed number of counts by corrections for: pressure of $C_2F_4Cl_2$, volume of bulb (11.1–13.3 ml.), irradiation time (59–63 min.), size of first aliquot (42.5–43.4%), and decay of S^{35} (22 to 29 days).

Table II: $O=C=S^{35}$ Yields from Recoil S^{35} in $CO_2-C_2F_4Cl_2$ Mixtures

Sample no.	Pressures, cm.			Observed activity, ^a counts	Relative $O=C=S^{35}$ activity ^b	% yield ^b
	$C_2F_4Cl_2$	CO_2	O_2			
315	63.4	10.5	0	1280 ± 50	86 ± 4	3.2
316	70.1	6.0	0	2500 ± 60	146 ± 2	5.5
317	76.1	1.1	0	2870 ± 70	152 ± 3	5.7
324	67.5	12.4	1.3	1020 ± 50	53 ± 3	2.0
325	74.9	4.5	1.3	890 ± 50	43 ± 2	1.6
326	76.5	2.2	1.3	1010 ± 50	47 ± 3	1.8

^{a, b} See footnotes *a* and *b* of Table I.

The ratio of CO or CO_2 to $C_2F_4Cl_2$ was varied in three samples each for an indication of relative efficiencies of reaction. A second set of three samples each with CO and with CO_2 was run in the presence of O_2 , on the plausible assumption that molecular oxygen might be a good scavenging agent for thermal S^{35} atoms.

The yields of OCS^{35} are quite high from CO -containing ampoules and have been estimated in the last column to account for as much as 85% of the total S^{35} production. These percentages have considerable uncertainty attached, because 100% is a calculated figure without independent experimental check. The neutron flux in the TRIGA reactor contains a large fast neutron component, for which the $Cl^{35}(n,p)S^{35}$ cross section approaches the thermal value,¹⁸ but no correction has been made. Accurate percentage calculations will require calibration of the S^{35} production rate for the neutron spectrum actually available in this reactor.

Discussion

Chemical Nature of the Reacting Sulfur Species.

While the radioactivity identifies with certainty the particular nuclide formed in the nuclear reaction, very little information is directly available about its precise properties at the time of chemical reaction. The charge state, electronic state, and kinetic energy are not definitely known *a priori*, but must be deduced from the experiments themselves.

The extensive measurements made with recoil tritium atoms have assumed that the observed chemical reactions are those of a neutral, ground-state atom with excess kinetic energy.^{7,8} However, the especially favorable circumstances for tritium (ionization potential > I.P. of most target compounds; first excited

(18) The cross section is given as 125 mbarns for 14-Mev. neutrons in D. L. Allan, *Nucl. Phys.*, **24**, 274 (1961).

electronic state > 10 e.v.) are not found in the case of atomic sulfur.

The initial charge state of the S^{35} formed by this (n,p) reaction is not completely certain. Ionization of a moving atom by virtue of its own high velocity can be crudely estimated from the relative velocities of the atom and its bound electrons.¹⁹ This calculation is often summarized by the rough rule-of-thumb that ionization begins when the recoil energy in kilovolts equals the mass in atomic mass units—the S^{35} atom is in the borderline region for which ionization cannot automatically be either excluded or assumed, although most of the atoms probably do not ionize.¹⁹

The ionization potential of the free S atom is 10.36 e.v.²⁰ and the neutralization of S^+ by reaction with other molecules will be endothermic in many materials, including all of those used in the present experiments.²¹

The ground state of the neutral sulfur atom is 3P_2 , with the 3P_1 and 3P_0 states about 1130 and 1640 kcal./mole higher.²⁰ Two more electronic states also need to be considered, 1D_2 at 26,390 kcal./mole and 1S_0 at 63,370 kcal./mole above the ground state. Some of the reactions of photolytically produced sulfur atoms (see below) have chemical behavior characteristic of singlet reactants and are assumed to involve 1D atoms.^{4,5}

The available evidence from spectroscopy and mass spectrometry thus suggests that the neutral species (3P , 1D , 1S) and S^+ (perhaps in various electronic states) cannot be readily eliminated from consideration as at least partial contributors to the observed reactions of recoil S^{35} .

Thermochemistry of OCS Reactions. The over-all reactions leading to the formation of OCS^{35} in these systems are reactions 1 and 2 if the initiating species is neutral.



The values of ΔH for these reactions are 67.2 kcal./mole endothermic for (1) and 59.6 kcal./mole exothermic for (2), with all species in the respective ground states.²² The ionic equation corresponding to (1), as given in eq. 3, is even more endothermic (142 kcal./mole) because of the differences in ionization potential.



Reactions of Energetic Atoms. The direct reaction of S^{35} atoms with CO_2 , as given in eq. 1 is sufficiently endothermic to eliminate it from consideration except as a reaction initiated by energetic atoms. The two chief possibilities are that (a) the reacting S^{35} species is in the 1S electronic state, thereby almost entirely

accounting for the energy deficit through the electronic excitation; or (b) the sulfur atom possesses extra kinetic energy sufficient to balance the energetics. Current interpretations of recoil tritium experiments suggest that even larger amounts of kinetic energy (5 e.v.) are possessed by some of the tritium atoms as they enter the bond-forming reaction.¹⁶

Experimentally, the OCS^{35} yields obtained from CO_2 - $C_2F_4Cl_2$ mixtures suggest the existence of such an energetic atom reaction, especially since the yields are relatively little affected by the introduction of O_2 into the system. Neither, however, is the OCS^{35} yield appreciably affected by the concentration of CO_2 in the gas mixture. The latter observation is compatible with the existence in the system of an energetic sulfur atom species, which is basically unreactive toward $C_2F_4Cl_2$, but which reacts readily with CO_2 according to eq. 1. The distinction between electronic excitation (1S) and excess kinetic energy (3P or 1D) cannot readily be made from the present experiments. Kinetically excited S atoms would be expected to lose energy rather rapidly in collisions with $C_2F_4Cl_2$, and hence not be "unreactive" in the sense required above. Electronically excited S atoms, however, might also be expected to be converted rapidly to 3P or 1D by collision, and hence also not be "unreactive." If the atom in either case is able to maintain its excess energy through about 10 or 20 collisions, then the observed experimental results can be rationalized. The chemical characteristics of S atoms in the 1S state, for which eq. 1 is only 3.8 kcal./mole endothermic, are totally unknown, so that it is not possible at present to ascertain independently its reactivity toward $C_2F_4Cl_2$. The approximately 2% yield of OCS^{35} may arise either from a specific reaction of a 2% fraction of atoms in this excited state, or as one of the products of reaction of a larger component of the total S^{35} atom flux.

The increase in OCS^{35} with decreasing CO_2 concentration in O_2 -free samples may include partial contributions from the reactions of S^{35} with small amounts of radiolytic CO .²³ The qualitative side observations

(19) See ref. 2; the calculated electron velocity is about 20% of the atomic velocity.

(20) Ionization potentials: O, 13.61 e.v.; S, 10.36 e.v.; data from "Atomic Energy Levels," N.B.S. Circular 467. Vol. 1, 1949.

(21) Ionization potentials: CO, 14.01 e.v.; CO_2 , 13.79 e.v.; O_2 , 12.2 e.v.; $C_2F_4Cl_2$, est. 12 e.v., from CCl_2F_2 , 11.8 ± 0.5 e.v., and $CClF_3$, 12.8 ± 0.2 e.v.; data from F. H. Field and J. L. Franklin, "Electron Impact Phenomena," Academic Press, New York, N. Y., 1957.

(22) ΔH_f values obtained from "Selected Values of Chemical Thermodynamic Properties," N.B.S. Circular 500 1952: S, 53.25 kcal./mole; O, 59.16; CO, -26.42; CO_2 , -94.05; OCS, -32.80.

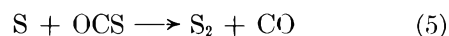
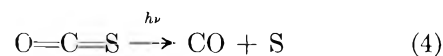
in the recoil tritium systems suggest that the scavenging reaction is quite efficient with trace components and hence difficult to regulate. The O_2 concentration in the other samples should be sufficient to divert the S^{35} atoms away from any CO impurity.

Scavenging Reaction of CO. The data of Table I show that recoil S^{35} is very efficiently converted to OCS^{35} in the presence of CO, presumably by reaction 2. The very high yields of labeled carbonyl sulfide indicate that the atomic sulfur species involved cannot react very efficiently with $C_2F_4Cl_2$, the major constituent of each sample. A similar statement can be made about CF_3Cl from our experiments, and has been made about SF_6 for S^{35} atoms formed through the $S^{34}(n,\gamma)$ nuclear reaction.⁶ Certainly, there is no insertion reaction into C-F and C-Cl bonds in these experiments that can approach the efficiency of 1D sulfur atom insertion into C-H bonds.^{4,5}

Reaction 2 is quite exothermic and requires eventually a third body collision for stabilization of the product. If extra kinetic or electronic energy were available, the molecule would be still more excited, and a faster decomposition rate could be anticipated, leading to the back reaction of eq. 2. Very probably, reaction 2 occurs primarily with thermal S^{35} atoms and illustrates an efficient method of scavenging these atoms to form a readily measured product.

An estimate of relative reaction efficiencies can be made by comparison of the percentage OCS^{35} yields vs. O_2 and CO concentrations. The OCS^{35} yield is rapidly diverted or suppressed by the O_2 , even when its concentration is much lower than that of CO. If this change is entirely attributed to the greater efficiency of reaction per O_2 collision than in CO collisions, a factor of about 10-20 is indicated, favoring reaction with O_2 . In view of the possible complexities in these systems (*e.g.*, radiation effects), other factors are likely also to be affecting these percentage yields.

Comparison with Photolytic S Atoms. Sulfur atoms have been produced from the photolysis of gaseous OCS by several groups of experimenters,^{3-5,24,25} and possibly analogous reactions have been known for nearly a century.²⁶ The scavenging reaction of eq. 2 was found to be negligible following photolysis of OCS at 228 $m\mu$, under the experimental conditions involved.²⁴ However, the mechanism for this photolysis reaction has been suggested to include reactions 4 and 5 as the first two steps.²⁵



Reaction 5 is not possible in our experiments since the OCS^{35} is present only in carrier-free tracer levels. The successful observation of a scavenger-type reaction in our system implies that competitive reactions similar to (5) must be nearly absent.

The recent observation of characteristic singlet reactions (insertion in cyclopropane and several alkanes to form mercaptans) have been convincingly interpreted as the reactions of photolytic sulfur atoms in the 1D state.^{4,5} Comparable experiments are now being carried out with recoil S^{35} as an aid to identification of the reactive S forms present in our systems.

Applications to Other Experiments: Synthesis of OCS^{35} ; Fast Separations in Nuclear Chemistry. The very high yields of carrier-free OCS^{35} obtained in CO scavenged chlorocarbons suggest that useful syntheses of this labeled molecule can be simply performed. None of these experiments has been carried out in high flux to determine the possible limits to the total activity available by such a technique; high *specific* activity seems assured, however, for both of the molecules required should be obtainable free from sulfur-containing impurities to a very high degree.

The high total yield of S^{35} activity in a simple, readily separable gaseous compound implies that these reactions can be used for very rapid isolation of sulfur radioactivities in nuclear chemistry problems. Carbon monoxide scavenging of tellurium and selenium isotopes seems quite likely to give $OCTe$ and $OCSe$ and could be useful for fast separations of short-lived fission products.

Acknowledgment. The neutron irradiations were carried out with the kind cooperation of the reactor staff of the Omaha Veterans Administration Hospital.

(23) Radiolysis of CO_2 leads to CO formation. See, for example, P. Harteck and S. Dondes, *J. Chem. Phys.*, **23**, 902 (1955); **26**, 1727 (1957).

(24) G. S. Forbes and J. E. Cline, *J. Am. Chem. Soc.*, **61**, 151 (1939).

(25) V. Kondratiev, *Acta Physicochim. URSS*, **16**, 272 (1942).

(26) G. Chevrier, *Compt. rend.*, **69**, 136 (1869). A mixture of sulfur vapor and carbon monoxide was sparked, with carbonyl sulfide reported as a product.

On the Viscosity of Branched Polymers Produced by High-Energy Irradiation

by J. G. Spiro,¹ D. A. I. Goring, and C. A. Winkler

Department of Chemistry, McGill University, and Physical Chemistry Division, Pulp and Paper Research Institute of Canada, Montreal, Canada (Received September 3, 1963)

Statistical calculations of the intrinsic viscosity of irradiated polymers were extended to study the effects of branching on $[\eta]$. It has become possible to test several theories by comparing calculated and experimental values of $[\eta]$ as a function of dose. It is concluded that formulas derivable from the Flory-Fox and Debye-Bueche treatments overestimate the influence of branching on viscosity. Zimm and Kilb's approximation gave good agreement with experimental data for solutions of irradiated polymers in poor solvents, while for solutions in good solvents the Stockmayer-Fixman treatment appeared to be better. Although the statistical treatment used was, in principle, limited to polymers of initially random distribution, experimental results obtained for irradiated samples of narrow distribution polystyrene indicate that the effect of molecular weight distribution is small. The fact that none of the above mentioned theories can explain the hydrodynamic behavior of branched molecules in solvents of different types is attributed to the inadequacy of the radius of gyration as a measure of hydrodynamic radius.

Introduction

A convenient technique for obtaining randomly branched polymers under controlled conditions is high-energy irradiation of certain linear polymers. Although samples prepared in this manner are polydisperse, the number and distribution of branch units are governed by statistical laws, permitting a detailed mathematical analysis of the changes which take place under irradiation. In particular, a considerable amount of theoretical work has been done to explain the variation of intrinsic viscosity ($[\eta]$) with dose in polymers cross linked by irradiation.²⁻¹⁰ The pertinent mathematical treatments have been based on several different theories concerning the effects of branching on $[\eta]$. However, the individual treatments differ not only in the suggested formulas for g' , the ratio of the intrinsic viscosity of a given branched molecule to that of a linear molecule having the same molecular weight, but also in the various approximations and statistical methods used. Moreover, since most of the calculations apply in principle only to polymers of the most probable distribution, it has been suggested⁶ that conclusions based on comparing theoretical and

experimental values of the intrinsic viscosity are of doubtful value when the molecular weight distributions of the samples used are not determined with some accuracy before irradiation. Hence, it has not yet been possible to reach clear conclusions about the effect of branching on polymer viscosity from the study of irradiated samples.

In the present work, the versatile statistical methods of Saito³ and Katsuura⁷ have been applied to some of the more important theories which correlate $[\eta]$ with branching. Strictly speaking, the equations used are valid only for polymers of initially random distri-

- (1) Mellon Institute, Pittsburgh, Pa.
- (2) (a) P. Y. Feng and J. W. Kennedy, *J. Am. Chem. Soc.*, **77**, 847 (1955); (b) A. R. Shultz, P. I. Roth, and G. B. Rathmann, *J. Polymer Sci.*, **22**, 495 (1956).
- (3) O. Saito, *J. Phys. Soc. Japan*, **13**, 1465 (1958).
- (4) M. Inokuti, *ibid.*, **14**, 79 (1959).
- (5) M. Inokuti and K. Katsuura, *ibid.*, **14**, 1379 (1959).
- (6) R. W. Kilb, *J. Phys. Chem.*, **63**, 1838 (1959).
- (7) K. Katsuura, *J. Phys. Soc. Japan*, **15**, 2310 (1960).
- (8) M. Dole, *J. Phys. Chem.*, **65**, 700 (1961).
- (9) A. M. Kotliar and S. Podgor, *J. Polymer Sci.*, **55**, 423 (1961).
- (10) A. M. Kotliar and S. Podgor, *ibid.*, **62**, S177 (1962).

bution. However, as will be shown later, there is strong evidence that the effect of initial distribution is negligible and that the computational technique used will be generally applicable to radiation-induced cross-linking processes.

Theory

For monodisperse linear polymers the intrinsic viscosity is given by the empirical relationship

$$[\eta] = KM^a \quad (1)$$

where K and a are constants and M is the molecular weight. Then, since $[\eta]$ is a weight average quantity, the value of $[\eta]$ for polydisperse linear polymers is given by

$$[\eta] = \frac{\sum_i [\eta]_i M_i n(M_i)}{\sum_i M_i n(M_i)} = K \frac{\sum_i M_i^{a+1} n(M_i)}{\sum_i M_i n(M_i)} \quad (2)$$

where M_i and $[\eta]_i$ are the molecular weight and intrinsic viscosity, respectively, of the i th species, and $n(M_i)$ is the number of molecules of molecular weight M_i .

When the intrinsic viscosity of cross-linked systems is calculated, the $[\eta]_i$ values of eq. 2 cannot be obtained directly from eq. 1. Statistically, however, the ratio of the viscosities of linear and branched molecules of equal molecular weight (g') depends only on the number of branches. Thus

$$[\eta]_{i,br} / [\eta]_{i,lin} = g'(m) \quad (3)$$

where m is the number of cross links and $g'(m)$ is the average value of g' for randomly branched molecules containing $2m$ cross-linked units. Moreover, if a relation can be found between the number of branch units and the average radius of gyration, then eq. 3 can be written as

$$[\eta]_{i,br} = [\eta]_{i,lin} \varphi(g) \quad (4)$$

where $g = g(m)$ is the ratio of the mean-square radii of the branched and unbranched molecules, and $\varphi(g) = \varphi[g(m)] = g'(m)$ is a function relating the hydrodynamic behavior to the radius of gyration. It is usually assumed that the value of g for a given species is largely independent of the solvent used. Accordingly, in computations of $[\eta]$, g is customarily replaced by g_θ , the random flight (θ -solvent) ratio of mean-square radii.

The intrinsic viscosity of the cross-linked system may then be expressed as

$$[\eta] = \frac{K \sum_m \sum_i \varphi(g) M_i^{a+1} n(M_{i,m})}{\sum_m \sum_i M_i n(M_{i,m})} \quad (5)$$

where $n(M_{i,m})$ is the number of molecules of molecular weight M_i which contain m cross links.

In the present work the following expressions for $\varphi(g)$ were considered

$$\varphi(g) = g^{1/2} \quad (6)$$

$$\varphi(g) = g^{2-a} \quad (7)$$

$$\varphi(g) = g^{1/2} \quad (8)$$

$$\varphi(g) = h^3 \quad (9a)$$

where

$$h = \sqrt{f}[2 - f + \sqrt{2}(f - 1)]^{-1} \quad (9b)$$

$$g = (3f - 2)/f^2 \quad (9c)$$

In eq. 9a, h is the ratio of the effective hydrodynamic radius of the branched molecule to that of the linear molecule of equal molecular weight, and it may be related to g through eq. 9b and 9c. In the latter equations, f is the number of branches of a given cruciform molecule, and g is the ratio of the mean-square radius of this molecule to that of a linear molecule of the same molecular weight.

Equations 6 and 7 correspond, respectively, to the direct application of the Flory-Fox¹¹⁻¹³ and Debye-Bueche¹⁴ theories to branched polymers, while eq. 8 was recently proposed by Zimm and Kilb.¹⁵ The use of eq. 9a, 9b, and 9c was suggested by Stockmayer and Fixman,¹⁶ on the basis of their calculation of the friction constant of cruciform molecules.

Computations of the intrinsic viscosity of irradiated polymers were made by the technique of Katsuura, based on eq. 5 and the mathematical treatments of Saito³ and Katsuura.⁷ While Katsuura's computations were limited to use of the $\varphi(g) = g^{2-a}$ correction factor for branching, his technique is applicable whenever the dependence of g' on the number of branch units can be described in terms of exponential functions.

The various theories under consideration give g' as a function of g , rather than directly as a function of the number of cross links in a given molecule, and therefore it was first necessary to compute g (i.e., g_θ) for a number of values of m . Katsuura calculated g from the theoretical results of Kataoka,¹⁷ however Zimm

(11) P. J. Flory, *J. Chem. Phys.*, **17**, 303 (1949).

(12) T. G. Fox, Jr., and P. J. Flory, *J. Phys. Chem.*, **53**, 197 (1949).

(13) P. J. Flory and T. G. Fox, Jr., *J. Am. Chem. Soc.*, **73**, 1904 (1951).

(14) P. Debye and A. M. Bueche, *J. Chem. Phys.*, **16**, 573 (1948).

(15) B. H. Zimm and R. W. Kilb, *J. Polymer Sci.*, **37**, 19 (1959).

(16) W. H. Stockmayer and M. Fixman, *Ann. N. Y. Acad. Sci.*, **57**, 334 (1953).

and Stockmayer's model¹⁸ appears to be more appropriate for highly branched molecules.

For tetrafunctionally branched molecules of random branch lengths Zimm and Stockmayer obtain

$$g(m) = \frac{3m!(2m+2)!}{(3m+3)!} \sum_{\nu=0}^m \binom{2m+\nu+2}{\nu} \quad (10)$$

the asymptotic form of which for large m is

$$g(m) \cong \frac{1}{2} \sqrt{\frac{3\pi}{m}} - \frac{2}{3m} \quad (11)$$

(Zimm and Stockmayer were able to simplify eq. 10 somewhat, but the alternative expression is not advantageous when digital computers are used.)

The formula of Kataoka corresponding to eq. 10 and 11 is

$$g(q) = \frac{3q^3 + 9q^2 - 18q + 8}{q(3q-1)(3q-2)} \quad (12)$$

where $q = m + 1$.

The two methods give similar or even identical results for low degrees of branching. However, as m increases, an increasing discrepancy is found between the two treatments. In the limit of an infinite number of branches, eq. 12 leads to $g = 1/3$, while the asymptotic equation of Zimm and Stockmayer (eq. 11) indicates that $\lim_{m \rightarrow \infty} g(m) = 0$. To evaluate the importance of differences between the two treatments, both methods of calculation were used in the present work.

Values of the correction factors $\varphi(g)$ were calculated for 40 different values of m , ranging from 0 to 115. In computations based on Zimm and Stockmayer's equations, the asymptotic formula was used for $m \geq 20$. The $\varphi(g) = \varphi[g(m)]$ functions (hereafter denoted merely by g') were expanded into sums of exponential functions of m by iterative least-squares analysis, using a modified form of a recently published computer program for the analysis of exponential growth and decay processes.¹⁹

Computations, including the numerical integrations involved in Katsura's technique, were made on the IBM 1410 computer of the McGill University Computer Center. The heavy burden on machine time limited somewhat the number of computations that could be made, but sufficient data were obtained to provide the information sought.

Results

I. Examination of Published Data. In Fig. 1 to 3, changes in the intrinsic viscosity on irradiation, as calculated on the basis of several theories, are compared with the experimental data of Shultz and col-

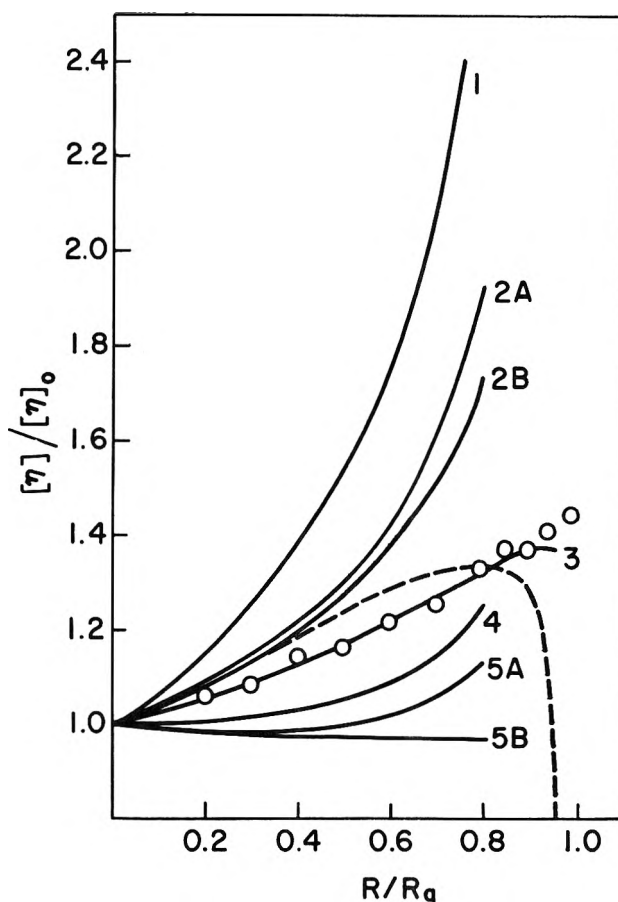


Figure 1. Comparison of experimental data for irradiated polystyrene in toluene, obtained by Shultz, *et al.*,^{2b} and theoretical curves, calculated from various equations proposed to describe the effects of branching on $[\eta]$. The theoretical curves were computed by assuming $\alpha = 0.74$ and $\beta/\alpha = 0.35$. For curves 2A, 4, and 5A, g -values were obtained from the formula of Kataoka (eq. 12), for curves 2B, 3, and 5B Zimm and Stockmayer's formulas (eq. 10 and 11) were employed. The following correction factors for branching were considered: curve 1, no correction [$g' = 1$]; curves 2A and 2B, $g' = g^{1/2}$; curve 3, $g' = h^3$; curve 4, $g' = g^{1.26}$; curves 5A and 5B, $g' = g^{3/2}$. The dashed curve represents the theoretical results of Shultz, *et al.*

laborators^{2b} and Kilb.⁶ Radiation doses (R) are expressed as fractions of the gelling dose, R_g . As mentioned in the Introduction, the computations apply, in principle, only to samples of initially random distribution. It may be assumed that, similarly to the dimethylsilicone fluid irradiated in Kilb's experiments,

(17) S. Kataoka, mimeographic circular on chemical physics in Japanese, *Busseironkenkyu*, **66**, 102 (1953); quoted in ref. 7.

(18) B. H. Zimm and W. H. Stockmayer, *J. Chem. Phys.*, **17**, 1301 (1949).

(19) P. C. Rogers, "FRANTIC Program for Analysis of Exponential Growth and Decay Curves," Technical Report No. 76, Massachusetts Institute of Technology, Laboratory for Nuclear Science, June, 1962.

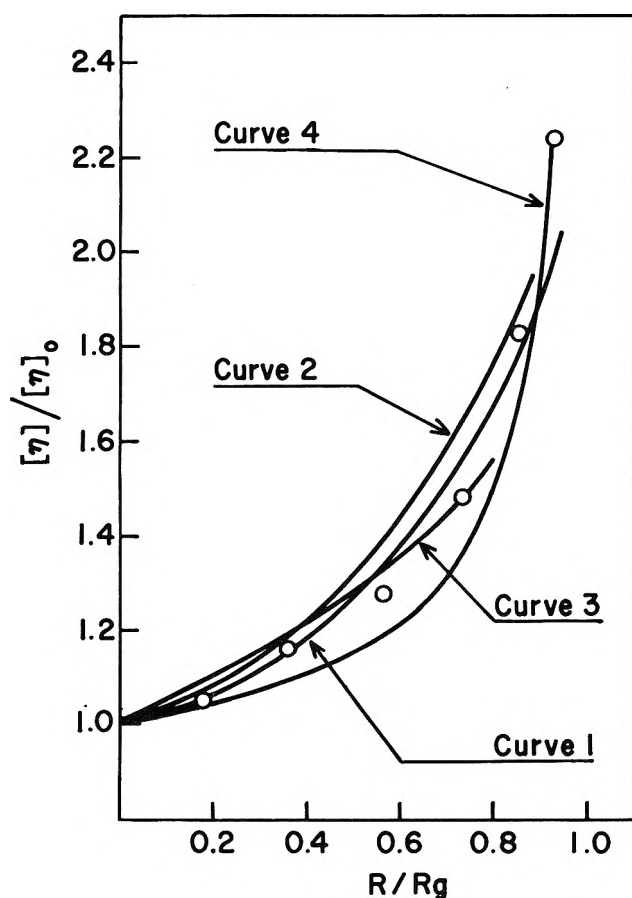


Figure 2. Comparison of experimental data for irradiated dimethylsilicone in toluene, obtained by Kilb,⁶ and theoretical curves, calculated from various equations proposed to describe the effects of branching on $[\eta]$. For the calculation of curves 1, 2, and 3, g -values were obtained from the formulas of Zimm and Stockmayer (eq. 10 and 11), for curve 4 Kataoka's formula (eq. 12) was employed. The following parameters and correction factors for branching were used: curve 1, $a = 0.79$, $\beta/\alpha = 0.75$, $g' = g^{1/2}$; curve 2, $a = 0.74$, $\beta/\alpha = 0.35$, $g' = g^{1/2}$; curve 3, $a = 0.79$, $\beta/\alpha = 0.0$, $g' = h^3$; curve 4, $a = 0.79$, $\beta/\alpha = 0.0$, $g' = g^{1.21}$.

Shultz's polystyrene samples satisfied this criterion reasonably well.

The most extensive calculations were made with the parameters of Shultz and collaborators. In their experiments, the extent of degradation was determined to be $\beta/\alpha = 0.35$, where β/α is the number of main chain scissions per cross-linked unit formed. The exponent a of the Mark-Houwink equation (eq. 1) was taken to be 0.74, as quoted by Shultz, *et al.* In Fig. 1, the data of curves 2A, 4, and 5A were computed by means of Kataoka's formula for g (eq. 12), while curves 2B, 3, and 5B were obtained from the parallel expressions of Zimm and Stockmayer (eq. 10 and 11).

In the calculation of curve 1 the effect of branching

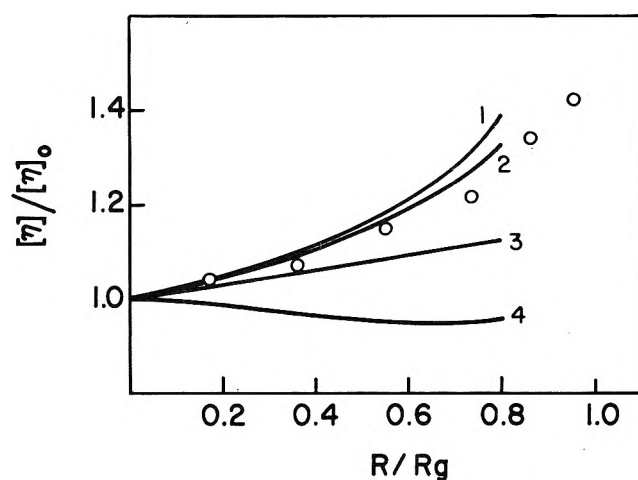


Figure 3. Comparison of experimental data for irradiated dimethylsilicone in θ solvent, obtained by Kilb,⁶ and theoretical curves, calculated from various equations proposed to describe the effects of branching on $[\eta]$. For the calculation of curves 1 and 4, g -values were obtained from the formula of Kataoka (eq. 12), for curves 2 and 3 Zimm and Stockmayer's formulas (eq. 10 and 11) were employed. In all computations, $a = 0.50$ and $\beta/\alpha = 0.0$ were assumed. The following correction factors for branching were used to compute the individual curves: curves 1 and 2, $g' = g^{1/2}$; curve 3, $g' = h^3$; curve 4, $g' = g^{3/2}$.

on viscosity was neglected, while, at the other extreme, curves 5A and 5B correspond to eq. 6, *i.e.*, to the Flory-Fox theory. It is obvious that branching lowers the viscosity considerably, but not nearly as much as predicted by eq. 6. The relation $g' = g^2 - a$ also appears to overestimate the effects of branching (curve 4). On the other hand, the Zimm-Kilb expression, which was used to calculate the values of curves 2A and 2B, gave higher viscosities than those observed in the experiments. The best, and, indeed, excellent agreement between calculated and experimental data was found when Stockmayer and Fixman's approximation was adopted. The results, shown in curve 3, are compared with the calculated values obtained by Shultz, *et al.*,^{2b} given as the dashed curve of Fig. 1. The computations of Shultz, *et al.*, were also based on Stockmayer and Fixman's treatment, but the mathematical approach was entirely different from that of the present work. It is interesting to note that both analyses predict a decrease in $[\eta]$ for high doses, which is at variance with the experimental data. However, for solutions in good solvents, and for doses not exceeding $R/R_g = 0.8$, the Stockmayer-Fixman treatment¹⁶ appears to be at least as satisfactory as the more recent formula, $g' = g^{1/2}$.

The differences between curves 2A and 2B, and between curves 5A and 5B, show that at large doses eq. 12 leads to values of $[\eta]$ that are significantly higher

than those obtainable on the basis of Zimm and Stockmayer's model. It will be noted that good agreement can be obtained with many of the experimental results given in Fig. 2, 3, and 5 to 7 if the correction factor $g' = g^{1/2}$ is used, with Zimm and Stockmayer's method of estimating g . Moreover, whenever the Zimm-Kilb correction fails (in good solvents), it appears to underestimate the decreasing effect of branching on viscosity. Therefore, its failure in these cases would be even more pronounced if Kataoka's formula for computing g were adopted. Also, as Zimm and Kilb¹⁵ pointed out in connection with the $g' = g^{1/2}$ formula, Zimm and Stockmayer's asymptotic expressions imply that $[\eta] = KM^{1/4}$ for highly branched polymers in θ solvents, a result which is in good agreement with a number of experimental data.²⁰⁻²² Thus, in computations of the type discussed in the present paper, Kataoka's formula seems to be less satisfactory than those of Zimm and Stockmayer.

Evaluation of the experimental data of Kilb⁶ is more difficult, since the extent of degradation could not be determined with accuracy in Kilb's experiments. Also, there appears to be some uncertainty²³ in the value of the viscosity exponent reported by Kilb for toluene solutions of dimethylsilicone.

Kilb's experimental data for irradiated dimethylsilicone in toluene solution, and the calculated values corresponding to these results, are given in Fig. 2. Curves 1 and 2 were calculated with $g' = g^{1/2}$, the values of g being obtained from the equations of Zimm and Stockmayer. Curve 1 was calculated by assuming $a = 0.79^6$ and $\beta/\alpha = 0.75$, while curve 2 corresponds to $a = 0.74$, and less degradation. Both curves are in quite satisfactory agreement with the experimental data. Curve 3, which was computed on the basis of the Stockmayer-Fixman treatment, with $a = 0.79$ and $\beta/\alpha = 0$, also agrees with the experiments.

It is difficult, then, to establish from the data of Fig. 2 whether $g' = g^{1/2}$ or eq. 9a-9c describe the effects of branching more satisfactorily. However, it is apparent from curve 4 of Fig. 2 that the Debye-Bueche correction factor, g^{2-a} , overestimates the influence of branching in decreasing $[\eta]$. The latter curve was calculated from eq. 12 of Kataoka for g , with $a = 0.79$ and $\beta/\alpha = 0$, yet, except near the gel point, the predicted increase in $[\eta]$ is considerably lower than that observed experimentally.

Kilb's results for irradiated dimethylsilicone in its θ solvent are given in Fig. 3, with the corresponding computed values. For calculation of the curves of Fig. 3, the extent of degradation was considered negligible. Curves 1 and 2 were computed from Zimm and Kilb's formula, using g -values obtainable from the

equations of Kataoka and of Zimm and Stockmayer, respectively. Curve 2 appears to be in good agreement with the experimental data even at high doses. However, the Stockmayer-Fixman approximation this time definitely overestimated the effect of branching on $[\eta]$ (curve 3). For curve 4, g was calculated from the Kataoka formula (eq. 12). It is obvious that the factor g^{2-a} , which, for θ solvents, is identical with the factor $g^{3/2}$ derivable from the Flory-Fox theory, grossly exaggerates the influence of branching.

It is of interest to compare the values given in curve 2 of Fig. 3 with theoretical results obtained by Kilb,⁶ who used the $g' = g^{1/2}$ approximation. The calculations of this author depended on assumptions similar to those of the present work but his mathematical analysis was based on Stockmayer's distribution function.²⁴ It can be seen from Table I that the agreement between the two treatments is good, except near the gel point, at $R/R_g = 0.95$. At such high doses, however, both methods are probably unreliable.

Table I: Increase of the Intrinsic Viscosity in Cross Linking without Degradation, as Computed by the Technique of Kataoka, Using Eq. 8, 10, and 11. The results are compared to values calculated by Kilb⁶

a	R/R_g	$[\eta]/[\eta]_0$	
		Present work	Kilb
0.50	0.20	1.05	1.06
0.50	0.40	1.11	1.13
0.50	0.60	1.19	1.22
0.50	0.80	1.32	1.36
0.50	0.90	1.42	1.48
0.50	0.95	1.47	1.58
0.68	0.20	1.08	1.10
0.68	0.40	1.20	1.23
0.68	0.60	1.38	1.41
0.68	0.80	1.69	1.74
0.68	0.90	1.98	2.09
0.68	0.95	2.14	2.43
0.75	0.20	1.10	1.11
0.75	0.40	1.25	1.27
0.75	0.60	1.47	1.51
0.75	0.80	1.89	1.95
0.75	0.90	2.30	2.46
0.75	0.95	2.54	3.00

(20) F. P. Price, S. G. Martin, and J. P. Bianchi, *J. Polymer Sci.*, **22**, 41 (1956).

(21) M. Wales, P. A. Marshall, and S. G. Weissberg, *ibid.*, **10**, 229 (1953).

(22) F. P. Price, J. H. Gibbs, and B. H. Zimm, *J. Phys. Chem.*, **62**, 972 (1958).

(23) A. J. Barry, *J. Appl. Phys.*, **17**, 1020 (1946).

(24) W. H. Stockmayer, *J. Chem. Phys.*, **11**, 45 (1943); **12**, 125 (1944).

The theoretical and experimental data of Fig. 1 to 3 leave little doubt that the correction factors $g' = g^{3/2}$ and $g' = g^2 - a$ strongly overestimate the decrease in $[\eta]$ due to branching. It is more difficult to choose between the Zimm-Kilb and Stockmayer-Fixman treatments. However, it appears that the former is preferable for solutions in poor solvents, while the latter may be superior for solutions in good solvents. Results given in the next section for samples of nonrandom initial distribution support this conclusion.

II. The Effect of Molecular Weight Distribution. Application of the mathematical analysis of Katsuura to samples of nonrandom initial distribution poses considerable difficulties. However, there are several indications that results computed for polymers of initially random distribution will be applicable to polymers of arbitrary distribution without introducing significant error. This seems to be shown particularly well by Charlesby's results on irradiated dimethylsilicone.²⁵

In an effort to determine experimentally whether

the initial molecular weight distribution influenced the change in $[\eta]$, Charlesby irradiated two kinds of silicone samples. One of them was a sample of molecular weight 28,000, probably of a near-random distribution. The second sample was a highly polydisperse mixture of silicone fluids: 80% by weight polymer of molecular weight 4000 and 20% by weight polymer of molecular weight 100,000. In spite of this very considerable difference in polydispersity, Charlesby's data show that the relative increase in $[\eta]$ was essentially the same for the two samples in question.

Kotliar and Podgor^{9,10} recently have developed a theoretical treatment of radiation effects in polymers of nonrandom initial distribution which enabled them to determine the molecular weight distribution of irradiated polymers of various polydispersities. However, application of their technique to the computation of intrinsic viscosities involves the approximation of using a simple step function to describe the dependence of $[\eta]$ on branching, and thus renders the quantitative validity of their results somewhat doubtful. Nevertheless, as shown in Fig. 4, their theoretical results, like the data of Charlesby, strongly indicate that initial distribution does not have an important role.

Thus, it seemed reasonable to assume that the theory developed for samples of the most probable distribution would be a good approximation for narrow range polymers. It was possible to test this assumption directly with a number of anionically polymerized polystyrene samples, obtained for some other studies, reported elsewhere.²⁶

The narrow distribution polystyrene samples were irradiated *in vacuo*, using one of the Gammacell Co⁶⁰ irradiation units of Atomic Energy of Canada Ltd., Ottawa, Canada. The exposure dose-rate was approximately 1,000,000 r./hr. Viscosities were determined at 25° for toluene and butanone solutions, and at 34°, the θ temperature, for cyclohexane solutions. Craig and Henderson suspended level viscometers²⁷ were used. Gelling doses were determined by extrapolation of viscosity-dose curves, while the extent of degradation ($\beta/\alpha = 0.14$) was estimated from osmotic measurements.

Results of the intrinsic viscosity determinations are shown in Fig. 5 to 7. Calculation of the theoretical curves given in these graphs was based on Zimm and

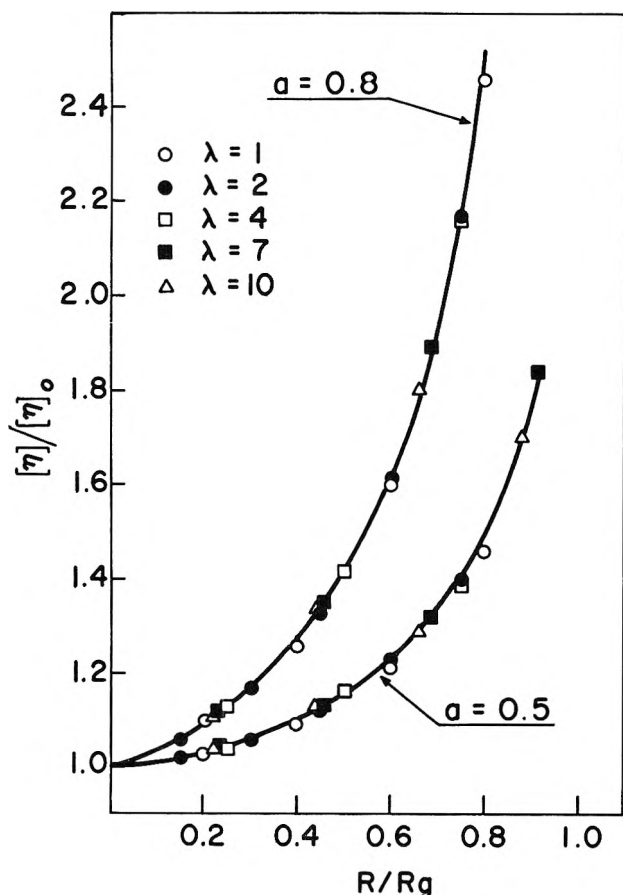


Figure 4. Increase of the intrinsic viscosity with dose in cross linking without degradation, as a function of initial polydispersity. The values plotted in this figure are based on those given in Table I of ref. 10.

(25) A. Charlesby, *J. Polymer Sci.*, 17, 379 (1955).

(26) J. G. Spiro and C. A. Winkler, *J. Appl. Polymer Sci.*, in press. We are most grateful to Dr. H. W. McCormick of the Dow Chemical Co. for providing these materials, and for the data, given in Table II, for the number and weight-average molecular weights.

(27) A. W. Craig and D. A. Henderson, *J. Polymer Sci.*, 19, 215 (1956).

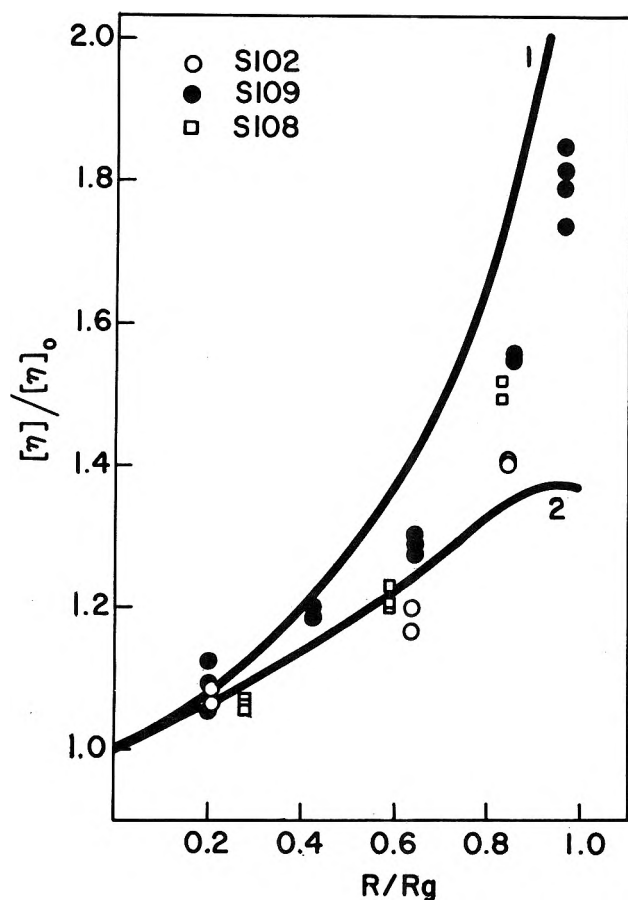


Figure 5. Comparison of experimental data for irradiated anionic polystyrenes in toluene, obtained in course of the present work, and theoretical curves, calculated from the theories of Zimm and Kilb (curve 1, $g' = g^{1/2}$) and Stockmayer and Fixman (curve 2, $g' = h^3$), with $a = 0.69$ and $\beta/\alpha = 0.14$. Values of g were estimated from the formulas of Zimm and Stockmayer (eq. 10 and 11).

Kilb's theory and the Stockmayer-Fixman approximation. Values of g were computed from the formulas of Zimm and Stockmayer (eq. 10 and 11). The exponents of the Mark-Houwink equations for toluene and butanone solutions were taken to be 0.69 and 0.58, respectively, as given by Outer, Carr, and Zimm.²⁸ The measurements in cyclohexane and toluene solutions were made for samples of various initial molecular weights, ranging approximately from $M = 80,000$ to 260,000. As expected from statistical considerations, any dissimilarities between data obtained for samples of different molecular weights appear to be within experimental error.

In Fig. 5 the increase of $[\eta]$ with dose is given for toluene solutions of the anionic polystyrenes. Calculations based on the Stockmayer-Fixman treatment (curve 2) are in good agreement with the experimental data, except at the largest doses. As with the

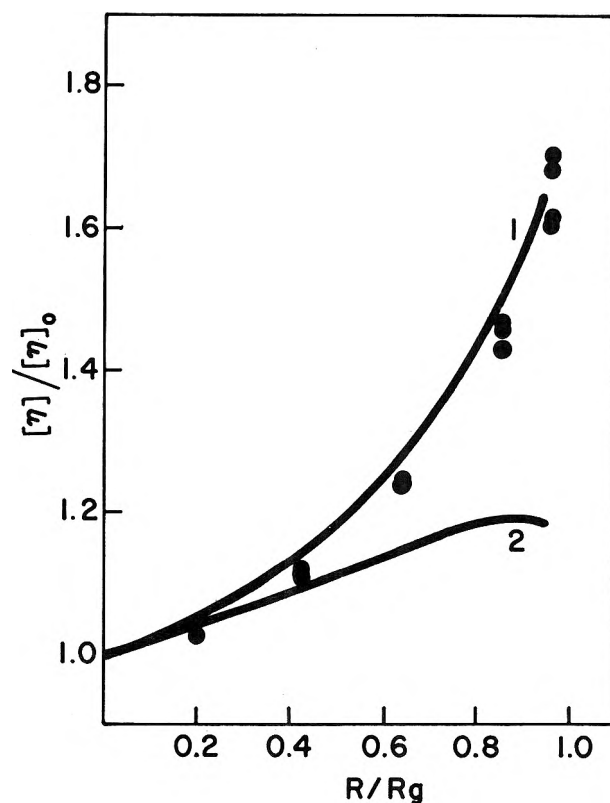


Figure 6. Comparison of experimental data for irradiated anionic polystyrene (sample S109) in butanone, obtained in course of the present work, and theoretical curves, calculated from the theories of Zimm and Kilb (curve 1, $g' = g^{1/2}$) and Stockmayer and Fixman (curve 2, $g' = h^3$), with $a = 0.58$ and $\beta/\alpha = 0.14$. Values of g were estimated from the formulas of Zimm and Stockmayer (eq. 10 and 11).

data of Fig. 1, the use of $g' = g^{1/2}$ leads to somewhat too high values (curve 1).

Table II: Number and Weight-Average Molecular Weights of the Narrow Range Polystyrene Samples

Sample	M_n	M_w
S102	78,500	82,500
S109	182,000	193,000
S108	247,000	267,000

In Fig. 6 and 7, theoretical and experimental data for butanone and cyclohexane solutions, respectively, are shown. Computations based on Zimm and Kilb's theory are in agreement with the experiments, while the Stockmayer-Fixman approximation leads to considerably lower values.

(28) P. Outer, C. I. Carr, and B. H. Zimm, *J. Chem. Phys.*, **18**, 830 (1950).

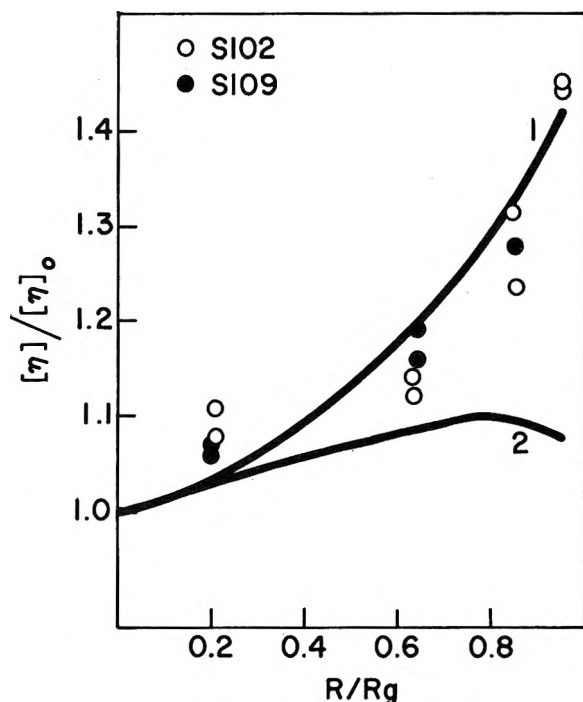


Figure 7. Comparison of experimental data for irradiated anionic polystyrenes in cyclohexane, obtained in course of the present work, and theoretical curves, calculated from the theories of Zimm and Kilb (curve 1, $g' = g^{1/2}$) and Stockmayer and Fixman (curve 2, $g' = h^3$), with $a = 0.50$ and $\beta/\alpha = 0.14$. Values of g were estimated from the formulas of Zimm and Stockmayer (eq. 10 and 11).

Since the relation between calculated and experimental results for the samples of narrow molecular weight distribution is similar to that observed in Fig. 1 to 3 for samples of initially random distribution, it may be concluded that, as predicted, molecular weight distribution has little effect on the relative change in $[\eta]$ caused by irradiation.

Discussion

Computation of the intrinsic viscosities of irradiated polymers clearly indicates that, as was earlier shown by several authors,^{15,16,29} direct application of the Flory-Fox theory to branched polymers is not feasible. In view of the results of the previous sections, there is little doubt that the $g' = g^{2-a}$ expression, derivable from the Debye-Bueche treatment, still considerably overestimates the effect of branching on $[\eta]$. While the Zimm-Kilb and Stockmayer-Fixman approximations are clearly in better agreement with the experiments, it appears that none of the theories considered can explain the hydrodynamic behavior of branched

polymers in solvents of different types. This implies no criticism of the Zimm-Kilb treatment, since the expression $g' = g^{1/2}$ was really developed for θ solvents, and its application to other solvents is only an extrapolation.¹⁵ Moreover, studies on star-shaped polymers^{30,31} have demonstrated the empirical value of the Zimm-Kilb formula, although some results in good solvents³² indicated discrepancies analogous to those found in the present work.

There is, however, a serious objection that can be raised against all the viscosity theories considered in this paper, namely that all of them attempt to correlate viscosity with the radius of gyration, rather than with the hydrodynamic radius. As Stockmayer and Fixman¹⁶ pointed out, a branched molecule of the same radius of gyration as a linear molecule has everywhere a greater mean segment density. This is likely to decrease the permeability of branched chains, and increase R_e , the equivalent hydrodynamic radius. Bueche³³ surmised that the influence of segment density is so pronounced that it is meaningless to express R_e as a function of the radius of gyration. The results of the present work, which indicate that none of the existing theories on the effects of branching is generally applicable, seem to agree with Bueche's conclusion. It appears, therefore, that the validity of the Zimm-Kilb approximation in poor solvents, as well as that of the Stockmayer-Fixman treatment in good solvents, is somewhat fortuitous. It is to be feared that a similar objection will also apply to modifications or extensions of the Flory-Fox theory. Accordingly, it will probably be necessary to study the effect of branching on the hydrodynamic permeability of the chain in detail, before a more satisfactory treatment of the viscosity of branched polymers may be developed.

Acknowledgments. This research was supported in part by Polymer Corporation Limited, Sarnia, Canada, and Atomic Energy of Canada Limited, Ottawa, Canada. Their support is gratefully acknowledged. Acknowledgment is also extended to the National Research Council of Canada, for financial assistance in the form of a studentship awarded to one of the authors.

(29) B. H. Zimm, *Ann. N. Y. Acad. Sci.*, **57**, 332 (1953).

(30) M. Morton, *et al.*, *J. Polymer Sci.*, **57**, 471 (1962).

(31) T. A. Orofino and F. Wenger, *J. Phys. Chem.*, **67**, 566 (1963).

(32) F. Wenger, Discussion Contribution No 187, Paper A41, International Symposium on Macromolecular Chemistry, July, 1961, Montreal, Canada; see *J. Polymer Sci.*, **57**, 481 (1962).

(33) F. Bueche, *ibid.*, **41**, 549 (1959).

Proton Magnetic Resonance Spectra of Aromatic and Aliphatic Thiols¹

by Sheldon H. Marcus² and Sidney I. Miller

Department of Chemistry, Illinois Institute of Technology, Chicago 16, Illinois (Received September 5, 1963)

The sulfhydryl proton resonance frequencies in c.p.s. from tetramethylsilane are shown to be represented by $\nu_{\text{SH}} = -17.0\sigma - 194.4$ for eleven thiophenols and by $\nu_{\text{SH}} = -47.2\sigma^* - 73.0$ for ten aliphatic thiols; four more compounds can be added to the aliphatic correlation providing the term $0.29n$ is included where n is the number of α carbon-carbon bonds. Deviation of representative aryl thiols from the correlation with σ^* is discussed in terms of conjugation and the magnetic anisotropy of the aromatic ring. Spin-spin coupling constants are evaluated for the phenyl protons of *para*-substituted thiophenols (A_2B_2 system) and generally fall into small ranges: 8.0–8.5, 2.2–2.5, and 0.2–0.6 c.p.s. for *ortho*, *meta*, and *para* couplings, respectively. Coupling constants between sulfhydryl and alkyl protons in the aliphatic series fall in the range 6.4–8.6 c.p.s. No correlation between coupling constants and substituent parameters is observed. An unusual case of a *para*-disubstituted benzene derivative in which all four phenylene protons are magnetically equivalent is found in *p*-chlorothiophenol.

Studies of rate,^{3,4} equilibrium⁵ and spectral properties⁶ of the thiol family have been reported. Proton magnetic resonance (p.m.r.) spectra of isolated thiols have been reported^{7–13} but no systematic survey is available. In this paper the p.m.r. spectra of about thirty aromatic and aliphatic thiols are discussed with respect to substituent effects on the proton resonance frequency (ν) and spin-spin coupling constant (J).

Experimental

Proton magnetic resonance spectra were produced on a Varian A60 analytical n.m.r. spectrometer operating at a frequency of 60.005 Mc.p.s. and equipped with a 4-4013A 12-in. electromagnet system and a 2100B regulated magnet power supply. Homogeneity adjustments were made using the Hewlett-Packard 405BR automatic d.c. digital voltmeter. All spectra were calibrated by the side-band technique using the Hewlett-Packard 200CDR wide range oscillator and 521C electronic counter. In all measurements the sample temperature was $28 \pm 1^\circ$, the radiofrequency amplitude was 0.07 gauss, and the scan rate was 1–2 c.p.s./sec. The samples were contained in 5-mm. o.d. n.m.r. tubes (high resolution type).

Carbon tetrachloride (Fisher certified) was the solvent except in two cases where it was necessary to use chloroform (Fisher certified) due to relative insolubility

in CCl_4 . Tetramethylsilane (K and K Laboratories) was the internal standard, eliminating the necessity for bulk magnetic susceptibility corrections. The thiols studied usually were commercial samples used directly from freshly opened bottles; purities are

- (1) Taken from the Ph.D. research of S. H. M.; supported in part by the U. S. Army Research Office (Durham); presented at the 144th National Meeting of the American Chemical Society, Los Angeles, Calif., April, 1963, p. 3P.
- (2) National Science Foundation Fellow, 1961–1963.
- (3) G. S. Krishnamurthy and S. I. Miller, *J. Am. Chem. Soc.*, **83**, 3961 (1961).
- (4) J. P. Danehy and C. J. Noel, *ibid.*, **82**, 2511 (1960).
- (5) M. M. Kreevoy, E. T. Harper, R. E. Duvall, H. S. Wilgres, and L. T. Ditsch, *ibid.*, **82**, 4899 (1960).
- (6) (a) S. I. Miller and G. S. Krishnamurthy, *J. Org. Chem.*, **27**, 645 (1962); (b) J. Jan, D. Hadzi, and G. Modena, *Ric. Sci.*, **30**, 1065 (1960).
- (7) L. H. Meyer, A. Saika, and H. S. Gutowsky, *J. Am. Chem. Soc.*, **75**, 4567 (1953).
- (8) S. Forsen, *Acta Chem. Scand.*, **13**, 1472 (1959).
- (9) L. D. Colebrook and D. S. Tarbell, *Proc. Natl. Acad. Sci. U. S.*, **47**, 993 (1961).
- (10) A. S. N. Murthy, C. N. R. Rao, B. D. N. Rao, and P. Venkateswarlu, *Trans. Faraday Soc.*, **58**, 855 (1962).
- (11) A. S. N. Murthy, C. N. R. Rao, B. D. N. Rao, and P. Venkateswarlu, *Can. J. Chem.*, **40**, 963 (1962).
- (12) R. Mathur, N. C. Li, E. D. Becker, and R. B. Bradley, Abstracts, 144th National Meeting of the American Chemical Society, Los Angeles, Calif., April, 1963, p. 1P.
- (13) W. Stacy and J. F. Harris, Jr., *J. Am. Chem. Soc.*, **85**, 963 (1963).

those given by the manufacturer: thiophenol (98%), *o*-methylthiophenol (96%), *p*-bromothiophenol (97%), *p*-*t*-butylthiophenol (98%), and *p*-nonylthiophenol (95%) were from Pitt Consol; *p*-aminothiophenol, *p*-acetamidothiophenol, and cyclohexyl mercaptan were from Aldrich Chemical; *p*-chlorothiophenol (97%), α -mercaptoacetic acid (98%), β -mercaptopropionic acid (99%), isooctyl α -mercaptoacetate (98.5%), isooctyl β -mercaptopropionate (99%), and α -mercaptopropionic acid (95%) were from Evans Chemetics; *n*-propyl, isopropyl *n*-butyl, *t*-butyl, *n*-amyl, and *n*-hexyl mercaptans were from Pennsalt; *p*-methylthiophenol, *m*-methylthiophenol, and β -mercaptoethanol were Eastman White Label; *p*-fluorothiophenol, b.p. 57–58° (10 mm.), (lit.¹⁴ b.p. 64–65° (12 mm.)), and *p*-nitrothiophenol, m.p. 75° (lit.¹⁵ m.p. 75°) were prepared by R. Wieseck. No p.m.r. spectrum showed any impurity signal of greater intensity than any sample peak.

Chemical shifts were obtained by taking the average of three values at each of three concentrations in the dilute range, below *ca.* 3 *M*, where there is little hydrogen bonding.^{8–11,16} Here the dependence of chemical shift on concentration approaches linearity and can be extrapolated to zero concentration. Thus, each infinite dilution value is the result of nine independent measurements. Spectra for the analysis of spin-spin coupling constants were obtained using the pure liquids or, in the case of solid compounds, concentrated solutions in carbon tetrachloride. The precision in the chemical shifts and coupling constants is ± 0.2 c.p.s.

Calculations. The fine structure of the ring protons of the thiophenols which lend themselves to an A_2B_2 analysis¹⁷ has been evaluated, using the Freqint IV program¹⁸ for solving the secular equations for the spin state energies. Required input in this program are chemical shifts and coupling constants; output consists of transition energies (resonance frequencies) and transition probabilities.

Results and Discussion

Aliphatic Thiols. The effect of substituents on the magnetic shielding of protons in aliphatic compounds is complex: electronegativity,^{19–22} magnetic anisotropy,²⁰ orientation,²³ and the number (*n*) of α -carbon-carbon bonds^{19,23} have all been implicated. The chemical shifts (ν_{SH}) for a series of organosilanes²⁴ have been correlated with Taft's σ^* values²⁵ and *n*. The effect of alkyl groups on the C¹³ resonance in the linear alkanes appears to be additive.²⁶

Our sulfhydryl p.m.r. frequencies (ν_{SH} in c.p.s. from tetramethylsilane at infinite dilution in carbon tetrachloride) and coupling constants (J_{HCSH} , in c.p.s.) between sulfhydryl and α -carbon protons are given in

Table I. An attempted correlation of ν_{SH} with σ^* was unsatisfactory (correlation coefficient $r = 0.854$); however, the equation $\nu_{\text{SH}} = -47.2\sigma^* - 73.0$ gives a more satisfactory correlation ($r = 0.980$) for ten unbranched compounds. The negative slope reflects the typical shift to higher fields due to increased electron shielding caused by electron-releasing groups. This is illustrated in Fig. 1. As in the case of the organosilanes the correlation for both unbranched and branched compounds may be improved ($r = 0.973$) by the inclusion of the *n* term, *i.e.*, $\nu_{\text{SH}} = -45.6(\sigma^* + 0.29n) - 60.6$. Unlike the organosilanes, however, the σ^* term is dominant over the *n* term. The *n* term reflects the dependence of ν_{SH} on presence of α carbon-carbon bonds. Such a dependence may be explained on the basis of the magnetic anisotropy of the carbon-carbon bond and/or the so-called carbon-carbon bond shift due to factors other than anisotropy. The present data do not enable one to make a choice between these alternatives. In any case, it is clear that for ν_{SH} inductive effects predominate over carbon-carbon bond effects, while for ν_{SiH} the reverse is true.

The proton-proton coupling constants have been shown to be dependent on the electronegativity of substituents in the case of the hexachlorobicyclo-[2.2.1]heptenes,²² but no regular dependence on substituent is observed for the cyclopropane derivatives.²¹ Substituent effects on C¹³ proton coupling have been found to be additive for both tetrahedrally and trigonally hybridized carbon,²⁷ and approximately so in the

- (14) G. Olah and A. Pavlath, *Acta Chim. Acad. Sci. Hung.*, **4**, 111 (1954).
- (15) C. C. Price and G. W. Stacy, *J. Am. Chem. Soc.*, **68**, 499 (1946).
- (16) S. H. Marcus, unpublished results.
- (17) J. A. Pople, W. G. Schneider, and H. J. Bernstein, "High Resolution Nuclear Magnetic Resonance," McGraw-Hill Book Co., Inc., New York, N. Y., 1959, p. 142.
- (18) (a) A. A. Bothner-By and C. Naar-Colin, *J. Am. Chem. Soc.*, **83**, 231 (1961); (b) adapted to the IBM 7090 by H. Kriloff, Illinois Institute of Technology.
- (19) J. R. Cavanaugh and B. P. Dailey, *J. Chem. Phys.*, **34**, 1099 (1961).
- (20) H. Spiessicke and W. G. Schneider, *ibid.*, **35**, 722 (1961).
- (21) J. D. Graham and M. T. Rogers, *J. Am. Chem. Soc.*, **84**, 2249 (1962).
- (22) K. L. Williamson, *ibid.*, **85**, 516 (1963).
- (23) W. C. Neikam and B. P. Dailey, *J. Chem. Phys.*, **38**, 445 (1963).
- (24) O. W. Steward, R. H. Baney, and E. B. Baker, Abstracts, 144th National Meeting of the American Chemical Society, Los Angeles, Calif., April, 1963, p. 3P.
- (25) R. W. Taft, Jr., "Steric Effects in Organic Chemistry," M. S. Newman, Ed., John Wiley and Sons, Inc., New York, N. Y., 1956, p. 619.
- (26) E. G. Paul and D. M. Grant, *J. Am. Chem. Soc.*, **85**, 1701 (1963).
- (27) E. R. Malinowsky, *ibid.*, **83**, 4479 (1961); **84**, 2649 (1962).

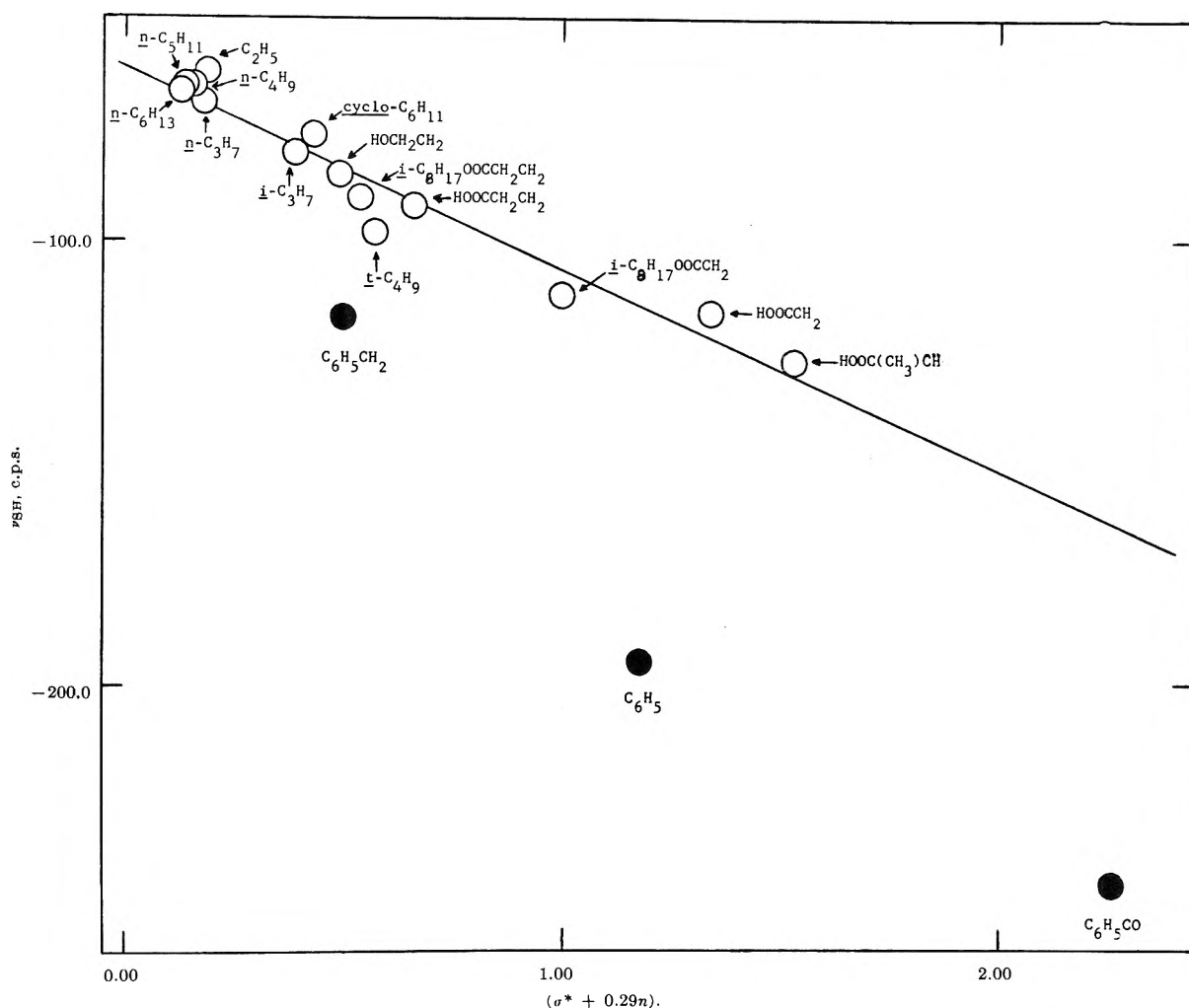


Figure 1. Graph of $\nu_{\text{SH}} = -45.6(\sigma^* + 0.29n) - 60.6$: O, aliphatic thiols; ●, aromatic thiols.

case of the substituted methanes.²⁸ As in the case of the cyclopropyl derivatives our J -values show no regular substituent effects.

Aromatic Effects. The aromatic thiols included in Fig. 1 show marked deviation from a plot of ν_{SH} vs. $(\sigma^* + 0.29n)$. The expression $(\sigma^* + 0.29n)$ contains the inductive substituent effect and the effect of neighboring carbon-carbon bonds. In the aromatic compounds there is a net deshielding due to other effects. Thiophenol, thiolbenzoic acid, and benzylmercaptan all experience the deshielding effect of the magnetic field induced by the electron current through the aromatic ring.²⁹ In the case of thiophenol there is a net deshielding of 67.0 c.p.s. A simple calculation²⁹ of the ring current correction was performed using the following geometry³⁰: C-C (aromatic), C-S, and S-H bond distances, 1.39, 1.82, and 1.33 Å., respectively; C-S-H bond angle, 100.3°. The resulting correction is 48 c.p.s., somewhat smaller than

observed. Though the simple calculation is known to underestimate the magnitude of the ring current correction,²⁹ it is not expected that this error be sufficient to account for the remaining deshielding. A further deshielding may result from conjugation of the sulfhydryl group with the aromatic ring placing a residual positive charge at the sulfur atom. In the case of benzyl mercaptan, the ring current effect is decreased, falling with the cube of the distance of the sulfhydryl proton from the center of the ring.²⁹ In addition, there is no conjugation between the sulfhydryl group and the ring. However, there may be an effect due to hyperconjugation between the methylene group and the ring placing a residual positive charge on the

(28) S. G. Frankiss, *J. Phys. Chem.*, **67**, 752 (1963).

(29) See ref. 17, pp. 180-183.

(30) "Tables of Interatomic Distances and Configuration in Molecules and Ions," The Chemical Society, London, 1958, pp. M114, M194-196. Values taken were for CH_3SH and $\text{C}_6\text{H}_5\text{Cl}$.

Table I: Chemical Shifts and Coupling Constants in the Aliphatic Series^a

Substituent	ν_{SH} , c.p.s.	J_{HCSH} , c.p.s.
<i>n</i> -C ₄ H ₉	-64.7	7.6
<i>cyclo</i> -C ₆ H ₁₁	-75.7	6.4
HOOCCH ₂	-116.1	8.2
HOOCCH ₂ CH ₂	-91.5	8.6
<i>i</i> -C ₈ H ₁₇ OOCCH ₂	-112.2	8.0
<i>t</i> -C ₄ H ₉	-97.5	...
<i>n</i> -C ₃ H ₇	-69.2	8.0
<i>i</i> -C ₃ H ₇	-80.2	5.8
<i>n</i> -C ₅ H ₁₁	-65.4	7.6
<i>n</i> -C ₆ H ₁₃	-65.5	7.7
HOOC(CH ₂)CH	-127.1	8.4
<i>i</i> -C ₈ H ₁₇ OOCCH ₂ CH ₂	-89.5	7.9
HOCH ₂ CH ₂ ^{b,f}	-84.9	8.4
C ₂ H ₅ ^{c,f}	-62.4	7.6
C ₆ H ₅	-195.4	
C ₆ H ₅ CH ₂ ^{d,f}	-117.4	
C ₆ H ₅ CO ^{e,f}	-245.2	

^a Representative aromatic thiols included for comparison^b

^b In CHCl₃. ^c See ref. 8. ^d See ref. 7. ^e See ref. 10. ^f Corrected to c.p.s. from tetramethylsilane at 60 Mc.p.s., zero concentration in carbon tetrachloride.

methylene protons. In the thiolbenzoic acid, the ring current effect is decreased as in benzyl mercaptan, there is no possibility of conjugation of the sulfhydryl group with the ring, or of any hyperconjugative effect. However, there can be conjugation between the sulfhydryl and carbonyl groups, placing residual positive and negative charges on the sulfur and oxygen atoms, respectively, as well as the effect of the anisotropy of the carbonyl group.

Aromatic Thiols. In aryl systems, the F¹⁹ resonance of substituted fluorobenzenes³¹ and other aromatic fluorine derivatives,³² the C¹³ and *para* proton resonance of monosubstituted benzenes,³³ and the proton resonance of substituted benzaldehydes³⁴ and anisoles³⁵ have been correlated with various σ -values while an absence of such correlation has been noted for the phenols.³⁶ The OH stretching frequency in the infrared has been correlated with σ for the phenols,³⁷ while only a trend has been noted for the sulfur analogs, the thiophenols.⁶ Our data for the sulfhydryl (ν_{SH}) and phenyl ($\nu_{\text{C}_6\text{H}_5}$, taken as the center of the multiplet structure) protons are given in Table II in c.p.s. from tetramethylsilane at infinite dilution in carbon tetrachloride. The range in ν_{SH} , *ca.* -220 to -180 c.p.s., may be compared with that of the aliphatic thiols (Table I), *ca.* -130 to -60 c.p.s. The aromatic series shows resonance at lower values of the applied magnetic field due to the deshielding effect of the mag-

netic field induced by electron currents in the π -system of the phenyl ring.¹⁷

Table II: Chemical Shifts in Substituted Thiophenols

Substituent	ν_{SH} , c.p.s.	$\nu_{\text{C}_6\text{H}_5}$, c.p.s.
4- <i>t</i> -C ₄ H ₉	-190.8	-430.1
4-CH ₃	-191.0	-423.0
3-CH ₃	-191.9	-420.6
H	-195.4	-430.0
4-Cl	-197.4	-431.0
4-C ₉ H ₁₉	-191.5	-427.9
4-F	-195.4	-424.2
4-Br	-197.2	-434.2
4-CH ₃ CONH ^a	-194.5
4-NO ₂	-217.0	-462.3
4-NH ₂	-184.8	-406.5

^a In CHCl₃; corrected to CCl₄ solution; solvent resonance swamped phenyl peak.

The relationship of ν_{SH} to Hammett's σ -values,³⁸ as shown graphically in Fig. 2, is given by $\nu_{\text{SH}} = -21.8\sigma - 195.1$ ($r = 0.952$). The correlation is improved by the use of the σ^- value for the *p*-nitro group: $\nu_{\text{SH}} = -17.0\sigma - 194.4$ ($r = 0.993$). In the light of these data it is puzzling that the infrared S-H stretching frequency in thiophenols shows only a rough trend with σ while the corresponding O-H frequency in phenols gives a fair correlation. As has been noted elsewhere, different measures of polarity are presumably involved in these different properties.

*For the present, the following simplified explanation of our correlation of ν_{SH} with σ seems to be adequate. An increase or decrease in the electron density or shielding of the sulfhydryl proton will require a higher or lower applied magnetic field, respectively, in order to achieve resonance at a fixed frequency. Since σ is a measure of electron releasing or withdrawing power of a substituent, ν_{SH} may be expected to show a trend

- (31) (a) H. S. Gutowsky, D. W. McCall, B. R. McGarvey, and L. H. Meyer, *J. Am. Chem. Soc.*, **74**, 4809 (1952); (b) L. H. Meyer and H. S. Gutowsky, *J. Phys. Chem.*, **57**, 481 (1953); (c) R. W. Taft, Jr., *J. Am. Chem. Soc.*, **79**, 1045 (1957); (d) R. W. Taft, Jr., E. Price, I. R. Fox, I. C. Lewis, K. K. Anderson, and G. T. Davis, *ibid.*, **85**, 709 (1963).
- (32) D. R. Eaton and W. A. Sheppard, *ibid.*, **85**, 1310 (1963).
- (33) H. Spiesscke and W. G. Schneider, *J. Chem. Phys.*, **35**, 731 (1961).
- (34) R. E. Klinck and J. B. Stothers, *Can. J. Chem.*, **40**, 1071 (1962).
- (35) C. Heathcock, *ibid.*, **40**, 1865 (1962).
- (36) W. G. Paterson and N. R. Tipman, *ibid.*, **40**, 2122 (1962).
- (37) C. N. R. Rao and R. Venkataraghavan, *ibid.*, **39**, 1757 (1961).
- (38) D. H. McDaniel and H. C. Brown, *J. Org. Chem.*, **23**, 420 (1958).

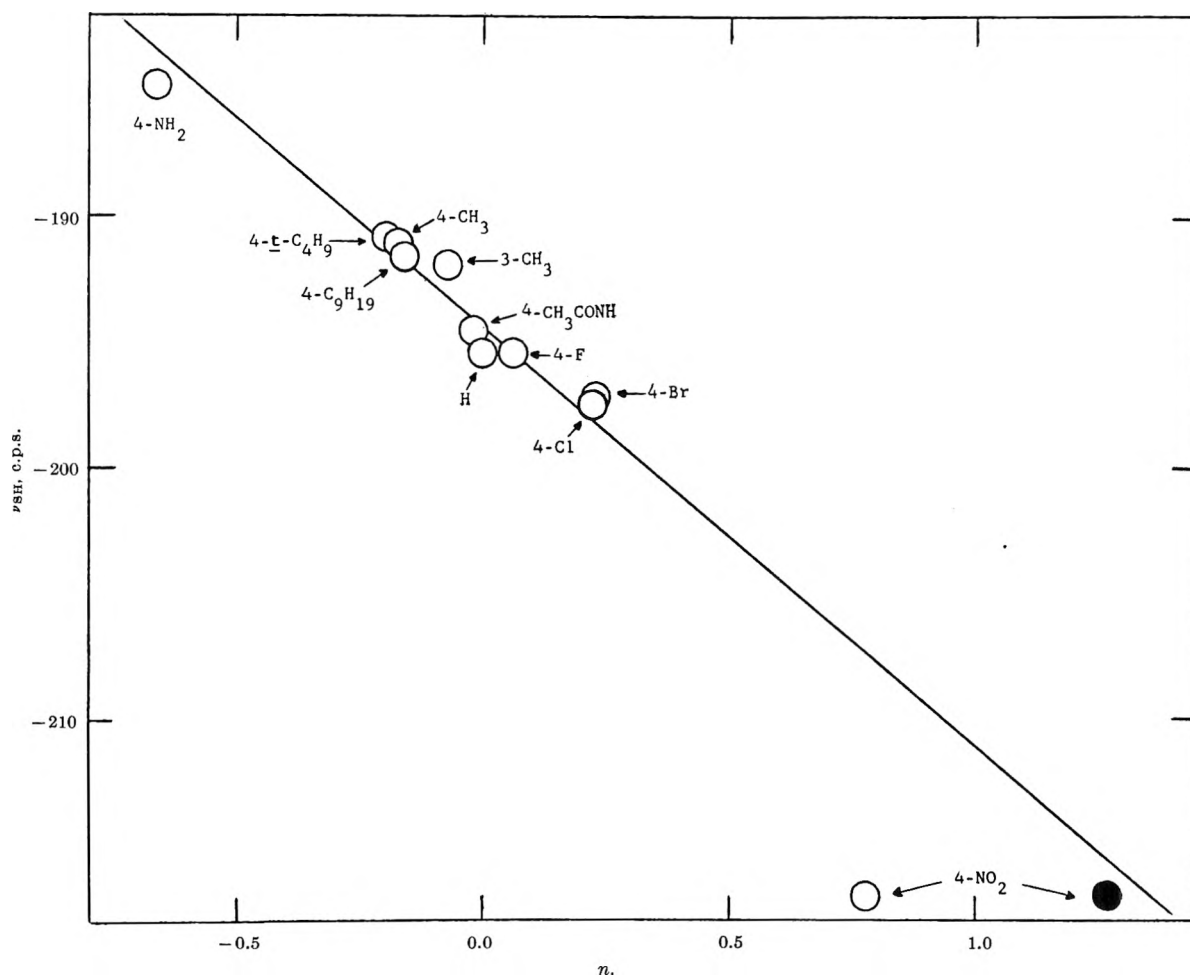


Figure 2. Graph of $\nu_{\text{SH}} = -17.0\sigma - 194.4$ for *meta*- and *para*-substituted thiophenols: O, σ ; ●, σ^- .

with σ ; and since σ is related to an energy difference ($\Delta\Delta F$), and ν_{SH} is in fact an energy difference, a regularity in the trend is expected and is indeed observed. The negative slope indicates that electron-releasing substituents shift the resonance position to higher applied magnetic fields due to an increase in electron density at the sulfhydryl proton. The necessity of using the σ^- value¹⁵ for the *para*-nitro substituent may be explained by an enhanced deshielding of the sulfhydryl proton due to direct conjugation between nitro and sulfhydryl groups in the *para* position in which a residual positive charge is on the sulfur atom. Further justification for such conjugation is given in the discussion of positional effects (see below).

Interpreting the slope ρ as the sensitivity of ν_{SH} to variation in substituent, the value for the thiophenols, -17.0 , may be compared with those of other proton resonances, the anisoles,³⁵ -13.2 , the benzaldehydes,³⁴ -14.5 , and the monosubstituted benzenes³³ (*para* proton), -41.4 . The resonance position of protons

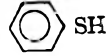
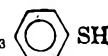
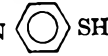



bound directly to the benzene ring is considerably more sensitive to substituent effects than that of protons removed from the ring by one or two atoms in functional groups. On the basis of the higher ρ -value, ν_{SH} for the thiophenols shows greater sensitivity toward variation in substituent than do ν_{CHO} and ν_{OCH_3} for the benzaldehydes and anisoles, respectively. The ring protons in this series being chiefly *ortho* and *meta*, $\nu_{\text{C}_6\text{H}_5}$ shows no correlation with σ . Previous work has demonstrated correlation for *para* protons only.³³

The effect of substituent position on resonance frequency in aromatic compounds has been examined and

Table III: Chemical Shifts in Methylthiophenols

Position	ν_{SH} , c.p.s.	ν_{CH_3} , c.p.s.
<i>ortho</i>	-186.3	-139.4
<i>meta</i>	-191.9	-138.4
<i>para</i>	-191.0	-138.3

Table IV: Spin-Spin Coupling Analysis of *para*-Substituted Thiophenols

Case ^a	Number of lines	Groups appearing as single lines	Relations ^b	Examples	—A ₂ B ₂ analysis ^c —				AB analysis ^c	
					ν_{AB}	J_{AB}	J_{meta}	J_{AB}'	ν_{AB}	J_{AB}
Ia ($\nu_{AB} > J_{AB}$)	20	(2, 3) (7, 8, 9) (12, 13, 14) (18, 19)	$d_{2,8} = J_{AB} + J_{AB}'$ $d_{4,7} = J_{AB} - J_{AB}'$ $d_{2,12} = \sqrt{\nu_{AB}^2 + J_{AB}^2 + J_{meta}^2 + J_{AB}'^2}$ $d_{1,6} = f(J_{meta})$	Br  SH CH ₃  SH	+13.7	8.3	2.4	0.4	+13.6	8.8
Ib ($\nu_{AB} \gg J_{AB}$)	20	(2, 3) (7, 8, 9) (12, 13, 14) (18, 19)	$d_{2,8} = J_{AB} + J_{AB}'$ $d_{4,7} = J_{AB} - J_{AB}'$ $d_{2,12} = \sqrt{\nu_{AB}^2 + J_{AB}^2 + J_{meta}^2 + J_{AB}'^2}$ $d_{1,6} = f(J_{meta})$	O ₂ N  SH H ₂ N  SH	+44.1	8.5	2.4	0.5	+44.3	8.9
II ($\nu_{AB} < J_{AB}$)	18	(6, 7, 8, 9, 10, 11, 12, 13)	$d_{2,8} = J_{AB} + J_{AB}'$ $d_{4,7} = J_{AB} - J_{AB}'$ $d_{4,5} = f(J_{meta})$ $d_{5,9} = g(\nu_{AB})$	<i>t</i> -C ₄ H ₉  SH	-3.6	8.0	3.8	0.6	≥ -0.2 < 0.0	9.3
III ($\nu_{AB} = 0$)	1			Cl  SH	0.0	0.0	...

^a $\nu_{AB} \equiv \nu_A - \nu_B$; H_A is *ortho* to SH. ^b $d_{i,j}$ is distance between lines *i* and *j* in c.p.s.; $J_{meta} = 1/2(J_{AA'} + J_{BB'})$; $J_{AB}' = J_{A'B}$; zero subscript refers to center of phenyl band. ^c All values in c.p.s.; *J*-values are absolute values.

explained on the basis of induction and conjugation.³⁹ The sulfhydryl and methyl proton resonance frequencies for the tolyl thiols are given in Table III. A shift of ν_{SH} to higher fields by the electron-releasing methyl group occurs in the order *ortho* > *para* > *meta*. The smallest effect is in the *meta* position which experiences minimal conjugation; the largest effect is in the *ortho* position which experiences both conjugation and induction, the latter to a greater degree than does the *para* position.

This presence of conjugation is added justification for the use of σ^- for the *para*-nitro group. The shift of ν_{CH_3} to lower fields by the sulfhydryl group occurs in the order *ortho* > *meta* \approx *para*. The sulfhydryl group, being electron-withdrawing by induction and electron-releasing by conjugation, appears to be close to a crossover region between net electron withdrawal and release where the *ortho*, *meta*, and *para* resonances tend to become unresolved. Indeed this is the case for the *meta* and *para* methyl resonances.

Spin-Spin Coupling. Coupling constants and chemical shifts have been evaluated for the ring protons of *para*-disubstituted benzenes by analysis of the p.m.r. spectra using AB and A₂B₂ models.⁴⁰⁻⁴² The results of our A₂B₂ analysis are given in Table IV. All values are for pure liquids or (in the case of solids) concentrated solutions in carbon tetrachloride, and are given in c.p.s. Lines are numbered in order from low field to high (the spectra are symmetric about the center). The data fall into four categories distinguished by the

magnitude of the chemical shift (ν_{AB}) between non-equivalent ring protons relative to the *ortho* coupling constant (J_{AB}). The number of lines in the theoretical spectrum is generally greater than that observed due to the presence of closely spaced lines which are not resolved experimentally but which result in a broadened signal. An extreme case of this is the *p-t*-butylthiophenol spectrum in which ν_{AB} is very small and the central lines are of relatively high intensity and very closely spaced. In these cases the resultant broadened signal is taken to be a weighted average of the theoretical lines.

A number of difference relations are observed between chemical shifts, coupling constants, and line spacings. Some of these are nonspecific functional dependences, e.g., $d_{1,5}$ (c.p.s.) = $f(J_{meta})$ as is found in cases Ia and Ib. $d_{1,5}$ is chosen as the line spacing most sensitive to changes in J_{meta} . Several calculations are then made keeping all other parameters constant at their determined values and varying J_{meta} in the region of its actual value. The calculated line spacings $d_{1,5}$ are then plotted vs. the corresponding J_{meta} values to obtain the functional dependence graphically. From the experimental value of $d_{1,5}$ the value of J_{meta} may

(39) See ref. 17, p. 260.

(40) J. Martin and B. P. Dailey, *J. Chem. Phys.*, **37**, 2594 (1962).

(41) D. M. Grant, R. C. Hirst, and H. S. Gutowsky, *ibid.*, **38**, 470 (1963).

(42) P. F. Cox, *J. Am. Chem. Soc.*, **85**, 380 (1963).

then be determined. The plots obtained in this manner generally show slight curvature.

Examination of the various relations shows that cases Ia and Ib differ only in the exchange of position of lines 2 and 3, the crossover occurring at some intermediate value of ν_{AB} .

Results of the evaluation are given in the last columns of Table III. A comparison is made, in the case of the chemical shift ν_{AB} and principal (*ortho*) coupling constant J_{AB} , to the results of an AB analysis⁴³ using the four most intense lines in the ring spectrum. The AB analysis is seen to give values of J_{AB} which are too high. The ν_{AB} values obtained in the AB analysis, however, are more successful, coming to within experimental error of the values obtained by A_2B_2 analysis, except in the case of *p-t*-butylthiophenol, where ν_{AB} is very small and the central lines have merged.

An average *meta* coupling constant $\frac{1}{2}(J_{AA'} + J_{BB'})$ is given in Table IV, it having been shown that the *meta* coupling constants are very close together in *para*-disubstituted benzenes.^{40,41} The *ortho*, *meta*, and *para* coupling constants in *para*-disubstituted benzenes have been shown to fall into small ranges (1.2, 1.1, and 0.3 c.p.s., respectively) and to be of the same sign. From Table IV, it is clear that a negligible substituent effect is observed for our J -values; the range of values (0.5 c.p.s. max.) is of the order of magnitude of the experimental error (0.2 c.p.s.) and falls into the range previously reported.^{40,42}

An interesting case is that of *p*-chlorothiophenol, which shows only a single line in the high resolution spectrum of the ring protons. Such behavior has been occasionally observed⁴⁴ in other *para*-disubstituted benzenes, *e.g.*, *p*-methoxyphenol.³⁶ Since the coupling constants show negligible substituent effects, it is to be expected that those for *p*-chlorothiophenol fall near the range¹ observed for the other derivatives. Indeed, the values of the *ortho*, *meta*, and *para* coupling constants for the oxygen analog, *p*-chlorophenol,⁴² 8.6,

2.8, and 0.3 c.p.s., respectively, fall in or very near the range observed for the *para*-substituted thiophenols. It is evident, therefore, that the four ring protons in *p*-chlorothiophenol are magnetically equivalent, *i.e.*, $\nu_{AB} = 0$, to within the resolution of the instrument. Simple substituent effects may not be used to explain this equivalence since the closeness of the *para*-bromo and chloro σ -values would predict similar behavior for *p*-bromothiophenol, which is not observed. Knowing unequivocally that ν_A (H_A *ortho* to SH) in *p*-chlorothiophenol is -431.0 c.p.s., and arguing by analogy, the resonance frequency closest to -431.0 c.p.s. in each pair of ring proton values in the *para*-substituted thiophenols is assigned to H_A ; thus, the sign of ν_{AB} is determined. The assignment is supported by the fact that ν_{AB} determined in this fashion shows a trend (but not a good correlation) with σ , as does ν_{AB} for the *para*-substituted phenols.

NOTE ADDED IN PROOF.—Subsequent to the acceptance of this work for publication, a set of n.m.r. substituent constants⁴⁵ for the chemical shift of ring protons in *para*-disubstituted benzenes has been brought to our attention. The values predicted for ν_{AB} (c.p.s.) in *para*-substituted thiophenols agree qualitatively with our experimentally determined values: Br, $+12.6$; CH_3 , -8.4 ; NO_2 , $+40.2$; NH_2 , -36.6 ; $t-C_4H_9$, -1.2 ; Cl, $+0.6$. Of special interest is the very small value of ν_{AB} predicted for *p*-chlorothiophenol.

Acknowledgment. We wish to thank Richard Wielesek for the preparation of two compounds and Pitt-Consol, Evans Chemetics, and Pennsalt Chemical Companies for their gifts of chemicals. S. H. M. wishes to thank the National Science Foundation for the grant of Cooperative Graduate Fellowships for the years 1961–1963.

(43) See ref. 17, p. 119.

(44) See ref. 17, p. 262.

(45) G. W. Smith, personal communication.

Studies of Chemically Reacting Systems on Sephadex. II.

Molecular Weights of Monomers in Rapid Association Equilibrium¹

by D. J. Winzor² and H. A. Scheraga

Department of Chemistry, Cornell University, Ithaca, New York (Received September 7, 1963)

In studies of proteins undergoing rapid, reversible association, estimation of the monomeric molecular weights by physicochemical methods is made difficult by the necessity of extrapolating the experimental data to zero concentration. Thus, the accuracy of such determinations depends to a large extent upon the lower limit of the concentration range which can be investigated by the particular method. It has been possible to study protein solutions with concentrations as low as 0.05 mg./ml. by a procedure employing gel filtration, in which the relationship between molecular weight and rate of elution is first determined. A study of α -chymotrypsin in acetate-chloride buffer, ionic strength 0.20, pH 3.86, has been used to check the validity of the procedure, which has then been applied to the estimation of the monomeric molecular weight of bovine thrombin in phosphate-chloride buffer, ionic strength 0.16, pH 7.0; a value of approximately 40,000 is obtained under these conditions.

Introduction

In solutions of proteins which undergo rapid, reversible association, the shift of the equilibrium position toward monomeric species is effectively complete only at infinitely low concentrations. Since physicochemical estimations of the monomeric molecular weight consequently require extrapolation of experimental data to zero concentration, great importance is attached to the results of experiments in which the lowest possible concentration of protein is used. In the techniques currently being used, this lower limit is 0.5–1.0 mg./ml. for light scattering studies^{3–6} and Archibald⁷ experiments,^{8,9} while concentrations as low as 0.2 mg./ml. have been used in sedimentation equilibrium studies of the association of insulin.¹⁰ The values of molecular weights obtained by extrapolations from these limiting concentrations are subject to a considerable degree of uncertainty^{3–6,8–11} and, accordingly, a method enabling the study at lower concentrations would be advantageous.

In preliminary studies of the association of α -chymotrypsin by gel filtration through columns of Sephadex G-100, the qualitative features of the theoretically predicted transport behavior^{12–14} have been observed.¹⁵ Gilbert¹³ has shown that for a protein

in rapid association equilibrium the elution rate of the advancing edge is a weight-average property of the system, and thus extrapolation of this quantity to zero

- (1) This work was supported by Grant HE-01362 from the National Heart Institute, National Institutes of Health, Public Health Service, and by Grant GB-75 from the National Science Foundation.
- (2) On leave from the Wheat Research Unit, Commonwealth Scientific and Industrial Research Organization, North Ryde, N.S.W., Australia, 1962–1963.
- (3) R. F. Steiner, *Arch. Biochem. Biophys.*, **53**, 457 (1954).
- (4) I. Tinoco, *ibid.*, **68**, 367 (1957).
- (5) R. Townend and S. N. Timasheff, *J. Am. Chem. Soc.*, **82**, 3168 (1960).
- (6) R. Townend, L. Weinberger, and S. N. Timasheff, *ibid.*, **82**, 3175 (1960).
- (7) W. J. Archibald, *J. Phys. Chem.*, **51**, 1204 (1947).
- (8) M. S. N. Rao and G. Kegeles, *J. Am. Chem. Soc.*, **80**, 5724 (1958).
- (9) D. B. S. Miller, *J. Biol. Chem.*, **237**, 2135 (1962).
- (10) P. D. Jeffrey and J. H. Coates, *Nature*, **197**, 1104 (1963).
- (11) M. A. Cohly and H. A. Scheraga, *Arch. Biochem. Biophys.*, **95**, 428 (1961).
- (12) G. A. Gilbert, *Discussions Faraday Soc.*, **20**, 68 (1955).
- (13) G. A. Gilbert, *Proc. Roy. Soc. (London)*, **A250**, 377 (1959).
- (14) J. L. Bethune and G. Kegeles, *J. Phys. Chem.*, **65**, 433, 1761 (1961).
- (15) D. J. Winzor and H. A. Scheraga, *Biochemistry*, **2**, 1263 (1963).

concentration should yield the migration rate of the monomeric species. Furthermore, Granath and Flodin¹⁶ have shown that the rate of elution is a function of molecular weight for a series of polymers. Because of the low concentrations which can be used in gel filtration when the protein content of the effluent is measured colorimetrically,¹⁷ it was anticipated that the molecular weight of monomeric species could be more accurately determined by this method provided that the relationship between migration rate and molecular weight was first established for the system under study. This paper presents data on the experimental test of the feasibility of this procedure using α -chymotrypsin in chloride-acetate buffer, ionic strength 0.20, pH 3.86, and on its application to the estimation of the monomeric molecular weight of bovine thrombin.

Experimental

Materials. Three times crystallized, salt-free α -chymotrypsin was obtained from Worthington Biochemical Corp., Freehold, N. J., and was used without further purification. Solutions were prepared by dissolving the crystals directly in buffer (0.18 *M* sodium chloride, 0.02 *M* sodium acetate, pH adjusted to 3.86 with acetic acid) and then dialyzing against more buffer for 12 hr. to prevent deviations in pH from the original buffer value.⁸

Bovine thrombin was prepared by the method of Schrier, *et al.*,¹⁸ from partially purified citrate thrombin solutions obtained in the frozen state (Sigma Chemical Co., St. Louis, Mo.). Equilibrium with pH 7.0, 1 *M* phosphate buffer (0.03 *M* K₂HPO₄, 0.02 *M* KH₂PO₄, 0.05 *M* KCl) was achieved by passage of the purified thrombin preparations through columns of Sephadex G-25 equilibrated with buffer.

Protein concentrations were estimated spectrophotometrically using the values 20.7 and 19.5 for the extinction coefficients ($E_{1\%}^{1\text{cm}}$) of chymotrypsin at 282 μ ,^{8,19} and thrombin at 280 μ ,²⁰ respectively.

Sedimentation. Molecular weights were estimated by the Klainer and Kegeles^{21,22} modification of the Archibald⁷ procedure, using a Spinco Model E ultracentrifuge equipped with phase-plate schlieren diaphragm and RTIC unit. The temperature of the rotor (approximately 21°C) was not controlled but was periodically recorded, and an average value was used in the calculations. Speeds in the range 9945 to 23,150 r.p.m. were used to effect marked changes in the concentration at the meniscus. For concentrations below 2 mg./ml. a cell with 30-mm. optical path was used, allowance being made for the greater optical sensitivity. The schlieren patterns were measured on a Gaertner two-dimensional comparator having a sensitivity of

0.001 mm. In the calculations of molecular weights, values of 0.731 and 0.735 were used for the partial specific volumes of chymotrypsin¹⁹ and thrombin,¹¹ respectively; the relevant buffer density data were also obtained from these two sources.

Column Procedure. The procedure for the conduct of gel filtration experiments and for the treatment of the experimental data has been described elsewhere.¹⁵ In the experiments with chymotrypsin a 32 \times 1.25-cm. column of Sephadex G-100 (Pharmacia Fine Chemicals, Inc., Rochester, Minn.) equilibrated with the pH 3.86 acetate-chloride buffer was used, while a 24 \times 1.25-cm. column of Sephadex G-100 equilibrated with pH 7.0 phosphate-chloride buffer was used for the study of thrombin. Sufficient protein solution was applied to the columns so that the resulting effluent profiles contained a plateau region in which the protein concentration was equal to that initially applied. By this procedure we were able to observe independently of each other the shapes of the advancing and trailing edges of a protein zone of known concentration. Fractions of approximately 0.3 ml. each were collected in previously weighed tubes, and elution was performed at approximately 6 ml./hr., no trailing of zones being observed at this flow rate with proteins not undergoing Gilbert-type association.¹⁵ In fact, from our observations¹⁵ with ovalbumin and soybean trypsin inhibitor, it would appear that proteins which are not in rapid association equilibrium yield gel filtration patterns in which the trailing edge is *sharper* than its advancing counterpart.²³

Typical elution profiles for α -chymotrypsin and bovine thrombin are shown in the upper curves of Fig. 1 and 2, respectively, the lower curves being the first difference curves obtained by using 0.50-ml. increments in volume. These patterns are characteristic of systems undergoing rapid, reversible dimerization^{12,13} in that the trailing boundary for each protein is more diffuse than the advancing edge²⁴ and is

- (16) K. Granath and P. Flodin, *Makromol. Chem.*, **48**, 160 (1961).
- (17) O. H. Lowry, N. J. Rosebrough, A. L. Farr, and R. J. Randall, *J. Biol. Chem.*, **193**, 265 (1951).
- (18) E. E. Schrier, C. A. Broomfield, and H. A. Scheraga, *Arch. Biochem. Biophys. Suppl.*, **1**, 309 (1962).
- (19) G. W. Schwert and S. Kaufman, *J. Biol. Chem.*, **190**, 807 (1951).
- (20) D. J. Winzor and H. A. Scheraga, *Arch. Biochem. Biophys.*, in press.
- (21) S. M. Klainer and G. Kegeles, *J. Phys. Chem.*, **59**, 952 (1955).
- (22) S. M. Klainer and G. Kegeles, *Arch. Biochem. Biophys.*, **63**, 247 (1956).
- (23) Further evidence for this postulate is provided by the results of an independent study (M. V. Tracey, private communication), in which this type of behavior was observed in gel filtration of bovine serum albumin monomer, ovalbumin, and lysozyme.

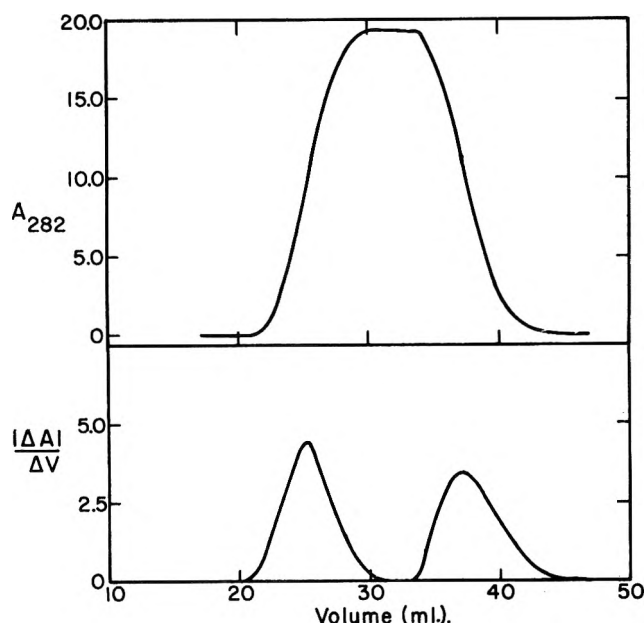


Figure 1.—Elution profile (upper curve) obtained in the chromatography of α -chymotrypsin (9.6 mg./ml.) on a 1.25×32 cm.-column of Sephadex G-100 previously equilibrated with acetate-chloride buffer, ionic strength 0.20, pH 3.86. The lower curves are the first difference plots, 0.50 ml. having been used as the increment in volume.

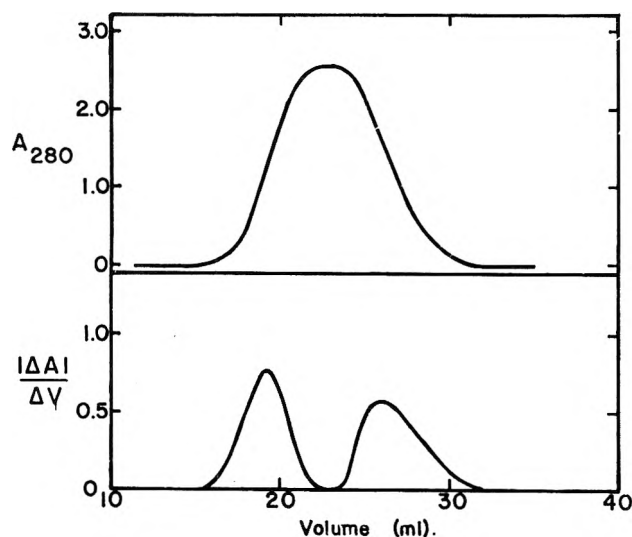


Figure 2. Elution profile (upper curve) obtained in the chromatography of bovine thrombin (1.3 mg./ml.) on a 1.25×24 cm.-column of Sephadex G-100 previously equilibrated with phosphate-chloride buffer, ionic strength 0.16, pH 7.0. The lower curves have the same significance as in Fig. 1.

decidedly asymmetric. As in the previous study,¹⁵ good correlation was found between the first difference curves for the trailing edge and the corresponding ultracentrifuge patterns. The trailing boundary in

Fig. 1 (derivative curve) resembles fairly closely the schlieren patterns for α -chymotrypsin under the same conditions,²⁵ while similar agreement is observed between the trailing boundary of Fig. 2 and Fig. 4 of ref. 11.

The migration rates of protein zones have been estimated as the ratio of the volume of solvent required for the elution of a protein (V_e) to the total volume of the column (V_t).²⁶ This quantity represents the fraction of the total column volume which is accessible to a particular type of molecule, and thus faster elution rates are indicated by smaller values of V_e/V_t . The data reported in this paper refer to the migration rate of the advancing edge, which is a weight average property of the system.¹³ Since the advancing boundaries of the protein zones were symmetrical (Fig. 1 and 2), V_e was taken as the volume at which the protein concentration reached half of the value attained in the plateau region.

Results

The results of direct Archibald molecular weight estimations on α -chymotrypsin in acetate-chloride, ionic strength 0.20, pH 3.86, are shown in Fig. 3. From the experimental data a value of approximately 35,000 for the molecular weight of monomeric chymotrypsin is indicated, whereas values from chemical^{27,28} and phys-

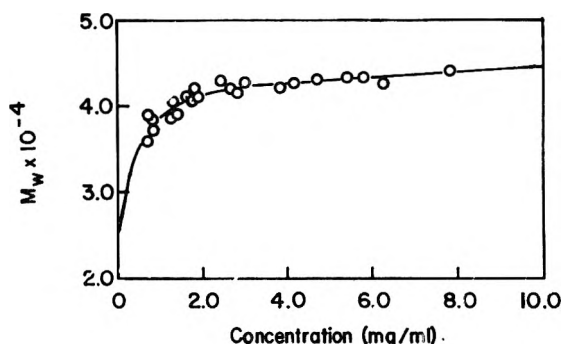


Figure 3.—The concentration dependence of the weight-average molecular weight (Archibald) of α -chymotrypsin in pH 3.86 acetate-chloride buffer, ionic strength 0.20. The circles refer to experimental values, the line being a theoretical curve calculated for a dimerizing system (see text).

(24) In the Gilbert theory, a hypersharp boundary is predicted for the advancing edge of a moving zone. Since for nonassociating proteins this boundary is the more diffuse, considerable sharpening has in fact taken place.

(25) G. W. Schwert, *J. Biol. Chem.*, **179**, 655 (1949).

(26) K. C. Pedersen, *Arch. Biochem. Biophys. Suppl.*, **1**, 157 (1962).

(27) E. F. Jensen, M. D. F. Nutting, R. Jang, and A. K. Balls, *J. Biol. Chem.*, **179**, 189 (1949).

(28) B. S. Hartley and B. A. Kilby, *Biochem. J.*, **60**, 672 (1952).

icochemical studies^{3,4,8,29,30} are in the range 22,000 to 27,000. The curve drawn through the data has been calculated for a monomer \rightleftharpoons dimer system using values of 24,000 for the monomeric molecular weight and 0.26 for the dissociation constant, the latter being calculated from the weight-average molecular weight data by the method of Rao and Kageles.⁸ For a dimerizing system, eq. 3 of ref. 8 becomes

$$K_2' = \frac{(2M_1 - M_w)^2 C}{(M_w - M_1) M_1}$$

where C is the total protein concentration, and M_1 and M_w are the monomeric and weight-average molecular weights, respectively. Thus, a plot of the quantity $(M_w - M_1)/(2M_1 - M_w)^2$ vs. C yields a line of slope $1/M_1 K_2'$, from which the dissociation constant (K_2') may be found. Figure 4 shows such a plot of the present molecular weight data, in which the deviation of the points from the line joining the origin with the point corresponding to the average ordinate and abscissa values is within experimental error.³¹

The gel filtration data on chymotrypsin, shown in Fig. 5, parallel fairly closely the sedimentation coefficient-concentration results obtained under the same conditions of pH and ionic strength.²⁵ At concentrations greater than 3 mg./ml. there is a slight negative dependence of migration rate upon concentration, while below 2 mg./ml. a rapid decrease in migration rate results from marked changes in the degree of association (Fig. 3). The close correspondence between molecular weight and rate of elution is illustrated by Fig. 6, in which the experimental value of V_e/V_t at a particular concentration is plotted against the

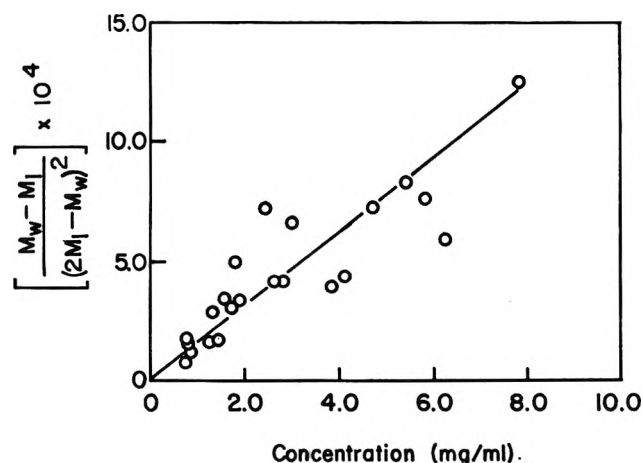


Figure 4. Plot of $(M_w - M_1)/(2M_1 - M_w)^2$ vs. concentration. The experimental points refer to the molecular weight data of Fig. 3, and the straight line joins the origin with the point defined by the average ordinate and abscissa values.

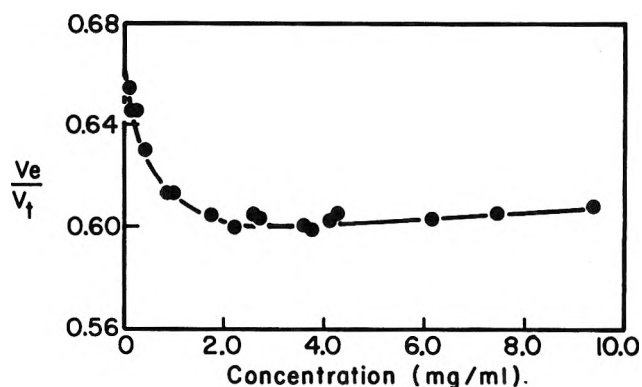


Figure 5. The concentration dependence of the migration rate of the advancing edge in the chromatography of α -chymotrypsin on Sephadex G-100; experimental conditions as in Fig. 1.

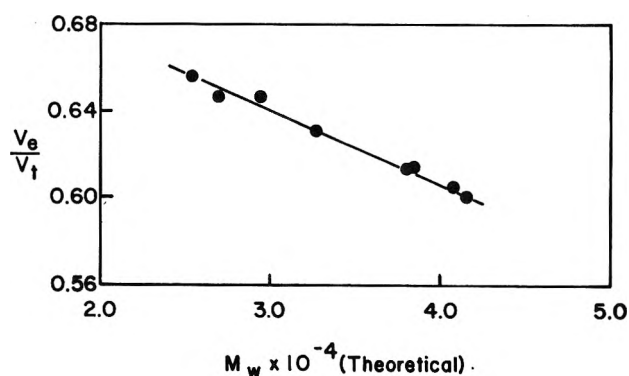


Figure 6. The relationship between molecular weight of chymotrypsin and the rate of elution from a column of Sephadex G-100.

theoretical molecular weight at the same concentration (Fig. 3). The data refer only to experiments in which the concentration was less than 3 mg./ml., since the changes in the degree of association above this concentration are insufficient to counteract the normal concentration dependence effects.³²

The linear relationship between V_e/V_t and molecular weight, evident in Fig. 6, provides the experimental test of the feasibility of estimating monomeric molecular weights by gel filtration experiments in conjunction with direct molecular weight determinations. Provided that the proportionality between the migration

(29) E. L. Smith and D. M. Brown, *J. Biol. Chem.*, **195**, 525 (1952).

(30) A. K. Balls and E. F. Jensen, *Advan. Enzymol.*, **13**, 321 (1952).

(31) In a plot of this kind, any discrepancies are greatly magnified. Since the data in Fig. 4 are obtained from the molecular weight values shown in Fig. 3, the deviation of a point from the line in Fig. 4 is only a greatly magnified measure of the same error between the corresponding experimental and theoretical molecular weights in Fig. 3.

(32) The negative concentration dependence of migration rate found in ultracentrifuge studies is also observed in gel filtration experiments on nonassociating systems.¹⁵

rate and molecular weight is first determined at higher concentrations, advantage can be taken of the gel filtration data at lower concentrations to assist in the extrapolation of molecular weight to zero protein concentration.

The relevant data for the application of the method to estimating the monomeric molecular weight of

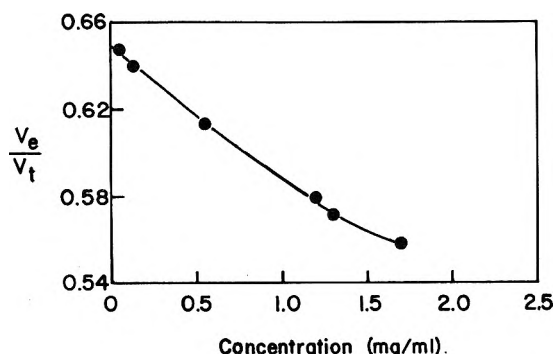


Figure 7. The concentration dependence of the migration rate of the advancing edge in the chromatography of bovine thrombin on Sephadex G-100; experimental conditions as in Fig. 2.

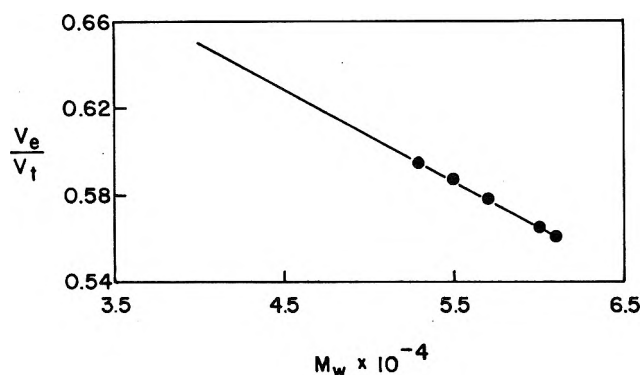


Figure 8. Relationship between molecular weight of bovine thrombin and rate of elution from a column of Sephadex G-100.

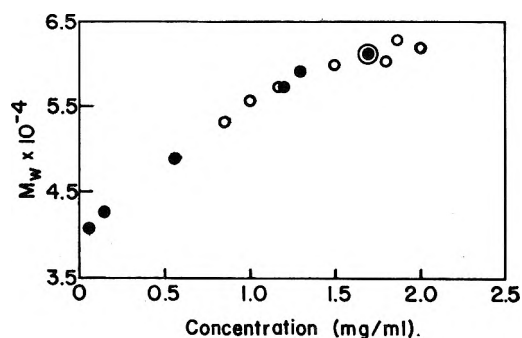


Figure 9. The concentration dependence of the molecular weight of bovine thrombin in pH 7.0 phosphate-chloride buffer of ionic strength 0.16: \circ , data from ultracentrifuge experiments; \bullet , values inferred from gel filtration studies.

bovine thrombin in phosphate-chloride buffer, ionic strength 0.16, pH 7.0, are shown in Fig. 7-9. The fundamental gel filtration results are given in Fig. 7, while Fig. 8 provides the relationship between V_e/V_t and molecular weight determined by the Archibald⁷ procedure. The combined results of molecular weight estimations by the two methods are depicted in Fig. 9, from which a value of approximately 40,000 is indicated for the molecular weight of thrombin at zero protein concentration.

Reference to the previous study of thrombin under the same conditions of ionic strength and pH¹¹ reveals qualitative similarity between the ultracentrifugal data,³³ and, accordingly, a monomeric molecular weight of 40,000 is consistent with both sets of experimental data. However, the present results seem to rule out the earlier interpretation whereby a value in the neighborhood of 33,000 was obtained for the molecular weight of bovine thrombin monomer. In the only other physicochemical study of thrombin under conditions where anomalous concentration dependence effects were observed,³⁴ a value of 33,700 was reported for the molecular weight, this value being calculated by combination of sedimentation coefficient data obtained in 0.1 M KCl with diffusion measurements performed in acetate-chloride buffer, pH 5.6.

Discussion

The molecular weight data on α -chymotrypsin, shown in Fig. 3, illustrate the difficulties which can be encountered in attempts to obtain monomeric molecular weights by extrapolation of results to zero protein concentration and emphasize the advantage of an estimation procedure whereby lower concentrations may be studied. This is further demonstrated by the experimental results obtained using the gel filtration technique (Fig. 5 and 6). In the present study, the lowest protein concentration studied by gel filtration was approximately 0.05 mg./ml., this limit being determined by the sensitivity of the colorimetric procedure¹⁷ used for protein estimation.

A disadvantage of the present method is that molecular weights can only be obtained indirectly, the fundamental quantity derived from the gel experiment being a rate of migration. As is also observed with sedimentation coefficients, the counterpart in ultracentrifuge studies, the magnitude of V_e/V_t is affected by factors other than molecular weight and thus cannot be used for molecular weight estimation without prior cali-

(33) The experimental scatter of the earlier data makes a more detailed comparison impractical.

(34) C. R. Harmison, R. H. Landaburu, and W. H. Seegers, *J. Biol. Chem.*, **236**, 1693 (1961).

bration by an absolute method. In this respect the migration rate through Sephadex is subject to more variation because of possible adsorption effects.³⁶⁻³⁷ However, the method provides data in a very important range of concentration not attainable by other methods, and is thus likely to prove a very useful supplementary procedure in molecular weight studies of rapidly associating systems by conventional techniques.

Normal concentration dependence of V_e/V_t , observed with ovalbumin¹⁵ and α -chymotrypsin, at higher concentrations (this study), will, of course, introduce an uncertainty in values obtained at high concentrations, and could conceivably introduce curvature into the calibration plot. For example, the point corresponding to the values of M and V_e/V_t for chymotrypsin at a concentration of 10 mg./ml. would deviate considerably from the straight line drawn in Fig. 6. However, from the practical point of view, there is usually no need to perform gel experiments at concentrations greater than 5 mg./ml., below which concentration sufficient molecular weight data should be obtained to establish the calibration curve. With ovalbumin, the correction for concentration dependence at this level is of the order of 0.02 in V_e/V_t .¹⁵ In a system with increasing degree of association at this concentration, no serious error would be introduced by ignoring a factor of this size, and thus V_e/V_t would still measure with sufficient precision the value of M . Since the concentration dependence of V_e/V_t values parallels quantitatively the sedimentation coefficient-concentration relationship for ovalbumin,¹⁵ which may be regarded as typical of fairly symmetrical proteins,³⁸ it is assumed that the concentration dependence factor is likely to be of importance only for more asymmetric molecules, *e.g.*, fibrinogen, where the effect is greater.³⁹

From the satisfactory agreement between the experimental data and the theoretical curve for the concentration dependence of the molecular weight (Fig. 3), it would appear that, under these conditions of pH and ionic strength, α -chymotrypsin is indeed a monomer-dimer system, as predicted from the shape of the

boundary observed in transport experiments.¹²⁻¹⁴ The results of this study thus differ from those obtained for chymotrypsin in phosphate buffer, pH 6.20, under which conditions it was necessary to postulate the presence of trimers as well as dimers to account for the molecular weight data,⁸ although the schlieren pattern obtained in sedimentation velocity experiments⁸ did not reveal apparent partial resolution of peaks, predicted for such a system.¹²⁻¹⁴

The main point of interest which prompted the investigation of the thrombin system was that there have been several indications of a value in the vicinity of 10,000 for the molecular weight of bovine thrombin. Such values have been obtained by direct measurement in buffers of high ionic strength,⁴⁰ in denaturing solvents,¹⁸ and also under acidic conditions.²⁰ Indirect measurements, involving a study of the binding of diisopropylphosphofluoridate to thrombin, have also indicated a similar value for the minimum molecular weight.⁴¹ The data of Fig. 9 are convincing evidence that a monomer of this size is not involved in the association equilibrium at pH 7.0, ionic strength 0.16, as was thought previously.⁴² However, under the other conditions cited, the monomer molecular weight may be in the neighborhood of 10,000; we plan to carry out gel filtration experiments of thrombin under these other conditions.

Acknowledgment. The technical assistance of Louise Krech is gratefully acknowledged.

- (35) B. Gelotte, *J. Chromatog.*, **3**, 330 (1960).
- (36) J. Porath, *Biochim. Biophys. Acta*, **39**, 193 (1960).
- (37) A. N. Glazer and D. Wellner, *Nature*, **194**, 862 (1962).
- (38) J. T. Edsall, "The Proteins," Vol. 1B, ed. by H. Neurath and K. Bailey, Academic Press, Inc., New York, N. Y., 1953, p. 549.
- (39) V. L. Koenig and K. O. Pedersen, *Arch. Biochem.*, **25**, 97 (1950).
- (40) L. Lorand, W. T. Brannen, Jr., and N. G. Rule, *Arch. Biochem. Biophys.*, **96**, 147 (1962).
- (41) J. A. Gladner, K. Laki, and F. Stohlman, *Biochim. Biophys. Acta*, **27**, 218 (1958).
- (42) H. A. Scheraga and M. A. Cohly, *Thromb. Diath. Haemorrhag.*, **5**, 609 (1961).

Hydrogenolysis of Ethane over Supported Platinum

by J. H. Sinfelt

Esso Research and Engineering Co., Linden, New Jersey (Received September 9, 1963)

The hydrogenolysis of ethane over two supported platinum catalysts, one employing silica as a support and the other alumina, was investigated in a flow reactor over the temperature range of 343 to 401°. The rate of hydrogenolysis to methane was found to increase with ethane partial pressure to a power in the range 0.7 to 0.9. However, the rate was found to decrease markedly with increasing hydrogen pressure. This has been interpreted in terms of a mechanism involving extensive dehydrogenation on the surface prior to a slow step in which carbon-carbon bonds are broken. The apparent activation energy of the reaction was found to be much higher over the silica-supported platinum, although the rates were not far different at the temperatures of this study. The difference in activation energies for the different supports suggests that the support interacts with platinum in some manner, and that silica differs from alumina with regard to such an interaction.

The catalytic hydrogenolysis of ethane to methane has been studied over nickel, cobalt, and iron catalysts by Taylor and co-workers.¹⁻⁴ From the results of these studies it was postulated⁴ that the initial step in the reaction involved dehydrogenation to form unsaturated surface radicals, and that the hydrogen content of the radicals varied with the metal. Since no data were reported for noble metal catalysts, it was decided to investigate the reaction over supported platinum. In addition, it was decided to investigate the effect of the support on the catalytic properties of the platinum, and hence studies were made with platinum supported on both alumina and silica. Although there is a widely held impression⁵ that the support does not interact with the metal in supported noble metal catalysts, data are presented here which refute this idea.

Experimental

Apparatus and Procedure. The reaction rate measurements were carried out in a flow system at atmospheric pressure. The reactor was a stainless steel tube approximately 1.0 cm. in diameter and 8 cm. in length. The reactor was held in a vertical position and was surrounded by a small electrical oven. The catalyst was centered with respect to the ends of the reactor, occupying a space approximately 1.5 to 4.0 cm. in length in the various runs. A fritted stainless steel disk was used to support the catalyst in the reactor, and quartz

wool was packed on top of the catalyst to hold it in place. A 3-mm. axial thermowell containing an iron-constantan thermocouple extended upward through the fritted steel disk into the catalyst bed, so that the tip of the thermowell was located at the center of the catalyst bed. The reaction gases were passed downflow through the catalyst bed, and the products were analyzed by a chromatographic unit coupled directly to the outlet of the reactor. The chromatographic column was 2 m. in length and 0.6 cm. in diameter. The column was packed with 100 mesh silica gel and was operated at 40°. Helium was used as a carrier gas, and a thermal conductivity detector was used with the column.

The reactant gases, ethane and hydrogen, were passed over the catalyst in the presence of helium diluent. Gas flow rates were measured using orifice-type flow meters with manometers. A total gas flow rate of 1 l./min. was used throughout. The run procedure consisted of passing the reactant gases over the catalyst for a period of 3 min., at which time a sample of the

- (1) K. Morikawa, W. S. Benedict, and H. S. Taylor, *J. Am. Chem. Soc.*, **58**, 1795 (1936).
- (2) E. H. Taylor and H. S. Taylor, *ibid.*, **61**, 503 (1939).
- (3) C. Kemball and H. S. Taylor, *ibid.*, **70**, 345 (1948).
- (4) A. Cimino, M. Boudart, and H. S. Taylor, *J. Phys. Chem.*, **58**, 796 (1954).
- (5) G. C. Bond, "Catalysis by Metals," Academic Press, Inc., London, 1962, p. 40.

product was taken for chromatographic analysis. The ethane was then cut out and hydrogen flow was continued for a period of 10 min. at the reaction temperature prior to another run. In this way, it was possible to minimize variation in catalyst activity from period to period. As an additional insurance against the complications due to varying catalyst activity, measurements at any given set of conditions were in most cases bracketed with runs at a standard set of conditions. In this way, the effect of changing a variable can be determined by comparison with the standard condition periods run immediately before and after the period in question. Before any reaction studies were made, the catalyst was pretreated in flowing hydrogen for 3 hr. at 500°.

Materials. The ethane used in this work was obtained from the Matheson Co. A chromatographic analysis of the ethane showed no detectable hydrocarbon impurities. It is estimated that a hydrocarbon impurity, *e.g.*, methane, would have been detected by the chromatographic analysis if it were present at a concentration above 0.01 wt. %. High purity hydrogen was obtained from the Linde Co. and was further purified by passing it through a Deoxo unit containing palladium catalyst to remove traces of oxygen as water, prior to passage through a molecular sieve dryer.

The platinum catalysts used in this work were supported on either silica or alumina. The platinum content of the catalysts was 0.60% by weight. The catalysts were prepared by impregnation of silica or alumina with aqueous chloroplatinic acid, followed by calcination in air. The Pt/SiO₂ catalyst was calcined at 538° for 1 hr., while the Pt/Al₂O₃ was calcined at 593° for 4 hr. The silica and alumina were prepared by heating either silica gel or β -alumina trihydrate, both obtained from Davison Chemical Co., for 4 hr. at 538 or 593°, respectively. The B.E.T. surface areas of the silica and alumina were 388 and 296 m.²/g., respectively. X-Ray diffraction measurements obtained in these laboratories indicated the alumina to be η -alumina.

Results

In studying the kinetics of the hydrogenolysis of ethane to methane, the approach taken was to measure initial rates of reaction at low conversion levels (0.05 to 5.9%). The reaction rate r is defined by the relation

$$r = \frac{F}{W}x \quad (1)$$

where F represents the feed rate of ethane to the reactor in g. moles/hr., W represents the weight in grams

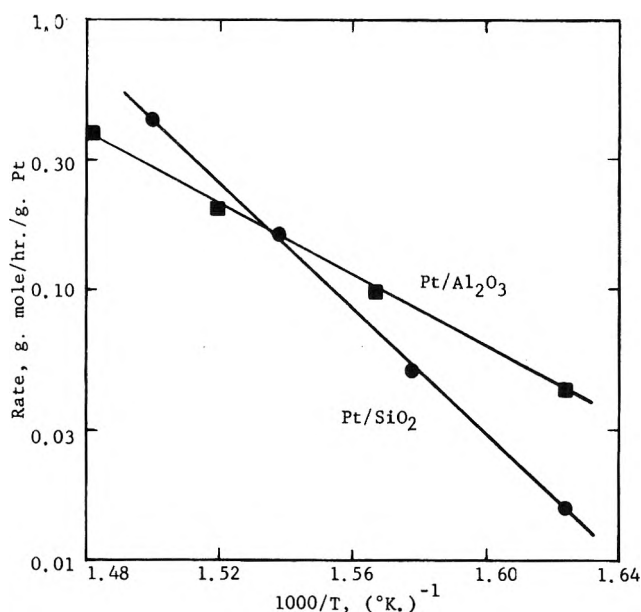


Figure 1. Effect of temperature on the rate of hydrogenolysis of ethane; H₂ pressure = 0.20 atm.; C₂H₆ pressure = 0.030 atm.

of platinum on the catalyst charged to the reactor, and x represents the fraction of the ethane converted to methane.

Data on the effect of temperature on rates for both the Pt/SiO₂ and Pt/Al₂O₃ catalysts are shown in the Arrhenius plots in Fig. 1. From the slopes of these plots, the apparent activation energies of the ethane hydrogenolysis reaction over the Pt/SiO₂ and Pt/Al₂O₃ catalysts are 54 and 31 kcal./mole, respectively.

Rate data showing the effects of hydrogen and ethane partial pressures, p_H and p_E , respectively, are summarized in Table I in the form of a ratio r/r_0 , where r is the rate at any given conditions and r_0 is the rate at a standard set of conditions ($p_H = 0.20$ atm., $p_E = 0.030$ atm.). The rate measurements at conditions different from the standard were bracketed by rate determinations at the standard conditions. Each r/r_0 value in Table I was obtained by dividing the rate determined in a given reaction period at a particular set of conditions by the average of the rate determinations at the standard conditions immediately before and after the given reaction period. This procedure served to minimize the effects of varying catalyst activity. While the variation in activity during any one reaction period was generally not large (10-20% at most), the cumulative activity decline over an extended period of time could have led to erroneous conclusions about the kinetics if the above procedure had not been adopted.

Table I: Relative Rates of C₂H₆ Hydrogenolysis as a Function of C₂H₆ and H₂ Partial Pressures

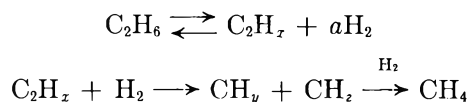
Catalyst	p_{H_2} atm.	$p_{\text{C}_2\text{H}_6}$ atm.	r/r_0^a
Pt/SiO ₂ (377°)	0.10	0.030	3.3
	0.20	0.030	1.0
	0.60	0.030	0.12
	0.20	0.0050	0.21
	0.20	0.010	0.37
	0.20	0.030	1.0
	0.20	0.100	2.6
Pt/Al ₂ O ₃ (366°)	0.10	0.030	2.6
	0.20	0.030	1.0
	0.40	0.030	0.24
	0.20	0.0050	0.27
	0.20	0.010	0.47
	0.20	0.030	1.0
	0.20	0.100	2.1

^a Rate relative to the rate at the standard conditions ($p_{\text{H}_2} = 0.20$ atm., $p_{\text{C}_2\text{H}_6} = 0.030$ atm.) for the particular catalyst and temperature in question; the r/r_0 values cannot be used by themselves to compare the activities of the catalysts.

For both the Pt/SiO₂ and the Pt/Al₂O₃ catalysts, the data in Table I show that the rate of ethane hydrogenolysis increases with increasing ethane partial pressure, but decreases markedly with increasing hydrogen partial pressure. The dependence of the rate on the partial pressures of ethane and hydrogen can be expressed as a simple power law, $r = kp_{\text{C}_2\text{H}_6}^n p_{\text{H}_2}^m$. Approximate values of the exponents n and m as derived from the experimental data are summarized below.

Catalyst	n	m
Pt/SiO ₂ (377°)	0.9	-1.8
Pt/Al ₂ O ₃ (366°)	0.7	-1.7

These results can be accounted for satisfactorily by the mechanism proposed by Cimino, Boudart, and Taylor.⁴ According to these authors, ethane hydrogenolysis over metals involves the reaction steps



where x , y , and z are integers and a is equal to $(6 - x)/2$ by stoichiometry. The species C₂H _{x} represents an adsorbed dehydrogenated radical which reacts with a molecule of hydrogen to form the surface fragments CH _{y} and CH _{z} . The latter are hydrogenated off the surface to form methane. By postulating that the initial dehydrogenation step was an equilibrated reaction and that the cracking of C₂H _{x} in the second step was rate controlling, the authors derived an approximate rate law of the form

$$r = kp_{\text{C}_2\text{H}_6}^n p_{\text{H}_2}^{(1-na)}$$

where $0 < n < 1$. Taking the experimental values of n for the Pt/SiO₂ and Pt/Al₂O₃ catalysts, and assuming a value for a , we can calculate the exponent $(1 - na)$ of p_{H_2} and compare with m , the experimental value. The best agreement is obtained if we assume $a = 3$, in which case the calculated exponents of p_{H_2} for the Pt/SiO₂ and Pt/Al₂O₃ catalysts are, respectively, -1.7 and -1.1, which are to be compared with the corresponding experimental m values of -1.8 and -1.7. The agreement is good for the Pt/SiO₂ catalyst but only fair for the Pt/Al₂O₃ catalyst.

Discussion

On the whole, we conclude that the kinetic formulation of Cimino, Boudart, and Taylor accounts satisfactorily for the results on ethane hydrogenolysis over supported platinum.

The most interesting finding of the present study is the marked difference in the apparent activation energy for the two platinum catalysts studied. While the degree of dispersion of the platinum may be different on alumina and silica, the difference in apparent activation energies cannot be rationalized readily on the basis of a difference in platinum surface areas alone, since this would be expected to affect only the magnitudes of the rates rather than the temperature dependence. It seems more likely that some specific interaction between platinum and support is involved. The widely held impression⁵ that supports do not interact with noble metals is thus open to considerable question.

Electron Paramagnetic Resonance Study of the Photolysis of

Nitromethane, Methyl Nitrite, and Tetranitromethane at 77°K.¹

by Benon H. J. Bielski and Richard B. Timmons

Chemistry Department, Brookhaven National Laboratory, Upton, New York (Received September 12, 1963)

Results have been obtained through the use of electron paramagnetic resonance spectroscopy which show that the initial step in the photolysis of nitromethane is dissociation into a methyl radical and nitrogen dioxide. The photolysis of methyl nitrite is also shown to produce free radicals. Evidence is presented which indicates that the methoxy radical is produced during photolysis. The primary step in the photolysis of tetranitromethane is postulated to be a split into NO₂ and C(NO₂)₃.

The purpose of this investigation was to obtain direct evidence for radical formation during the photolysis of aliphatic nitro compounds by the use of electron spin resonance spectroscopy. Particular emphasis was placed on keeping the present conversion low so as to ensure that no secondary photolysis would obscure the results.

Before presenting the results of this work, it is appropriate first to review briefly the previous research on the photolysis of the three compounds mentioned in the title. Considerable interest has been shown in recent years on the photolysis of aliphatic nitro and nitrite compounds and major attention has been centered on nitromethane and methyl nitrite. A clear understanding of the photolytic decomposition of these compounds provides a valuable key to the elucidation of the photochemical processes involved in the case of the more complex molecules. For the sake of clarity, each compound mentioned above will be discussed individually.

Nitromethane

Recently, Rebbert and Slagg² have published a detailed account of the photolysis of nitromethane both in the gas phase and in the liquid phase. From the product formation observed, they suggest that the initial step in the photolysis is a split into a methyl radical and nitrogen dioxide



This suggestion agrees with the previous work of

Gray, *et al.*,³ and Nicholson,⁴ who also propose the same primary step.

A dissenting view had been proposed by Brown and Pimentel,⁵ who suggested that the initial step is an intramolecular rearrangement to methyl nitrite when photolysis was carried out at 20°K. in an argon matrix. However, in a later report Pimentel and Rollefson,⁶ after studying the gas phase photolysis of nitromethane, have concluded that both the gas phase and the matrix studies can be explained in terms of an initial fragmentation to CH₃ and NO₂. Then, because of the matrix cage effect, some of the CH₃ and NO₂ can recombine to form CH₃ONO or CH₃NO₂ in the low temperature work.

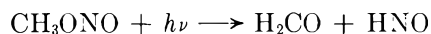
In all of the gas phase studies nitrogen dioxide was not observed as one of the reaction products. It also was not observed in the matrix studies of Brown and Pimentel.⁵ It is to be expected that because of the high reactivity of NO₂, its steady-state concentration would always be quite low. This is especially true for the

- (1) Research performed under the auspices of the U. S. Atomic Energy Commission.
- (2) R. E. Rebbert and N. Slagg, *Bull. soc. chim. Belges*, **71**, 709 (1962).
- (3) P. Gray, A. D. Yoffe, and L. Roselaar, *Trans. Faraday Soc.*, **51**, 1489 (1955).
- (4) A. J. C. Nicholson, *Nature*, **190**, 143 (1961).
- (5) H. W. Brown and G. C. Pimentel, *J. Chem. Phys.*, **29**, 883 (1958).
- (6) G. C. Pimentel and G. Rollefson, "Formation and Trapping of Free Radicals," ed. by A. M. Bass and H. P. Broida, Academic Press, New York, N. Y., 1960, Chapter 4, p. 97.

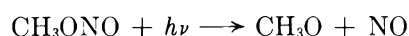
gas phase studies. It was hoped that the NO₂ concentration in the present study would be sufficiently high to allow for its detection by e.p.r. spectroscopy.

Methyl Nitrite

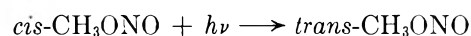
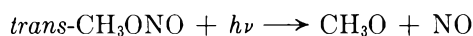
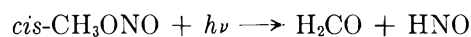
Several different primary steps have been suggested for the photolysis of methyl nitrite. For example, Thompson and Purkis⁷ have suggested an initial split into formaldehyde and nitroxyl



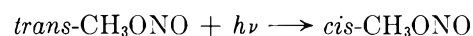
On the other hand, Gray and Style⁸ have proposed the following mechanism



Brown and Pimentel⁵ were the first to take into account that methyl nitrite exists as two distinct rotational isomers⁹ and have suggested the following sequence to explain their results of the photolysis of methyl nitrite at 20°K. in an argon matrix



Their assignment of the *cis*- and *trans*-methyl nitrite was based on Tarte's assumption that the *cis* isomer is the more stable one.⁹ However, later work indicates that actually the *trans*-methyl nitrite is the more stable form.¹⁰⁻¹² Therefore, the results of Brown and Pimentel should be interpreted in terms of this new assignment. For example, if a reaction such as reaction 6 is important, then it should be written as



Hanst and Calvert¹³ have studied the photolysis of methyl nitrite both in the presence and absence of oxygen and in the presence of excess NO. Their results lend strong support for an initial split into methoxy radicals and nitric oxide.

Recently, McMillan¹⁴ has shown that the photolysis of *t*-butyl nitrite proceeds with an initial split into *t*-butoxy radicals and nitric oxide. The evidence in this particular case seems to be quite convincing.

Tetranitromethane

The structure of tetranitromethane is generally accepted to consist of four true nitro groups arranged tetrahedrally about a central carbon atom. Occasionally, workers have suggested that one of these nitro groups is different from the other three.¹⁵⁻¹⁷ However, Nicholson has shown¹⁸ that most probably the tetranitromethane used in these cases was very impure.

He has reported that when a sample of tetranitromethane is carefully purified, the measured physical properties can all be explained in terms of each nitro group as being equivalent.

Little work has been performed on the photolysis of tetranitromethane. Nicholson observed the formation of N₂, NC₂, NO, CO, and CO₂ when tetranitromethane was photolyzed to 100% decomposition.¹⁹ The major product was NO₂ with only small amounts of N₂ being formed. The exact mechanism for photodecomposition of this compound is not known; however, Nicholson favors an initial split into NO₂ and a C(NO₂)₃ radical.²⁰ It is interesting but difficult to account for the formation of N₂, CO, and CO₂. However, under the experimental conditions of complete decomposition of tetranitromethane, appreciable secondary photolysis of nitrogen dioxide would occur giving rise to oxygen atoms and O₂ molecules. Thus these products could conceivably be produced by the oxidation of the C(NO₂)₃ radical.

It is to be noted that in the majority of the photolytic work discussed above, large per cent conversions of sample were carried out and the primary step was thus inferred from the presence or absence of certain reaction products. The only previous report in which the radical intermediates were directly observed was in the work of Style and Ward,²¹ who observed fluorescence of methoxyl on the photolysis of methyl nitrite in the Schumann region.

In the present work, information concerning the primary step was sought from the structure of the e.p.r. spectra obtained. Samples of CH₃NO₂, CH₃ONO, and C(NO₂)₄ were photolyzed as pure compounds and also in various matrices. In each case e.p.r. spectra

- (7) H. W. Thompson and C. H. Purkis, *Trans. Faraday Soc.*, **32**, 1466 (1936).
- (8) J. A. Gray and D. W. G. Style, *ibid.*, **48**, 1137 (1952).
- (9) P. Tarte, *J. Chem. Phys.*, **20**, 1570 (1952).
- (10) L. H. Piette, J. D. Ray, and R. O. Ogg, Jr., *ibid.*, **26**, 1341 (1957).
- (11) P. Gray and M. W. T. Pratt, *J. Chem. Soc.*, 3403 (1958).
- (12) R. F. Grant and D. W. Davidson, *J. Chem. Phys.*, **33**, 1713 (1960).
- (13) P. L. Hanst and J. C. Calvert, *J. Phys. Chem.*, **63**, 2071 (1959).
- (14) G. R. McMillan, *ibid.*, **67**, 931 (1963).
- (15) H. Mark and W. Noethling, *Z. Krist.*, **65**, 435 (1927).
- (16) I. E. Coop and L. E. Sutton, *J. Chem. Soc.*, 1269 (1938).
- (17) G. L. Lewis and C. P. Smyth, *J. Am. Chem. Soc.*, **61**, 3067 (1939).
- (18) A. J. C. Nicholson, *J. Chem. Soc.*, 1553 (1949).
- (19) A. J. C. Nicholson, Ph.D. Thesis, Cambridge University, 1949.
- (20) A. J. C. Nicholson, private communication.
- (21) D. W. G. Style and J. C. Ward, *Trans. Faraday Soc.*, **49**, 999 (1953).

were obtained which clearly indicated the primary step in the photolysis of these compounds.

Experimental

The nitromethane, nitroethane, and 1-nitropropane were of Eastman Kodak spectroscopic grade. The methyl nitrite was prepared by a standard procedure described in the literature.²² The CH_3ONO was collected at -80° and was further purified by distillation. It was stored at -80° in order to prevent any decomposition. Tetranitromethane was obtained from K and K Laboratory, Inc., and was further purified by a method described by Bielski and Allen.²³

The samples were prepared as follows: flat "Supersill" quartz tubes (dimensions: 20-mm. height, 2.5-mm. width, and 0.5-mm. thickness) were filled with the aliphatic nitro compound, frozen in liquid nitrogen, and placed into optical dewars, in which they were photolyzed at 77°K . Photolysis was carried out using both a high pressure GE B-H6 mercury lamp and a low pressure mercury lamp.

All e.p.r. measurements were carried out on a Varian Model V 4500 e.p.r. spectrometer and the first derivative of the microwave absorption spectrum was recorded.

The g -values of the absorption lines were determined by the standard procedure of comparison with 1,1-diphenyl-2-picrylhydrazyl (DPPH) whose g -value is 2.0036.²⁴

Results

Nitromethane was photolyzed at 77°K . as a pure compound, in a water matrix and in a carbon tetrachloride matrix. The photolysis times were varied from 5 sec. to 10 min. While there was an increase in signal strength with increasing time of photolysis, no changes in number or positions of peaks in the e.p.r. spectra could be observed during this short time interval. However, when photolysis was carried out for longer time periods (over 30 min.) more complex e.p.r. spectra were obtained. The spectra observed did not in any way depend upon the matrix employed.

The e.p.r. spectrum of photolyzed nitromethane is given in Fig. 1, which represents a plot of the first derivative curve with the magnetic field strength increasing to the right. As can be seen, a rather complex structure is observed. Theoretically, one would expect only a triplet of lines for NO_2 and a quartet for the methyl radical. However, previous observations^{25,26} of the e.p.r. spectrum of nitrogen dioxide revealed that it can have as many as six lines. The exact reason for the existence of the additional triplet is not known. An explanation advanced by Sharpatyi

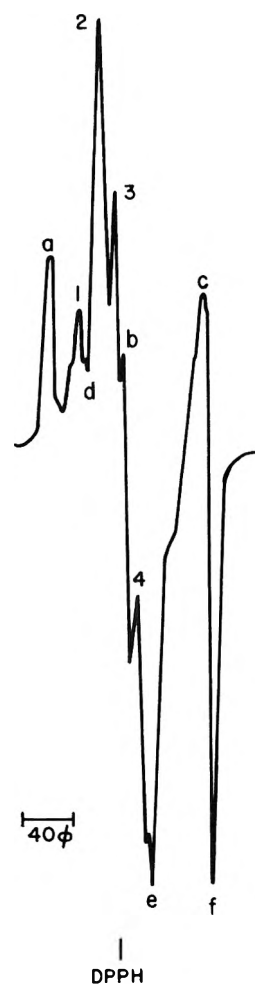


Figure 1. E.p.r. spectrum of nitrogen dioxide and the methyl radical produced during the photolysis of nitromethane at 77°K .

and Molin²⁵ is that perhaps different molecular structures of nitrogen dioxide were involved.

The spectrum of Fig. 1 was labeled as in Jen, *et al.*,²⁶ with a, b, and c referring to the main triplet of lines and d, e, and f to the other triplet. The average separation of the a-b-c triplet lines is 58 gauss. This agrees well with the reported value of 57.8 gauss.²⁵ The corresponding value for the d-e-f triplet is 46 gauss, which is also in close agreement with the value of 45 gauss estimated from the work of Jen, *et al.*²⁶

Removal of these six lines from the e.p.r. spectrum shown in Fig. 1 leaves only a quartet of lines. The

- (22) J. Slater, *J. Chem. Soc.*, 117, 590 (1920).
 (23) B. H. J. Bielski and A. O. Allen, to be published.
 (24) C. A. Hutchison, Jr., R. G. Pastor, and A. G. Kowalsky, *J. Chem. Phys.*, 20, 534 (1952).
 (25) V. A. Sharpatyi and K. N. Molin, *Russ. J. Phys. Chem.*, 35, 621 (1961).
 (26) C. K. Jen, S. N. Foner, E. L. Cochran, and V. A. Bowers, *Phys. Rev.*, 112, 1169 (1958).

total separation of these four lines is 65 gauss. This again is in close agreement with values reported in the literature for the methyl radical.^{26,27}

As a sensitive test of the validity of the above analysis, the sample was annealed at -80° for 1 hr. and the e.p.r. spectrum again recorded (Fig. 2). It then consisted solely of a triplet of lines of total separation about 116 gauss. This value of 116 gauss establishes that nitrogen dioxide molecules remain. The annealing broadened the lines, but this is to be expected from increased dipolar interaction between nitrogen dioxide molecules and from changes in crystalline anisotropy. The center line corresponds to a g -value of 2.0035 in reasonable agreement with the published value for nitrogen dioxide of 2.0037.²⁶

Because of the broad line width after annealing, it was impossible to resolve the spectrum into the two triplets mentioned previously. If Sharpatyi and Molin²⁵ are correct concerning the existence of more than one structural isomer of nitrogen dioxide at 77°K ., then, conceivably, annealing the sample at -80° has put all the nitrogen dioxide molecules into the same structural isomeric state. However, the agreement of total line separation and g -value with the reported values identifies this triplet as due to nitrogen dioxide.

A pure sample of methyl nitrite was photolyzed for periods up to 10 min. at 77°K . and the resulting spectrum is given in Fig. 3; unfortunately, it was impossible to obtain better resolution. The spectrum consists only of a poorly resolved quartet of lines but is clearly quite different from the photolyzed nitromethane spectrum shown in Fig. 1. It was observed that when the methyl nitrite sample was annealed at -80° for 10 sec., no e.p.r. absorption spectra could be observed. This can be interpreted as further evidence

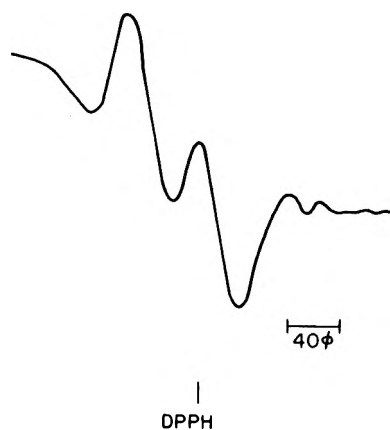


Figure 2. E.p.r. spectrum of nitrogen dioxide at 77°K . This spectrum was obtained after annealing the photolyzed nitromethane sample shown in Fig. 1 at -80° .

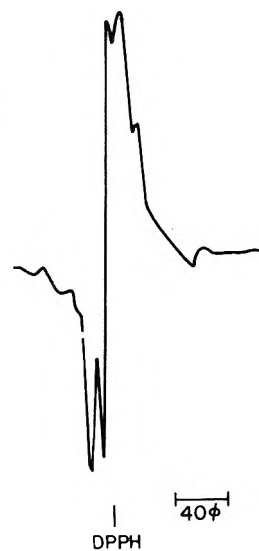


Figure 3. E.p.r. spectrum of photolyzed methyl nitrite at 77°K .

that photolysis of nitromethane and methyl nitrite proceeds by different mechanisms. The fact that no free radical signal was observed after such a short annealing period is also good evidence that no appreciable amounts of NO_2 were produced in the methyl nitrite photolysis.

Pure samples of nitroethane and nitropropane were photolyzed at 77°K . The spectra for these compounds were very complex. However, by annealing the samples at -80° it was possible to show that here too NO_2 had been produced during photolysis. The increased complexity of the e.p.r. spectra compared to the CH_3NO_2 case can be interpreted as arising from the presence of the increased number of protons of the ethyl and propyl radicals resulting in additional number of peaks.

Samples of tetranitromethane were photolyzed as a pure compound and also in H_2O and CH_3OH matrices. The same spectrum was obtained in each case and this spectrum is shown in Fig. 4. The spectrum is identical with the reported spectrum of nitrogen dioxide²⁵ and no additional peaks were observed. It was noticed that in a matrix of $\text{C}(\text{NO}_2)_4$ and in the water matrix a distinct pink color was visible after photolysis. In the methanol matrix a bright yellow color was obtained.

Discussion

The present work on the nitromethane photolysis confirms the previous postulates¹⁻³ that the primary step in the photolysis of this compound is dissociation into a methyl radical and nitrogen dioxide. Brown

(27) A. J. Tench, *J. Phys. Chem.*, **67**, 923 (1963).



Figure 4. E.p.r. spectrum of photolyzed tetranitromethane at 77°K.

and Pimentel⁵ do not report observing infrared bands attributable to nitrogen dioxide in their experiments; however, it is conceivable that the steady-state concentration of nitrogen dioxide is always very low and thus is detected only with the more sensitive e.p.r. measurements. Indeed, it was observed in the present investigation that the peak height of the e.p.r. spectrum of nitrogen dioxide soon reached a maximum and would then remain relatively constant during the short photolysis times employed. If samples were photolyzed for longer periods, then the spectra became more complex. This most probably resulted from reactions of oxygen atoms which, in turn, came from photolysis of NO₂.

No measurable change in coupling constant for the methyl radical could be observed in the different matrices employed. This is in agreement with the results of Jen, *et al.*²⁶ Also, as suggested by these workers, the relative constancy of this coupling constant allows for ready identification of the methyl radical by e.p.r. spectroscopy.

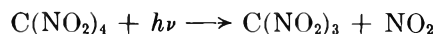
Of the several alternatives available in the case of the methyl nitrite, the e.p.r. results obtained in the present study tend to favor an initial split into a methoxy radical and nitric oxide. The methoxy radical might be expected to appear as a quartet of lines with relative peak heights in the ratio 1:3:3:1 caused by the presence of the three equivalent protons. However, if the odd electron is localized mainly on the oxygen atom, then only a broad singlet would be obtained. Gray and Williams²⁸ have suggested that such localization on the oxygen atoms does occur in alkoxy radicals.

Attempts to observe the e.p.r. spectrum of nitric oxide in a solid matrix have been unsuccessful even though at 77°K. the ²π_{3/2} paramagnetic state of NO is expected to have an appreciable population. Failure to observe resonance has been attributed to the crystalline anisotropy of the matrix field causing the resonance lines of the π state to be spread out too much for identification.²⁶

In the present investigation, a quartet of lines of total separation 43 gauss was obtained in the photolysis of methyl nitrite (Fig. 3). The only reported observation of the e.p.r. spectrum of the methoxy radical²⁵ was shown to have a total width of 45 gauss. Although the spectrum shown in Fig. 3, as well as the one reported in the literature, is not well resolved, it is suggested that this is the methoxy radical e.p.r. spectrum and it would appear that the odd electron is localized mainly on the oxygen atom. Thus the detection of the methoxy radical provides strong support for the work of Gray and Style⁸ and that of Hanst and Calvert.¹³

Because no detectable amount of NO₂ could be observed in the methyl nitrite photolysis confirms the results of Hanst and Calvert that C-O bond cleavage is not important in the methyl nitrite photolysis.

Photolysis of tetranitromethane shows clear evidence for nitrogen dioxide formation. Hence the primary step in the photolysis of this compound is suggested to be



No detectable signal could be obtained for the C(NO₂)₃ radical and this is rather puzzling. One possible explanation of this might be that there is a considerable interaction of this radical with the different matrices used. This might then account for the fact that samples of pure tetranitromethane and of tetranitromethane in water turned pink when photolyzed at 77°K.; however, tetranitromethane in methanol turned yellow.

The fact that a definite signal for NO₂ was observed in the photolysis of nitroethane confirms the suggestion of Rebbert and Slagg² that at least one of the primary steps in the decomposition of this molecule is



Photolysis of 1-nitropropane also yielded nitrogen dioxide and hence it is shown that the photolysis of all

(28) P. Gray and A. Williams, *Chem. Rev.*, **59**, 240 (1959).

(29) Sr. P. J. Sullivan and W. S. Koski, *J. Am. Chem. Soc.*, **84**, 1 (1962).

aliphatic nitro compounds used in this investigation results in the formation of nitrogen dioxide. It is reasonable, therefore, to expect that the primary step

in the photolysis of the more complex aliphatic nitro compounds will also involve carbon-nitrogen bond scission and the formation of NO_2 .

On the Sonochemical Formation of Hydrogen Peroxide in Water

by M. Anbar and I. Pecht

The Weizmann Institute of Science, Rehovoth, Israel (Received September 20, 1963)

The sonochemical formation of hydrogen peroxide was investigated in H_2O^{18} solutions containing $\text{H}_2\text{O}_2^{16,16}$. It was found that nonvolatile OH scavengers do not affect the production of H_2O_2 , in contrast to volatile organic solutes. It was concluded that H_2O_2 is not formed by recombination of OH radicals in solution. The sonochemical formation of H_2O_2 under oxygen was studied using H_2O^{18} and $\text{O}_2^{18,18}$. It was shown that H_2O_2 is formed by three parallel pathways: from the water, from oxygen atoms, and from oxygen molecules. Oxygen atoms formed on sonolysis were shown to form ozone to a limited extent.

Hydrogen peroxide is known to be formed in water undergoing sonolysis both under oxygen and under other gases.¹⁻⁴ The yield of hydrogen peroxide was shown to be dependent on solutes and on the composition of the gas over the solution. It was suggested that hydrogen peroxide is formed under argon by the recombination of OH radicals.^{1,2} The submission of water to the action of ultrasonics under oxygen produces additional pathways for the formation of H_2O_2 . These pathways have been investigated using oxygen-18 as tracer,² and it was claimed that two-thirds of the H_2O_2 produced originates from the oxygen gas and that the O-O bond is not cleaved during this reaction. On the other hand, it was claimed that ozone is formed sonochemically⁵ under similar conditions, which obviously implies the cleavage of the O-O bond. Thus, further isotope experiments were required to clarify this point.

The mechanism of formation of hydrogen peroxide was discussed by Weissler,³ who also concluded that H_2O_2 is formed under argon by the recombination of OH radicals. This conclusion was arrived at in view of the fact that acrylamide, formic acid, and allylthiourea, which are efficient OH scavengers, inhibit the formation

of H_2O_2 . It has been pointed out that the behavior of the sonolyzed systems, which are not completely homogenous, differs significantly from the same systems undergoing radiolysis.³ As all three scavengers examined by Weissler are volatile compounds, it remained an open question whether H_2O_2 is formed in the liquid or in the gas phase. It was suggested, therefore, to study the formation of H_2O_2 in the presence of non-volatile OH scavengers, *e.g.*, thallos and formate ions.

The sonochemical yield of H_2O_2 determined in all previous studies is the net result of the yield of formation and of the presumable decomposition of H_2O_2 . Applying a technique developed in radiation chemistry,⁶ dilute solutions of $\text{H}_2\text{O}_2^{16,16}$ in H_2O^{18} were subjected to

- (1) A. Henglein, *Naturwiss.*, **43**, 277 (1956); **44**, 179 (1957).
- (2) M. Del Duca, E. Yeager, M. O. Davis, and F. Hovorka, *J. Acoust. Soc. Am.*, **30**, 301 (1958).
- (3) A. Weissler, *J. Am. Chem. Soc.*, **81**, 1077 (1959).
- (4) M. Haissinsky, R. Klein, and P. Rivayrand, *J. Chim. Phys.*, **59**, 611 (1962).
- (5) M. Haissinsky and A. Mangeot, *Nuovo Cimento*, [10] **4**, 1086 (1954).
- (6) M. Anbar, S. Guttman, and G. Stein, *J. Chem. Phys.*, **30**, 703 (1961).

ultrasonics. Thus, it was possible to obtain the net yield of formation of hydrogen peroxide.

Experimental

Materials. O^{18} -enriched water between 92 and 97 atom % O^{18} was obtained from the isotope distillation plant of the Weizmann Institute. Oxygen-18 gas 97 atom % was prepared by electrolysis, followed by enrichment by thermal diffusion. The oxygen-enriched water contained practically 100 atom % deuterium and was thus nearly pure D_2O^{18} . It has been shown that the sonolytic decomposition of water does not involve any deuterium isotope effect.⁷ In order to simplify formulas, we shall refer to this water as H_2O^{18} .

The H_2O_2 was BDH microanalytical reagent 100 volumes solution. All the water used was triple-distilled. The methanol, Tl_2SO_4 , and $NiSO_4$ were BDH Analar and the sodium formate and K_2SO_4 were Baker analyzed reagents. The gases used were of the highest purity available (Matheson Co. Ltd.).

Ultrasonic Irradiation. The ultrasonic generator was a Model T 200 (Lehfeldt and Co. GMBH) with a water-cooled quartz transducer operating at 800 kc. A special concentrator was adapted to focus the ultrasonic energy to a limited volume. The irradiation vessel was thermostated by circulating water at $20 \pm 1^\circ$. The irradiation vessel used in all experiments was a small Pyrex bulb (volume 7 ml.) connected to an inlet tube. The Pyrex bulb was of minimal thickness in order to reduce sonic absorption. The bulb was fitted at a constant position in the focus of the ultrasonic concentrator. The energy input was 1.6×10^9 ergs/sec./cm.² in all the experiments. The yield of H_2O_2 , under argon, under these conditions was 4.2×10^{-6} mole/l./min.

Analysis. The procedure adopted was identical with that used in a previous study.⁶ After sonolysis, an aliquot of the solution was decomposed over platinum black in a vacuum system. The formate-containing H_2O_2 solutions were decomposed by ceric ions, as the formate or its decomposition products inhibited the catalytic action of platinum black. The O_2 evolved in this procedure originates only from the H_2O_2 and no oxygen exchange between differently labeled H_2O_2 molecules takes place during the decomposition.⁸ The oxygen was collected and its isotopic composition was determined by mass spectrometry.

The mass spectrometric analysis was carried out with a CEC Model 21-401 mass spectrometer. The isotopic abundance was determined by scanning masses 28 to 40. Masses 28 (N_2) and 40 (Ar) were determined to check on the air and argon contamination. Obviously, air causes dilution of the isotopic composition of oxy-

gen, whereas argon introduces an error in the determination of mass 36 ($O_2^{18,18} = Ar^{36}$).

In all experiments H_2O_2 of normal isotopic composition was used. Oxygen which originated from the initial H_2O_2 contained consequently 0.4% $O^{16}O^{18}$ and virtually no $O^{18}O^{18}$. The H_2O^{18} used contained 3 to 8 atom % O^{16} and consequently the H_2O_2 which originated from water contained 6 to 16% $H_2O_2^{16,18}$. Allowance for these dilution factors was made in all calculations.⁶

In the remainder of the sonolyzed solution, the H_2O_2 concentration was determined spectrophotometrically by either the titanate sulfate⁹ or the triiodide¹⁰ methods.

Results and Discussion

The yield of hydrogen peroxide $H_2O_2^{18,18}$ formed under argon in the presence of different additives is given in Table I. It has been found that $H_2O_2^{18,18}$ is formed under our conditions at a yield of 4.9 μ moles/l./min., which is independent of the total energy absorbed and of the concentration of H_2O_2 , within the measured range. Under the same conditions, the yield of H_2O_2 was determined by nonisotopic methods, in the absence of initial H_2O_2 in solution, and was found to be 4.2 μ moles/l./min.; this means that about 0.7 μ mole/l./min. of H_2O_2 are destroyed under the given conditions, irrespective of its concentration.

The addition of $7.5 \times 10^{-2} M$ $NiSO_4$ to the sonolyzed solution did not affect the yield of $H_2O_2^{18,18}$. Nickel ions were shown to interact with electrons¹¹ and with excited water molecules in solution.¹² The absence of any effect of nickel ions on the yield of $H_2O_2^{16,18}$ implies that the latter species is not a precursor of $H_2O_2^{18,18}$ in solution.

Thallos ions were found to decrease the yield of $H_2O_2^{18,18}$ to a certain extent and this effect might be attributed to their fast reaction with OH radicals.¹³ When, however, the effect of thallos ions is compared with that of potassium ions, it is found that the latter have even a more conspicuous effect on the yield of $H_2O_2^{18,18}$. It has to be concluded, therefore, that the effect of thallos ions is analogous to that of potassium ions and is due to a change in water structure, which affects the cavitation process.^{5,14}

(7) M. Anbar and I. Pecht, *J. Chem. Phys.*, in press.

(8) M. Anbar, *J. Am. Chem. Soc.*, **83**, 2031 (1961).

(9) P. Bonnet-Maury, *Compt. rend.*, **218**, 117 (1944); A. Weissler, *Ind. Eng. Chem., Anal. Ed.*, **17**, 695 (1954).

(10) A. O. Allen, C. J. Hochanadel, J. A. Ghorriley, and T. W. Davies, *J. Phys. Chem.*, **56**, 575 (1952).

(11) J. H. Baxendale and R. S. Dixon, *Proc. Chem. Soc.*, 148 (1963).

(12) M. Anbar and D. Meyerstein, Israel AEC Report IA-901 (1963).

(13) T. J. Sworsky, *Radiation Res.*, **4**, 483 (1956).

If $\text{H}_2\text{O}_2^{18,18}$ would be formed by recombination of OH radicals in the bulk of the solution, one would expect that the yield of $\text{H}_2\text{O}_2^{18,18}$ would strongly depend on the presence of $\text{H}_2\text{O}_2^{16,16}$. In other words, the yield of H_2O_2 would be expected, like under radiolytic conditions,⁶ to fall *below* the yield of H_2O_2 in the absence of initial hydrogen peroxide. Further, $5 \times 10^{-2} M \text{Ti}^+$ should bring it down to zero.

The experiments with formate ions show that these do hardly affect the yield of H_2O_2 even at 0.5 M formate. When formate-containing solutions were irradiated for long periods, the yield of $\text{H}_2\text{O}_2^{18,18}$ was found to diminish. This is most probably due to the effect of carbon monoxide formed from formate¹⁵ on the production of H_2O_2 .¹⁶

The experiments with thallos ions and with formate ions, both of which are efficient OH scavengers, point to the fact that if H_2O_2 is formed by recombination of OH radicals, these are not accessible by scavengers in solution. On the other hand, Weissler has shown that the precursors of H_2O_2 are *completely* scavengable by formic acid, acrylamide, and allylthiourea, all of which are efficient scavengers of OH radicals. The only difference is that these reagents are volatile, in contrast to formate and thallos ions. Our experiments with methanol, which is a relatively poor scavenger for OH radicals, as compared with acrylamide,¹⁷ show that the formation of H_2O_2 may be abolished completely in the presence of any organic volatile compound. The last results are in accord with previous findings on the effect of volatile organic solutes on the sonochemical formation of H_2O_2 .¹⁸ In other words, if H_2O_2 is formed by the recombination of OH radicals, this does not take place in the liquid phase.

The effect of oxygen at small concentrations (2.5%) on the yield of $\text{H}_2\text{O}_2^{18,18}$ corroborates the conclusion that hydrogen peroxide is produced in the cavitation and not in the liquid phase. Moreover, as there is no plausible reaction between oxygen and OH radicals, the latter are unlikely to be the species scavenged by O_2 . It seems reasonable to suggest excited water molecules as plausible precursors of H_2O_2 in the gas phase. These were previously suggested as the precursors of the "molecular" H_2O_2 under radiolysis⁶ and were shown to react both with oxygen and with organic solutes.¹² The formation of excited water molecules in cavitation is not surprising in view of the transient high temperatures involved.^{7,16}

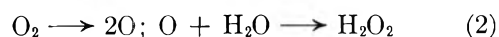
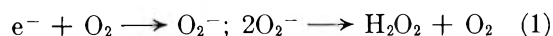
From the previous results, it is concluded that the yield of $\text{H}_2\text{O}_2^{18,18}$ formed from water is considerably diminished under oxygen. On the other hand, it has been shown that the yield of H_2O_2 under oxygen is a little higher than that under argon.³ This would

Table I: The Sonochemical Formation of $\text{H}_2\text{O}_2^{18,18}$ in H_2O^{18} under Argon in the Presence of $\text{H}_2\text{O}_2^{16,16}$

Duration of sonolysis, min.	$[\text{H}_2\text{O}_2]$, moles/l. $\times 10^3$	Additive	$[\text{Additive}]$, moles/l. $\times 10^2$	$\text{H}_2\text{O}_2^{18,18}$ formed, ^a moles/l./min. $\times 10^5$
20	2.5	4.95
60	2.5	4.95
80	6.3	5.05
120	2.7	4.75
60	2.3	NiSO_4	7.5	5.00
85	2.0	Ti_2SO_4	1.0	4.80
30	2.3	Ti_2SO_4	2.0	4.50
90	1.9	Ti_2SO_4	2.0	4.00
100	1.9	Ti_2SO_4	5.0	3.70
93	1.9	Ti_2SO_4	15.0	3.30
100	2.5	K_2SO_4	2.0	3.90
90	2.5	K_2SO_4	15.0	2.90
85	2.5	HCOONa	5.0	3.80
85	2.5	HCOONa	20.0	2.50
10	2.3	HCOONa	50.0	4.50
100	2.3	MeOH	10.0	0.58
100	2.3	MeOH	50.0	0.06
81	2.3	O_2	2.5%	3.60

^a Normalized to 100% O^{18} .

imply the formation of hydrogen peroxide from the oxygen by different mechanisms. There are two mechanisms for the formation of H_2O_2 from O_2 , which may be distinguished by isotopic tracer experiments.



In the first case, the hydrogen peroxide formed will have the isotopic composition of the oxygen without any cleavage of the O-O bond, whereas in the second, the hydrogen peroxide formed should have a mixed isotopic composition. Del Duca, *et al.*,² have attempted to investigate this problem; however, owing to the unavailability of highly enriched oxygen-18 their results are of low significance. Consequently, we have repeated them using oxygen and water 96-97% in O^{18} . The results are given in Table II.

It has been found (Table II) that under 1 atm. of $\text{O}_2^{16,16}$ over H_2O^{18} the yield of $\text{H}_2\text{O}_2^{18,18}$ drops to 1.15 $\mu\text{moles/l./min.}$ At the same time $\text{H}_2\text{O}_2^{16,16}$ of mixed isotopic origin is formed at a yield of 1.25 $\mu\text{moles/l./min.}$

(14) M. Anbar and I. Pecht, to be published.

(15) A. Weissler, *J. Acoust. Soc. Am.*, **32**, 1082 (1960).

(16) M. E. Fitzgerald, V. Griffing, and J. Sullivan, *J. Chem. Phys.*, **25**, 926 (1955).

(17) C. Ferradini, *Advan. Inorg. Chem. Radiochem.*, **3**, 171 (1961).

(18) A. Henglein and R. Schulz, *Z. Naturforsch.*, **8B**, 277 (1953).

Table II: The Sonochemical Formation of H_2O_2 under Oxygen in the Presence of $\text{H}_2\text{O}_2^{16,16}$

Oxygen, atom % O^{18}	H_2O , atom % O^{18}	$\text{H}_2\text{O}_2^{16,18}$ formed, ^a moles/l./min. $\times 10^6$	$\text{H}_2\text{O}_2^{18,18}$ formed, ^b moles/l./min. $\times 10^6$
0.2	96.2	1.25	1.15
97.0	0.2	1.3	3.3

^a Corrected for $\text{H}_2(\text{O})_2^{16,18}$ from $\text{H}_2\text{O}_2^{16,16}$ (0.2 atom %), for $\text{H}_2\text{O}_2^{16,18}$ originating from $\text{H}_2\text{O}_2^{18,18}$ (3-4 atom %) and $\text{H}_2\text{O}_2^{17,17}$ (accompanying the $\text{H}_2\text{O}_2^{18,18}$). ^b Normalized to 100% O^{18} .

On the other hand, under 1 atm. of $\text{O}_2^{18,18}$ over H_2O^{16} , the yield of $\text{H}_2\text{O}_2^{18,18}$ originating from $\text{O}_2^{18,18}$ reaches 3.3 $\mu\text{moles/l./min.}$, whereas the $\text{H}_2\text{O}_2^{16,18}$ of mixed isotopic origin amounts to 1.3 $\mu\text{moles/l./min.}$ It may be concluded, therefore, that under oxygen, hydrogen peroxide is produced by three different mechanisms, including both pathways suggested above. At an O_2 pressure of 1 atm., the relative yields of the three pathways are $(\text{H}_2\text{O}):(\text{O}_2):(\text{O}) = 1:3:1.2$. The proportions are expected to change with the partial pressure of oxygen. The over-all yield of H_2O_2 under oxygen, 5.8 $\mu\text{moles/l./min.}$, is about 20% higher than the yield under argon, in accord with previous results.³

The formation of H_2O_2 of mixed isotopic origin suggests the existence of oxygen atoms under cavitation conditions. If oxygen atoms are formed, they may either react with oxygen to form ozone⁵ or with water to form H_2O_2 . If ozone is formed, it will induce isotopic exchange between different oxygen molecules by a chain reaction.¹⁹ We have checked on this possibility by sonolyzing a gas mixture of $\text{O}_2^{16,16}$ and $\text{O}_2^{18,18}$ over water and determined the yield of $\text{O}_2^{16,18}$ produced. $\text{O}_2^{16,18}$ was produced in this reaction, which was carried out under conditions identical with the previous experiments, with a yield of 6.5 $\mu\text{moles/l./min.}$, which is comparable to the yield of H_2O_2 . This low yield of isotopic "scrambling" does not allow the existence of appreciable amounts of ozone in the sonochemical process. Furthermore, it may be concluded that the rate of reaction of oxygen atoms with water is rather fast and competes effectively with the $\text{O} + \text{O}_2$ reaction. This result is in accord with former findings that water acts as an inhibitor for radiolytically induced $\text{O}_2^{16,16}$ - $\text{O}_2^{18,18}$ isotopic exchange.⁶

Acknowledgment. The authors wish to thank Mrs. V. Fischeff and Mrs. O. Asher for their devoted help in the mass spectrometric analysis.

(19) R. A. Ogg, Jr., and W. T. Stuppen, *Discussions Faraday Soc.*, 17, 47 (1954).

Solvolysis of the Tetrachloronickelate(II) Anion

by Charles P. Nash and Myrna S. Jenkins

Department of Chemistry, University of California, Davis, California (Received September 23, 1963)

Thermodynamic data have been obtained for the replacement of one chloride on the tetrachloronickelate(II) anion by either acetonitrile or dimethylacetamide. The entropy change makes a major contribution to the free energy of solvolysis in both solvents. It is suggested that the inability of the solvents to solvate chloride ion is a major factor in determining the position of the octahedral-tetrahedral equilibrium of the nickel ion in these media. Theoretical calculations which use the Born equation to determine the electrostatic entropy of solution of the anions yield entropy changes for the two solvolysis reactions which are in good agreement with experiment.

Introduction

In recent years there has accumulated overwhelming evidence for the existence of tetrahedral complexes of nickel(II)¹ containing from two to four halide ions and from zero to two other ligands such as triphenylphosphine,^{2,3} triphenylphosphine oxide,⁴ and triphenylarsine oxide.⁵ Many of these complexes can be obtained in the crystalline state,^{6,7} and tetrahedral anions can also exist in solution in dipolar aprotic solvents such as acetonitrile,^{7,8} nitromethane,^{7,8} dimethylformamide,^{7,9,10} and dimethylacetamide.¹⁰

In a recent paper, Goodgame, Goodgame, and Cotton⁸ suggest that the NiCl_4^{-2} ion undergoes solvolysis in acetonitrile (An) to form NiCl_3An^- , also tetrahedral. Since no quantitative information yet exists regarding the thermodynamics of formation of any of the tetrahedral nickel species, we have chosen to study the solvolysis of tetrachloronickelate(II) by acetonitrile and dimethylacetamide (DMA) using spectrophotometric methods. We have also attempted, unsuccessfully, to obtain thermodynamic data for the octahedral-tetrahedral transformation of the nickelous ion in acetonitrile. Our qualitative observations, however, suggest that this process is endothermic, in agreement with the observations of Furlani and Morpurgo.⁷ These workers have demonstrated a substantial increase in the amount of tetrahedral nickel species present in ethanol and dimethylformamide solutions containing halide as the temperature was increased to *ca.* 100°.

Experimental

Materials. Spectro grade acetonitrile (Matheson Coleman and Bell) was shaken for a prolonged period with magnesium sulfate which had previously been oven dried at 400° for 18 hr. Dimethylacetamide and dimethylformamide (Eastman White Label) were redistilled and treated in a like manner. The gas chromatograms of all three solvents showed only a single peak.

Reagent grade nickel perchlorate hexahydrate (G. Fredrick Smith) was recrystallized from triply distilled water and vacuum dried. A nickel analysis by standard methods¹¹ showed the material to be hexahydrated. Nickelous chloride dihydrate was prepared by controlled dehydration of the hexahydrate (Baker and Adamson Special Reagent grade). Its composition was confirmed by chloride analysis.

- (1) N. S. Gill and R. S. Nyholm, *J. Chem. Soc.*, 3997 (1959).
- (2) L. M. Venanzi, *ibid.*, 719 (1958).
- (3) F. A. Cotton, O. D. Faut, and D. M. L. Goodgame, *J. Am. Chem. Soc.*, **83**, 344 (1961).
- (4) F. A. Cotton and D. M. L. Goodgame, *ibid.*, **82**, 5771 (1960).
- (5) D. M. L. Goodgame and F. A. Cotton, *ibid.*, **82**, 5774 (1960).
- (6) D. M. Gruen and R. L. McBeth, *J. Phys. Chem.*, **63**, 393 (1959).
- (7) C. Furlani and G. Morpurgo, *Z. physik. Chem.*, **28**, 93 (1961).
- (8) D. M. L. Goodgame, M. Goodgame, and F. A. Cotton, *J. Am. Chem. Soc.*, **83**, 4161 (1961).
- (9) L. I. Katzin, *J. Chem. Phys.*, **36**, 3034 (1962).
- (10) S. Buffagni and T. M. Dunn, *Nature*, **188**, 937 (1960).
- (11) I. M. Kolthoff and V. A. Stenger, "Volumetric Analysis," Vol. II, Interscience Publishers, Inc., New York, N. Y., 1947, p. 283.

Tetraethylammonium chloride was prepared from the iodide by refluxing it with a 1.5-fold excess of silver chloride, filtering, and evaporating the filtrate to dryness. The crude product was repeatedly recrystallized from a mixture of acetonitrile and acetone and vacuum dried at 60°. Tetraethylammonium perchlorate was prepared by mixing a concentrated aqueous solution of tetraethylammonium chloride with a saturated solution of sodium perchlorate. The crude product was recrystallized from water and vacuum dried at 60°. Qualitative tests showed no evidence of either sodium or halide ions.

Tetraethylammonium tetrachloronickelate(II) was precipitated by adding ether to a dimethylacetamide solution which initially contained $4 \times 10^{-2} M$ nickel chloride dihydrate and $8 \times 10^{-2} M$ tetraethylammonium chloride. The identity of the vacuum-dried product was confirmed both by its absorption spectrum in 0.01 *F* solution in acetonitrile⁸ and by a chloride analysis.

Physical Measurements. All spectra were obtained with a Cary Model 14 recording spectrophotometer using matched sets of 0.1, 1.0, 2.0, and 10.0-cm. glass-stoppered silica absorption cells. Temperature control ($\pm 0.2^\circ$) was obtained by circulating thermostated water. Temperature measurements were made with a copper-constantan thermocouple whose junction projected into the air chamber on the "sample" side of the cell compartment of the spectrophotometer. Solubilities were determined by stripping the solvent from weighed portions of saturated solutions which had been prepared by agitating solid-solvent mixtures for 2-5 days in a constant temperature bath.

Results

Solvolysis Reactions. The spectrum which we observe for a 0.01 *F* solution of tetraethylammonium tetrachloronickelate(II) in acetonitrile is in excellent agreement with that reported previously by Goodgame, *et al.*⁸ Two absorption maxima of equal intensity (ϵ 160) appear at 657.5 and 702.5 $m\mu$ with a shoulder at about 620 $m\mu$. A very different spectrum is observed in a $4 \times 10^{-4} F$ solution. Only a single absorption maximum appears at 615 $m\mu$ (ϵ 150), there is a shoulder *ca.* 572 $m\mu$, and the region where the previous maxima occurred displays only a tapering general absorption having $\epsilon \sim 90$. When a $4 \times 10^{-2} F$ solution is subjected to 10-, 20-, and 100-fold dilutions and the spectra are recorded in correspondingly lengthened cells, the four spectra exhibit an isobestic point at 628 $m\mu$. A typical set of spectra is reproduced in Fig. 1.

The spectrum of a saturated solution ($M \approx 2 \times$

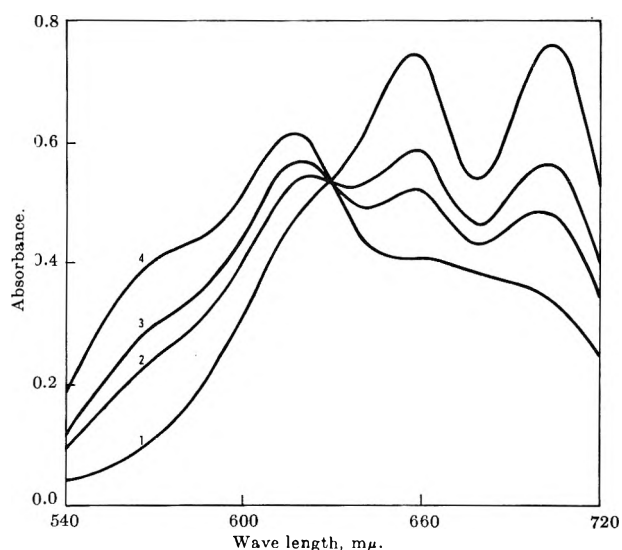


Figure 1. Concentration dependence of the spectrum of tetrachloronickelate(II) in acetonitrile: curve 1, $4 \times 10^{-2} M$ solution in 0.1-cm. cell; curve 2, $4 \times 10^{-3} M$ solution in 1.0-cm. cell; curve 3, $2 \times 10^{-3} M$ solution in 2.0-cm. cell; curve 4, $4 \times 10^{-4} M$ solution in 10.0-cm. cell.

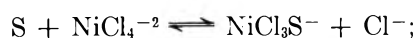
10^{-2}) of tetraethylammonium tetrachloronickelate in dimethylacetamide indicates that virtually all the nickel is present in this system as the solvolyzed tetrahedral species, since upon a 60-fold dilution Beer's law is obeyed to better than 2%. This spectrum is characterized by a single maximum (ϵ 155) at 627.5 $m\mu$, a shoulder *ca.* 586 $m\mu$, and a flat absorption ($\epsilon \sim 100-105$) extending from 655 to 700 $m\mu$. The qualitative similarity between this spectrum and the one observed in very dilute acetonitrile solution is unmistakable. In contrast to the report of Buffagni and Dunn¹⁰ we find little evidence for a reversion to octahedral coordination in dilute solution in dimethylacetamide.

When a $4 \times 10^{-3} F$ solution of the tetrachloronickelate salt in DMA is diluted with stock solutions of tetraethylammonium chloride at initial concentration levels $3-5 \times 10^{-2} M$, again with appropriate variations in the optical path, a family of spectra is obtained which display an isobestic point at 631 $m\mu$ and the two long wave length maxima characteristic of $NiCl_4^{-2}$ are developed.

If it is assumed that only two interconverting species are present in each of our solvent systems, it is a simple matter to use the appropriate form of Beer's law to obtain an equilibrium constant for the reactions. The extinction coefficients of the three nickel-containing anions at the wave lengths chosen may be obtained by on the one hand using a 20-fold excess of chloride ion to produce "entirely" $NiCl_4^{-2}$, and on the other

working at such high dilution that Beer's law is obeyed by the solvolyzed species. At 658 $m\mu$ we obtain a value for the extinction coefficient of NiCl_4^{-2} of 200 in each solvent (lit.⁸ 196). The solvolyzed species containing acetonitrile has extinction coefficient 90 and the dimethylacetamide analog has extinction coefficient 105 at this same wave length. At 705 $m\mu$ we find the extinction coefficient of NiCl_4^{-2} to be 206 (lit.⁸ 202) while the solvolyzed ions have extinction coefficients 77 and 100 in the same order as before.

In Table I we summarize the (dimensionless) equilibrium constants and thermodynamic data for the solvolysis reactions written in the sense



$$K = \frac{(\text{NiCl}_3\text{S}^-)(\text{Cl}^-)}{(\text{NiCl}_4^{-2})(\text{S})} \quad (1)$$

Solvent molarities were computed for acetonitrile from data in standard sources,¹² and for dimethylacetamide from the 25° value given by Lester, Gover, and Sears¹³ together with a coefficient of thermal expansion estimated from the absorption spectrum of the solvolyzed anion at 25 and 68° (10% expansion over this range). Activity coefficients have been omitted.

Table I: Summary of Thermodynamic Data for Solvolysis of NiCl_4^{-2}

Solvent	$K_{25} \times 10^4$	$K_{68} \times 10^4$	ΔF° , kcal. mole ⁻¹	ΔH° , kcal. mole ⁻¹	ΔS° , e.u.
Dimethyl- acetamide	28 ± 2	32 ± 3	3.5	0.6	-9.7
Acetonitrile	1.0 ± 0.1	2.4 ± 0.3	5.5	3.8	-5.7

Octahedral Chloride Complexes. An attempt was made to study the equilibrium corresponding to the addition of one chloride ion to octahedral nickelous ion in acetonitrile, but the results were less than satisfactory. There is little doubt that at least one chloride coordinates, since additions of up to one mole of chloride ion per mole of nickel produce a color change from pale violet to light green. It is even possible to obtain a rough value of a dimensionless equilibrium constant $K \approx 4 \times 10^{-5}$ for the process of removing the chloride ion at room temperature. Unfortunately, no really convincing isosbestic point is obtained, and the "near miss" shifts by almost 20 $m\mu$ when the system is heated to 68°. The difficulty probably arises because the presence of six water molecules per nickel ion leads to the formation of mixed solvates in the "pure" perchlorate starting solution. In fact, Popov and Geske¹⁴

have reported that there are two distinct waves in the polarogram of hydrated nickel perchlorate in acetonitrile solution.

Because it is impossible to define the starting species it is meaningless to attempt to evaluate ΔH for the octahedral-tetrahedral conversion. Qualitative experiments leave little doubt, however, that this conversion is endothermic. When an acetonitrile solution containing 2-2.5 moles of chloride per mole of nickel is heated to boiling, a decided bluish tint indicative of (probably) NiCl_3An^- develops. These results are qualitatively similar to those found in the ethanol and dimethylformamide solvent systems by Furlani and Morpurgo.⁷

Effect of Water Addition. It has been suggested by Gill and Nyholm¹ that the formation of tetrahedral halo complexes of nickel does not occur in aqueous solution because of the very high heat of hydration of the chloride ion, which must be supplied at least three times over in order to get to a tetrahedral product. To verify this conjecture we have studied the effect of additions of water to the present nonaqueous solutions.

When water is added to a $4 \times 10^{-3} M$ solution of the solvolyzed trichloronickelate anion in dimethylacetamide, about 10% of the color intensity is lost up to a water content of 0.5 M . Subsequent additions of water produce a more efficient bleaching characterized by a linear plot of absorbance *vs.* water content having a slope such that 15% of the original intensity still remains when the water molarity is 2.8. The successive spectra show no evidence for any alteration in the nature of the absorbing species; there is simply less of it. At the 2.8 M level the nature of the solvent has been changed rather drastically, as it now contains about 10 mole % water. Our results are in general agreement with the behavior found by Pflaum and Popov¹⁵ for solutions of cobaltous chloride in dimethylformamide. After an initial addition which produced only a small effect, the absorbance declined linearly with the water content, and at roughly the same rate which we observe in the trichloronickelate-dimethylacetamide system.

When a $4 \times 10^{-3} F$ solution containing both NiCl_4^{-2} and NiCl_3An^- in acetonitrile is treated with water, the first 0.5 M portion decreases the average absorb-

(12) "International Critical Tables," Vol. III, McGraw-Hill Book Co., Inc., New York, N. Y., 1928, p. 28.

(13) G. R. Lester, T. A. Gover, and P. G. Sears, *J. Phys. Chem.*, **60**, 1076 (1956).

(14) A. I. Popov and D. H. Geske, *J. Am. Chem. Soc.*, **79**, 2074 (1957).

(15) R. T. Pflaum and A. I. Popov, *Anal. Chim. Acta*, **13**, 165 (1955).

ance by about 30% and alters the spectrum by intensifying the short wave length maximum characteristic of a solvolyzed species. A water addition which should yield a 1 *M* solution causes instead a total bleaching of the blue color and the formation of a second (aqueous) liquid phase into which virtually all the nickel ion has been extracted. Other experiments show that a very concentrated aqueous solution of nickel chloride is immiscible with acetonitrile whereas a concentrated solution of nickel nitrate or nickel perchlorate, even one which is saturated with tetraethylammonium perchlorate, is completely miscible with acetonitrile. Evidently acetonitrile will go to great lengths to rid itself of chloride ion.

Discussion

The discussion of these experimental results segregates naturally into two more or less distinct aspects. First we discuss the conclusions which may be drawn regarding the stability of the tetrahedral structure for the nickel ion. We then show that the entropy changes we find for the solvolysis reactions can be accounted for in a very satisfactory way by using conventional statistical mechanical methods.

The Stability of NiCl₄⁻². The thermodynamic quantities in Table I demonstrate quite clearly that the entropy change plays an important part in the formation of NiCl₄⁻² from its solvolyzed tetrahedral precursor. It is virtually the governing quantity in dimethylacetamide and makes a significant contribution in acetonitrile. To the extent that the enthalpy changes in Table I reflect the differences in the strengths of the Ni-Cl and Ni-solvent bonds, the relative magnitudes are consistent with the relative stabilities of solid coordination complexes containing these two organic molecules as ligands. Whereas transition metal complexes containing dimethylacetamide may be prepared simply by ether precipitation from a solution of the corresponding salt in the amide,¹⁶ an elaborate procedure devised by Hathaway and Underhill^{17,18} seems to be required to isolate acetonitrile-containing solids.

The entropy change must also play the dominant role in forcing the octahedral-tetrahedral equilibrium far to the right side in our two solvents. We have found that the enthalpy change for this conversion is positive, while the free energy change is so negative that no evidence for octahedral coordination is found in these systems when Cl⁻/Ni⁺² ≥ 4. On the basis of the enthalpy change recorded in Table I for the dimethylacetamide system, we must question the generality of a recent conclusion of Katzin.^{9,19} He has proposed that the great stability of tetrahedral anions in dipolar aprotic solvents arises largely because the bind-

ing energy of the ligands is much greater in a tetrahedral configuration. Our results show that from an enthalpy standpoint there is virtually nothing to differentiate dimethylacetamide from the fourth chloride. Provided that rather small enthalpy changes also attend replacement of the lower-lying chloride ions, so that there is nothing particularly special about the last one, it follows from Katzin's argument that a large fraction of the nickel ions in dimethylacetamide solution, even in the presence of an "indifferent" anion such as perchlorate, should be tetrahedrally coordinated. No experimental evidence to support this conclusion has yet been reported.

Our results suggest that the most important aspect governing the stability of tetrahedral nickel in solution is the incompatibility of the solvent with chloride ions. Prue and Sherrington²⁰ have analyzed conductance data obtained in several dipolar aprotic solvents, including the dialkylated amides, and conclude that anions are not solvated in these media. Furthermore, the recent experiments of Bull, *et al.*,¹⁶ indicate that water coordinates to transition metal ions more strongly than does dimethylacetamide, and yet an enormous excess of water is required to destroy the tetrahedral configuration of the nickel ion in this solvent. Moreover, the linear decline in the concentration of tetrahedral nickel with increasing water content is not consistent with a mass-action expression as complex as one would envision to describe the reversion to octahedral geometry. This behavior is, however, consistent with the supposition that the primary role of water is to provide a favorable environment for free halide ion.

Our proposal that the chemical potential of the chloride ion is a major factor in determining the position of the octahedral-tetrahedral equilibrium of nickel also explains the behavior of 1:4 nickel-chloride mixtures in dimethylformamide. It has been well established that in this solvent a significant fraction of the nickel ion (~40%) is octahedrally coordinated,^{7,9,10} in contrast to the behavior we find in dimethylacetamide. Since dimethylacetamide is the stronger base²¹ and forms the more stable complexes with iodine²² and

(16) W. E. Bull, S. K. Madan, and J. E. Willis, *Inorg. Chem.*, **2**, 303 (1963).

(17) B. J. Hathaway and A. E. Underhill, *J. Chem. Soc.*, 3091 (1961).

(18) B. J. Hathaway, D. G. Holah, and A. E. Underhill, *ibid.*, 2444 (1962).

(19) L. I. Katzin, *J. Chem. Phys.*, **35**, 467 (1961).

(20) J. E. Prue and P. J. Sherrington, *Trans. Faraday Soc.*, **57**, 1795 (1961).

(21) T. Higuchi, C. H. Barnstein, H. Ghassemi, and W. E. Perez, *Anal. Chem.*, **34**, 400 (1962).

phenol,²³ it is *a priori* probable that the higher fraction of octahedral coordination should occur in dimethylacetamide. Solubility measurements, however, indicate that the chloride ion is significantly more stable in dimethylformamide than in dimethylacetamide. We find that at 25° the ratio of the saturation mole fractions of tetraethylammonium chloride to tetraethylammonium perchlorate is 0.27 in dimethylacetamide and 1.15 in dimethylformamide, while the absolute solubility of the perchlorate is higher in dimethylformamide by a factor of 1.55. Evidently the formamide is a somewhat better solvent than the acetamide for ions in general, but is more than four times better in the case of the compact chloride ion. If all other factors are approximately equal, it follows on the basis of our proposal that the higher degree of octahedral coordination should be found in the solvent which most effectively retains chloride ions. These are just exactly the experimental facts.

Entropies of Solvolysis. The relative magnitudes of the entropy changes for the two solvolysis reactions seem, at first sight, rather too close together when one considers that the absolute entropy of gaseous acetonitrile is 58.0 e.u.,²⁴ while that of gaseous dimethylacetamide may be estimated as 80–85 e.u.²⁵ Because the anionic species which enter into eq. 1 are presumably not solvated, this having been demonstrated experimentally for the chloride ion,²⁰ the present solvolysis reactions seem to afford a reasonable chance for a theoretical calculation of the entropy changes to succeed.

Throughout the calculations we shall ignore any vibrational contributions to the entropy change. This is equivalent to an assumption that the sum of the vibrational entropies of the solvent molecule and the tetrachloronickelate anion is the same as the vibrational entropy of the solvolyzed product. The error contributed by this assumption is impossible to assess.

The entropy terms which remain to be evaluated are the translational contribution, the rotational contribution, the contribution of internal rotation in the solvolyzed anions, and the electrostatic entropy of solution. The translational contribution to the value of ΔS is easily determined from the Sakur–Tetrode equation to be -1.95 e.u. in DMA and -0.15 e.u. in An.

The rotational entropy of dimethylacetamide may be calculated by assuming that all atoms save hydrogen lie in a plane with bond distances and bond angles as given by Pauling.²⁶ In the methyl groups we assume tetrahedral geometry with one hydrogen lying directly above the prolongation of the appropriate C–C or C–N bond, and a C–H bond length of 1.09 Å. Moments of inertia and products of inertia about an

arbitrary set of orthogonal axes through the center of mass²⁷ were used to compute the rotational entropy of DMA as 28.8 e.u. at 298°K.

The rotational entropy of acetonitrile at 298°K. has been given by Gunthard and Kovats²⁴ as 18.53 e.u., including the contribution arising from the C_{3v} symmetry of the molecule.

We assume a regular tetrahedral structure for the tetrachloronickelate ion with a Ni–Cl bond length of 2.24 Å. This value is midway between the values 2.26 and 2.22 Å. found for the Co–Cl and Cu–Cl bond lengths in crystals containing the tetrachlorocobaltate²⁸ and tetrachlorocuprate²⁹ anions. The calculated rotational entropy of the tetrachloronickelate ion is 25.2 e.u., including the contribution of a symmetry number of 12.

For the species $NiCl_3DMA^-$ we assume that the amide coordinates through oxygen, in accordance with the findings of Bull, *et al.*¹⁶ The structure of the anion for which the calculations were made is the one in which the plane defined by the Ni–O bond and the center of mass of the DMA molecule is parallel to the line defined by two chlorine atoms. This anion has no symmetry elements. The Ni–O bond distance was estimated by subtracting from the Ni–Cl distance the Cl radius (0.99 Å.) and adding the single bond radius of oxygen (0.74 Å.). The calculated rotational entropy of this anion is 32.1 e.u. at 298°K.

A similar procedure was used to compute the Ni–N bond length in $NiCl_3An^-$ as 1.99 Å. We find the rotational entropy of this species to be 28.8 e.u. at 298°K., including a symmetry number of 3.

The possibility of internal rotation about the Ni–O and Ni–N bonds in the two solvolyzed anions cannot be overlooked. The method summarized by Aston and Fritz³⁰ may be used with each anion, in-

(22) R. S. Drago, D. A. Wenz, and R. L. Carlson, *J. Am. Chem. Soc.*, **84**, 1106 (1962).

(23) M. D. Joesten and R. S. Drago, *ibid.*, **84**, 2696 (1962).

(24) H. Gunthard and E. Kovats, *Helv. Chim. Acta*, **35**, 1190 (1952).

(25) From the entropy of formamide given by J. C. Evans, *J. Chem. Phys.*, **22**, 1228 (1954), and the group contributions of methyl substituents given by I. M. Klotz, "Chemical Thermodynamics," Prentice-Hall, Inc., New York, N. Y., 1950, p. 173.

(26) L. Pauling, "The Nature of the Chemical Bond," 3rd Ed., Cornell University Press, Ithaca, N. Y., 1960, p. 282. This treatise is the source of all structure data not specifically referenced.

(27) N. Davidson, "Statistical Mechanics," McGraw-Hill Book Company, Inc., New York, N. Y., 1962, p. 171.

(28) M. A. Porai-Koshits, *Kristallografiya*, **1**, 291 (1956).

(29) L. Helmholz and R. F. Kruh, *J. Am. Chem. Soc.*, **74**, 1176 (1952).

(30) J. G. Aston and J. J. Fritz, "Thermodynamics and Statistical Thermodynamics," John Wiley and Sons, Inc., New York, N. Y., 1959, pp. 387–392.

cluding a symmetry number of three in each case, to yield the values 5.4 and 3.7 e.u. for completely free internal rotation in the anions containing dimethylacetamide and acetonitrile, respectively.

At this point the values cited above may be subtotaled to yield values of ΔS for reaction 1 in the gas phase of -18.45 e.u. for the reaction with DMA and -11.4 e.u. for the reaction with acetonitrile. We now assume that these same values would be observed in a condensed phase if all the species were neutral molecules. This assumption is about as good as Trouton's rule. Because three anions enter into reaction 1, some means must be found to include the electrostatic entropies of these species in solution.

The electrostatic entropy change which attends the immersion of a charge q on a conducting sphere of radius r in a structureless dielectric continuum having dielectric constant D is³¹

$$\Delta S_{e1}^{\circ} = \frac{q^2}{2rD} \left(\frac{\partial \ln D}{\partial T} \right)_p \quad (2)$$

It is well known that this expression fails to account satisfactorily for entropies of solvation of anions in water. Various explanations which involve perturbation of the local dielectric constant or the water structure in the vicinity of the ion have been given, and several empirical approaches have been offered to replace eq. 2.³²⁻³⁴ In the present instances, however, it would seem that eq. 2 has a reasonable chance to yield meaningful answers, since the anions are not solvated in a specific sense.

Dielectric constant data for the solvents have been taken from Maryott and Smith³⁵ (acetonitrile) and Leader and Gormley³⁶ (DMA). The ionic radius used for the chloride ion is 1.81 \AA ., and the calculated electrostatic entropies of solvation of this ion are -13.6 e.u. in DMA and -8.2 e.u. in An. For the tetrachloronickelate ion we use a radius of 3.25 \AA ., approximately the sum of the Ni-Cl bond length and the covalent

radius of chlorine. The corresponding electrostatic entropies are -30.3 e.u. in DMA and -18.2 e.u. in An.

There is some difficulty in deciding what radius one should ascribe to the solvolyzed anions. If the negative charge is restricted to the (NiCl_3) portion of the ion and the bonded amide or nitrile behaves rather like another solvent molecule, then a radius of 3.5 \AA . is about right. If the entire ion is assumed to interact with the dielectric, then scale models indicate that a radius of 5 \AA . should be used in dimethylacetamide and 4.5 \AA . in acetonitrile. The corresponding values of ΔS_{e1} lie in the range -7.0 to -5.0 in DMA and -4.2 to -3.3 in An.

When the cited electrostatic entropies are added to the subtotals given above, we find theoretical values for the entropies of solvolysis of tetrachloronickelate in the range -8.8 to -6.8 e.u. in dimethylacetamide solution and -5.6 to -4.7 e.u. in acetonitrile. These values are to be compared to the experimental values -9.7 and -5.7 e.u., respectively.

When the approximations inherent in the calculations are examined—neglect of vibrational contributions, equal entropies of condensation of all species, completely free internal rotation, and particularly the use of the Born equation to obtain the electrostatic entropies—the agreement between theory and experiment is all that could be desired. There is every reason to believe that similar methods could be used successfully on a variety of problems involving anionic intermediates or transition states in dipolar aprotic solvents.

(31) See ref. 27, p. 525.

(32) R. A. Robinson and R. H. Stokes, "Electrolyte Solutions," Academic Press, Inc., New York, N. Y., 1959, pp. 63-71.

(33) R. M. Noyes, *J. Am. Chem. Soc.*, **84**, 513 (1962).

(34) E. Whalley, *J. Chem. Phys.*, **38**, 1400 (1963).

(35) A. A. Maryott and E. R. Smith, National Bureau of Standards Circular No. 514, National Bureau of Standards, Washington, D. C., 1951.

(36) G. R. Leader and J. F. Gormley, *J. Am. Chem. Soc.*, **73**, 5731 (1951).

Photometric Study of the Reaction of Iodine with Active Nitrogen¹

by C. G. Freeman and L. F. Phillips

Department of Chemistry, University of Canterbury, Christchurch, New Zealand (Received September 23, 1963)

Photometric observations have been made on the flame produced when iodine vapor is mixed with active nitrogen from a microwave discharge. A mechanism (reactions 1-7) is proposed for the over-all reaction. The rate constants for reactions 1 and 5 are found to be $k_1 = 9 \times 10^{-14} \text{ cm.}^3 \text{ molecule}^{-1} \text{ sec.}^{-1}$ and $k_5 = 3.4 \times 10^{-13} \text{ cm.}^3 \text{ molecule}^{-1} \text{ sec.}^{-1}$, respectively. The most conspicuous feature of the reaction flame is intense emission in the blue and ultraviolet, arising from reactions 5 and 6. Pink emission from the point of mixing is mainly due to reaction 7. The reaction is suggested as a means of producing $A(^3\Sigma_u^+)$ nitrogen molecules in order to study their behavior in the absence of nitrogen atoms.

Introduction

The intense blue reaction flame of iodine and active nitrogen was among the first to be investigated by Strutt (Lord Rayleigh)² 50 years ago. The results of this and later work³ have shown that the processes responsible for producing the flame are extremely rapid, that the only products of the reaction are nitrogen and iodine, and that the flame spectrum consists of bands and continua of molecular iodine between 2100 and 6000 Å., with lines of atomic iodine at 2062 and 1850 Å.

In the present work it has been found that the flame may be divided into two regions, in the first of which nitrogen atoms are consumed and nitrogen molecules in the metastable $A(^3\Sigma_u^+)$ state are produced. Here the flame usually appears pink rather than blue, although emission in the blue and ultraviolet does occur. In the second region the blue emission predominates and its intensity decays gradually, in a manner which parallels the gradual decay of the A-state molecules. The lifetime of the blue emission increases with decreasing iodine concentration and the results may be extrapolated to a value of about 1 sec. at zero iodine concentration, in agreement with current estimates of the lifetime of the A-state.

Although most of the reactivity of discharged nitrogen is attributed to the presence of ground state nitrogen atoms, it has been shown that there are several reactions in which excited molecules are of prime importance.⁴⁻⁶ A-state molecules are normally present in active nitrogen as a result of termolecular recombination of atoms, either directly or by way of the Lewis-

Rayleigh afterglow,⁷ and as a result of excitation in the discharge.⁸ The present system is unusual in that the A-state molecules are produced from atoms by a series of rapid, bimolecular reactions. Since it should be possible to freeze out the iodine while removing only a fraction of the A-state molecules, this introduces the possibility of studying the reactions of this important species in the absence of atomic nitrogen.

Experimental

A diagram of the reaction vessel is given in Fig. 1. It consists essentially of a 30-cm. length of 1-cm. i.d. Pyrex tubing down which the reacting gases travel with velocities of between 3 and 7 m./sec. at pressures between 1 and 3 mm. Active nitrogen from a microwave discharge passes a light trap and enters the reaction vessel at A. Jet B is used to introduce nitric oxide for visual titration of nitrogen atoms.⁹ Iodine

- (1) Presented in part at the 37th Congress of the Australian and New Zealand Association for the Advancement of Science, Canberra, January, 1964.
- (2) R. J. Strutt and A. Fowler, *Proc. Roy. Soc. (London)*, **A86**, 105 (1911).
- (3) (a) A. Elliott, *ibid.*, **A174**, 273 (1940); (b) L. H. Easson and R. W. Armour, *Proc. Roy. Soc. Edinburgh*, **48**, 1 (1928).
- (4) K. D. Bayes, *Can. J. Chem.*, **39**, 1074 (1961).
- (5) A. N. Wright, R. L. Nelson, and C. A. Winkler, *ibid.*, **40**, 1082 (1962).
- (6) L. F. Phillips, *ibid.*, **41**, 732 (1963); **41**, 2060 (1963).
- (7) K. R. Jennings and J. W. Linnett, *Quart. Rev. (London)*, **12**, 116 (1958).
- (8) H. B. Dunford, *J. Phys. Chem.*, **67**, 258 (1963).
- (9) G. B. Kistiakowsky and G. G. Volpi, *J. Chem. Phys.*, **27**, 1141 (1957); F. Kaufman and J. R. Kelso, *ibid.*, **27**, 1209 (1957).

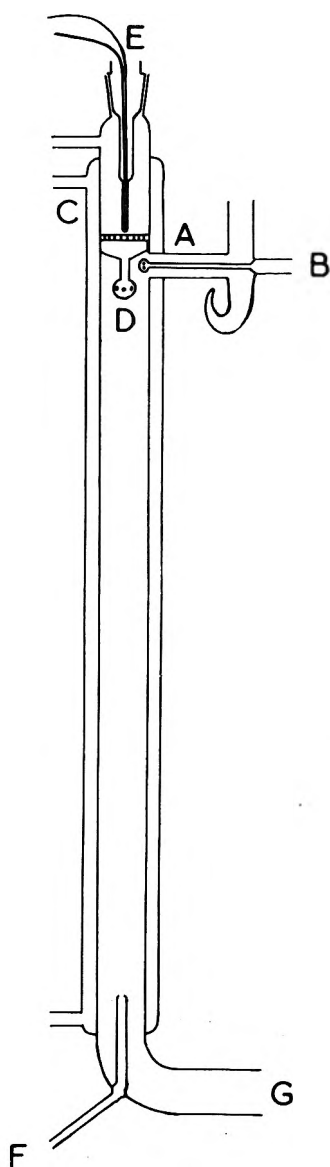


Figure 1. Reaction vessel: A, active nitrogen inlet; B, NO inlet; C, iodine saturator; D, iodine inlet; E, thermocouple; F, connection to McLeod gage; G, connection to cold trap and pump.

crystals are contained above a sintered glass disk at C. Iodine vapor is carried through the sinter by a stream of argon and enters the vessel through jet D. Identical results are obtained when nitrogen is used as the carrier gas instead of argon. The pressure drop across the iodine saturator is measured with a dibutyl phthalate manometer. The temperature of saturation is measured with a glass-enclosed thermocouple, E, whose sensitive junction is buried in the solid iodine. Complete saturation is assumed on the grounds that the same results are obtained with a high argon flow

and low saturator temperature as with a low argon flow and high saturator temperature. This applies particularly to the results of Fig. 7. Tube F leads to a McLeod gage and has also served as an auxiliary means of introducing nitric oxide. A water jacket is provided for temperature control, measurements having been made between 15 and 35°. This amount of temperature variation does not affect the reaction and has been used to widen the range of iodine pressures that could be covered. Tube G leads to a large cold trap and a rotary vacuum pump.

The intensity of light emission from the reaction vessel is measured with a 1P21 photomultiplier in combination with various filters. For the blue emission a Wratten No. 50 filter ($\lambda_{\max} = 4600 \text{ \AA.}$) is used, while for the nitrogen afterglow a Spectrolab Type P interference filter of 15 Å. half-width at 6250 Å. is used. This wave length was selected for minimum interference from iodine emission. An Ilford spectrum red filter, No. 608, was used for preliminary measurements of afterglow intensity but was not suitable for observations close to the inlet jet. The photomultiplier, with its filtering and collimating system, can be moved along the length of the reaction vessel so that the emission intensity can be studied as a function of time. The output of the photomultiplier is taken through a cathode-follower to a 0-250 $\mu\text{a.}$ meter.

Flame spectra have been photographed using a Hilger medium quartz spectrograph with Ilford Astra III and HP3 plates. For this purpose the Pyrex vessel of Fig. 1 was replaced by a plain quartz tube with a single inlet jet.

Analytical reagent grade iodine, commercial 99.9% argon and Matheson prepurified nitrogen ($\text{O}_2 < 8 \text{ p.p.m.}$) are used. Purer nitrogen tends to produce the highly energetic "pink afterglow"¹⁰ in the reaction vessel and this is undesirable for the present work.

After a few hours' operation the walls of the reaction vessel near the iodine inlet become coated with a white translucent solid. A similar deposit forms very rapidly when iodine vapor is introduced into discharged oxygen. The solid material, which is readily soluble in water and which evaporated from the quartz tube when it was warmed with a flame, is assumed to be I_2O_5 . Nitric oxide is purified by distillation from soda asbestos at -80° .

Typical partial pressures of iodine, atomic nitrogen, argon, and nitrogen are 10^{-2} , 3×10^{-2} , 0.2, and 2 mm. respectively, at the entrance to the reaction tube.

(10) G. E. Beale and H. P. Broida, *J. Chem. Phys.*, **31**, 1030 (1959); H. P. Broida and I. Tanaka, *ibid.*, **36**, 236 (1962).

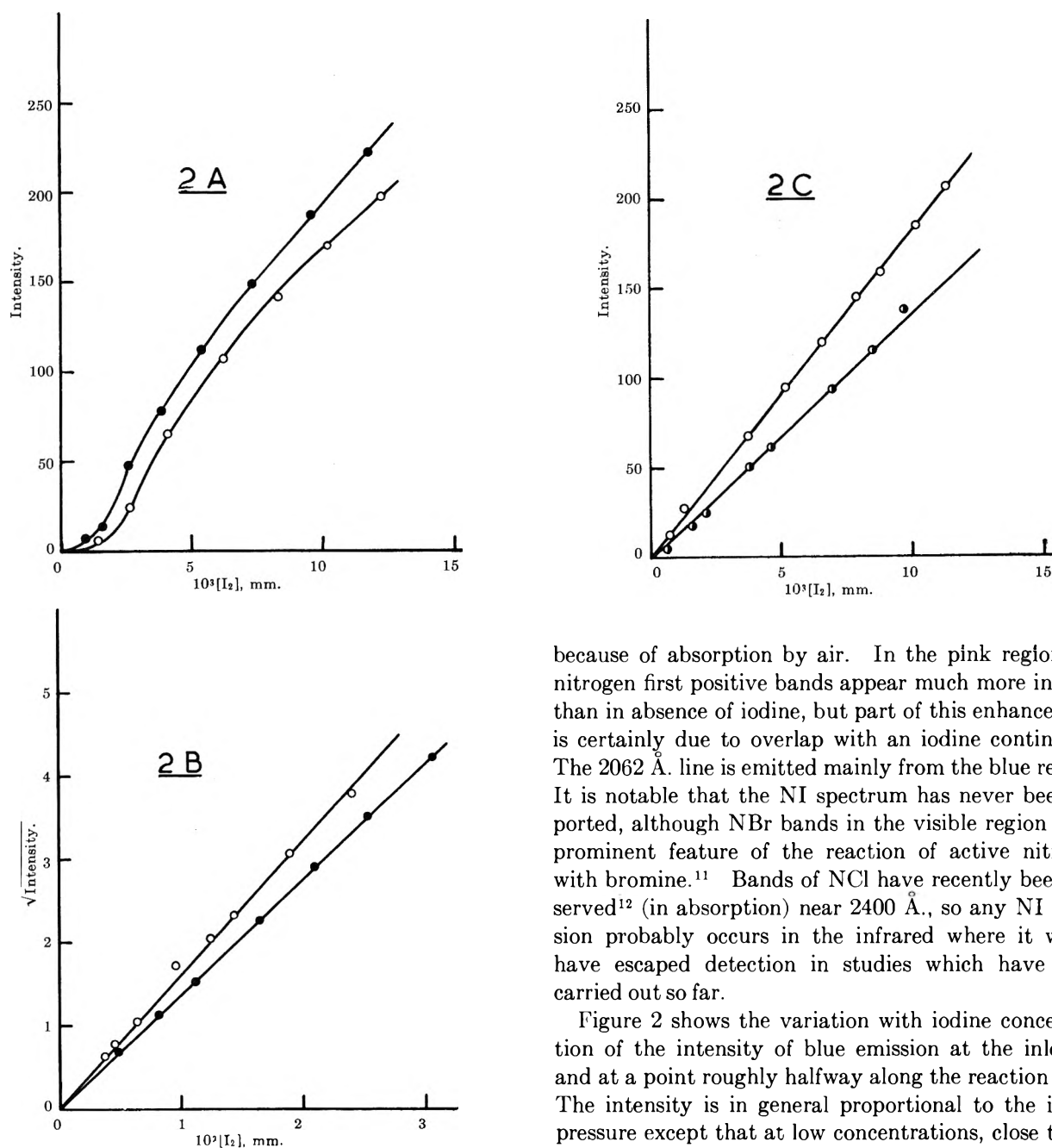


Figure 2. Dependence of blue intensity on iodine pressure: A, intensity at iodine inlet; B, square root of intensity at iodine inlet, low iodine pressures; C, intensity 15 cm. along reaction tube; points: O, 1.85 mm. of N_2 ; \bullet , 2.35 mm. of N_2 ; \bullet , 2.80 mm. of N_2 .

Results

At the point of mixing, the reaction flame appears pink, changing to intense blue a few centimeters downstream. The spectroscopic features of the flame were found to be as previously described except that the iodine line at 1850 \AA . was not observed, probably

because of absorption by air. In the pink region the nitrogen first positive bands appear much more intense than in absence of iodine, but part of this enhancement is certainly due to overlap with an iodine continuum. The 2062 \AA . line is emitted mainly from the blue region. It is notable that the NI spectrum has never been reported, although NBr bands in the visible region are a prominent feature of the reaction of active nitrogen with bromine.¹¹ Bands of NCl have recently been observed¹² (in absorption) near 2400 \AA ., so any NI emission probably occurs in the infrared where it would have escaped detection in studies which have been carried out so far.

Figure 2 shows the variation with iodine concentration of the intensity of blue emission at the inlet jet and at a point roughly halfway along the reaction tube. The intensity is in general proportional to the iodine pressure except that at low concentrations, close to the inlet jet, the intensity varies as the square of the iodine pressure. At high iodine pressures the flame shortens and the intensity halfway along the tube begins to fall off.

Figure 3 shows the effect on the iodine emission near the inlet jet of varying the nitrogen atom concentration by varying the amount of power supplied to the discharge. It is apparent that the intensity varies only slowly with the nitrogen atom concentration.

(11) E. V. Milton, H. B. Dunford, and A. E. Douglas, *J. Chem. Phys.*, **35**, 1202 (1961).

(12) R. G. W. Norrish, private communication, 1963.

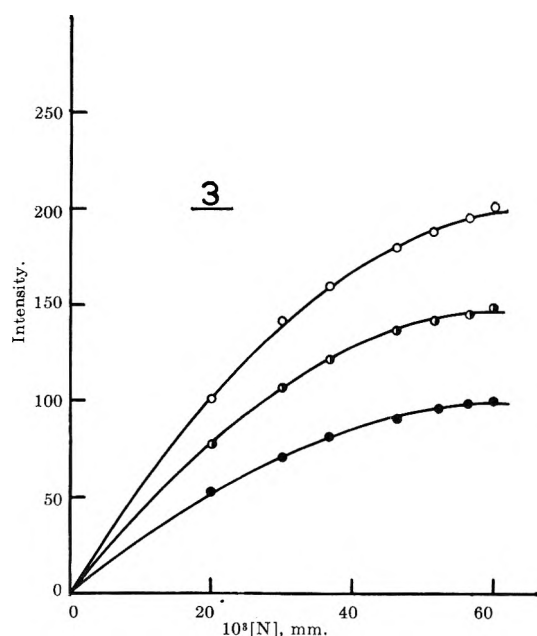


Figure 3. Dependence of blue intensity on nitrogen atom concentration; intensity at iodine inlet; points: \circ , 10.1×10^{-3} mm. of I_2 ; \bullet , 5.5×10^{-3} mm. of I_2 ; \bullet , 2.4×10^{-3} mm. of I_2 .

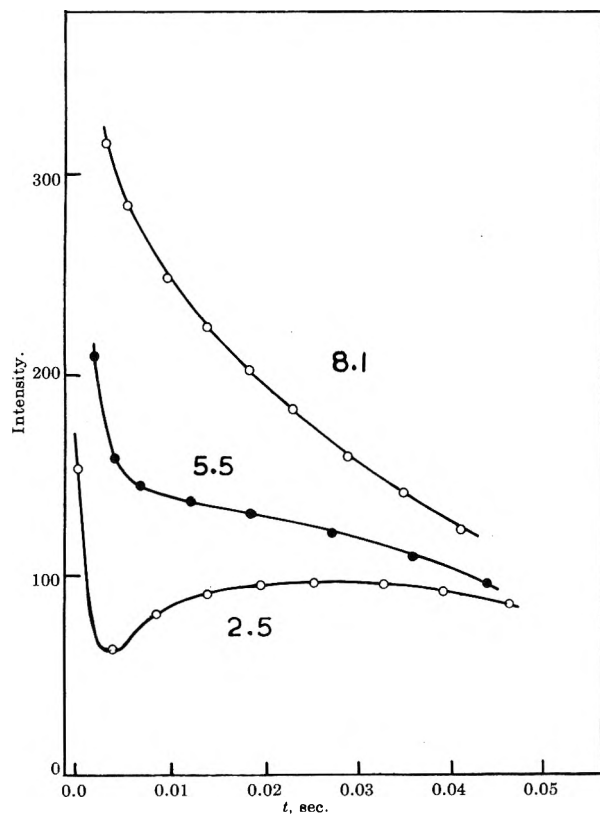


Figure 4. Variation of blue intensity with time at constant $[I_2]$ and $[N]$. Values of $10^3[I_2]$ (mm.) are marked on the curves; 1.85 mm. of N_2 , 0.030 mm. of N ; N atom concentration refers to zero time.

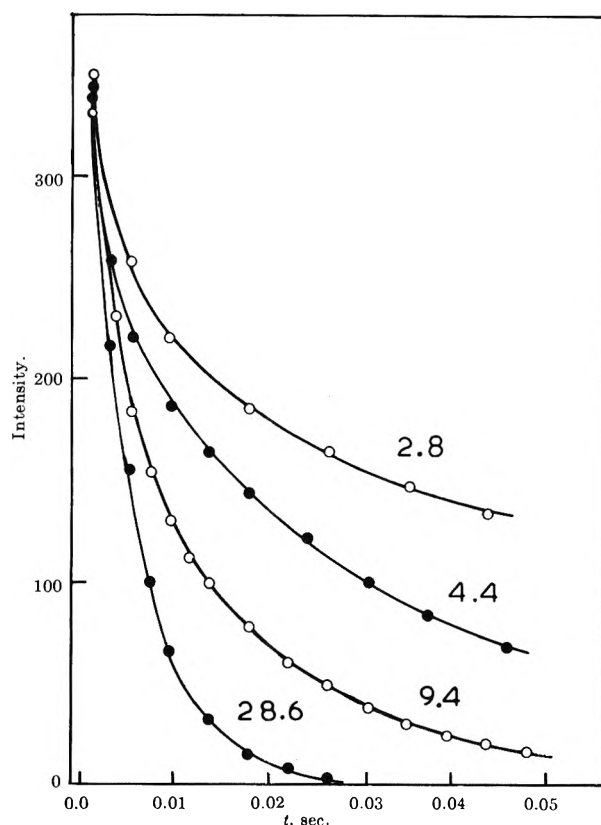


Figure 5. Variation of nitrogen afterglow with time. Values of $10^3[I_2]$ are marked on the curves; 1.85 mm. of N_2 , 0.030 mm. of N .

The variation of intensity with time is shown for the blue emission in Fig. 4 and for the nitrogen afterglow in Fig. 5. It is seen that the nitrogen afterglow, and hence the nitrogen atom concentration, always decreases steadily with time. In contrast, the blue emission intensity passes through a minimum at low iodine concentrations, beginning to decrease again only when most of the nitrogen atoms have been consumed. Once the nitrogen atoms have been removed, the blue emission decays exponentially, as shown in Fig. 6, the rate of decay increasing with increasing iodine concentration.

Discussion

The slow exponential decay of Fig. 6 and the results for low iodine concentration in Fig. 4 indicate that the blue emission in the latter part of the flame is due to the presence of some long-lived energetic species which is produced in the first part of the flame. An obvious candidate for identification as this energetic species is the $A(^3\Sigma_u^+)$ state of N_2 . It has a lifetime of the order of 1 sec.^{5,8,13} and an energy of 142 kcal./mole in its lowest vibrational level, sufficient to excite radiation down to 2020 Å. Furthermore, as shown below, the

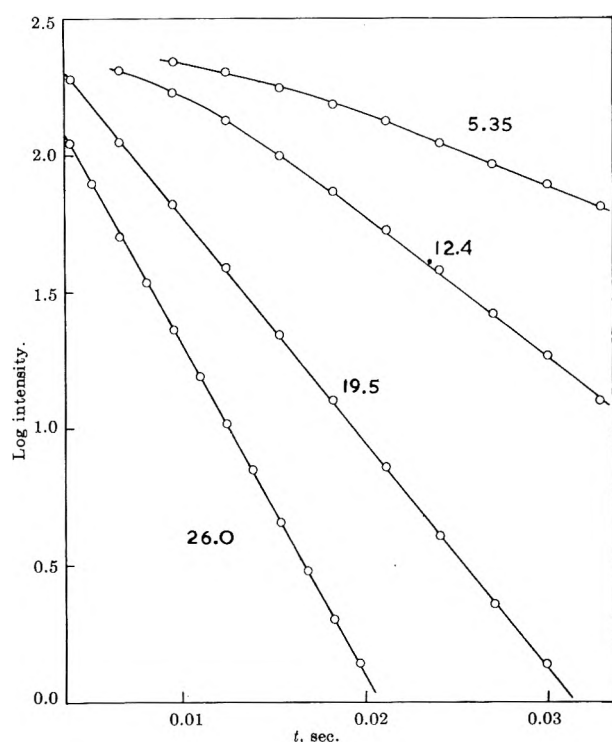
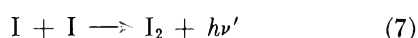
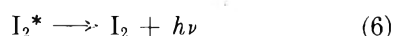
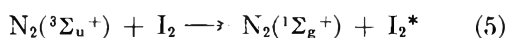
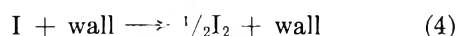
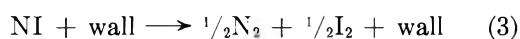
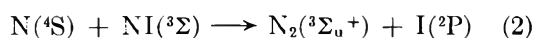


Figure 6. Typical graphs showing exponential decay of the blue I_2 emission. Values of $10^3[I_2]$ (mm.) are marked on the curves; 2.80 mm. of N_2 .

production of this species can readily be accounted for in terms of the probable reaction mechanism. Figure 7 shows that the rate of decay of the metastable species depends linearly on the iodine concentration and that the results may be extrapolated to a lifetime in the neighborhood of 1 sec. at zero iodine concentration. If the long-lived species were a metastable iodine molecule, the intensity of emission could be proportional to the iodine concentration as in Fig. 2, assuming some sort of cascade emission process, but the rate of decay would be unlikely to depend linearly on the iodine concentration.

The following mechanism is proposed to account for these observations.



The assignment to NI of a $^3\Sigma$ ground state follows

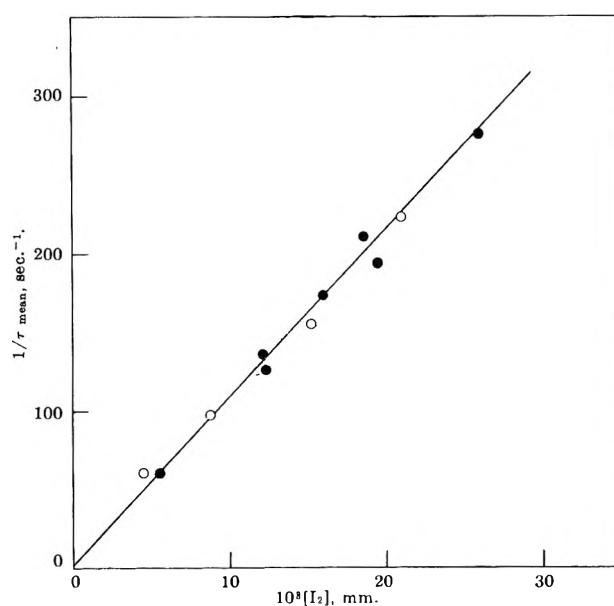


Figure 7. Variation of rate of decay of blue emission with iodine pressure; points: \circ , 1.85 mm. of N_2 ; \bullet , 2.80 mm. of N_2 ; from the slope of the line, $k_6 = 3.4 \times 10^{-13}$ cm.³ molecule⁻¹ sec.⁻¹.

the example of Milton, Dunford, and Douglas¹¹ for NBr . Reaction 2 differs from that proposed by these authors for the analogous NBr reaction in that N_2 is produced in the A-state rather than in the $X(^1\Sigma_g^+)$ ground state. A simple calculation based on conservation of angular momentum suggests that reaction 2 should produce A-state molecules eleven times out of fifteen.

Termolecular recombination reactions are considered to be too slow to be important in the present system; however, wall recombination of iodine atoms is required to be efficient in order to explain the rapid removal of atomic nitrogen by somewhat smaller amounts of iodine. Wall recombination of chlorine and bromine atoms has been found to be very fast in a Pyrex vessel,¹⁴ and it is assumed in the present work that iodine is present almost entirely in the form of I_2 .

Since the dissociation energy¹⁵ of I_2 is only 35.55 kcal./mole, it is likely that many of the excited molecules produced by reaction 5 dissociate instead of radiating. There is not sufficient energy available, however, to dissociate the molecule and simultaneously excite the atomic line at 2062 Å. Excitation of this line may occur on the wall. The quantity of iodine

(13) N. P. Carleton and O. Oldenberg, *J. Chem. Phys.*, **36**, 3460 (1962); J. F. Noxon *ibid.*, **36**, 926 (1962); E. C. Zipl, Jr., *ibid.*, **38**, 2034 (1963); P. G. Wilkinson and R. A. Mulliken, *ibid.*, **31**, 674 (1959).

(14) E. A. Ogryzlo, *Can. J. Chem.*, **39**, 2556 (1961).

(15) A. G. Gaydon, "Dissociation Energies," Chapman and Hall, London, 1953.

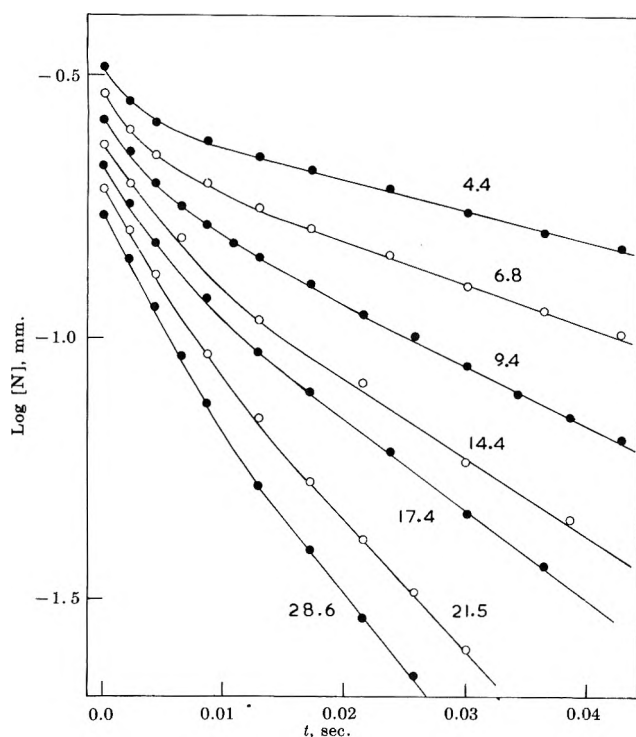


Figure 8. Variation of $\log [N]$ with time at different iodine pressures. Values of $10^3 [I_2]$ (mm.) are marked on curves; 1.85 mm. of N_2 . Successive curves have been displaced upward for clarity; otherwise, they should all have the same intercept at $t = 0$.

which is able to be held as atoms in a monolayer¹⁶ is similar to the amount which has been added to the gas phase in the present experiments.

Reaction 7 is included to account for the dependence of intensity on the square of the iodine concentration in the pink region of the flame.

It remains to consider the kinetics of the disappearance of atomic nitrogen in the presence of iodine. Ordinary termolecular recombination with I_2 as third body is unlikely to have a rate constant greater than about 10^{-31} cm.⁶ molecule⁻² sec.⁻¹ and should not be important in the present system.¹⁷ If the only fate of NI is to be converted to N_2 by reactions 2 and 3, then the rate of consumption of N is given by

$$-d[N]/dt = k_1[N][I_2] \left\{ 1 + \frac{k_2[N]}{k_2[N] + k_3} \right\} \quad (8)$$

According to eq. 8 a graph of $\ln [N]$ vs. time should be a curve which tends to a line of slope $-2k_1[I_2]$ at high values of $[N]$ and to a line of slope $-k_1[I_2]$ at low values of $[N]$. Typical graphs of $\log [N]$ vs. time are shown in Fig. 8. Nitrogen atom concentrations were calculated from the square root of the afterglow intensity at 6250 Å., the proportionality factor

being determined by NO titration in absence of I_2 . The graphs have the predicted shape, and the final slopes yield reasonable values for k_1 , assuming constant $[I_2]$, as shown in Table I. The initial slopes are not sufficiently well defined to be useful for calculation, presumably because the nitrogen atom concentrations are not great enough. The difference between the results for 1.8 and 2.8 mm. of N_2 probably reflects the slower diffusion of NI to the wall at the higher pressure. It should also be noted that the reaction only produces significant quantities of A-state molecules when nitrogen atoms are present in relatively high concentrations.

Table I: Rates of Nitrogen Atom Consumption

$[N_2]$, mm.	$[N]_0$, mm.	$10^3 [I_2]$, mm.	Final slope, ^a sec. ⁻¹	k_1 , cm. ³ molecule ⁻¹ sec. ⁻¹ × 10 ⁻¹⁴
1.85	0.029	3.3	13	9.8
1.85	0.029	6.8	18	8.5
1.85	0.029	9.4	26	8.8
1.85	0.029	14.4	34	7.5
1.85	0.029	17.4	42	7.7
1.85	0.029	21.5	59	8.7
1.85	0.029	28.6	79	8.8
2.80	0.044	6.6	22	10.7
2.80	0.044	15.2	53	11.1
2.80	0.044	27.0	100	11.8

^a Final slopes refer to graphs of $\ln [N]$ vs. time. ^b Mean $k_1 = 9.3 \times 10^{-14}$ cm.³ molecule⁻¹ sec.⁻¹.

Further work is intended to extend these observations to the reactions of active nitrogen with chlorine and bromine and to measure the lifetime of the A-state at very low iodine concentrations. A preliminary attempt has also been made to investigate the possible reactivity of the A-state toward nitric oxide⁵ by introducing NO into the blue flame through jet F. No evidence was found for destruction of NO by the A-state, although the blue emission was completely quenched. This experiment is to be repeated in a system from which the iodine has been removed with a suitable cold trap.

Acknowledgment. This work was supported by grants from the New Zealand Universities Research Committee and the United States Air Force Office of Scientific Research.

(16) J. S. Campbell, R. L. Moss, and C. Kemball, *Trans. Faraday Soc.*, **56**, 1481 (1960).

(17) S. W. Benson, "The Foundations of Chemical Kinetics," McGraw-Hill Book Co., Inc., New York, N. Y., 1960, p. 310.

The Extraction of Acids by Basic Organic Solvents. IV. Tributyl

Phosphate and Trioctyl Phosphine Oxide-HAuCl₄ and HAuBr₄¹

by M. I. Tocher, D. C. Whitney, and R. M. Diamond²

Lawrence Radiation Laboratory, University of California, Berkeley, California (Received September 23, 1963)

A study has been made of the extraction of tracer amounts of HAuCl₄ and HAuBr₄ from aqueous solutions of the corresponding hydrohalic acids into dilute solutions of tributyl phosphate (TBP) in xylene, CCl₄, and isooctane, and of trioctyl phosphine oxide (TOPO) in CCl₄. It was found that the extracting species has the formula $H^+ \cdot 3R_3PO \cdot xH_2O \cdots AuX_4^-$, where R is the butoxy or octyl group and X is Br or Cl. Such a trisolvated species is almost certainly analogous to the trisolvated hydronium species previously found for HClO₄, HReO₄, and HBr extracted into dilute TBP solutions and for HClO₄ and HReO₄ into dilute TOPO solutions, so that its formula can be written $H_3O^+ \cdot 3R_3PO \cdot yH_2O \cdots AuX_4^-$, and it conforms to the model for strong acid extraction proposed in previous papers in this series.

Introduction

A class of compound which shows high extraction into basic oxygenated organic solvents (ethers, ketones, organophosphorus esters, etc.) is the monobasic halometallic acids, HMX₄, where M is a transition metal and X is a halogen; examples are HFeCl₄, HAuBr₄, HSbCl₆, etc. Considerable data have been published on their extraction, but many of the studies involved elemental analysis of the extracting species in the pure organic solvent, which in general precludes the possibility of determining the role of the solvent in the metal complex. In addition, the problem of being certain that the analysis corresponds to only a single species may make the interpretation of such data a difficult task.

Of the work which draws its conclusions mainly from organic phase stoichiometry, probably the most extensive is that of Clark, *et al.*,^{3,4} on the Fe(III) complexes in ethers. These workers have identified HFeCl₄·5H₂O and HFeBr₄·4H₂O as the extracting species into ethyl and isopropyl ethers. Fomin and Morgunov,⁵ on the other hand, found that HFeCl₄·3-4H₂O was the principal species extracting into ethyl, butyl, and isoamyl ethers and have questioned some of Clark's results. Another type of work, but of significance to these studies, is the report by McCusker, *et al.*,⁶ on the crystallization of a species from dioxane solu-

tions which they characterize as [FeCl₂(dioxane)₂·(H₂O)(HCl)]⁺[Cl]⁻·dioxane; further comment on this structure is reserved for the Conclusions.

Hesford and McKay⁷ have described a method involving the extraction of tracer amounts of the acid into organic solvents diluted with inert liquids which allows treatment of the organic phase as a quasi-ideal system. That is, simple equilibrium expressions may be used to describe the extraction, and in these, the activities of the organic phase solutes may be replaced by concentrations. In several reported examples of halometallic acid extraction, this method of concentration variation has been used, but the metal ion concentrations were so high as to cast some doubt on the validity of the assumption that the organic phases were quasi-ideal. Also, in several cases there is no

- (1) This work was supported by the U. S. Atomic Energy Commission.
- (2) Author to whom requests for reprints should be addressed.
- (3) A. H. Laurene, D. E. Campbell, S. E. Wiberly, and H. M. Clark, *J. Phys. Chem.*, **60**, 901 (1956).
- (4) G. S. Golden and H. M. Clark, *ibid.*, **65**, 1932 (1961).
- (5) V. V. Fomin and A. F. Morgunov, *Russ. J. Inorg. Chem.*, **5**, 670 (1960).
- (6) P. A. McCusker, T. J. Lane, and S. M. S. Kennard, *J. Am. Chem. Soc.*, **81**, 2974 (1959).
- (7) E. Hesford and H. A. C. McKay, *Trans. Faraday Soc.*, **54**, 573 (1958).

indication that corrections were made for the coextraction of the hydrohalic acid or for loading of the extractant. As pointed out by Hesford, *et al.*,⁸ results under these conditions may give an inaccurate picture of the nature of the extracting species, and caution may have to be used in interpreting such data. Reports of this type include the identification of $\text{HFeCl}_4 \cdot 3\text{TBP}$ at low (2–4 *M*) HCl concentrations but $\text{HFeCl}_4 \cdot 2\text{TBP}$ at high (6–9 *M*) HCl concentrations,⁹ and $\text{HFeCl}_4 \cdot 2\text{TOPO}$ at very high Fe concentrations,¹⁰ where TBP and TOPO stand for tributyl phosphate and trioctyl phosphine oxide, respectively.

The final set of reported results includes those which more or less fulfill the requirements outlined by Hesford. These actually cover the widest range of examples; the reported species are $\text{HTlCl}_4 \cdot 3\text{TBP}$,¹¹ $\text{HFeCl}_4 \cdot 3[\text{butyl ether}]$,¹² $\text{HMCl}_4 \cdot 3[\text{diisopropyl carbinol}]$ ($M = \text{Pa, Fe, Au}$),¹³ $\text{HAuCl}_4 \cdot 3\text{TBP}$,¹⁴ $\text{HMF}_6 \cdot 3\text{TBP}$ and $\text{HMOF}_4 \cdot 3\text{TBP}$ ($M = \text{Nb, Ta}$),¹⁵ and $\text{HCrO}_3\text{X} \cdot 3\text{TBP}$ ($X = \text{Br or Cl}$) at low HX concentrations (1–3 *M*).¹⁶ It may be noted that in every case the acid shows a solvation (as opposed to hydration) number of 3; in none of these examples was the hydration of the acid determined.

Other papers in this present series on strong acids have dealt with the extraction of simple mineral acids into dilute (<0.3 *M*) tributyl phosphate (TBP) and trioctyl phosphine oxide (TOPO) solutions. In these studies, it was shown that very strong acids such as HClO_4 ,^{17,18} HReO_4 ,^{17,18} and HBr ¹⁹ extract with the trisolvated, and in the case of TBP, partially hydrated, hydronium ion as the cation. Acids not quite as strong, such as HNO_3 ,^{20,21} however, extract primarily as the anhydrous, monosolvated molecular acid. An interpretation was presented in terms of a competition for solvating the proton among the water molecules, the basic organic extractant, and the anions.

In this paper the study is extended to the mixed acid systems $\text{HAuCl}_4\text{--HCl}$ and $\text{HAuBr}_4\text{--HBr}$, where the metal acid is in tracer concentration and is the species being investigated. The results reported herein, plus those reported by the other authors cited, can be formulated in terms of the previously proposed model, and this is done in the Conclusions.

Experimental

Reagents. All acids and salts used were reagent grade. Of the diluents, the xylene was a reagent grade mixture of the three isomers (see the Results section for comments on the purity), while the isoctane and CCl_4 were of spectroscopic quality. The tributyl phosphate (Fisher Scientific Co.) was purified as described previously,¹⁷ while the trioctyl phosphine oxide

(Eastman White Label) was used as purchased. The Au^{138} tracer was prepared by neutron irradiation of 99.9% Au foil in the Livermore pool-type reactor or the General Electric test reactor, Vallecitos, and was certified radiochemically pure by half-life and γ -ray spectrum measurements. The $\text{HAuCl}_4\text{--HCl}$ solutions were prepared by dissolving the gold foil in aqua regia, taking to dryness three times with 6 *M* HCl , and finally dissolving the resulting HAuCl_4 in HCl of the desired concentration. These solutions were stored in the dark to prevent any possible decomposition.

Procedure. Between 5 and 10 μl . of tracer solution was injected with a micropipet into a two-phase mixture consisting of equal volumes of acid solution and extractant solution (generally 5.00 ml. of each phase) in a 60-ml. glass-stoppered bottle. The samples were shaken on a mechanical wrist-type shaker for 15–30 min., transferred to 12-ml. centrifuge cones, and centrifuged for 2 min. Duplicate 2.00-ml. aliquots were taken from the upper phase, and one 2.00-ml. aliquot was taken from the lower phase, the aliquots being placed in 1-dram screw cap vials. The vials were γ -counted using a well-type $\text{Na}(\text{Tl})\text{I}$ scintillation counter and a single channel pulse-height analyzer; the ratio of the counts/min. in each phase (after correction for background) is the distribution ratio, *D*, for the tracer acid.

Since in some cases a variation in the value of *D* was observed with a change in the tracer gold concentration over the range 10^{-7} to 10^{-2} *M*, most of the

- (8) E. Hesford, H. A. C. McKay, and D. Scargill, *J. Inorg. Nucl. Chem.*, **4**, 321 (1957).
- (9) S. K. Majumdar and A. K. De, *Talanta*, **7**, 1 (1960); H. Specker and M. Cremer, *Z. anal. Chem.*, **167**, 110 (1959).
- (10) W. J. White and J. C. Ross, ORNL-2382 (1957).
- (11) K. S. Venkateswarlu and P. C. Das, *J. Inorg. Nucl. Chem.*, **25**, 730 (1963).
- (12) V. V. Fomin, P. A. Zagorets, A. F. Morgunov, and I. I. Ter-tishnik, *Russ. J. Inorg. Chem.*, **4**, 1038 (1959).
- (13) A. T. Casey and A. G. Maddock, *Trans. Faraday Soc.*, **58**, 918 (1962); A. G. Maddock, W. Smulek, and A. J. Tench, *ibid.*, **58**, 923 (1962); A. G. Goble and A. G. Maddock, *J. Inorg. Nucl. Chem.*, **7**, 94 (1958).
- (14) D. G. Tuck and R. M. Diamond, UCRL-8897 (1959); D. G. Tuck, *J. Inorg. Nucl. Chem.*, **11**, 164 (1959).
- (15) G. P. Giganov and V. D. Ponomarev, *Tr. Inst. Met. Obogashch. Akad. Nauk Kaz. SSR*, **5**, 119, 125 (1962); *Chem. Abstr.*, **58**, 9671h (1963).
- (16) D. G. Tuck and R. M. Walters, *J. Chem. Soc.*, 1111 (1963).
- (17) D. C. Whitney and R. M. Diamond, *J. Phys. Chem.*, **67**, 209 (1963).
- (18) M. I. Tocher, T. J. Conocchioli, and R. M. Diamond, to be published.
- (19) D. C. Whitney and R. M. Diamond, *J. Phys. Chem.*, in press.
- (20) D. C. Whitney and R. M. Diamond, to be published.
- (21) T. J. Conocchioli and R. M. Diamond, unpublished work.

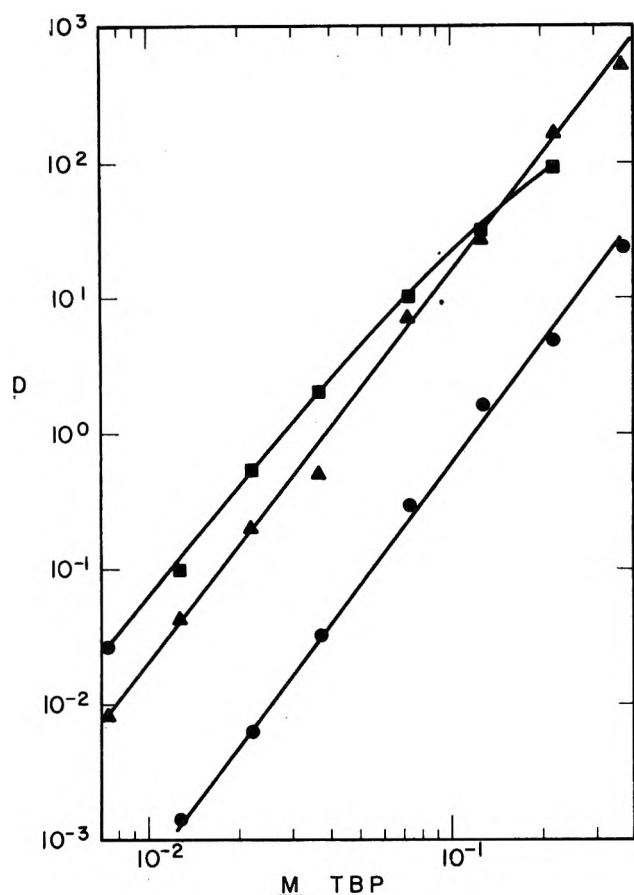


Figure 1. Variation of distribution ratio of HAuCl_4 with total TBP concentration (in isoctane) for initial aqueous Au concentration of $1 \times 10^{-5} M$ and acid concentrations of: ●, 2.0 M HCl; ▲, 6.0 M HCl; ■, 10.0 M HCl.

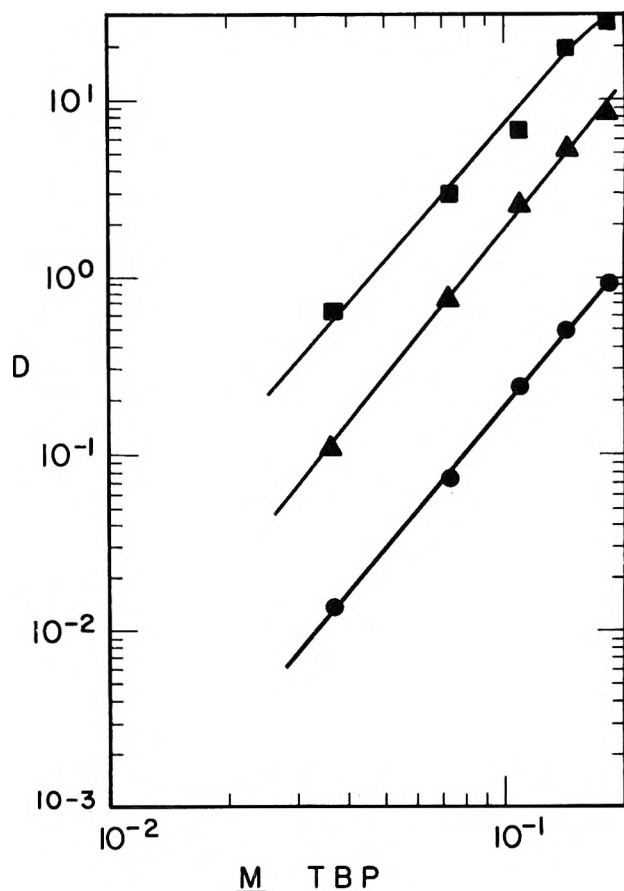


Figure 2. Variation of distribution ratio of HAuCl_4 with total TBP concentration (in xylene) for initial aqueous Au concentration of $1 \times 10^{-6} M$ and acid concentrations of: ●, 2.0 M HCl; ▲, 6.0 M HCl; ■, 10.0 M HCl.

work reported in this paper was done at a fixed gold concentration, namely, $10^{-5} M$.

The time required for the samples to come to equilibrium is presumably of the order of a few minutes or less, since variation of the shaking time over the range of 5–120 min. did not produce significant differences in distribution ratios. The normal range of 15–30 min. used in these experiments was a convenient period. The centrifugation time was also arbitrarily chosen, since longer times showed no changes in the distribution ratios except for a tendency to promote evaporation of the organic phase. The reproducibility of the distribution ratios in the range 10^{-2} to 10^2 was 5%; for larger or smaller ratios the spread in values was greater.

Analysis of the HAuCl_4 complex was done by shaking a 6 M LiCl–0.4 M HCl–0.01 M HAuCl_4 solution with 10% TBP in isoctane, back-extracting the complex completely into H_2O , and determining the H:Au:Cl ratios by standard analytical methods—namely, Au^{+3}

by peroxide precipitation and weighing of the metal, Cl^- by the Volhard method, and H^+ by titration using a pH meter. Blanks were determined in the same manner for 6 M LiCl–0.4 M HCl extractions. The results gave a net ratio of 1.02:1.00:3.98, see Table I. (LiCl solutions were used in order to lower the amount of HCl extracting into the TBP solution in competition with the HAuCl_4 .) Analyses were not done on HAuBr_4 , but it can be assumed to be analogous to HAuCl_4 .

All experimental work was done at room temperature, $23 \pm 2^\circ$, with no apparent changes in extraction occurring over this small temperature range.

Results

The distribution ratios, D , of the gold tracer as a function of the TBP or TOPO concentration in various organic solvents for various aqueous hydrohalic acid concentrations are shown as log–log plots in Fig. 1–6.

In some cases (notably some xylene solutions) the

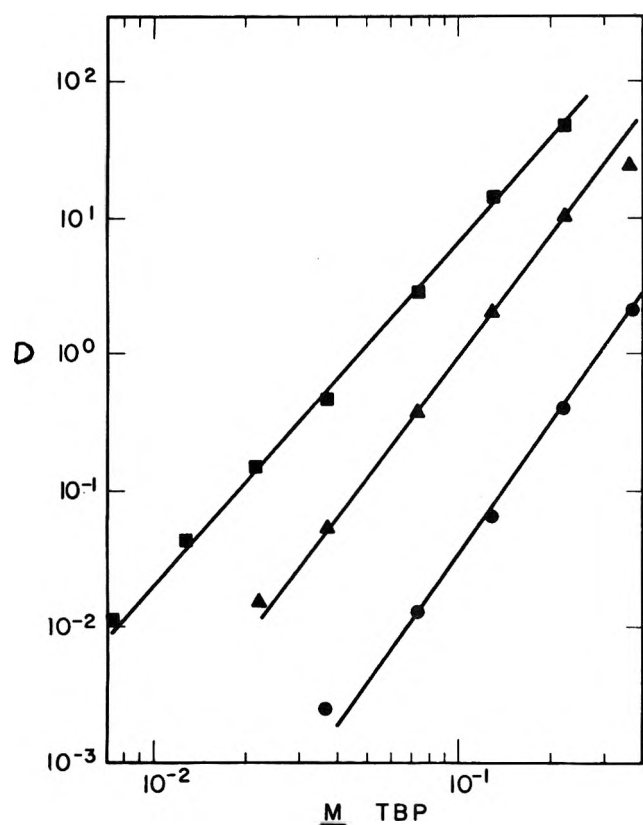


Figure 3. Variation of distribution ratio of HAuCl_4 with total TBP concentration (in CCl_4) for initial aqueous Au concentration of $1 \times 10^{-5} M$ and acid concentrations of: ●, 2.0 M HCl; ▲, 6.0 M HCl; ■, 10.0 M HCl.

Table I

Aqueous phase			10% TBP in isoctane phase		
M LiCl	M HCl	M HAuCl_4	M H^+	M Au(III)	M Cl^-
6.0	0.40	0.010	0.063	0.061	0.244
6.0	0.40	0.0009	0.0009
Net organic phase concn.			0.062	0.061	0.243
Net organic phase ratios			1.02	1.00	3.98

inert diluent was found to yield an appreciable distribution ratio, even with no extractant present. This same problem was noted by Tuck¹⁴ in HAuCl_4 -TBP extractions using xylene diluent and is possibly due to basic impurities in the solvent; no such behavior was found when spectroscopic grade *m*-xylene was used in place of reagent grade mixed xylenes. Whatever the cause, the distribution ratios obtained for the pure solvents were subtracted from those with extractant present to yield the corrected distribution ratios which are plotted in the figures.

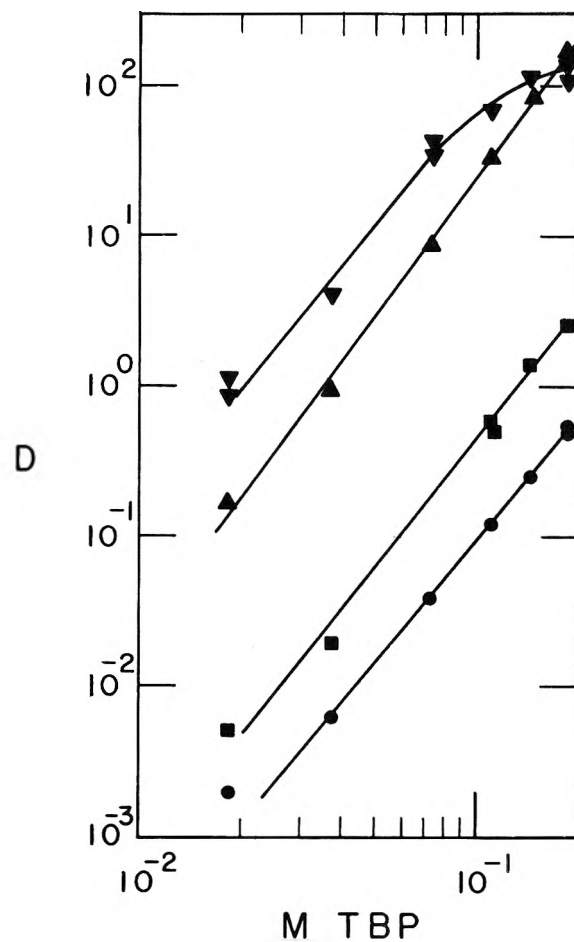
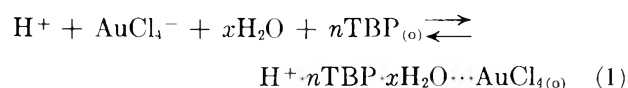


Figure 4. Variation of distribution ratio of HAuBr_4 with total TBP concentration (in xylene) for initial aqueous concentrations of: ●, 1.1 M HBr, $1 \times 10^{-5} M$ HAuBr_4 ; ■, 2.0 M HBr, $1 \times 10^{-6} M$ HAuBr_4 ; ▲, 4.1 M HBr, $1 \times 10^{-5} M$ HAuBr_4 ; ▼, 6.3 M HBr, $1 \times 10^{-6} M$ HAuBr_4 .

Discussion

In the following derivation of the equations describing the extraction system, only those for TBP and HAuCl_4 will be shown explicitly. Completely analogous equations would apply if TBP is replaced by TOPO or HAuCl_4 is replaced by HAuBr_4 , since the types of equations are general. Due to the low dielectric constants ($\epsilon \sim 2$) of the solvents, the extracting species in these systems will probably be in the form of an ion pair, as has been established earlier for the extracting species of HClO_4 , HReO_4 , and HBr under these conditions.¹⁷⁻¹⁹

The equation for the extraction can be written then as



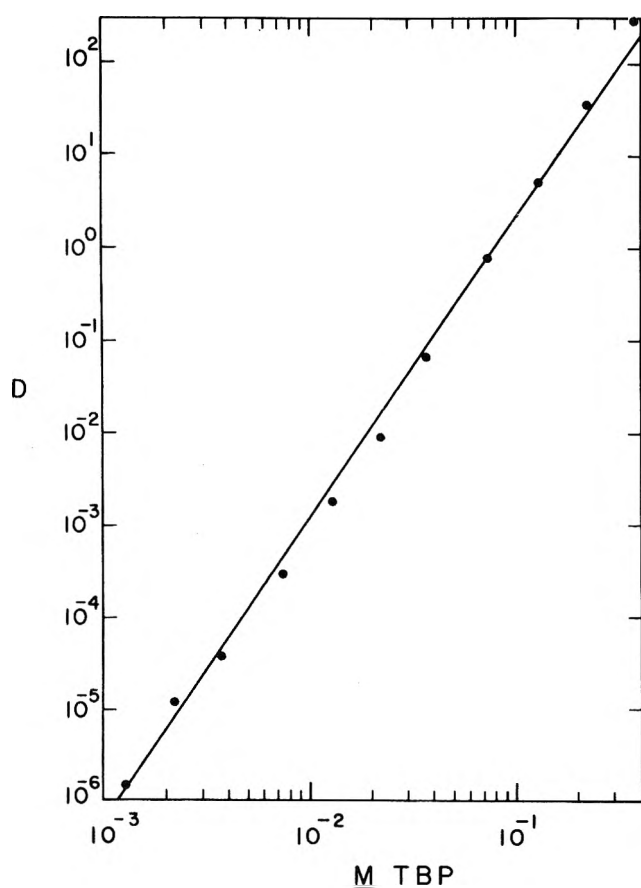


Figure 5. Variation of distribution ratio of HAuCl_4 with total TBP concentration (in iso-octane) from 6.0 M LiCl-0.1 M HCl solutions, 1×10^{-5} M HAuCl_4 initial aqueous concentration.

where (o) denotes the organic phase, and aqueous ion hydration has been omitted. The corresponding equilibrium constant is

$$K_{\text{HAuCl}_4} = \frac{[\text{H}^+ \cdot n\text{TBP} \cdot x\text{H}_2\text{O} \cdots \text{AuCl}_4^-]_{(o)}}{[\text{H}^+][\text{AuCl}_4^-](\text{H}_2\text{O})^x[\text{TBP}]_{(o)}^n} \quad (2)$$

$$= \frac{[\text{H}^+ \cdot n\text{TBP} \cdot x\text{H}_2\text{O} \cdots \text{AuCl}_4^-]_{(o)} \gamma_{(o)}}{[\text{TBP}]_{(o)}^n \gamma_{\text{TBP}}^n (\text{H}_2\text{O})^x [\text{H}^+] [\text{AuCl}_4^-] \gamma_{\text{H}^+} \gamma_{\text{AuCl}_4^-}}$$

where parentheses represent activities, and brackets stand for concentrations. By the proper choice of conditions, it is possible to simplify eq. 2 considerably. Since HCl extracts relatively poorly, $(\text{H}_2\text{O})^x [\text{H}^+] \gamma_{\text{H}^+}$ is constant for a given HCl concentration. Also, since HAuCl_4 is in dilute (tracer) concentration, $\gamma_{\text{AuCl}_4^-}$ is very close to being constant for a given $[\text{H}^+]$. As long as the concentration of all acid in the organic phase is kept small compared to the TBP concentration, the equilibrium TBP concentration, $[\text{TBP}]$, will be proportional to the total TBP concentration,

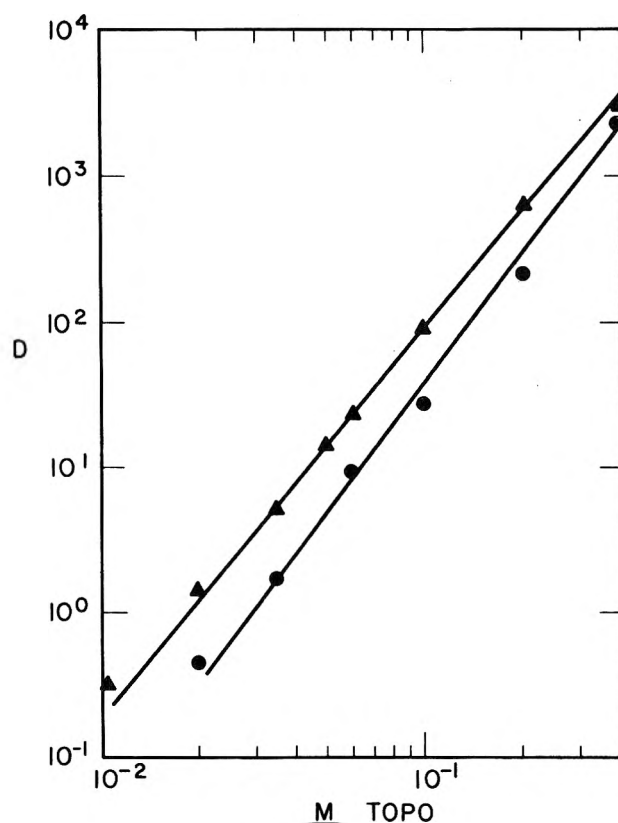


Figure 6. Variation of distribution ratio of HAuCl_4 with total TOPO concentration (in CCl_4) for initial aqueous Au concentration of 1×10^{-6} M and acid concentrations of: ●, 0.05 M HCl; ▲, 0.20 M HCl.

differing only by the amount of $\text{TBP} \cdot \text{H}_2\text{O}$ formed (the proportion of the latter depends on $a_{\text{H}_2\text{O}}$ and the equilibrium constant for the extraction of water by TBP; see ref. 17). Little is known concerning the activity coefficients of inorganic species in organic solvents, so it has been assumed that for the dilute organic phases used in this study, the ratio of activity coefficients of the two species present, *i.e.*, $\gamma_{(o)}/\gamma_{\text{TBP}}^n$, is a constant. When these various considerations are applied to eq. 2, and it is noted that $[\text{H}^+ \cdot n\text{TBP} \cdot x\text{H}_2\text{O} \cdots \text{AuCl}_4^-]_{(o)}/[\text{AuCl}_4^-]$ is the distribution ratio for gold, D , the resulting expression is

$$K'_{\text{HAuCl}_4} = \frac{D}{[\text{TBP}]^n} \quad (3)$$

Taking logarithms

$$\log D = n \log [\text{TBP}] + \log K'_{\text{HAuCl}_4} \quad (4)$$

Thus, a plot of $\log D$ vs. $[\text{TBP}]$ should yield a straight line of slope n , giving the dependence of the extracting species (if it is an ion pair) on TBP. Such plots are shown for HAuCl_4 extracting from 2, 6, and 10 M

HCl into TBP in isoctane (Fig. 1), xylene, (Fig. 2), and CCl_4 (Fig. 3), and for HAuBr_4 extracting from 1, 2, 4, and 6 M HBr into TBP in xylene (Fig. 4); the slopes are seen to range in value from 2.8 to 3.2.

The tendency for the curves from 10 M HCl solutions to bend over to a slope below 3.0 has its explanation in the assumption that the extraction of HCl is negligibly small. Although this is certainly true in 2 M HCl (where $[\text{H}^+]_{(o)} \approx 10^{-4} M$ for 0.15 M TBP in isoctane, $[\text{H}^+]_{(o)}$ denoting organic phase HCl concentration), the extraction has started to become appreciable ($[\text{H}^+]_{(o)} \approx 0.003 M$) at 6 M and is actually quite large ($[\text{H}^+]_{(o)} \approx 0.04 M$) at 10 M . Since this extracted HCl coordinates with some of the TBP, decreasing the concentration of available TBP molecules, the result is a lowering of the D values for HAuCl_4 in 10 M HCl below their expected values by a factor of 5 or more for the most concentrated TBP solutions; the same effects, although somewhat smaller due to the lower extraction of HCl, are also noticeable for xylene and CCl_4 solutions. The rapid reduction of HCl extraction with decrease in TBP concentration ($\alpha[\text{TBP}]^3$) causes this effect to diminish and the D values to become closer to the expected values as the TBP concentration is reduced. The effect is even more apparent in the 6.3 M HBr system (Fig. 4), since HBr extracts better than HCl.

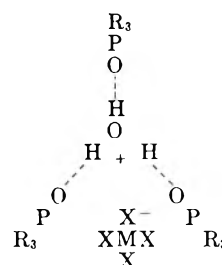
This problem could be avoided in some cases by doing the extraction from a 6.0 M LiCl-0.1 M HCl aqueous phase. The results of such an experiment are shown in Fig. 5, and it is seen that good results are achieved in isoctane solutions of TBP (slope ~ 3.2).

Extraction of HAuCl_4 from aqueous HCl solutions was also made into trioctyl phosphine oxide (TOPO) dissolved in CCl_4 . Equation 3 may be used to represent the extraction, provided [TOPO] is substituted for [TBP]. The results of plotting $\log D$ vs. $\log [\text{TOPO}]$ for these systems are shown in Fig. 6 and again slopes near, but usually below, 3 were found. The lowered values of the slopes can again be ascribed to the extraction of HCl, which, because of the greater basicity of TOPO, extracts from a 0.2 M solution to give a value of $[\text{H}^+]_{(o)} \approx 0.005 M$ for 0.1 M TOPO, corresponding to a complexing of 15% of the total TOPO. Actually, because of TOPO's greater extraction of water ($[\text{TOPO} \cdot \text{H}_2\text{O}] \approx 0.35[\text{TOPO}]$),¹⁸ this amounts to a 25% reduction of the actual equilibrium TOPO concentration.

Thus, it is seen that in each case involving a complex haloauric acid and either TBP or TOPO there are three extractant molecules per gold atom. Since the formula for the extracting chloro acid was shown to be HAuCl_4 (and most surely the bromo complex is HAuBr_4), this leaves only the number of water molecules unac-

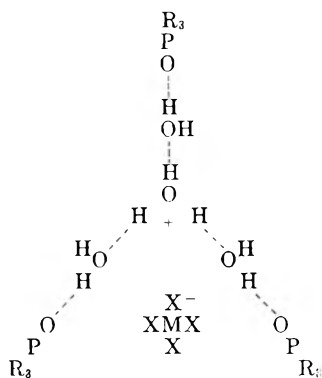
counted for. Unfortunately, it is difficult to determine water in submilligram quantities in the presence of an easily reducible metal ion, and such measurements were not attempted. However, it is possible to make a reasonable inference as to the minimum amount of water present in the complex.

From the fact that there are three TBP or TOPO molecules per HAuCl_4 , it may be assumed that there are three acidic bonding sites in the extracting acid. Since AuCl_4^- would not be expected to be an electron acceptor, the basic extractant molecules must be bonding to the proton. As tricoordinate protons are highly unlikely species, especially in view of the steric hindrance among the TBP (TOPO) molecules, it seems reasonable to assign to the proton an additional water molecule, making the cationic species H_3O^+ . Each TBP (TOPO) molecule is thus coordinated to one of the protons of the hydronium ion to make a total of three TBP (TOPO) per H_3O^+ . Indeed, in the previous studies of HClO_4 -TBP,¹⁷ HBr-TBP,¹⁹ and HClO_4 -TOPO,¹⁸ it was shown that the proton is extracted as the hydronium ion, with a TBP or TOPO molecule hydrogen bonded to each of the three hydrogen atoms. It seems that this model should also apply to HAuCl_4 , since the only difference in this case is that the metal complex acid probably is a slightly stronger acid and will extract better because of its larger size. By this reasoning, it is apparent that the minimum value of x in the haloauric systems may be set at 1, leading to the structure shown below.



This species should occur when the extractant is basic enough to compete with the water molecules for coordination to the hydrogen atoms of the hydronium ion. These conditions are met by the use of dilute TOPO solutions in CCl_4 , octane, etc., and so this is the species found for HClO_4 extracted by such systems¹⁸ and is the species assumed for the similar extraction of the haloauric acids. But with solutions of a more weakly basic extractant, additional molecules of water may appear in the complex. For example, the less basic nature of TBP enables water to compete more successfully with TBP for coordination to the H_3O^+ ion. As a result, in the studies of the HClO_4 -TBP and HBr-TBP systems,^{17,19} it was found that the

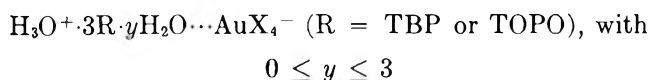
number of water molecules per proton extracted increased from 1 at an infinitely dilute TBP solution to about 2.5 at 10% by volume TBP in CCl_4 . The limiting case in pure TBP might well correspond to the fully trihydrated hydronium ion shown below which has the three TBP molecules hydrogen bonded to the first shell of water molecules. Several accounts of the existence and unusual stability of the ion $\text{H}_3\text{O}(\text{H}_2\text{O})_3^+$ in aqueous solution have been published,²²⁻²⁶ and



several authors have reported a ratio of $4\text{H}_2\text{O}/\text{H}^+$ for extraction into pure TBP.²⁷⁻²⁹ Again it might be expected that the haloauric acids would behave similarly to HClO_4 , and that the number of water molecules bound in the extracting complex would vary from 1 to 4 as the experimental conditions were varied.

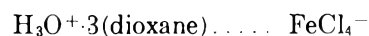
Conclusions

It thus appears that the formula for the extracting species can best be written as



and that a similar formula can be written for almost all of the other halometallic acids mentioned in the Introduction. That is, the general case will involve the extraction and trisolvation of a hydronium ion; the extent of hydration of the hydronium ion in the organic phase depends upon the base strength of the extractant and upon its concentration in the organic phase. It is worth noting at this point that the ratio $3\text{TBP}/\text{H}^+$ is not confined to acids of the general formula HMX_4 , but should be found for any strong acid. Preliminary studies on the extraction of Ag^+ from HBr solutions as, presumably, HAgBr_2 have also shown slope 3 in $\log\text{-}\log$ plots of D vs. TBP.³⁰ It appears that HSbCl_6 may also behave similarly,³⁰ although the experimental difficulties in the latter case are much greater.

Special mention should be made of the crystalline compound obtained by McCusker, *et al.*,⁶ since it is one of the few reported cases of the isolation from solution of a hydrated halometallic acid. The structure indicated in the Introduction seems a rather unlikely one for this type of compound, and, on the basis of the ideas presented in this paper, it might perhaps be more reasonable to formulate it as



Lastly, a comment should be made on the role of the anion in such strong acid extraction systems. If the anion is large, and very weakly basic, it passes into and remains in the organic phase as an ion. It does not coordinate with the basic extractant, but is essentially ejected from the aqueous into the organic phase because of its disturbance of the hydrogen-bonded water structure, much as is a molecule of CCl_4 . (The halometallic anions are similar to a molecule of CCl_4 carrying a single negative charge.) The degree of extraction is greater the larger, more weakly basic, and more hydrophobic is the anion. In low dielectric constant solvents, such as the CCl_4 , isooctane, and xylene of the present work, the anion ion pairs with the hydronium complex; in higher dielectric constant media, the ions are dissociated.²¹ If the anion is moderately basic, it will enter into the competition with water and extractant for solvating the proton. If it wins, forming the molecular acid, the extracting species into dilute extractant solutions will be monosolvated (*e.g.*, $\text{TBP} \cdot \text{HONO}_2$, $\text{TBP} \cdot \text{HO}_2\text{CCl}_3$, $\text{TOPO} \cdot \text{HONO}_2$), as there is then only one acidic site with which the extractant can bond.

Acknowledgment. The authors wish to acknowledge the aid of Mrs. Ursula Abed and Mrs. Eileen Burnett of the Lawrence Radiation Laboratory Analytical Group in the HAuCl_4 analyses.

- (22) M. Eigen and L. de Maeyer in "The Structure of Electrolytic Solutions," W. J. Hamer, Ed., John Wiley and Sons, Inc., New York, N. Y., 1959.
- (23) E. Wicke, M. Eigen, and T. Ackermann, *Z. physik. Chem.* (Frankfurt), **1**, 340 (1954).
- (24) M. Eigen and L. de Maeyer, *Proc. Roy. Soc. (London)*, **A247**, 505 (1958).
- (25) R. Grahn, *Arkiv Fysik*, **19**, 13 (1962).
- (26) H. D. Beckey, *Z. Naturforsch.*, **14a**, 712 (1959).
- (27) S. Siekierski and R. Gwózdź, *Nukleonika*, **5**, 205 (1960).
- (28) D. G. Tuck and R. M. Diamond, *J. Phys. Chem.*, **65**, 193 (1961).
- (29) W. H. Baldwin, C. E. Higgins, and B. A. Soldano, *ibid.*, **63**, 118 (1959).
- (30) D. C. Whitney and R. M. Diamond, unpublished work.

The Effect of Pressure on the Dissociation of Lanthanum Ferricyanide Ion Pairs in Water

by S. D. Hamann, P. J. Pearce, and W. Strauss

C.S.I.R.O. Chemical Research Laboratories, Division of Physical Chemistry, Fishermen's Bend, Melbourne, Australia, and Department of Chemical Engineering, University of Melbourne, Melbourne, Australia
(Received September 23, 1963)

This paper describes conductometric measurements of the influence of pressure on the molal dissociation constant K_m of lanthanum ferricyanide ion pairs in water at 25°. The value of K_m increases by a factor of 1.7 between 1 and 2000 atm., and the initial trend corresponds to a change in partial molar volume of -8.0 cm.³/mole for dissociation at 1 atm. The results agree quite well with the predictions of the ion-association theories of Bjerrum and of Fuoss, if it is assumed that the "contact distance," a , is independent of pressure and that the change of K_m arises only from the increases in dielectric constant and density which occur when water is compressed.

When two oppositely charged ions in solution separate from an associated state into a free ionic state, there is inevitably an increase in the total electrostatic interaction between the ions and their surrounding solvent molecules. It is this factor which is responsible for the large decrease of entropy which usually occurs when ion pairs dissociate.¹ It might be expected also that the increase in electrostriction would reduce the volume of the solution as a whole and, as a corollary, that an increase in hydrostatic pressure would shift the dissociation equilibrium toward the free-ion state. Fisher,² working in these laboratories, has observed such a displacement in aqueous solutions of the 2:2 electrolyte MgSO₄, for which the dissociation constant is almost doubled by raising the pressure from 1 to 2000 atm. at 25°.

In the present paper we report some similar measurements on solutions of the 3:3 electrolyte LaFe(CN)₆, which we expected to show rather larger pressure effects than MgSO₄ because of its higher valence.

Experimental

Method. The measurements were made by a conductivity method similar to that used by Fisher.²

To obtain the data needed to estimate the degree of dissociation of LaFe(CN)₆ under pressure it was necessary (i) to establish the way in which pressure alters the equivalent conductance Λ^0 of LaFe(CN)₆ at infinite

dilution, and (ii) to measure the equivalent conductance of LaFe(CN)₆ at particular pressures and at different finite concentrations of the salt.

The first end was achieved indirectly by measuring the conductances of aqueous solutions of KCl,² K₃Fe(CN)₆ and LaCl₃. For each salt the ratio Λ_P/Λ_1 of the equivalent conductance at the pressure P atm. to that at 1 atm. was determined at several concentrations. The results were then extrapolated to zero concentration and the ratios Λ_P^0/Λ_1^0 thus obtained were multiplied by the known values of Λ_1^0 for these salts (149.85,³ 172.6,⁴ and 146.0,³ respectively) to obtain Λ_P^0 . Then, by Kohlrausch's law

$$\Lambda_P^0[1/3\text{LaFe(CN)}_6] = \Lambda_P^0[1/3\text{LaCl}_3] + \Lambda_P^0[1/3\text{K}_3\text{Fe(CN)}_6] - \Lambda_P^0[\text{KCl}]$$

The values of $\Lambda_P[1/3\text{LaFe(CN)}_6]$ at finite concentrations were measured directly.

The details of the experimental arrangement and procedure have already been described by Fisher.²

Materials. Water. Conductivity water was ob-

- (1) G. H. Nancollas, *Discussions Faraday Soc.*, **24**, 108 (1957).
- (2) F. H. Fisher, *J. Phys. Chem.*, **66**, 1607 (1962).
- (3) R. A. Robinson and R. H. Stokes, "Electrolyte Solutions," Butterworths, London, 1959, p. 466.
- (4) J. C. James and C. B. Monk, *Trans. Faraday Soc.*, **46**, 1041 (1950).

tained from a mixed-bed deionizing column and had a conductivity of less than 5×10^{-7} mho.

Potassium Ferricyanide. Analytical grade salt was recrystallized from water and dried under reduced pressure over phosphorus pentoxide.

Lanthanum Ferricyanide. Following the method of Marsh,⁵ lanthanum oxide was dissolved in an equivalent amount of HCl and the solution diluted to give an oxide concentration of 100 g./l. To this solution, at 45°, the stoichiometric quantity of cold saturated $K_3Fe(CN)_6$ was added drop by drop, with vigorous stirring. The temperature was held between 40 and 50° and the stirring continued until sufficient red-brown precipitate had formed. The product was washed with water and dried between filter papers for several weeks. The lanthanum content was determined by titration with EDTA using xylenol orange as an indicator, and the ferricyanide content was determined by reaction with potassium iodide and back-titration with standard potassium thiosulfate. The analyses showed that the salt had the composition $LaFe(CN)_6 \cdot 5H_2O$, in agreement with the conclusion of Davies and James,⁶ and not $LaFe(CN)_6 \cdot 4.5H_2O$, as suggested by Prandtl and Mohr.⁷

Lanthanum Chloride. A solution was prepared by treating an excess of lanthanum oxide with HCl. The solution was filtered, diluted to about 0.1 N, and standardized by titration with silver nitrate using fluorescein as an adsorption indicator.

Results

The results are listed in Tables I–III and shown, in part, in Fig. 1 and 2. The values of Λ_P have been corrected for the change of conductance of the solvent and for the change of cell constant with changing pressure.^{2,8}

Table I: Relative Equivalent Conductance Λ_P/Λ_1 of Potassium Ferricyanide in Water at 25°

P, atm.	Concentration at 1 atm., equiv./l.					
	0.0441	0.0220	0.00500	0.00100	0.00050	0
1	1.0000	1.0000	1.0000	1.0000	1.0000	1.000
480	1.0126	1.0106	1.0121	1.0103	1.0115	1.011
985	1.0139	1.0108	1.0112	1.0072	1.0075	1.007
1495	1.0054	1.0013	0.9966	0.9942	0.9952	0.993
2000	0.9903	0.9845	0.9782	0.9748	0.9758	0.973

It should be noted that these corrections introduce some uncertainty into the results and that the absolute errors in the final data may be as great as $\pm 0.5\%$, although the reproducibility was better than that.

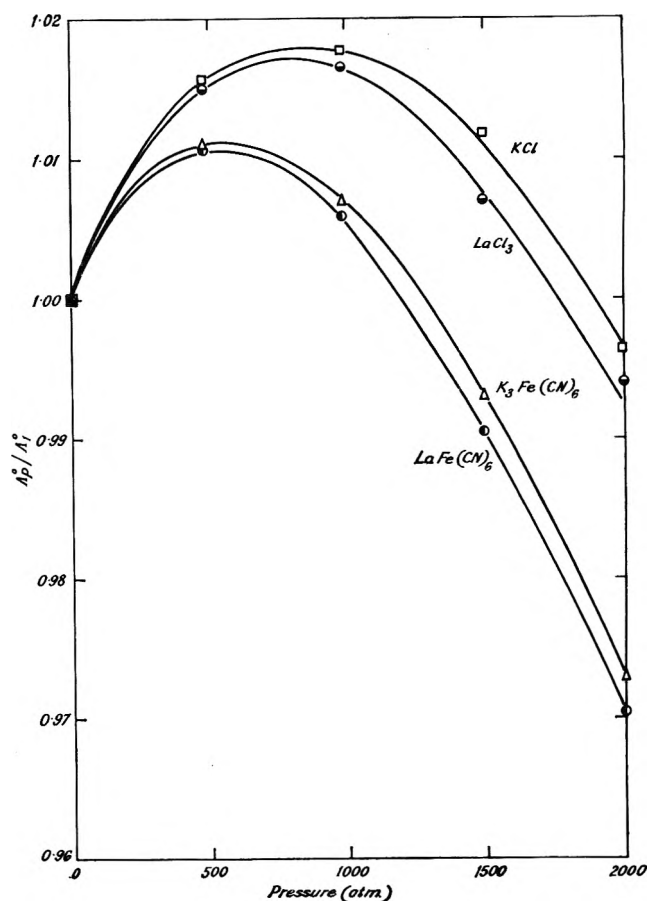


Figure 1. Limiting equivalent conductance ratios of several salts.

Table II: Relative Equivalent Conductance Λ_P/Λ_1 of Lanthanum Chloride in Water at 25°

P, atm.	Concentration at 1 atm., equiv./l.				
	0.0100	0.00502	0.00100	0.000502	0
1	1.0000	1.0000	1.0000	1.0000	1.000
480	1.0196	1.0202	1.0167	1.0164	1.015
985	1.0241	1.0239	1.0189	1.0187	1.016
1495	1.0200	1.0185	1.0120	1.0123	1.007
2000	1.0071	1.0063	0.9975	0.9985	0.994

Treatment of Results

There are several ways of treating the experimental data to derive values of the molal ion-pair dissociation constant K_m . Some of these procedures are based on

- (5) J. K. Marsh, *J. Chem. Soc.*, 1084 (1947).
- (6) C. W. Davies and J. C. James, *Proc. Roy. Soc. (London)*, **A195**, 116 (1949).
- (7) W. Prandtl and S. Mohr, *Z. anorg. allgem. Chem.*, **236**, 247 (1938).
- (8) S. D. Hamann and W. Strauss, *Trans. Faraday Soc.*, **51**, 1684 (1955).

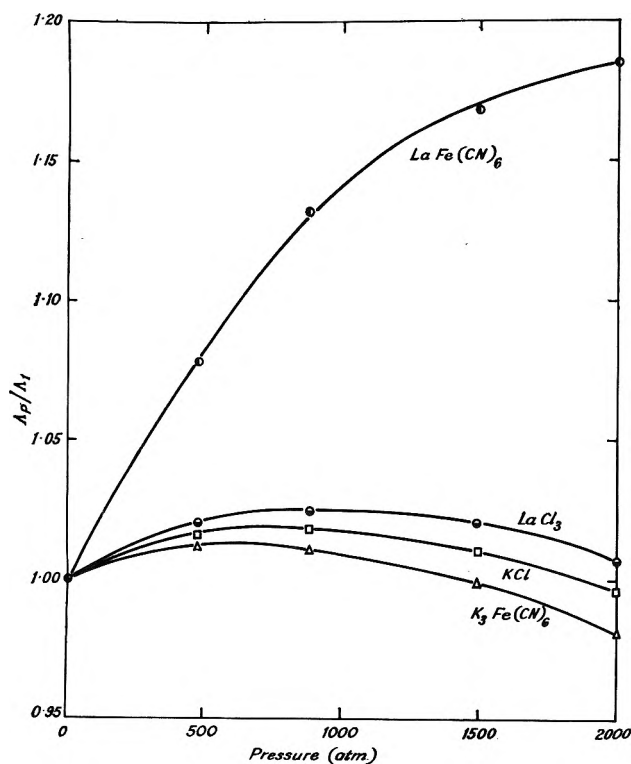


Figure 2. Equivalent conductance ratios of several salts at the concentration $c = 0.01 N$.

Table III: Equivalent Conductance Δp of Lanthanum Ferricyanide in Water at 25°

P, atm.	Concentration at 1 atm., equiv./l.					
	0.0102	0.00510	0.00204	0.00102	0.000510	0
1	58.3	67.2	83.2	97.5	112.1	168.7
480	62.8	71.9	88.2	102.7	117.1	170.5
985	66.0	75.2	91.6	105.9	119.8	169.7
1495	68.1	77.3	93.5	107.3	120.7	167.1
2000	69.1	78.3	94.3	107.6	120.3	163.7

empirical relations (e.g., Davies⁹ equation for activity coefficients) which involve parameters that may vary in an unknown way with a change of pressure: clearly they are unsuitable for the present purpose. Other, more rigorous, methods involve rather long computations which are hardly justified by the limited accuracy of our measurements. Here we have compromised by adopting the following method.

(i) For a pure aqueous solution of $\text{LaFe}(\text{CN})_6$ we define K_m by

$$K_m = \frac{m\alpha^2\gamma_{\pm}^2}{1 - \alpha} \quad (1)$$

where m denotes the molality of $\text{LaFe}(\text{CN})_6$, α denotes the degree of dissociation, and γ_{\pm} denotes the mean

molal activity coefficient of the free ions. This definition assumes that the activity coefficient of ion pairs is unity.

(ii) We further assume that γ_{\pm} may be replaced by f_{\pm} , the mean rational activity coefficient. The error introduced by this assumption is no greater than 0.03%.

(iii) We assume that f_{\pm} is given by the Debye-Hückel formula

$$-\log f_{\pm} = \frac{1.8246 \times 10^6 |z_1 z_2| I^{1/2}}{(\epsilon T)^{3/2} (1 + BqI^{1/2})} \quad (2)$$

in which $B = 5.029 \times 10^9 / (\epsilon T)^{1/2}$ cm.⁻¹ mole^{-1/2} l.^{1/2} (deg.)^{1/2}; z is ionic valence; ϵ is the dielectric constant; T is the temperature in °K.; I = ionic strength (= $3ac$); c is concentration in equiv./l.; and q is the distance of closest approach of the free hydrated ions, in cm.

(iv) Following Robinson and Stokes,¹⁰ we have put q equal to the Bjerrum critical separation

$$q = \frac{|z_1 z_2| e^2}{2\epsilon kT} \quad (3)$$

where k is Boltzmann's constant and e is the electronic charge. For a 3:3 electrolyte $q = 32.18 \text{ \AA.}$ at 25° and 1 atm.

(v) We assume that

$$\alpha = \Lambda_{\text{exptl}} / \Lambda_{\text{theor}}$$

where Λ_{theor} can be calculated from the relation

$$\Lambda_{\text{theor}} = \Lambda^0 - \left[\frac{R\Lambda^0}{1 + Bq(I/2)^{1/2}} + E \right] \frac{I^{1/2}}{1 + BqI^{1/2}} \quad (4)$$

used by Davies, Otter, and Prue.¹¹ Here

$$R = \frac{8.204 \times 10^{-7} |z_1 z_2|}{(\epsilon T)^{3/2}}$$

$$E = \frac{41.25 (|z_1| + |z_2|)}{\eta(\epsilon T)^{1/2}}$$

and η = viscosity of the solution.

In applying these formulas we have, in every instance, allowed for the influence of pressure on the values of ϵ^{12-15} and η^{16} and its effect on Λ^0 (Table III)

(9) C. W. Davies, *J. Chem. Soc.*, 2093 (1938).

(10) See ref. 3, p. 407.

(11) W. G. Davies, R. J. Otter, and J. E. Prue, *Discussions Faraday Soc.*, 24, 103 (1957).

(12) We have assumed that, at 25°, ϵ is given by the formula $\epsilon_p = \epsilon_1 / [1 - 0.4060 \log(1 + P/2885 \text{ atm.})]$, which is based on Owen and Brinkley's¹³ analysis of the high pressure measurements of Kyropoulos.¹⁴ The recent data of Owen, Miller, Milner, and Cogan¹⁵ are undoubtedly more accurate than those of Kyropoulos, but unfortunately it is impossible to extrapolate them safely beyond the experimental pressure limit of 1000 atm.

and c .^{17,18} The values of K_m so obtained are listed in Table IV and plotted on a logarithmic scale against $c^{1/2}$ and P in Fig. 3 and 4. It will be seen from Fig. 3 that K_m is by no means independent of c , which suggests that one or more of the assumptions used in deriving K_m is wrong. Nevertheless, it is probably justifiable to suppose that the intercepts in Fig. 3 are close to the true values of K_m . It is, in any case, clear from Fig. 4 that the pressure dependence of K_m (in which we are primarily interested) is independent of the concentration. Table IV includes values of the change of standard partial molar volume $\Delta \bar{V}^0$ for the dissociation of ion pairs, derived from the relation

$$\Delta \bar{V}^0 = - \frac{\partial RT \ln K_m}{\partial P}$$

Discussion

Figure 1 shows that, at infinite dilution, the conductivity ratios Λ_P^0/Λ_1^0 of the four salts all lie within

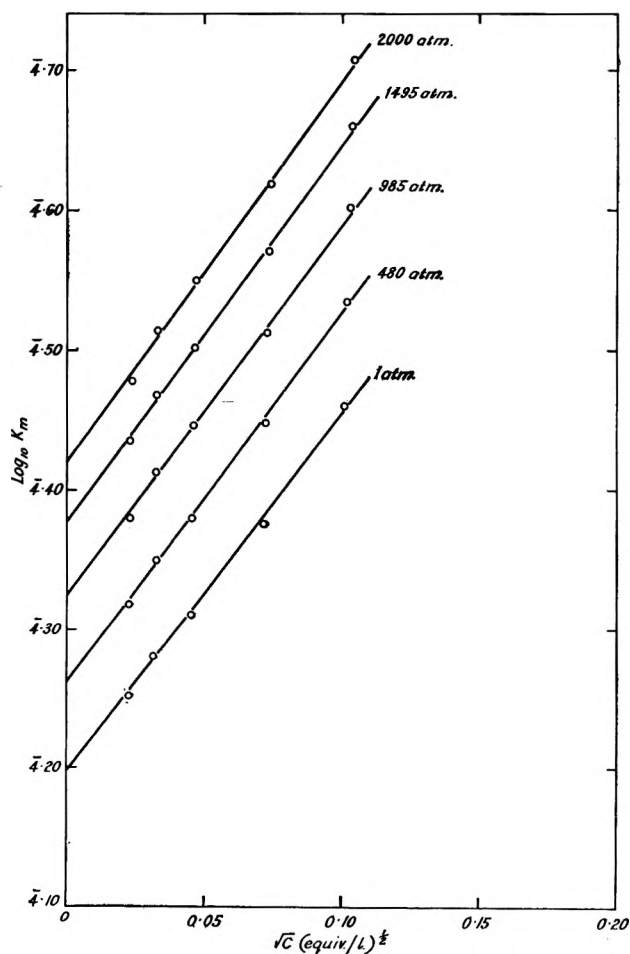


Figure 3. The molal dissociation constant of $\text{LaFe}(\text{CN})_6$ as a function of concentration at various pressures.

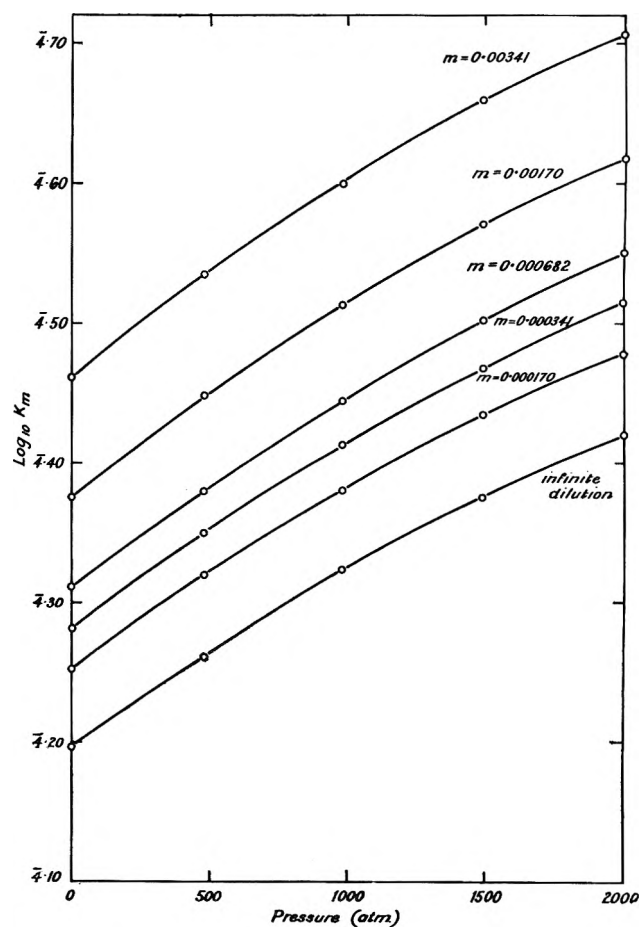


Figure 4. The molal dissociation constant of $\text{LaFe}(\text{CN})_6$ as a function of pressure at various molalities, m .

Table IV: Values of K_m and $\Delta \bar{V}^0$ for the Dissociation of Lanthanum Ferricyanide in Water at 25°

P, atm.	Concentration at 1 atm., equiv./l.					
	0.0102	0.00510	0.00204	0.00102	0.000510	0
1	2.889	2.382	2.048	1.909	1.788	1.574
480	3.432	2.804	2.398	2.239	2.086	1.824
985	3.989	3.258	2.784	2.591	2.402	2.109
1495	4.570	3.725	3.177	2.936	2.721	2.377
2000	5.088	4.155	3.549	3.270	3.007	2.630
	$\Delta \bar{V}^0$, cm. ³ /mole					
1	-9.2	-8.4	-8.2	-8.3	-8.1	-8.0
2000	-4.9	-5.0	-5.1	-4.8	-4.5	-4.6

- (13) B. B. Owen and S. R. Brinkley, *Phys. Rev.*, **64**, 32 (1943).
- (14) S. Kyropoulos, *Z. Physik*, **40**, 507 (1926).
- (15) B. B. Owen, R. C. Miller, C. E. Milner, and H. L. Cogan, *J. Phys. Chem.*, **65**, 2065 (1961).
- (16) P. W. Bridgman, *Proc. Am. Acad. Arts Sci.*, **61**, 57 (1926).
- (17) The change of c is very nearly proportional to the change in density of water, which we have taken from the tables of Dorsey.¹⁸
- (18) E. N. Dorsey, "Properties of Ordinary Water-Substance," Reinhold Publ. Co., New York, N. Y., 1940, p. 207.

1 or 2% of each other. The maxima in the curves are quite usual for salts in water and are probably associated with the minimum in the viscosity of water which Bridgman¹⁶ observed at about 1000 atm. There appears to be a small but real difference between the behavior of the chlorides and the ferricyanides, possibly caused by the bulkiness of the ferricyanide ions.

In contrast to the curves in Fig. 1, those in Fig. 2 show that at a finite concentration $\text{LaFe}(\text{CN})_6$ behaves quite differently from the other salts. Its conductivity rises much more steeply with increasing pressure; in fact, the salt behaves more like a weak acid or a weak base than a strong electrolyte.¹⁹ Irrespective of any detailed theory we can confidently ascribe the effect to an increase in the concentration of free ions with increasing pressure. From the quantitative treatment presented in the last section, it appears that the abnormal increase in conductivity of $\text{LaFe}(\text{CN})_6$ arises from a 1.7-fold increase in K_m between 1 and 2000 atm., corresponding to a volume change $\Delta \bar{V}^0$, for dissociation, of $-8.0 \text{ cm}^3/\text{mole}$ at 1 atm. Surprisingly, this value is remarkably close to the value $-7.3 \text{ cm}^3/\text{mole}$ for the dissociation of MgSO_4 .² Originally, we had expected the dissociation of a 3:3 electrolyte to cause a much greater increase of electrostriction than that of a 2:2 electrolyte; the fact that it does not indicates that factors other than the purely electrostatic one operate.

In this connection it is informative to consider the results in terms of the theories of ion association advanced by Bjerrum²⁰ and Fuoss.²¹ Bjerrum's model supposes that oppositely charged ions can be considered to be associated when their centers come within a critical distance q of each other, q being defined by eq. 3. The dissociation constant on the volume concentration scale is then given by

$$K_c = \frac{1000}{4\pi N Q(b)} \left(\frac{\epsilon k T}{|z_1 z_2| e^2} \right)^3 \quad (5)$$

where N denotes Avogadro's number and $Q(b)$ is a tabulated function of $b = 2q/a$, a being the distance between the centers of the ions when they are actually in contact. The remaining symbols have the same meanings as in eq. 2 and 3.

Fuoss,²¹ on the other hand, suggested that the ions should only be considered to form pairs when their centers are within the "contact distance" a of each other. From this criterion he arrived at the formula

$$K_c = \frac{3000}{4\pi N a^3 e^b} \quad (6)$$

The values of K_m corresponding to (5) and (6) are given

to a good approximation by dividing K_c by the density ρ of water at the temperature and pressure of the system.

For a given electrolyte in water at a fixed pressure and temperature, the theoretical value of K_m depends only on the distance of closest approach a , which is usually regarded as a parameter adjustable to fit the experimental value of K_m . Applying eq. 5 and 6 to our data and to those of Fisher,² we find the following values of a in water at 25° and 1 atm.

	Bjerrum	Fuoss
MgSO_4	4.19 Å.	3.87 Å.
$\text{LaFe}(\text{CN})_6$	7.04 Å.	7.36 Å.

If, now, we assume that a is independent of pressure, we can calculate the way in which K_m should vary with pressure, simply by allowing for the corresponding changes in ϵ^{22} and ρ .¹⁸ In particular we can estimate theoretical values of $\Delta \bar{V}^0$ from the derivatives

$$\begin{aligned} -\frac{\partial \ln K_m}{\partial P} &= \frac{\Delta \bar{V}^0}{RT} \\ &= \frac{\partial \ln \rho}{\partial P} + \frac{\partial \ln Q(b)}{\partial \epsilon} \frac{\partial \epsilon}{\partial P} - 3 \frac{\partial \ln \epsilon}{\partial P} \\ &\quad \text{(Bjerrum)} \\ &= \frac{\partial \ln \rho}{\partial P} + \frac{\partial b}{\partial \epsilon} \frac{\partial \epsilon}{\partial P} \\ &\quad \text{(Fuoss)} \end{aligned}$$

The first term in these formulas is simply the compressibility of the solution and the remaining terms depend only upon ϵ and $\partial \epsilon / \partial P$. Table V lists the calculated and experimental values of $\Delta \bar{V}^0$ at 1 atm. and Fig. 5 compares the calculated and experimental values of K_m over a range of pressures.

Table V: Values of $\Delta \bar{V}^0$ for the Dissociation of Ion Pairs in Water at 25° and 1 Atm.

	$\Delta \bar{V}^0, \text{ cm}^3/\text{mole}$		
	Bjerrum	Fuoss	Exptl.
MgSO_4	-4.86	-7.42	-7.3
$\text{LaFe}(\text{CN})_6$	-6.89	-8.98	-8.0

(19) S. D. Hamann, "Physico-Chemical Effects of Pressure," Butterworths, London, 1957, p. 129.

(20) See ref. 3, p. 393.

(21) See ref. 3, p. 551.

(22) Because the calculations are particularly sensitive to the way in which ϵ varies with P , we have based them on the accurate dielectric constant data of Owen, *et al.*¹⁵ As we mentioned in footnote 12, Owen's measurements were made to only 1000 atm. and to obtain the curves in Fig. 5 it was necessary to extrapolate the data to 2000 atm. The right-hand parts of the curves must therefore be considered to be only tentative.

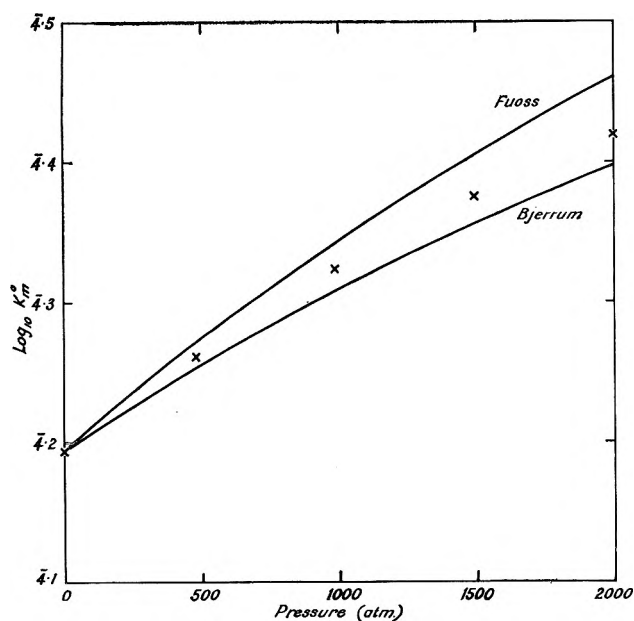


Figure 5. A comparison of the experimental results (shown as crosses) with the predictions of the theories of Bjerrum and of Fuoss.

The following points emerge from this analysis. First, the value of a is considerably greater for $\text{LaFe}(\text{CN})_6$ than for MgSO_4 and in consequence b (which is

proportional to $|z_1 z_2|/a$) is only slightly larger despite the higher valence of $\text{LaFe}(\text{CN})_6$. This compensation of effects explains the similarity in behavior of the two salts under pressure. The reason for the larger value of a may lie either in the bulkiness of the $\text{Fe}(\text{CN})_6^{3-}$ ion or in the existence of a permanent hydration shell around La^{3+} . It has been suggested previously¹ that the observed entropy of dissociation of $\text{LaFe}(\text{CN})_6$ is consistent with the idea that its ion pairs contain hydrated lanthanum ions and it is certainly significant that the solid salt contains water of crystallization (see the Experimental part of this paper). In this connection, also, the small value of $-\Delta\bar{V}^0$ (about half the volume of a water molecule) suggests that the ions are almost fully hydrated in the ion-pair state. From all this evidence, it is reasonable to suppose that an ion pair contains at least one water molecule sandwiched between the two ions.

Second, Table V and Fig. 5 show that both the theories of Bjerrum and of Fuoss agree sufficiently well with experiment to be useful in predicting ion-association equilibria at high pressures. It would, of course, be possible to obtain an exact fit of the present experimental data by allowing a to vary with pressure, but this would necessarily be an arbitrary procedure since there is no known theoretical relationship between a and the pressure.

Reactions of Deuterium Atoms with Olefins in Liquid Propane at 90° K.

Relative Rate Constants of the Addition

by T. T. Kassal and M. Szwarc

*Department of Chemistry, State University College of Forestry at Syracuse University, Syracuse 10, New York
(Received July 22, 1963)*

The addition of D atoms to a series of olefins and dienes was studied at 90°K. The deuterium atoms were formed on a hot tungsten wire in the gas phase and thereafter diffused into liquid propane where a homogeneous reaction took place. The relative rate constants of D atom addition to propylene, butene-1, pentene-1, hexene-1, and 3-methylbutene-1 were found to be nearly identical, the addition to isobutene and butadiene were found to be 5 and 25 times faster than to the terminal olefins, while the addition to pentene-2 and hexene-2 were half as high. Allene was found to be less reactive than the internal olefins. The usual pattern of reactivities is maintained even at this low temperature.

During the past five years, Klein and Scheer¹⁻⁶ have published a series of most interesting papers describing the reactions of a variety of olefins with H atoms. The substrates were condensed at temperatures below 100°K., while the atoms were produced in the gas phase by the dissociation of H₂ on a hot tungsten filament. Their results indicated a most unusual gradation of the reactivities of the investigated olefins and dienes. For example,² the reactivities toward H atoms at 77°K. appeared to decrease as follows: propylene > butene-1 > isobutene > 3-methylbutene-1 >> butadiene, while hexene-1 did not react at all. These findings aroused our interest since they are at variance with the normally observed gradations in reactivities of olefins and dienes toward free atoms and radicals.

The reactivity of a substrate was measured by the rate of hydrogen uptake, $\Delta p/\Delta t$, at a constant amount of the hydrogenated substance. However, many other factors might influence the result of such an experiment, e.g., the roughness coefficient of the surface, the transmission and solubility coefficients of the atoms, etc. In fact, the pronounced effect of the matrix on the apparent reactivity of an olefin was demonstrated in a recent paper by Klein and Scheer.⁷

It was decided, therefore, to develop a liquid system in which the investigated olefin or diene is dissolved and reacts under standard conditions. In such a system the rate of hydrogen uptake should correctly determine the relative reactivity of a substrate.

The Liquid Phase System. After an extensive investigation, it was found that liquid propane forms the most convenient solvent for low temperature experiments. Its melting point was reported to be 83°K., and carefully deaerated liquid propane containing a sufficient amount of solute remains fluid even at 77°K. Its inertness to D atoms at 90°K. was demonstrated by exposing the liquid to a high partial pressure of D atoms for periods as long as 1000 sec. Neither decrease of pressure nor the appearance of HD was observed.

The hydrogenation experiments were carried out in an apparatus shown in Fig. 1. A flat bottomed tube served as a reactor in which the solvent and the reagent were condensed. To standardize our procedure, we used the same amount of solvent in all the runs. The mixture was stirred magnetically at a constant, although rather slow rate, and it was demonstrated that small variations in the rate of stirring did not affect the results.

The tungsten filament used for production of D atoms was placed 12 cm. above the solvent's surface.

- (1) R. Klein and M. D. Scheer, *J. Am. Chem. Soc.*, **80**, 1007 (1958).
- (2) R. Klein and M. D. Scheer, *J. Phys. Chem.*, **62**, 1011 (1958).
- (3) M. D. Scheer and R. Klein, *ibid.*, **63**, 1517 (1959).
- (4) R. Klein, M. D. Scheer, and J. G. Waller, *ibid.*, **64**, 1247 (1960).
- (5) R. Klein and M. D. Scheer, *ibid.*, **65**, 324 (1961).
- (6) M. D. Scheer and R. Klein, *ibid.*, **65**, 375 (1961).
- (7) R. Klein and M. D. Scheer, *ibid.*, **66**, 2677 (1962).

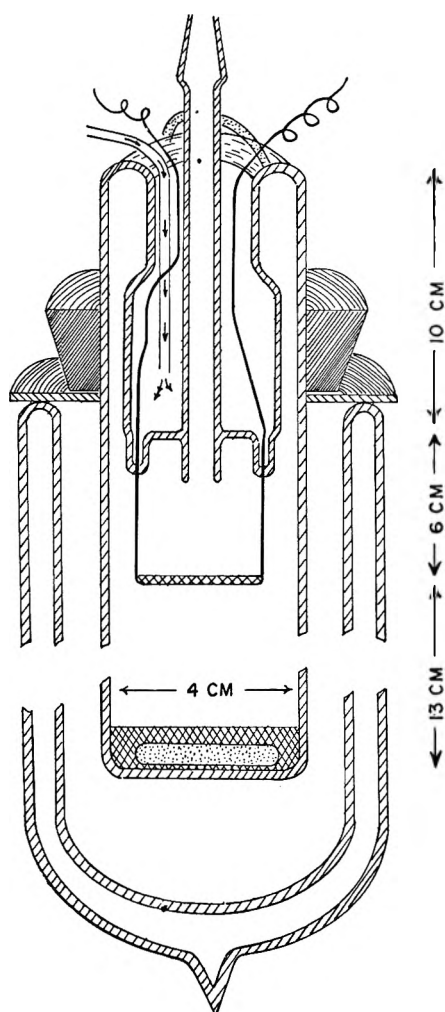


Figure 1.

In earlier experiments, a shield was introduced between the filament and the liquid to protect the solution from the heat radiation. However, it was found that this precaution is superfluous; even if the radiation slightly raised the temperature of the stirred liquid, the effect would be undetectable within the limits of our accuracy. No solvent evaporation was observed, since no cracking of the propane or the reagent on the hot filament was noticed.

In our technique it was essential to maintain a constant and reproducible partial pressure of D atoms in each series of experiments. This required constancy of filament temperature, standardization of the initial pressure of D_2 , and preservation of a fixed geometry of our apparatus. It was found that the temperature of the wire was constant for a constant voltage drop across the filament. The latter was maintained at the required level by a constant voltage transformer and by manually regulated Variacs. The heat was removed

from the filament mainly by radiation and by conductivity through the heavy leads; only a small fraction of the dissipated energy was carried away by the gas. The leads were kept at constant temperature by blowing air through the inner space leading to the electrodes (see Fig. 1), and the rest of the apparatus was thermostated by its immersion in the refrigerating liquid. The level of the coolant was kept constant during the experiment and during the period when the hydrogen pressure was measured. Moreover, an asbestos plate and a rubber stopper isolated the refrigerating liquid from the outside, thus preventing any cooling of walls not immersed in the dewar (see Fig. 1).

The constancy of the deuterium atom flux into the liquid was periodically checked by determining the D-uptake of pentene-1 at a constant concentration of the olefin. Whenever the filament had to be changed, the results were normalized by reinvestigating the addition to pentene-1 under a new set of conditions.

Thorough degassing of the solvent and solute was essential for reliability and reproducibility of the experiments. Chemically pure propane was first deaerated by the conventional freeze and thaw technique and by high vacuum distillation. The investigated olefin was treated similarly. The hydrocarbons then were distilled to thermostated pipets and from there into the reactor. In the reactor the liquid was stirred for about 1 hr. at $90^\circ K$. while the apparatus was connected to high vacuum pumps.

In a typical experiment, the investigated olefin and the solvent were condensed on the bottom of the reactor tube while the refrigerant covered only this part of the vessel that contained the investigated solution (about 1.25 cm. above the bottom of the reactor) and the stopcock leading to the vacuum line was closed. The walls of the tube above the surface of the cooled liquid then were heated with a hot air blower while the level of refrigerant was maintained on the level of the solution. This procedure removed any olefins condensed on the wall. Thereafter, the dewar was raised to a position shown in Fig. 1 and additional refrigerant was added if necessary and the system was pumped for a while. The required amount of deuterium was admitted into the reactor and the filament switched on for about 1000 sec. During this time any olefin molecules adsorbed on the wall were hydrogenated and thereafter the drop of pressure reflected the genuine rate of reaction in the liquid phase. The pressure was measured at various times and, of course, each reading was taken a few minutes after switching off the filament to allow the system to reach its standard state. A typical plot of Δp vs. time is shown in Fig. 2.

Three factors, namely, solubility, reactivity, and

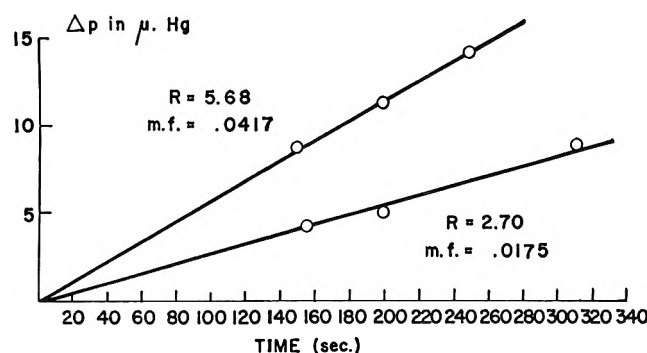


Figure 2. 3-Methylbutene-1 + propane.

volatility, impose a limitation upon the range of substrates which could be investigated by this technique. For example, ethylene was found too volatile to be studied in our system, whereas tetramethylethylene was not sufficiently reactive within the limits of its solubility.

Calculation of the Relative Rate Constants of D Atom Addition. At a fixed temperature of the wire and pressure of D_2 a stationary concentration of D atoms is established above the liquid propane. The partial pressure, p_D , of the atoms may be calculated with a reasonable accuracy from Langmuir's equation⁸ giving the equilibrium constant, K_{diss} , of the dissociation process $D_2 \rightleftharpoons 2D$ at the temperature of the wire, T_w , as a function of T_g , the temperature of the gas, and $\bar{\omega}$, the total rate of atom destruction by all the processes but their combination on the wire. The equation has the form $K_{diss} = (T_w/T_g)^{1/2}(p_D - \text{const.} \times \bar{\omega}T_g^{1/2})^2/p_{D_2}$, and it may be shown that $\bar{\omega}$ is sufficiently small to make p_D only slightly smaller than the value calculated on the basis $\bar{\omega} = 0$.

As a result of the diffusion of the atoms into the liquid a stationary state is established in which the concentration of the atoms, C_x , in a layer at depth x is given by the differential equation, $\mathcal{D}(d^2C_x/dx^2) = k_r C_x^2 + f_x k_{add}[\text{Olef}]C_x$. Here, \mathcal{D} denotes the diffusion constant of D atoms in the liquid, k_r is their bimolecular rate constant of recombination, k_{add} is their rate constant of addition to a substrate present at a concentration $[\text{Olef}]$, and f_x is a coefficient, determined by C_x and $k_{add}[\text{Olef}]$, which gives the fraction of the radicals formed in a layer at depth x that become hydrogenated through the addition of a second D atom. The solution of this equation, with the appropriate boundary conditions, gives C_x as a function of x and of the variable parameter $r = k_{add}[\text{Olef}]$. Denoting this function by the symbol $F(x,r)$ we may express the rate of D atom uptake by the integral

$$D \text{ atom uptake} = k_{add}[\text{Olef}] \int_0^\infty f_x F(x,r) dx = G(r)$$

It is implied that the olefin concentration remains constant throughout the whole liquid, an assumption which appears to be justified since the total amount of atoms reacting in a single experiment is much smaller than the amount of a substrate present in a layer as thin as 5×10^{-4} cm.

It was shown that no HD is formed under our experimental conditions, and therefore the experimentally measured $\Delta p/\Delta t$ is proportional to $G(r)$, the proportionality factor being determined by the volume of the reactor, the area of the liquid, and the temperature of the gas. Hence, if the same rate of pressure drop is observed in two experiments involving different substrates, say (1) and (2), the respective r_1 and r_2 must be identical, *i.e.*

$$k_{add, 2}/k_{add, 1} = [\text{Olef}_1]/[\text{Olef}_2] (\Delta p/\Delta t = \text{const.}) \quad (1)$$

Equation 1 permits the determination of the relative rate constants of D atom addition to a series of substrates. In our experiments pentene-1 was chosen as the standard olefin and all the relative rate constants refer to k_{add} for pentene-1 as unity. Finally, it should be noted that eq. 1 remains valid even if other transport processes participate in the reaction, assuming, of course, their reproducibility under standard conditions of the experiments.

Results

The drop of pressure Δp was measured for various time intervals Δt at a constant concentration of the substrate and at fixed operating conditions of the apparatus. From the resulting linear plot, illustrated in Fig. 2, $\Delta p/\Delta t$ was determined for a particular concentration of a substrate. By keeping the operating conditions constant but varying the substrate's concentration, a functional relationship was established for $\Delta p/\Delta t$ and the concentration, as exemplified by Fig. 3 and 4. The graphs, such as Fig. 4, allow the determination of the concentrations of various substrates corresponding to a constant $\Delta p/\Delta t$, and hence give the values of the respective k_{add} . Alternatively, these constants are given by the initial slopes of the lines shown in Fig. 4.

All the data obtained by this technique are collected in Table I. It should be noticed that in a series of substrates of nearly identical reactivity, the experimental points in graphs of $\Delta p/\Delta t$ vs. $[\text{Olef}]$ fall on a common line; see, *e.g.*, Fig. 4. Such lines perhaps give the best experimental evidence for closely similar reactivity of such olefins as propylene, butene-1, pentene-1,

(8) I. Langmuir, *J. Am. Chem. Soc.*, **37**, 417 (1915).

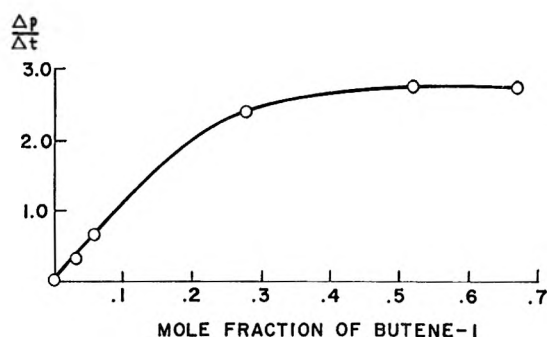


Figure 3. Total flux of D atoms at low filament temperature.

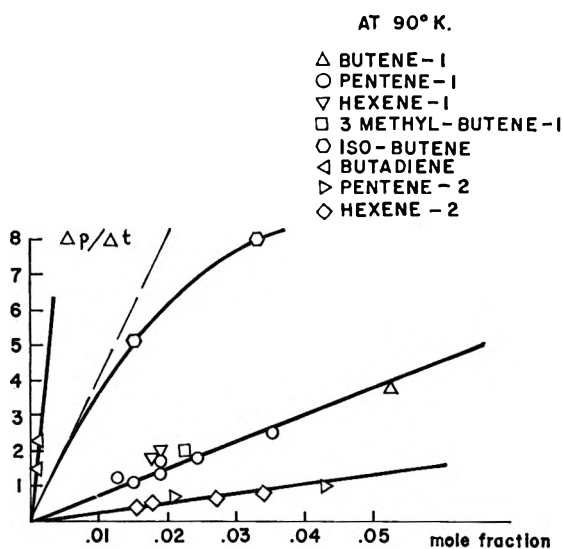


Figure 4. All lines with the exception of that observed for isobutene represent extrapolations of initial tangents. The curvature is observed only for isobutene, since in other experiments the rate, $\Delta p/\Delta t$, was too low to give appreciable deviation from linearity.

Table I: The Relative Rate Constants of D Atom Addition to Olefins in Liquid Propane at 90°K., the Rate Constant of Addition to Pentene-1 Being Taken as Unity

Olefin	k_{oc} (relative)
Propylene	1.0
Butene-1	0.95
Pentene-1	(1.00)
Hexene-1	1.4
3-Methylbutene-1	1.2
Isobutene	4-5
Butadiene	25
Pentene-2	0.5
Hexene-2	0.5
Allene	~0.4

hexene-1, 3-methylbutene-1, etc., or pentene-2 and hexene-2.

Discussion

The results shown in Table I or in Fig. 4 prove that even at this low temperature the α -monoolefins possessing the terminal group $-\text{CH}=\text{CH}_2$ are equally reactive toward D atom addition. The small variations in the observed rate constant may be real, although they are within the experimental uncertainties. Isobutene was found to be 4-5 times as reactive as the olefins of the previous class and butadiene was the most reactive substrate in the investigated series of compounds. The normal pattern of reactivity, as illustrated by their methyl affinities⁹ determined in the temperature range 0-100°, is preserved even at 90°K.

The olefins with internal double bonds $-\text{CH}=\text{CH}-$ are by a factor of two less reactive than the terminal olefins, *i.e.*, the reactivity per carbon center seems to decrease by a factor of ~ 4 . The low reactivity of allene parallels its low methyl affinity¹⁰ which was found to be lower than that of propylene or butene-1.

It seems, therefore, that the low temperature does not introduce any anomalies in kinetic behavior.

Acknowledgment. We wish to thank the Office of Ordnance Research Durham, for financial support of this work through Grant DA-ORD-31-124-61-G72.

Appendix

The Transmission Coefficient for D Atom Penetration through the Surface of Liquid Propane. Increase in the olefin concentration leads eventually to trapping of all the atoms that penetrated through the liquid surface. Under these conditions C_0 , the concentration of the atoms in the highest layer of the liquid, falls down to zero. For practical reasons, experiments leading to trapping of all the atoms may be performed only at low temperature of the wire; otherwise, the required concentration of the scavenger would be impossibly high.

The pertinent experiments were performed at $T_w = 1400^\circ\text{K}$. and are presented graphically in Fig. 3. The plateau value corresponds to flux of 2.2×10^{-10} mole of D/cm² sec., the concentration in the gas phase was calculated from Langmuir's equation to be 5×10^{-12} mole of D/cm³, and hence the transmission coefficient for D atom penetration through the surface of liquid propane at 90°K. is about 10^{-3} .

The existence of a plateau proves that the reaction takes place *in* the liquid and not *on* the surface.

(9) M. Feld and M. Szwarc, *J. Am. Chem. Soc.*, **82**, 3791 (1960).

(10) A. Rajbenbach and M. Szwarc, *Proc. Roy. Soc. (London)*, **A251**, 394 (1959).

Calculation of the Ostwald Solubility Coefficient for Hydrogen Atoms and the Absolute Rate Constants of Their Addition to Propylene

by M. Szwarc

*Department of Chemistry, State University College of Forestry at Syracuse University, Syracuse, New York
(Received November 8, 1963)*

The Ostwald solubility coefficient for H atoms in butane at 77°K. was calculated from the data of Klein and Scheer. The results show that the heat of solution of H atoms is about 0.1 kcal./mole, *i.e.*, the polarizability of H is higher than that of He or H₂ and slightly lower than that of argon. The absolute rate constant of H atom addition was calculated to be 1×10^8 cc./mole. sec., *i.e.*, it seems to be only slightly higher than the value proposed by Klein and Scheer.

In an elegant paper, Klein, *et al.*,¹ attempted to determine the absolute rate constant for H atom addition to propylene dissolved in butane at 77°K. They assumed that the addition of H atoms is much faster than their combination and on this basis they found $k_{\text{add}}[\text{H}] = 2.5 \times 10^{-2}$ sec.⁻¹ and $(k_{\text{add}}\mathcal{D})^{1/2}[\text{H}] = 8 \times 10^{-8}$ mole^{1/2} cm.^{-1/2} sec.⁻¹. The derivation of the absolute rate constant was then based on an arbitrary assumption, namely that the Ostwald solubility coefficient of H atoms in butane is unity at 77°K.

We shall show now that this assumption, which turned out to be nearly correct, is unnecessary and further information may be derived from Klein and Scheer's data. It is essential to prove that the basic assumption of the relatively slow combination of H atoms is correct. This is shown by Klein and Scheer in their following paper² where the absence of the reaction $\text{C}_3\text{H}_6\text{D} + \text{D} \rightarrow \text{C}_3\text{H}_6\text{D}_2$ was demonstrated in the system in which the reaction $\text{C}_3\text{H}_6 + \text{D} \rightarrow \text{C}_3\text{H}_6\text{D}$ did occur. On this basis, we may write the inequality

$$k_{\text{add}}[\text{propylene}] \geq 10k_r[\text{H}]$$

where k_r denotes the bimolecular recombination constant of H atoms in butane, the coefficient 10 indicating that no more than 10% of the atoms recombine. The recombination is diffusion-controlled and hence

$$k_r/\mathcal{D} = 4\pi\rho N$$

where \mathcal{D} is the diffusion constant of H atoms, ρ their collision radius, and N the Avogadro number. Taking

the reasonable value $\rho = 0.5 \text{ \AA.}$, one finds $k_r/\mathcal{D} = 3.8 \times 10^{16}$ and this in conjunction with the findings of Klein, *et al.*,¹ *i.e.*, $k_{\text{add}}/\mathcal{D} = 10^{11}$, leads to $k_r/k_{\text{add}} = 3.8 \cdot 10^5$. Substituting this value into the above inequality and knowing the concentration of propylene to be 10^{-3} mole/cc. we find $[\text{H}] \leq 2.6 \times 10^{-10}$ mole/cc.; $k_{\text{add}} \geq 10^8$ cc./mole sec.; $\mathcal{D} \geq 1 \times 10^{-3}$ cm.²/sec.; and $k_r \geq 3.8 \times 10^{13}$ cc./mole sec.

It is improbable that either \mathcal{D} or k_r would be much greater than their limit and hence the lower limits give the approximate values of these constants. This scheme is, of course, self-consistent, giving the rate of addition 10 times greater than the rate of H recombination.

The concentration of H atoms in the gas phase is calculated on the basis of Langmuir's equation³ to be 2×10^{-10} mole/cc. Therefore, the Ostwald solubility coefficient of H atoms at 77°K. is only slightly larger than unity. The entropy change for this process may be taken to be the same as for the transfer of He from the gas phase into the equal concentration of He atoms in liquid butane. The latter may be calculated from the data of Gross, *et al.*,⁴ and gives $\Delta s = 1.5$ e.u. Hence, the heat of solution of H atoms in

- (1) R. Klein, M. D. Scheer, and J. G. Waller, *J. Phys. Chem.*, **64**, 1247 (1960).
- (2) R. Klein and M. D. Scheer, *ibid.*, **65**, 324 (1961).
- (3) I. Langmuir, *J. Am. Chem. Soc.*, **37**, 417 (1915). The calculation given in ref. 1 leads to $[\text{H}]_g = 5 \times 10^{-10}$ since the factor $(T_l/T_g)^{1/4}$ of Langmuir's equation was omitted.
- (4) H. L. Clever, R. Battino, J. H. Saylor, and P. M. Gross, *J. Phys. Chem.*, **61**, 1078 (1957).

liquid butane is +0.1 kcal./mole. This value compares reasonably with $\Delta H = +1.8$ kcal./mole determined⁴ from the solubility of He in hydrocarbon solvents and $\Delta H = -0.3$ kcal./mole for Ar. The polarizability of H atom seems, therefore, to be larger than that of He and of H₂ ($\Delta H \sim 1.5$ kcal./mole⁵), and it is only slightly smaller than that of argon.

In the system of Kassal and Swarc⁶ at 90°K., the concentration of D atoms is calculated to be 5×10^{-11} mole/cc. in the gas phase.

The rate of the addition was 2×10^{-10} mole of D/cc. sec. for [propylene] = 5×10^{-4} mole/cc. Accepting the activation energy of the addition to be 1.4 kcal./mole (*i.e.*, the apparent activation energy, determined by Klein and Scheer,⁷ minus $\Delta H = 0.1$) we anticipate the rate constant of the addition to be 4×10^8 moles/cc. sec. The addition is therefore ~ 20 times as fast as the atom recombination in the highest level of the liquid, if $C_0 = C_{\text{gas}}$. The system is therefore represented by the equation

$$\mathfrak{D}(d^2C_z/dz^2) = k_{\text{add}}[\text{olefin}]Cx$$

leading to the rate of D uptake = $(k_{\text{add}}[\text{olefin}]\mathfrak{D})^{1/2}$, C_0 . We may now calculate the concentration C_0 of D atoms in the highest layer of the liquid propane. Having the values for the concentration of propylene and the rate of D atom uptake and accepting the above

values for k_{add} and \mathfrak{D} , we find $C_0 = 3 \times 10^{-11}$ mole/cc. From the plateau D atom uptake shown in Fig. 3 of the preceding paper, we calculate that the exchange of atoms between the gaseous and liquid phase is 10 times faster than the rate of the addition, and therefore the saturation value for $C_0 = 3.3 \times 10^{-11}$ mole/cc. The Ostwald solubility coefficient again is approximately unity.

It may be remarked that the system of Kassel and Swarc could be treated on the assumption that the recombination is much faster than the addition. The results derived on that basis were internally self-consistent⁸ but led to the Ostwald solubility coefficient of about 10^3 and $\Delta H = -1.5$ kcal./mole. The k_{add} derived on this basis was $\sim 7 \times 10^5$ cc./mole sec. at 90°K. and the activation energy increased to ~ 3 kcal./mole. The absence of HD in the products was, however, the strongest argument against the assumption: rate of combination \gg rate of addition.

Acknowledgment. We wish to thank the Office of Ordnance Research, Durham, for financial support of this work through Grant DA-ORD-31-12461-G72.

-
- (5) S. Peter and M. Weinert, *Z. physik. Chem.*, **5**, 114 (1955).
 - (6) T. T. Kassal and M. Swarc, *J. Phys. Chem.*, **68**, 381 (1964).
 - (7) R. Klein and M. D. Scheer, *ibid.*, **65**, 375 (1961).
 - (8) T. T. Kassel, Ph.D. Thesis, Syracuse University, 1963.

Calorimetric Investigations of Molten Salts

by Teh Hu, Hon Chung Ko, and Loren G. Hepler

Department of Chemistry, Carnegie Institute of Technology, Pittsburgh, Pennsylvania
(Received July 15, 1963)

A calorimeter for measurement of heats of solution and heats of reaction in molten salts at temperatures up to about 400° is described. This calorimeter has been used for measurements of the heat of solution of NaCl(c) and NaNO₃(liq) at 350° ($\Delta H^\circ = 6.04$ kcal./mole), heat of fusion of NaNO₃ ($\Delta H^\circ = 3.57$ kcal./mole), and heat of precipitation of AgCl in NaNO₃-KNO₃ eutectic mixture at 320° ($\Delta H^\circ = -18.9$ kcal./mole). Some thermodynamic calculations for the NaCl-NaNO₃ system are reported.

Most of the relatively small number of calorimetric investigations of systems involving molten salts have been carried out by means of drop calorimetry. Accurate heats of fusion of a number of salts have been obtained by drop calorimetry and can be so determined for many other salts, but materials that are slow to reach a well defined thermodynamic state in the room temperature part of a drop calorimeter present difficulties. Further, the drop method is not generally well suited for obtaining heat of solution and reaction data for molten salt systems. Partly because of these difficulties associated with investigations of molten salt systems and partly to obtain data relevant to earlier work, we have built a solution calorimeter for use with molten salts and have used this apparatus for three kinds of investigations. These are (i) the determination of the heat of fusion of a salt, (ii) the determination of the heat of solution of a solid salt in a molten salt, and (iii) the determination of the heat of precipitation of a slightly soluble salt.

We believe that the recent work of Kleppa and Jordan, some of which is discussed below, and our work reported here illustrate clearly the value of investigations of molten salt systems by means of solution calorimetry.

Experimental

Our apparatus may be described in outline as a furnace containing a massive aluminum block in which the calorimeter (a dewar vessel) is placed. A complete account by Hu¹ of the construction and operation of this apparatus is summarized below.

The calorimeter furnace consists of an aluminum

barrel that is surrounded by Kaylo insulation and enclosed in a chemical drum that is itself enclosed in a wooden box. Grooves have been made on the top, side, and bottom of the furnace to accommodate aluminum tubes. Inside each aluminum tube a nichrome wire heater is strung through a 4-hole porcelain tube. One of the heaters is controlled by a Minneapolis-Honeywell Pyr-O-Vane temperature controller that is actuated by a chromel-alumel thermocouple connected to the inside wall of the side of the furnace. The other heaters were controlled manually by Variacs, which were adjusted by trial and error until temperature gradients in the furnace were eliminated as determined by various differential thermocouples attached to the walls. Temperature fluctuations of the furnace were generally less than 1° and always less than 2°.

Sitting inside the furnace on three stainless steel legs is a cylindrical aluminum block that was kindly donated to us by J. A. Nock, Jr., of the Alcoa Research Laboratories. This block has been grooved to accommodate heaters like those on the furnace. These heaters are used to bring the block up to the desired temperature but are never used during the course of a calorimetric run. A chromel-alumel thermocouple is connected to the block. Two cavities have been machined in the block to accommodate two silvered, highly evacuated dewar vessels that hold about 280 ml. each. The block weighs 25 kg. and the two plugs mentioned below weigh 4 kg. each.

Two aluminum plugs that fit into the cavities above

(1) T. Hu, Ph.D. Thesis, Department of Chemistry, Carnegie Institute of Technology, 1963.

the dewars in the block are permanently fastened to the larger aluminum plate that serves as lid for the chemical drum and wooden box. Kaylo insulation is fastened between the upper plate and the furnace lid.

Holes have been drilled in the plugs and lids to permit introduction of the calibrated resistance thermometer, the Pyrex stirrers, sample containers, and lead wires for calibration heaters.

Calibration heaters of 190–200 ohms have been made by winding Secon 0.075-mm. diameter alloy 406 ceramic insulated wire on a welding rod to make coils of wire which were slipped off the rod and inserted in Pyrex coils made of 5-mm. tubing. These glass coils were then fastened in holes in the undersides of the plugs over the dewar vessels. After the heaters were in place, the insulation was cured by heating.

The sample containers for the material to be dissolved in the molten salt in the dewar were 5×16 -mm. Pyrex test tubes blown to have thin-walled bottoms. These tubes were suspended from the bottoms of the plugs by means of nichrome wire hooks that fit through small holes near the top of each tube. The hooks and tubes were of such length that the samples were about 2 cm. below the surface of the molten salts in the dewars. The samples were introduced at the appropriate time by breaking the bottom of the sample tube with a 6-mm. Pyrex tube that extended through the entire upper assembly. Gold pellets could also be introduced by dropping them into the tube used for breaking the sample container.

Resistances of the platinum resistance thermometer were determined with a Leeds and Northrup G-2 Mueller bridge with HS2284-d galvanometer. Thermocouple measurements were made with a Leeds and Northrup K-3 potentiometer and Type E galvanometer. The K-3 and Type E instruments were also used for determining power input in the calibration heaters, which were powered by five 6-v. storage batteries. The durations of the heating periods were determined with a standard electric timer that could be read to 0.01 sec.

The block was made with two cavities to hold two dewars so that two experiments could be made when the apparatus was heated up and so that the apparatus can later be used for twin calorimetry.

Our operating procedure for the calorimetric apparatus described here was as follows. First the furnace and block (with dewar vessels) were brought to and maintained at the desired temperature. Then the top plate and furnace lid were lifted so the dewars could be filled with known amounts of the appropriate pre-heated molten salt and loaded sample tubes hung from the nichrome hooks. After the top plate and

furnace lid were back in place, the entire assembly was allowed to stand for at least 1 hr. to approach thermal equilibrium before actual measurements were begun. The first measurements consisted of determination of the thermometer resistance as a function of time until a satisfactorily steady temperature drift was observed. Temperature drifts were ordinarily about 6×10^{-3} deg./min. and drift uncertainties less than 4×10^{-4} deg./min. After a steady temperature drift had been observed for several minutes, calibration was begun. This calibration was usually accomplished electrically, but was done a few times by dropping a known mass of gold into the calorimeter. During a heating period potential measurements were made across a resistance in series with the heater and across the smaller of two resistances in parallel with the heater. Heating periods were of 60–150 sec. duration. Temperature drifts were obtained after the heating period and then the sample was introduced by breaking the sample tube. After a steady temperature drift was again observed, the calibration procedure was repeated. Then the same procedure was followed for the second dewar.

All of the reactions studied were rapid; steady drifts being observed 2–3 min. after the sample was introduced. Observed values of ΔT were about 0.01° for solution of $\text{NaNO}_3(\text{liq})$ in the $\text{NaNO}_3\text{--KNO}_3$ mixture and were between 0.08 and 0.44° for the other reactions.

Results and Discussion

Heats of solution of $\text{NaCl}(\text{c})$ in 470–510 g. of molten NaNO_3 at 350° have been measured with results given in Table I. On the basis of these data, ΔH_{soln} to form an infinitely dilute solution at 350° is taken to be 6.04 ± 0.06 kcal./mole, where 0.06 is thrice the average deviation from the average.

Table I: Heats of Solution of $\text{NaCl}(\text{c})$ in $\text{NaNO}_3(\text{liq})$ at 350°

NaCl. g.	Mole fraction of NaCl	ΔH , kcal./mole
0.8312	0.002510	6.04
0.7386	0.002315	6.04
0.6393	0.001938	6.07
0.5325	0.001619	5.99

Kleppa and Meschel² have measured heats of solution of NaCl in NaNO_3 at 454° . In their experiments, the mole fraction of NaCl ranged between 0.1 and 0.2, compared to our measurements in which the mole

(2) O. J. Kleppa and S. V. Meschel, *J. Phys. Chem.*, **67**, 688 (1963).

fraction of NaCl ranged from 0.0016 to 0.0025. Kleppa and Meschel extrapolated their results to obtain a limiting $\Delta H_{\text{soln}} = 6.40$ kcal./mole at 454° . They have also deduced that $\Delta C_p = 2.2$ cal./deg. mole for solution of NaCl in NaNO_3 . Using their value of ΔC_p , it is here calculated from their data that $\Delta H_{\text{soln}}^\circ = 6.17$ kcal./mole at 350° , which is in good agreement with our results.

Previous investigations³ of the solubility of NaCl in NaNO_3 from 300 to 440° yielded data that can be used with the solubility equation for ideal solutions to estimate that $\Delta H_{\text{soln}} \cong 6.4$ kcal./mole. Since this value is close to that determined calorimetrically, indicating that the NaCl- NaNO_3 system is close to ideal, we are led to the following calculation.

The van't Hoff equation for the temperature coefficient of solubility can be written

$$\frac{d \ln N_2 \gamma}{dT} = \frac{\Delta H_{\text{soln}}^\circ}{RT^2}$$

where N_2 is the mole fraction of solute in saturated solution and γ is the appropriate activity coefficient. Integration of the above equation gives

$$\ln N_2 \gamma = -\frac{\Delta H_{\text{soln}}^\circ}{RT} + C$$

The above mentioned indication that the NaCl- NaNO_3 system is nearly ideal suggests that $\ln \gamma$ might be expressed as the first term in a power series of the mole fraction of solute; that is

$$\ln \gamma = kN_2 + \dots$$

Combining the two preceding equations and rearranging gives

$$\ln N_2 + \frac{\Delta H_{\text{soln}}^\circ}{RT} = -kN_2 + C \quad (1)$$

A plot of the left side of (1) (solubility data from Hu and Ko,³ $\Delta H_{\text{soln}}^\circ$ from this paper) against N_2 at temperatures ranging from 310 to 360° gives a straight line from whose slope it is calculated that $k \cong -1.5$, leading to

$$\ln \gamma \cong -1.5N_2; \log \gamma \cong -0.65N_2 \quad (2)$$

At 350° N_2 for saturated solution is 0.102 and it is calculated from (2) that $\gamma = 0.86$ for NaCl in this saturated solution.

The heat of fusion of NaNO_3 has been determined calorimetrically by measuring the heats of solution of solid and liquid NaNO_3 in NaNO_3 - KNO_3 eutectic. Results of measurements of heats of solution of solid NaNO_3 at temperatures below the melting point of

NaNO_3 (307°) are given in Table II. Results of measurements of heats of mixing liquid NaNO_3 with the KNO_3 - NaNO_3 eutectic at temperatures above 307° are given in Table III.

Table II: Heats of Solution of $\text{NaNO}_3(\text{c})$ in KNO_3 - NaNO_3 Eutectic

g. of NaNO_3 / 500 g. of eutectic	t , $^\circ\text{C}$.	ΔH , kcal./mole
1.1433	297.4	3.51
1.2076	294.7	3.49
1.3231	294.2	3.50
1.6555	293.8	3.55
0.9981	292.4	3.52

Table III: Heats of Solution of $\text{NaNO}_3(\text{liq})$ in KNO_3 - NaNO_3 Eutectic

g. of NaNO_3 / 500 g. of eutectic	t , $^\circ\text{C}$.	ΔH , kcal./mole
1.0384	321.0	-0.043
1.2009	313.0	-0.029
1.4880	322.2	-0.047

The data in Table II lead to $\Delta H_{\text{soln}} = 3.53$ kcal./mole for solution of $\text{NaNO}_3(\text{c})$ at 307° . In obtaining this result, ΔC_p of solution was taken to be 1.3 cal./deg. mole as for melting.⁴ Taking $\Delta C_p = 0$ for mixing liquid NaNO_3 with the liquid eutectic, we obtain $\Delta H_{\text{mix}} = -0.04$ kcal./mole at 307° . Then $\Delta H_{\text{fusion}} = \Delta H_{\text{soln}} - \Delta H_{\text{mix}} = 3.57$ kcal./mole for NaNO_3 .

Various earlier workers have reported values of ΔH_{fusion} of NaNO_3 ranging from 3.16 to 3.80 kcal./mole, as discussed previously.³

In our own earlier work³ in which $\Delta H_{\text{fusion}} = 3.60 \pm 0.10$ kcal./mole was calculated from freezing points of dilute solutions of NaCl and other salts in NaNO_3 , it was implicitly assumed that activity coefficients were nearly unity. The mole fraction of NaCl in those experiments ranged from 0.002 to 0.01. For a value of $N_2 = 0.005$, eq. 2 yields $\gamma_2 = 0.993$.

From the Gibbs-Duhem equation relating activities of the components of a solution⁵

- (3) H. C. Ko, T. Hu, J. G. Spencer, C. Y. Huang, and L. G. Hepler, *J. Chem. Eng. Data*, **8**, 364 (1963); M.S. Thesis of T. Hu, University of Virginia, 1961; M.S. Thesis of H. C. Ko, University of Virginia, 1961.
- (4) K. K. Kelley, "Contributions to Data on Theoretical Metallurgy," U. S. Bureau of Mines, Bulletin 584, 1960.
- (5) I. M. Klotz, "Chemical Thermodynamics," Prentice-Hall, Inc., Englewood Cliffs, N. J., 1950.

$$\ln \gamma_1 = - \int_{N_2=0}^{N_2} \frac{N_2}{N_1} d \ln \gamma_2 \quad (3)$$

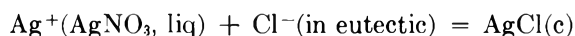
where subscripts 1 and 2 refer to components we call solvent and solute. Combination of $d \ln \gamma_2 = kdN_2$ from eq. 2 with eq. 3 and integration leads to

$$\log \gamma_1 = -0.65N_2 - 1.5 \log N_1 \quad (4)$$

For $N_2 = 0.005$ and $N_1 = 0.995$, we calculate from eq. 4 that $\gamma_1 = 1.0001$.

These calculations support previous assumptions by ourselves and others that dilute solutions of NaCl (and other salts used in the freezing point experiments³) in NaNO₃ may be treated as being thermodynamically ideal and that solutions having $N_2 = 0.1$ are not far from ideal.

We have measured the heat of precipitation of AgCl(c) in the NaNO₃-KNO₃ eutectic at 320°. To make these measurements, a slight excess of NaCl was dissolved in the eutectic and then the heat associated with adding liquid AgNO₃ to the eutectic solution was measured. The calorimetric reaction may be written

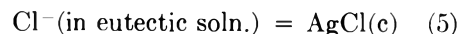


The calorimetric results are given in Table IV.

Table IV: Heats of Precipitation of AgCl at 320°

g. of AgNO ₃ / 500 g. of eutectic	ΔH , kcal./mole
0.7298	-18.80
0.7806	-18.93
0.5523	-18.83
0.9566	-18.90

Since Kleppa, Clarke, and Hersh⁶ have shown that mixing liquid AgNO₃ with liquid NaNO₃ or KNO₃ is slightly endothermic, we take $\Delta H_{\text{ppt}} = 18.9 \pm 0.1$ kcal./mole for the reaction



Blander, Braunstein, and Silverman⁷ have recently applied rigorous thermodynamic methods to analysis of solubility and e.m.f. data on AgCl in KNO₃ and have calculated $\Delta H^\circ = +19.2 \pm 0.6$ kcal./mole for solution of AgCl(c) in molten KNO₃ in the temperature range from 350 to 440°. Except for differences in solvent and temperature, their ΔH° refers to a reaction that is just the reverse of our reaction 5 for which we find $\Delta H^\circ = -18.9$ kcal./mole at 320°. Since ΔC_p for this reaction is about 2 cal./deg. mole and the effect of changing solvent from pure KNO₃ to KNO₃-NaNO₃ is small (heats of mixing in the KNO₃-NaNO₃ system are small⁸), our heat of precipitation is in good agreement with the value calculated by Blander and co-workers.⁷

Jordan^{9,10} and his co-workers have recently investigated heats of precipitation of AgCl in various molten nitrate systems at various temperatures and have reported results for ΔH ranging from -18 to -20 kcal./mole.

Flengas and Rideal¹¹ have conducted electrometric titrations in KNO₃-NaNO₃ eutectic at various temperatures and have calculated that $\Delta H = +18.3$ kcal./mole for solution of AgCl.

Acknowledgment. We are grateful to the Atomic Energy Commission for support of this research.

- (6) O. J. Kleppa, R. B. Clarke, and L. S. Hersh, *J. Chem. Phys.*, **35**, 175 (1961).
- (7) M. Blander, J. Braunstein, and M. D. Silverman, *J. Am. Chem. Soc.*, **85**, 895 (1963).
- (8) O. J. Kleppa, *J. Phys. Chem.*, **64**, 1937 (1960).
- (9) J. Jordan, J. Meier, E. J. Billingham, and J. Pendergrast, *Nature*, **187**, 318 (1960).
- (10) J. Jordan, J. Meier, E. J. Billingham, and J. Pendergrast, *Anal. Chem.*, **32**, 651 (1960); **31**, 1439 (1959).
- (11) S. N. Flengas and E. Rideal, *Proc. Roy. Soc. (London)*, **A233**, 443 (1956).

On the Mechanism of Fluorescence Quenching.

Tyrosine and Similar Compounds

by Jehuda Feitelson

Department of Physical Chemistry, The Hebrew University, Jerusalem, Israel (Received July 15, 1963)

Quenching of the fluorescence of tyrosine, phenylalanine, and related compound solutions was investigated under various conditions. In particular, the effect of weak acids, of their salts, and of pH was studied. The results show that quenching by bases (in the general sense) occurs through their catalytic action upon the dissociation of the tyrosine hydroxyl group. These bases have no influence upon phenylalanine. Quenching of amino acid fluorescence by their own undissociated carboxyl groups is observed both for tyrosine and for phenylalanine. It seems therefore to involve the aromatic ring itself and not the phenolic hydroxyl group. A mechanism by which quenching might occur is suggested.

Factors influencing the ultraviolet fluorescence of aqueous tyrosine solutions were investigated in some detail. This seemed to be of interest both because of its possible importance in photobiological processes¹ and also because aromatic amino acids constitute a convenient system for the study of vicinal group effects upon chromophore fluorescence. Most of the previous work in this field was done by Weber,² who dealt with the pH dependence and influence of various quenching agents upon the fluorescence of tyrosine, tryptophane, and their parent compounds phenol and indole.

We tried to gain some insight into the mechanism of the quenching process by measuring the influence of strong and weak acids, their anions, and weak bases upon the fluorescence intensity of tyrosine. Other compounds, where one of the three reactive groups of tyrosine—hydroxyl, amino, or carboxyl—were either missing or blocked, were investigated in a similar manner.

It was found that the fluorescence of the various compounds differs mainly in two aspects. First, there are great differences between the quantum yields of the various tyrosine derivatives while their absorption spectra are very similar. Secondly, the changes in fluorescence caused by changes in solution pH and added quenching agent differ greatly for the various compounds. The results obtained enable us to draw conclusions about the reactivity and interactions of the

various parts of the molecule in its first excited (singlet) state.

Experimental

Tyrosine from Nutritional Biochem. Corp. was twice recrystallized from water. Tyrosine methyl ester, phenylalanine, and phenylalanine methyl ester HCl were recrystallized and chromatographically pure Yeda-Rehovot (Israel) products. Tyramine (purissimum grade) and γ -(*p*-hydroxyphenyl)propionic acid (purum grade) were obtained from Fluka AG Buchs, SG (Switzerland). Hydrocinnamic acid was laboratory synthesized and twice recrystallized from petroleum ether (m.p. 47–48°). All added substances were of analytical grade. Triply distilled water was used as solvent.

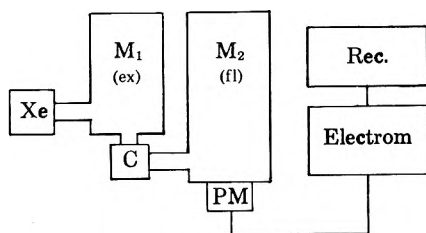
In order to eliminate interactions between the fluorescent solute molecules, very low concentrations were used (tyrosine, 9×10^{-6} M, tyrosine derivatives, 4.5×10^{-5} M, phenylalanine and derivatives, 9×10^{-5} M). Concentrations of quenching substances were in the 0.0–0.2 M range except for tyrosine methyl

(1) T. Bucher and J. Kaspers, *Biochem. Biophys. Acta*, **1**, 21 (1947); G. Weber and F. J. W. Teale, *Discussions Faraday Soc.*, **27**, 134 (1959).

(2) G. Weber, summarized in (a) Symposium on Light and Life, Johns Hopkins Press, Baltimore, Md., 1961; (b) preprint of Papers of Symposium on Reversible Photochemical Processes, Durham, N. C., 1962.

ester quenched by HCOOH, where the formic acid concentration reached 0.4 *M*.

The apparatus for fluorescence measurements is shown in the block diagram.



Light from a 375-w. Siemens Ediswan Xe-arc was focussed on the entrance slit of a Bausch and Lomb 250-mm. focal length monochromator. The exciting light of appropriate wave length (278 $m\mu$ for tyrosine, 257 $m\mu$ for phenylalanine, band width 12 $m\mu$) entered the cell compartment containing a Spectrosil grade (Thermal Syndicate) rectangular quartz cell with the solution. The fluorescence (at 303 $m\mu$ for tyrosine, 282 $m\mu$ for phenylalanine) emitted at right angle entered a second (Bausch and Lomb 500-mm. focal length) monochromator and hence an EMI 6256B photomultiplier. The voltage signal was measured at the ends of a 10-megohm load resistor by a vibrating reed EIL electrometer and either read directly on the meter scale or fed into a Kipp Model BD2 recorder. All parts of the apparatus were kept in mutually fixed positions by mounting them on an optical table. Slow drifts in the light source intensity were taken into account by measuring the fluorescence of a reference solution at frequent intervals. Fast fluctuations were filtered out.

In order to check any possible influence of dissolved oxygen on the fluorescence yield, aqueous solutions of all the compounds under investigation were measured after careful deaeration. The solutions, contained in the side arm of a modified Thunberg cell, were stirred and repeatedly evacuated until the equilibrium oxygen pressure over the solution was less than 0.001 mm. Comparison with the fluorescence of similar solutions in equilibrium with air showed no difference. The measurements therefore were carried out in nondeaerated solutions.

Absorption spectra were measured with a Hilger Uvispek spectrophotometer in 2-cm. optical path quartz cells.

pH measurements were carried out with a Metrohm E-187 pH meter. Standard buffers of pH 1.10 and 2.10 (HC⁻-KCl), pH 4.00 (K biphthalate), pH 6.68 (KH₂PO₂-Na₂HPO₄), and pH 10.02 (NaHCO₃-Na₂CO₃) were used.³

Results

The absorption and emission curves of the tyrosine and also of the phenylalanine derivative series were similar in shape. No significant wave length shifts were found, but differences in intensity between the different compounds were observed. It therefore was often sufficient to compare the ratio of molar extinction coefficients for two compounds with the ratio of their emission maxima when calculating the quantum yields of one substance relative to that of another. By accepting the values of Weber and Teale⁴ for the parent compounds, tyrosine and phenylalanine, the fluorescence quantum yields presented in Table I were obtained for neutral aqueous solutions.

Table I: Fluorescence Quantum Yields and Lifetimes of Tyrosine-like Substances in Aqueous Solution

	Quantum yield, <i>F</i>	Lifetime, $m\mu\text{sec.}$
Tyrosine	0.21	7.5
Tyrosine methyl ester	0.022	0.8
Tyramine	0.22	8.0
γ -(<i>p</i> -Hydroxyphenyl)-propionic acid	0.20	7.0
Phenylalanine	0.04	8.0
Phenylalanine methyl ester	0.028	5.6
Hydrocinnamic acid	0.04	8.0

In the absence of direct lifetime measurements of the excited states for the various compounds, approximate values of the natural lifetimes were calculated from absorption curves.⁵ Together with the quantum yields of column two (Table I), they yielded the actual excited state lifetimes in water.

The dependence of tyrosine and phenylalanine derivative fluorescence upon pH is shown in Fig. 1 and 2. The quantum yields indicated are relative values with respect to the parent compound—tyrosine or phenylalanine—at neutral pH. In the low pH range perchloric acid solutions were added. The data at high pH were obtained from the fluorescence in NH₄Cl-NH OH mixtures of various concentration ratios, which were extrapolated to zero buffer concentration. NH₄Cl and NaClO₄ had even at comparatively high (>1 *N*) concentration only a negligible effect upon the

(3) V. Gold, "pH Measurements, their Theory and Practice," Methuen, London, 1956, Appendix.

(4) F. W. J. Teale and G. Weber, *Biochem. J.*, **65**, 476 (1957).

(5) T. Förster, "Fluoreszenz Organischer Verbindungen," Vandenhoeck and Ruprecht, Göttingen, 1951, Chapter VIII.

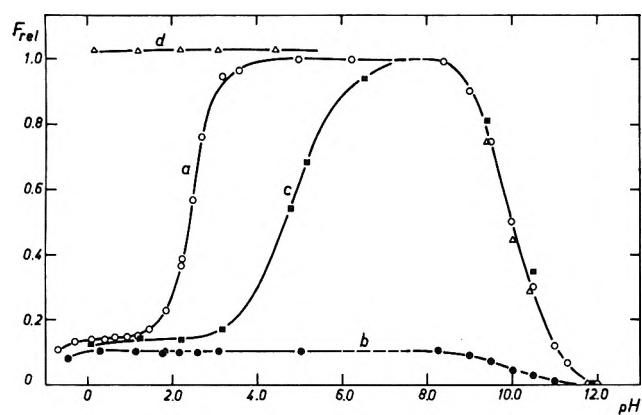


Figure 1. The dependence of fluorescence upon pH: a, tyrosine; b, tyrosine methyl ester; c, γ -(*p*-hydroxyphenyl)propionic acid; d, tyramine.

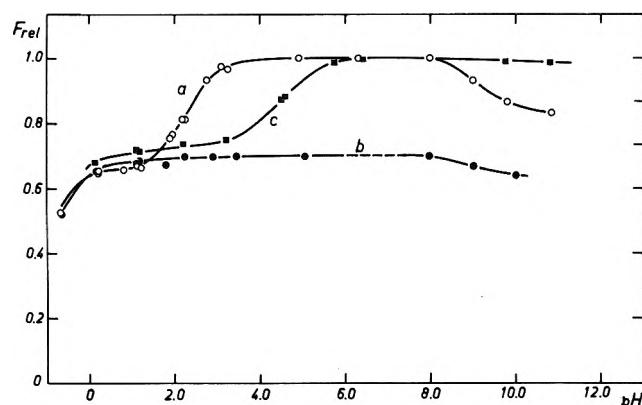
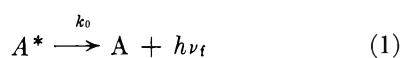


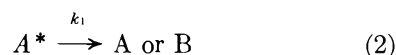
Figure 2. The dependence of fluorescence upon pH: a, phenylalanine; b, phenylalanine methyl ester; c, hydrocinnamic acid.

fluorescence of our substances. The figures show a strong decrease of fluorescence with the appearance of the un-ionized carboxyl groups. (pK_{COOH} of tyrosine is about 2.3, of γ -(*p*-hydroxyphenyl)propionic acid, 4.9, of phenylalanine, 2.2, and of hydrocinnamic acid, 4.7). In the basic range the fluorescence of tyrosine-like compounds disappears near the phenolic $pK \approx 10$ while in phenylalanine it decreases somewhat when the amino group becomes un-ionized (pH range 8–9). It is noteworthy that the compounds carrying a nonionized or esterified carboxyl group have low quantum yields and can be grouped together. The same substances without any carboxyl or with an ionized COO^- group fluoresce intensely.

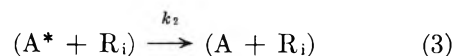
The following reactions of the excited molecule A^* were considered



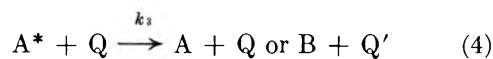
Fluorescence



Radiationless deactivation or photochemical reaction yielding product B



Quenching by group R_i which belongs to A but is not directly attached to chromophore. Here R_i is COOH or NH_2



Quenching by (solute) Q which might or might not involve a chemical transformation.

The fluorescence yield is calculated from stationary state kinetics. The ratio of the quantum yields in the absence (F') and in the presence of a quenching agent (F) takes the form

$$F'/F = 1 + (k_2/k_1')\alpha_R + (k_3/k_1')[Q] \quad (5)$$

$k_1' = k_1 + k_0$ is the reciprocal of the excited state lifetime, corresponding to F' , and k_3/k_1' , the experimental quenching constant. α_R is the fraction of excited molecules which under the given experimental conditions carry group R_i . In our case, for example, the fraction of tyrosine molecules with un-ionized COOH groups, α_{COOH} , changed from unity at low pH, through intermediate values in the vicinity of the carboxyl pK , to zero in neutral solutions.

The theory of diffusion-controlled reactions^{6,7} shows that k_3 obtained in this way represents only approximately the stationary bimolecular constant. In fast reactions, transient terms, due to an initial reactant distribution which is unrepresentative of the stationary state, have to be taken into account. These terms, which make the experimental value of k_3 too large, gain in importance at high quencher concentrations and at short excited state lifetimes. Therefore, by working at a concentration of quenching agent not exceeding 0.2 M it was thought that the simple, though approximate, equation could be adopted. The quenching constant was found from a plot of F'/F vs. concentration of Q. k_3 was found by inserting k_1' ($=1/\tau$) values from Table I. Measurements were usually carried out in the plateau regions $\alpha \approx 0$ or $\alpha \approx 1$ and k_2/k_1' could be estimated from the intercept. The use of eq. 5 was justified both by the similar values of k_3 obtained at intermediate and low pH ($\tau \approx 8 \mu\text{sec}$).

(6) R. M. Noyes, reviewed in "Progress in Reaction Kinetics," Vol. I, G. Porter, Ed., Pergamon Press, London, 1961.

(7) A. Weller, reviewed in (a) *Z. Elektrochem.*, **64**, 55 (1960); (b) "Progress in Reaction Kinetics," Vol. 1, G. Porter, Ed., Pergamon Press, London, 1961.

and 1 μ sec., respectively) and by the straight lines resulting in F'/F -concentration plots.

The addition of weak acid anions and un-ionized weak bases causes a great decrease in fluorescence of the tyrosine series compounds, but does not influence the phenylalanine derivatives. It should be noted that the only difference between the two series of compounds lies in the presence or absence of the aromatic hydroxyl in the molecule.

Since the fluorescence of tyrosine itself is very pH dependent in basic solution, the data for NH_4OH quenching are somewhat less accurate than those for the other substances. In order to obtain reliable results the fluorescence was measured in NH_4Cl - NH_4OH buffer mixtures of different concentrations but at constant pH.

Table II: Quenching of Tyrosine and Related Compound Fluorescence by Bases^a

	Base	k_3/k_1'	$k_3 \times 10^{-8}$, l./mole sec.
Tyrosine	CH_3COO^-	6.4	8.5
Tyrosine methyl ester	CH_3COO^-	0.6	7.5
Tyramine	CH_3COO^-	7.0	8.7
γ -(<i>p</i> -Hydroxyphenyl)- propionic acid	CH_3COO^-	4.1	5.9
Tyrosine	HCOO^-	4.8	6.4
Tyrosine	$\text{CH}_2\text{ClCOO}^-$	4.2	5.6
Tyrosine	$\text{NH}_3^+\text{CH}_2\text{COO}^-$	1.5	2.1
Tyrosine	H_2PO_4^-	2.7	3.6
Tyrosine	HPO_4^{2-}	9.0	12.0
Tyrosine	NH_2OH	2.2	2.9
Tyrosine	NH_4OH	6.0	8.0
Tyrosine methyl ester	NH_4OH	~ 1.0	~ 11.0
Tyramine	NH_4OH	6.3	7.9
γ -(<i>p</i> -Hydroxyphenyl)- propionic acid	NH_4OH	5.0	7.2

^a NaCl and NH_4Cl at concentrations $< 0.2 N$ did not influence the fluorescence.

Of the substances mentioned in Table II only NH_2OH had any influence on the fluorescence of the phenylalanine series compounds. Contrary to the tyrosine derivatives, no dependence upon ammonia concentration was observed.

The quenching by acids conjugate to the bases of Table II was also investigated. In order to avoid changes in quantum yield due to the changing pH (Fig. 1) the measurements were carried out in buffer solutions of constant acid to salt ratio but varying over-all concentration. From the composite value of k_3/k_1' so obtained and the already known anion quenching constant (Table II), the constants due to acid

Table III: Quenching of Phenylalanine and Phenylalanine Methyl Ester by Hydroxylamine and by Chloroacetic Acid

System	k_3/k_1'	$k_3 \times 10^{-8}$, l./mole sec.
Phenylalanine- NH_2OH	0.55	0.7
Phenylalanine- NH_3^+OH	< 0.1	
Phenylalanine- CH_2ClCOOH	3.0	3.7
Phenylalanine methyl ester- NH_2OH	0.6	1.0
Phenylalanine methyl ester- NH_3^+OH	< 0.1	
Phenylalanine methyl ester- CH_2ClCOOH	2.3	4.1

quenching were found. Experiments, where the acids were added at the lower pH plateau ($< \text{pH } 2$) gave the same results. The data are presented in Table IV.

Table IV: Quenching of Tyrosine and Related Compound Fluorescence by Weak Acids

	Acid	k_3/k_1'	$k_3 \times 10^{-8}$, l./mole sec.
Tyrosine	H_2PO_4^-	2.7	3.6
Tyrosine	$\text{NH}_2\text{OH}\cdot\text{HCl}$	< 0.3	< 0.4
Tyrosine	CH_3COOH	0.6	0.8
Tyramine	CH_3COOH	0.65	0.8
Tyrosine	HCOOH	5.3	7.1
Tyrosine methyl ester	HCOOH	0.7	8.6
Tyrosine	CH_2ClCOOH	16.0	21
Tyrosine methyl ester	CH_2ClCOOH	2.5	30

Of the quenching agents mentioned in Table IV only CH_2ClCOOH had any appreciable influence upon the fluorescence of phenylalanine or phenylalanine methyl ester.

The accuracy of the fluorescence intensity measurements was better than $\pm 2\%$. In those cases in which a strong decrease in fluorescence was observed upon addition of quenching agent, this resulted in an average error of about $\pm 3\%$ in the quenching constant. In our case this applies roughly to k_3/k_1' values between 5 and 10. In the range where the fluorescence decreased only slightly on addition of quencher (and a correspondingly small change in meter deflection was observed), the relative error of our measurements was of course greater. For k_3/k_1' values of unity or less the error might reach a magnitude of $\pm 20\%$. In addition the inherent uncertainty in k_1' ($= 1/\tau$) must be kept in mind when discussing k_3 values.

Discussion

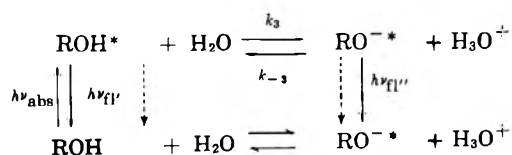
We shall discuss here the two main features of our experimental results. One is the strong quenching of

the tyrosine-like compounds by bases in the general sense, which is entirely absent in similar compounds lacking the aromatic hydroxyl group. The second, common both to the tyrosine and phenylalanine compounds, is the decrease of fluorescence due to the presence of un-ionized carboxyl or ester groups. These groups either constitute a part of the fluorescing molecule or are added in the form of un-ionized acid to the solution.

As shown by Förster,⁸ and later elaborated by Weller,⁹ the dissociation constant for aromatic hydroxyls in the excited state is often many times larger than in the ground state. In the case of β -naphthol the un-ionized molecule and the naphtholate ion fluoresce at different wave lengths. The emission spectrum of the latter begins to appear near pH 2 while at the same time the naphthol fluorescence decreases. Since the pK of β -naphthol in its ground state is about 9.2, this indicates clearly that even at low pH partial dissociation is attained in the excited state.

Sandorfy tried to correlate Förster's results with the charge distributions of phenol and β -naphthol in their ground and first excited states.¹⁰ His calculations show that whereas in the ground state the phenol oxygen carries a formal negative charge of 0.25 unit, this changes in the first excited state to a slightly positive value. The charge on the adjacent H atom is practically unaffected by the transition. An increase in dissociation can therefore be anticipated for phenols in the first excited state; this should also apply to tyrosine.

A rough estimate of ΔpK ($pK_{\text{excit. st.}} - pK_{\text{ground st.}}$) can be obtained from the difference in wave length between the absorption peaks of the un-ionized and the ionic form of the molecule.⁸ The scheme below shows the various processes which occur in such an illuminated aqueous solution. An asterisk indicates the excited state and dashed arrows the radiationless deactivation of the excited state.



For tyrosine an approximate value of $\Delta pK \approx 5$ is obtained. The *o*-ionized tyrosine molecule is non-fluorescent. We anticipate, therefore, an increased -OH dissociation in the excited state and a simultaneous decrease in quantum yield at pH values much lower than pH 10 (the pK of the aromatic hydroxyl). The absence of this decrease led to the opinion that no change in the dissociation constant occurs upon excitation.¹¹ Returning to the reaction scheme, it is

seen that equilibrium cannot be attained in the excited state. First, no back reaction can take place since the excited RO^{-*} is very rapidly deactivated. Secondly, and of more importance to us, is the fact that the forward (dissociation) rate constant, k_3 , is rather small. If we estimate the value of the (hypothetical) excited state equilibrium constant to be $K^* \approx 10^{-5}$, and assume a reasonable diffusion-controlled rate constant for the back reaction of say $k_{-3} = 10^{10}$ l./mole sec., we obtain $k_3 = 10^5$ sec.⁻¹. Since the lifetime of the excited tyrosine, as calculated from oscillator strength and quantum yield, is only about 10 m μ sec., we see that no appreciable dissociation can occur during this period. The fluorescence should therefore persist with increasing pH until in the vicinity of the ground state pK the nonfluorescent RO^- becomes predominant. On the other hand, the observation that tyrosine emission is quenched by weak acid anions can be satisfactorily explained. The above mentioned dissociation is generally base catalyzed. Anions of weak acids and other bases should therefore promote the process and thereby act as quenching agents in the case of tyrosine. The fluorescence of phenylalanine and related compounds, which do not carry aromatic hydroxyls, should not be quenched by this mechanism. Our experiments are in agreement with these expectations (Table II).

The ground state pK values and the wave length shifts of the absorption maxima when dissociation takes place are almost identical for all the tyrosine derivatives. Under these circumstances the proposed quenching mechanism is also supported by the fact that similar constants, k_3 , were obtained for a given base and different tyrosine derivatives although the fluorescence yields differed from case to case.

From Brönsted's catalytic law we might expect the catalytic power of a base to be related to the dissociation constant of its conjugate acid. The rates of our quenching reactions, however, fall already into a range of velocities which are to a large extent diffusion controlled. Smoluchovsky has proposed an equation for these border cases between activation and diffusion-controlled reactions.¹² It shows that the measured rate constants can still be influenced to some extent by the hypothetical activation-governed constant which would apply were it not for the slow diffusion step.¹³

(8) T. Förster, *Z. Elektrochem.*, **54**, 41, 531 (1950).

(9) A. Weller, *ibid.*, **56**, 662 (1952); see also ref. 7a for further references.

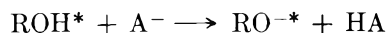
(10) C. Sandorfy, *Can. J. Chem.*, **31**, 439 (1953).

(11) A. White, *Biochem. J.*, **71**, 217 (1960).

(12) M. V. Smoluchovsky, *Z. physik. Chem.*, **92**, 129 (1917).

Our results for the carboxylate ions show indeed that their catalytic power increases slowly with their strength as bases. Brönsted's relation applies usually to catalysts of similar chemical structure. It is therefore not surprising that ammonia and NH_2OH , although in mutually correct order, do not fall into place when compared with the carboxylate bases.

When examining Weller's rate constants for the catalyzed naphthol dissociation



we see that our quenching constants for tyrosine are somewhat smaller than the corresponding naphthol values and that the differences between the bases A^- are more pronounced.¹⁴ This shows that the tyrosine dissociation is controlled by diffusion to a smaller degree and more influenced by activation energy. The lower $\text{p}K^*$ of β -naphthol ($\text{p}K^* = 2.8$ vs. $\text{p}K^* \simeq 5$) does indeed indicate a smaller activation energy for the forward reaction in $\text{ROH}^* + \text{H}_2\text{O} \rightleftharpoons \text{RO}^{-*} + \text{H}_3\text{O}^+$. (The back reactions are usually very fast and of comparable rate).

By inspecting Fig. 1 and 2 it is seen that the appearance of an un-ionized COOH group in tyrosine or hydroxyphenylpropionic acid depresses the chromophore fluorescence to about 15% of its previous value. Only at very high acid concentration (~ 2 N HClO_4) is a further decrease in fluorescence observed. A qualitatively similar but smaller effect is found in the phenylalanine series. We believe, therefore, that this kind of quenching must be attributed to an attack upon the aromatic ring itself. The phenolic OH group is here of importance only insofar as its increased dissociation and the calculations by Sandorfy, mentioned previously, indicate an appreciable electron drift into the ring upon excitation. However, quenching can also be observed when adding carboxylic acids to a solution of compounds which do or do not contain a carboxyl group of their own (see Tables III and IV). This shows that primarily we are not dealing with an inductive effect through the carbon chain.¹⁵ Such an effect, due to substitution at a carbon in position β with respect to the chromophore, would in any case be rather weak.

Summarizing the experimental findings we see that: (1) the excited ring interacts with carboxylic acids; this effect increases with the strength of the acid; (2) the tyrosine ring, carrying an excess negative charge in the excited state, interacts more strongly than phenylalanine both with added RCOOH and with its own $-\text{COOH}$ group; (3) protons *per se* have a very weak effect (see the low pH end of Fig. 1 and 2); (4) the methyl esters of tyrosine and phenylalanine have a quantum yield which is independent of pH and similar

to that of the unesterified compounds with undissociated carboxyl groups.

The contribution of polar structures in the excited state of aromatic molecules is greater than in the ground state. Together with points 1 and 2, this indicates an electrostatic effect between the reactive parts of the quencher molecule and the chromophore. Observations 3 and 4, however, show that this does not consist in a simple proton donation to the aromatic acceptor¹¹ and that the quenching is therefore probably due to interactions between the carboxyl groups proper and the excited ring.

We cannot at present prove the quenching mechanism rigorously, but the following suggestions are in accord with our experimental findings.

Transfer of the electronic excitation energy to the quencher can be ruled out in our case. The available energy would be insufficient even for the long wave length ($n \rightarrow \pi^*$)_{carbonyl} excitation of the carboxyl group. However, quenching of fluorescence can occur through intermolecular charge transfer.¹⁶ In our system, no differences indicative of a charge-transfer band were observed when comparing the absorption spectra of the compounds with the spectrum of their mixture. But even when the probability for direct charge transfer is low, the same result can be achieved through interactions between the acceptor and the excited donor. In the first excited singlet state, the highest bonding and the lowest antibonding orbitals are singly occupied. Given the necessary wave function overlap and local symmetry, these orbitals can conceivably also interact with a corresponding lone pair or excited state orbital of the quenching molecule. In principle, both electron transfer from the quencher lone pair to the bonding aromatic π -orbital or from the aromatic π^* to the quencher excited state orbital are possible. Inspection of the relation between energy levels of phenol, benzene, and acetic acid reveals that the ionization potentials of carboxylic acids are appreciably higher than those for benzene or phenol. The first excited states are, however, very close together. If benzene and phenol can be used as models for tyrosine and phenylalanine, these data, together with our experimental results (points 1 and 2), show that

(13) In the treatment by Weller, this fact is incorporated through his parameter, γ , which measures the probability that reaction takes place during an encounter.

(14) Compare Table III with Weller's (ref. 7a) data: naphthol quenched by CH_3COO^- , $k_3 = 2.9 \times 10^9$ l./mole sec.; by HCOO^- , $k_3 = 2.4 \times 10^9$ l./mole sec.

(15) R. W. Cowgill, *Arch. Biochem. Biophys.*, **100**, 36 (1963).

(16) L. E. Orgel, *Quart. Rev. (London)*, **8**, 422 (1954); in ref. 5, Chapter X, p. 47, the various quenching mechanisms are discussed in detail.

Table V: Ionization Potentials and Energy Levels of First Excited State for Aromatic Compounds and Carboxylic Acids^{17b}

	Benzene	Phenol	Acetic acid	Formic acid
Ionization potential (e.v.)	9.5	9.0	10.70	11.3
First excited state (-e.v.)	4.0 ^a	4.5	4.7	5.3

^a -4.0 e.v. which is here used for the first excited level of benzene is in fact the mean value for the first group of excited states.

the quenching by carboxyl groups *via* electron donation to the quencher is the more probable process. The possibility of intermolecular electron transfer to $-C=O$ groups has been demonstrated by the electron scavenging action of acetone and of formic acid in irradiated solutions.¹⁸ The differences in quenching ability between the various acids could be due to either of two causes. The same factors which determine the strength of carboxylic acids will also influence their attraction for electrons. On the other hand, the quenching power of a carboxylic acid might depend on its tendency to act as solvating agent for the chromophore. Interactions between aromatic substances and carboxylic acids have been reported in the literature.^{2b,19} From solubility measurements it seems that this effect also increases with the strength of the acid.²⁰

In the basic range, the strong decrease in tyrosine fluorescence which is due to $-OH$ dissociation obscures any other effect. However, for phenylalanine and phenylalanine methyl ester, the quantum yield is observed to decrease somewhat near the amino group pK (pH 8-9). This effect seems therefore to derive from the un-ionized RNH_2 group. Also the quenching of phenylalanine by NH_2OH in the un-ionized form is probably of the same origin. On the other hand, the ionized NH_3OH^+ as well as the attached $-RNH_3^+$ groups have no influence upon the chromophore fluorescence. (Compare in Fig. 2 phenylalanine with hydrocinnamic acid in the neutral and basic ranges and see Table III.)

Acknowledgment. The author wishes to thank Prof. G. Stein for helpful discussions during the progress of this work. This research was supported in part by the U. S. Atomic Energy Commission.

- (17) S. Nagakura and J. Tanaka [(a) *J. Chem. Phys.*, **22**, 236 (1954); (b) **23**, 1441 (1955)] have charted energy level diagrams for various molecules. The ground state energies are obtained from ionization potentials and the higher levels from absorption spectra.
- (18) J. Rabani and G. Stein, *J. Chem. Phys.*, **37**, 1865 (1962).
- (19) R. West, *J. Am. Chem. Soc.*, **81**, 1614 (1959); S. Wada, *Bull. Chem. Soc. Japan*, **35**, 710 (1962).
- (20) See ref. 2b. Our own unpublished results show an increase of the solubility of benzene in water upon addition of carboxylic acids. The solubility in 0.2 *N* acid solution increases in the direction acetic acid \leq formic acid $<$ chloroacetic acid.

Activity, Density, and Relative Viscosity Data for Several Amino Acids, Lactamide, and Raffinose in Aqueous Solution at 25°

by H. David Ellerton, Gundega Reinfelds, Dennis E. Mulcahy, and Peter J. Dunlop

*Department of Physical and Inorganic Chemistry, University of Adelaide, Adelaide, South Australia
(Received August 12, 1968)*

Isopiestic vapor pressure measurements, densities, and relative viscosities are reported for aqueous solutions of glycine, glycyglycine, α -amino-*n*-butyric acid, *dl*-valine, lactamide, and raffinose at 25°. Osmotic and activity coefficients have been computed from isopiestic vapor pressure measurements and compared where possible with the data previously published. Apparent and partial molar volume data have been obtained from the density measurements.

The rate at which relative motion of the two components of a binary solution takes place under the influence of chemical potential gradients was first described in terms of a diffusion coefficient, D , by Fick's first law.¹ It has been pointed out, however, that the diffusion coefficients in both binary and ternary diffusion depend on the frame of reference used, and coefficients on various frames of reference have been defined.^{2,3}

It has also been shown that the above transport process may be described in terms of a set of mutual frictional coefficients which are independent of the frame of reference used.⁴⁻⁹ These mutual frictional coefficients may be obtained by combining the diffusion coefficients with certain activity and density data. It is the purpose of this paper to report activity data for the binary systems glycine-H₂O, glycyglycine-H₂O, α -amino-*n*-butyric acid-H₂O, *dl*-valine-H₂O, lactamide-H₂O, and raffinose-H₂O at 25° for use in computing mutual frictional coefficients for these systems (see companion paper¹⁰). Density and relative viscosity data are also reported for four of the above systems. These binary systems were chosen so that comparisons could be made with other data for amino acids, isomers of amino acids, and sugars previously reported in the literature.

Experimental

Materials. All reagents used, except raffinose, were recrystallized from doubly distilled water until successive recrystallizations were indistinguishable

by the isopiestic method.¹¹ The solutions were prepared by weighing and the weights were corrected to weight *in vacuo*. Doubly distilled water was always used as the solvent. In the case of the activity measurements, the solutions were prepared so that they were initially reasonably close to their equilibrium values. The densities of the solids used for the vacuum corrections are reported in row 8 of Table II, and the molecular weights¹² used for calculating the solution concentrations are in row 9 of the same table.

Sodium chloride (reference solute) was A.R. grade and was recrystallized once from doubly distilled water, dried *in vacuo*, and fused in a platinum crucible. Using

- (1) A. Fick, *Pogg. Ann.*, **94**, 59 (1855).
- (2) J. G. Kirkwood, R. L. Baldwin, P. J. Dunlop, L. J. Gosting, and G. Kegeles, *J. Chem. Phys.*, **33**, 1505 (1960).
- (3) R. P. Wendt and L. J. Gosting, *J. Phys. Chem.*, **63**, 1287 (1959).
- (4) O. Lamm, *ibid.*, **61**, 948 (1957); *Acta Chem. Scand.*, **11**, 362 (1957).
- (5) R. W. Laity, *J. Phys. Chem.*, **63**, 80 (1959).
- (6) R. J. Bearman, *ibid.*, **65**, 1961 (1961).
- (7) A. Klemm, *Z. Naturforsch.*, **8a**, 397 (1953).
- (8) S. Ljunggren, *Trans. Royal Inst. Technol. Stockholm*, **No. 172** (1961).
- (9) P. J. Dunlop, *J. Phys. Chem.*, **68**, 26 (1964).
- (10) H. D. Ellerton, G. Reinfelds, D. E. Mulcahy, and P. J. Dunlop, *ibid.*, **68**, 403 (1964).
- (11) R. A. Robinson and R. H. Stokes, "Electrolyte Solutions," Butterworths Scientific Publications, London, 1959, pp. 177-181.
- (12) Using atomic weights compiled in International Union of Pure and Applied Chemistry, Information Bulletin No. 14b (1961).

the isopiestic method the once recrystallized material was found to be identical with a sample that had been twice recrystallized. Sucrose was BDH microanalytical grade and was used without further purification. Glycine was obtained from British Drug Houses and this A.R. material was recrystallized once from doubly distilled water. Samples of the first and second recrystallizations were indistinguishable by the isopiestic method.¹¹ Glycylglycine was obtained from British Drug Houses and was recrystallized four times. α -Amino-*n*-butyric acid was obtained from the Sigma Chemical Corp., U. S. A., and was recrystallized three times. *dl*-Valine was purchased from Nutritional Biochemicals Corp., U. S. A., and was also recrystallized three times. Lactamide was part of a sample prepared for diffusion measurements by Wendt and Gosting³ and had been recrystallized three times. Raffinose was obtained from the Pfanstiehl Laboratories, Inc., U. S. A., and was used without further purification.

Osmotic and Activity Coefficients. Osmotic coefficient measurements are of importance since they may be combined with density data to obtain the factor $(1 + C \partial \ln y / \partial C) = (1 + \bar{C} \partial \ln y / \partial \bar{C})$ which is used in the computation of mutual frictional coefficients. Here C and \bar{C} are solute concentrations in moles/cc. and moles/1000 cc., respectively, and y is the corresponding activity coefficient. The activity data were obtained from the osmotic coefficients determined by the isopiestic vapor pressure method which has been described in detail previously.¹¹

The silver dishes used for containing the solutions had bases which had been ground to a high degree of flatness. These dishes were approximately 3.5 cm. in diameter and 2 cm. in height. Each dish had a close-fitting lid which had been ground so as to fit perfectly. Usually eight dishes were used for each experiment, four containing the reference solution and four containing the solution with unknown osmotic coefficient. Approximately 5 ml. of prepared solution was used per dish.

In order to determine whether any interaction was taking place between the silver dishes and the solutions, several gold-plated silver dishes were used simultaneously in a number of the experiments. No difference could be detected between the behavior of the solutions in the silver and the gold-plated dishes.

The dishes were placed on a flat silver-plated copper block of about 3-cm. thickness which was contained in a glass vacuum desiccator. With the lids removed and the desiccator sealed, evacuation of the apparatus was commenced, and was generally carried out over a period of several hours to avoid splattering caused by

degassing of the solutions. After evacuation, the desiccator and contents were placed in a large thermostat bath, controlled at 25° to approximately $\pm 0.002^\circ$, and rocked gently. Stirring of the solutions was effected by 4-mm. stainless steel ball bearings rolling across the bottom of the dishes under the influence of the rocking motion. It was observed that if no ball bearings were used in the dishes, the results were the same as those in which either one or two ball bearings had been used. However, a much longer time was needed for the solutions to attain equilibrium when the ball bearings were absent. Also, the results were unaffected by whether the ball bearings were wholly or partially immersed in the solutions.

The time required for equilibrium to be attained depended on the concentration of the solution. For the more concentrated solutions, 5 to 7 days was required before the final weights were taken, but for the more dilute ones as much as 2 weeks was sometimes necessary.

Sodium chloride was used as the reference solute for all systems except in the case of raffinose, for which sucrose was found to be the most suitable reference solute.

The experimental values of the equilibrium molalities, m , of all the solutes studied and the molalities of the corresponding reference solutions, m_{NaCl} or m_{sucrose} , at 25° are given in Table I. To represent the osmotic coefficients, ϕ , which were computed from the equilibrium solute concentrations and the values of the osmotic coefficients of the reference materials,^{13,14} equations of the form

$$\phi = 1 + \sum_{i=1}^5 A_i m^i \quad (1)$$

were used and the coefficients A_i obtained by the method of least squares.¹⁵ Values of the constants for eq. 1, together with the percentage deviations of the experimental points from the equations, are given in Table II.

It can be shown that

$$\ln \gamma = (\phi - 1) + \int_0^m (\phi - 1) d \ln m \quad (2)$$

and hence using eq. 1

$$\ln \gamma = \sum_{i=1}^5 \left(\frac{i+1}{i} \right) A_i m^i \quad (2a)$$

(13) See ref. 11, p. 476.

(14) R. A. Robinson and R. H. Stokes, *J. Phys. Chem.*, **65**, 1954 (1961).

(15) An IBM 7090 electronic computer was used to least square all data.

Table I: Summary of Isoopiestic Results at 25°

Glycine		Glycylglycine		Glycylglycine		α -Amino-n-butyric acid		dl-Valine		Lactamide		Raffinose	
<i>m</i>	<i>m</i> _{NaCl}	<i>m</i>	<i>m</i> _{NaCl}	<i>m</i>	<i>m</i> _{NaCl}	<i>m</i>	<i>m</i> _{NaCl}	<i>m</i>	<i>m</i> _{NaCl}	<i>m</i>	<i>m</i> _{NaCl}	<i>m</i>	<i>m</i> _{sucrose}
0.2064	0.1088	0.1030	0.05328	1.1794	0.5548	0.2191	0.1184	0.09997	0.05328	0.2039	0.1088	0.1212	0.1222
0.3272	0.1718	0.1047	0.05416	1.1942	0.5614	0.3792	0.2072	0.1016	0.05415	0.3216	0.1718	0.1263	0.1273
0.3298	0.1732	0.2093	0.1071	1.3318	0.6229	0.6107	0.3382	0.3040	0.1662	0.3243	0.1732	0.1299	0.1306
0.3327	0.1747	0.2127	0.1088	1.3468	0.6291	0.9586	0.5357	0.3089	0.1688	0.5098	0.2720	0.1837	0.1857
0.5230	0.2720	0.3061	0.1549	1.3744	0.6417	1.0619	0.5950	0.3869	0.2134	0.7464	0.3969	0.1868	0.1891
0.7757	0.3969	0.3121	0.1580	1.3967	0.6513	1.3925	0.7855	0.3909	0.2156	1.2902	0.6729	0.1901	0.1924
0.8282	0.4232	0.4035	0.2021	1.4897	0.6933	1.6644	0.9426	0.4363	0.2412	1.6009	0.8254	0.2287	0.2312
1.1174	0.5616	0.4090	0.2045	1.5057	0.7003	2.0796	1.1860	0.5196	0.2896	1.6357	0.8429	0.2330	0.2359
1.1368	0.5705	0.5096	0.2517	1.6038	0.7447			0.5124	0.2856	1.8370	0.9382	0.2243	0.2275
1.7304	0.8429	0.5151	0.2544	1.6220	0.7521			0.6033	0.3386	2.4089	1.2049	0.2301	0.2329
1.9424	0.9382	0.6124	0.2996	1.6255	0.7543			0.5977	0.3352	2.6009	1.2914		
2.1476	1.0286	0.6238	0.3048							3.0295	1.4814		
2.1657	1.0365	0.7109	0.3442							4.0949	1.9253		
2.4059	1.1414	0.7229	0.3498							4.6065	2.1247		
2.7772	1.3014	0.8183	0.3934							4.7473	2.1792		
2.8094	1.3155	0.8358	0.4011										
3.0854	1.4313	1.0213	0.4845										
3.1139	1.4433	1.0368	0.4911										

Table II: Constants for the Least-Squared Equations of Osmotic Coefficients vs. Molarity at 25°

	Glycine	Glycylglycine	α -Amino-n-butyric acid	dl-Valine	Lactamide	Raffinose
$A_1 \times 10$	-0.960	-2.682	0.251	0.383	-0.3202	1.333
$A_2 \times 10^2$	3.334	27.595	0.876	0.48	0.4954	...
$A_3 \times 10^3$	-6.08	-228.8	-1.76	40.6	-0.6771	...
$A_4 \times 10^4$	4.55	1214.4	0.521	...
$A_5 \times 10^2$...	-2.630
% deviation	± 0.05	± 0.03	± 0.03	± 0.07	± 0.06	± 0.12
Range	3.1	1.6	2.0	0.6	4.7	0.23
Solid density ^a	1.601	1.561	1.231	1.316	1.138	1.465
Molecular weight ^b	75.068	132.120	103.122	117.149	89.095	504.446

^a The density of solid NaCl was taken as 2.165 g./cc. and sucrose as 1.588 g./cc. ^b The molecular weights of NaCl and sucrose were taken as 58.443 and 342.303, respectively.

Thus, without any graphical integration, molal activity coefficients, γ , may be calculated using eq. 2a and the parameters A_i in Table II. Molar activity coefficients, y , may be computed with the aid of the density data for each system. It is believed that the activity coefficients computed by eq. 2a are accurate to within 0.1%.

Density Measurements. All density measurements were performed in triplicate or quadruplicate with single stem pycnometers, each having a volume of approximately 30 cc. These pycnometers were calibrated at 25° assuming the density of water, d_0 , to be 0.997048 g./cc. They were cleaned before use with chromic acid, and over a period of about a year the volumes changed by less than 0.004%.

The density values for each system were fitted to equations of the form

$$d = d_0 + \sum_{i=1}^3 B_i \bar{C}^i \quad (3)$$

by the method of least squares. The densities, d , are in g./cc. The values of the constants, B_i , in eq. 3, together with the concentration limits and the percentage deviations of the experimental points from the equations, are given in Table III.

Apparent molar volumes for the solutes, Φ_1 , are given by the relation

$$\Phi_1 = \frac{1000}{\bar{C}} \left(\frac{d_0 - d}{d_0} \right) + (M/d_0) \quad (4)$$

where M is the molecular weight of the solute. By combining eq. 1 and 2, the apparent molar volumes may be expressed by equations of the form

Table III: Constants for the Equations of Density and Apparent Molar Volume vs. Concentration at 25°^a

	Glycine	Glycylglycine	α -Amino- <i>n</i> -butyric acid	<i>dl</i> -Valine
$B_1 \times 10^2$	3.1978	5.6007	2.7718	2.6642
$B_2 \times 10^3$	-1.044	-2.165	-0.460	-0.249
$B_3 \times 10^4$	0.964	2.63
% deviation of densities	± 0.0007	± 0.003	± 0.0005	± 0.0002
Φ_1^0	43.217	76.338	75.628	90.775
D_1	1.0473	2.1713	0.4613	0.2501
D_2	-0.0967	-0.2643
Range	2.1	1.4	1.1	0.5

^a Density data for lactamide and raffinose solutions have been reported previously: F. T. Gucker, Jr., and T. W. Allen, *J. Am. Chem. Soc.*, **64**, 191 (1942); P. J. Dunlop, *J. Phys. Chem.*, **60**, 1464 (1956).

$$\Phi_1 = \Phi_1^0 + \sum_{i=1}^2 D_i \hat{C}_i \quad (5)$$

where

$$\Phi_1^0 = (M - 1000B_1)/d_0 \quad (5a)$$

and the constants D_i are given by

$$D_1 = -(1000B_2)/d_0 \quad (5b)$$

$$D_2 = -(1000B_3)/d_0 \quad (5c)$$

Values for Φ_1^0 , D_1 , and D_2 are given in Table III.

Partial molar volumes of the solute, \bar{V}_1 , and of the solvent, \bar{V}_0 , may be computed using the equations of Geffcken¹⁶ and the values of Φ_1^0 , D_1 , and D_2 .

$$\bar{V}_1 = \Phi_1 + \hat{C} \left[\frac{1000 - \hat{C}\Phi_1}{1000 + \hat{C}^2 \frac{\partial \Phi_1}{\partial \hat{C}}} \right] \frac{\partial \Phi_1}{\partial \hat{C}} \quad (6a)$$

$$\bar{V}_0 = \frac{1000 \bar{V}_0^0}{1000 + \hat{C}^2 \frac{\partial \Phi_1}{\partial \hat{C}}} \quad (6b)$$

where \bar{V}_0^0 is the partial molar volume of the pure solvent. The partial molar volumes of the solvent are given in a companion paper¹⁰ where they are used to compute mutual frictional coefficients.

Viscosity Measurements. Two Ubbelohde viscometers with water flow times of 288.7 and 328.5 sec., respectively, were used for the measurements. A small kinetic energy correction was applied to each result.

It can be shown that

$$(\eta/dt) = A - (B/t^2) \quad (7)$$

where η , d , and t are the viscosity, density, and flow time for a given solution, and A and B are constants. The kinetic energy correction, K , is given by $K = (B/A)$. The values of (η/dt) vs. $(1/t^2)$ for water were plotted at 20, 25, and 30° to obtain A and B and hence K for each viscometer. The value obtained was 530 sec.² in each case.

The experimental relative viscosity values were fitted to equations of the form

$$\eta_r = 1 + \sum_{i=1}^3 F_i \hat{C}_i \quad (8)$$

by the method of least squares. The viscosity data, together with the concentration limits and percentage deviations of the experimental points from eq. 8, are given in Table IV.

Table IV: Constants for the Least-Squared Equations of Relative Viscosity vs. Concentration at 25°

	Glycylglycine	α -Amino- <i>n</i> -butyric acid	<i>dl</i> -Valine	Lactamide
$F_1 \times 10$	3.151	3.606	4.052	1.984
$F_2 \times 10^2$	5.45	0.89	14.09	2.668
$F_3 \times 10^3$	36.7	67.8	98.0	3.97
Range	1.4	1.0	0.4	2.1
% deviation	± 0.13	± 0.07	± 0.06	± 0.12

Discussion

Osmotic coefficients for the systems glycine-H₂O, glycylglycine-H₂O, α -amino-*n*-butyric acid-H₂O, and *dl*-valine-H₂O have been reported previously.¹⁷⁻¹⁹ These measurements depended on the use of osmotic coefficients of sucrose solutions as a reference, as determined from earlier vapor pressure measurements. However, in order to achieve the maximum accuracy in computation of the frictional coefficients (see companion paper), a completely new series of measurements has been made using as the reference recently published osmotic coefficient data for sodium chloride¹³ and sucrose¹⁴ solutions. When the osmotic coefficients calculated from this work were plotted as a function of molality, it was found that the points lay on smooth curves of a similar type to those obtained earlier by

(16) W. Geffcken, *Z. physik. Chem.*, **A155**, 1 (1931).

(17) E. R. B. Smith and P. K. Smith, *J. Biol. Chem.*, **117**, 209 (1937).

(18) P. K. Smith and E. R. B. Smith, *ibid.*, **121**, 507 (1937).

(19) E. R. B. Smith and P. K. Smith, *ibid.*, **135**, 273 (1940).

Smith and Smith.¹⁷⁻¹⁹ Their points, however, showed considerable scatter, and in some regions their values, after correction to the new standard, differed by as much as 1.5% for glycine, 1.3% for glycyglycine, 1.7% for α -amino-*n*-butyric acid, and 0.4% for *dl*-valine, from the values obtained in this work.

It is of interest to compare the osmotic coefficients of lactamide with those of glycolamide.²⁰ The additional methyl group on the lactamide molecule seems to have little effect on the vapor pressure of the solutions, as the osmotic coefficients are almost identical with those of glycolamide solutions. However, the relative viscosities of lactamide solutions showed greater concentration dependence than those of glycolamide.²¹

The densities of glycine solutions have been reported previously.²² The results of this work show an average deviation from eq. 3 of $\pm 0.0007\%$ while those of the previous workers showed an average deviation from their least-squared equation of $\pm 0.009\%$. The two sets of results agree very closely at low and high concentrations but differ by as much as 0.012% in the region of $C = 1$. The densities and relative viscosities of glycyglycine solutions and α -amino-*n*-butyric acid solutions at several concentrations have also been reported previously.²³ The densities agree with this work to within 0.003% for glycyglycine solutions, and 0.007% for α -amino-*n*-butyric acid solutions, whereas the relative viscosities agree to within 0.5 and 0.3%, respectively.

It is of interest to compare the apparent molar volumes of glycyglycine with those of two isomers, asparagine and methylhydantoic acid. The limiting apparent molar volume, Φ_1^0 , for glycyglycine obtained from this work was 76.33 cc./mole, whereas values of apparent molar volumes of 78.0 and 94.2 cc. per mole

have been quoted for asparagine²⁴ and methylhydantoic acid²⁵ at unspecified concentrations. Of the three isomers, glycyglycine has a much greater dipole moment than asparagine, which is an α -amino acid, whereas the methylhydantoic acid molecule, according to McMeekin, *et al.*,²⁶ bears no electric charge. The charged condition of the first two molecules results in electrostriction of the solvent, and the apparent molar volumes are smaller than that of the uncharged methylhydantoic acid, whose volume is close to that expected from empirical calculations.²⁶ The somewhat larger molecular volume of asparagine compared to glycyglycine has been attributed²⁷ to the closer proximity of its $-\text{NH}_3^+$ and $-\text{COO}^-$ groups.

Acknowledgments. The authors wish to thank Mr. E. W. Gooden for performing some of the experiments with α -amino-*n*-butyric acid and Dr. B. J. Steel for many helpful discussions and his criticism of the manuscript. This work was supported in part by grants from the Colonial Sugar Refining Co. Ltd. of Australia and the United States Institutes of Health (AM-06042-02).

- (20) R. H. Stokes, *Trans. Faraday Soc.*, **50**, 565 (1954).
- (21) P. J. Dunlop and L. J. Gosting, *J. Am. Chem. Soc.*, **75**, 5073 (1953).
- (22) F. T. Gucker, Jr., W. L. Ford, and C. E. Moser, *J. Phys. Chem.*, **43**, 153 (1939).
- (23) J. Daniel and E. J. Cohn, *J. Am. Chem. Soc.*, **58**, 415 (1936).
- (24) J. P. Greenstein and J. Wyman, *ibid.*, **58**, 463 (1936).
- (25) T. L. McMeekin, E. J. Cohn, and J. H. Weare, *ibid.*, **57**, 626 (1935).
- (26) E. J. Cohn and J. T. Edsall, "Proteins, Amino Acids and Peptides," Reinhold Publishing Corporation, New York, N. Y., 1943, p. 157.
- (27) E. J. Cohn, T. L. McMeekin, J. T. Edsall, and M. H. Blanchard, *J. Am. Chem. Soc.*, **56**, 784 (1934).

The Mutual Frictional Coefficients of Several Amino Acids

in Aqueous Solution at 25°

by H. David Ellerton, Gundega Reinfelds, Dennis E. Mulcahy, and Peter J. Dunlop

Department of Physical and Inorganic Chemistry, University of Adelaide, Adelaide, South Australia
(Received August 12, 1963)

Diffusion and refractive index data at 25° are reported for the binary systems glycine-H₂O, glycyglycine-H₂O, α -amino-*n*-butyric acid-H₂O, and *dl*-valine-H₂O. The diffusion data are combined with other available thermodynamic data to compute mutual frictional coefficients for these systems. These mutual frictional coefficients are compared with those for other binary systems which have been calculated from the data in the literature. A relationship between relative frictional coefficients and relative viscosity is tested.

Many papers in recent years have reported diffusion coefficients for both binary and ternary isothermal diffusion. For binary diffusion these coefficients, which are defined by Fick's first law,¹ relate the flow of a given component to the corresponding concentration gradient when relative motion of the components is taking place. It has been emphasized that, when reporting diffusion coefficients, the frame of reference should be specified^{2,3} and coefficients for several frames of reference have been given in the literature, both for binary³ and ternary diffusion.⁴⁻¹³ However, as has been previously indicated, it is possible to define mutual frictional coefficients,¹⁴⁻²⁰ independent of the frame of reference, which may be computed from the measured diffusion coefficients and certain corresponding thermodynamic data. It is the purpose of this paper to report frictional and diffusion coefficients for the systems glycine-H₂O, glycyglycine-H₂O, α -amino-*n*-butyric acid-H₂O, and *dl*-valine-H₂O and to compare these frictional coefficients with others which may be computed from the diffusion and thermodynamic data in the literature.

Experimental

Apparatus. Almost all the diffusion measurements were made with a Gouy diffusimeter²¹ which was supported and aligned on a 9-m. lathe bed. This optical bench was mounted kinematically on three stainless steel ball bearings, 7.6 cm. in diameter, which rested

in steel supports on top of three concrete pillars which were isolated from the floor of the room and set 1.8 m. into the earth.

- (1) A. Fick, *Pogg. Ann.*, **94**, 59 (1855).
- (2) J. G. Kirkwood, R. L. Baldwin, P. J. Dunlop, L. J. Gosting, and G. Kegeles, *J. Chem. Phys.*, **33**, 1505 (1960).
- (3) R. P. Wendt and L. J. Gosting, *J. Phys. Chem.*, **63**, 1287 (1959).
- (4) P. J. Dunlop and L. J. Gosting, *J. Am. Chem. Soc.*, **77**, 5238 (1955).
- (5) I. J. O'Donnell and L. J. Gosting, "The Structure of Electrolytic Solutions," W. J. Hamer, Ed., John Wiley and Sons, Inc., New York, N. Y., Chapman and Hall, London, 1959.
- (6) P. J. Dunlop, *J. Phys. Chem.*, **61**, 994 (1957).
- (7) P. J. Dunlop, *ibid.*, **61**, 1619 (1957).
- (8) P. J. Dunlop, *ibid.*, **63**, 612 (1959).
- (9) L. A. Wolf, D. G. Miller, and L. J. Gosting, *J. Am. Chem. Soc.*, **84**, 317 (1962).
- (10) R. P. Wendt, *J. Phys. Chem.*, **66**, 1279 (1962).
- (11) P. J. Dunlop and L. J. Gosting, *ibid.*, **63**, 86 (1959).
- (12) D. G. Miller, *ibid.*, **63**, 570 (1959).
- (13) L. A. Wolf, *ibid.*, **67**, 273 (1963).
- (14) O. Lamm, *Acta Chem. Scand.*, **11**, 362 (1957).
- (15) S. Ljunggren, *Trans. Royal Inst. Technol., Stockholm*, No. 172 (1961).
- (16) A. Klemm, *Z. Naturforsch.*, **8a**, 397 (1953).
- (17) R. W. Laity, *J. Phys. Chem.*, **63**, 80 (1959).
- (18) R. J. Bearman, *ibid.*, **65**, 1961 (1961).
- (19) L. Onsager, *Ann. N. Y. Acad. Sci.*, **46**, 241 (1945).
- (20) P. J. Dunlop, *J. Phys. Chem.*, **68**, 26 (1964).
- (21) This apparatus gave diffusion coefficients and refractive index increments for sucrose which agreed to better than 0.1% with those of Gosting and Akeley (see ref. 24).

A Wratten 77A filter was used to isolate the green mercury line, $\lambda = 5460.7 \text{ \AA}$, of an AH-4 mercury vapor lamp which was supported in a water-cooled housing. Light from the lamp was focused onto a Gaertner bilateral slit which was then focused, by means of a high quality lens,²² through the water bath and cell onto the photographic plate. The optical distance, b , from the center of the diffusion cell to the photographic plate was measured and found to be 304.82 cm.²³ The two quartz cells A and B, which were used for the diffusion measurements, had thicknesses, a , along the optic axis equal to 2.5032 and 2.4950 cm., respectively. The values of the diffusion and refractometer corrections, δ and δ' , were approximately 18 μ and appeared to be essentially independent of the concentration of the diffusing material.

Calculations. A paper from another laboratory²⁴ has adequately described the methods used for computing the differential diffusion coefficients, D , and the refractive increments, $\Delta n/\Delta \hat{C}$. The values of the relative fringe deviations for each Gouy experiment, Ω_i ,²⁴ were generally in the range $\pm 2 \times 10^{-4}$ for each value of the reduced fringe number $f(\zeta)$.²⁴ The bath temperature, which at all times was within a hundredth of a degree of 25°, remained constant to $\pm 0.005^\circ$ during the course of each diffusion experiment. Observed diffusion coefficients, D , at each temperature, T , were corrected to 25.00° using the Stokes-Einstein relation $(D\eta/T)_{25^\circ} = (D\eta/T)_{\text{exptl}}$, where η is the viscosity of water. Frictional coefficients for binary diffusion, $R_{01} = R_{10}$,²⁰ were computed from the measured coefficients, the corresponding partial molar volumes of the solvent, \bar{V}_0 , the values of the osmotic coefficients, ϕ ,^{25,26} and the solution densities, d . These calculations are described in more detail below. The value of the gas constant used was 8.3144×10^7 ergs deg.⁻¹ mole⁻¹ and the absolute zero was taken as being -273.16° .

Materials and Solutions. All solutes were of Analar grade, wherever possible, and were recrystallized from distilled water before use. Further details of the materials used in this work can be found in a companion paper.²⁶ All solutions were made up by weight using doubly distilled water as solvent. The weights were converted to weights *in vacuo* before calculating the solute concentrations, \hat{C} , in moles/1000 cc. The molecular weights of glycine, glycyglycine, α -amino-*n*-butyric acid, and *dl*-valine were taken as 75.068, 132.120, 103.122, and 117.149, respectively. Densities, d , and relative viscosities, η_r , were measured for several of the above systems and have been reported previously.²⁶

Results

Values of the experimental diffusion coefficients, D obtained at mean solute concentrations $\hat{C}_m = [(\hat{C}_A + \hat{C}_B)/2]$ and solute increments $\Delta \hat{C} = (\hat{C}_B - \hat{C}_A)$ are tabulated for each of the systems studied in column 5 of Table I. Here A and B denote the upper and

Table I: Experimental Diffusion Data at 25°

C_m	$\Delta \hat{C}$	$(\Delta n/\Delta \hat{C}) \times 10^3$	J	$D \times 10^5$
(A) Glycine ^a				
0.049990 ^b	0.099990	13.568	61 77	1.0504
0.10000 ^b	0.20000	13.540	123 29	1.0411
0.24999 ^c	0.14999	13.444	92 55	1.0128
0.49960 ^c	0.14911	13.290	91 01	0.9696
0.80712	0.22247	13.126	133 86	0.9293
1.24982	0.13954	12.884	82 41	0.8767
1.99858	0.13891	12.567	80 02	0.8130
(B) Glycyglycine ^a				
0.022680	0.045359	25.273	52 55	0.7863
0.036434	0.072868	25.240	84 31	0.7815
0.24442	0.077440	24.950	88 57	0.7112
0.24443	0.077440	24.945	88 55	0.7117
0.47962	0.079430	24.674	89 85	0.6647
1.00043	0.083750	24.157	92.74	0.5810
(C) α -Amino- <i>n</i> -butyric acid				
0.031044 ^d	0.062088	17.958	101 89	0.8258
0.048620 ^e	0.097240	17.981	80 15	0.8230
0.062380 ^d	0.12476	17.967	204 84	0.8220
0.24642 ^d	0.057370	17.936	94.03	0.7922
0.48234 ^d	0.057710	...	93.57	0.7586
0.49893 ^e	0.10056	17.843	82.25	0.7587
0.81540 ^d	0.062530	17.745	101.40	...
0.99912 ^e	0.099770	17.702	80.96	0.6962
(D) <i>dl</i> -Valine ^a				
0.027708	0.055416	20.596	52.32	0.7682
0.045235	0.090470	20.612	85.48	0.7657
0.12666	0.078715	20.594	74.31	0.7538
0.36638	0.095770	20.582	90.36	0.7190

^a Cell A was used for all experiments, except where otherwise indicated. ^b See ref. 28. ^c See ref. 9. ^d These experiments were performed with the Spinco electrophoresis-diffusion apparatus (see ref. 27) in which the light passed through the cell twice. Cell B was used for these experiments. ^e Cell A was used for these experiments.

(22) Supplied by the Perkin-Elmer Corp., U. S. A.

(23) This distance was measured by the Standards Laboratory of the South Australian Government Railways.

(24) L. J. Gosting and D. F. Akeley, *J. Am. Chem. Soc.*, **75**, 5685 (1953).

(25) R. A. Robinson and R. H. Stokes, "Electrolyte Solutions," Butterworths Scientific Publications, London, 1959, p. 29.

(26) H. D. Ellerton, G. Reinfelds, D. E. Mulcahy, and P. J. Dunlop, *J. Phys. Chem.*, **68**, 398 (1964).

Table II: Constants for the Least-Squared Equations of D vs. \hat{C} at 25°

	D^0	$A_1 \times 10$	$A_2 \times 10$	$A_3 \times 10$	$A_4 \times 10$	% dev.
Glycine	1.0609	-2.1097	0.7248	-0.2151	0.0352	±0.06
Glycylglycine	0.7963	-4.708	6.581	-6.411	2.399	±0.11
α -Amino- <i>n</i> -butyric acid	0.8305	-1.545	0.2127	±0.09
<i>dl</i> -Valine	0.7722	-1.454	±0.01

lower solutions, respectively, used in each diffusion experiment. As previously stated, almost all the diffusion measurements were performed with the Gouy diffusimeter; however, several measurements were performed for the system α -amino-*n*-butyric acid with a modified Spinco electrophoresis-diffusion apparatus which has been described previously.²⁷ The agreement between the two types of apparatus was quite satisfactory. By means of a 7090 IBM electronic computer the experimental diffusion coefficients were fitted by the method of least squares to polynomials of the form

$$D \times 10^5 = D^0 + \sum_{i=1}^4 A_i \hat{C}^i \quad (1)$$

where D^0 is the value of the diffusion coefficient at infinite dilution. The constants A_i for all materials together with the average deviations of the experimental points from the smooth curves are given in Table II. Some of the diffusion data for glycine in Table I have been reported previously.^{9,28}

Refractive index increments per mole were calculated using the relationship $(\Delta n/\Delta \hat{C}) = (\lambda J/a\Delta \hat{C})$, where J is the total number of fringes in a Gouy or an integral fringe pattern and λ is the wave length of the green mercury line. The refractive increments for all systems are given in column 3 of Table I and are referred to the refractive index of air as unity. These increments may be represented by equations of the form

$$(\Delta n/\Delta \hat{C}) \times 10^3 = (\Delta n/\Delta \hat{C})^0 + \sum_{i=1}^3 B_i \hat{C}^i \quad (2)$$

where $(\Delta n/\Delta \hat{C})^0$ is the value of the refractive increment at infinite dilution. Values for the constants B_i for all materials, together with the average deviations of the experimental points from the smooth curves, are given in Table III.

Discussion

One formal method of defining a set of mutual frictional coefficients, R_{ik} , for isothermal diffusion¹⁷⁻²⁰ provides the equations

$$X_i = \sum_{k=0}^q C_k R_{ik} [(v_i)_v - (v_k)_v] \quad (i = 0, 1, \dots, q) \quad (3)$$

for a system of q solutes in a solvent 0. The X_i are the gradients of chemical potential causing diffusion

$$X_i = -(\partial \mu_i / \partial x)_{T,P} \quad (4)$$

and here the C_k ²⁹ are the solute concentrations in moles/cc., the μ_i are the chemical potentials of the various components, and the $(v_i)_v$ are diffusion velocities with respect to the volume frame of reference defined by²

$$\sum_{i=0}^q \bar{V}_i (J_i)_v = \sum_{i=0}^q \bar{V}_i C_i (v_i)_v = 0 \quad (5)$$

where the \bar{V}_i are the partial molar volumes of the components and the $(J_i)_v$ are flows in the x direction.

For a binary system consisting of a solute, 1, and a solvent, 0, it has been shown^{18,20} that eq. 3 becomes³⁰

$$\begin{aligned} R_{01} &= [RT \bar{V}_0 (1 + C \partial \ln y / \partial C) / D] \\ &= [RT \bar{V}_0 (1 + \hat{C} \partial \ln y / \partial \hat{C}) / D] \end{aligned} \quad (6)$$

where R_{01} is the mutual frictional coefficient for binary diffusion, R is the gas constant, y is the solute activity coefficient on the volume concentration scale, and D is the experimentally measurable mutual diffusion coefficient. It is clear from eq. 3 that, even though the mutual diffusion coefficients depend on the frame of reference used for measurement, the R_{01} values are independent of such reference frames since velocity differences appear in the above equations.

Equation 6 has been used to compute frictional coefficients, R_{01} , for the systems reported in this paper

(27) J. M. Creeth, L. W. Nicol, and D. J. Winzor, *J. Phys. Chem.*, **62**, 1546 (1958).

(28) P. J. Dunlop, *J. Am. Chem. Soc.*, **77**, 2994 (1955).

(29) It should be noted that this concentration variable C differs from the concentration variable \hat{C} ($\hat{C} = 1000C$). The variable \hat{C} is more useful for experimental purposes.

(30) Here and in the following discussion we choose to delete the subscript 1 from all concentrations and activity coefficients.

Table III: Constants for the Least-Squared Equations of $(\Delta n/\Delta \hat{C})$ vs. \hat{C} at 25°

	$(\Delta n/\Delta \hat{C})^a$	B_1	B_2	B_3	% dev.	Concn. limit
Glycine	13.603	-0.6561	0.0685	...	±0.02	2.0
Glycylglycine	25.305	-1.6125	0.749	-0.287	±0.01	1.0
α -Amino- <i>n</i> -butyric acid	17.985	-0.286	±0.05	1.0
<i>dl</i> -Valine	20.595	±0.05	0.36

Table IV: Summary of Frictional Coefficient and Relative Viscosity Data at 25°

\hat{C}	$(1 + \hat{C} \frac{\partial \ln \eta}{\partial \hat{C}})$	\bar{V}_0^a	D^b	$(R_{01} \times 10^{-16})^c$	R_r	η_r
(A) Glycine						
0.0	1.000	18.068	1.0609	4.222	1.000	1.000
0.2	0.973	18.067	1.0214	4.269	1.011	1.029
0.4	0.953	18.065	0.9868	4.327	1.025	1.060
0.6	0.939	18.061	0.9562	4.398	1.042	1.093
0.8	0.930	18.055	0.9289	4.481	1.061	1.127
1.0	0.925	18.047	0.9044	4.576	1.084	1.163
1.2	0.924	18.037	0.8822	4.682	1.109	1.202
1.4	0.926	18.025	0.8620	4.798	1.136	1.242
1.6	0.930	18.010	0.8438	4.920	1.165	1.284
1.8	0.936	17.993	0.8274	5.045	1.195	1.329
2.0	0.943	17.973	0.8130	5.169	1.224	1.376
(B) Glycylglycine						
0.0	1.000	18.068	0.7963	5.625	1.000	1.000
0.1	0.962	18.067	0.7552	5.706	1.014	1.032
0.2	0.933	18.066	0.7237	5.776	1.027	1.067
0.3	0.912	18.065	0.6989	5.846	1.039	1.104
0.4	0.898	18.062	0.6784	5.927	1.054	1.141
0.5	0.889	18.059	0.6603	6.029	1.072	1.180
0.6	0.885	18.056	0.6433	6.157	1.095	1.220
0.7	0.884	18.052	0.6269	6.312	1.122	1.262
0.8	0.887	18.048	0.6109	6.493	1.154	1.307
0.9	0.892	18.043	0.5957	6.695	1.190	1.356
1.0	0.899	18.038	0.5824	6.906	1.228	1.409
(C) α -Amino- <i>n</i> -butyric Acid						
0.0	1.000	18.068	0.8305	5.394	1.000	1.000
0.2	1.027	18.068	0.8004	5.746	1.065	1.073
0.4	1.057	18.067	0.7721	6.131	1.137	1.150
0.6	1.090	18.065	0.7454	6.550	1.214	1.234
0.8	1.126	18.063	0.7204	7.002	1.298	1.329
1.0	1.166	18.060	0.6972	7.486	1.388	1.437
(D) <i>dl</i> -Valine						
0.0	1.000	18.068	0.7722	5.801	1.000	1.000
0.1	1.017	18.068	0.7577	6.013	1.037	1.042
0.3	1.035	18.068	0.7432	6.239	1.076	1.087
0.3	1.054	18.068	0.7286	6.479	1.117	1.137
0.4	1.074	18.067	0.7141	6.734	1.161	1.191

^a The partial molar volumes, \bar{V}_0 , have units of cm.³ mole⁻¹.

^b The diffusion coefficients, D , have units of cm.² sec.⁻¹. ^c The frictional coefficients, R_{01} , have units of ergs cm. sec. mole⁻².

and the results are tabulated in column 5 of Table IV. The values of \bar{V}_0 were calculated from the density equations reported in a companion paper²⁶ and the thermodynamic factor was computed from the equations for the osmotic coefficients given in the same paper. The constants in Table II were used to compute the D values at round values of \hat{C} . All computations were performed with the aid of an IBM 1620 electronic computer. Inspection of Table IV shows that the frictional coefficients so obtained show a much larger concentration dependence than do the corresponding diffusion coefficients.

Frictional coefficients were also computed from the thermodynamic and diffusion data in the literature^{3,26,31} for the systems α -alanine-H₂O, lactamide-H₂O, β -alanine-H₂O, glycolamide-H₂O, sucrose-H₂O, raffinose-H₂O, urea-H₂O, and biphenyl-benzene. Table V gives values of the frictional ratio $R_r = (R_{01}/R_{01}^0)$ for these systems at round values of the concentration, \hat{C} . Here R_{01}^0 is the value of the frictional coefficient which is found by extrapolating the experimental values to infinite dilution. Table IV includes values of R_r and also η_r at round concentrations for the systems glycine-H₂O, glycylglycine-H₂O, α -amino-*n*-butyric acid-H₂O, and *dl*-valine-H₂O.

Now if we assume that Stokes' law can be used to predict the variation of the frictional coefficients with concentration and if we also assume that the shape of

- (31) (a) L. J. Gosting and M. S. Morris, *J. Am. Chem. Soc.*, **71**, 1998 (1949); (b) L. J. Gosting and D. F. Akeley, *ibid.*, **74**, 2058 (1952); (c) P. J. Dunlop and L. J. Gosting, *ibid.*, **75**, 5073 (1953); (d) P. J. Dunlop, *J. Phys. Chem.*, **60**, 1464 (1956); (e) F. J. Gutter and G. Kegeles, *J. Am. Chem. Soc.*, **75**, 3893 (1953); (f) C. L. Sandquist and P. A. Lyons, *ibid.*, **76**, 4641 (1954); (g) H. C. Donoian and G. Kegeles, *ibid.*, **83**, 255 (1961); (h) L. S. Mason, P. M. Kampmeyer, and A. L. Robinson, *ibid.*, **74**, 1287 (1952); (i) F. T. Gucker, Jr., F. W. Gage, and C. E. Moser, *ibid.*, **60**, 2582 (1938); (j) F. T. Gucker, Jr., and T. W. Allen, *ibid.*, **64**, 191 (1942); (k) R. H. Stokes, *Trans. Faraday Soc.*, **50**, 565 (1954); (l) F. T. Gucker, Jr., and W. L. Ford, *J. Phys. Chem.*, **45**, 309 (1941); (m) R. A. Robinson, *J. Biol. Chem.*, **199**, 71 (1952); (n) D. H. Everett and M. F. Penney, *Proc. Roy. Soc. (London)*, **A212**, 164 (1952); (o) H. T. Briscoe and W. T. Rinehart, *J. Phys. Chem.*, **46**, 387 (1942); (p) E. R. B. Smith and P. K. Smith, *J. Biol. Chem.*, **132**, 47 (1940); (q) G. Scatchard, W. J. Hamer, and S. E. Wood, *J. Am. Chem. Soc.*, **60**, 3061 (1938).

Table V^a: Values of Relative Frictional Coefficients for Several Two-Component Systems at 25°

\hat{C}	α -Alanine	Lactamide	β -Alanine	Glycol- amide	Sucrose	Raffinose	Urea	Biphenyl ^b
0.0	1.000	1.000	1.000	1.000	1.000	1.000	1.000	1.000
0.1	1.093	1.150
0.15	1.144
0.2	1.041	1.031	1.036	1.015	^c	^d	1.004	1.032
0.4	1.086	1.064	1.074	1.031			1.009	1.065
0.6	1.135	1.100	1.117	1.048			1.014	1.101
0.8	1.186	1.137	1.164	1.066			1.019	1.138
1.0	1.242	1.176	1.215	1.085			1.025	1.179
1.2	1.304	1.218	1.271	1.106			1.031	1.222
1.4	1.375	1.262	1.332	1.127			1.038	1.269
1.6	1.463	1.309	1.398	1.150			1.045	1.318
1.8	^e	1.358	1.469	1.174			1.052	1.372
2.0		1.409	1.546	1.200			1.059	1.428
2.2		^f	1.628	1.226			1.067	1.489
2.4			1.717	1.254			1.076	1.550
2.6			1.811	1.283			1.086	1.625
2.8			1.911	1.314			1.097	1.701
3.0			2.018	1.345			1.108	1.783
3.2			2.131	1.378			1.119	^g
3.4			2.251	1.411			1.131	
3.6			2.378	1.445			1.143	
3.8			2.514	1.479			1.156	
4.0			2.660	1.512			1.169	

^a References to the data used for computing the relative frictional coefficients and the corresponding relative viscosities are given at the bottom of each column. ^b The solvent for biphenyl was benzene (see ref. 31f). ^c See ref. 31a, q. ^d See ref. 26 and 31d. ^e See ref. 31e, h, and m. ^f See ref. 3, 26, and 31j. ^g See ref. 31f, n, and o. ^h See ref. 31g, h, and p. ⁱ See ref. 31i, c, k, and l. ^j See ref. 31b and q.

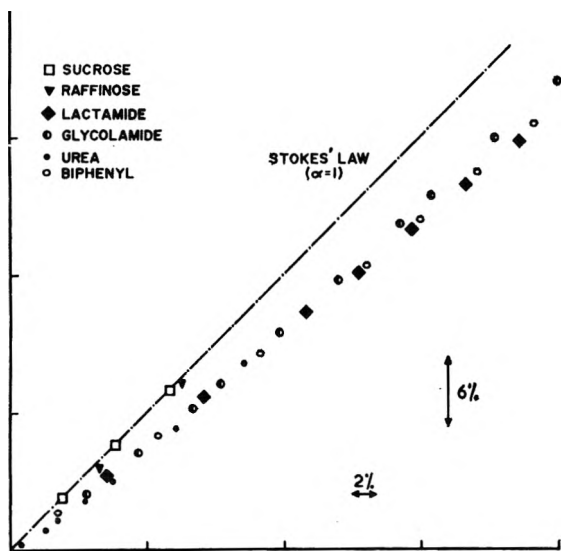


Figure 1. Values of $\log(R_r)$ vs. $\log(\eta_r)$ for several uncharged solutes in water at 25°. The solvent for biphenyl is benzene.

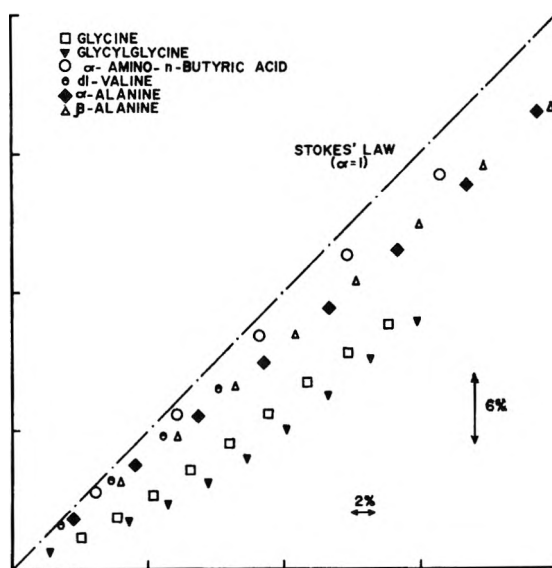


Figure 2. Values of $\log(R_r)$ vs. $\log(\eta_r)$ for several amino acids in water at 25°.

the diffusing entity is independent of concentration, then we would expect that

$$R_r \equiv (R_{01}/R_{01}^0) = (\eta_r)^\alpha \tag{7}$$

where $\alpha = 1$. Hence a graph of $\log(R_r)$ vs. $\log(\eta_r)$ would be a straight line with a slope of unity, and deviations from this slope would then be a measure of the

deviations from Stokes' law. Accordingly, in Fig. 1 and 2 graphs of $\log(R_r)$ vs. $\log(\eta_r)$ have been made for the systems reported in this paper and for those systems selected from the literature (see Table V).²² It is estimated that the error in each frictional coefficient is $\pm 0.3\%$ and that the error in each value of the relative viscosity is $\pm 0.2\%$. Thus the error in the relative frictional coefficients is $\pm 0.6\%$. These limits have been clearly marked in Fig. 1 and 2.

Inspection of Fig. 1 shows that of all the substances considered, sucrose is the only one which, in agreement with Stokes' law, gives a value of $\alpha = 1$. It is interesting to note that the α -values for all the other systems containing solutes with relatively small dipole moments, but excluding the system raffinose-H₂O, are approximately equal to 0.8. Figure 2 gives a similar graph for the amino acid-H₂O systems. However, while some of the relative frictional coefficients for the amino acids

give α -values of approximately 0.8, *dl*-valine and α -amino-*n*-butyric acid give values which lie between 0.8 and 1.0, while glycine and glycyglycine give α -values which are considerably less than 0.8, particularly at low concentrations. The marked change in slope for glycine and glycyglycine is interesting in view of the fact that the other amino acids show an essentially linear dependence of $\log(R_r)$ on $\log(\eta_r)$.

Acknowledgments. The authors wish to thank Mr. E. W. Gooden for performing some of the experiments with α -amino-*n*-butyric acid and Dr. B. J. Steel for many helpful discussions and his criticism of the manuscript. This work was supported in part by grants from the Colonial Sugar Refining Co. Ltd. of Australia and the United States Institutes of Health (AM-06042-02).

(32) The relative viscosity data are given in ref. 31.

NOTES

The Solubility of Mercury in Hydrocarbons

by Robert R. Kuntz and Gilbert J. Mains

Departments of Chemistry, University of Missouri, Columbia, Missouri, and Carnegie Institute of Technology, Pittsburgh 13, Pennsylvania (Received August 21, 1963)

The solubility of mercury in hydrocarbon solvents is of interest to the solution thermodynamicist in his efforts to understand the nature and extent of solvent-solute interactions¹ and, more recently, to the photochemist in his studies of mercury photosensitization of liquid hydrocarbons.^{2,3} Because the solubility is very low, of the order of micromoles per liter at 25°, earlier experimental measurements have involved the absorption of mercury from a large volume of saturated solution by gold foil⁴ or radioactive tracer techniques.⁵ A summary of these solubilities is given in the first column of Table I. The purpose of this note is to point out that the optical density at 2560 Å. of a saturated solution of mercury in hydrocarbon is a reliable measure of the solubility and, furthermore, that it is possible to estimate these solubilities using the Hildebrand equation for "regular" solutions.

Experimental

Phillips "pure grade" hydrocarbon solvents were made optically pure by passing through silica gel which had been previously baked and cooled *in vacuo*. Each solvent was degassed and distilled into a vessel which had been fused to a 100-mm. quartz absorption cell and contained a drop of mercury. Saturation was accomplished by vigorous shaking of the vessel for 20 min. at the desired temperature. Absorption spectra were taken with a Beckman DU spectrophotometer.

Results and Discussion

The absorption spectra of mercury in hydrocarbon solvents all exhibit a broad absorption in the 2537 Å. region which can be resolved into two overlapping peaks on most spectrographs.^{2,4,6} Maximum absorption

- (1) J. H. Hildebrand and R. L. Scott, "The Solubility of Nonelectrolytes," 3rd Ed., Reinhold Publishing Co., New York, N. Y., 1950.
- (2) M. K. Phibbs and B. deB. Darwent, *J. Chem. Phys.*, **18**, 679 (1950).
- (3) R. Kuntz and G. J. Mains, *J. Am. Chem. Soc.*, **85**, 2219 (1963).
- (4) H. Reichardt and K. F. Bonhoffer, *Z. Physik*, **67**, 780 (1931).
- (5) H. C. Moser and A. Voigt, U.S.A.E.C. Rept. ISC-892 (1957).
- (6) R. Kuntz, Ph.D. Thesis, Carnegie Institute of Technology, 1962.

Table I: The Solubility of Mercury in Some Organic Solvents

Solvent	T, °C.	Solubilities, $\mu\text{moles/l.}$		
		Experi- mental measure- ment	Calcd. from O.D. at 2560 Å.	Calcd. from eq. 1
<i>n</i> -Pentane	25		5.8	5.0
<i>n</i> -Hexane	25	6.4	(6.4)	5.9
<i>n</i> -Hexane ^c	40	13.5		
<i>n</i> -Hexane ^c	63	50.8		
Isopentane	25		5.5	3.3
3-Methylpentane	25		5.1	7.4
2,2-Dimethylbutane	25		5.0	4.3
2,3-Dimethylbutane	25		6.0	6.0
Cyclohexane ^b	25	11.0		15.8
<i>n</i> -Decane ^c	25		5.5	1.5
Water ^b	25	0.3	0.1	15.7×10^6
Water ^a	120	5.0		
Methanol ^d	25	0.78	1.52	0.97
Methanol ^a	40	3.0		
Methanol ^a	63	18.0		
Toluene ^b	25	12.5		43.7
Benzene ^b	25	12.0		66.7
CCl ₄ ^b	25	7.5		15.0
Perfluorodimethyl- cyclobutane	25		0.34	0.46

^a From ref. 4. ^b From ref. 5. ^c Extrapolated from the data in ref. 2. ^d Extension of $\log C$ vs. $1/T$ for data from ref. 4.

occurs at 2560 Å. for *n*-pentane, *n*-hexane, isopentane, 3-methylpentane, 2,2-dimethylbutane, 2,3-dimethylbutane, and *n*-decane.⁶ This absorption, assigned to the $6^1S_0 \rightarrow 3^1P_1$ transition in the gas phase, is considerably pressure broadened and split into two components by the strong electric fields of the solvent. This broadening and Stark splitting have been discussed quantitatively⁴ and will not be reviewed here. In the case of a series of C_5H_{12} and C_6H_{14} isomers the broadening and electric field splittings might be expected to be essentially the same and, therefore, the breadth of the absorption and the splitting of the two overlapping peaks to be the same. This is the experimental observation. Therefore, it may be concluded that the extinction coefficient of mercury does not vary significantly from one hydrocarbon solvent to another and, once it has been determined, a measurement of the optical density of a solution of mercury in hydrocarbon solvents at 2560 Å. permits a calculation of the solubility by assuming the Beer-Lambert absorption equation to be applicable.

The optical density of a saturated solution of mercury in *n*-hexane was measured⁶ and, when combined with the solubility measured by Moser and Voigt, gives an extinction coefficient, $\epsilon_{2560} = 7.35 \times 10^3$ l./mole cm. at 25°. This value was then used to calculate the solu-

bility of mercury in the other hydrocarbon solvents for which optical density measurements were available. The results of these calculations are given in the second column of Table I. It is unfortunate that water and methanol are the only solvents for which both optical density and experimental data are available for comparison since these solvents show considerably greater broadening of the peak and Stark splitting. Nonetheless, the order of magnitude predictions based upon the poor assumption that the extinction coefficient is the same in water, methanol, and hydrocarbon are in encouraging agreement with the experimental solubilities.

If mercury in hydrocarbons forms a "regular" solution, then values for the solubility may be calculated from the Hildebrand equation,¹ viz.

$$\ln a_2 = \ln x_2 + \frac{\phi_1 V_1 (\delta_2 - \delta_1)^2}{RT} \quad (1)$$

where a_2 is the activity of the solute; x_2 is the mole fraction of the solute; ϕ_1 is the volume fraction of the solvent; $\delta = (\Delta E_{\text{vap}}/V)^{1/2}$, the solubility parameter; and V_1 is the molal volume of the solvent. If the solubility of liquid hydrocarbon in mercury is neglected, $a_2 = 1$. Furthermore, because the solutions are so dilute it is possible to set $\phi_1 = 1$. Since the solubility parameters for mercury and most solvents have been tabulated,¹ it is possible to calculate the solubility of mercury based upon this equation. The values so calculated are given in the third column of Table I. The agreement between the experimental measurements and the values calculated from the equation is not at all bad except for the cases of the aromatic solvents and, of course, water. Indeed, except for water, the Hildebrand equation gives an "order of magnitude" approximation. Without exception, the values predicted by the Hildebrand equation are high for the polar compounds, a behavior similar to that observed in the case of iodine solutions.¹ The agreement between the solubility values calculated from optical density measurements and that predicted by the Hildebrand equation for "regular" solutions is quite remarkable and it appears unlikely that it is fortuitous. It would seem that, in spite of the wide discrepancy between the van der Waals interactions of hydrocarbon molecules and the metallic bonds in liquid mercury, no aggregation of mercury occurs in solution and the solute molecules are randomly dispersed in solution. The absence of spectrographic evidence for clustering of the mercury atoms was discussed by Reichardt and Bonhoffer.⁴ The solubility, therefore, is determined by the heat of solution of mercury in the hydrocarbon solvent. This conclusion is in accord with the large changes in the heat of solution of mercury in passing from methanol to hexane or water

as solvents. From the temperature dependence of the solubilities given in Table I the heats of solution in methanol, hexane, and water are 16.5, 10.3, and 6.9 kcal./mole, respectively.

Acknowledgments. R. Kuntz wishes to thank the Petroleum Research Fund for supporting the allied research which led to the measurements reported here. Special thanks are due Miss Pamela Wormington and Mr. Jonas Dedinas for determination of the absorption spectra of mercury in water, methanol, and perfluorodimethylcyclobutane.

Ionization of Some Weak Acids in Water-Heavy Water Mixtures¹

by Pentti Salomaa,² Larry L. Schaleger, and F. A. Long

Department of Chemistry, Cornell University, Ithaca, N. Y. (Received August 26, 1963)

In connection with a recent study on acid-base equilibria and kinetics in mixtures of light and heavy water³ it was established that the glass electrode method of measuring acid dissociation constants permits precision determinations in these solvents. In this paper three additional sets of equilibrium data obtained by this method are reported.

The results are collected in Table I. The pK values determined for the three acids in the solvent water, given in the table, are in good agreement with previously recorded values.⁴ The relative ionization constants K_H/K_D reported earlier for chloroacetic acid, *viz.*, 3.08⁴ and 2.76,⁵ compare well with the value 2.69 of Table I. On the other hand, the earlier values for hydrazoic acid,⁶ 2.14 (at 20°), and for ammonium ion,⁷ 3.1, are in poor agreement with the present data.

According to the equilibrium theory of solvent isotope effects developed originally by Gross and co-workers⁸ and revised recently by a number of authors,⁹⁻¹² the relative ionization constants K_H/K_n in mixed H₂O-D₂O solvents can be expressed in terms of the fractionation factors l and φ as

$$\frac{K_H}{K_n} = \frac{(1 - n + n\varphi)}{(1 - n + nl)^3}; \quad \frac{K_H}{K_D} = l^{-3}\varphi \quad (1)$$

$$l = \left(\frac{[D_3O^+]}{[H_3O^+]} \right)^{1/3} \frac{1 - n}{n}; \quad \varphi = \frac{[DA]}{[HA]} \frac{1 - n}{n} \quad (2)$$

Table I: Observed and Calculated Values for the Relative Ionization Constants K_H/K_n of some Weak Acids in H₂O-D₂O Mixtures at 25°

n	ClCH ₂ COOH		HN ₃		NH ₄ ⁺	
	$pK_H = 2.809$ Obsd.	Calcd.	$pK_H = 4.694$ Obsd.	Calcd.	$pK_H = 9.264$ Obsd.	Calcd.
0.099	1.07	1.08	1.10	1.09	1.11	1.13
.197	1.16	1.18	1.20	1.19	1.24	1.27
.296	1.27	1.29	1.32	1.31	1.41	1.45
.395	1.39	1.41	1.46	1.44	1.62	1.65
.494	1.56	1.55	1.62	1.60	1.88	1.89
.593	1.71	1.71	1.82	1.78	2.19	2.18
.692	1.95	1.90	2.03	2.00	2.49	2.51
.792	2.17	2.12	2.23	2.23	2.91	2.92
.891	2.40	2.37	2.54	2.52	3.39	3.42
.990	2.66		2.86		4.00	
1.000 ^a	(2.69)		(2.89)		(4.06)	

^a Extrapolated values.

in which the value of l is approximately 0.67.^{9,13} The calculated values given for chloroacetic and hydrazoic acids in Table I are based on these equations. Agreement between the observed and calculated values is excellent.

It has recently been shown that the application of the simple Gross theory is not justified in cases in which the acid and its conjugate base contain several exchangeable hydrogens.³ General equations, which depend on the number and character of exchangeable hydrogens in these species, were shown to be derivable without assumptions about fractionation factors. Ammonium ion provides an interesting application of the general equations since the number of exchangeable hydrogens in the acid and its conjugate base are four

- (1) The support of the Atomic Energy Commission is gratefully acknowledged.
- (2) On leave from the University of Turku, Turku, Finland.
- (3) P. Salomaa, L. L. Schaleger, and F. A. Long, *J. Am. Chem. Soc.*, **86**, 1 (1964).
- (4) A. O. McDougall and F. A. Long, *J. Phys. Chem.*, **66**, 429 (1962).
- (5) D. C. Martin and J. A. V. Butler, *J. Chem. Soc.*, 1366 (1939).
- (6) D. Dunn, F. S. Dainton, and S. Duckworth, *Trans. Faraday Soc.*, **57**, 1131 (1961).
- (7) G. Schwarzenbach, A. Epprecht, and H. Erlenmeyer, *Helv. Chim. Acta*, **19**, 1292 (1936).
- (8) P. Gross, *et al.*, *Trans. Faraday Soc.*, **32**, 877, 883 (1936).
- (9) E. L. Purlee, *J. Am. Chem. Soc.*, **81**, 263 (1959).
- (10) V. Gold, *Trans. Faraday Soc.*, **56**, 255 (1960).
- (11) C. G. Swain and R. F. W. Bader, *Tetrahedron*, **10**, 182 (1960).
- (12) E. A. Halevi, F. A. Long, and M. A. Paul, *J. Am. Chem. Soc.*, **83**, 305 (1961).
- (13) According to a personal communication of Dr. V. Gold, n.m.r. studies lead to essentially the same value for l as that derived from other sources.

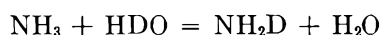
and three, respectively. In this particular case, the equations take the form

$$\frac{K_H}{K_n} = \frac{(1 - n + n\varphi_1)^4}{(1 - n + nl)^3(1 - n + n\varphi_2^3)} \quad (3a)$$

$$\frac{K_H}{K_D} = l^{-3}\varphi_1^4\varphi_2^{-3} \quad (3b)$$

$$\varphi_1 = \left(\frac{[\text{ND}_4^+]}{[\text{NH}_4^+]} \right)^{1/4} \frac{1 - n}{n}; \quad \varphi_2 = \left(\frac{[\text{ND}_3]}{[\text{NH}_3]} \right)^{1/3} \frac{1 - n}{n} \quad (4)$$

The fractionation factor for ammonia, φ_2 , can be estimated independently. The equilibrium constant for the reaction



in the gas phase at 25° is 1.61,¹⁴ from which the equilibrium constant for the liquid phase is

$$K = 1.61 \left(\frac{P_{\text{HDO}}}{P_{\text{H}_2\text{O}}} \right) \left(\frac{P_{\text{NH}_3}}{P_{\text{NH}_2\text{D}}} \right)$$

where the P 's are the vapor pressures at 25° of the species involved. By the rule of the geometric mean¹⁵

$$\varphi_2 = 2K/3 = 1.004(P_{\text{NH}_3}/P_{\text{NH}_2\text{D}})$$

in which the known value¹⁶ of $P_{\text{H}_2\text{O}}/P_{\text{HDO}}$, 1.069, has been introduced.

The vapor pressure of NH_2D has not been measured directly, but its value relative to that of NH_3 can be computed in the following way. The boiling points of NH_3 and ND_3 at atmospheric pressure are -33.48 and -31.11° , respectively.¹⁷ It is reasonable to assume that the successive substitution of protium by deuterium atoms in ammonia effects approximately equal elevations in the boiling points¹⁸; therefore, the boiling point of NH_2D cannot significantly differ from -32.69° . The entropy of vaporization¹⁷ of NH_3 at its boiling point is 23.3 cal. mole⁻¹ deg.⁻¹, and using the same value for NH_2D ,¹⁹ *i.e.*, adopting Trouton's rule, one can calculate the vapor pressure ratios for different temperatures from the Clausius-Clapeyron equation. In this way, a value of 1.032 is obtained for $P_{\text{NH}_3}/P_{\text{NH}_2\text{D}}$ at 25°, which gives $\varphi_2 = 1.04$. Combining this value with the known values of l and K_H/K_D , a value of 1.083 is obtained from eq. 3b for the fractionation factor of ammonium ion, φ_1 .

With the fractionation factors available, K_H/K_n values for all intermediate solvent compositions can be calculated from eq. 3a. The results are given in the last column of Table I. The values thus obtained are in excellent agreement with those directly measured.

This agreement does not firmly establish eq. 3 and 4 as correct, the reason being that for ammonium ion, with the large K_H/K_D ratio of 4.06, the simple Gross equation gives nearly as good fit to the data as does the general equation. (So also does the equation for a "linear" theory.¹²) However, since data on other polybasic acids, *e.g.* H_3PO_4 and H_3AsO_4 , confirm the correctness of the general equations, the point of particular interest is that the general equation *when combined with an independently estimated fractionation factor* gives an excellent fit.

- (14) I. Kirschenbaum, "Physical Properties and Analysis of Heavy Water," McGraw-Hill Book Co., Inc., New York, N. Y., pp. 58-59.
- (15) J. Bigeleisen, *J. Chem. Phys.*, **23**, 2264 (1955).
- (16) I. Kirshenbaum, ref. 14, Chapter 1.
- (17) I. Kirshenbaum and H. C. Urey, *J. Chem. Phys.*, **10**, 706 (1942).
- (18) This can be shown to be true of the isotopically different waters. From the known values of $P_{\text{H}_2\text{O}}/P_{\text{HDO}}$ at different temperatures¹⁶ and the values of $P_{\text{H}_2\text{O}}$, the normal boiling point of HDO calculates to be 100.71°, which is just the average of the boiling points of H_2O and D_2O , 100.00 and 101.43°.
- (19) The experimental value for the entropy of vaporization¹⁷ of ND_3 , 23.9 cal. mole⁻¹ deg.⁻¹, does not materially differ from that of NH_3 , and the difference between NH_3 and NH_2D must therefore be even smaller.

Particle to Particle Migration of Hydrogen Atoms on Platinum-Alumina Catalysts from Particle to Neighboring Particles

by S. Khoobiar

Esso Research and Engineering Company, Process Research Division, Linden, New Jersey (Received August 29, 1963)

The dissociation of H_2 to H atoms on noble metal wires at high temperatures has been suggested by many authors. The removal of H atoms from a hot wire is widely observed and accepted.

This note reports results of a simple and direct experiment which strongly indicates that H_2 dissociates on Pt/ Al_2O_3 (0.5 wt. % Pt) catalyst at room temperature and that active H atoms migrate readily from parent particles to neighboring particles and initiate chemical reactions. These findings have not been observed previously.

Experimental

WO_3 and MnO_2 are known to be good indicators for detection of H atoms because H atoms readily reduce these oxides with a collision efficiency of unity to

lower valence states¹ and the reduced oxide has a different color from that of the unreduced oxide. Thus, WO_3 has a yellow color and reduces initially to blue W_2O_{11} and then to brown WO_2 . Hydrogen molecules accomplish the reduction above 200° , but not at room temperature.²

The Pt- Al_2O_3 catalyst used in this work is a reforming catalyst prepared as described in the literature.³ The catalysts were made by impregnation of the support with aqueous chloroplatinic acid followed by drying at 550° for 1 hr. The support is a γ - Al_2O_3 and is commercially available.

The pure hydrogen was passed over WO_3 or mixtures of WO_3 with either Al_2O_3 or Pt- Al_2O_3 at room temperature in a 1×5 in. glass tube. Table I shows the results for equal volumes of the various mixtures.

Table I

Mixture ^a	Vol. % WO_3	Vol. % Al_2O_3	Vol. % Pt- Al_2O_3	Initial color	Time, min.	Final color
A	100	Yellow	300	Yellow
B	50	50	..	Yellow	300	Yellow
C	50	..	50	Yellow	1	Blue

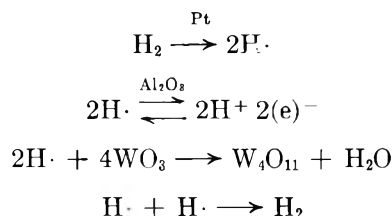
^a All the powders were dried at 150° in drying ovens prior to use and had a grain size of 500–800 μ . The powders were thoroughly mixed at room temperature manually.

These results demonstrate directly that H_2 at room temperature does not reduce WO_3 when it is alone or mixed with Al_2O_3 , but does reduce WO_3 readily in the presence of Pt- Al_2O_3 . When the temperature is increased to 50° , mixture C converts instantaneously to a blue color, but in order to change the color of A and B, higher temperatures are required (200 – 500°). The effectiveness of Pt- Al_2O_3 in bringing about the color change is attributed to dissociation of the hydrogen on Pt, followed by migration of H atoms to WO_3 .

Discussion of Results

The dissociation of H_2 on Pt- Al_2O_3 can be inferred from H_2 chemisorption studies⁴ and from various related studies including the known ability of these systems to catalyze reactions such as H_2 - D_2 exchange. The present experiments offer direct and conclusive evidence for this dissociation even at room temperature and, more important, for a subsequent migration of the dissociated products. Unpublished data from this laboratory⁵ based on electrical conductivity measurements have shown that hydrogen can exist as H^+ on Al_2O_3 . Although the details of the migration are of course unknown, one can postulate migration of either

$\text{H}\cdot$ or H^+ as a two-dimensional gas on the surface and diffusion through interparticle contacts from particle to particle. One possible mechanism would be



This finding is very important since it sheds some light on the more elusive steps involved in catalytic reactions involving H_2 on supported metal catalyst systems.

- (1) H. W. Melville and J. C. Robb, *Proc. Roy. Soc. (London)*, **A196**, 445 (1956).
- (2) L. G. Austin, *Ind. Eng. Chem.*, **53**, 660 (1961).
- (3) F. G. Ciapetta and C. J. Plank, "Catalysis," Vol. 1, Reinhold Publishing Corp., New York, N. Y., 1954, p. 315.
- (4) L. Spenadel and M. Boudart, *J. Phys. Chem.*, **64**, 204 (1960).
- (5) S. Khoobiar, P. J. Lucchesi, and J. L. Carter, to be published.

Hartley Band Extinction Coefficients of Ozone in the Gas Phase and in Liquid Nitrogen, Carbon Monoxide, and Argon

by William B. DeMore and Odell Raper

California Institute of Technology Jet Propulsion Laboratory,
Pasadena, California (Received September 5, 1963)

In the course of work on the photolysis of O_3 , we have determined the O_3 extinction coefficients in the region 2000–3100 \AA . in liquid N_2 and CO at 77.4°K . and in liquid Ar at 87.5°K . Previously, O_3 extinction coefficients have been reported in aqueous solvents^{1–4} and in CCl_4 ,⁵ but the only data for low temperature solvents are those of Kirshenbaum and Streng⁶ for the visible absorption of O_3 in liquid O_2 .

In the gas phase, differing extinction coefficients in the Hartley band were reported by Ny and Choong,⁷

- (1) H. Taube, *Trans. Faraday Soc.*, **53**, 656 (1957).
- (2) J. Weiss, *ibid.*, **31**, 668 (1935).
- (3) M. G. Alder and O. R. Hill, *J. Am. Chem. Soc.*, **72**, 1884 (1950).
- (4) M. L. Kilpatrick, C. C. Herrick, and M. Kilpatrick, *ibid.*, **78**, 1784 (1956).
- (5) G. W. Robinson, M.S. Thesis, Georgia Institute of Technology, 1949.
- (6) A. O. Kirshenbaum and A. G. Streng, *J. Chem. Phys.*, **35**, 1440 (1961).
- (7) T.-Z. Ny and S.-P. Choong, *Chinese J. Phys.*, **1**, 38 (1933).

Vigroux,⁸ and Inn and Tanaka.⁹ The Inn and Tanaka results have subsequently been verified closely by Hearn⁹ at six wave lengths and are considered to be the most reliable values available. We have measured the gas phase extinction coefficients throughout the region 2000–3100 Å. and our results are in close agreement with those of Inn and Tanaka.

Experimental

Reagents. Ozone was prepared by a Tesla coil discharge in purified O₂ and stored at 77°K. Transfer of O₃ to the absorption cells was accomplished by distillation from a liquid argon bath and collection at 77°K. Following the transfer, residual traces of O₂ were removed by pumping on the O₃ under high vacuum.

The solvents (N₂, Linde high purity dry; CO, Matheson C.P.; Ar, Linde tank grade) were passed through a Drierite-Ascarite column, liquefied, and further purified by two distillations, taking the center fraction in each case. Argon was handled using liquid argon as a coolant.

Apparatus. Spectra were recorded on a Cary Model 11 spectrophotometer. The wave length scale was calibrated by means of a low pressure mercury arc, and the wave lengths reported in this work are considered reliable to ±2 Å.

Gas phase spectra were taken in a 5-cm. cylindrical quartz cell, the O₃ being sealed off in the cell under vacuum.

The liquid cell was a 1-cm. cylindrical quartz cell, with an annular quartz jacket for the coolant, suspended in a vacuum canister with quartz windows. The entire unit could be placed in the spectrophotometer. Since the light path did not pass through the coolant and the solution was free of turbulence, the quality of the spectra was comparable to that of ordinary room temperature solvents. Optical densities of aqueous solutions of chromium nitrate were found to be identical within 0.5% in the above cell and in standard 1-cm. cylindrical cells, with an appropriate zero correction.

Measurement of gaseous O₂, from decomposed O₃, was done by means of a calibrated gas buret which was similar in construction to a McLeod gage, with the exception that the measuring stem had a stopcock to permit the O₂ to be collected by Toepler pump action. Calibration of the gas buret was checked by measurement of known samples in a standard volume at a pressure measured on a 0–20 mm. Wallace and Tiernan gage which was calibrated by means of a McLeod gage. The gas buret is considered accurate to 2% or better.

Methods. Ozone concentrations in the low temperature solvents were determined by separately measuring

the amount of O₃ spectrophotometrically in gas cells, using the relation

$$[\text{O}_3]_{\text{solvent}} = [\text{O}_3]_{\text{gas}} V_{\text{gas}} / V_{\text{solvent}}$$

The volumes, V_{gas} and V_{solvent} , were determined by filling the cells with water from a buret or by weighing the water. To ensure against errors due to loss of O₃ in transfer, the following three separate methods were employed in the initial experiments with N₂ solvent.

Method 1. The O₃ peak optical density (2553 Å.) was measured in a sealed-off gas cell and the O₃ was then transferred to the liquid cell at 77°K., using glass blown connections and break-off seals exclusively. In transfers of this type all glassware in contact with the O₃ sample was pre-exposed to O₃ at higher pressures. The solvent was then condensed into the cell and the spectrum was recorded. Zero corrections for the liquid spectra were made by taking the spectrum of the cell containing solvent only.

Method 2. The spectrum was first recorded in solution, followed by removal of the solvent by pumping at 77°K. and subsequent transfer of the O₃ to the gas cell. Although more difficult than method 1, this technique gave results which were within 1% of those of method 1. Since methods 1 and 2 give upper and lower limits, respectively, for O₃ concentrations in solution, convergence of the results eliminates the possibility of error due to O₃ loss in transfer.

Method 3. In this method, which was the simplest experimentally, gaseous O₃ was placed in the low temperature cell and the spectrum was recorded. The O₃ was then condensed by addition of coolant to the annular jacket and the solvent was condensed into the cell, and the spectrum was then taken. Although this method suffered somewhat from an unfavorable volume ratio (the volume of O₃ in the light path was about 1/6 the total gaseous volume), the results were equal to within 1% of those from methods 1 and 2. Therefore, method 3 was used exclusively for the solvents Ar and CO.

Ozone concentrations in the gas phase were determined by converting the O₃ to O₂, by means of heat or a Tesla spark coil, and then measuring the O₂ in the gas buret. The technique was as follows: a sample of pure O₃ was sealed off in the (well-baked out) 5-cm. cell with two break-off seals attached, and the peak (2553 Å.) was measured. The cell was immediately placed in liquid N₂ to quench O₃ decomposition, and the

(8) E. Vigroux, *Ann. phys.*, **8**, 709 (1953).

(9) E. C. Y. Inn and T. Tanaka, "Ozone Chemistry and Technology," *Advances in Chemistry Series*, No. 21, American Chemical Society, Washington, D. C., 1959, p. 263; *J. Opt. Soc. Am.*, **43**, 870 (1953).

cell was then opened to high vacuum by means of one of the break-off seals. After removal of any O_2 or other volatile gases, the cell was resealed (while pumping) and the O_3 was decomposed. The cell was then placed in a Dry Ice bath and attached to the gas buret, and the O_2 was admitted to the gas buret through the second break-off seal.

Extinction coefficients at other wave lengths in the region 2000–3100 Å. were then determined relative to the peak value by taking the spectrum of O_3 with about 10 cm. added O_2 (no pressure effect was noted). This method has the advantage that O_3 decomposition is sufficiently inhibited so that no corrections are necessary.

Table I: Ozone Extinction Coefficients Obtained by Different Workers (cm. NTP)⁻¹

Wave length, Å.	Inn and Tanaka	Present work	Hearn
2102	6.39	6.33	
2152	11.7	12.1	
2202	21.0	21.4	
2252	34.3	34.8	
2302	52.8	53.5	
2352	73.6	74.6	
2362	78.2	79.8	
2372	83.2	84.1	
2382	86.2	88.9	
2392	90.1	93.1	
2402	95.3	97.3	
2412	98.9	102	
2422	103	105.5	
2432	107	110	
2452	116	118	
2478	124	125	
2500	130	130	
2519	133	134.5	
2537	(133.1) ^a	135	133.9
2539	134	135	
2553	135	137	
2587	133	134.5	
2604	128	129	
2624	123	123.5	
2643	118	117.5	
2675	103	103	
2702	89.1	91.1	
2752	66.6	66.9	
2802	43.6	45.6	
2852	27.5	28.0	
2894	(17.1) ^a	17.3	17.2
2902	15.5	15.6	
2952	8.33	8.5	
2967	(6.72) ^a	6.85	6.97

^a As interpolated by Hearn, ref. 9.

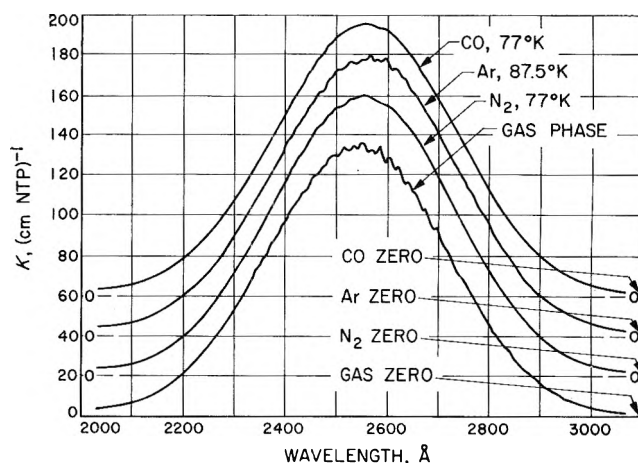


Figure 1. Extinction coefficients of ozone. (To obtain K values for N_2 , Ar, or CO, subtract 20, 40, or 60, respectively, from the value indicated on the ordinate.)

Results and Discussion

The extinction coefficients of O_3 in liquid N_2 , CO, and Ar, and in the gas phase, are shown in Fig. 1. The concentration ratios were determined to within 2% and therefore, coupled with a 2% uncertainty in the gas phase extinction coefficients, the solvent values are believed to be reliable to within 4%.

Values for the gas phase extinction coefficients obtained by Inn and Tanaka, Hearn, and in the present study are listed at several wave lengths in Table I. Our results are for the most part 1 or 2% higher than the Inn and Tanaka values, and near the maximum seem to be in better agreement with the values found by Hearn. Agreement with the Inn and Tanaka results is poorest in the region from about 2375 to 2450 Å., where the Inn and Tanaka values fall as much as 3% below ours. We have rechecked our data in this region and find no error.

Concerning the Densities and Temperature Coefficients of Liquid Barium and Calcium

by A. V. Grosse and P. J. McGonigal¹

The Research Institute of Temple University, Philadelphia, Pennsylvania (Received June 14, 1968)

The density of liquid barium has been measured recently by Addison and Pulham² and the density of liquid calcium was measured previously by Culpin³ in connection with his viscosity studies. No other data are available. The present authors have had

occasion to question the accuracy of these data with regard to the slopes of the density *vs.* temperature lines.

The situation here is similar to that which existed in the case of magnesium and which was discussed by the authors previously.⁴ However, in contrast, there was an abundance of experimental density data for liquid magnesium and it was the *very great discrepancies* between values reported by various workers that first attracted our attention. It was possible to *predict* values for the density at the normal boiling point, critical density, and slope of the density *vs.* temperature line or the temperature coefficient of density for magnesium and these predictions were found subsequently to agree rather closely with our experimental results and extrapolations based thereon. Our calculated results for barium and calcium, obtained by methods to be discussed below, are contrasted with the experimental values in Table I. The discrepancy is substantial.

Table I: Data for Barium and Calcium

	Barium	Calcium
Melting point, °K.	1002 ^a	1123 ^b
Reference density at m.p., g./cm. ³	3.320	1.364
-dD/dT × 10 ⁴ g./cm. ³ °K.	2.14	8.87
Calculated:		
Method 1	5.04	2.18
Method 2	5.10	2.20
Method 3	5.64	2.24
Critical density, g./cm. ³		
Method 1	0.722	0.304
Method 2	0.712	0.299
Method 3	0.620	0.292
Estimated critical temp., °K.	4720 ± 10%	4590 ± 10%
Density at normal boiling point, g./cm. ³		
Method 1	2.862	1.224
Method 2	2.857	1.223
Method 3	2.806	1.220
Normal boiling point, °K.	1910 ^c	1765 ^c
Reduced temperature at normal boiling point	0.405	0.384
ΔH _{vap} at normal boiling point, cal./g. atom	36,070 ^c	35,840 ^c

^a D. T. Peterson and J. A. Hinkebein, *J. Phys. Chem.*, **63**, 1360 (1959). ^b O. Kubaschewski and R. Hörnle, *Z. Metallk.*, **42**, 129 (1951). ^c D. R. Stull and G. C. Sinke, "Thermodynamic Properties of the Elements," Advances in Chemistry Series, No. 18, American Chemical Society, Washington, D. C., 1956.

It has been shown⁵⁻⁷ that critical temperatures of metals can be estimated to a fair degree of reliability

by application of the *theorem of corresponding states* to entropy of vaporization data. Critical temperatures estimated on this basis show good agreement with those estimated by use of extrapolated liquid and vapor densities and the law of the rectilinear diameters.

The metal selected as a reference for the application of the theorem of corresponding states is mercury, the only metal whose critical constants have been experimentally determined.⁸ The most reliable data for the entropy of vaporization of mercury are those of Busey and Giaque.⁹ The estimated critical temperatures of barium and calcium together with some other pertinent physical properties are shown in Table I.

Treatment of the data reported by Culpin³ yielded the equation

$$D \text{ (g./cm.}^3\text{)} = 2.360 - 8.87 \times 10^{-4}T \text{ (}^\circ\text{K.)} \quad (1)$$

for the density of liquid calcium. The melting point observed by Culpin was 1075°K., which is considerably lower than 1123°K. as reported by Kubaschewski and Hörnle. No subsequent data have been reported. Without introduction of significant error, the reference density of liquid calcium will be taken as 1.364 g./cm.³ at 1123°K.

The data of Addison and Pulham² fit the equation

$$D \text{ (g./cm.}^3\text{)} = 3.534 - 2.14 \times 10^{-4}T \text{ (}^\circ\text{K.)} \quad (2)$$

for the density of liquid barium. Their measurements covered the range 1013-1103°K. and a slight extrapolation yields a reference density of 3.320 g./cm.³ at the melting point (1002°K.).

It is noted that the temperature coefficient for calcium is very steep and indeed extrapolation of the rectilinear diameter indicates that it crosses the temperature axis at 2660°K., which is well below the critical temperature. The slope in the case of barium, on the other hand, is very slight and leads to a very high

- (1) A report of this work will constitute a portion of a dissertation to be submitted by P. J. McGonigal to the Graduate Board of Temple University in partial fulfillment of the requirements for the degree of Doctor of Philosophy.
- (2) C. C. Addison and R. J. Pulham, *J. Chem. Soc.*, 3873 (1962).
- (3) M. F. Culpin, *Proc. Phys. Soc. (London)*, **203**, 1079 (1957).
- (4) P. J. McGonigal, A. D. Kirshenbaum, and A. V. Grosse, *J. Phys. Chem.*, **66**, 737 (1962).
- (5) A. V. Grosse, *J. Inorg. Nucl. Chem.*, **22**, 23 (1961).
- (6) A. V. Grosse, "The Liquid Range of Metals, and Some of their Physical Properties at High Temperatures," Paper No. 2159, A.R.S., Space Flight Report to the Nation, New York, N. Y., October 9-15, 1961.
- (7) A. V. Grosse, "The Liquid Range of Metals and Some of their Physical Properties at High Temperatures," Report of the Research Institute of Temple University, October 19, 1960.
- (8) F. Birch, *Phys. Rev.*, **41**, 641 (1932).
- (9) R. H. Busey and W. F. Giaque, *J. Am. Chem. Soc.*, **75**, 806 (1953).

critical density or requires the assumption of a very high critical temperature.

In view of these facts, the critical densities, temperature coefficients of the density *vs.* temperature lines (which are valid up to at least the normal boiling points), and the densities at the normal boiling points were estimated by three separate but related methods. The *first* method was the same as used by us in the work on magnesium.⁴ An average reduced rectilinear diameter *vs.* reduced temperature line for six metals (Hg, Bi, Ag, Pb, Sn, and Ga) was constructed and assumed to be fairly representative of the reduced density *vs.* reduced temperature behavior of metals in general. The *second* method is the same as the first except that the average line was constructed from data for sodium, potassium, and magnesium. The *third* method involved application of a generalized relation between reduced density and temperature which is valid for liquid metals as well as other classes of liquids.¹⁰

Table I shows our calculated density data for barium and calcium. It is seen that the three methods yield results which agree rather closely with each other. The reliability of our calculations is, of course, dependent upon the accuracy of the experimental reference density as well as errors in estimation of critical temperatures which are discussed elsewhere.⁵ Although our calculated data are given to three or four significant figures to illustrate the agreement of the three methods, it should be remembered that the error possibility may be $\pm 10\%$.

The final results calculated for the density *vs.* temperature relationship may be expressed by the equation

$$D_{Ba} \text{ (g./cm.}^3\text{)} = 3.847 - 5.26 \times 10^{-4} T \text{ (}^\circ\text{K.)} \quad (3)$$

for barium, and

$$D_{Ca} \text{ (g./cm.}^3\text{)} = 1.613 - 2.21 \times 10^{-4} T \text{ (}^\circ\text{K.)} \quad (4)$$

for calcium.

The differences between the experimental and calculated temperature coefficients, -8.87×10^{-4} *vs.* -2.21×10^{-4} g./cm.³ °K., respectively, for calcium and -2.14×10^{-4} *vs.* -5.26×10^{-4} g./cm.³ °K. for barium, are substantial.

These differences between the experimental and calculated results are even more striking if the coefficients of cubical expansion, $-1/D \text{ d}D/\text{d}T$, which would be expected to have similar values for barium and calcium, are compared. The coefficients of cubical expansion at the melting point obtained from an average of calculated data are very similar (1.58×10^{-4} °K.⁻¹ for barium and 1.62×10^{-4} °K.⁻¹ for calcium) while the values obtained from the experimental data differ

by a factor of ten (0.645×10^{-4} °K.⁻¹ and 6.49×10^{-4} °K.⁻¹, respectively). These discrepancies serve to illustrate the difficulties inherent in measuring the physical properties of liquid metals, especially for the first time, at elevated temperatures.

Acknowledgment. We gratefully acknowledge the financial support of U. S. Atomic Energy Commission Grant AT(30-1)-2082.

(10) P. J. McGonigal, *J. Phys. Chem.*, **66**, 1686 (1962), and further unreported work in progress.

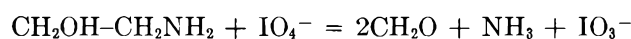
The Kinetics of the Periodate Oxidation of 2-Aminoethanol

by George Dahlgren and John M. Hodson

Department of Chemistry, University of Alaska, College, Alaska
(Received July 29, 1963)

The periodate oxidation of aminoalcohols and vicinal diamines has received scant attention in the literature, and kinetic papers on the subject are nearly nonexistent. Nicolet and Shinn¹ studied the periodate oxidation of substituted aminoethanols and found that tertiary amine groups slowed the reaction considerably. They attributed this retardation to the protonated form of the amine being nonoxidizable. Aminoalcohols with a single alkyl group on the nitrogen reacted rapidly. Fleury, *et al.*,² found the reaction of ethylenediamine with periodate at 100° to be a relatively slow reaction accompanied by side reactions. McCasland and Smith³ investigated the effect of *cis-trans* isomerism on the rate of periodate oxidation of 2-aminocyclohexanol and 2-aminocyclopentanol. The *cis* isomers were found to react faster than their *trans* counterparts, an effect also observed in the case of substituted cyclopentene glycols.⁴ Maros, *et al.*,⁵ have studied the stoichiometry of periodate oxidation of aminoalcohols and found that the reaction followed the scheme

- (1) B. H. Nicolet and L. A. Shinn, *J. Am. Chem. Soc.*, **61**, 1615 (1939).
- (2) P. Fleury, J. Courtois, and M. Grandchamp, *Bull. soc. chim. France*, **88** (1949).
- (3) G. E. McCasland and D. A. Smith, *J. Am. Chem. Soc.*, **73**; 5164 (1951).
- (4) V. C. Bulgrin and G. Dahlgren, *ibid.*, **80**, 3883 (1958).
- (5) L. Maros, I. Molnar-Perl, and E. Schulek, *Acta Chim. Acad. Sci. Hungary*, **30**, 119 (1962).



In an attempt to elucidate the mechanism of the periodate oxidation of aminoalcohols we have investigated the reaction of 2-aminoethanol.

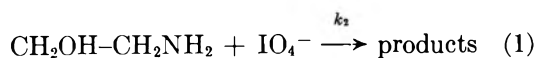
Experimental

Materials. Fisher 2-aminoethanol was distilled in a 53-plate column. The fraction used in this work boiled at 84.5° at 18 mm. and was 99.8% pure by gas chromatography (n_D^{25} 1.4510). Inorganic materials were the best grade available.

Rate Determinations. The reaction was studied by the same procedure used in the rate studies previously noted. The runs were made using acetate buffers to maintain a pH ± 0.02 throughout the run. The ionic strength of the reaction mixtures for the pH variation runs was maintained at 0.2 by the addition of sodium nitrate.

Results and Discussion

If the reaction of periodate with aminoalcohols involves the nonprotonated aminoalcohol as suggested by McCasland and Smith³ for aminocyclanols and a negative periodate ion (assumed here to be IO_4^-), as originally suggested by Duke,⁶ then a consideration of the reaction scheme



leads to the second-order rate expression

$$\frac{-d(P)_T}{dt} = k_2(\text{IO}_4^-)(\text{AE}) = k_2(P)_T(\text{AE})/(1 + 1/K_D) \quad (2)$$

where $(P)_T$ is the total periodate concentration as determined by analysis, (AE) is the concentration of nonprotonated 2-aminoethanol, and the factor $(1 + 1/K_D)$ is the correction term for the availability of IO_4^- in the pH range 3-7.⁷ Since the $\text{p}K_a$ for 2-aminoethanol is approximately 10,⁸ the concentration of the nonprotonated species is given by $(\text{AE}) = K_a(\text{AEH}^+)/(\text{H}^+)$, where (AEH^+) is the total concentration of 2-aminoethanol in the pH range 3-7. Substitution of this expression into eq. 2 yields

$$\frac{-d(P)_T}{dt} = k_2K_a(\text{AEH}^+)(P)_T/(\text{H}^+)(1 + 1/K_D) \quad (3)$$

For runs at constant pH and in which the 2-aminoethanol is present in sufficient excess so as to remain essentially constant throughout the run, the rate is given by the first-order expression

$$\frac{-d(P)_T}{dt} = k_1'(P)_T \quad (4)$$

where $k_1' = k_2K_a(\text{AEH}^+)/(\text{H}^+)(1 + 1/K_D)$. Excellent pseudo-first-order plots were obtained for runs in which the 2-aminoethanol was present in four- to sevenfold molar excess over the periodate. Mean values for $k_1'/(\overline{\text{AEH}^+})$, where $(\overline{\text{AEH}^+})$ is the average concentration of 2-aminoethanol over the observed portion of the run, for several temperatures are recorded in Table I along with the calculated values for k_2 . The deviations from the mean values are well within the experimental error and therefore the first-order dependence of the 2-aminoethanol appears established.

The first-order dependence of the rate on pH suggested by eq. 3 was verified experimentally at 0° using a fourfold molar excess 2-aminoethanol, a constant ionic strength of 0.2, and a pH range 3.6 to 6.4. A plot of the log of the pseudo-first-order rate constant vs. the pH for ten runs gave a good straight line of unit slope and an intercept of $k_2K_a(\text{AEH}^+)/(1 + 1/K_D)$. The value of k_2 obtained from the intercept was $7.5 \pm 0.8 \times 10^3$, in reasonable agreement with the value of $8.2 \pm 0.2 \times 10^3$ obtained from the data above at constant pH.

Table I: Rate Constants and Equilibrium Constants for the Periodate Oxidation of 2-Aminoethanol. ($k_2 = k_1'(\text{H}^+)(1 + 1/K_D)/(\overline{\text{AEH}^+})K_a$; $(\text{AEH}^+)_0$ (range) 0.08-0.14 M $(P)_T$ (initial) = 0.0202 M)

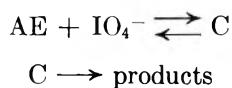
	T, °C. ($\pm 0.05^\circ$)		
	0.0°	12.5°	25.0°
K_D°	7.9	18.3	39.6
$K_a \times 10^{11b}$	4.95	13.1	32.0
pH_{av}	4.14	4.16	4.15
$(k_1'/(\overline{\text{AEH}^+})) \times 10^3, \text{sec.}^{-1}$	4.97 ± 0.10 (7 runs)	11.0 ± 0.5 (6 runs)	20.4 ± 0.9 (6 runs)
$k_2 \times 10^{-3}, \text{l. mole}^{-1} \text{sec.}^{-1}$	8.2 ± 0.2	6.1 ± 0.3	4.6 ± 0.2

^a C. Crouthamel, A. Hayes, and D. S. Martin, *J. Am. Chem. Soc.*, **73**, 82 (1951). ^b See ref. 8 of this work.

The thermodynamic functions of activation are listed in Table II. The enthalpy of activation was obtained over the temperature range 0-25°; the free energy and entropy of activation were calculated using data obtained at 0°. The negative enthalpy of activation suggests that the rate-determining step is preceded by

- (6) F. R. Duke, *J. Am. Chem. Soc.*, **69**, 3054 (1947).
 (7) F. R. Duke and V. C. Bulgrin, *ibid.*, **76**, 3803 (1954).
 (8) R. G. Bates and G. D. Pinching, *J. Res. Natl. Bur. Std.*, **46**, 349 (1951).

an equilibrium, possibly similar to that demonstrated kinetically for ethylene glycol by Duke and Bulgrin.⁷ By analogy to their work, we suggest the following scheme which accounts for the observed data.

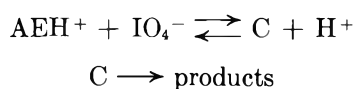


However, the method used for determining the presence of the activated complex C in the ethylene glycol work⁷ fails with 2-aminoethanol due to the very low concentration of C which would be present at any time.

Table II: Thermodynamic Functions of Activation at 0° for the Periodate Oxidation of 2-Aminoethanol via the

Reaction	$\text{AE} + \text{IO}_4^- \xrightarrow{k_s} \text{products}$
ΔH^* , kcal./mole	-4.3 ± 0.2
ΔG^* , kcal./mole	11.0 ± 0.0
ΔS^* , e.u.	-56 ± 1

Many mechanisms can be postulated which would account for the observed kinetics. Although no conclusive experimental evidence was found for it, one of these schemes is worthy of note at this time, for it suggests a new reactive species, the protonated form of the aminoalcohol. The negative temperature effect and the first-order pH dependence can be accounted for by a pre-equilibrium between the protonated form of the aminoalcohol and the periodate species, followed by the disproportionation of the complex in a rate-determining step, *viz.*



Acknowledgment. The authors gratefully acknowledge the financial assistance of the Research Corporation in support of this work.

Transport of Aqueous Solutions at a Mercury-Glass Interface, Induced by Electric Polarization

by Robert J. Good and William G. Givens

General Dynamic/Astronautics, San Diego 12, California
(Received August 7, 1963)

In the course of a study of the effect of electric polarization on the interfacial tension between mercury and

electrolyte solutions, an interesting effect was observed to occur at the mercury-glass interface. This was the transport of the aqueous electrolyte solution, between mercury and the wall of the containing tube, when the mercury was polarized negatively with respect to the aqueous solution.

Experimental

The apparatus used is shown in Fig. 1. The mercury contained in the U-tube was connected to the negative pole of a d.c. source and the mercury pool (C) was connected to the positive pole. Transport of the aqueous solution was observed, with the solution moving between the mercury and the walls of the U-tube, from the interface at A to the opposite side of the U-tube. The effect has been observed with U-tubes of glass, Tygon, and Teflon, and with solutions of tetramethylammonium chloride, tetramethylammonium iodide, hexadecyltrimethylammonium bromide, sodium chloride, lithium chloride, hydrochloric acid, and mixtures of these substances, at concentrations of 0.001 to 0.1 M. It was observed with triple-distilled mercury and with 99.99999% pure mercury (purchased from United Minerals and Chemicals Co.).

As voltage was increased from zero, the contact angle (measured through the aqueous phase) at the mercury solid-aqueous solution line decreased markedly. The voltage at which the contact angle reached zero was apparently the threshold voltage for transport, which was approximately 1.5 v. in glass tubes for the systems tested. This threshold showed variations of only 0.1 or 0.2 v., typically, among the various solutions in glass; it was reproducible in a particular system to within about 0.1 v. (This degree of repro-

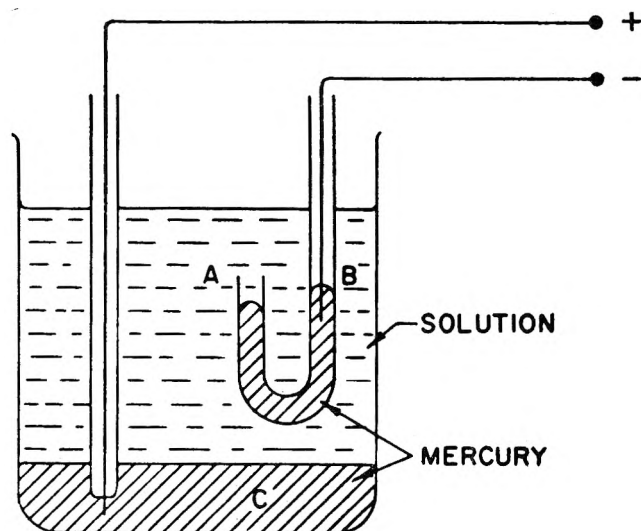


Figure 1.

ducibility was due in part to hysteresis and in part to uncertainty of observation of the start of transport.) At voltages high enough to cause continuous pumping, *e.g.*, about 2 v., a definite waist, shown exaggerated in Fig. 2, was visible below the top of the mercury column.

Teflon showed a threshold of around 2 v., as did Tygon which had been washed with a hot detergent solution. Untreated Tygon in one case showed a threshold of 0.5 v. with 0.01 *M* tetramethylammonium chloride; while we were not able to repeat this low value, addition of organic oils such as dinonyl phthalate to the solution, or to the plastic tubing, decreased the threshold from near 2 v. to approximately 1 v. (It was difficult to obtain consistent values of this reduction in threshold voltage, however.)

U-tubes having inside diameters from 0.28 to 7 mm. were used, with transport occurring in all. In the smaller tubes, with i.d. about 1 mm. or less, the mercury column tended to break up and pulsate in the tube, whereas in the larger tubes continuous stable flow was obtained.

Removal of the dissolved oxygen from the solution by bubbling nitrogen through it did not change the effect qualitatively. The current was reduced somewhat, and the depth to which the aqueous solution was carried below the mercury surface, at a given voltage, was increased.

The transport of water could be made to occur against a very considerable pressure head. At 1.75 v. in a 4-mm. glass U-tube, deoxygenated 0.01 *M* tetramethylammonium chloride penetrated to a depth of 37 mm. in about 2 hr. (This appeared to be the limiting depth, under these conditions.) At 3.0 v., the solution penetrated past the 37-mm. depth in about 10 min. Both the rate of transport and the head against which the pumping could take place increased rapidly with increasing voltage. One measurement of the rate of

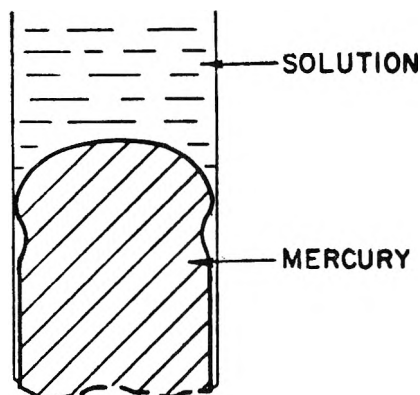


Figure 2. Configuration of mercury surface at voltages above 3 v. (schematic).

transport was made. With a U-tube 7 mm. in diameter and a mercury depth of 2 mm., 0.016 ml./min. of 0.01 *M* tetramethylammonium chloride was transferred to the other side of the U-tube, when 3 v. was applied. The current was 0.24 ma. Analysis showed no change in the chloride concentration (within 5%) and a pH change from 6.5 to 8 between the starting electrolyte and that transported under the mercury.

The effect has also been observed with liquid gallium, in glass, though with considerably greater difficulty. The threshold voltage was about 0.5 v. higher than with mercury; and with several samples of gallium it was not possible to get the pumping to start at all. There usually remained regions of Ga-glass interface where the solution had not displaced the metal. Presumably this behavior of the gallium occurred because of the strong tendency of gallium to form oxide coatings which adhere to glass.

Discussion

Changes in the mercury-aqueous solution interfacial tension with an applied potential are well known, as is the circulation of a mercury surface under the influence of interfacial tension gradients.¹⁻³ Hence, a mechanism for the transport may be proposed in terms of the interfacial tension gradients. If the contact angle in the aqueous phase is zero, and if the interfacial tension at the edge of the meniscus is greater than that nearer the center, a surface flow will occur toward the edge of the meniscus. The mercury and aqueous phase near the surface will be carried along and the aqueous phase can be dragged in between the mercury and the wall. The waist in the mercury surface shown in Fig. 2 provides visible evidence of circulation beneath the mercury surface, since such a profile could not be stable if the system were static.

The contact angle in the aqueous phase is normally positive, as indicated by a sharp edge to the meniscus on observation with a microscope. With increasing voltage, the contact angle visibly decreases and the edge disappears into a continuous curve (indicating a zero contact angle) when the voltage is reached at which transport sets in. This decrease in contact angle is to be expected, since the interfacial tension between the mercury and the aqueous phase is reduced by the negative polarization of the mercury (past the electrocapillary maximum) and this causes the spreading co-

- (1) G. W. C. Milner, "The Principles and Applications of Polarography," Longmans, Green and Co., London, 1957, p. 70 ff.
- (2) I. M. Kolthoff and J. J. Lingane, "Polarography," Interscience Publishers, Inc., New York, N. Y., 1952, p. 168 ff.
- (3) J. J. Bickerman, "Surface Chemistry," Academic Press, New York, N. Y., 1958, p. 441 ff.

efficient for the aqueous phase to increase. An analogous effect was reported⁴ for the mercury-water-hydrogen gas contact angle.

The proposed gradient in surface tension would be generated by a gradient in polarization and adsorption over the surface. The geometrical restriction of the available path for electric current, near the edges of the tube, will cause a lower current density near the edge of the meniscus than in the center, with the lowest current density nearest the edge where the mercury comes in contact with the tube walls. The polarization of the interface decreases with decreasing current density, and with it the adsorption of counterions, so the interfacial tension will be higher at the edge of the meniscus than nearer the center.

The magnitude of the driving force leading to the observed pumping action could be estimated with the aid of published electrocapillary curves¹⁻³ if the exact potential distribution over the surface were known. The increase of negative potential past the electrocapillary maximum causes a very marked decrease in interfacial tension, *e.g.*, as much as 100 dynes/cm. v.⁵ If a difference in tension acted on a sufficiently thin layer of liquid, a very considerable pressure could be developed. For example, a 1 dyne/cm. (interfacial) tension acting along a film 10^4 Å. thick corresponds to a pressure of about 8 cm. A detailed hydrodynamic analysis would be required to give a quantitative account of the rate of flow in relation to the actual surface tension gradient; but this calculation shows that the magnitude of the force available is quite adequate to account for the effect observed.

Acknowledgment. This work was supported by the U. S. Atomic Energy Commission under Contract AT(04-3)-297. Thanks are expressed to Dr. Donald Lewis for stimulating discussions which led, serendipitously, to the work here reported.

(4) H. G. Moller, *Ann. Physik* (4) 25, 725 (1908).

(5) J. T. Davies and E. K. Rideal, "Interfacial Phenomena," Academic Press, New York, N. Y., 1961, pp. 97, 361-362.

Deactivation of Palladium-Alumina Catalysts

by Donald G. Manly and Fred J. Rice, Jr.

The John Stuart Research Laboratories of The Quaker Oats Company, Barrington, Illinois (Received September 12, 1963)

In the course of a catalytic study carried out in these laboratories it was observed that a deactivated pal-

ladium-alumina catalyst could not be brought back to original activity by regeneration with air. In view of the loss of activity of platinum catalysts which have undergone growth of the platinum metal particles,¹ and the somewhat lower Tamman temperature of palladium (460° vs. 540°), crystal growth might be expected to be a major problem. Johnson and Keith² have explained the various data obtained on platinum by showing that an increase in oxidation severity will result in more platinum oxide-alumina complex formation and, therefore, provide a more dispersed platinum upon reduction, if one does not exceed the temperature at which the oxygen pressure is less than the dissociation pressure of platinum oxide.

On this basis, similar crystal growth would not be expected below 790°, since it has been demonstrated that the dissociation pressure of palladium oxide is 0.2 atm. at 789°.³ However, our results indicate crystal growth of palladium at temperatures below 400° in the presence of air. Therefore, it must be concluded that the explanation of crystal growth for platinum put forth by Johnson and Keith² is not applicable to palladium.

Experimental

A commercial palladium-alumina (Harshaw Pd-0501) catalyst containing 0.3% palladium in 3-mm. tablet form was used for all experiments.

Adsorption experiments were run on approximately 20 g. of catalyst. The catalysts were heat treated in a muffle furnace (flow system for oxygen treatment) by gradually raising the temperature to the desired level and holding for 48 hr. The catalysts were then reduced in a flow of hydrogen for 2 hr. and then evacuated for 2 hr. Carbon monoxide was then introduced to the evacuated system in 1.426-cc. increments at 5-min. intervals and the adsorption calculated from the pressure increase.

Analysis of fresh and regenerated catalysts showed no change in palladium content and no increase in foreign metal content. Attempted determination of crystal size by both X-ray and electron microscopy failed to detect palladium. Pore volume and surface area determination on a catalyst which had been through ten production-regeneration cycles showed a definite but small collapse of the support. It is felt that such an effect on one treatment is insignificant.

- (1) G. A. Mills, S. Weller, and E. B. Cornelius, "Second International Congress on Catalysis," Vol. II, Paris, 1960, Paper 113.
- (2) M. F. L. Johnson and C. D. Keith, *J. Phys. Chem.*, **67**, 200 (1963).
- (3) L. Wöhler, *Z. Elektrochem.*, **11**, 839 (1905); C. B. Alcock and G. W. Hooper, *Proc. Roy. Soc. (London)*, **A254**, 551 (1960), concluded that the vapor pressure of PdO was probably less than that of the metal.

Regeneration consisted of heating the spent catalyst to 650° in a muffle furnace and holding at that temperature for 13 hr.

Results and Discussion

A fresh catalyst sample was used for each treatment to give the results shown in Table I. The theoretical adsorption based upon 0.88 CO molecule per Pd atom⁴ was calculated to be 0.554 cc./g. The results of Table I show that there is no crystal growth of palladium at 450° under vacuum, since practically the theoretical adsorption was obtained. The 90% of theoretical obtained on the fresh catalyst was perhaps caused by previously adsorbed CO from the atmosphere.

Table I: Effect of Catalyst Treatment on CO Adsorption

Temp., °C.	Conditions	H ₂ treatment, °C.	Cc. STPCO/g.
25	Air, 1 atm.	100	0.496 ± 0.021 ^a
300	Air, 1 atm.	100	0.524 ± 0.029 ^a
300	Oxygen, 1 atm.	100	0.191 ± 0.042 ^a
450	Air, 1 atm.	100	0.441 ± 0.034 ^a
450	Vacuum	100	0.55 ^b
450	Oxygen, 1 atm.	100	0.20 ^b
650	Air, 1 atm.	100	0.267 ± 0.023 ^a
650	Air, 1 atm.	300	0.34 ^b
650	Air, 1 atm.	350 (24 hr.)	0.25 ^b

^a Average deviation on triplicate analyses. ^b Single determination.

That oxygen is the major cause of the decrease in palladium surface is demonstrated by a comparison of the results obtained using air at 1 atm. vs. oxygen at 1 atm. at a given temperature. For example, at 450° under vacuum, essentially theoretical adsorption occurred, while in air the adsorption dropped to 80% and in oxygen to 36%. This effect of oxygen cannot be attributed to the formation of higher oxides of palladium, since these are known to be unstable and readily reduced with hydrogen at room temperature.⁵ It is possible, however, that a palladium oxide-alumina complex exists which is difficult to reduce, since a 300° reduction temperature on the 650° catalyst gave 60% of theoretical adsorption as compared with 50% when reduced at 100°. Additional time of hydrogen treatment, as shown by that which was treated 24 hr. at 350°, did not show any benefit.

In view of the data presented, it is concluded that far greater differences exist between palladium and platinum-alumina catalysts than might be inferred from differences in Tamman temperature and other physical properties. Although the possibility of a

palladium alumina compound, which is not reducible with hydrogen, has not been eliminated, crystal growth is the preferred explanation for the data observed. It is also concluded that crystal growth of the palladium metal particles can occur at temperatures below 400° and that oxygen is an accelerator for this process. The exact nature of the reactions involved is not understood at this time, but it is believed that palladium oxide may be considerably more mobile than the metal itself, leading to increased crystallite formation as the oxygen severity is increased.

Acknowledgment. The authors wish to express their appreciation to the Harshaw Chemical Co. for their cooperation and assistance in sample preparation and analytical problems.

(4) J. J. F. Scholten and A. Van Montfoort, *J. Catalysis*, **1**, 85 (1962).

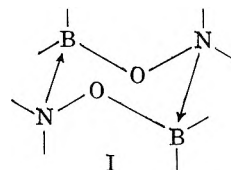
(5) N. V. Sidgwick, "The Chemical Elements and Their Compounds," Vol. II, Oxford University Press, London, 1950, p. 1558

The Electric Dipole Moment and Molecular Conformation of the Heterocycle Boron-Oxygen-Nitrogen-Boron-Oxygen-Nitrogen

by H. Bradford Thompson,¹ Lester P. Kuhn, and Masahiro Inatome

Alfred Nobel Science Laboratories, Gustavus Adolphus College, St. Peter, Minnesota, and the Ballistics Research Laboratories, Aberdeen Proving Ground, Maryland (Received July 31, 1963)

Synthesis and structural proof of two compounds having the cyclic structure I have been reported,² and the name Bon-Bon proposed for this ring system.



This structure should be nonpolar if the chair form prevails. Accordingly, we have measured the electric dipole moments in solution for the two known Bon-Bons, the dimers of (aminoxy)di-*n*-butylborane and (*n*-butylaminoxy)di-*n*-butylborane. Results are summarized in Table I.

(1) Department of Chemistry, Iowa State University, Ames, Iowa.

(2) L. P. Kuhn and M. Inatome, *J. Am. Chem. Soc.*, **85**, 1206 (1963).

Table I: Electric Dipole Moment Data and Results

Concn. $\times 10^5$, mole/ml.	n^{25D}	ϵ	S^a	Moment, D.
(R ₂ BONH ₂) ₂ in CCl ₄ (R = <i>n</i> -butyl)				
Solvent	1.45783	2.20820		
0.16C	1.45786	2.20824		
0.31E	1.45790	2.20817		
0.47C	1.45790	2.20829	0.0	0.0 \pm 0.2
(R ₂ BONHR) ₂ in CCl ₄ (R = <i>n</i> -butyl)				
Solvent	1.45786	2.20847		
0.15C	1.45783	2.20847		
0.337	1.45783	2.20863		
0.582	1.45780	2.20832	0.0	0.0 \pm 0.2

^a Slope for $(\epsilon - n^2)/(\epsilon + 2)(n^2 + 2)$ vs. concn. See ref. 7.

Discussion

It is apparent that both Bon-Bons have very small electric dipole moments. Since the moment is proportional to the square root of the orientation polarization, the uncertainty (both relative and absolute) in a dipole moment is quite large when the moment is small. Nonetheless, the data clearly suffice to establish a nonpolar conformation. This should be either a chair or a flexible form; a planar structure seems most unlikely for tetravalent nitrogens and borons.

It is clear that the chair form will have a small or zero moment, since, ignoring possible orientations of the butyl groups, it has a center of symmetry. The moment of the flexible form is somewhat more difficult to predict; to estimate this we have assumed the bond parameters in Table II.³⁻⁵

Table II: Bond Lengths and Moments Assumed

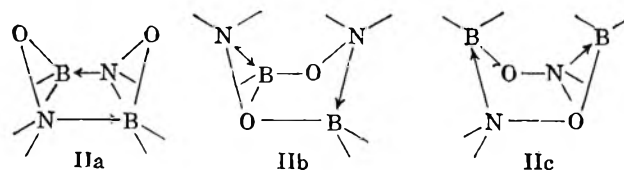
Bond	Moment	Ref.	Length	Ref.
R-B	0.0	Estimate ^a		
R-N	0.6	3		
B-O	1.0	Estimate ^a	1.36	4b
N-O	0.30	3	1.36	4b
N-B	2.55	5	1.55	4c
H-B	1.31	3		

^a From electronegativity differences and by analogy with data in ref. 3.

Bond angles about boron, oxygen, and nitrogen atoms have been assumed to be tetrahedral. In each case this seems to be a reasonable mean between published values in analogous compounds.^{4a}

On this basis, the boat form IIa should have an

electric moment of 2.4 D. and the form IIb, 5.4 D. The moment of IIc would be 2.6 D. and forms inter-



mediate between IIa and IIc could have moments somewhat lower, but IIc involves very close approach of the side chains in the "flagpole" positions and is thus sterically an unlikely contributor. Consequently, a flexible form would have a moment in excess of 2 D. at the very least. It thus appears that the Bon-Bon ring system is chair form.

Experimental

Electric moments were determined by Guggenheim's method,⁶ using procedure⁷ and apparatus⁸ described previously. The solvent carbon tetrachloride was fractionally distilled from analytical reagent grade using a column of about eight theoretical plates, dried over CaCl₂, again fractionated, collected, and stored over CaCl₂. The fraction used boiled over a range of less than 0.03°: n^{25D} 1.4578. Purity check by vapor chromatography indicated no detectable volatile impurity at the 0.01% level or above. Solutes prepared as described previously² were again recrystallized from dry CCl₄ before preparing the solutions.

Errors in n and ϵ as reported in Table I are estimated to be less than 0.0001 and 0.0002, respectively. The internal consistency of the data is somewhat better, corresponding to errors of 0.00003 and 0.0001, respectively.

In view of the startlingly small variation in ϵ and in n over the concentration range, two of the (aminoxy)-di-*n*-butylborane solutions were evaporated after the measurements, and the presence of the solute was verified.

(3) C. P. Smyth, "Dielectric Behavior and Structure," McGraw-Hill Book Co., Inc., New York, N. Y., 1955, p. 244.

(4) (a) "Tables of Interatomic Distances and Configuration in Molecules and Ions," L. E. Sutton, Ed., The Chemical Society, London, 1958; (b) from "Table of Selected Bond Lengths"; (c) mean of four molecules containing analogous B-N single bonds.

(5) H. J. Becher, *Z. anorg. allgem. Chem.*, **270**, 273 (1952).

(6) E. A. Guggenheim, *Trans. Faraday Soc.*, **45**, 714 (1948).

(7) H. B. Thompson, L. Everson, and J. V. Dahlen, *J. Phys. Chem.*, **66**, 1634 (1962).

(8) H. B. Thompson and C. C. Sweeney, *ibid.*, **64**, 221 (1960).

Participation of the SO_2^- Radical Ion in the Reduction of *p*-Nitrophenol by Sodium Dithionite

by C. R. Wasmuth, Charles Edwards, and Richard Hutcherson

*Physical Sciences Section of the University of Tennessee
Martin Branch, Martin, Tennessee (Received August 9, 1963)*

The SO_2^- radical ion is a reaction intermediate in some mechanisms¹ that have been proposed for the autoxidation of sodium dithionite, a reagent that can be used for the reduction of nitrophenols to aminophenols in alkaline solution.² In this paper, kinetic evidence is presented that gives an indication that the SO_2^- radical ion is also a reaction intermediate in the reduction of *p*-nitrophenol by sodium dithionite. The detection of this possible reaction intermediate together with aromatic nitro radical anions in alkaline solutions prepared by mixing aqueous solutions of sodium hydroxide and sodium dithionite with acetone solutions of nitrobenzene or of any of a number of *para*-substituted nitrobenzenes has recently been reported by Kolker and Waters.³

Experimental

Materials. Baker purified sodium dithionite and Eastman White Label *p*-nitrophenol were obtained for the kinetic measurements and were used without further purification. Analysis of the sodium dithionite by the method of Hahn⁴ indicated that the $\text{Na}_2\text{S}_2\text{O}_4$ content was $90 \pm 1\%$.

Kinetic Measurements. Each of the reaction mixtures was prepared from 325 ml. of an aqueous sodium hydroxide solution, 10 ml. of an aqueous sodium hydroxide solution containing *p*-nitrophenol at a concentration in the range of 0.0008 to 0.001 *M*, and a weighed 100 to 700-mg. sample of sodium dithionite. Each reaction was started by the addition of the 10 ml. of *p*-nitrophenol solution to a freshly mixed solution of the freshly weighed sodium dithionite in the 325 ml. of sodium hydroxide solution. The sodium hydroxide solution was kept under a nitrogen atmosphere and brought to a temperature of 25° in a constant temperature bath before the addition of the sodium dithionite. Boiled deionized water was used in the preparation of all of the solutions in order to minimize autoxidation of the sodium dithionite.

Samples of the reaction mixtures were transferred to an absorption cell having a path length of 25 mm. for the rate measurements, which were carried out with

a Coleman Model 6A spectrophotometer. The cell compartment of the spectrophotometer was not thermostated. The reaction runs were of short duration, however, and the effect of temperature variation was kept small by limiting the time interval over which data were taken for the calculation of rate constants. Reaction rates were measured by following the decrease in absorbance at 410 $m\mu$, a wave length close to the *p*-nitrophenolate ion absorption maximum at 403 $m\mu$. This change in absorbance corresponded to the decrease in concentration of the *p*-nitrophenolate ion in the reaction mixture.

The variation with concentration of the *p*-nitrophenolate ion absorbance at 410 $m\mu$ measured by the Coleman spectrophotometer showed an apparent deviation from Beer's law not found for absorbance measurements taken for comparison with a Beckman DU spectrophotometer operated at a wave length band width setting much narrower than that provided in the Coleman instrument. It was found, however, that this deviation from a linear relationship between absorbance and concentration in the concentration range used could very nearly be completely removed by the addition of two terms to the observed *p*-nitrophenolate ion absorbance, a_{obsd} . Each corrected absorbance value, a , used in the calculation of rate constants was accordingly

$$a = a_{\text{obsd}} + 0.05a_{\text{obsd}}^2 + 0.13a_{\text{obsd}}^3$$

For a reaction run each *p*-nitrophenolate ion absorbance value, a_{obsd} , was obtained as the difference between the total absorbance of the reaction mixture at the time of the measurement and the total absorbance of the mixture ten half-times after the time of the initial measurement. These total absorbance values included a contribution from the absorbance of an impurity apparently present in the original sodium dithionite and presumably colloidal sulfur, which caused the reaction solutions to be slightly turbid. The absorbance contribution of this impurity was approximately 0.1 for the reaction solution having the highest initial concentration of sodium dithionite.

Results and Discussion

The kinetic measurements established that the reaction of sodium dithionite with *p*-nitrophenol in dilute aqueous sodium hydroxide solution with the sodium dithionite in great excess is first order in the *p*-

- (1) R. G. Rinker, T. P. Gordon, D. M. Mason, R. R. Sakaida, and W. H. Corcoran, *J. Phys. Chem.*, **64**, 573 (1960).
- (2) E. Grandmougin, *Ber.*, **39**, 3561 (1906).
- (3) P. L. Kolker and W. A. Waters, *Proc. Chem. Soc.*, 55 (1963).
- (4) F. L. Hahn, *Anal. Chem. Acta*, **3**, 62 (1949).

nitrophenolate ion and one-half order in the dithionite ion.

The order in *p*-nitrophenolate ion was determined by plotting the logarithm of the *p*-nitrophenolate ion absorbance, *a*, against reaction time for the data from each of the reaction runs. Reasonably linear plots typical of first-order reactions were obtained. Such plots based upon the data from representative runs are presented in Fig. 1.

A plot of the logarithm of the pseudo-first-order rate constant against the logarithm of the initial concentration of sodium dithionite is given in Fig. 2. The first-order rate constant values were obtained by least squares calculations of the slopes of the best straight lines through plots of $\log a$ against time for time intervals ending 60 sec. after the initial absorbance measurement of each reaction run. A value of 0.52 for the order in dithionite ion was obtained by a similar least squares calculation of the slope of the best straight line through the points in Fig. 2 that correspond to the reactions run at a sodium hydroxide concentration of 0.098 *M*. The average value for the over-all three-halves-order rate constant was 0.21 $\text{l.}^{1/2} \text{mole}^{-1/2} \text{sec.}^{-1}$. The data from the other reaction runs gave an indication that the rate is not strongly dependent upon pH in the pH region in which the reaction orders were determined.

Initial steps of the *p*-nitrophenol reduction consistent

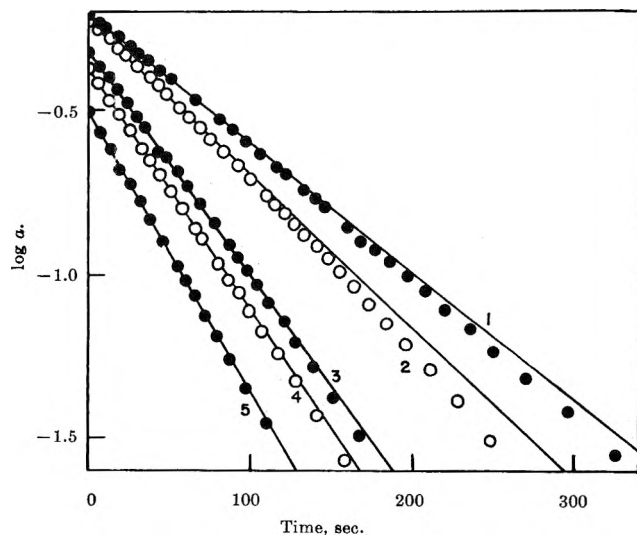


Figure 1. Typical plots of logarithm of corrected *p*-nitrophenol absorbance, *a*, vs. time. The best straight lines through the points plotted for the initial 60-sec. periods beginning with the first absorbance measurements are shown. These measurements were taken approximately 30 to 40 sec. after the addition of *p*-nitrophenol to the reaction mixtures. (See Fig. 2 for reagent concentrations.)

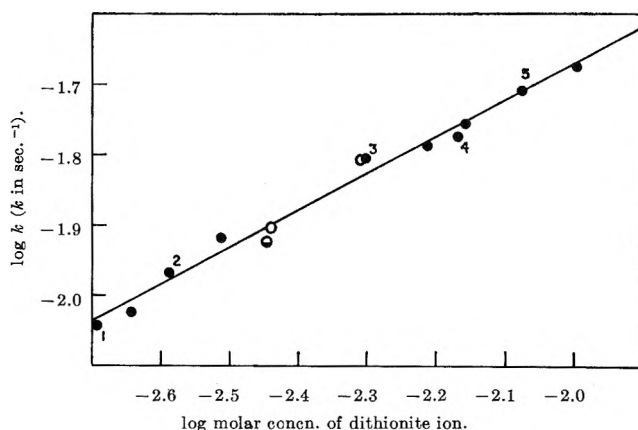
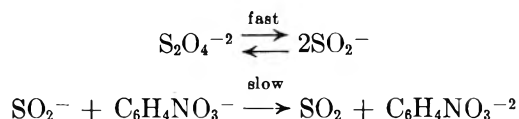


Figure 2. Logarithm of first-order rate constant, *k*, vs. logarithm of dithionite ion concentration for the reduction of *p*-nitrophenol in solutions: ●, 0.098 *M* in NaOH; ○, 0.194 *M* in NaOH; ⊙, 0.098 *M* in NaOH, 0.100 *M* in NaClO₄. The numbered points were obtained from data presented in Fig. 1.

with the measured reaction orders in *p*-nitrophenolate ion and in dithionite ion are



According to this interpretation of the kinetic orders, a nitro radical ion is produced by an electron-transfer reaction between the *p*-nitrophenolate ion and the SO_2^- radical ion. The SO_2^- radical ion is thought to be formed by an equilibrium dissociation^{1,5} of the dithionite ion and thus would be proportional in concentration to the square root of the dithionite ion concentration.

The Brønsted equation relating reaction rate to ionic strength at low levels of ionic strength for the proposed reaction sequence would be

$$\log \frac{k_1}{k_0} = 0.51I^{1/2}$$

where k_1 and k_0 are the three-halves order rate constants for reactions in solutions having ionic strengths of *I* and zero.⁶ Ionic strength effects were not investigated in detail, but some consideration was given to the variation of ionic strength with sodium dithionite concentration in the relatively high ionic strength reaction mixtures prepared for the kinetic runs. It was concluded that the effect of this variation was small since

(5) R. G. Rinker, T. P. Gordon, D. M. Mason, and W. H. Corcoran, *J. Phys. Chem.*, **63**, 302 (1959).

(6) A. A. Frost and R. G. Pearson, "Kinetics and Mechanism," 2nd Ed., John Wiley and Sons, Inc., New York, N. Y., 1961, p. 150.

sodium perchlorate at a concentration more than equivalent in ionic strength to the highest sodium dithionite concentration used had little if any effect on the reaction rate.

Nuclear Magnetic Resonance Studies of Ion-Exchange Resins. II. Electrolyte Invasion

by Robert H. Dinius¹ and Gregory R. Choppin

Department of Chemistry, Florida State University, Tallahassee, Florida (Received August 16, 1963)

The proton magnetic resonance spectra of samples of the cation-exchange resin Dowex-50 in varying degrees of hydration were reported in our first paper.² The observed chemical shift as a function of the degree of hydration indicated that the polystyrenesulfonic acid resin functions as a very strong acid. In addition, there was evidence for a greater degree of disorder in the water structure in the resin phase compared to pure water. We have extended these n.m.r. studies to resin samples containing imbibed electrolyte as well as water in order to gain additional insight into the effects of invading electrolytes on the resin phase.

Experimental

Solutions. All reagents used were of analytical grade and were diluted to the desired concentrations with distilled water. The concentrations of all the acid solutions were determined by titration with standard (carbonate-free) sodium hydroxide.

Resin. The hydrogen form cation-exchange resin, Dowex-50 (4% divinylbenzene), was purchased from Bio-Rad Laboratories Co. The preparation of the resin for use has been described previously.³

Electrolyte Invasion. To measure directly the extent of electrolyte invasion of the resin, approximately 3 g. of dried resin was transferred to small weighed tubes which were closed at one end with glass wool and which fitted into 40-ml. centrifuge tubes. The tube was weighed to obtain the dry resin weight, then the electrolyte solution of known molarity was passed through the resin bed until equilibrium was reached between resin phase and solution phase. The tube was centrifuged to constant weight in a clinical centrifuge.⁴ The normal procedure was to centrifuge for 2 min., wipe the tube dry, and weigh. Five repetitions of this procedure were sufficient to reach constant weight (when the change was less than 2-4 mg.). Following

this, the resin was washed with water to remove all invaded electrolyte and the washings were titrated with standard base. From the sample weights and the titrations, it was possible to calculate the composition of the resin in terms of moles of water and of invaded electrolyte per equivalent of resin exchange sites. Since our experiments were concerned only with systems in which the extent of electrolyte invasion was appreciable, a small amount of surface absorption of the solution phase on the resin beads should not change the results.

Nuclear Magnetic Resonance Spectra. The samples used for the n.m.r. spectra studies were prepared by passing electrolyte solution through the resin until equilibrium had been attained. A portion of this resin was transferred to an n.m.r. sample tube and enough of the electrolyte solution with which it was in equilibrium was added to completely cover the resin.

The procedure for recording the n.m.r. spectrum and the spectrometer used have been described previously.⁵ The external reference was cyclohexane. The chemical shift values for perchloric and hydrochloric acid in the aqueous phase reported by Hood and co-workers, corrected for magnetic susceptibilities, were used as standards.⁶ The ion-exchange resins are spherical beads; consequently, no corrections for magnetic susceptibility are needed.²

Results

The results of the electrolyte invasion measurements are presented in Table I and those of the n.m.r. measurements in Table II. In these tables the quantities tabulated are: m_s , the molality of the solution phase; m_r , the molality of the resin phase (number of moles of resin sites per kg. of absorbed water); m_+ , the molality of the mobile cations in the resin phase; m_- , the molality of the mobile anions in the resin phase. For cation-exchange resin, $m_r = m_+ - m_-$. N_x and N_w are the moles of electrolyte and the moles of water per equivalent of resin. $S_{\text{obsd}(r)}$ and $S_{\text{obsd}(s)}$ are the chemical shifts for the resin and solution phase acid protons. The chemical shifts are calculated with respect to pure water as the zero reference point using the nondimen-

- (1) Department of Chemistry, Auburn University, Auburn, Alabama.
- (2) R. H. Dinius, M. T. Emerson, and G. R. Choppin, *J. Phys. Chem.*, **67**, 1178 (1963).
- (3) G. R. Choppin and R. H. Dinius, *Inorg. Chem.*, **1**, 140 (1962).
- (4) H. P. Gregor and M. H. Gottlieb, *J. Am. Chem. Soc.*, **75**, 3539 (1953).
- (5) R. H. Dinius and G. R. Choppin, *J. Phys. Chem.*, **66**, 268 (1962).
- (6) G. C. Hood, O. Redlich, and C. A. Reilly, *J. Chem. Phys.*, **22**, 2067 (1954).

sional unit.⁷ P is the fraction of all exchangeable protons present in the form of hydronium ions calculated from $P = 3m_+ / [2(55.6) + m_+]$.

Discussion

Electrolyte Invasion. The experimental values of the electrolyte invasion of the resin phase by HCl and HClO₄ are shown in Fig. 1 as a function of aqueous phase concentration. The invasion by HCl is less than

Table I: Electrolyte Invasion of the Resin Phase

m_s	m_+	m_r	m_-	N_w	N_x
Dowex-50 (4% DVB) and HClO ₄					
0.58	3.75	3.58	0.17	15.5	0.047
1.20	4.20	3.87	0.33	14.4	0.086
1.64	4.65	4.05	0.60	13.7	0.15
3.33	6.27	4.65	1.62	12.0	0.35
5.58	8.50	5.50	3.00	10.1	0.55
7.85	11.00	6.90	4.10	8.05	0.60
8.70	12.65	7.53	5.12	7.37	0.68
9.45	14.10	8.00	6.10	6.94	0.76
11.5	18.0	9.85	8.10	5.65	0.83
14.8	24.1	12.6	11.5	4.40	0.91
Dowex-50 (4% DVB) and HCl					
1.15	3.10	2.97	0.13	18.7	0.044
2.64	4.60	3.81	0.79	14.6	0.21
3.60	5.62	4.24	1.38	13.1	0.33
5.99	9.37	5.56	3.81	10.0	0.69
6.45	9.83	5.59	4.24	9.95	0.76
9.65	13.89	6.17	7.72	9.00	1.25

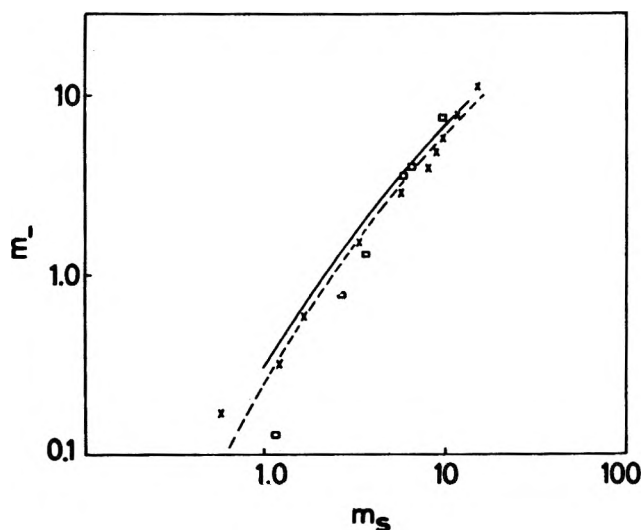


Figure 1. Graph of the amount of solute invasion of Dowex-50 resin as a function of aqueous phase concentration: ---, HClO₄ (calcd.); ×, HClO₄ (exptl.); ———, HCl (calcd.); - - -, HCl (exptl.); m_s is the molality of the solution phase; m_- is the molality of mobile anions in the resin phase.

that by HClO₄. A possible explanation for this behavior is found in the relative effects of HCl and HClO₄ on the structure of liquid water. Infrared studies of absorption bands of liquid water in the 1.2- μ region have shown that HClO₄ has a net effect

Table II: Chemical Shifts of Dowex-50-Electrolyte Systems

m_s	m_r	m_+	$S_{(s)}$ ($\times 10^6$)	$S_{(r)}$ ($\times 10^6$)	P_s	P_r
Dowex-50 (4% DVB) and HClO ₄						
1.64	4.05	4.65	0.38	0.934	0.044	0.12
3.33	4.65	6.27	0.75	1.33	0.087	0.16
7.85	6.90	11.0	1.74	2.32	0.198	0.27
11.5	9.85	18.0	2.40	3.09	0.281	0.42
Dowex-50 (4% DVB) and HCl						
1.15	2.97	3.10	0.35	0.956	0.031	0.08
2.64	3.81	4.60	0.72	1.29	0.069	0.12
6.45	5.59	9.83	1.74	2.16	0.164	0.24
9.65	6.17	13.89	2.52	3.00	0.239	0.33

of decreasing slightly the extent of ordering of the solvent water, whereas HCl has a net effect of increasing the ordering.⁸ In our earlier paper,² we concluded that water in the resin phase of Dowex-50 is also more disordered than the pure liquid state. Thus, it would seem logical that the disordering solute, HClO₄, would more easily enter the resin phase with its greater disorder than would the ordering solute HCl.

It has been suggested that the resin phase may function as a differentiating medium to strong acids.⁹ As the resin phase becomes more concentrated due to electrolyte invasion and water expulsion, it is probable that HCl would become associated. At this point, the absorption of HCl would increase as the structure-promotion effect is largely nullified by the association. This would explain the higher resin phase molality for HCl relative to HClO₄ at high solution phase concentrations since HClO₄, being a stronger acid, should be less associated.

The curves in Fig. 1 were calculated using the equation

$$m_- = \left[\frac{m_r^2}{4} + m_s^2 \right]^{1/2} - \frac{m_r}{2}$$

This is a simplified version of an equation derived by Helfferich¹⁰ by treating the resin-electrolyte solution as

- (7) J. A. Pople, W. G. Schneider, and H. J. Bernstein, "High Resolution Nuclear Magnetic Resonance," McGraw-Hill Book Co., New York, N. Y., 1959, p. 87.
- (8) G. R. Choppin and K. Buys, *J. Chem. Phys.*, **39**, 2042 (1963).
- (9) B. Chu and R. M. Diamond, *J. Phys. Chem.*, **63**, 2021 (1959).

a Donnan equilibrium system. Helfferich's full equation has m_s^2 multiplied by a term for the ratio of the mean ionic activity coefficients for the electrolyte in the aqueous and the resin phases and a term involving the water activities in the two phases and the partial molal volumes of water and electrolyte. In our systems, neglect of this latter term should not be serious. The good agreement between the calculated curve and the experimental values for HClO_4 indicates that the ratio of mean activity coefficients must be very close to unity. The agreement between the calculated curve and the experimental values for HCl is less satisfactory. Nevertheless, the values calculated by using the simple equation do agree well with experimental values for the amount of invasion of the resin phase by both HCl and HClO_4 for solution phase concentrations above 5 m .

A difference in the behavior of imbibed HCl and HClO_4 is seen also in Fig. 2. For values of N_x between 0.1 and 0.5, the slopes are similar for both solutes, indicating a water expulsion rate of approximately 12 moles of H_2O per mole of solute. At higher values of N_x , HClO_4 continues this expulsion rate whereas the

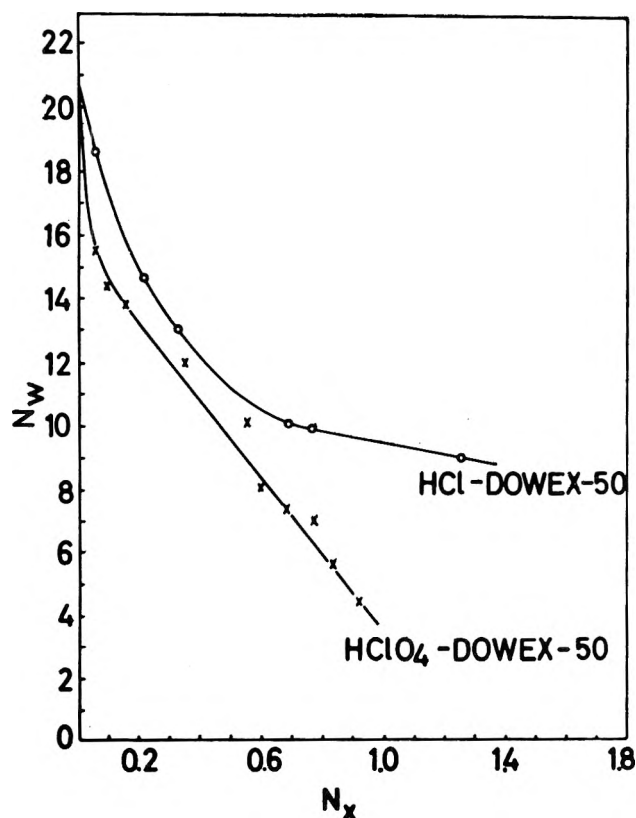


Figure 2. The number of moles of H_2O per resin equivalent, N_w , as a function of the number of moles of invaded solute per resin equivalent, N_x .

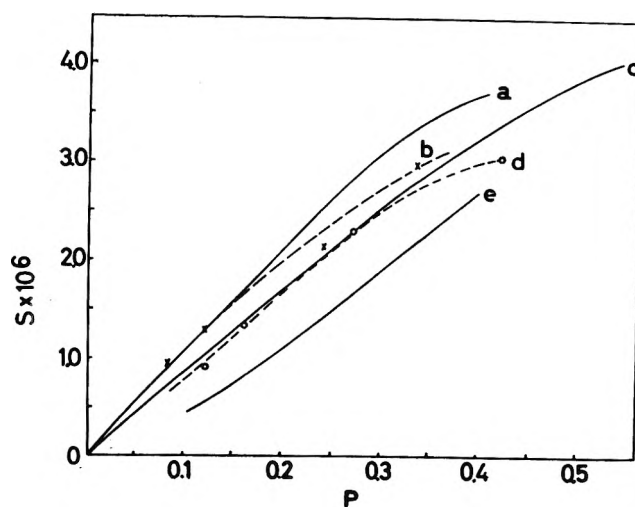


Figure 3. The chemical shift S as a function of the fraction P of exchangeable protons in the form of H_3O^+ ions for HCl and HClO_4 in aqueous solutions and on the heterogeneous systems of solution and resin: a, aqueous HCl ; b, $\text{HCl} + \text{H}_2\text{O}$ in Dowex-50; c, aqueous HClO_4 ; d, $\text{HClO}_4 + \text{H}_2\text{O}$ in Dowex-50; e, hydrated Dowex-50.

rate of HCl decreases to 2 moles of H_2O per mole of solute. This is consistent with the model which assumes association of HCl but not of HClO_4 in the resin phase. It would seem significant that this change in expulsion rate coincides with an aqueous solution concentration between 6 and 8 m HCl and that reversal of the relative molalities of HCl and HClO_4 in the resin phase also occurs in this region (Fig. 1).

The n.m.r. shift data are shown in Fig. 3. Hood, *et al.*,⁶ interpreted the lower slope as $P \rightarrow 0$ of the $\text{HClO}_4(\text{aq})$ curve relative to that of the $\text{HCl}(\text{aq})$ curve to be a result of the greater effect of perchlorate ion in decreasing the extent of structure in the liquid water. This is in agreement with the low slope of the hydrated Dowex-50 curve since it has been concluded that the water is quite disordered in the resin phase. The order of the slopes $(\text{HCl} + \text{HR}) > (\text{HClO}_4 + \text{HR}) > \text{HR}$ could be interpreted to reflect that both HCl and HClO_4 would have a net structure promoting effect in the resin phase because of the higher concentration of H^+ but, as noted earlier, this would be more pronounced for HCl than for HClO_4 .

The deviation from linearity of the curves at high values of P is due to association. In aqueous HCl this becomes obvious at a P value corresponding to about 11 m . In the resin curve, the onset of the deviation

(10) F. Helfferich, "Ion Exchange," McGraw-Hill Book Co., New York, N. Y., 1962, pp. 142-143.

corresponds to the resin phase in equilibrium with approximately 7 to 8 *m* aqueous phase in agreement with the interpretation of the curves in Fig. 1 and 2.

For the system $\text{HClO}_4 + \text{HR}$, the deviation in Fig. 3 corresponds to an external aqueous phase concentration of approximately 10 *m* HClO_4 . The ClO_4^- concentration in the resin phase is about 8 *m* compared to a value of only about 4 *m* for HCl when the HCl curve deviates. We cannot be certain that the deviation in the $\text{HClO}_4 + \text{HR}$ curve is not due to RSO_3H association rather than HClO_4 , since it was possible only to ascertain the qualitative acid strength for Dowex-50 (4% DVB) resin²



Acknowledgment. We wish to acknowledge the financial assistance of contracts from the U. S. Atomic Energy Commission and the Office of Naval Research. Drs. Merle T. Emerson and Ernest Grunwald are to be thanked for their assistance and interest.

Thermodynamic Study of Germanium Monotelluride Using a Mass Spectrometer¹

by R. Colin and J. Drowart

Laboratoire de Chimie Physique Moléculaire, Université Libre de Bruxelles, Brussels, Belgium (Received August 26, 1963)

As a part of a study² of the composition of the vapors in equilibrium with the group IVB-group VIB compounds and of the thermochemical determination of the dissociation energy of the corresponding gaseous molecules and of their polymers, the vapor over germanium monotelluride, for which pressures were recently measured,^{3,4} was analyzed mass spectrometrically. The heat of formation of $\text{GeTe}(\text{s})$, the dissociation energy of $\text{GeTe}(\text{g})$, and the atomization energy of $\text{GeTe}_2(\text{g})$ were obtained from these measurements.

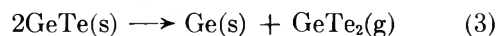
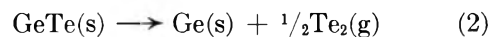
The germanium monotelluride, synthesized from the elements, was vaporized from quartz Knudsen cells^{2a} between 624 and 964°K. The mass spectrometer, experimental procedure, and methods of interpreting the data were described previously.⁵⁻⁸

The ionic species formed by electron impact from the neutrals in the molecular beam coming from the cell were Ge^+ , Te^+ , GeTe^+ , Te_2^+ , and GeTe_2^+ . Their approximate appearance potentials, 12.6 ± 0.5 , 13.3 ± 0.5 , 10.1 ± 0.5 , 8.4 ± 0.6 , and 10.8 ± 0.5 e.v.,

respectively, indicate GeTe^+ , Te_2^+ , and GeTe_2^+ to be parent ions and Ge^+ and Te^+ fragment ions, the difference between the appearance and ionization potentials,⁹ 4.5 ± 0.5 and 4.3 ± 0.5 e.v., respectively, being approximately equal to the dissociation energy of GeTe to be obtained below. For nominal 30-e.v. electrons, the relative ion intensities, which did not vary much with temperature, were approximately 1.0, 8.9×10^{-2} , and 1.3×10^{-2} for GeTe^+ , Te_2^+ , and GeTe_2^+ , respectively. The intensity of the ions corresponding to $(\text{GeTe})_n$ polymers was less than 2.5×10^{-5} that of GeTe^+ ions. Hence, GeTe vaporizes mainly according to the reaction



like most group IVB-group VIB compounds,^{2b} as was assumed by Hirayama³ and concluded by Ch'un-hua, *et al.*,⁴ from the X-ray examination of a sample after part of it had been vaporized. Less extensive reactions are



The complete evaporation of two 100-mg. samples gave GeTe pressures of 1.45×10^{-6} and 4.69×10^{-6} atm. at 713 and 740°K., respectively, in agreement with the average of the two literature determinations,^{3,4} which agree within a factor of approximately three. After these experiments, about 10% of the initial germanium content of the sample remained in the cells as a result of reactions 2 and 3. The Te_2 and GeTe_2 partial pressures, a typical set of which is given in Table I, were calculated from the relative ion intensities and the average total pressures of the literature.^{3,4} The relative ionization cross sections, $\sigma_{\text{Ge}}/\sigma_{\text{Te}_2}/\sigma_{\text{GeTe}_2} = 1.00/1.16/1.35$, required for the calculation were based on the calculated values of Otvos and Stevenson¹⁰

- (1) This work was sponsored in part by the Wright Air Division of The Aeronautical Systems Division A.F.S.C., U. S. Air Force, through its European Office.
- (2) (a) R. Colin and J. Drowart, *J. Chem. Phys.*, **37**, 1120 (1962); (b) R. Colin and J. Drowart, Technical Note No. 10, AF 62(052)-225, February 28, 1963.
- (3) C. Hirayama, *J. Phys. Chem.*, **66**, 1563 (1962).
- (4) L. Ch'un-hua, A. S. Pashinkin, and A. V. Novoselova, *Zh. Neorgan. Khim.*, **7**, 963 (1962).
- (5) J. Drowart and R. E. Honig, *J. Chem. Phys.*, **61**, 980 (1957).
- (6) J. Drowart and P. Goldfinger, *J. chim. phys.*, **55**, 721 (1958).
- (7) M. Ackerman, F. E. Stafford, and J. Drowart, *J. Chem. Phys.*, **33**, 1784 (1960).
- (8) M. G. Inghram and J. Drowart, "Proceedings of a Symposium on High Temperature Technology," McGraw-Hill Book Co., Inc., New York, N. Y., 1960, p. 219.
- (9) C. E. Moore, National Bureau of Standards Circular 467, U. S. Government Printing Office, Washington, D. C., 1949.

and on the measured value,¹¹ $\sigma_{\text{Te}_2}/\sigma_{\text{Te}}$. The relative secondary electron multiplier yields, $\gamma_{\text{Ge}}/\gamma_{\text{Te}_2}/\gamma_{\text{GeTe}_2} = 1.00/0.88/0.85$, were based on a calibration curve¹² and on molecular effects evaluated as suggested by Stanton, Chupka, and Inghram.¹³

Table I: Partial Pressures and Reaction Enthalpies

T, °K.	-log P, atm.			$\Delta H^\circ_{298(1)}$,	$\Delta H^\circ_{298(2)}$,	$\Delta H^\circ_{298(3)}$,
	GeTe ^a	Te ₂	GeTe ₂	kcal./ mole	kcal./ mole	kcal./ mole
788	4.56	5.72	6.41	26.0	55.5	
805	4.30	5.36	6.23	25.8	55.6	
819	4.05	5.05	5.88	25.7	55.3	
870	3.33	4.33	5.08	25.8	56.2	
				48.6 ^b	25.8	55.8

^a See ref. 3 and 4. ^b See text.

The enthalpy of reaction 1 was taken as the average of the literature second-law values $\Delta H^\circ_{758} = 46.9 \pm 2.0^3$ and $\Delta H^\circ_{794} = 45.8 \pm 3.0^4$ kcal./mole. This value, $\Delta H^\circ_{776} = 46.4 \pm 2.0$ kcal./mole, combined with $\Delta G^\circ_{776} = 16.82 \pm 0.7$ kcal./mole gives $\Delta S^\circ_{776} = 38.2 \pm 2.1$ e.u., whence $S^\circ_{776}(\text{GeTe(s)}) = 31.3 \pm 2.1$ e.u. The heat capacity of GeTe(s) was estimated, assuming¹⁴ $C_p = 6.35$ cal./deg. g.-atom at 298°K. and $C_p = 7.13$ cal./deg. g.-atom at the first transition point, here the melting point at 998°K., giving $C_p(\text{GeTe(s)}) = 12.0 + 2.3 \times 10^{-3}T$ (298–998°K.). With the heat content and high temperature entropy estimated accordingly, $\Delta H^\circ_{298(1)} = 48.6 \pm 2.1$ kcal./mole and $S^\circ_{298} = 18.8 \pm 2.2$ e.u., close to the sum of the standard entropies of the elements, were obtained. The enthalpies of reactions 2 and 3, $\Delta H^\circ_{298} = 25.8 \pm 2.2$ and $\Delta H^\circ_{298} = 55.8 \pm 3.0$ kcal./mole, respectively, were calculated by the third law. The necessary free energy functions for Ge(s), Te₂(g), and GeTe(g) were taken from the literature.^{15–17} The free energy function for GeTe₂(g) was calculated from statistical mechanical formulas. A symmetric linear model was considered by analogy with CO₂ and CS₂.¹⁸ The stretching force constant k was taken the same as in GeTe¹⁹; the ratio of the bending to stretching force constant divided by the square of the internuclear distance (2.6 Å.) was estimated by analogy with CO₂ and CS₂.¹⁸ The vibration frequencies obtained are 197, 110 (doubly degenerate), and 418 cm.⁻¹. The numerical values for the free energy function $-(G_T^\circ - H^\circ_{298}/T)$ are 77.2, 78.3, and 79.5 e.u. at 700, 800, and 900°K., respectively.

Together with the heats of sublimation of germa-

nium,¹⁵ $\Delta H^\circ_{298} = 90.0 \pm 1.0$, and of Te₂,¹⁵ $\Delta H^\circ_{298} = 39.6 \pm 1.5$, and the dissociation energy of Te₂,^{11,20} $D^\circ_{298} = 52.5 \pm 2.5$ kcal./mole, the heat of formation of solid GeTe, $\Delta H^\circ_{298.f} = -6.0 \pm 2.3$ kcal./mole, the dissociation energy of gaseous GeTe, $D^\circ_{298}(\text{GeTe}) = 93.5 \pm 2.0$ kcal./mole or $D^\circ_0(\text{GeTe}) = 92.5 \pm 2.0$ kcal./mole, and the heat of atomization of GeTe₂, $\Delta H^\circ_{298.at}(\text{GeTe}_2) = 138.3 \pm 3.0$ or $\Delta H^\circ_{0.at}(\text{GeTe}_2) = 137.0 \pm 3.0$ kcal./mole, were calculated from the enthalpies of reactions 2, 1, and 3, respectively (Table I).

It has been shown for the group IVB–group VIB molecules PbO,²¹ PbS,^{2a,22} SnS,^{2a} GeS,^{2b} SnSe,^{2b} PbSe,^{2b} and SnO²³ that the electronically excited E-states, shown to be analogous,²⁴ most probably correlated with the ³P₁ + ³P₁ sublevels of the atoms. For the tellurides, the convergence limit of this state is, however, not as accurately known as for the sulfides and selenides. For the E-state of GeTe, for which vibrational levels are known up to 4.38 e.v., a convergence limit was estimated¹⁹ at 4.49 e.v. by a graphical Birge–Spencer extrapolation made by analogy with GeS and GeSe. If a linear Birge–Spencer extrapolation is made, in spite of the uncertainty on the vibrational frequency and anharmonicity constant,¹⁹ the convergence limit is at 4.67 ± 0.25 e.v. On adding to the thermochemical value of the dissociation energy of the ground state the excitation energy of the ³P₁ levels of Ge and Te, 0.07 and 0.58 e.v., respectively,⁹ the value 4.66 ± 0.09 e.v. is obtained, showing that again here the E-state most probably correlated with the ³P₁ sublevels of the atoms.

- (10) J. W. Otvos and D. P. Stevenson, *J. Am. Chem. Soc.*, **78**, 546 (1956).
- (11) R. Colin, *Ind. Chim. Belge*, **26**, 51 (1961).
- (12) M. Ackerman, F. E. Stafford, and J. Drowart, Technical Note No. 1, AF 61(052)-225, February 29, 1960.
- (13) H. E. Stanton, W. A. Chupka, and M. G. Inghram, *Rev. Sci. Instr.*, **27**, 109 (1956).
- (14) O. Kubaschewski and L. L. Evans, "Metallurgical Thermochemistry," Pergamon Press, New York, N. Y., 1958, p. 183.
- (15) D. R. Stull and G. C. Sinke, *Advances in Chemistry Series*, No. 18, American Chemical Society, Washington, D. C., 1956.
- (16) K. K. Kelley, U. S. Bureau of Mines Bulletin 584, U. S. Government Printing Office, Washington, D. C., 1960.
- (17) K. K. Kelley and E. G. King, *ibid.*, Bulletin 592, 1961.
- (18) G. Herzberg, "Infrared and Raman Spectra," D. Van Nostrand Co., Inc., Princeton, N. J., 1945.
- (19) G. Drummond and R. F. Barrow, *Proc. Phys. Soc. (London)*, **65A**, 277 (1952).
- (20) R. F. Porter, *J. Chem. Phys.*, **34**, 583 (1961).
- (21) R. F. Barrow, J. L. Deutsch, and D. N. Travis, *Nature*, **191**, 374 (1961).
- (22) R. F. Barrow, P. W. Fry, and R. C. Le Bargy, *Proc. Phys. Soc. (London)*, **81**, 697 (1963).
- (23) R. F. Barrow, private communication.
- (24) R. F. Barrow and H. C. Rowlinson, *Proc. Roy. Soc. (London)*, **A224**, 374 (1954).

Acknowledgment. The authors acknowledge Professor P. Goldfinger's interest in this work. They thank the Union Minière du Haut Katanga for the germanium used in this investigation.

Heat Capacities and Thermodynamic Properties of Globular Molecules. XI. Melting of 3-Azabicyclo[3.2.2]nonane

By Claus A. Wulff and Edgar F. Westrum, Jr.¹

Department of Chemistry, University of Michigan, Ann Arbor, Michigan (Received September 3, 1963)

A previous paper in this series² presented the low-temperature heat capacity of 3-azabicyclo[3.2.2]-nonane (AZBN) and revealed a solid-solid transition at 297.78°K. with an entropy increment of 11.68 cal./mole °K.). The transition was ascribed to a rotational reorientation process leading to a plastically crystalline phase (crystal I). Further evidence for the plastically crystalline nature of this phase has been obtained by determination of the thermodynamics of melting and the heat capacities of crystal I and the liquid.

The thermal properties of AZBN were determined between 280 and 490°K. by adiabatic calorimetry using the previously described³ Mark IV intermediate range thermostat, a silver calorimeter (laboratory designation W-22), and a capsule-type platinum-resistance thermometer (laboratory designation A-7). Also described elsewhere are the quasi-adiabatic calorimetric method⁴ and the computer program for the conversion of data to thermodynamic functions.⁵ The measurements were made on a single loading of 55.1265 g. (*in vacuo*) of an AZBN sample previously characterized,² which contained 0.21 mole % impurity as determined by fractional melting. The heat capacity of the sample exceeded 75% of the total measured over the entire range. All calculations are based upon a calorie defined as 4.1840 j., an ice point temperature of 273.15°K., and a gram formula mass of 125.216 g.

The heat capacity data presented in Table I have been adjusted for curvature and for vaporization into the free volume of the calorimeter on the basis of a preliminary survey of the sublimation pressure.⁶

The data agree to 0.1% with the low-temperature results over the common range between 285 and 350°K. Comparison of enthalpy-type runs with the integration of the heat capacity data given in Table II indicates good accord. Five determinations of the enthalpy

Table I: Heat Capacity of AZBN. [Units: cal., mole, °K.]

<i>T</i>	<i>C_p</i>	<i>T</i>	<i>C_p</i>	<i>T</i>	<i>C_p</i>
Δ <i>H</i> Run A		467.57	148.3	430.63	63.42
				438.92	64.22
Series I		Series III		447.07	65.44
				455.06	67.64
459.54	74.5				
464.94	290	470.86	72.18		
466.33	1442	475.41	72.95	Series V	
469.53	113.2	479.88	73.17		
		484.59	74.13	329.79	56.53
		489.43	74.53	338.85	56.59
Δ <i>H</i> Run B				347.88	56.77
				356.87	57.09
Δ <i>H</i> Run C		Δ <i>H</i> Run D		365.80	57.60
				374.31	58.17
Series II		Δ <i>H</i> Run E		Fusion Runs G	
459.61	71.8	Δ <i>H</i> Run F			
462.37	96.5				
464.47	205			Series VI	
465.56	487	Series IV			
466.08	924			383.60	58.86
466.35	1822	406.17	60.86	392.77	59.64
466.50	2309	413.75	61.59	401.84	60.45
		422.25	62.52	410.80	61.27

Table II: Enthalpy Runs for AZBN. [Units: cal., mole, °K.]

Run	<i>T</i> ₁	<i>T</i> ₂	Δ <i>H</i>	∫ <i>C_p</i> d <i>T</i>
A	284.43	325.60	5647	5650
B	319.12	403.30	4868	4865
C	432.38	458.21	1693	1693
D	400.58	447.27	2933	2930

of melting, including two fractional melting series, are summarized in Table III. The sample melted under its own vapor pressure at 466.55°K. Assuming the

- (1) To whom correspondence concerning this work should be addressed.
- (2) C. M. Barber and E. F. Westrum, Jr., *J. Phys. Chem.*, **67**, 2373 (1963).
- (3) E. F. Westrum, Jr., and J. C. Trowbridge, *Rev. Sci. Instr.*, in press.
- (4) E. F. Westrum, Jr., J. B. Hatcher, and D. W. Osborne, *J. Chem. Phys.*, **21**, 419 (1953).
- (5) B. H. Justice, Appendix to Ph.D. dissertation, University of Michigan; cf. U. S. Atomic Energy Commission Report TID. 12722, 1961.
- (6) Three series of static sublimation pressure measurements made by James R. Trudell as an undergraduate research problem accord with the equation, $\log P(\text{cm.}) = 7.907 - 2727/T$, within 1% over the range 303 to 443°K. and were used as the basis for the vaporization corrections. These values indicate a triple point pressure of 1.28 atm. which accords with the reported sublimation of this substance prior to melting (cf. Technical Data Report No. X-119, Eastman Chemical Products, Inc., Kingsport, Tennessee, May, 1962).

impurities to be liquid-soluble solid-insoluble, the triple point of the pure substance is $467.12 \pm 0.01^\circ\text{K}$. The five determinations of the enthalpy of melting yield a mean value of 1653 ± 2 cal./mole and 3.549 cal./mole $^\circ\text{K}$. for the enthalpy and entropy of melting.

Table III: Melting Data for AZBN. [Units: cal., mole, $^\circ\text{K}$.]

Designation	T_1	T_2	$H_{T_2} - H_{T_1}^a$
Series I	455.31	472.53	3040.4
Series II	458.21	473.14	3037.1
Fusion Run E	455.61	479.72	3039.1
Fusion Run F	457.05	474.30	3036.6
Fusion Run G	454.75	476.46	3038.5
			Av. = 3038.3 ± 1.5
			$\Delta H_m = 1653 \pm 2$

^a Corrected for enthalpy increments between T_1 and 455°K ., T_2 and 475°K ., and for quasi-adiabatic drifts.

Since the value of ΔS_m is below the (arbitrary) limit of 5 cal./mole $^\circ\text{K}$. prescribed by Timmermans⁷ for the definition of a plastic crystal phase, AZBN meets all the macroscopically observable criteria for plastic crystallinity, *i.e.*, solid-solid transition, low entropy of fusion, high melting temperature, and high vapor pressure. The substance is one of a number of compounds related to bicyclooctane that are being investigated in this laboratory. Discussion of the molecular disordering process leading to the plastic crystal phases will be deferred until more experimental evidence becomes available.

A brief summary of the thermodynamic properties is made in Table IV; those for the gaseous phase also involve the sublimation pressure data.⁶

Table IV: Thermodynamic Properties of AZBN. [Units: cal., mole, $^\circ\text{K}$.]

T	C_p	S°	$H^\circ - H^\circ_0$	$-(G^\circ - H^\circ_0)/T$
Crystal I				
350	56.83	65.61	12992	28.49
400	60.28	73.40	15809	33.63
450	65.84	80.79	19052	38.46
467.12	...	83.30	20201	40.05
Liquid				
467.12	...	86.84	21854	40.05
500	(75.92) ^a	(91.86)	(24281)	(43.30)
Vapor				
400	...	101.0 ^b	28290 ^b	30.3 ^b

^a Values in parentheses are extrapolated from *ca.* 495°K .

^b Not corrected for deviation from ideality; *i.e.*, $S_{\text{vapor}} - S_{\text{crystal}} = R \ln P + \Delta H_s/T = R \ln 0.1629 \text{ atm.} + 12480/400$.

Acknowledgment. The authors gratefully acknowledge the partial financial support of the Division of Research of the United States Atomic Energy Commission and C. A. W. acknowledges the support of the Institute of Science and Technology of the University of Michigan in the form of a postdoctoral fellowship.

(7) *Cf.* J. Timmermans, *J. Phys. Chem. Solids*, **18**, 1 (1961).

The Synthesis and Infrared and Nuclear Magnetic Resonance Spectra of Ammonium Dicyanamide

by James W. Sprague, Jeanette G. Grasselli, and William M. Ritchey

The Standard Oil Company (Ohio), Research Department, Cleveland, Ohio (Received October 2, 1963)

The metallic salts of dicyanamide have been known in well characterized forms for many years.¹ Their infrared spectra have recently been described.² Metallic salts are prepared by methods such as the alkali fusion of cyanamide with melon (or other highly condensed members of this carbon-nitrogen system) or the reaction of disodium cyanamide with cyanogen halide followed by metathetical exchange with an appropriate salt. These reactions were not appropriate to the ammonium salt although a crude sample had been prepared.^{1,3} We have found that the salt may be obtained by the addition of concentrated solutions of cyanogen bromide to liquid ammonia.

Over a period of 1.5 hr. 150 ml. of a glyme (1,2-dimethoxyethane) solution containing 100 g. of cyanogen bromide was added to 250 ml. of liquid ammonia with vigorous stirring. The ammonia evaporated slowly from the reaction mixture which then stood over a weekend. Two phases separated. The supernatant solution was decanted from the solids and discarded. The solids which consisted primarily of ammonium bromide and ammonium dicyanamide were extracted with a mixture of 200 ml. of ethyl acetate and 200 ml. of acetone which was evaporated to about

(1) W. Madelung and E. Kern, *Ann.*, **427**, 1 (1922).

(2) M. Kuhn and R. Mecke, *Chem. Ber.*, 3010 (1961).

(3) The synthesis of the ammonium salt and its infrared spectrum as a KBr pellet have been presented recently by M. B. Frankel, *et al.*, *J. Org. Chem.*, **28**, 2428 (1963). The bands listed by these authors in the $\text{C}\equiv\text{N}$ stretching frequency region differ slightly from ours, but it is not possible to determine if partial cation exchange has occurred in their pellet without data in the 900-950 cm^{-1} region.

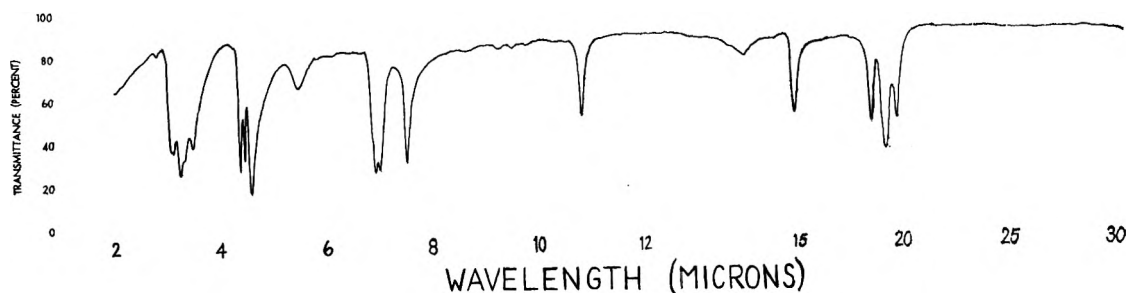


Figure 1. Infrared spectrum of ammonium dicyanamide, split mull.

50 ml. and allowed to crystallize. The crude ammonium bromide amounted to 78 g. or 85% of theoretical.

The crystals from the concentrated extracts were filtered, washed with a little acetone, and recrystallized from hot acetone. Ammonium dicyanamide, white crystals weighing 8 g., was obtained in 20% yield from cyanogen bromide. *Anal.* Calcd. for $C_2H_4N_4$: C, 28.6; H, 4.8; N, 66.6. Found: C, 29.6; H, 5.4; N, 64.2; melting range: 139–140° to clear melt which solidified to dicyandiamide, identified by its infrared spectrum.

The infrared spectrum of ammonium dicyanamide shows characteristic frequencies of the ammonium ion and of the dicyanamide anion. The latter can be assigned as in the excellent discussion of Kuhn and Mecke,² and the notation of these authors has been followed in listing the bands in Table I. As expected, shifts in the anion frequencies are observed for the ammonium salt, and it is of interest to note that they fall between the values for the K^+ (see below) and Na^+ salts. The bands due to the ammonium ion⁴ are found at 3212, 3160, 3052, 2962, 2842, 1818, 1710, 1451, 1438, 1421, 1377, and 1342 cm^{-1} . The band positions listed were obtained from a split mull (halocarbon oil, 2–7.4 μ ; nujol, 7.4–38 μ) on a Perkin-Elmer 221-G using an expanded abscissa of 25 cm^{-1}/cm . Positions are reproducible to 2 cm^{-1} . Figure 1 shows the infrared spectrum of the split mull on the Perkin-Elmer 21 (15–38 μ on PE 221-G with CsBr optics) where it was recorded for comparison with the spectrum of the sample as a KBr pellet. The spectrum of ammonium dicyanamide in water was very similar to that of the mull.

The infrared spectrum of the ammonium dicyanamide was first obtained as a KBr pellet on a Perkin-Elmer 21 spectrophotometer. When the high resolution spectrum to obtain accurate band positions was later run on the Perkin-Elmer 221-G with the sample as a mull, some unusual spectral changes were immediately noted. Detailed investigation of these led to the conclusion that almost complete cation exchange occurs

Table I: Anion Frequencies for Ammonium Dicyanamide $[N(CN)_2]^-$ Structure, C_{2v}

cm^{-1} ^a	Assignment ^b
505 m	$B_2 \Gamma$ } N-CN
519 m	$A_1 \Delta$ } N-CN
538 m	$B_1 \Delta$ N-CN
668 m	$A_1 \Delta$ C-N-C
927 m	$A_1 \omega_s$ } C-N
1328 s	$B_1 \omega_s$ } C-N
2171 s	$A_1 \omega_s$ } C≡N
2229 s	$B_1 \omega_s$ } C≡N
2234 s	
2274 s	$\omega_s + \omega_a$ (C-N)
3538 w	ω_s (CN) + ω_s (C≡N)

^a Intensities given are s, strong; m, medium; w, weak.

^b Γ , Δ = bond deformations; ω_s = symmetrical stretch; ω_a = asymmetrical stretch.

in the pellet⁵ resulting in NH_4Br and $KN(CN)_2$. Such occurrences are not uncommon and this observation serves only to emphasize the well documented⁶ need for caution when interpreting spectra of solids in KBr pellets.⁷ The bands due to the potassium dicyanamide are observed at 662, 910, 1316, 1339, and 3460 cm^{-1} and approximately at 2114, 2160, 2188, and 2232 cm^{-1} in the nitrile stretching region (bands too intense for accurate measure).

The n.m.r. spectra were obtained on a fully equipped Varian V-4300C spectrometer operating at a frequency

- (4) E. L. Wagner and D. F. Hornig, *J. Chem. Phys.*, **18**, 296 (1950); **18**, 305 (1950).
- (5) (a) L. H. Jones and M. M. Chamberlain, *ibid.*, **25**, 365 (1956); (b) J. A. A. Ketelaar, C. Haas, and J. van der Elsken, *ibid.*, **24**, 624 (1956); (c) F. Vrátný, *J. Inorg. Nucl. Chem.*, **10**, 328 (1959).
- (6) (a) A. W. Baker, *J. Phys. Chem.*, **61**, 450 (1957); (b) H. Röpke and W. Neudert, *Z. anal. Chem.*, **170**, 78 (1959); (c) A. Tolks, *Spectrochim. Acta*, **17**, 511 (1961).
- (7) Although Kuhn and Mecke present the spectrum of $Na[N(CN)_2]$ as a KBr pellet, no cation exchange is observed (comparing band positions listed by them for Na^+ salt and those observed by us in exchanged NH_4^+ salt spectrum). This is probably due to the conditions used in preparing pellets.

of 60 Mc./sec. The compound was examined at $25.0 \pm 0.5^\circ$ in dilute solutions ($\sim 10\%$ wt. vol.) in both dimethyl sulfoxide- d_6 (DMS) and D_2O utilizing tetramethylsilane (TMS) as the reference, internally in DMS and externally in D_2O . Radiofrequency power was held well below saturation intensity and a sweep rate of approximately 0.95 c.p.s./sec. was employed. The spectra were calibrated by linear interpolation between the reference and its 600-c.p.s. side band.

A triplet with broad resonances of equal intensity at approximately 7.7 p.p.m. below TMS with a coupling constant of approximately 50 c.p.s. was observed in DMS spectra. No other resonances were observed which were not due to the solvent or the reference. Upon examination in acidified D_2O , the triplet coalesced with the H_2O resonance and the resulting singlet was observed shifted slightly downfield from the normal location of the H_2O resonance line. These results are interpreted^{8,9} as being due to the presence of protons attached to a quaternary nitrogen and indicating that no other protons are present in the compound.

Spectroscopic as well as chemical evidence therefore has characterized the ammonium salt of dicyanamide:

Acknowledgment. The authors wish to acknowledge the experimental assistance of Mr. Harry Adams, Miss Patricia L. Neibecker, and Mr. Herb Grossman.

(8) E. Grunwald, A. Loewenstein, and S. Meiboom, *J. Chem. Phys.*, **27**, 630 (1957).

(9) J. A. Pople, W. G. Schneider, and H. J. Bernstein, "High-Resolution Nuclear Magnetic Resonance," McGraw-Hill Book Co., Inc., New York, N. Y., 1959, p. 455.

A New Class of Photochromic Substances: Metal Carbonyls¹

by M. A. El-Sayed

Contribution No. 1632, Chemistry Department, University of California, Los Angeles 24, California. (Received October 2, 1963)

Photochromism² is defined as the reversible coloring of compounds on irradiation with ultraviolet light, γ -rays,^{3a} or electrons.^{3b} There are a great number of organic molecules and, to a lesser extent, a smaller number of inorganic compounds which undergo these reversible color changes. The mechanism for color changes is not unique and differs from one class of compounds to the other.²

In this communication we report a class of compounds which undergo a reversible color change under the in-

fluence of ultraviolet irradiation. The set of compounds used are metal hexacarbonyls of Cr, Mo, and W. Irradiation is carried out with a 1-kw. high pressure Hg lamp (AH₆) in 1:1 ether-isopentane mixture at room and at liquid nitrogen temperatures. The electronic spectrum is obtained using the Beckman spectrometer Model DK1.

At 77°K., the formation of a yellow color is observed as soon as the glass is exposed to ultraviolet light. It is formed also *in vacuo* and at different wave lengths of excitation. The yellow color is relatively independent of the metal that is bound to the carbon monoxide molecules. It disappears a few minutes after the glass is allowed to warm up to room temperature. Exposure at room temperature in ether-isopentane is also found to produce the yellow color.

Figure 1 (A) shows the electronic absorption spectra of $Mo(CO)_6$ solution in 1:1 ether-isopentane mixture at room temperature before exposure. This carbonyl has two structureless bands at 2892 and 2270 Å. and

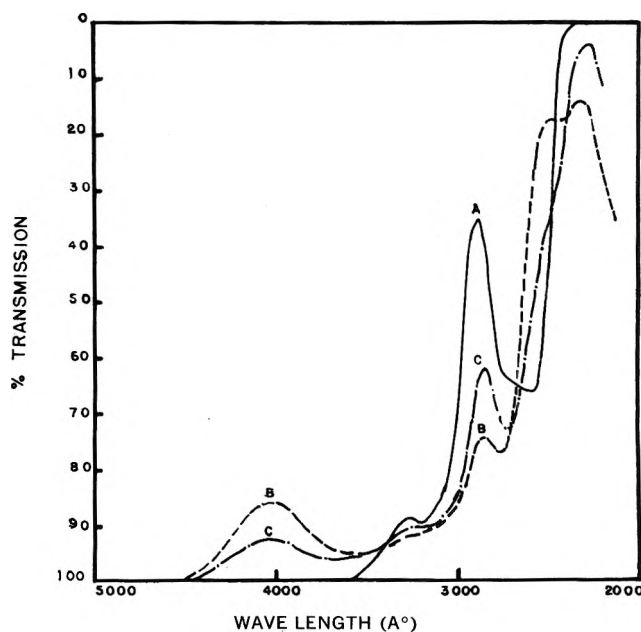


Figure 1. The electronic spectra of ultraviolet-irradiated $Mo(CO)_6$ solutions in 1:1 ether-isopentane mixture: A, spectrum of 415×10^{-3} mole/l. unexposed solution; B, of the same solution immediately after 20-sec. exposure; C, a few minutes after exposure.

(1) Work supported by the U. S. Atomic Energy Commission, partly from a contract with the University of California at Los Angeles and partly from a contract to Florida State University, Tallahassee, Fla.

(2) For a review on the subject see G. Brown and W. Shaw, *Rev. Pure Appl. Chem.*, **11**, 2 (1961).

(3) (a) Y. Hirshberg, *Bull. Res. Council Israel*, **7A**, 228 (1958); (b) *J. Chem. Phys.*, **27**, 758 (1957).

a shoulder of longer wave length. Figure 1 (B) shows the spectrum of the same solution exposed for 20 sec. in the Beckman cell and obtained soon after exposure. This spectrum shows clearly the appearance of two new bands at 4095 and 2469 Å. and a decrease in the intensity of the original bands. Figure 1 (C) shows the spectrum taken 4 min. after the exposure has been ceased. The peaks resulting from ultraviolet exposure decrease in intensity while those present before exposure increase.

The colored species may be a bimolecular photo-product of the excited molecule,² a photodissociation or photoionization product. Among the possibilities for photoreaction is the reaction with the solvent, with oxygen (photooxidation), or with another unexcited carbonyl (phototransformation into a polynuclear carbonyl). The known behavior of $\text{Fe}(\text{CO})_5$ toward light and the fact that most binuclear carbonyls are yellowish in color argues in favor of the formation of the binuclear carbonyl. However, the yellow color in the binuclear carbonyls is found to be due to a tail in the visible which belongs to a broad absorption at the edge of the ultraviolet and not due to a well defined sharp band in the visible as observed in this study. Also, the very dilute concentrations used cannot explain the instantaneous formation of the yellow color which appears even at 77°K.

Photooxidation seems improbable on the basis of the following observations. (1) If two tubes are filled with identical carbonyl solutions, oxygen passed through one and the other thoroughly vacuum degassed, then exposed to the ultraviolet source, each of the tubes develops the yellow color at the same rate. (2) Chromium, molybdenum, and tungsten carbonyls all form the yellow color on exposure, whereas chromium has no known yellow oxide. (3) Accompanying the formation of the yellow color, new $\text{C}\equiv\text{O}$ stretching absorptions are observed in the infrared which disappear after exposure at the same rate as the yellow color.

Two possibilities should now be considered; first, the reversible formation of a relatively weak complex with the solvent, and second, the dissociation to $\text{M}(\text{CO})_5$ species. In solvents with strong coordinating power such as acetonitrile, the carbonyl compounds cannot be defined as photochromic material since the color change is not completely reversible. After removing the exciting light, the yellow color fades slowly, but the solution never recovers its colorless initial appearance as it does in saturated nonpolar solvents. It is shown in this case that an actual compound with the solvent molecule has been formed.⁴

The infrared spectra of these species in isopentane-ether and in hexane have been obtained.^{5,6} The number

of bands could be in agreement with a square pyramidal structure.^{5,6} This fact, together with other chemical and physical arguments, leads to the conclusion⁵⁻⁷ that the new species is $\text{M}(\text{CO})_6$. If this is the case, the application of flash photolysis techniques to obtain the spectra of $\text{M}(\text{CO})_6$ in the vapor phase of these compounds should be interesting.

From the electronic spectrum (Fig. 1), one can estimate an approximate value of the molar extinction coefficient (ϵ) of the colored species. Assuming that upon the absorption of a photon each $\text{M}(\text{CO})_5$ molecule gives one molecule of the colored form, ϵ for the maximum of the band at 4095 Å. is found to be ~ 200 . The quantum yield, however might be very different from unity; the value estimated for the molar extinction coefficient should be taken as a lower limit.

Because of the great similarity in bonding between the different carbonyls, photochromism from other metal carbonyls and perhaps other organometallic compounds in nonreactive deoxygenated solvents is expected.

Acknowledgment. The author wishes to thank Professor R. K. Sheline for valuable discussions.

- (4) G. Dobson, M. A. El-Sayed, I. Stolz, and R. K. Sheline, *Inorg. Chem.*, **1**, 526 (1962).
- (5) M. A. El-Sayed and R. K. Sheline, unpublished work, summer, 1959.
- (6) I. Stolz, G. Dobson, and R. K. Sheline, *J. Am. Chem. Soc.*, **84**, 3589 (1962).
- (7) C. Bamford and C. Finch, *Trans. Faraday Soc.*, **59**, 118 (1963).

Electrolyte-Solvent Interaction. XIII. Conductance of Amine Picrates in Ethylene Chloride at 25°¹

by James J. Zwolenik and Raymond M. Fuoss

Contribution No. 1745 from the Sterling Chemistry Laboratory of Yale University, New Haven, Connecticut
(Received November 9, 1963)

In the search for a reproducible high-resistance system for use as a secondary standard in calibrating² conductance cells with small cell constants, several amine picrates were examined in solution in ethylene chloride ($D = 10.35$, $\eta = 0.00783$) and in *o*-dichlorobenzene ($D = 10.07$, $\eta = 0.01324$ at 25°). It was found that the resistance of dilute solutions of tribenzyl-, triethyl-, tri-*n*-propyl-, and tri-*n*-butylamine picrates increased slowly with time; these changes were small

(of the order of tenths of a per cent per hour) but too great for precision standards. The conductances at concentrations above that corresponding to the conductance minimum, however, were stable. The observed drift in conductance in the dilute solutions is probably due to oxidation of the amines to the corresponding amine oxide³ to an equilibrium concentration of the latter.

Experimental

Tribenzylammonium picrate was prepared by mixing 10% ethanol solutions of recrystallized picric acid (m.p. 121°) and recrystallized tribenzylamine (m.p. 92°). It was recrystallized from 7:3 95% ethanol-acetone (3.5 g./100 ml.) and from 7:3 95% ethanol-water (1.5 g./100 ml.); m.p. 194°. Triethylammonium picrate and tri-*n*-propylammonium picrate were also prepared in ethanol and recrystallized from ethanol; m.p. 178 and 118°, respectively.

Conductances were measured in a Nichol cell^{2,4} using electrical equipment already described.⁵ All solutions were made up by weight. In order to minimize the effects of drifting conductance, concentration runs, made by adding successive portions of picrate to the cell, were made. Densities at 25° were calculated from the following data, assuming linear dependence of density on weight concentration: ethylene chloride, $\rho_0 = 1.2460$; 0.05 *N* Bz₃NHPi in C₂H₄Cl₂, $\rho = 1.2484$; 0.2 *N* Et₃NHPi in C₂H₄Cl₂, $\rho = 1.2468$; *o*-dichlorobenzene, $\rho_0 = 1.3010$; 0.1 *N* Pr₃NHPi in *o*-C₆H₄Cl₂, $\rho = 1.3008$. Salt densities: Bz₃NHPi, 1.20; Et₃-

NHPi, 1.39. The conductance data are summarized in Table I.

Both tribenzyl- and triethylammonium picrates show minima in their conductances at about 0.05 *N* in ethylene dichloride, which is nearly the same behavior as that shown by tributylammonium picrate.⁶ Plots of $\Lambda c^{1/2}$ against *c* are linear⁷ for these systems. From the intercepts at *c* = 0, and assuming $\Lambda_0(\text{Bz}_3\text{NHPi}) = 50$ and $\Lambda_0(\text{Et}_3\text{NHPi}) = 70$, association constants $K_A(\text{Bz}_3\text{NHPi}) = 1.5 \times 10^7$ and $K_A(\text{Et}_3\text{NHPi}) = 4.8 \times 10^7$. Since $K_A(\text{Bu}_3\text{NHPi})$ is also 4.8×10^7 , the indication is that the aryl-substituted amines are less associated than the alkyls. The interesting feature of the results is the relatively low conductance shown by Pr₃NHPi in *o*-dichlorobenzene. One would expect $K_A(\text{Pr}_3\text{NHPi})$ to be about 5×10^7 in ethylene dichloride; it clearly must be much larger than this in the isodielectric solvent *o*-dichlorobenzene. The data are all at concentrations above the conductance minimum; an estimate from the $\Lambda c^{1/2}$ -*c* plot, using $\Lambda_0(\text{Pr}_3\text{NHPi}) = 35.5$ from Walden's rule and data for tetrapropylammonium picrate in ethylene dichloride,⁸ gives $K_A \approx 9 \times 10^9$ for Pr₃NHPi in dichlorobenzene, over two orders of magnitude higher than in ethylene chloride. This is an even more striking difference between isodielectric solvents than the one reported by Ramsey⁹ for ethylene chloride and ethylidene chloride or *o*-dichlorobenzene, and represents another case of specific solvent-electrolyte interaction. Possibly both the ion-pair dissociation and the molecular dissociation of the amine picrates depend on the chemical nature of the solvent.

Table I: Conductance of Amine Picrates

10 ³ <i>c</i> Bz ₃ NHPi in C ₂ H ₄ Cl ₂	Λ	<i>c</i> Et ₃ NHPi in C ₂ H ₄ Cl ₂	Λ
0.349	0.682	0.02090	0.1081
0.742	.504	.02888	.1003
1.178	.414	.03771	.0963
1.617	.361	.05533	.0944
2.119	.321	.09356	.1010
5.169	.1984		
10.177	.1557	<i>n</i> -Pr ₃ NHPi in <i>o</i> -C ₆ H ₄ Cl ₂	
26.88	.1225	0.0538	0.01398
32.62	.1196	.0989	.01799
49.16	.1177	.1295	.02105
		.2253	.03148
		.3144	.04102

- (1) (a) This note is abstracted from a thesis submitted to the Graduate School of Yale University by J. J. Zwolenik, in partial fulfillment of the requirements for the degree of Doctor of Philosophy; (b) grateful acknowledgment is made for National Science Foundation Fellowships.
- (2) J. J. Zwolenik and R. M. Fuoss, *J. Phys. Chem.*, in press.
- (3) M. M. Davis and H. B. Hetzer, *J. Am. Chem. Soc.*, **76**, 4247 (1954).
- (4) J. C. Nichol and R. M. Fuoss, *J. Phys. Chem.*, **58**, 696 (1954).
- (5) J. E. Lind, Jr., and R. M. Fuoss, *ibid.*, **65**, 999 (1961).
- (6) D. J. Mead, R. M. Fuoss, and C. A. Kraus, *J. Am. Chem. Soc.*, **61**, 3257 (1939).
- (7) R. M. Fuoss and C. A. Kraus, *ibid.*, **55**, 2387 (1933).
- (8) L. M. Tucker and C. A. Kraus, *ibid.*, **69**, 454 (1947).
- (9) J. B. Ramsey and E. L. Colichman, *ibid.*, **69**, 3041 (1947); Y. H. Irami, H. K. Bodenseh, and J. B. Ramsey, *ibid.*, **83**, 4745 (1961).

Reduction of Platinum Oxide by Organic Compounds. Catalytic Self-Activation in Deuterium Exchange Reactions

Sir: Recently, the use of platinum oxide prereduced with hydrogen has been evaluated as a catalyst for exchange reactions between isotopic water and organic compounds.^{1,2} A new π -complex chemisorption theory has been proposed to account for the observed reactivities.^{3,4} The technique is a valuable tool for the preparation of deuterated compounds for mass spectrometry and magnetic resonance spectroscopy and also yields a convenient source of tritiated intermediates for tracer studies in chemical and biological fields.⁵

From the viewpoint of fundamental catalytic theory, we now wish to report a novel reaction involving the reduction of platinum oxide ($\text{PtO}_2 \cdot 2\text{H}_2\text{O}$) by organic compounds and the subsequent use of this "self-activated" catalyst in exchange reactions. At 30° , unreduced platinum oxide ($\text{PtO}_2 \cdot 2\text{H}_2\text{O}$) does not catalyze exchange reactions between organic compounds such as benzene and deuterium oxide, whereas this reaction is virtually complete in 18 hr. when platinum oxide prereduced with hydrogen is used in the usual reagent amounts shown below. Above 90° , reduction of platinum oxide by benzene readily occurs and the resulting catalyst leads to complete equilibrium between isotopic water and benzene in 24 hr. at 120° . In a typical experiment, benzene (2.0 g.) and heavy water (1.5 g.) are added to platinum oxide (0.05 g.) and the reaction vessel vacuum sealed and shaken at 120° for 24 hr. The organic layer is then analyzed by mass spectrometry to determine the deuterium distribution, total deuterium content, and identity of the reaction products.

During the process of "self-activation," the catalyst is not completely reduced since catalyst exposure to hydrogen after self-activation yields an explosive reaction at 30° . This effect is further evidence in an accumulating body of knowledge concerning the specificity of different sites in catalytic exchange reactions.^{6,7} Furthermore, platinum oxide, self-activated by benzene at 120° , does not catalyze exchange between benzene and heavy water at 30° . These data are consistent with the results of a platinum catalyst which was activated by prereduction with hydrogen and then exposed to benzene at 120° . When cooled to 30° and the benzene removed, this catalyst was not effective in benzene-deuterium oxide exchange at this lower temperature.⁷

There is a considerable variation in the relative reactivities of various commercial platinum oxides in self-activation. Of three commercial varieties examined, that supplied by Bishop and Co., New York, N. Y., was very much faster in both reduction and exchange than the remaining two under identical conditions. When equilibration was achieved with the Bishop catalyst (100% reaction), the other two products showed 25% reaction. However, both latter reactions were readily completed if exchange was continued for a longer period of time or if the temperature was increased to 130° .

In preliminary studies, benzene, biphenyl, dibenzyl, cyclohexene, *n*-octane, cyclohexane, and naphthalene self-activated unreduced platinum oxide with or without the presence of water at 120° . The first four compounds also exchange readily under these conditions while *n*-octane and cyclohexane react only slowly, although more efficiently than in the presence of a prereduced platinum catalyst. Naphthalene self-activates platinum oxide but does not appreciably exchange with D_2O , this behavior being consistent with the ready poisoning characteristics of this compound in terms of the π -complex theory of heterogeneous catalysis.⁷⁻¹⁰ Pyridine and nitrobenzene neither "self-activate" nor exchange with D_2O in the presence of unreduced PtO_2 at 120° .

In terms of catalytic theory, the important aspect of this "self-activation" process is that hydrogen for reduction of the platinum catalyst must be supplied by the organic compound through C-H bond rupture, *i.e.*, a dissociative type process. The lack of reactivity of pyridine and nitrobenzene confirms the conclusions drawn in our earlier work^{11,12} where it was shown that

- (1) J. L. Garnett, L. J. Henderson, and W. A. Sollich, "Proc. Intern. Atomic Energy Agency Tritium Symposium, Tritium in the Physical and Biological Sciences," Vol. II, Vienna, 1961, p. 47.
- (2) J. L. Garnett, L. J. Henderson, W. A. Sollich, and G. V. D. Tiers, *Tetrahedron Letters*, **15**, 516 (1961).
- (3) J. L. Garnett and W. A. Sollich, *Australian J. Chem.*, **14**, 441 (1961).
- (4) J. L. Garnett and W. A. Sollich, *J. Catalysis*, **2**, 350 (1963).
- (5) J. L. Garnett, *Nucleonics*, **20**, No. 12, 86 (1962).
- (6) J. R. Anderson and C. Kemball, *Advan. Catalysis*, **9**, 51 (1957).
- (7) J. L. Garnett and W. A. Sollich, *J. Catalysis*, **2**, 339 (1963).
- (8) J. L. Garnett, *Proc. Royal Aust. Chem. Inst.*, **28**, No. 8, 328 (1961).
- (9) E. Crawford and C. Kemball, *Trans. Faraday Soc.*, **58**, 2452 (1962).
- (10) J. J. Rooney, *J. Catalysis*, **2**, 53 (1963).
- (11) J. L. Garnett and W. A. Sollich, *Australian J. Chem.*, **15**, 56 (1962).
- (12) R. A. Ashby and J. L. Garnett, *ibid.*, **16**, 549 (1963).

the adsorption characteristics and hence the exchange properties of the heterocycles and nitrobenzene were different from other substituted aromatics and aliphatics. From π -complex chemisorption theory, it is significant that aromatic compounds in general are more reactive than aliphatics in self-activation and exchange. In conclusion, the "self-activation" process offers a convenient tritiation procedure for a large range of compounds without the necessity for hydrogen pre-activation of the catalyst.

A full discussion of the process of "self-activation" using a variety of organic compounds and different catalysts as model systems will be published in detail elsewhere.

Acknowledgment. The authors are grateful to the Australian Institute of Nuclear Science and Engineering (Mr. E. A. Palmer) for assistance in the purchase of the heavy water, the New South Wales State Cancer Council for the use of their facilities, and Mr. J. Mason for instrumentation advice.

SCHOOL OF CHEMISTRY
THE UNIVERSITY OF NEW SOUTH WALES
KENSINGTON, N.S.W., AUSTRALIA

J. L. GARNETT
W. A. SOLLICH

RECEIVED OCTOBER 29, 1963

Carbon-13 Chemical Shifts and Intramolecular Hydrogen Bonding

Sir: In a comprehensive study of C^{13} chemical shifts in a variety of molecular systems, Lauterbur¹ measured the shift of the carbonyl carbon in a series of *ortho*-substituted methyl benzoates. He found that for the series with *ortho* substituents H, OCH₃, I, Br, NO₂, Cl, and OH, the variation in the carbonyl carbon shift was only 0.8 p.p.m., probably within experimental error, except when the *ortho* substituent was a hydroxyl group. For that case, methyl salicylate, he reported a shift of the carbonyl carbon of about 5 p.p.m. to lower field and rationalized it as an effect of intramolecular hydrogen bonding between the carbonyl oxygen atom and the hydroxyl hydrogen. Because of our interest in the effect of hydrogen bonding on carbonyl chemical shifts, and in C^{13} chemical shifts in general, we have investigated the validity of Lauterbur's interpretation and the scope of the effect in these systems.

That the original interpretation is *a priori* subject to question rests on the fact that the measurement of C^{13} shifts in methyl salicylate does not establish conclusively the value of the shift of the carbonyl carbon,

since there are two resonance peaks in the spectrum of this compound which appear in the region characteristic of carbonyls. One of these is about 4 p.p.m. downfield and the other about 4 p.p.m. upfield from the position of resonance of the carbonyl carbon atom in methyl benzoate. It is reasonable to suppose that these two peaks correspond to the two carbon atoms bonded to the electronegative oxygen atoms, the "carbonyl carbon" and the "hydroxyl carbon." Without additional data the correct assignment of these peaks remains a moot point. One could either argue that the well known intramolecular hydrogen bond in this compound causes a downfield shift of the carbonyl carbon and the upfield peak is due to the hydroxyl carbon (as Lauterbur did), or that the hydrogen bond shifts the resonance of the carbonyl carbon to higher field and that the low-field peak is due to the carbon atom bound to the hydroxyl group involved in the hydrogen bond.

To distinguish between these two possibilities, we obtained the carbon-13 n.m.r. spectra of a series of compounds in which strong intramolecular hydrogen bonds are known to exist between a carbonyl group attached to a benzene ring and a hydroxyl group situated *ortho* to the carbonyl group.² These compounds were selected in such a way as to vary the group attached to the benzoyl (carbonyl) carbon atom through a range of inductive and resonance characteristics. Thus the attachment of OCH₃, H, CH₃, and C₆H₅ to the benzoyl (carbonyl) carbon atom should affect the chemical shift of the carbonyl carbon appreciably, approximately as predicted by the work done in this laboratory³ on the C^{13} chemical shifts of carbonyl compounds. On the other hand, the effect of these substituents on the hydroxyl carbon atom could be expected reasonably to be of the second order in magnitude. The compounds investigated and the corresponding chemical shifts are presented in Fig. 1.

The shifts summarized in Fig. 1 were obtained in natural abundance on 1:3 mole fraction solutions of solute in benzene at ν measuring frequency of 15.1 Mc./sec. using the rapid passage, dispersion mode technique described previously by Lauterbur. Shifts were measured in a concentric-sphere sample container to eliminate bulk susceptibility effects, with respect to an external reference of saturated aqueous NaO₂- $C^{13}CH_3$ (53.3 p.p.m. downfield from benzene) in the center sphere, using the side-band technique. Only

- (1) P. C. Lauterbur, *Ann. N. Y. Acad. Sci.*, **70**, 841 (1958).
- (2) L. Pauling, "The Nature of the Chemical Bond," 3rd Ed., Cornell University Press, Ithaca, N. Y., 1960.
- (3) G. B. Savitsky and R. M. Pearson, unpublished results.

COMPOUND	LINE POSITIONS ^a		Δ ^b
		15.8 C=O	
		11.4 X 19.6 Y	-4.4
		12.8 C=O	-3.0
	-13.3 C=O -2.2 C=O		17.2 C-OCH ₃
	-20.6 C=O -9.5 C=O		19.8 C-OH
		-14.9 C=O	
	-22.0 C=O		18.3 C-OH
		-13.8 C=O	
	-20.7 C=O		20.4 C-OH

δ^b ppm

Figure 1. C^{13} chemical shifts of carbonyl groups in some aromatic systems demonstrating effects of intramolecular H-bonding: ^a chemical shift with respect to standard $NaO_2C^{13}CH_3$; ^b shift due to intramolecular hydrogen bonding with *ortho* hydroxyl group or amino group.

peaks in the -24 to $+24$ -p.p.m. region with respect to the external reference are represented in Fig. 1. These shifts are the average result of at least five field scans in both increasing and decreasing sense and can be considered accurate to about ± 0.3 p.p.m. All samples were Eastman White Label, used without further purification.

In Fig. 1, we have labeled the two resonance peaks of interest in methyl salicylate as *x* and *y*. We see that in the hydroxy-containing compounds there is in each case a resonance peak in the relatively narrow region from 18.3 to 20.4 p.p.m. with respect to the reference. All the other low-field peaks in these hydroxy compounds vary considerably from compound to compound but are invariably downfield from the 18.3–20.4-p.p.m. region. Also, in the case of anisaldehyde and salicylaldehyde the low-field peaks appear as doublets with a separation of 11.1 p.p.m. and are undoubtedly due to the carbonyl carbon, split by spin-spin interaction with the formyl proton. In the spectrum of methyl anthranilate the assignment of the peak at 12.8 p.p.m. to the carbonyl group seems unambiguous, since no other peaks appear in the region represented in Fig. 1.

Thus, all the data clearly indicate that Lauterbur's original interpretation was correct, that peak *x* is due to the carbonyl carbon in methyl salicylate, and that intramolecular hydrogen bonding shifts the C^{13} resonance of the carbonyl group downfield by amounts ranging from 3 to 7 p.p.m. This result is in accord with C^{13} n.m.r. studies of intermolecular hydrogen bonding to carbonyl groups where shifts of this magnitude and direction are observed.⁴ An investigation is now under way to determine the effect of ring substituents on these intramolecular hydrogen bonding shifts.

(4) G. E. Maciel and G. C. Ruben, *J. Am. Chem. Soc.*, **85**, 3903 (1963)

DEPARTMENT OF CHEMISTRY
UNIVERSITY OF CALIFORNIA
DAVIS, CALIFORNIA

G. E. MACIEL
G. B. SAVITSKY

RECEIVED OCTOBER 10, 1963

Plutonyl Species in Molten Chloride Salt Solutions¹

Sir: A previous spectrophotometric investigation of the chemistry of plutonium in molten chloride salt solution demonstrated the existence of Pu(IV) as well as Pu(III) in such solutions, but no evidence for the existence of higher oxidation states was obtained.² We have recently prepared molten chloride salt solutions containing plutonyl(V) and plutonyl(VI) by reaction of dissolved Pu(III) and (IV) with an O_2-Cl_2 gas stream. These oxidation states were identified by comparison of the absorption spectra of the molten salt solutions with spectra of these oxidation states in other media.³⁻⁵ Additional verification of the existence of plutonyl species in molten chloride salt solutions was supplied by the observation that PuO_2 can be obtained by electroreduction of the plutonium in O_2-Cl_2 sparged solutions,⁶ in analogy to the electroreduction of uranyl(VI) to UO_2 .⁷

The spectra of two LiCl-CsCl eutectic solutions containing plutonyl(V) and (VI) are shown in Fig. 1

- (1) Work performed under Contract No. AT(45-1)-1350 for the U. S. Atomic Energy Commission.
- (2) D. M. Gruen, R. L. McBeth, J. Kooi, and W. T. Carnall, *Ann. N. Y. Acad. Sci.*, **79**, 941 (1960).
- (3) D. Cohen, *J. Inorg. Nucl. Chem.*, **18**, 211 (1961).
- (4) W. E. Keder, *ibid.*, **24**, 561 (1962).
- (5) J. L. Ryan, *Inorg. Chem.*, **2**, 348 (1963).
- (6) G. E. Benedict, Hanford Laboratories, unpublished data.
- (7) R. G. Robins, *J. Nucl. Mater.*, **3**, 294 (1961).

along with those containing Pu(III) and Pu(IV) for comparison. These spectra were obtained with a solution 0.0089 *M* in total plutonium species in a 3.8-cm. absorption cell at 400°, using a Cary 14 H spectrophotometer. Spectrum A of Pu(III) was obtained by

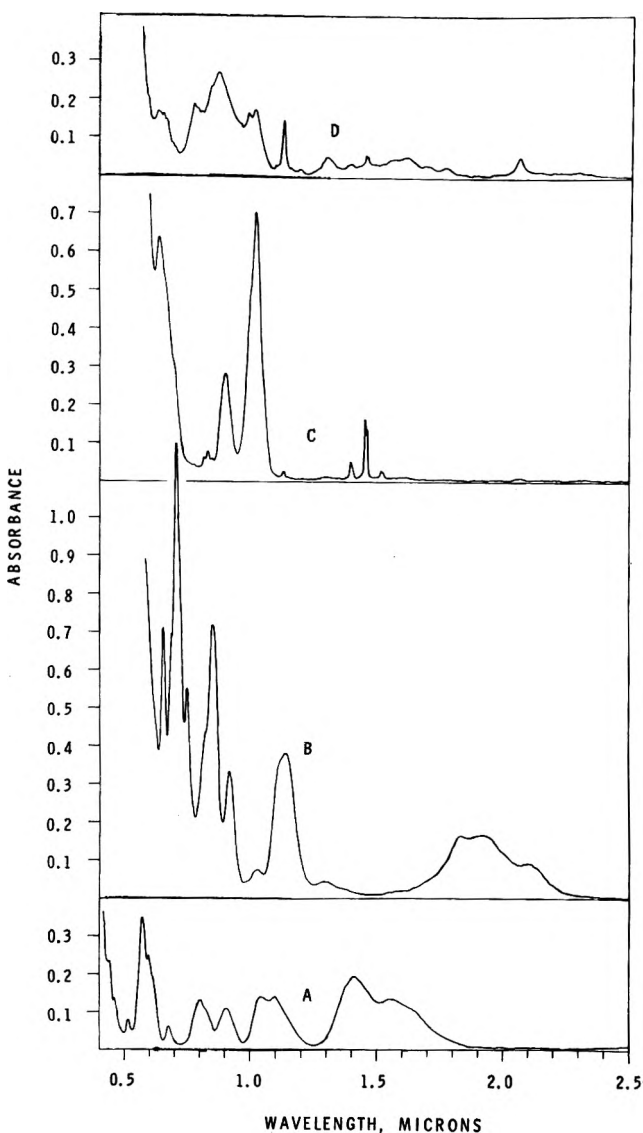


Figure 1. Absorption spectra of Pu ions in LiCl-CsCl eutectic at 400°. A is Pu(III), B is Pu(IV), C is predominantly plutonyl(VI), and D is predominantly plutonyl(V).

dissolving PuCl₃ in the eutectic and sparging with 2% H₂ in HCl to assure the absence of Pu(IV). Spectrum B of Pu(IV) was obtained by sparging with Cl₂ to oxidize the Pu(III) to Pu(IV); the spectrum indicates that at least 90% of the plutonium was oxidized. The plutonium was then oxidized to plutonyl species,

predominantly plutonyl(IV), by sparging with 33% O₂ in Cl₂; when the reaction was complete, spectrum C was obtained. Removal of Cl₂ from the solution by sparging with He resulted in diminution of the plutonyl(VI) and growth of the plutonyl(V) peaks and eventually in the precipitation of a portion of the plutonium as PuO₂. This behavior is attributed to shifts in the equilibria



Spectrum D, which is predominantly that of plutonyl(V), was obtained shortly before precipitation began.

The behavior of the plutonyl species under various conditions was studied spectrophotometrically. The ratio of plutonyl(V) to plutonyl(VI) in O₂-Cl₂ sparged solutions was found to vary inversely with the square root of the concentration of Cl₂ in the sparge gas. With a given O₂-Cl₂ composition, the ratio increases with temperature and also depends on the composition of the solution, being greater in LiCl-KCl eutectic than in LiCl-CsCl eutectic. In solutions sparged only with Cl₂, reduction of the plutonyl species to Pu(III) and Pu(IV) occurs. This reduction proceeds quite slowly at low temperature. Sparging with HCl results in rapid reduction of the plutonyl species, initially to Pu(IV), then to Pu(III).

HANFORD LABORATORIES
HANFORD ATOMIC PRODUCTS OPERATION
GENERAL ELECTRIC COMPANY
RICHLAND, WASHINGTON

J. L. SWANSON

RECEIVED DECEMBER 6, 1963

On the Delayed Fluorescence of Pyrene Solutions. A Correction

Sir: The rate parameters describing the prompt and delayed fluorescence of pyrene in ethanol have been evaluated¹ from experimental data on the spectra² and on k_{FM} and k_{FD} , the rate parameters of the monomer and excimer fluorescence, respectively, for pyrene in cyclohexane.³ In this analysis no correction was applied to allow for the difference in the refractive index n of cyclohexane ($n = 1.43$) and ethanol ($n =$

- (1) J. B. Birks, *J. Phys. Chem.*, **67**, 2199 (1963).
- (2) C. A. Parker and C. G. Hatchard, *Trans. Faraday Soc.*, **59**, 284 (1963).
- (3) J. B. Birks, D. J. Dyson, and I. H. Munro, *Proc. Roy. Soc. (London)*, **A275**, 575 (1963).

1.36) and its influence on the values of k_{JM} and k_{JD} . The analysis has now been repeated, taking⁴ k_f proportional to n^2 , and the following revised values for the rate parameters of pyrene in ethanol are obtained: $k_{JM} = 0.136 \times 10^7 \text{ sec.}^{-1}$; $k_{JD} = 1.05 \times 10^7 \text{ sec.}^{-1}$; $k_{DM} = 6 \times 10^9 \text{ l. mole}^{-1} \text{ sec.}^{-1}$; $k_{tM} = 0.073 \times 10^7 \text{ sec.}^{-1}$; $k_{tD} = 0.86 \times 10^7 \text{ sec.}^{-1}$; $k_{MD} = 0.83 \times 10^7 \text{ sec.}^{-1}$; $q_M = 0.65$, $q_D = 0.55$, and $c_h = 5 \times 10^{-4} M$, as in the previous analysis,¹ but values of $\alpha = 1.94$ and $\alpha = 2.02$ (instead of $\alpha = 1.45$ and $\alpha = 1.52$) are obtained from K_2 and K_3 , respectively. It thus appears

that the triplet-triplet quenching results in the initial formation of excimers and excited monomers in the ratio of 2:1, respectively, and not in the ratio 1.5:1 as originally estimated.¹

(4) J. B. Birks and D. J. Dyson, *Proc. Roy. Soc. (London)*, **A275**, 136 (1963).

THE PHYSICAL LABORATORIES
UNIVERSITY OF MANCHESTER
MANCHESTER 13, ENGLAND

J. B. BIRKS

RECEIVED DECEMBER 21, 1963